

THE SYNTHESSES AND REACTIONS OF
CARBONYL(PHOSPHINE)(THIOLATO)RUTHENIUM(II)
COMPLEXES

By

PHILIP GREGORY JESSOP

B.Sc., The University of Waterloo, 1986

A THESIS SUBMITTED IN PARTIAL FULFILLMENT OF
THE REQUIREMENTS FOR THE DEGREE OF
DOCTOR OF PHILOSOPHY

in

THE FACULTY OF GRADUATE STUDIES
(Department of Chemistry)

We accept this thesis as conforming
to the required standard

THE UNIVERSITY OF BRITISH COLUMBIA

February 1991

© Philip Gregory Jessop, 1991

In presenting this thesis in partial fulfilment of the requirements for an advanced degree at the University of British Columbia, I agree that the Library shall make it freely available for reference and study. I further agree that permission for extensive copying of this thesis for scholarly purposes may be granted by the head of my department or by his or her representatives. It is understood that copying or publication of this thesis for financial gain shall not be allowed without my written permission.

Department of Chemistry

The University of British Columbia
Vancouver, Canada

Date 22 April 1991

ABSTRACT

The chemistry of homogeneous transition metal systems offer parallels to the reactions on the surfaces of industrial hydrodesulphurization catalysts. The reactions of several ruthenium complexes with sulphur-containing reagents are described, with an emphasis on the kinetics and mechanisms thereof. The complex $\text{Ru}(\text{CO})_2(\text{PPh}_3)_3$ (**2**), for example, reacts quickly with thiols and disulphides, producing *cct*- $\text{RuH}(\text{SR})(\text{CO})_2(\text{PPh}_3)_2$ (**9**) and *cct*- $\text{Ru}(\text{SR})_2(\text{CO})_2(\text{PPh}_3)_2$ (**14**), respectively, although **2** fails to react with unstrained thioethers. Reactions of the related complex $\text{Ru}(\text{CO})_2(\text{PPh}_3)(\text{dpm})$ ($\text{dpm}=\text{Ph}_2\text{PCH}_2\text{PPh}_2$) are complicated by the lability of all of the three different ligands.

The two dihydrides *cct*- $\text{RuH}_2(\text{CO})_2(\text{PPh}_3)_2$ (**3**) and $\text{RuH}_2(\text{dpm})_2$, as a *cis/trans* mixture (**7**), react with thiols to produce the hydrido-thiolato complexes **9** and $\text{RuH}(\text{SR})(\text{dpm})_2$ (**13**), respectively. The mechanisms appear to depend on the basicity of the hydride ligands; the more basic dihydride, **7**, is probably protonated by the thiol, giving an unobserved molecular hydrogen intermediate, while **3** reacts by slow reductive elimination of H_2 . The same rate constant, rate law, and activation parameters are found for the reaction of **3** with thiols, CO or PPh_3 . The reaction of **3** with RSSR produces mostly **9**, with small amounts of **14**.

The complete characterization of several members of the series **9** and **14** is described, including the crystal structure of the *p*-thiocresolate example of each. The reactions of **9** with other thiols, $\text{P}(\text{C}_6\text{H}_4\text{pCH}_3)_3$, CO, RSSR , HCl, PPh_3 , and H_2 , are also reported. The first three of these reactions share the same rate law and rate constant, the common rate determining step probably being initial loss of PPh_3 . Some equilibrium constants for the exchange reactions of **9d** ($\text{R}=\text{CH}_2\text{CH}_3$) with other thiols were determined, the K_{eq} values increasing with the acidity of the incoming thiol.

The mercapto hydrogens of **9a** and **14a** (R=H) exchange with the acidic deuterons of added CD₃OD. The hydridic and ortho-phenyl hydrogens exchange more slowly, presumably by intramolecular processes.

Complex **14b** (R=C₆H₄*p*CH₃) is unstable in the presence of light, exchanges phosphines rapidly with added P(C₆H₄*p*CH₃)₃, exchanges thiolate groups with added thiols, and is converted by high pressures of H₂ to a mixture of **9b** and **3**.

Intermediates proposed for the mechanism of the thiol exchange reactions of **9** and **14** contain two or three thiolate groups sharing a proton. A related complex, [Ru(CO)₂(PPh₃)(μSEt)₂(μ₃SEt)Na(THF)]₂, which contains three thiolate groups on a ruthenium centre sharing a sodium cation, was isolated from the reaction of *cct*-RuCl₂(CO)₂(PPh₃)₂ with sodium ethanethiolate. In acetone, **9b** and **14b** can be formed cleanly from *cct*-RuHCl(CO)₂(PPh₃)₂ and *cct*-RuCl₂(CO)₂(PPh₃)₂, respectively, by reaction with *p*-thiocresolate.

Complex **3** or cheaper analogues could be used as catalysts for the reduction of disulphides by H₂, or as recyclable reagents for the non-oxidative extraction of thiols from thiol-containing mixtures such as oil fractions. The chemistry described above will help to guide future researchers to systems that more closely parallel the processes occurring on the surfaces of industrial hydrodesulphurization catalysts.

to my family

TABLE OF CONTENTS

Abstract	ii
List of Tables	x
List of Figures	xiii
List of Abbreviations	xxii
Numerical Key to Ruthenium Complexes	xxvii
Acknowledgements	xxix
1 INTRODUCTION	1
1.1 Sulphur	2
1.1.1 History and applications	2
1.1.2 Natural occurrence	4
1.1.3 Nomenclature of sulphur compounds	7
1.2 The extraction of sulphur from fossil fuels	8
1.2.1 Reasons for sulphur extraction	8
1.2.2 Sulphur extraction from petroleum	11
1.3 Reactions of sulphur-containing organics with transition metal complexes	22
1.3.1 Reactions involving S-H bond cleavage	23
1.3.2 Reactions involving S-S bond cleavage	27
1.3.3 Reactions involving S-C bond cleavage	31
2. GENERAL EXPERIMENTAL PROCEDURES	34
2.1 Materials	34
2.2 Equipment and techniques	35

2.2.1	Reaction conditions	35
2.2.2	Spectroscopy and chromatography	36
2.2.3	Kinetic measurements	38
2.2.4	Data handling for kinetic experiments	41
2.3	Syntheses of the precursor complexes	45
2.3.1	<i>cct</i> -RuCl ₂ (CO) ₂ (PPh ₃) ₂	45
2.3.2	Ru(CO) ₂ (PPh ₃) ₃	46
2.3.3	<i>cct</i> -RuH ₂ (CO) ₂ (PPh ₃) ₂	48
2.3.4	<i>cct</i> -RuH(Cl)(CO) ₂ (PPh ₃) ₂	49
2.3.5	<i>cis</i> - and <i>trans</i> -RuCl ₂ (dpm) ₂	50
2.3.6	<i>cis</i> - and <i>trans</i> -RuH ₂ (dpm) ₂	52
2.3.7	An attempted new synthesis of RuH ₂ (dpm) ₂ : the synthesis of trans-RuH(η ¹ BH ₄)(dpm) ₂	53
3.	THE REACTIONS OF RUTHENIUM COMPLEXES WITH THIOLS	63
3.1	The reaction of Ru(CO) ₂ (PPh ₃) ₃ with H ₂ S and thiols	63
3.2	The characterization of RuH(ER)(CO) ₂ (PPh ₃) ₂	64
3.3	The reaction of RuH ₂ (CO) ₂ (PPh ₃) ₂ with H ₂ S and thiols	77
3.4	The reaction of RuH ₂ (dpm) ₂ with H ₂ S and thiols	89
3.5	The thiol exchange reactions of <i>cct</i> -RuH(SR)(CO) ₂ (PPh ₃) ₂	103
3.6	The slower reaction of RuH(SR)(CO) ₂ (PPh ₃) ₂ with H ₂ S and thiols	110
3.7	The reaction of RuH(SH)(dpm) ₂ with H ₂ S	115
3.8	The thiol exchange reactions of <i>cct</i> -Ru(SR) ₂ (CO) ₂ (PPh ₃) ₂	119
3.9	The reactions of other carbonyl(phosphine)ruthenium(0) complexes with H ₂ S and thiols	133

3.10	Experimental details	138
4.	REACTIONS OF CARBONYL (PHOSPHINE) RUTHENIUM COMPLEXES WITH DISULPHIDES, THIOETHERS, AND RELATED REAGENTS	152
4.1	The reactions of $\text{Ru}(\text{CO})_2(\text{PPh}_3)_3$ with disulphides	152
4.2	The characterization of $\text{cct-Ru}(\text{SR})_2(\text{CO})_2(\text{PPh}_3)_2$	158
4.3	The reaction of $\text{cct-RuH}_2(\text{CO})_2(\text{PPh}_3)_2$ (3) with disulphides	168
4.4	The reaction of $\text{cct-RuH}(\text{SR})(\text{CO})_2(\text{PPh}_3)_2$ with disulphides	170
4.5	The reactions of carbonyl (phosphine) ruthenium complexes with strained cyclic thioethers	170
4.6	The non-reactions of carbonyl (phosphine) ruthenium complexes with unstrained thioethers	172
4.7	The reactions of carbonyl (phosphine) ruthenium complexes with other neutral sulphur-containing reagents	172
4.8	Experimental details	173
5.	THE METATHESIS REACTIONS OF CHLORORUTHENIUM COMPLEXES WITH THIOLATE SALTS	180
5.1	Introduction	180
5.2	The reactions of $\text{cct-RuCl}_2(\text{CO})_2(\text{PPh}_3)_2$ with sodium thiolates	182
5.3	The characterization of $[\text{Ru}(\text{SEt})_3(\text{CO})_2(\text{PPh}_3)\text{Na}(\text{THF})]_2$	188
5.4	The reactions of other ruthenium chloro complexes with sodium thiolates	212
5.5	Experimental details	213

6.	THE REACTIONS OF THIOLATO RUTHENIUM(II) COMPLEXES WITH NON-SULPHUR-CONTAINING REAGENTS	218
6.1	The reactions of <i>cct</i> -RuH(SR)(CO) ₂ (PPh ₃) ₂ (9)	218
6.1.1	P(C ₆ H ₄ <i>p</i> CH ₃) ₃	218
6.1.2	CO	227
6.1.3	PPh ₃	233
6.1.4	H ₂	234
6.1.5	Acids	234
6.1.6	CD ₃ OD	235
6.2	The reactions of <i>cct</i> -Ru(SR) ₂ (CO) ₂ (PPh ₃) ₂ (14)	239
6.2.1	Light	239
6.2.2	P(C ₆ H ₄ <i>p</i> CH ₃) ₃	245
6.2.3	H ₂	249
6.2.4	CD ₃ OD	249
6.3	Experimental details	253
7.	GENERAL CONCLUSIONS AND RECOMMENDATIONS FOR FUTURE RESEARCH	259
7.1	Potential applications for the complexes in sulphur chemistry	259
7.2	Parallels to surface chemistry	260
7.3	Conclusions	262
7.4	Recommendations for future research	264
8.	REFERENCES	266

APPENDIX 1	Summary of crystallographic data	282
APPENDIX 2	Atomic coordinates for <i>cct</i> -RuH(SC ₆ H ₄ <i>p</i> CH ₃)(CO) ₂ (PPh ₃) ₂ (9b)	284
APPENDIX 3	Atomic coordinates for <i>cct</i> -Ru(SC ₆ H ₄ <i>p</i> CH ₃) ₂ (CO) ₂ (PPh ₃) ₂ (14b)	288
APPENDIX 4	Atomic coordinates for [(CO) ₂ (PPh ₃)Ru(SEt) ₃ Na(THF)] ₂ (21)	294
APPENDIX 5	Kinetic data	298

LIST OF TABLES

1.1	Estimated concentrations of selected sulphur compounds identified in Wasson, Texas, crude oil	5
1.2	Nomenclature of compounds containing sulphur, carbon and hydrogen	9
1.3	Canadian nationwide emissions of sulphur oxides, in 1972	12
2.1	Fragments detected in the FAB/mass spectrum of RuH(BH ₄)(dpm) ₂	55
2.2	¹ H NMR data for <i>trans</i> -RuH(X)(dpm) ₂	55
3.1	³¹ P{ ¹ H} and ¹ H NMR data for <i>cis</i> -RuH(ER)(CO) ₂ (PPh ₃) ₂ complexes in C ₆ D ₆ at 20°C and 300 MHz	67
3.2	FT-IR data for <i>cis</i> -RuH(ER)(CO) ₂ (PPh ₃) ₂ complexes in Nujol, HCB, or CH ₂ Cl ₂ at room temperature	67
3.3	Selected bond lengths (Å) with estimated standard deviations in parentheses, for RuH(SC ₆ H ₄ pCH ₃)(CO) ₂ (PPh ₃) ₂ (9b)	73
3.4	Selected bond angles (°) with estimated standard deviations in parentheses, for RuH(SC ₆ H ₄ pCH ₃)(CO) ₂ (PPh ₃) ₂ (9b)	73
3.5	³¹ P{ ¹ H} and ¹ H NMR data for RuH(SEt)(CO) ₂ L ₂	73
3.6	Kinetic data for the reaction of RuH ₂ (CO) ₂ (PPh ₃) ₂ (3) with various reagents in C ₆ D ₆ at 26°C	85
3.7	NMR data for Ru(X)(Y)(dpm) ₂ complexes	96
3.8	Published <i>pK_a</i> values for selected thiols in aqueous solution	106
4.1	NMR spectroscopic data for complexes of the series <i>cis</i> -Ru(SR)(SR')(CO) ₂ (PPh ₃) ₂	159
4.2	Selected bond lengths (Å) for <i>cis</i> -Ru(SC ₆ H ₄ pCH ₃) ₂ (CO) ₂ (PPh ₃) ₂ (14b)	166

4.3	Selected bond angles ($^{\circ}$) for <i>cct</i> -Ru(SC ₆ H ₄ <i>p</i> CH ₃) ₂ (CO) ₂ (PPh ₃) ₂ (14b)	166
4.4	Selected bond lengths (Å) for <i>cct</i> -Ru(SH) ₂ (CO) ₂ (PPh ₃) ₂ (14a)	167
4.5	Selected bond angles ($^{\circ}$) for <i>cct</i> -Ru(SH) ₂ (CO) ₂ (PPh ₃) ₂ (14a)	167
5.1	Fragments detected in the FAB-Mass spectrum of <i>cct</i> -RuCl(SEt)(CO) ₂ (PPh ₃) ₂	187
5.2	NMR and IR spectral data for Ru(X)(SEt)(CO) ₂ (PPh ₃) ₂	187
5.3	Fragments detected in the FAB-Mass spectrum of [(CO) ₂ (PPh ₃)Ru(SCH ₂ CH ₃) ₃ Na(THF)] ₂	197
5.4	Selected bond lengths (Å) for 21	201
5.5	Selected bond angles ($^{\circ}$) for 21	201
A2.1	Final atomic coordinates (fractional) and B(eq) (9b)	284
A2.2	Calculated hydrogen coordinates and B(iso) (9b)	286
A3.1	Final atomic coordinates (fractional) and B(eq) (14b)	288
A3.2	Calculated hydrogen coordinates and B(iso) (14b)	291
A4.1	Final atomic coordinates (fractional) and B(eq) (21)	294
A4.2	Calculated hydrogen coordinates and B(iso) (21)	296
A5.1	The reaction of <i>cct</i> -RuH ₂ (CO) ₂ (PPh ₃) ₂ (3) with <i>p</i> -thiocresol	298
A5.2	The reaction of <i>cct</i> -RuH ₂ (CO) ₂ (PPh ₃) ₂ (3) with ethanethiol	298
A5.3	The reaction of <i>cct</i> -RuH ₂ (CO) ₂ (PPh ₃) ₂ (3) with carbon monoxide	299
A5.4	The reaction of <i>cct</i> -RuH ₂ (CO) ₂ (PPh ₃) ₂ (3) with triphenyl phosphine	299
A5.5	The reaction of <i>cct</i> -RuH(SCH ₂ CH ₃)(CO) ₂ (PPh ₃) ₂ (9d) with thiophenol at 22 $^{\circ}$ C	299
A5.6	The reaction of <i>cct</i> -Ru(SH) ₂ (CO) ₂ (PPh ₃) ₂ (14a) with thiophenol at 25 $^{\circ}$ C	300
A5.7	The reaction of Ru(CO) ₂ (PPh ₃) ₃ (2) with <i>p</i> -tolyl disulphide (RSSR) at 25 $^{\circ}$ C	300

- A5.8 The reaction of *cct*-RuH(SR)(CO)₂(PPh₃)₂ (**9**) with P(C₆H₄*p*CH₃)₃ (L') at 45°C 300
- A5.9 The reaction of *cct*-RuH(SR)(CO)₂(PPh₃)₂ (**9**) with 1 atm carbon monoxide 301

LIST OF FIGURES

1.1	The spirit of sulphur	3
1.2	The dependence of sulphur content of three crude oils on the fraction distilled	5
1.3	An overview of a petroleum refinery, emphasizing the placement of desulphurization units	13
1.4	Hydroprocessor flow plan	14
1.5	The dependence of the HDS activity of the transition metal sulphides on their heat of formation	16
1.6	Transition metal complexes exhibiting different modes of thiophene coordination	18
1.7	The Lipsch-Schuit mechanism for thiophene HDS	20
1.8	The Angelici mechanism for thiophene HDS	21
2.1	Anaerobic UV/vis. cell	37
2.2	Constant pressure gas uptake apparatus	39
2.3	FAB mass spectrum of RuH(BH ₄)(dpm) ₂ in <i>p</i> -nitrobenzyl alcohol	56
2.4	¹ H NMR spectrum of RuH(BH ₄)(dpm) ₂ under H ₂ at 20°C, 300 MHz	57
2.5	¹ H NMR (300 MHz) spectra of RuH(BH ₄)(dpm) ₂ in C ₆ D ₅ CD ₃ below ambient temperatures	59
2.6	FT-IR spectra of HCB mulls of a) RuH(BH ₄)(dpm) ₂ and b) RuD(BD ₄)(dpm) ₂ (88% deuteration)	61
3.1	¹ H NMR spectrum of <i>cct</i> -RuH(SEt)(CO) ₂ (PPh ₃) ₂ (9d) in C ₆ D ₆ at 20°C and 300 MHz	65
3.2	¹ H NMR spectrum of <i>cct</i> -RuH(SCH ₂ Ph)(CO) ₂ (PPh ₃) ₂ (9e) in C ₆ D ₆ at 20°C and 300 MHz	66
3.3	FT-IR spectrum of <i>cct</i> -RuH(SR)(CO) ₂ (PPh ₃) ₂ (9) in HCB where a) R=Me and	

	b) R=Ph.	69
3.4	$^{13}\text{C}\{^1\text{H}\}$ NMR spectrum of <i>cct</i> -RuH(SEt)(CO) ₂ (PPh ₃) ₂ (9d) in CD ₂ Cl ₂ at 20°C and 75 MHz	71
3.5	X-ray crystallographic structure of <i>cct</i> -RuH(SC ₆ H ₄ pCH ₃)(CO) ₂ (PPh ₃) ₂ (9b)	72
3.6	Stereo-view of the structure of <i>cct</i> -RuH(SC ₆ H ₄ pCH ₃)(CO) ₂ (PPh ₃) ₂ (9b)	72
3.7	Relationship between the ^{31}P NMR chemical shift and the Ru-P bond length of thiolato-phosphine ruthenium complexes	75
3.8	The UV/vis. spectra of <i>cct</i> -RuH(ER)(CO) ₂ (PPh ₃) ₂ in THF at room temperature, where ER = SC ₆ H ₄ pCH ₃ (9b), SCH ₃ (9c), or SeC ₆ H ₅ (9h). The spectra of Ru(CO) ₂ (PPh ₃) ₃ (2) and RuH ₂ (CO) ₂ (PPh ₃) ₂ (3) are included for comparison	75
3.9	^1H NMR spectra acquired during the reaction of <i>cct</i> -RuH ₂ (CO) ₂ (PPh ₃) ₂ (3) with H ₂ S in C ₆ D ₆	78
3.10	Plot absorbance at 400 nm versus time during the reaction of <i>cct</i> -RuH ₂ (CO) ₂ (PPh ₃) ₂ (3) with ethanethiol in THF at 26°C	80
3.11	Logarithmic plot of absorbance at 400 nm for the reaction of <i>cct</i> -RuH ₂ (CO) ₂ (PPh ₃) ₂ (3) with ethanethiol in THF at 26°C	80
3.12	Dependence of the <i>pseudo</i> -first order rate constant on the concentration of <i>cct</i> -RuH ₂ (CO) ₂ (PPh ₃) ₂ (3) for the reaction with ethanethiol in THF at 26°C	81
3.13	Dependence of the <i>pseudo</i> -first order rate constant on the thiol concentration for the reaction of <i>cct</i> -RuH ₂ (CO) ₂ (PPh ₃) ₂ (3) with ethanethiol in THF at 26°C	81
3.14	Logarithmic plot of absorbance at 400 nm versus time for the reaction of <i>cct</i> -RuH ₂ (CO) ₂ (PPh ₃) ₂ (3) and <i>p</i> -thiocresol in THF at 26°C	82
3.15	Dependence of the <i>pseudo</i> -first order rate constant on the concentration of <i>cct</i> -RuH ₂ (CO) ₂ (PPh ₃) ₂ (3) for the reaction with <i>p</i> -thiocresol in THF at 26°C	83
3.16	Dependence of the <i>pseudo</i> -first order rate constant on thiol concentration for the reaction of <i>cct</i> -RuH ₂ (CO) ₂ (PPh ₃) ₂ (3) with <i>p</i> -thiocresol in THF at 26°C	83
3.17	Eyring plot for the reactions of <i>cct</i> -RuH ₂ (CO) ₂ (PPh ₃) ₂ (3) with several reagents	

- 3.18 Logarithmic plot of absorbance at 350 nm versus time for the *pseudo*-first order reaction of *cct*-RuH₂(CO)₂(PPh₃)₂ (**3**) with CO in THF at 26°C 87
- 3.19 Logarithmic plot of absorbance at 400 nm versus time for the *pseudo*-first order reaction of *cct*-RuH₂(CO)₂(PPh₃)₂ and PPh₃ in THF at 26°C 87
- 3.20 a) ¹H NMR spectra (hydride region) for the reaction of *cis*- and *trans*-RuH₂(dpm)₂ with H₂S in C₆D₆ at 25°C and 300 MHz 91
- b) ¹H NMR spectra (methylene region) for the reaction of *cis*- and *trans*-RuH₂(dpm)₂ with H₂S in C₆D₆ at 25°C and 300 MHz 92
- 3.21 ¹H NMR spectra (hydride region) for the reaction of RuH₂(dpm)₂ with PhCH₂SH in C₆D₆ at 25°C 93
- 3.22 ¹H NMR spectrum (300 MHz) of a sample of RuH(SPh)(dpm)₂ prepared *in situ* from RuH₂(dpm)₂ and thiophenol in C₆D₆ 94
- 3.23 a) ³¹P{¹H} NMR spectrum of a sample of RuH(SPh)(dpm)₂ (**13**) prepared *in situ* from RuH₂(dpm)₂ and thiophenol in toluene-*d*₈ 95
- b) Simulated spectrum for *cis*-**13b**
- 3.24 Time dependence of concentrations during the reaction of RuH₂(dpm)₂ with thiophenol in C₆D₆ at 25°C 98
- 3.25 Time dependence of the concentration of *cis*-RuH₂(dpm)₂ (*cis*-**7**) in the reaction with thiols in C₆D₆ at 25°C 98
- 3.26 The ¹H NMR spectrum (hydride region) acquired during the reaction of RuH₂(dpm)₂ with *p*-toluenesulphonic acid 101
- 3.27 ¹H NMR spectra acquired during the reaction of *cct*-RuH(SEt)(CO)₂(PPh₃)₂ with thiophenol in C₆D₆ at 22°C 105
- 3.28 Time dependence of concentrations during the reaction of *cct*-RuH₂(CO)₂(PPh₃)₂ with PhSH and EtSH in C₆D₆ at 36°C 106
- 3.29 Logarithmic plot of concentrations versus time for the *pseudo*-first order reaction of *cct*-RuH(SEt)(CO)₂(PPh₃)₂ and PhSH in C₆D₆ at 22°C 108

- 3.30 Dependence of the *pseudo*-first order rate constant on [PhSH] for the reaction with *cct*-RuH(SEt)(CO)₂(PPh₃)₂ in C₆D₆ at 22°C 108
- 3.31 ¹H NMR spectra (hydride region) acquired during the reaction of *cct*-RuH(SH)(CO)₂(PPh₃)₂ (**9a**) with H₂S in C₆D₆ at 60°C 112
- 3.32 a) ¹H NMR spectra (hydride region) acquired during the reaction of RuH(SH)(dpm)₂ (**13a**) with H₂S in C₆D₆ at 60°C 116
- b) ¹H NMR spectra (methylene region) acquired during the reaction of RuH(SH)(dpm)₂ (**13a**) with H₂S in C₆D₆ at 60°C 117
- 3.33 Logarithmic plot of concentration of *trans*-RuH(SH)(dpm)₂ (**13a**) during the reaction of that compound with H₂S at 60°C in C₆D₆ 118
- 3.34 The ³¹P{¹H} NMR spectrum of Ru(SH)₂(dpm)₂ (**15**) in C₆D₆ 118
- 3.35 ³¹P{¹H} NMR spectra acquired during the reaction of *cct*-Ru(SH)₂(CO)₂(PPh₃)₂ (**14a**) with PhSH at 25°C in C₆D₆ 121
- 3.36 UV/vis. spectra acquired at 1 min intervals during the reaction of *cct*-Ru(SH)₂(CO)₂(PPh₃)₂ (**14a**) with PhSH at 25°C in THF 122
- 3.37 Time dependence of the concentrations of species detected by ³¹P{¹H} NMR during the reaction of *cct*-Ru(SH)₂(CO)₂(PPh₃)₂ (**14a**) with PhSH at 25°C in C₆D₆
- a) at 77 mM PhSH 123
- b) at 690 mM PhSH 123
- c) at 1700 mM PhSH 124
- d) at 2900 mM PhSH 124
- e) at 810 mM PhSH and 470 mM PPh₃ 125
- 3.38 The log plot of the concentration of *cct*-Ru(SH)₂(CO)₂(PPh₃)₂ (**14a**) during its reaction with thiophenol in C₆D₆ at 25°C 125
- 3.39 The dependence on [PhSH] of the observed initial rate constant for the loss of *cct*-Ru(SH)₂(CO)₂(PPh₃)₂ (**14a**) during the reaction with PhSH at several

	concentrations of added PPh_3	126
3.40	Phosphine dependence of the inverse of the observed initial rate constant for the loss of $cct\text{-Ru}(\text{SH})_2(\text{CO})_2(\text{PPh}_3)_2$ (14a) during the reaction with PhSH at several $[\text{PhSH}]$	126
3.41	Thiol dependence of the calculated rate constant k_B for the second step of the reaction of $cct\text{-Ru}(\text{SH})_2(\text{CO})_2(\text{PPh}_3)_2$ with thiophenol at 25°C in C_6D_6	130
3.42	^1H NMR spectrum (hydride region) of the products of the reaction of $\text{Ru}(\text{CO})_2(\text{dpm})(\text{PPh}_3)$ with ethanethiol	136
3.43	$^{31}\text{P}\{^1\text{H}\}$ NMR spectrum of the products of the reaction of $\text{Ru}(\text{CO})_2(\text{dpm})(\text{PPh}_3)$ with ethanethiol	137
4.1	The logarithmic dependence of the concentration of $\text{Ru}(\text{CO})_2(\text{PPh}_3)_3$ (2 , $[\mathbf{2}]_0 = 7.5 \text{ mM}$) during its reaction with <i>p</i> -tolyl disulphide in C_6D_6 at 18°C with or without a free-radical trap	153
4.2	The UV/visible absorption spectrum of a solution of $\text{Ru}(\text{CO})_2(\text{PPh}_3)_3$ and <i>p</i> -tolyl disulphide in THF at 26°C	155
4.3	The dependence on $[\mathbf{2}]$ of the initial rate of the reaction $\text{Ru}(\text{CO})_2(\text{PPh}_3)_3$ (2) with <i>p</i> -tolyl disulphide in THF at 26°C	156
4.4	a) The dependence on $[\text{RSSR}]$ of the initial rate of the reaction of $\text{Ru}(\text{CO})_2(\text{PPh}_3)_3$ (2) with <i>p</i> -tolyl disulphide in THF at 26°C b) Plot of $1/(\text{initial rate})$ against $1/[\text{RSSR}]$ for the same reaction	157
4.5	^1H NMR spectrum of $cct\text{-Ru}(\text{SC}_6\text{H}_4\text{pCH}_3)_2(\text{CO})_2(\text{PPh}_3)_2$ (9b), in C_6D_6	161
4.6	FT-IR spectrum of $cct\text{-Ru}(\text{SC}_6\text{H}_4\text{pCH}_3)_2(\text{CO})_2(\text{PPh}_3)_2$ in HCB	162
4.7	a) The structure of $cct\text{-Ru}(\text{SC}_6\text{H}_4\text{pCH}_3)_2(\text{CO})_2(\text{PPh}_3)_2$ (14b) b) A stereoscopic view of the same structure	164
4.8	The structure of $cct\text{-Ru}(\text{SH})_2(\text{CO})_2(\text{PPh}_3)_2$	165

- 5.1 a) ^1H NMR spectrum of *cct*-RuCl(SEt)(CO)₂(PPh₃)₂
b) Expanded region of the ^1H NMR spectrum of a sample of *cct*-Ru(SEt)₂(CO)₂(PPh₃)₂ containing 20% *cct*-RuCl(SEt)(CO)₂(PPh₃)₂ 184
- 5.2 a) The FT-IR spectrum of *cct*-RuCl(SEt)(CO)₂(PPh₃)₂ in Nujol mull
b) Carbonyl region of the FT-IR spectrum of a sample of *cct*-Ru(SEt)₂(CO)₂(PPh₃)₂ containing 20% of *cct*-RuCl(SEt)(CO)₂(PPh₃)₂ in a Nujol mull 185
- 5.3 The FAB-Mass spectrum of *cct*-RuCl(SEt)(CO)₂(PPh₃)₂ in a *p*-nitrobenzyl alcohol matrix 186
- 5.4 The ^1H NMR spectrum of a C₆D₆ solution of [(CO)₂(PPh₃)Ru(SCH₂CH₃)₃Na(THF)]₂ at 20°C 189
- 5.5 The ^1H COSY NMR plot for a C₆D₆ solution of [(CO)₂(PPh₃)Ru(SCH₂CH₃)₃Na(THF)]₂ 190
- 5.6 The methylene region of ^1H NMR spectra of a C₆D₆ solution of [(CO)₂(PPh₃)Ru(SCH₂CH₃)₃Na(THF)]₂ 191
- 5.7 Simulated ^1H NMR spectra of a) the CH_{2a} protons, and b) the CH_{2b} protons of [(CO)₂(PPh₃)Ru(SCH₂CH₃)₃Na(THF)]₂ 193
- 5.8 The FT-IR spectrum of [(CO)₂(PPh₃)Ru(SCH₂CH₃)₃Na(THF)]₂ in Nujol 194
- 5.9 The FAB-Mass spectrum of [(CO)₂(PPh₃)Ru(SCH₂CH₃)₃Na(THF)]₂ in a *p*-nitrobenzyl alcohol matrix 196
- 5.10 The structure of one half of a molecule of [(CO)₂(PPh₃)Ru(SCH₂CH₃)₃Na(THF)]₂ 198
- 5.11 The structure of [(CO)₂(PPh₃)Ru(SCH₂CH₃)₃Na(THF)]₂ 199
- 5.12 Stereoscopic view of the structure of [(CO)₂(PPh₃)Ru(SCH₂CH₃)₃Na(THF)]₂ 200
- 5.13 a) ^{13}C solid state (CP/MAS) NMR spectrum of [(CO)₂(PPh₃)Ru(SCH₂CH₃)₃Na(THF)]₂

	b) ^{13}C solid state (CP/MAS) NQS NMR spectrum of $[(\text{CO})_2(\text{PPh}_3)\text{Ru}(\text{SCH}_2\text{CH}_3)_3\text{Na}(\text{THF})]_2$	203
5.14	$^{13}\text{C}\{^1\text{H}\}$ NMR spectrum of $[\text{Ru}(\text{CO})_2(\text{PPh}_3)\text{Ru}(\text{SEt})_3\text{Na}(\text{THF})]_2$ in C_6D_6 at 20°C	204
5.15	^{13}C APT NMR spectrum of $[\text{Ru}(\text{CO})_2(\text{PPh}_3)\text{Ru}(\text{SEt})_3\text{Na}(\text{THF})]_2$ in C_6D_6 at 20°C	205
5.16	The Heteronuclear Correlation ($^{13}\text{C}/^1\text{H}$) NMR plot for $[\text{Ru}(\text{CO})_2(\text{PPh}_3)\text{Ru}(\mu\text{SEt})_2(\mu_3\text{SEt})\text{Na}(\text{THF})]_2$ in C_6D_6	206
5.17	The ^1H $[\text{Ru}(\text{CO})_2(\text{PPh}_3)\text{Ru}(\mu\text{SEt})_2(\mu_3\text{SEt})\text{Na}(\text{THF})]_2$ in toluene- d_8 at -78°C	210
6.1	$^{31}\text{P}\{^1\text{H}\}$ NMR spectra acquired during the reaction of <i>cct</i> - $\text{RuH}(\text{SCH}_2\text{Ph})(\text{CO})_2(\text{PPh}_3)_2$ (9e) with $\text{P}(\text{C}_6\text{H}_4\text{pCH}_3)_3$ in C_6D_6 at 45°C	220
6.2	^1H NMR spectra acquired during the reaction of <i>cct</i> - $\text{RuH}(\text{SCH}_2\text{Ph})(\text{CO})_2(\text{PPh}_3)_2$ (9e) with $\text{P}(\text{C}_6\text{H}_4\text{pCH}_3)_3$ in C_6D_6 at 45°C	221
6.3	Time dependence of the concentrations of observed complexes during the reaction of <i>cct</i> - $\text{RuH}(\text{SCH}_2\text{Ph})(\text{CO})_2(\text{PPh}_3)_2$ (9e) with $\text{P}(\text{C}_6\text{H}_4\text{pCH}_3)_3$ in C_6D_6 at 45°C	222
6.4	Log plot of [9e] during the reaction of <i>cct</i> - $\text{RuH}(\text{SCH}_2\text{Ph})(\text{CO})_2(\text{PPh}_3)_2$ (9e) with $\text{P}(\text{C}_6\text{H}_4\text{pCH}_3)_3$ in C_6D_6 at 45°C	222
6.5	The dependence of $d[\text{12e}]/dt$ on [22e] during the reaction of <i>cct</i> - $\text{RuH}(\text{SCH}_2\text{Ph})(\text{CO})_2(\text{PPh}_3)_2$ (9e) with $\text{P}(\text{C}_6\text{H}_4\text{pCH}_3)_3$ in C_6D_6 at 45°C	225
6.6	Time dependence of the concentration of observed complexes during the reaction of <i>cct</i> - $\text{RuH}(\text{SCH}_2\text{Ph})(\text{CO})_2(\text{PPh}_3)_2$ (9e) with $\text{P}(\text{C}_6\text{H}_4\text{pCH}_3)_3$ in the presence of PPh_3 in C_6D_6 at 45°C	226
6.7	Time dependence of Q_1 and Q_2 during the reaction of <i>cct</i> - $\text{RuH}(\text{SCH}_2\text{Ph})(\text{CO})_2(\text{PPh}_3)_2$ (9e) with $\text{P}(\text{C}_6\text{H}_4\text{pCH}_3)_3$ in the presence of PPh_3 in C_6D_6 at 45°C	226

- 6.8 UV/vis. spectra acquired every 900 s during the reaction of *cct*-RuH(SEt)(CO)₂(PPh₃)₂ and CO in THF at 26°C 228
- 6.9 Log plot of absorbance versus time for the reaction of *cct*-RuH(SEt)(CO)₂(PPh₃)₂ (**9d**) and CO in THF at 26.5°C 229
- 6.10 Eyring plot for the reactions of *cct*-RuH(SR)(CO)₂(PPh₃)₂ (**9**) with CO in THF 231
- 6.11 ¹H NMR spectrum acquired 30 min after the start of the reaction of *cct*-RuH(SC₆H₅)(CO)₂(PPh₃)₂ (**9i**) with excess HBF₄/H₂O in C₆D₆ at room temperature 236
- 6.12 The time dependence of the intensity of the ¹H NMR signals due to *cct*-RuH(SH)(CO)₂(PPh₃)₂ in 4% v/v CD₃OD/C₆D₆ at 19°C 237
- 6.13 The log plot of the intensity of the ¹H NMR signals due to *cct*-RuH(SH)(CO)₂(PPh₃)₂ in 4% v/v CD₃OD/C₆D₆ at 19°C 237
- 6.14 UV/vis. absorbance spectra of a THF solution of *cct*-Ru(SC₆H₄*p*CH₃)₂(CO)₂(PPh₃)₂ at 25°C being irradiated at 430 nm 240
- 6.15 FAB Mass spectrum of the solid residue from a THF solution of *cct*-Ru(SC₆H₄*p*CH₃)₂(CO)₂(PPh₃)₂ irradiated for 90 min under a Hanovia lamp 241
- 6.16 a) Observed isotopic pattern for the fragment *m/z* = 1149±4
b) The predicted isotopic patterns for four possible formulations for the fragment 242
- 6.17 ³¹P{¹H} NMR spectra acquired during the reaction of *cct*-Ru(SH)₂(CO)₂(PPh₃)₂ (**14a**) with P(C₆H₄*p*CH₃)₃ in C₆D₆ at 25°C 246
- 6.18 ¹H NMR spectra acquired during the reaction of *cct*-Ru(SH)₂(CO)₂(PPh₃)₂ (**14a**) with P(C₆H₄*p*CH₃)₃ in C₆D₆ at 25°C 247
- 6.19 The time dependence of the concentrations of the observed complexes during the reaction of *cct*-Ru(SH)₂(CO)₂(PPh₃)₂ (**14a**) with P(C₆H₄*p*CH₃)₃ in C₆D₆ at 25°C 248
- 6.20 ¹H NMR spectrum of a C₆D₆ solution of the product from the reaction

- of a THF solution of *cct*-Ru(SC₆H₄pCH₃)₂(CO)₂(PPh₃)₂ with H₂ 250
- 6.21 ³¹P{¹H} NMR spectrum of C₆D₆ solution of the product from the
reaction of a THF solution of *cct*-Ru(SC₆H₄pCH₃)₂(CO)₂(PPh₃)₂
with H₂ 251
- 6.22 The time dependence of the intensity of the ¹H NMR signals due to
cct-Ru(SH)₂(CO)₂(PPh₃)₂ in 4% v/v CD₃OD/C₆D₆ at 25°C 252

LIST OF ABBREVIATIONS

A	=	absorbance
A_{∞}	=	absorbance after infinite reaction time
alkyl/polym.	=	polymerization unit
APT	=	attached proton test (^{13}C NMR pulse sequence)
AT	=	acquisition time during an FT-NMR pulse sequence
atm.	=	atmosphere(s)
atm. dist.	=	atmospheric pressure distillation tower (Fig. 1.3)
B_{eq}	=	isotropic equivalent thermal parameters
B, B_{iso}	=	isotropic thermal parameters
BDH	=	British Drug Houses Chemicals Ltd.
bipy	=	2,2'-bipyridyl
br.	=	broad
Bu	=	butyl
buS ₄	=	1,2-bis((3,5-di-tert-butyl-2-mercapto-phenyl)thio)ethanato(2-)
Bz	=	benzyl ($\text{CH}_2\text{C}_6\text{H}_5$)
<i>c</i>	=	<i>cis</i>
C	=	a constant
calcd.	=	calculated
<i>ccc</i>	=	<i>cis, cis, cis</i>
<i>cct</i>	=	<i>cis, cis, trans</i>
CDE	=	cyclododecene
CDT	=	1,5,9-cyclodecatriene
COD	=	1,5-cyclooctadiene
COSY	=	Homonuclear Correlated Spectroscopy (FT-NMR experiment)

COT	=	1,3,5-cyclooctatriene
Cp	=	cyclopentadienyl
CP/MAS	=	cross-polarization/magic angle spinning (^{13}C solid state NMR technique)
<i>ctc</i>	=	<i>cis, trans, cis</i>
δ	=	bending mode (IR) or chemical shift (NMR)
d	=	doublet (NMR) or bond distance
D	=	deuterium
D1, D2	=	delay times in an FT-NMR pulse sequence
DBU	=	1,8-diazabicyclo-[5,4,0]-undec-7-ene
DEA	=	diethanolamine
deC4	=	unit for the separation of C-4 hydrocarbons
def	=	deformation
dipp	=	1,3- <i>bis</i> (diisopropylphenylphosphino)propane
dma	=	N,N-dimethylacetamide
dmdppe	=	1-dimethylphosphino-2-diphenylphosphinoethane
dmpe	=	1,2- <i>bis</i> (dimethylphosphino)ethane
dms	=	dimethylsulphoxide
dpm	=	<i>bis</i> (diphenylphosphino)methane
dppe	=	1,2- <i>bis</i> (diphenylphosphino)ethane
dq	=	doublet of quartets
dt	=	doublet of triplets
ϵ	=	molar extinction coefficient
Elem. Anal.	=	elemental analysis
est.	=	estimated
Et	=	ethyl
F(000)	=	electrons per unit cell
FAB/MS	=	fast-atom bombardment mass spectroscopy

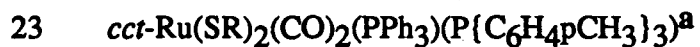
FT	=	Fourier transform
GC	=	gas chromatograph(y)
gof	=	goodness of fit indicator
h	=	hour
ΔH^\ddagger	=	enthalpy of activation
H _b	=	bridging hydrogen atom
HCB	=	hexachloro-1,3-butadiene
HDN	=	hydrodenitrogenation
HDO	=	hydrodeoxygenation
HDS	=	hydrodesulphurization
HETCOR	=	heteronuclear correlation (FT-NMR experiment)
H _t	=	terminal hydride ligand
H ₂ TPP	=	tetraphenylporphyrin
I	=	intensity
IR	=	infra-red (spectroscopy)
IUPAC	=	International Union of Pure and Applied Chemistry
J	=	coupling constant (NMR)
K _{eq}	=	equilibrium constant
KMS	=	Kezdy-Mangelsdorf-Swinbourne method
k _{obs}	=	observed <i>pseudo</i> -first order rate constant
l	=	path length (spectroscopy)
L	=	ligand (usually PPh ₃ in this work)
μ	=	absorption coefficient
m-	=	<i>meta</i> -
M	=	metal, or unit of molarity
MCB	=	Matheson, Coleman and Bell
m/z	=	mass to charge ratio

Me	=	methyl
Merox	=	mercaptan oxidation process
min	=	minutes
mol	=	moles or molecular
MSD	=	Merck, Sharp and Dohme
multi.	=	multiplet
n	=	order of the rate dependence on free ligand concentration
NMR	=	nuclear magnetic resonance
nOe	=	nuclear Overhauser effect
<i>o</i> -	=	<i>ortho</i> -
<i>p</i> -	=	<i>para</i> -
P1, P2	=	duration of pulses in an FT-NMR pulse sequence
Ph	=	phenyl
PPh ₃	=	triphenylphosphine
ppm	=	parts per million
ppth	=	parts per thousand
Py	=	-2-C ₅ H ₄ N
q	=	quartet
Q	=	quotient (defined in Section 6.1.1)
qn	=	quintet
ρ	=	density
R	=	alkyl or aryl group, or rate of change of absorbance (<i>dA/dt</i>)
R, R _w	=	agreement factors (defined on page 283)
rearr.	=	rearrangement
RNA	=	ribonucleic acid
s	=	singlet
ΔS‡	=	entropy of activation

θ	=	Bragg angle
<i>t</i>	=	<i>trans</i>
t	=	triplet
T	=	constant delay time or temperature
T ₁	=	longitudinal relaxation time
THF	=	tetrahydrofuran
THT	=	tetrahydrothiophene
TMS	=	tetramethylsilane
tol	=	<i>p</i> -tolyl (-C ₆ H ₄ <i>p</i> CH ₃)
<i>ttt</i>	=	<i>trans, trans, trans</i>
UV/vis.	=	ultra-violet or visible absorption (spectroscopy)
V	=	volume (of the unit cell)
v/v	=	concentration by volume
vac. dist.	=	vacuum distillation tower (Fig. 1.3)
ν	=	frequency or stretching mode (IR)
ν_D/ν_H	=	isotopic shift
w _{0.5}	=	peak width at half-height
wt.	=	weight
Z	=	formulas per unit cell

NUMERICAL KEY TO THE RUTHENIUM COMPLEXES

- 1 *cct*-RuCl₂(CO)₂(PPh₃)₂
- 2 Ru(CO)₂(PPh₃)₃
- 3 *cct*-RuH₂(CO)₂(PPh₃)₂
- 4 *cct*-RuH(Cl)(CO)₂(PPh₃)₂
- 5 *cis*-RuCl₂(dpm)₂
- 6 *trans*-RuCl₂(dpm)₂
- 7 *cis*- or *trans*-RuH₂(dpm)₂
- 8 *trans*-RuH(BH₄)(dpm)₂
- 9 *cct*-RuH(ER)(CO)₂(PPh₃)₂^a
- 10 Ru(CO)₃(PPh₃)₂
- 11 *cct*-RuH(ER)(CO)₂(PPh₂Py)₂^a
- 12 *cct*-RuH(ER)(CO)₂{P(C₆H₄pCH₃)₃}₂^a
- 13 *cis*- or *trans*-RuH(ER)(dpm)₂
 - a R = H (*trans* only)
 - b C₆H₅
 - c CH₂C₆H₅
- 14 *cct*-Ru(SR)₂(CO)₂(PPh₃)₂^a
- 15 *cis*- or *trans*-Ru(SH)₂(dpm)₂
- 16 Ru(CO)₂(PPh₃)(dpm)
- 17 isomer of RuH(SCH₂CH₃)(CO)(PPh₃)(dpm)
- 18 isomer of RuH(SCH₂CH₃)(CO)(PPh₃)(dpm)
- 19 *cct*-RuS₂(CO)₂(PPh₃)₂
- 20 *cct*-RuCl(SCH₂CH₃)(CO)₂(PPh₃)₂
- 21 [Ru(CO)₂(PPh₃)(SEt)₃Na(THF)]₂
- 22 *cct*-RuH(SR)(CO)₂(PPh₃)(P{C₆H₄pCH₃}₃)^a



a Complexes 9, 11, 12, 14, and 22 through 24 are further identified by one of the following letters, which indicate the thiolate or selenolate group (ER). In the case of complexes 14 with two different thiolate ligands, two such initials are shown in the abbreviation.

a	SH	f	SC ₆ H _{4o} CH ₃
b	SC ₆ H _{4p} CH ₃	g	SC ₆ H _{4m} CH ₃
c	SCH ₃	h	SeC ₆ H ₅
d	SCH ₂ CH ₃	i	SC ₆ H ₅
e	SCH ₂ C ₆ H ₅	j	SC ₆ F ₅

ACKNOWLEDGEMENTS

I offer my sincerest thanks to the following people for the assistance they have provided me during my studies and the preparation of this thesis: my supervisor, Dr. Brian R. James, and the members of his research group, for their guidance and input; Dr. Chung-Li Lee of the Pulp and Paper Research Institute of Canada, who started the project, for his continuing support and advice; three undergraduate researchers, Mr. Marc Prystay (the PPh₂Py systems), Miss Kavita Khajuria (the light sensitivity of *cis*-Ru(SR)₂(CO)₂(PPh₃)₂), and Miss Golnar Rastar (the reaction of *cis*- and *trans*-RuH₂(dpm)₂ with H₂S); Dr. S. Rettig, for the X-ray crystallography; Mr. P. Borda, for the elemental analyses; the technical and administrative staff of the chemistry department; several employees of Imperial Oil Ltd. for useful discussions and help with Figure 1.3; Johnson-Matthey for a loan of ruthenium trichloride; the National Sciences and Engineering Research Council and the University of British Columbia for funding; and my wife for her patience and help in preparing the figures and list of references.

1. INTRODUCTION

The mechanism of the hydrodesulphurization (HDS) of sulphur-containing organics in fuel remains a mystery, even after decades of research. Even the kinetics of the reaction, outside of the adsorption and desorption steps, are not understood. Analogies to the reactions of homogeneous complexes can lead to greater understanding of heterogeneous catalysts. Such analogies are central to a mechanism proposed recently¹ for thiophene HDS. Although such research has emphasized thiophenes because of their resistance to desulphurization, three decades of related research into the coordination chemistry of thiols, thioethers, disulphides, and other sulphur compounds have identified many modes of coordination in, and reactions of, their complexes. The kinetics of the formation and subsequent reactions of such complexes have been largely ignored. It is the purpose of the research described in this thesis to assist in this regard.

Two ruthenium complexes, $\text{RuH}_2(\text{CO})_2(\text{PPh}_3)_2$ and $\text{Ru}(\text{CO})_2(\text{PPh}_3)_3$, were chosen because of the high HDS activity of ruthenium sulphide (Fig. 1.6), and because of the ease by which the two complexes and their reaction products could be identified by IR and NMR spectroscopies. The reactions of these and related complexes with thiols, disulphides, thioethers, thiophenes and sulphur itself were to be observed and monitored kinetically if possible. In addition, the products and their properties and reactivities were further subjects for study. Finally, the effect of ligand choice on reactivity and rate was to be examined.

This first chapter reviews the applications, natural occurrence, and nomenclature of sulphur compounds, the industrial use of HDS, some theories on the mechanism of the reaction, and the coordination chemistry of simple sulphur-containing compounds.

1.1 SULPHUR

1.1.1 History and Applications

Sulphur (Fig. 1.1) can be both beneficial and harmful, according to popular belief. Sulphurous hot springs have long been used as healing baths. This, along with the natural fumigating action of sulphurous vapours, led to myths about sulphur's medicinal properties. Pliny the Elder, in his "Natural History" (c. 77 A.D.), reported the use of sulphur for medicine, fumigation, and religious ceremonies.³ However, the production of sulphur from the gases of volcanoes and fumaroles naturally suggested an association with hell and the centre of the earth. Apollonius of Tyana (AD 17-97) believed that "volcanoes are caused by a mixture of bitumen and sulphur in the earth, which smokes by its own nature."⁴ The connection of volcanoes, "brimstone" (probably sulphur), and hell is a common theme in the Bible (Gen. 19:24, Rev. 14:9-11; 20:10; 21:8). The presence of sulphur within the earth, according to the alchemical sulphur-mercury theory of metals, was essential for the natural production of gold.³

Although our understanding of sulphur and its compounds has increased, the element still retains its two-sided nature. Much of the recent research into sulphur chemistry has been aimed at sulphur removal, rather than the practical applications of its compounds. Large amounts of sulphur are removed from natural gas, petroleum, and coal-based fuels, not for the price the sulphur will fetch, but to prevent catalyst fouling, pipe corrosion, and environmental damage.

The production of sulphur as waste from fuel processing has the result of keeping down the price of sulphur, and consequently the price of sulphuric acid. In fact, 80% of sulphur is converted to sulphuric acid, which is used as a reagent in the production of phosphate fertilizers, synthetic fibres (Rayon, Nylon 6), white pigments, and steel pickling.⁵ U.S. production of sulphuric acid in 1988 (86×10^9 lb) was larger than for any other chemical. Other sulphur chemicals used industrially are hydrogen sulphites and sulphates (pulping processes), sulphites (tanning, sugar refining, etc.), sodium



Fig. 1.1 The Spirit of Sulphur 2

thiosulphate (photography), sulphur dioxide and carbon disulphide (solvents), sulphur hexafluoride (transformer oil), xanthates (fungicides), thiokols (plastics), and several compounds used in the treatment of rubber.⁵

1.1.2 Natural Occurrence

Sulphur occurs as the native element, as well as in organic and inorganic compounds. Sulphur is mined or extracted by the Frasch process as the native element at a number of sites, such as Sicily and Louisiana. It is also "recovered as a byproduct in smelting sulfide ores, from sour natural gas, and from pyrite."⁶ The United States, with its reserves of elemental sulphur, relies on the Frasch process. Canada, on the other hand, obtains 85% of its sulphur from the desulphurization of natural gas.⁷

The sulphur-containing minerals, other than sulphur itself, are sulphides (e.g. pyrite FeS_2), sulpharsenides (e.g. cobaltite $(\text{Co,Fe})\text{AsS}$), sulphosalts (e.g. tetrahedrite $\text{Cu}_{12}\text{Sb}_4\text{S}_{13}$) and sulphates (e.g. gypsum CaSO_4).⁶

Sulphur-containing organics, hydrogen sulphide, and even elemental sulphur⁸ are found in petroleum. The sources of these compounds are the sulphur compounds in the original biological matter, and the biogenic reduction of sulphate minerals to hydrogen sulphide, followed by reactions with components of petroleum.⁸ The type of functional group and the concentration of the sulphur compound depend on the fraction of petroleum studied. "Sulfur in the lower-boiling straight-run distillates is mainly in the form of mercaptans, sulfides, and disulfides, whereas thermally-cracked distillates contain the more refractory thiophene type, in addition to the thiophenols that occur in catalytically cracked distillates."⁹ A thorough study by the U. S. Bureau of Mines described the relationship between sulphur content (weight percent) and boiling point of the fuel fraction (Fig. 1.2), and identified 200 individual sulphur compounds contained in

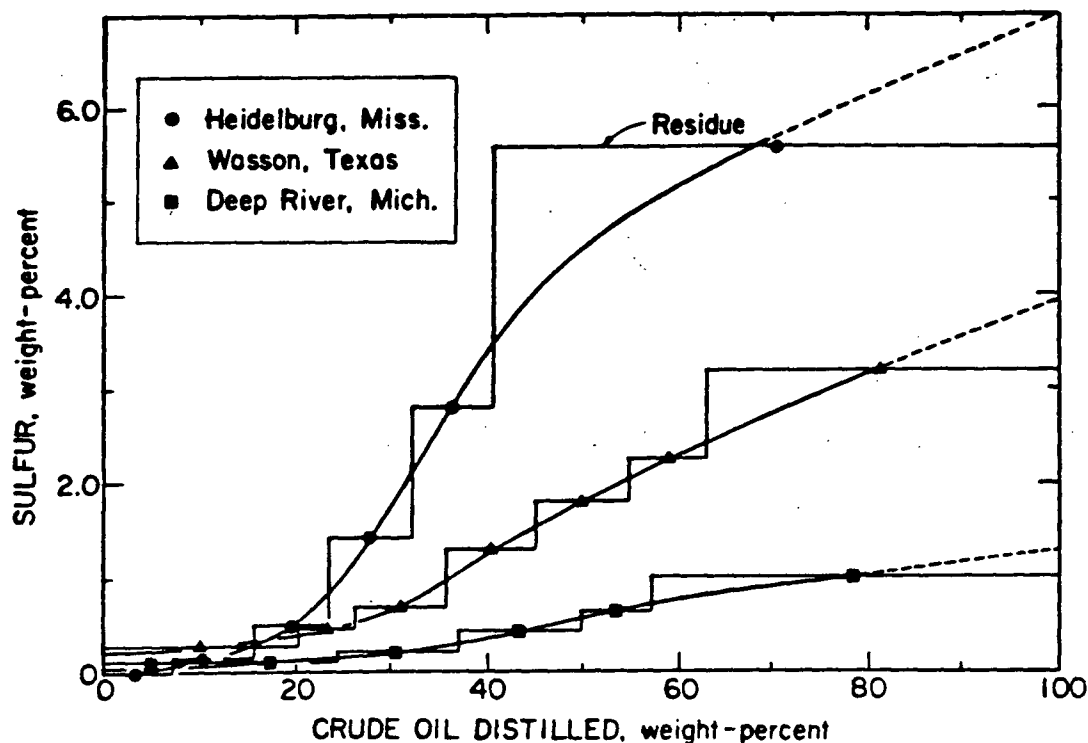


Fig. 1.2 The dependence of sulphur content of three crude oils on the fraction distilled.⁸

Table 1.1 Estimated Concentrations of Selected Sulphur Compounds Identified in Wosson, Texas, crude oil.^a

Name	b.p. (°C)	ppm by wt.
methanethiol	5.9	24.0
ethanethiol	35.0	53.0
2-thiopropane	37.4	8.8
2-propanethiol	52.6	19.9
2-thiabutane	66.7	22.2
2-butanethiol	85.0	38.6
2-pentanethiol	112.4	14
2,3-dithiapentane ^b	133. (est.)	-
2-methylthiacyclopentane	133.2	23
2-hexanethiol	138.9	28
<i>trans</i> -2,5-dimethylthia-cyclopentane	142.0	25
<i>cis</i> -2,5-dimethylthiacyclopentane	142.3	24
2-methylthiacyclohexane	153.0	29
cyclohexanethiol	158.7	12
2-methylbenzo[b]thiophene	243. (est.)	24.8
3-methylbenzo[b]thiophene	246. (est.)	9.5
2,4-dimethylbenzo[b]thiophene	-	9.4
2,5- and/or 2,7-dimethylbenzo-[b]thiophene	-	10.1

a) Ref. 8

b) Tentative identification only.

four crude oils (Table 1.1).⁸ Although thiophene itself is low boiling, heterocyclic compounds such as thiophene are usually more common in the heavier fractions of oil because of their ability to form hydrogen bonds.¹⁰

Coal contains up to 10 wt. % sulphur, consisting of sulphate sulphur (sulphates of iron, calcium, and others, less than 0.1 wt. %), pyritic sulphur (pyrite and marcasite, up to 8.0 wt. %), and organic sulphur (thiols, sulphides, and thiophenes, up to 6.0 wt. %).¹¹⁻³ The first two classes of sulphur compounds can be extracted by washing and gravity separation. Of the organic sulphur in bituminous coal, thiols make up 10-30%, sulphites 5-27%, and thiophenes 40-70%.¹³ These compounds, especially the thiophenes, are difficult to remove. Conventional coal-cleaning processes, such as leaching, have had only mediocre success. The only effective technique is conversion to coal-derived liquids, followed by hydrodesulphurization (Section 1.2.2).¹⁴

A wide variety of sulphur-containing chemicals is found in biology. Sulphur minerals are oxidized by weathering to sulphates, which are required by most plants and some micro-organisms. Plants convert these sulphates to the amino acids L-cystine, L-cysteine, and L-methionine, which are required, with the vitamins thiamine and biotin, by the higher animals. These organic sulphur compounds are "largely degraded to hydrogen sulfide as a result of microbial action on plants and animals after their death."¹⁵ The classes of sulphur-containing compounds, a few examples, and the materials in which they have been found are the following:

a) Thiols: 3-methyl-1-butanethiol (skunk),¹⁶ ergothioneine (cereal grains), glutathione (widespread), transfer RNA (bacteria), a variety of enzymes, and the amino acids L-cysteine and homocysteine.

b) Disulphides: the amino acids cystine and homocystine, lipoic acid (widespread), thiamine disulfide, and several antibiotics.¹⁷

c) Sulphides: pheromones, the amino acid methionine, vitamins thiamine and biotin, the penicillin and cephalosporin classes of antibiotics,¹⁷ and many of the odoriferous volatiles in foods, such as kahweofuran (coffee).

d) Thiophenes: more than 150 thiophene derivatives isolated from Compositae and fungi.¹⁸

e) Thioesters: the thioesters of the two thiols Coenzyme A and acyl carrier protein "are involved in the functioning of oxidoreductases, transferases, hydrolases, ligases, lyases, and isomerases."¹⁷

f) Coordination Compounds: The sulphur-containing ligands found in metalloproteins are S²⁻ and the residues of the amino acids cysteine and methionine. Methionine-coordinated metal ions can be found in some cytochromes c (heme Fe atoms)¹⁹ and in blue copper proteins such as azurin and plastocyanin.²⁰ Cysteine-bound metal ions are found in metallothioneins (Cd),²¹ liver alcohol dehydrogenase (Zn),²² rubredoxin (Fe),²³ azurin and plastocyanin (Cu),²⁰ and zinc fingers such as those in the yeast protein ADR1.²⁴ Ferredoxins contain sulphide-bridged iron atoms bound to cysteine or other ligands.²⁵⁻⁷ The structure of the FeMo cofactor of nitrogenase is not known, but estimates of the stoichiometry of its thiolate-bound core are in the range 1Mo, 6-8Fe, 6-9S.^{25,28-9}

1.1.3 Nomenclature of Sulphur Compounds

The nomenclature of sulphur chemistry was invented by the devil. If one omits for the moment the difference between "sulphur" (British) and "sulfur" (American), and ascribes the thiol vs. mercaptan problem to the vagaries of a nomenclature system built around historical labels, one is still faced with a bewildering array of systematic and trivial names. An extreme example is the word "sulphide", which means a binary

metal/sulphur compound to a geochemist, a thioether complex to a coordination chemist, an S^{2-} ion to an inorganic chemist, a thiol to some biochemists,¹⁷ and either a thioether or a thiolate salt to an organic chemist. IUPAC confusingly allows its use for thioethers, thiolate salts and S^{2-} ligands.³⁰ Table 1.2 presents a summary of the terms used to refer to compounds or ligands which contain only sulphur, carbon, hydrogen, and/or metal atoms. In the following work, the terms thiol, thioether, thiolate anion, and disulphide are used to refer to the organic species RSH, RSR, RS^- , and RSSR. The term sulphide is reserved for complexes containing the ligand S^{2-} . The "ph" spelling is used, except in direct quotes from sources that use the other convention.

1.2 THE EXTRACTION OF SULPHUR FROM FOSSIL FUELS

1.2.1 Reasons for Sulphur Extraction

The deleterious effects of high-sulphur-content fossil fuels are catalyst fouling, corrosion of pipes and reactor vessels, undesirable properties of the fuel products, and air pollution during processing or after combustion. As the world reserves of low-sulphur fuels are consumed and the demands of environmental legislation and the public become more stringent, the use of desulphurization will increase.

1.2.1.1 Catalyst Fouling

Noble metal catalysts in the catalytic reformer,³³ some hydrocracking units,⁹ and the butadiene hydrogenator section of the alkylation unit of the refinery are poisoned by sulphur-containing compounds. It is the poisoning of the reformer catalyst which is the economic incentive for hydrodesulphurization.

Table 1.2 Nomenclature of Compounds Containing Sulphur, Carbon and Hydrogen

Formula	Name	Notes	Reference
RSH	alkanethiol	suffix	30
RSH	alkyl hydrosulfide	5	32, 30
RSH	thio(alcohol)	trivial	30
RSH	alkyl mercaptan	outdated	30
RSH	mercapto-	prefix	30
RSH	sulfide	biochemistry	17
RSSH	alkyl hydrodisulfide		32, 30
RSSH	alkyldisulfane	1	30
RSSH	alkylpersulfide		32
RSR	dialkyl sulfide	4,5	30
RSR	dialkyl thioether	outdated	30
RSR	alkylthio-	prefix	30
RSR	thia-	prefix, 6	30
RSR	thio-	trivial	30
RSR	epithio-	prefix, 2	30
RSSR	dialkyl disulfide	5	30
RSSR	dialkyldisulfane	1	30
RSSR	dithiodi-	prefix, 3	30
RSSR	disulfaneyldi-	prefix, 1, 3	30
RSSR	epidithio-	prefix, 2	30
RSSR	alkyldisulfanyl-	prefix, 1	30
RS·	alkylsulfanyl	free radical	30
RS·	alkanesulfenyl	free radical	30
RS·	alkylthio	free radical	30
RS+	alkylsulfanyl	cation	30
RS+	alkanesulfenyl	cation	30
RS+	alkylsulfanylium	cation	30
RS+	alkanesulfenylium	cation	30
R ₃ S ⁺	trialkylsulfonium	cation, suffix	30
R ₃ S ⁺	dialkylsulfonio-	cation, prefix	30
S ²⁻	sulfide	anion	31
S ²⁻	thio	ligand	31
S ₂ ²⁻	disulfide	anion	31
S ₂ ²⁻	disulfido-	ligand	31
HS-	hydrogensulfide	anion	31
HS-	mercapto-	ligand	31
RS-	alkanethiolate	suffix, anion	31
RS-	alkyl sulfide	anion	30
RS-	sulfido-	anion, prefix	30
RS-	alkylthio-	ligand	31
RS-	alkanethiolato-	ligand	31

Notes: 1. S-S chain is straight, not branched.

2. S atom bridges two carbons already in a ring.

3. Identical R groups.

4. Compounds of the formula $RS(CH_2)_nSR'$ have been referred to as disulphides.¹³⁰

5. Radicofunctional nomenclature.

6. For use when an S atom replaces a CH_2 group in the parent formula.

1.2.1.2 Corrosion

Corrosion in the refinery due to sulphur compounds occurs at high temperatures or pressures. Regions where these conditions exist, such as pipe still heaters, fractionators, and reactors, are prone to iron oxide and iron sulphide scale formation. At low temperatures, acid attack by HCl, H₂S, or CO₂ in condensates is the principal cause of corrosion.³⁴

1.2.1.3 Undesirable Properties of Fuel Products

Fuel products high in hydrogen sulphide, thiols, and volatile sulphides have distinctly unpleasant odours. This problem is rectified by either extraction of the sulphur, or conversion of the thiols to the non-volatile disulphides, which are often allowed to remain in the fuel product.⁹ The stability of fuel products is compromised if H₂S, disulphides, or polysulphides are present. The last two species "actively promote the formation of sludges."³⁵ Sulphur compounds are removed from kerosenes to decrease smoke formation.³⁶ The effectiveness of alkyl-lead anti-knock agents is inhibited by thiols and disulphides.³⁷ However, since the use of alkyl-lead compounds is diminishing, this inhibition is no longer a justification for desulphurization.

1.2.1.4 Air Pollution

The bulk of anthropogenic emissions of sulphur gases in the U.S. are of sulphur dioxide.³⁸ Although industrial emissions of hydrogen sulphide are in sufficient quantities to cause concern, they represent only 1% of the total anthropogenic sulphur emissions in Canada.³⁹ The gaseous products of fossil fuel combustion contain sulphur dioxide and sulphur trioxide in ratios of between 40:1 and 80:1.¹⁴ Fuel combustion in

stationary sources, such as heating systems in buildings, and power generating stations, is responsible for greater emissions than combustion by mobile sources such as transportation vehicles (Table 1.3). In the United States, where coal combustion plays a greater role in power generation, the stationary source emissions are significantly greater than in Canada.

Stack gases of fluid catalytic crackers are a major source of sulphur oxides. These emissions can be reduced by scrubbing of the gases, or hydrotreating of the cracker feedstock.⁴¹

Once emitted, SO_2 is oxidized in the atmosphere to SO_3 in a reaction catalyzed by metallic oxide particulates. Sulphur trioxide reacts with water or particulates to form sulphuric acid or sulphates, respectively. Both products cause reduced visibility, corrosion of materials, and acid rain. The observed useful life of galvanized sheet steel at 65% humidity and $13 \text{ g/m}^3 \text{ SO}_2$ (rural setting) is 30-35 years. At $1040 \text{ g/m}^3 \text{ SO}_2$ (heavily industrial setting), the useful life is reduced to 3-5 years.⁴² The effects of sulphur oxides on the environment are more difficult to measure, but the serious consequences of large scale damage are sufficient to keep the subject under intense scientific and political scrutiny.

1.2.2 Sulphur Extraction from Petroleum

The removal of organic sulphur from petroleum is accomplished by amine treatment, caustic treatment, molecular sieve adsorption, or catalytic hydrotreating.⁴³ The last mentioned process is the most effective at removing sulphur and therefore is used to treat feedstocks of the catalytic reformer, and refinery product streams which need to be particularly low in sulphur. The placement of desulphurization units within a simplified refinery flow-plan is shown in Fig. 1.3. Hydrotreating (Fig. 1.4) involves passing the feed over catalysts of nickel, cobalt or molybdenum oxides on alumina, under high

Table 1.3 Canadian Nationwide Emissions of Sulphur Oxides, in 1980^a

Source	Emissions (x 10⁶ kg SO₂)	Percent of Total
COMBUSTION IN VEHICLES		
marine	60	1.4
diesel	39	0.9
gasoline	19	0.5
railroad	3	0.1
aircraft	2	0.1
subtotal	123	2.9
STATIONARY SOURCES		
power generation by utilities	696	16.5
residential, commercial and industrial	556	13.2
fuel wood	2	0.1
subtotal	1,255	29.8
INDUSTRIAL PROCESSES		
Cu, Ni production	1,723	40.9
natural gas processing	348	8.3
Fe production	219	5.2
other metals	167	4.0
tar sands operations	136	3.2
pulping	104	2.5
petroleum production/refining	100	2.4
other	38	0.9
subtotal	2,837	67.3
solid waste incineration	3	0.1
TOTAL	4,218	100.0

^a Adapted from reference 39b.

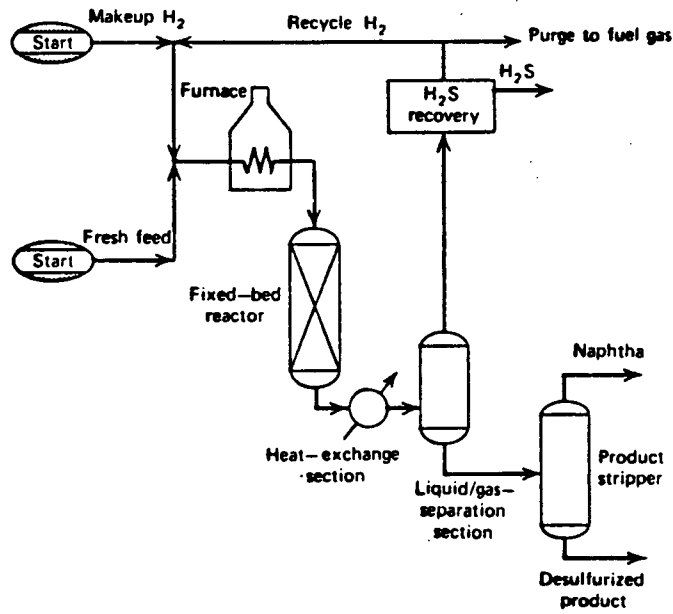


Fig. 1.4 Flow plan for a naphtha hydrotreater.45

pressures of hydrogen. If the temperature is kept below 300°C, only the thiols are converted to H₂S, and the process is called hydrosweetening.⁴⁴ Naphtha (catalytic reformer feedstock) hydrotreating usually occurs at catalyst bed temperatures of up to 370°C.⁴³ At these temperatures, the following reactions take place:

a) Hydrodesulphurization (HDS)



b) Hydrodenitrogenation (HDN)

c) Hydrodeoxygenation (HDO)

d) Hydrogenation of olefins and some aromatics

e) Hydrocracking⁴⁶



After conversion, the products are separated; hydrogen is recycled; and H₂S is converted to sulphur in a Claus plant.

The HDS catalysts are usually MoO₃, with CoO as a promoter, deposited from an ammonia solution onto a high surface area alumina support. The oxides are converted to sulphides by presulphiding the catalyst with H₂/H₂S mixtures.⁴⁶ Heavy metals in the feed poison the HDS catalyst, but this is preferable to poisoning of the expensive reformer catalyst.

The sulphides of Ru, Os, Rh, and Ir are far more efficient HDS catalysts than those of either Co or Mo, possibly because of the intermediate heats of formation of the noble metal sulphides (Fig. 1.5).⁴⁷⁻⁹ However, the success of catalysts containing both Co and Mo, and the cost of the noble metal catalysts, prohibit their use industrially.

The mechanism of the hydrodesulphurization reaction is not known. Thiophene is the model substrate of choice, because it is the parent molecule of the least easily desulphurized class of molecules. The hydrocarbon products of the reaction of thiophene with 1 atm of hydrogen, over cobalt molybdate on alumina at 288°C, are butadiene (2%),

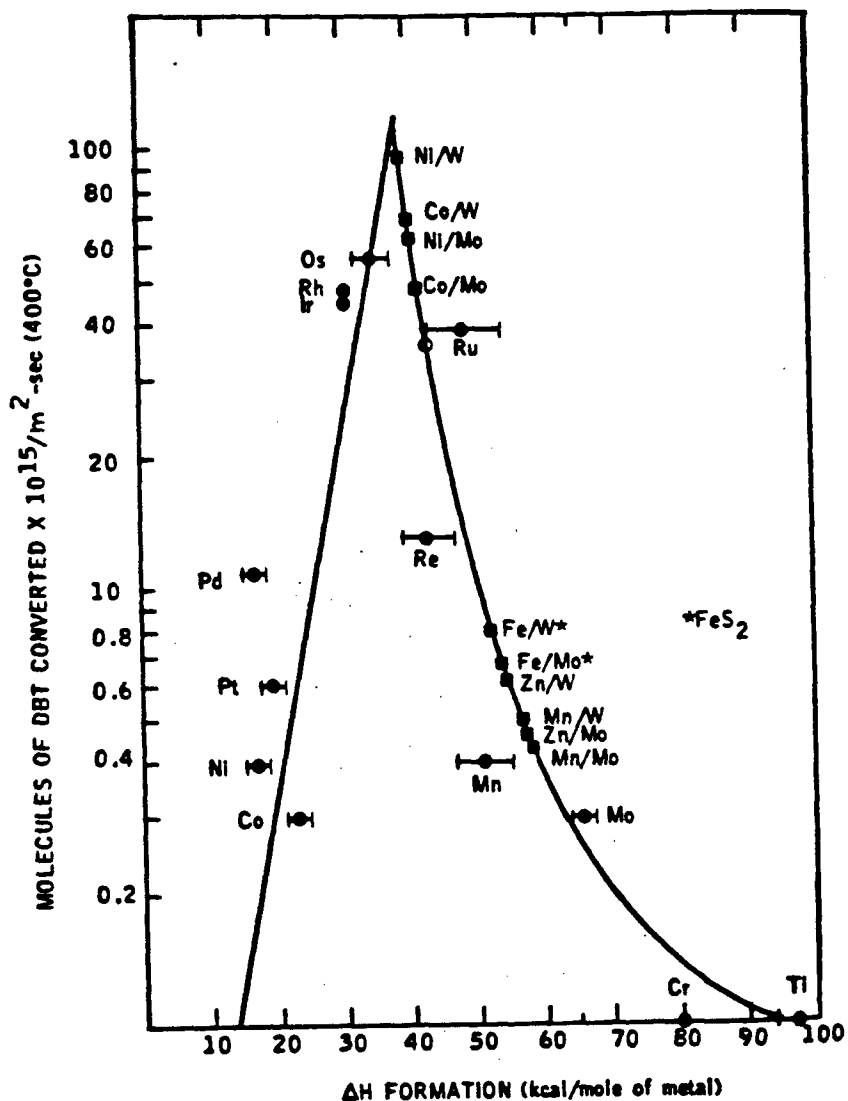


Fig. 1.5 The dependence of the HDS activity of the transition metal sulphides on their heat of formation (DBT = dibenzothiophene).⁴⁷ Mixtures of metal sulphides are shown as filled squares at the average of the heats of formation of the individual sulphides. The commercial catalyst is shown as a hollow circle.

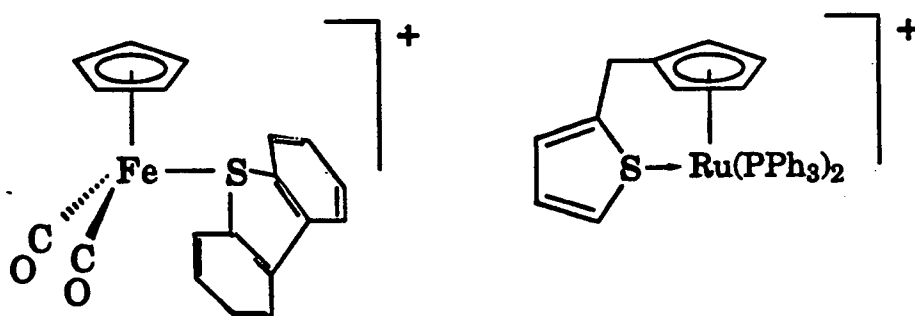
1-butene (48%), *cis*-2-butene (20%), *trans*-2-butene (24%), and butane (6%).⁵⁰ Central to the debate over the mechanism are the mode of coordination of thiophene to the surface and the nature of the first step in the reaction pathway.

Studies of thiophene adsorption onto clean or sulphided surfaces of various metals found examples of S-bound perpendicular, S-bound tilted, and η^5 -bound thiophenes.¹ IR studies on molybdenum sulphide catalysts showed evidence for thiophenes coordinated by one (η^2 or η^3) or two (η^4 or η^5) double bonds.⁵¹ Perpendicular binding through the S atom is preferred in molybdenum sulphide anion vacancies, according to quantum chemical extended Hückel theory studies.⁵² Coordination complex analogues for four of these binding modes have been reported (Fig. 1.6).³⁰³ It is likely that the mode of binding on surfaces varies depending on the adsorbed species. One study⁵³ of thiophenes and thianthrenes adsorbed on commercial CoMo/Al₂O₃ catalysts at normal operating conditions divided the molecules into those concentrating their electron density at the sulphur, and those having their electron density delocalized over an extensive π system. The former group would bind by the sulphur atom. The latter group, especially if steric hindrance existed around the sulphur, would bind in the manner of a π complex. This is consistent with observations in coordination chemistry: benzothiophene and dibenzothiophene, which fall in the latter group, bind to metal atoms by the benzene, not thiophene, ring.⁵⁴⁻⁶

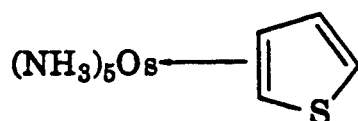
Angelici¹ used parallels with coordination chemistry to argue in favour of η^5 coordinated thiophenes in HDS. He argued that a) η^5 coordination is stronger and more activating than the η^1 coordination, and that b) product distributions of exchange reactions of D₂ with thiophene bound to HDS catalyst surfaces are very similar to those of exchange reactions of CD₃OD with Ru(Cp)(η^5 -thiophene)⁺.

After adsorption, what is the first step in the HDS of thiophene; desulphurization to butadiene followed by hydrogenation, or hydrogenation to di- or tetrahydrothiophene followed by desulphurization? Studies by Desikan and Amberg⁶³ suggest the former,

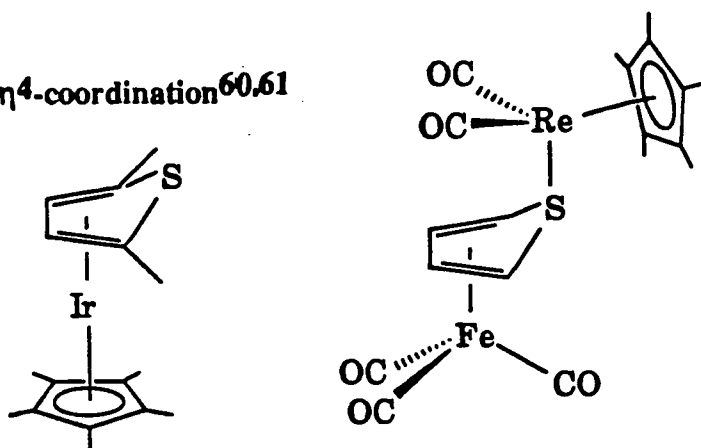
a) η^1 -coordination^{57,58}



b) η^2 -coordination⁵⁹



c) η^4 -coordination^{60,61}



d) η^5 -coordination⁶²

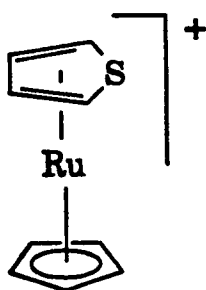


Fig. 1.6 Transition metal complexes exhibiting different modes of thiophene coordination.

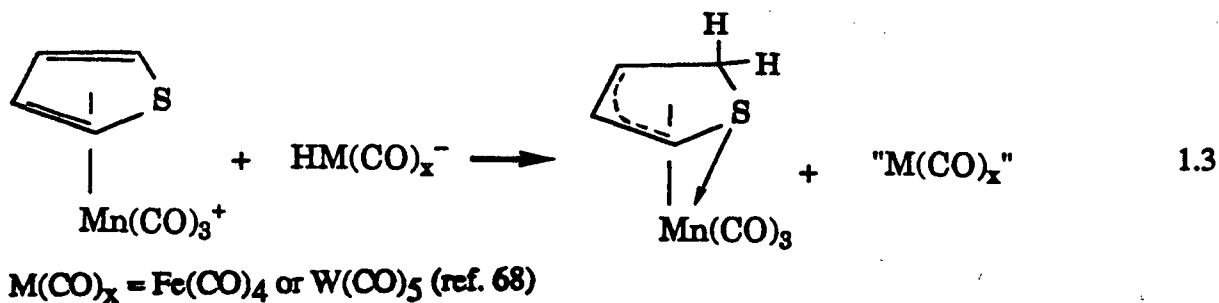
because the HDS of tetrahydrothiophene gives a different product distribution than the HDS of thiophene. However, results with benzothiophene⁶⁴ and the presence of tetrahydrothiophene in thiophene HDS effluent⁶⁵ suggest that both pathways are being followed simultaneously.

It is likely that two kinds of sites exist. One type, responsible for desulphurization, is poisoned by H₂S, thiophene, pyridine and NH₃. The other, weakly electrophilic site, responsible for hydrogenation, is poisoned only by NH₃ or alkali.⁶³

The Lipsch-Schuit mechanism⁶⁶ proposes η^1 -coordination of the thiophene, followed by H atom donation from an OH or SH group to the α carbon, causing C-S bond cleavage. This would be repeated, liberating butadiene. The sulphur atom would then be removed from the surface by hydrogenation (Fig. 1.7). This mechanism has been criticized for its use of S-bound thiophene species⁶⁷⁻⁸, and because the hydrogenation of the sulphide on the surface would be rate limiting.⁶⁹

Kolboe⁷⁰ proposed intramolecular β -elimination of H₂S from thiophene, which would produce adsorbed diacetylene. This is supported by IR detection of an acetylene on the surface of the catalyst,⁶⁶ but would require unstable benzyne species if it were the pathway of reaction of benzothiophenes.^{46,67}

Mechanisms involving η^2 - or η^5 -coordination of the thiophene have since been proposed.^{67,71} Angelici¹ has developed a mechanism (Fig. 1.8) based on observed reactions of thiophene coordination complexes, including the donation by hydride complexes of H⁻ to bound thiophene complexes (reaction 1.3),^{68,72} the protonation of the allyl sulphide intermediate (reaction 1.4)⁶⁸, and the elimination of butadiene from Fe(CO)₄(2,5-dihydrothiophene) (reaction 1.5).^{1,73}



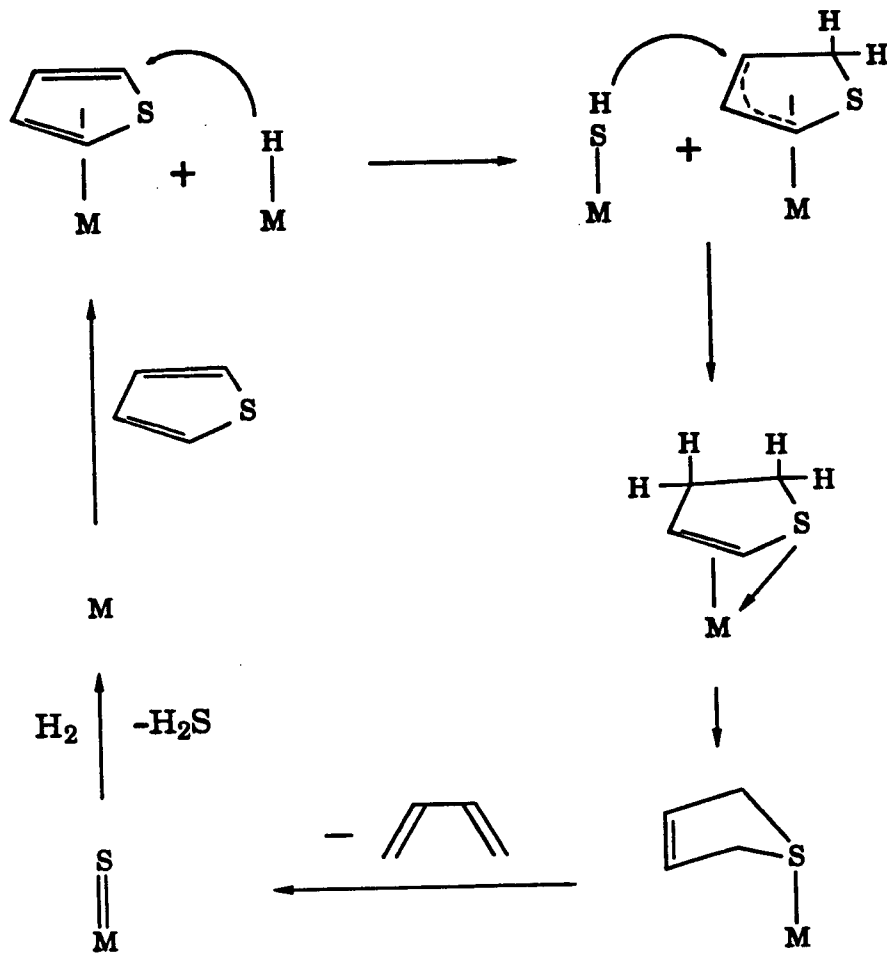
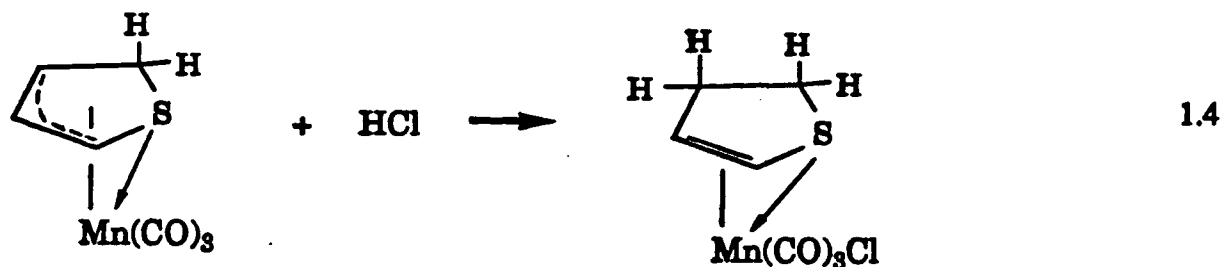


Fig. 1.8 The Angelici mechanism for thiophene HDS.1



The mechanism assumes that hydride species would be available on the surface of the catalyst "as a result of dissociative adsorption of H_2 ."¹ The mechanism does not satisfy the concerns of Gellman *et al.*⁶⁹, about the slow rate of hydrogenation of sulphide species on the surface.

More recently, Wang and Angelici⁵⁵ have used analogies from coordination chemistry to study the more difficult problem of the mechanism of the HDS of dibenzothiophene.

1.3 REACTIONS OF SULPHUR-CONTAINING ORGANICS WITH TRANSITION METAL COMPLEXES

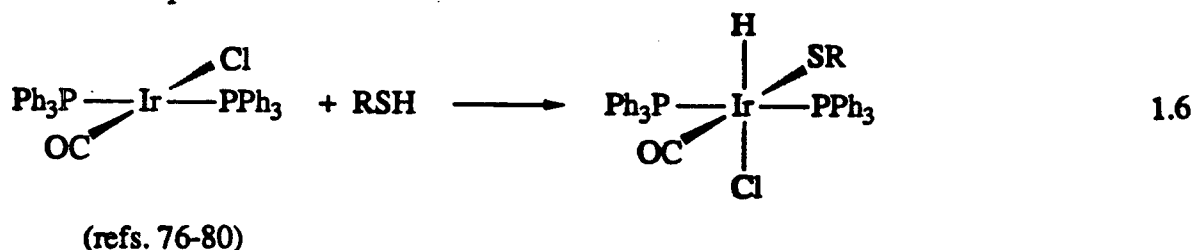
The reactions which occur on the surface of the HDS catalyst involve thiols, sulphides and disulphides. Their reactivity is affected by their coordination to the surface. These reactivity changes are most easily studied in the chemistry of the analogous homogeneous systems.

The coordination of sulphur compounds to transition metal centres is usually, but not always, followed by S-H, S-S or S-C bond cleavage. Despite the fact that, of the three groups, the S-H bonds have the greatest bond dissociation energies (83-91 kcal/mol),⁷⁴

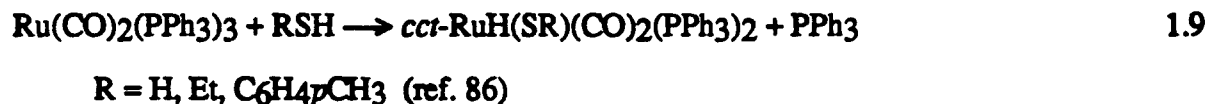
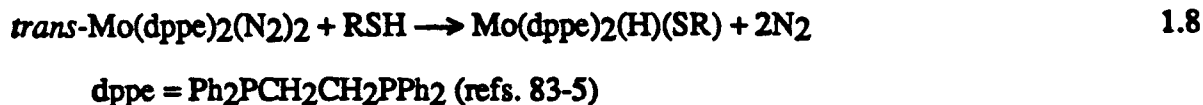
they are the most easily cleaved because of their ionic character. Thiols are acidic in aqueous solution, with pK_a 's of 6.6, 7.0 and 10.7 for aryl thiols, hydrogen sulphide and alkyl thiols, respectively (Table 3.8). The S-S bonds of di- and poly-sulphides are also easily cleaved, having a bond strength of 66 kcal/mol (for HSSH).⁷⁵ Sulphur-carbon bonds (61-77 kcal/mol),⁷⁴ on the other hand, are rarely cleaved. Coordinated thioethers ($M-SR_2$) are more common than organometallic thiolato complexes ($M(R)(SR)$) that result from oxidative addition of thioethers to metal centres. The following sections describe reactions with transition metal complexes in which S-H, S-S or S-C bonds have been cleaved.

1.3.1 Reactions Involving S-H Bond Cleavage

Oxidative addition of thiols has been known since the early 1960's, for example, with Vaska's compound.



Similar reactions are:



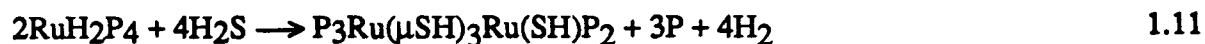
Reaction 1.9 will be more fully described in Sections 3.1 and 3.2 of this work.

Examples of H₂S or thiol coordination without cleavage of the S-H bond, such as that in equation 1.7, are rare, although that type of structure is proposed to be the intermediate in all such reactions. A few observed compounds of this type are Fe(RSH)(CO)₄,⁸⁷ [Ru(NH₃)₅(HSEt)]²⁺,⁸⁸ (PhCH₂SH)Rh(μO₂CCH₃)₄Rh(HSCH₂Ph),⁸⁹ [CpRu(PPh₃)₂(H₂S)]⁺,⁹⁰ and possibly Fe(TPP)(PhSH)(SPh) (H₂TPP=tetraphenylporphyrin).⁹¹

Oxidative addition of thiols is often followed by dimerization, because thiolate ligands have a tendency to adopt bridging positions.⁹²



M=Rh or Ir (refs. 93-4)



P=PPhMe₂ (ref. 95)



L=CO or H₂ (refs. 96-7)

The hydrido-thiolato products of the oxidative addition may react with excess thiol in a second step.



(ref. 86)



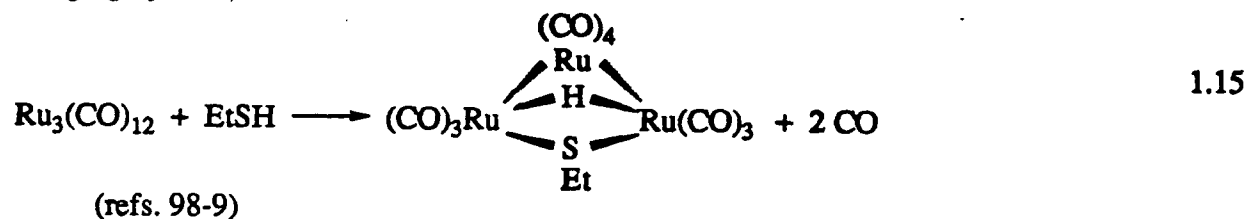
(refs. 83-5)

This type of reaction can be inhibited by the use of bulky thiols, or the use of exactly one equivalent of thiol in the initial reaction. This problem of subsequent reaction, along

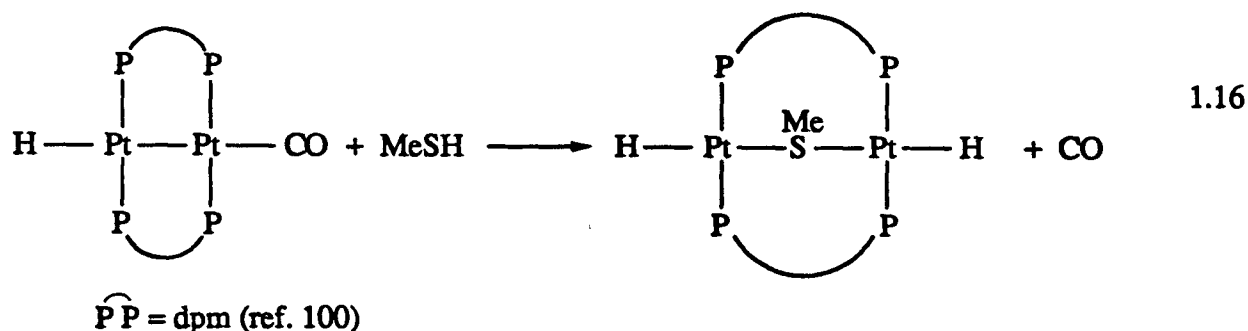
with the tendencies of these complexes either to dimerize or eliminate thiol, restricts the number of well-characterised hydrido thiolato complexes.

The kinetics of the oxidative addition reaction are rarely studied. The reaction of *trans*-Mo(dppe)₂(N₂)₂ with *n*-propyl or phenyl thiol (reaction 1.8 followed by reaction 1.14) was monitored by UV.⁸⁴ The rate had a first-order dependence on the concentration of the complex, and zero to first-order dependence on the thiol concentration. The proposed mechanism (Scheme 1.1) included two unobserved species [MoH(SR)(dppe)₂] and [MoH₂(SR)₂(dppe)₂], modelled after the known complexes [MoH(tpbt)(dppe)₂] (tpbt = 2,4,6-*i*Pr₃C₆H₂S⁻) and [MoH₂Cl₂(dppe)₂].

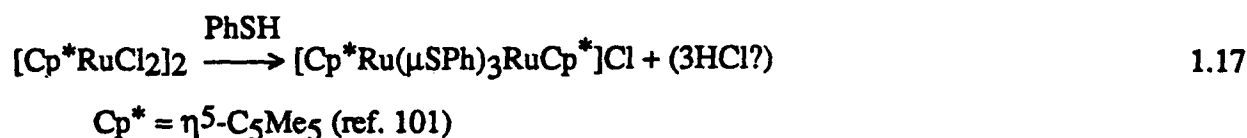
Addition of thiols across a metal-metal bond produces a bridging thiolate and either a bridging hydride,



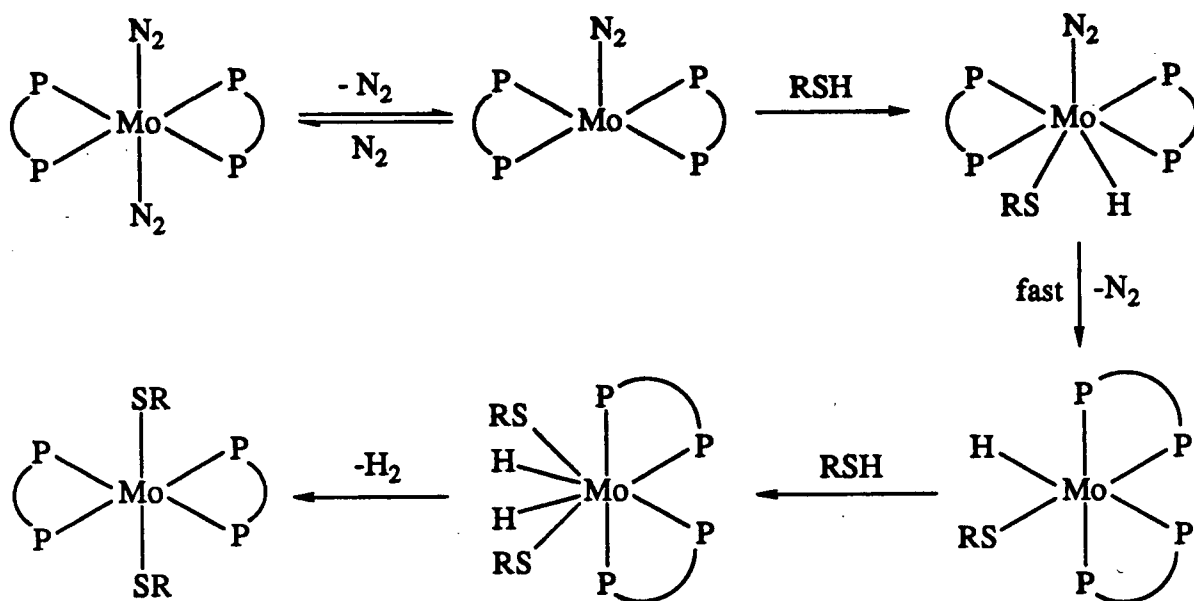
a terminal hydride,



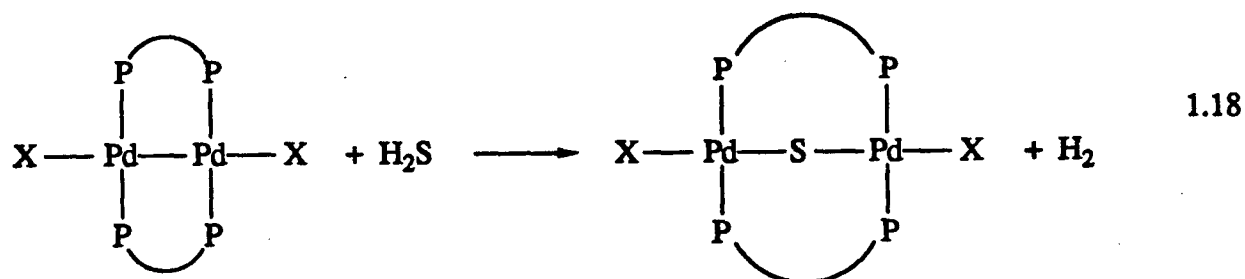
or no hydride ligand.



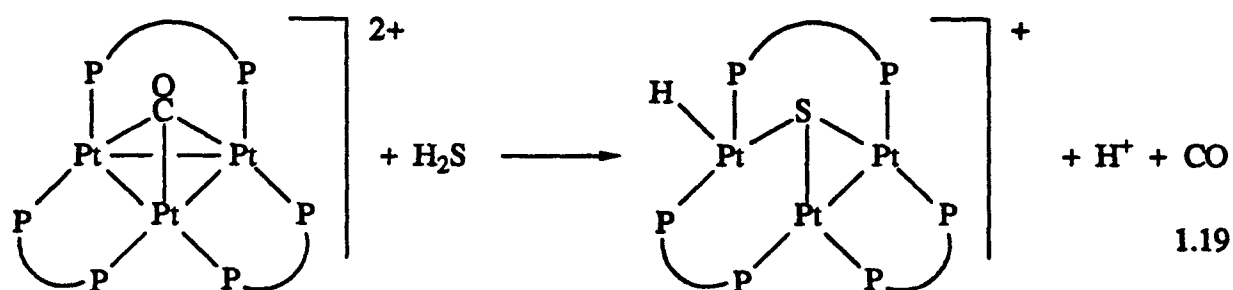
Scheme 1.1 The proposed mechanism for the reaction of *trans*-Mo(dppe)₂(N₂)₂ with thiols (adapted from ref. 84).



Similarly, one or both of the S-H bonds in H₂S may be cleaved, and one or both of the hydrogens eliminated.



X = Cl, Br; $\widehat{\text{P}}\widehat{\text{P}} = \text{dpm}$ (refs. 102-5)

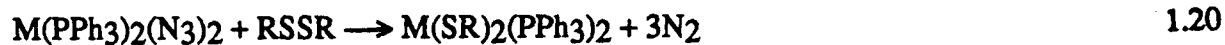


$\widehat{\text{P}}\widehat{\text{P}} = \text{dpm}$ (ref. 106)

During the conversion of H₂S to elemental sulphur, the production of hydrogen gas in a process based on this type of chemistry would be preferable to the production of water as found in modern Claus plants.

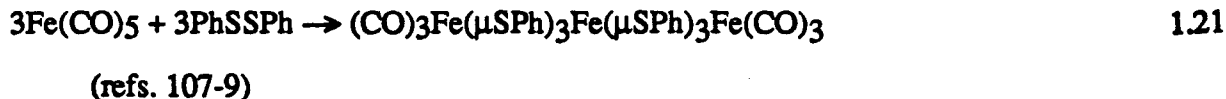
1.3.2 Reactions Involving S-S Bond Cleavage

Oxidative addition of disulphides involves cleavage of S-S bonds, forming two terminal thiolate ligands,

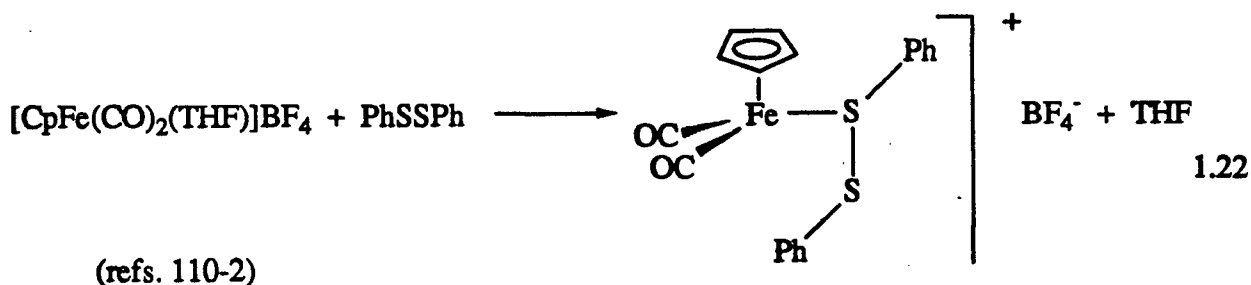


R = Me, Bu or Ph; M = Pd or Pt (ref. 95)

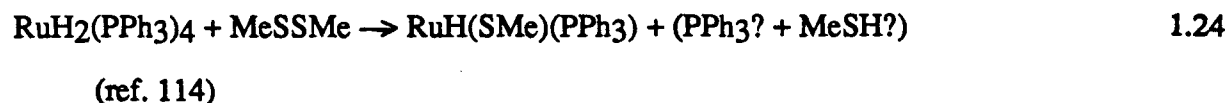
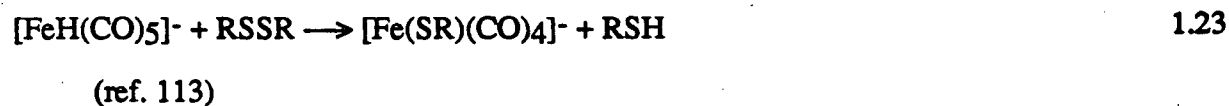
or forming a thiolate-bridged structure.



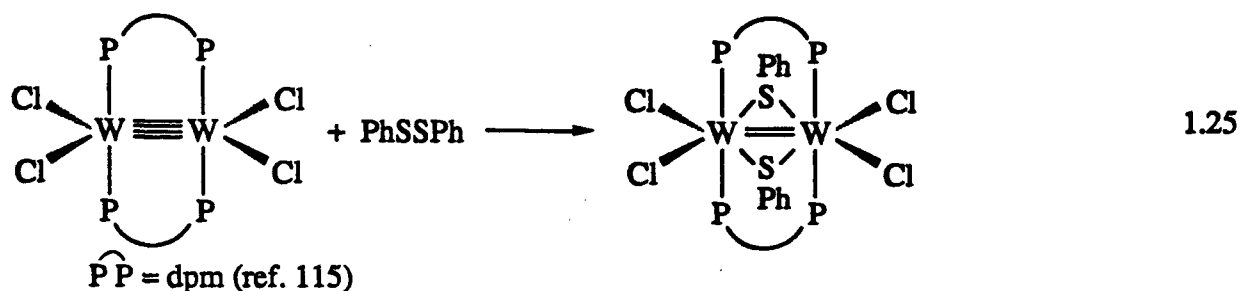
The intermediate in disulphide oxidative addition reactions may be a disulphide coordinated by one or two sulphur atoms to the metal. This is usually not observed; but such compounds have been isolated.

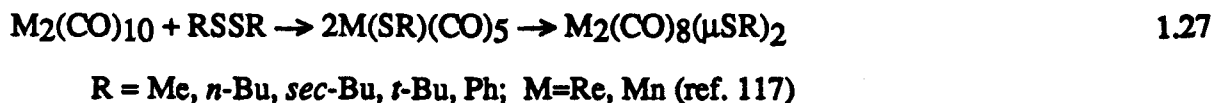
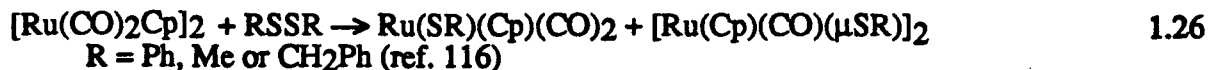


Reactions of disulphides with metal hydrides produce a thiolate complex and one equivalent of liberated thiol.



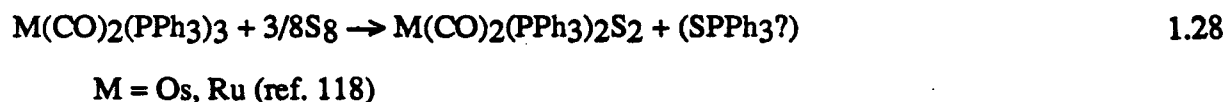
Addition of disulphides across metal-metal bonds leads to thiolate-bridged structures, either directly or through a monomeric thiolate complex.



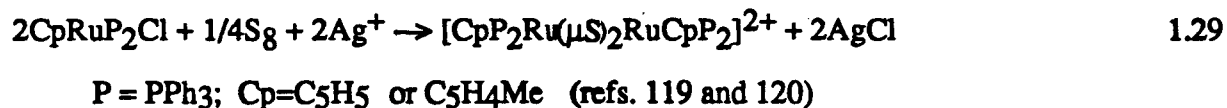


The first steps in reaction 1.27 were photolytic cleavage of the dimer to form M(CO)₅, followed by RS group transfer from RSSR. *Pseudo*-first-order kinetics showed that the rate decreased with the bulk of the alkyl group of the disulphide, although diphenyl disulphide reacted more quickly than the dialkyl disulphide due to either its weaker S-S bond or "the electron accepting capability of the phenyl group" which would favourably affect the rate of the donation of an electron from M(CO)₅ to the disulphide.¹¹⁷

The reactions of elemental sulphur with transition metal complexes also involve S-S bond cleavage. Sulphur has been widely used as an S atom donor, along with ethylene and propylene sulphides, and alkyl trisulphides. The products are mononuclear,



dinuclear,



or polynuclear inorganic sulphides.



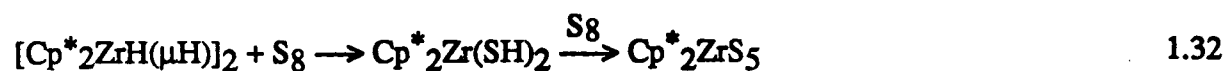
(ref. 82)

The resulting sulphur bridge in dinuclear complexes can be unsupported and of several atoms.

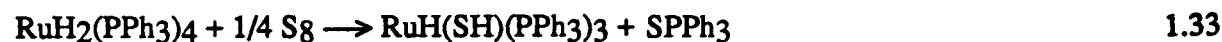


(ref. 121)

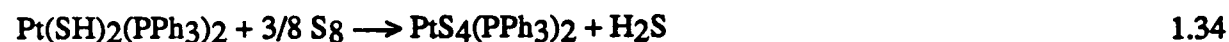
Metal hydrides react with sulphur to yield mercapto complexes, some of which react further to give inorganic sulphido complexes.



$\text{Cp}^* = \eta^5\text{-C}_5\text{H}_4\text{tBu}$ (ref. 122-3)



(ref. 18)



(ref. 124)

There are even reports of the sequential insertion of sulphur into the M-C bonds of metal alkyl complexes.

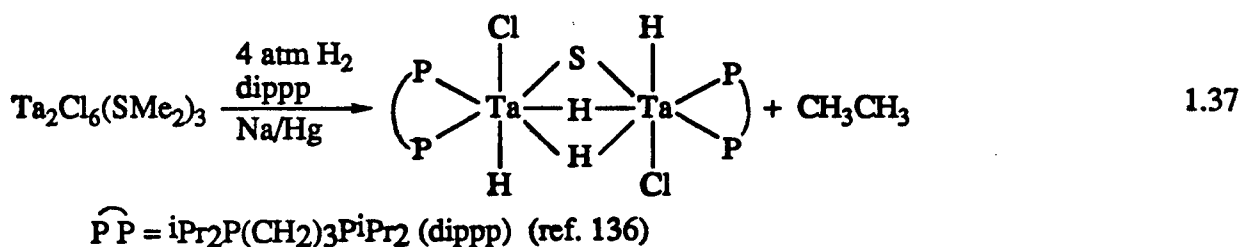
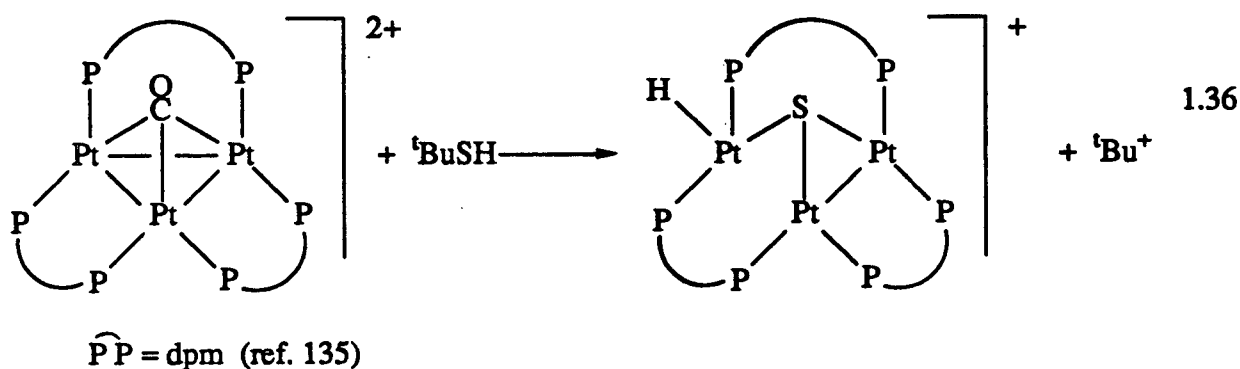


$\text{R} = \text{CH}_2\text{SiMe}_3$ (refs. 125-6)

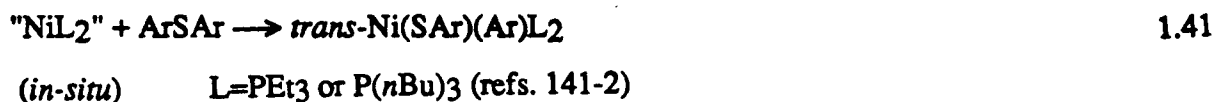
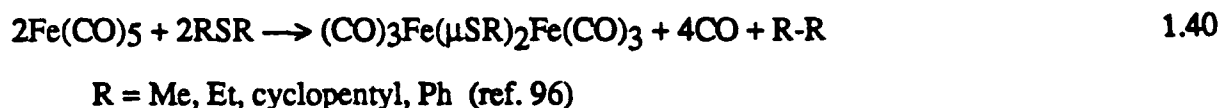
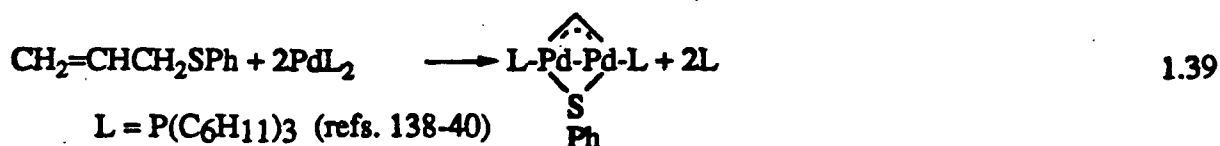
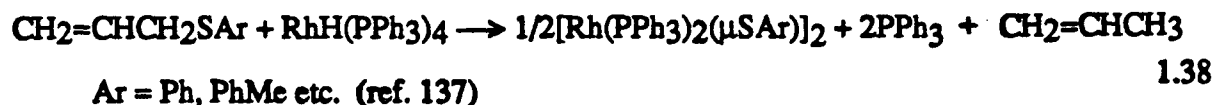
1.3.3 Reactions Involving S-C Bond Cleavage

The $\text{Pd}_2\text{X}_2(\text{dpm})_2$ dimers which extracted sulphur from hydrogen sulphide (reaction 1.18) failed to extract sulphur from thiols or sulphides,¹⁰³ because of the greater resistance to cleavage of S-C bonds compared to S-H and S-S bonds. The same reason can be given for the stability of metal thioether complexes relative to their thiol or disulphide cousins. Examples of stable ruthenium thioether complexes include $[\text{Ru}(\text{NH}_3)_5\text{L}]^{2+}$ ($\text{L}=\text{Me}_2\text{S}$, tetrahydrothiophene (THT), thiophene),^{88,127} *cis*- and *trans*- $[\text{Ru}(\text{bipy})_2\text{L}_2]^{2+}$ ($\text{bipy}=2,2'$ -bipyridyl, $\text{L}=\text{MeSPh}$, phenothiazine, 1,4-dithiane),¹²⁸ $[\text{CpRu}(\text{PPh}_3)_2\text{L}]^+$ ($\text{L}=\text{THT}$, ethylene sulphide),¹²⁹ *mer*- $[\text{RuCl}_3\text{L}_3]$ ($\text{L}=\text{Me}_2\text{S}$, Et_2S , PhSMe , THT, etc.),¹³⁰⁻² and $[\text{RuCl}_3(\text{Et}_2\text{S})_2]_2$.¹³¹ In addition, a large number of transition metal crown thioether complexes have been reported.¹³³

Stoichiometric sulphur extraction from thiols and thioethers is known (see also Jang *et al.*).¹³⁴



A reaction similar to 1.37, but involving sulphur atom abstraction from PhSSPh has been reported.³⁰⁸ Oxidative addition reactions of thioethers involving cleavage of only one S-C bond (especially an allyl-S bond) are far more common than reactions involving cleavage of 2 S-C bonds.



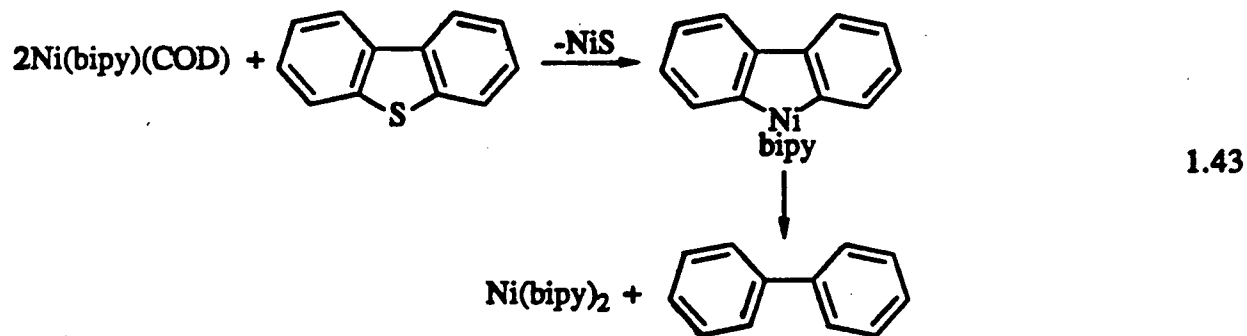
Strained-ring thioethers such as ethylene and propylene sulphides are a special case.

Although coordinated ethylene sulphide exists¹²⁹ in the complex

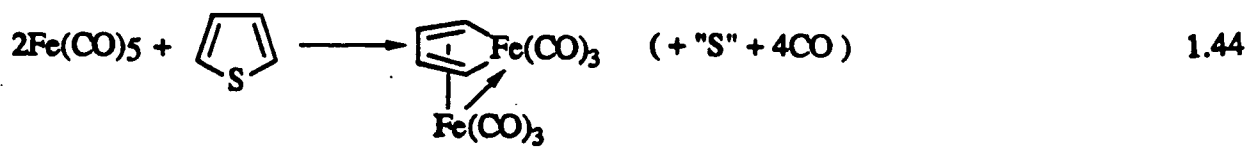
[CpRu(PPh₃)₂(SC₂H₄)]⁺, it more typically donates the sulphur atom, liberating ethylene.



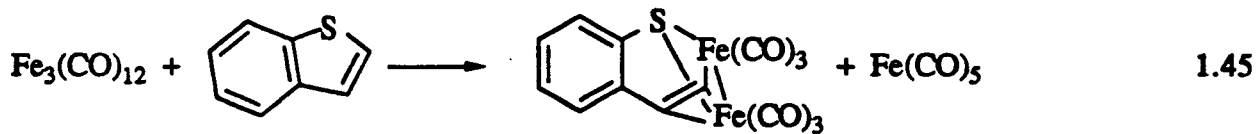
Thiophenes are another special case. A few of their transition metal complexes have been mentioned (section 1.2.2). Examples of reactions in which one or both of the S-C bonds of a thiophene group have been cleaved by reaction with transition metal complexes are shown below.



(ref. 144)



(ref. 145)



(ref. 146)

2. GENERAL EXPERIMENTAL PROCEDURES

The materials, the general techniques common to most of the experiments, and the syntheses of the non-sulphur-containing ruthenium complexes, are described in this chapter. Details of individual experiments can be found in the last section of each subsequent chapter.

2.1 MATERIALS

All of the ruthenium complexes were synthesized from $\text{RuCl}_3 \cdot 3\text{H}_2\text{O}$, supplied by Johnson Matthey. Thiophene, benzyl trisulphide, benzene selenol, triphenyl phosphine sulphide, and the thiols, sulphides, and disulphides were supplied by Aldrich. Diphenyl sulphide was purified before use by mixing 1:1 with acetone, adding a concentrated acetone solution of KMnO_4 until it stayed purple, filtering and fractionally distilling under vacuum. Elemental analysis and NMR spectroscopy showed the thioether to be pure. Other chemicals used were benzophenone (BDH), dpm (Aldrich), fluoboric acid (MCB), sodium borohydride (BDH), sodium tetraphenylboron (Fisher), tetrafluoroboric acid diethyl ether complex (Aldrich), triphenyl phosphine (BDH), *tris-p*-tolyl phosphine (Strem) and sodium methylate (Fisher). Sodium ethyl and *p*-tolyl thiolates were synthesized by the reaction of the thiol with an excess of sodium in undistilled diethyl ether under N_2 . After 1 h, unreacted sodium was removed with tweezers and the white suspension filtered. The salt was dried under vacuum overnight and stored under N_2 or Ar. Na/Hg amalgam was prepared by dissolving Na slivers into Hg under Ar until the solution solidified. Then extra Hg was added until the solution could be easily stirred. Tetra-*n*-butyl ammonium tetrafluoroborate was synthesised by Mr. A. Pacheco of this research lab, from the reaction of tetra-*n*-butyl ammonium hydroxide with tetrafluoroboric acid, followed by recrystallization (twice) from ethyl acetate and *n*-pentane.

The solvents, analytical or glass distilled grade, were dried by refluxing for several days over drying agents under N_2 , and distilling from the drying agent immediately before use.

Tetrahydrofuran or "THF" (supplied by BDH), toluene (Omnisolve), benzene (BDH), diethyl ether (BDH), and hexanes (BDH) were dried over sodium and benzophenone. Pentane was dried over phosphorus pentoxide. Acetone was dried over K_2CO_3 . Methanol (BDH, glass distilled) was dried over magnesium turnings treated with iodine. *N,N*-dimethylacetamide (BDH) to be used in the synthesis of $RuH(Cl)(CO)_2(PPh_3)_2$ was not distilled, but only degassed by repeated freeze/thaw cycles under hydrogen. C_6D_6 , CD_2Cl_2 , CD_3OD , D_2O , $C_6D_5CD_3$, $(CD_3)_2CO$, and THF-d₈ were supplied by Cambridge or MSD Isotopes. All of these, except CD_3OD and D_2O , were received as ampoules, and transferred to storage vessels and thence to the NMR sample tubes under an inert gas (N_2 or Ar). CD_3OD and D_2O were received in bottles and were not stored under anaerobic conditions.

Gases (N_2 , Ar, H_2 , O_2 , CO, H_2S , HCl, and MeSH) were used as received from Matheson.

The thiols and thiolate salts are extremely smelly, and all of the sulphur-containing organics are extremely toxic. Hydrogen sulphide and methanethiol must be handled with particular care because of the fatal consequences of accidental exposure to these gases. Selenium-containing compounds such as benzene selenol are even more toxic than their sulphur-containing analogues.

2.2 EQUIPMENT AND TECHNIQUES

2.2.1 Reaction Conditions

Except where noted, synthetic scale reactions were performed in THF at room temperature and under one atmosphere of an inert gas (either N_2 or Ar), using standard Schlenk tube techniques. NMR scale *in situ* experiments were performed in the following manner. Into a wide-mouth Schlenk tube was placed a 5 mm glass NMR tube containing a known weight of the solid reagents, or the unknown to be characterized. After evacuation of the Schlenk tube, the gas was admitted. The cap to the Schlenk tube was removed, with the gas flow sufficiently high to

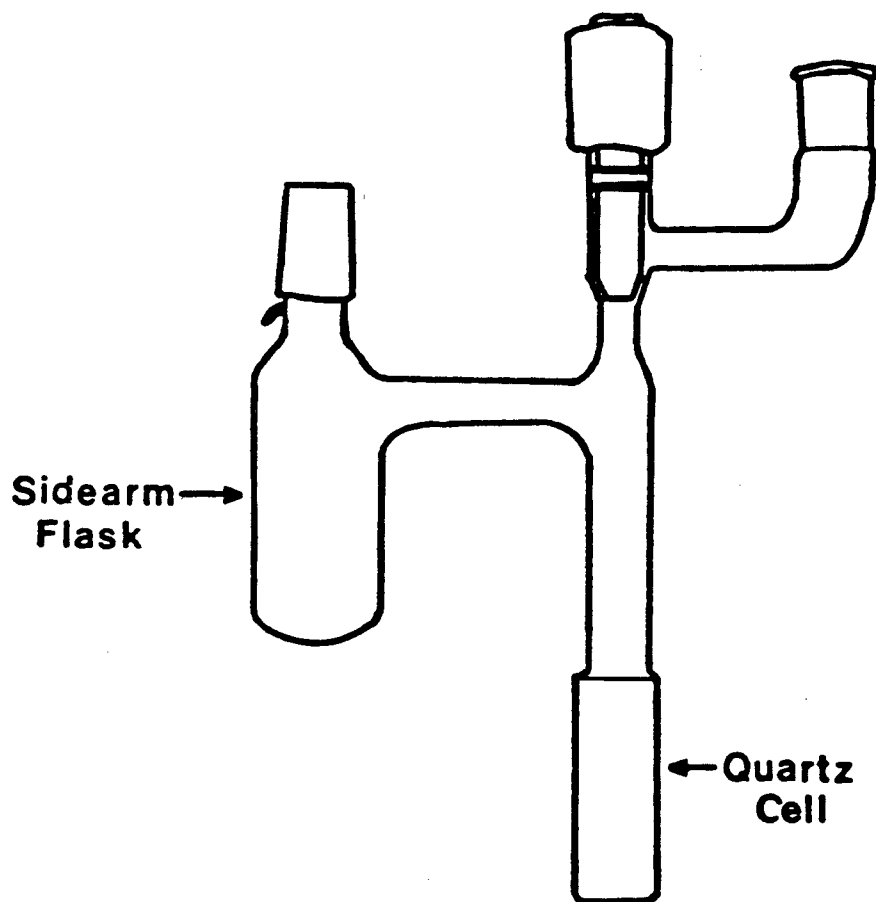
prevent the entry of air. The solvent, usually C_6D_6 , was pipetted into the NMR tube, which was sealed with a septum flushed with an inert gas. The liquid reagent was then injected through the septum to start the reaction.

2.2.2 Spectroscopy and Chromatography

All NMR spectra were acquired at 19°C and using a Varian XL-300 at 300 MHz (1H) or 121 MHz (^{31}P nuclei) unless otherwise stated. Other NMR spectrometers used were a Bruker AC-200, a Bruker WH-400 for special experiments requiring greater field strength, and a Bruker AMX-500 for ^{31}P -decoupled 1H spectra. Solid state ^{13}C NMR spectra were acquired using a Bruker MSL-400 operated by Dr. L. Randall; the spectrometer contained zirconium spinners and a standard MAS probe tuned to 100.6 MHz. The solid state spectra were obtained with adamantane as external reference, and reported with respect to TMS. Solution NMR chemical shifts were measured with respect to TMS in C_6D_6 for 1H and ^{13}C , triphenyl phosphine in C_6D_6 for ^{31}P , and $BF_3:(C_2H_5)_2O$ in 1:1 $C_6D_6:(C_2H_5)_2O$ for ^{11}B nuclei, all as external references. The ^{31}P chemical shifts, however, are reported here with respect to 85% H_3PO_4 aqueous solution which shows a resonance, in the XL-300 at room temperature (20°C), at 6.05 or 5.46 ppm downfield of PPh_3 in C_6D_6 or CD_2Cl_2 , respectively. The deuterium lock signal was the solvent itself. All of the ^{31}P and ^{13}C spectra were 1H broad-band decoupled. The chemical shift of triphenylphosphine in C_6D_6 with respect to aqueous 85% H_3PO_4 was determined by acquiring the ^{31}P spectrum of a 10 mm NMR tube containing the former solution, with a 5 mm NMR tube containing the latter solution held inside it by plastic O-rings. The chemical shift of PPh_3 has been reported previously.¹⁴⁷

UV/vis spectra were measured taken in specially designed 1 cm or 1 mm quartz or glass cells (Fig. 2.1) sealed under the desired gas. The spectrometer, a Perkin Elmer 552A, contained an electronically temperature controlled cell holder accurate to $\pm 0.2^\circ C$.

Fig. 2.1 Anaerobic UV/vis. cell.



Infrared spectra of Nujol or hexachloro-1,3-butadiene mulls, or THF, toluene, or CH_2Cl_2 solutions were taken in a Nicolet 5DX FTIR internally calibrated with a He/Ne laser.

Fast Atom Bombardment Mass Spectra (FAB-MS) were acquired by Ms. C. Beaulieu of this department, using an AEI MS 9 mass spectrometer with a 6 kV ion source, a 7-8 kV, 1 mA xenon gun, and a 10 s/decade scan rate. The samples were contained in a *p*-nitrobenzyl alcohol matrix. The theoretical isotope patterns were predicted using the simulation program PEEKS-1982.148

The experimental conditions of the X-ray crystallography experiments will be described in the sections which detail their results.

The conductivity of solutions was measured with a Yellow Springs Instrument Co. 3403 Cell (with a cell constant of 1 cm^{-1}) and a Serfass Conductivity Bridge Model RCM 15B1.

Organic products were separated in a Hewlett Packard HP 5890A gas chromatograph with a 15 m OV101 column at 30°C with helium carrier gas, a split/splitless injector, and a flame ionization detector. The injection volume of liquids was $0.1 \mu\text{L}$. Hydrogen gas was detected qualitatively with a 10 ft molecular sieve column and a thermal conductivity detector.

Quantitative measurement of gas production was achieved using a constant pressure gas-uptake apparatus, described in section 2.2.3.

Microanalyses were performed by Mr. P. Borda of this department.

2.2.3 Kinetic Measurements

The reaction rates were monitored by one or more of three methods; UV/vis. spectroscopy, NMR spectroscopy, and gas-uptake measurements. Times were recorded from an electronic stopwatch during the NMR experiments, and from a Lab-Chron 1400 timer during uptake and UV/vis. experiments.

The constant pressure gas-uptake apparatus (Fig. 2.2) has been briefly described in the literature^{149,150}. This equipment can be used to measure the rate of gas-uptake or evolution at

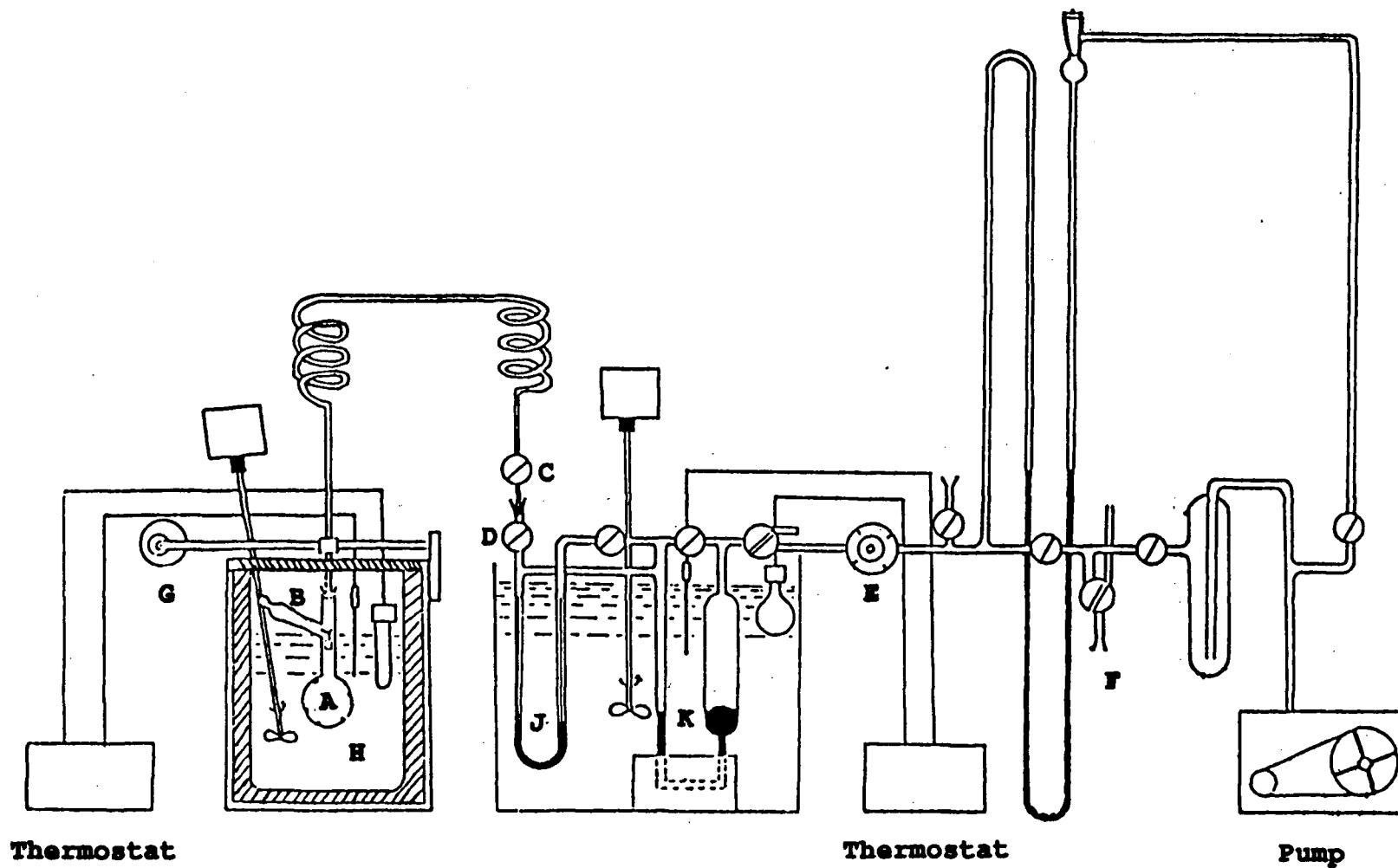


Fig. 2.2 Constant pressure gas uptake apparatus. The following parts are labelled:
A reaction flask, **B** hook, **C** stopcock, **D** stopcock, **E** fine valve, **F** two-way valve to a gas cylinder, **G** agitating motor and mechanism, **H** temperature-controlled oil bath, **J** *n*-dibutyl phthalate manometer, **K** mercury manometer.

constant gas pressure. A solution of the required concentration of reagent (thiol or phosphine) was placed in reaction flask A, and a glass bucket containing the ruthenium complex was suspended from a hook inserted through sidearm B. A ground glass joint sealed the hook to the flask while allowing the hook to be rotated to drop the bucket. The flask was attached to coiled glass tubing, which in turn was attached via valve C to valve D. With the needle valve E closed, the solution was degassed three times by freezing, evacuating, and adding 400 torr of the desired gas (usually N₂ or Ar) through valve F. Then the coils and valve C (closed) were reattached to valve D, and the reaction flask was clamped to a shaker mechanism G and immersed in the oil bath H at the reaction temperature ($\pm 0.05^\circ\text{C}$). After 20 min of temperature equilibration, the section of the system between C and F was evacuated and filled to 400 torr. Then valve C was opened, the system set to the final reaction pressure, the bucket dropped, and the timer and shaker started. As gas evolved, the height of the liquid (*n*-dibutyl phthalate) in the left column of manometer J decreased. Gas was withdrawn slowly through needle valve E to restore the balance in manometer J. The resulting dip in the mercury manometer K was measured by a Precision Tool Vernier Microscope Type 2158. Both manometers were suspended in a water bath at 25°C. Calibration permitted the conversion of mercury height measurements to millimoles of gas produced.

The monitoring of reaction kinetics by FT-NMR spectroscopy requires the assumption that the areas under the peaks in the spectra are proportional to the concentrations of the respective nuclei. This is true only if

- 1) all of the peaks to be compared are due to protons with identical T₁ values (and identical nOe effects for ³¹P NMR), or
- 2) the time between pulses is greater than five times the longest T₁ value of the relevant nuclei.¹⁵¹⁻²

The time between pulses was 1.364 s and 0.750 s for the ¹H and ³¹P{¹H} NMR experiments respectively. Because the T₁ values of most of the nuclei involved were greater than 1/5th of these times, condition 2 was not satisfied for most of the experiments described herein. The

error involved is small, however, if the T_1 values of the reactants and products are almost identical. This occurs in a series of related complexes if the varying group does not significantly affect the magnetic environment around the nucleus being measured. For example, it was shown that the ratios of concentrations in mixtures of complexes of the type $cct\text{-RuH}(\text{SR})(\text{CO})_2(\text{PPh}_3)_2$ can be accurately measured by $^{31}\text{P}\{^1\text{H}\}$ or ^1H NMR. Thus, a known C_6D_6 solution of $cct\text{-RuH}(\text{SCH}_3)(\text{CO})_2(\text{PPh}_3)_2$ and $cct\text{-RuH}(\text{SC}_6\text{H}_4\text{-}p\text{-CH}_3)(\text{CO})_2(\text{PPh}_3)_2$ containing 55% of the latter, was analyzed by comparing the intensities of the hydride triplets, the methyl singlets, and the $^{31}\text{P}\{^1\text{H}\}$ singlets. The results (58%, 57% and 60%, respectively), show that the accuracy is sufficient for kinetic experiments. The error is greater when comparing complexes with greater differences in structure, or when comparing complexes and free ligands. In particular, free triphenylphosphine in solution has a very large T_1 value of 26 s.¹⁵³

2.2.4 Data Handling for Kinetic Experiments

Many of the reactions in coordination chemistry are of the type



where M, L, and P are a metal complex, a reagent, and a product, respectively. If the reaction rate is first order with respect to [M] and n^{th} order with respect to [L],

$$-\frac{d[\text{M}]}{dt} = k[\text{M}][\text{L}]^n \quad \text{Eqn. 2.1}$$

and if $[\text{L}] > 10 [\text{M}]$ (*pseudo*-first order conditions), then the rate law can be simplified.

$$-\frac{d[\text{M}]}{dt} = k_{\text{obs}}[\text{M}] \quad \text{where } k_{\text{obs}} = k[\text{L}]^n \quad \text{Eqn. 2.2}$$

The integrated rate law can be expressed in terms of [M],

$$\ln[M]_t = \ln[M]_0 - k_{\text{obs}}t \quad \text{Eqn. 2.3}$$

or in terms of a measurable quantity A (hereafter referred to as absorbance) such as IR or UV/vis. absorbance, if one assumes that L does not absorb, A_∞ is the final absorbance, $[M]_\infty$ is zero (the reaction goes to completion), and C_m and C_p are proportionality constants for the absorbances of M and P (i.e. for UV/vis., $C = \epsilon \cdot l$, where ϵ is the extinction coefficient and l is the path length).

$$\begin{aligned} A_t &= C_m[M]_t + C_p[P]_t \\ A_t - A_\infty &= C_m[M]_t + C_p[P]_t - C_m[M]_\infty - C_p[P]_\infty \\ &= C_m[M]_t + C_p([M]_0 - [M]_t) - C_p[M]_0 \\ &= (C_m - C_p)[M]_t \\ A_0 - A_\infty &= (C_m - C_p)[M]_0 \end{aligned}$$

Inserting these expressions into the integrated rate law (Eqn. 2.3), one obtains the final expression.

$$\ln(A_t - A_\infty) = \ln(A_0 - A_\infty) - k_{\text{obs}}t \quad \text{Eqn. 2.4}$$

A plot of $\ln(A_t - A_\infty)$ or $\ln[M]_t$ versus time is referred to as a *pseudo*-first order log plot, and is linear if the reaction is *pseudo*-first order. The slope of the line is equal to $-k_{\text{obs}}$.

There are at least six methods for the calculation of k_{obs} . The first three use the *pseudo*-first order plot, but differ in the way that A_∞ is determined. The error involved in the determination of A_∞ is the weakest point of these methods. These three methods are:

1. Waiting for five or more half lives, and directly measuring A_∞ ,
2. Calculating A_∞ from $[M]_0$ and the C_p of an independently synthesized and characterized sample of the product,
3. Optimizing the straightness (correlation coefficient) of the *pseudo*-first order log plot by varying the value of A_∞ . The value of A_∞ which gives the straightest line should be similar to that determined by methods 1 or 2.

The other three methods calculate k_{obs} directly, and thereby avoid the problem of error in A_{∞} . These methods are based on two series of absorbance readings at times t_1, t_2 , etc., and at times $t_1 + T, t_2 + T$, etc., where T is a constant delay time. Applying equation 2.4, one obtains

$$(A_{\infty} - A_t) = (A_{\infty} - A_0)e^{-k_{\text{obs}} \cdot t} \quad \text{Eqn. 2.5}$$

and

$$(A_{\infty} - A_{t+T}) = (A_{\infty} - A_0)e^{-k_{\text{obs}}(t+T)} \quad \text{Eqn. 2.6}$$

Subtracting these equations, one obtains¹⁵⁴

$$(A_{t+T} - A_t) = (A_{\infty} - A_0)(1 - e^{-k_{\text{obs}} \cdot T})e^{-k_{\text{obs}} \cdot t}$$

$$\ln(A_{t+T} - A_t) = \ln\{(A_{\infty} - A_0)(1 - e^{-k_{\text{obs}} \cdot T})\} - k_{\text{obs}} \cdot t \quad \text{Eqn. 2.7}$$

The application of these methods, however, can place undue weight on the less accurate late data points. Ordinary or weighted least squares linear regression can lead to a bias.¹⁵⁵ The type of linear regression which should be used is therefore a concern, as is the choice of T .¹⁵⁵ These methods for calculating k_{obs} are:

4. The Guggenheim method,^{154,156} in which a plot of $\ln(A_{t+T} - A_t)$ versus time has a slope of $-k_{\text{obs}}$ (Eqn. 2.7),

5. The Kezdy-Mangelsdorf-Swinbourne (KMS) method,^{154-5,157-9} in which a plot of A_t versus A_{t+T} has a slope of $e^{k_{\text{obs}} \cdot T}$,

$$A_t = A_{\infty}(1 - e^{k_{\text{obs}} \cdot T}) + A_{t+T} e^{k_{\text{obs}} \cdot T} \quad \text{Eqn. 2.8}$$

and

6. The R/R method,¹⁶⁰ in which k_{obs} is determined from the average value of R_t/R_{t+T} . The rates are determined from the tangents to the plot of the time dependence of $[M]$.

$$R_t/R_{t+T} = e^{k_{\text{obs}} \cdot T} \quad \text{Eqn. 2.9}$$

where

$$R_t = (dA/dt)_t = (A_0 - A_\infty)(-k)e^{-k_{\text{obs}} \cdot t} \quad \text{Eqn. 2.10}$$

Equation 2.8 is obtained by dividing equation 2.5 by equation 2.6, and rearranging.¹⁵⁴ Equation 2.10 can be derived from equation 2.4 by rearranging to equation 2.11 and then taking the derivative.¹⁶⁰

$$A_t = (A_0 - A_\infty)e^{-k_{\text{obs}} \cdot t} + A_\infty \quad \text{Eqn. 2.11}$$

In order to compare these six methods, k_{obs} was calculated using each method, from the UV/vis. absorbance data for the reaction of *cct*-RuH₂(CO)₂(PPh₃)₂ (1.0 mM) with ethanethiol (94.5 mM) at 26°C in THF to give *cct*-RuH(SEt)(CO)₂(PPh₃)₂ (see section 3.3 and Fig. 3.10). The values of k_{obs} , obtained from the absorbance data at 400 nm taken up to 3400 s after the reaction started, and using a delay time (T) of 1600 s, are 7.01, 7.63, 6.73, 6.61, 6.58, and 6.50 x 10⁻⁴ s⁻¹ calculated by methods 1 through 6, respectively. The first two methods are the least accurate because they rely heavily on the accuracy of a single point, A_∞ . The differences (3 %) between the other four are considered to be of the same order as the experimental error. Method 3 was used to calculate the A_∞ and k_{obs} values reported in this thesis.

Rate constants from multiple experiments are quoted with 90 % confidence limits, calculated with the use of t-factors.¹⁵⁴

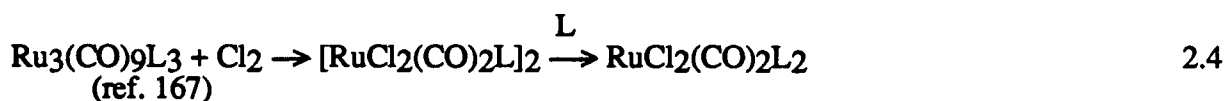
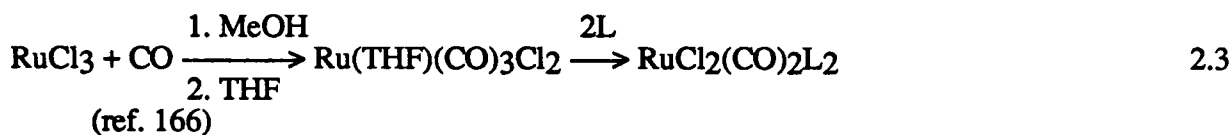
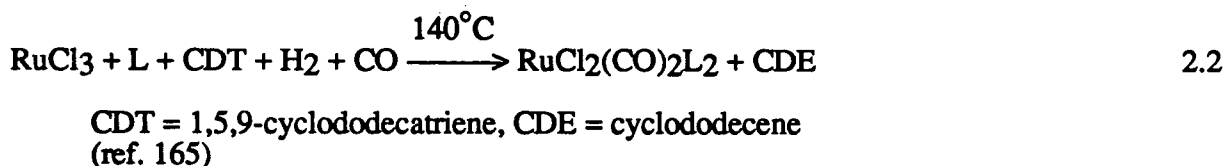
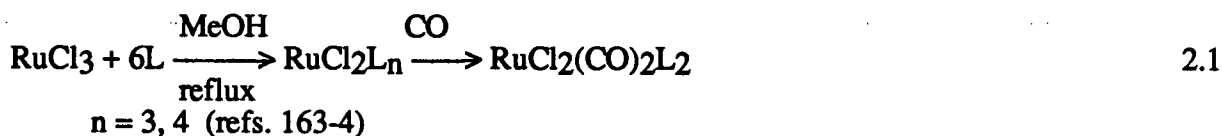
Plots of k_{obs} versus [M] are linear and horizontal for all reactions *pseudo*-first order in [M]. Plots of k_{obs} versus [L] should be linear and horizontal (n=0), linear through the origin (n=1), or curved (0<n<1 or n>1).

2.3 SYNTHESSES OF THE PRECURSOR COMPLEXES

Throughout the equations in section 2.3, the abbreviation "L" will be used for triphenyl phosphine.

2.3.1 *cct*-RuCl₂(CO)₂(PPh₃)₂

The *cct* isomer of this complex (**1**) has been synthesized through a variety of routes:¹⁶¹⁻²



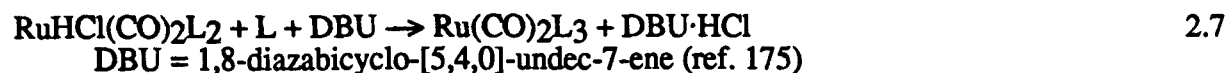
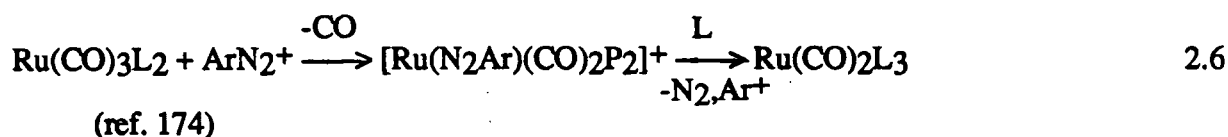
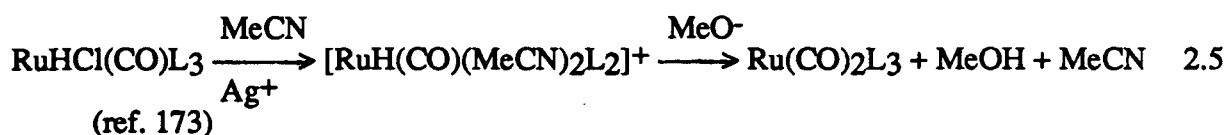
Other methods give other isomers of the complex, often the yellow *mtt* isomer¹⁶¹ which can be converted by heating in solution¹⁶⁸⁻⁹ or in the solid state¹⁷⁰ to the white *cct* isomer.

Although the *cis* positions of the carbonyls are evident from the two stretching bands in the IR spectrum, it requires ¹³C NMR to prove the *cct* geometry. The substituted, *o*- and *m*- carbons of the phenyl groups appear in that spectrum as triplets,¹⁶⁵ a phenomenon characteristic of complexes with *trans* triphenylphosphine ligands.¹⁷¹ No X-ray crystallographic structure has been reported of this complex.

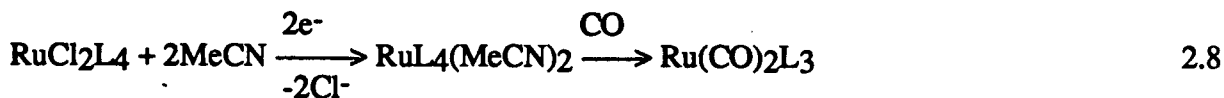
The method used in this work, based upon reaction 2.1, was used previously in this laboratory.¹⁷² The complex $\text{RuCl}_3 \cdot x\text{H}_2\text{O}$ (3 g, 10 mmol) was dissolved in reagent methanol (400 mL) under air, and the solution refluxed for 15 min. To the cooled solution was added triphenylphosphine (20 g, 76 mmol), and the mixture was refluxed for 1 h; the resulting dark brown suspension was filtered and washed with methanol (150 mL). The $\text{RuCl}_2(\text{PPh}_3)_3$ thus isolated was dissolved in CH_2Cl_2 (300 mL) under N_2 . The flask was flushed with CO and the solution stirred overnight. The resulting yellow solution was concentrated by vacuum distillation of half of the solvent. A pale yellow precipitate appeared. Methanol (40 mL) was added to encourage the precipitation. The white product was collected by filtration and dried over 24 h under vacuum. The yield was 6 g, or 80%. IR (Nujol) 2057, 1994 cm^{-1} $\nu(\text{CO})$; IR (CH_2Cl_2) 2059, 1996 cm^{-1} $\nu(\text{CO})$; $^{31}\text{P}\{^1\text{H}\}$ NMR (C_6D_6) δ 15.65 ppm (s). The IR frequencies are within the range of reported values.¹⁶⁵

2.3.2 $\text{Ru}(\text{CO})_2(\text{PPh}_3)_3$

The direct reaction of phosphines with $\text{Ru}(\text{CO})_5$ does not proceed past the disubstituted product.¹⁷³ Other methods are used for the synthesis of $\text{Ru}(\text{CO})_2(\text{PPh}_3)_3$ (2).



Another method¹⁷⁶ used $\text{Ru}(\text{PPh}_3)_4(\text{MeCN})_2$ generated by the electrochemical reduction of $\text{RuCl}_2(\text{PPh}_3)_4$ in acetonitrile.

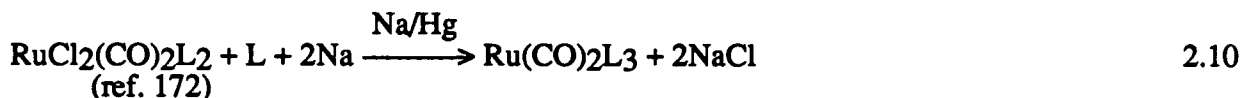


A method which appears obvious in hindsight is the reaction of *cis*- $\text{RuH}_2(\text{CO})_2(\text{PPh}_3)_2$ (Section 2.3.3) with PPh_3



which has not yet been reported, although the reverse reaction was observed as long ago as 1972.¹⁷³ The details and kinetics of reaction 2.9 are described in Section 3.3.

The method used in the present work was only reported fairly recently.



Samples of *cis*- $\text{RuCl}_2(\text{CO})_2(\text{PPh}_3)_2$ (2 g, 2.6 mmol) and PPh_3 (1.4 g, 5.2 mmol) were dissolved in distilled and dried THF (400 mL) under an inert gas. Sodium/mercury amalgam (15 to 20 mL) was added, and the mixture stirred for 2 to 3 days. The suspension was allowed to settle, and the supernatant solution was transferred to a separate flask and filtered through diatomaceous earth. The orange filtrate was reduced in volume to 100 mL by vacuum distillation. Addition of hexanes (140 mL) induced the formation of a deep yellow precipitate, which was collected by filtration and dried under vacuum overnight. The yields were 60 to 80%. Elem. Anal. Calcd. for $\text{RuP}_3\text{O}_2\text{C}_56\text{H}_45$: C, 71.3; H, 4.8. Found: C, 71.0; H, 4.8. IR (Nujol) 1902 cm^{-1} $\nu(\text{CO})$; $^3\text{P}\{^1\text{H}\}$ NMR (C_6D_6) δ 49.26 ppm (s); UV/vis. (THF) λ_{max} 345 nm ($\epsilon=17,000\text{ M}^{-1}\text{ cm}^{-1}$). The $\nu(\text{CO})$ stretch falls within the range of reported values for this complex.^{173-4,177}

The geometry of this 5-coordinate complex is believed to be trigonal bipyramidal. The single carbonyl stretching band in the IR spectrum indicates *trans* and therefore axial carbonyls. The

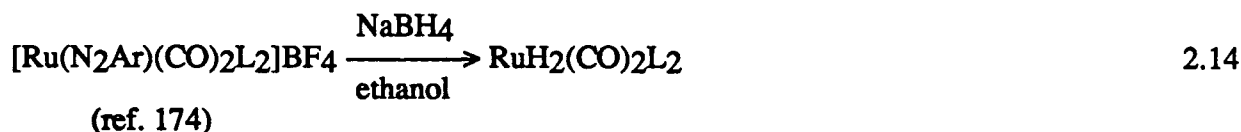
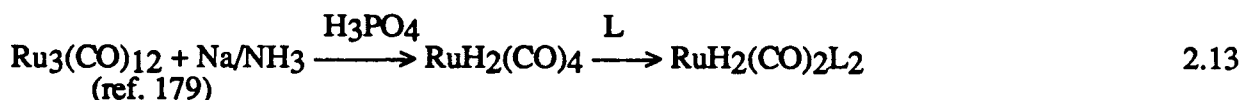
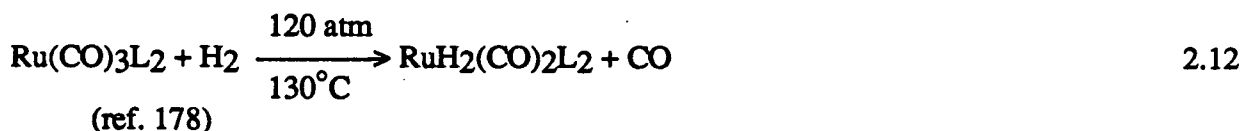
single peak in the $^{31}\text{P}\{^1\text{H}\}$ NMR spectrum indicates equivalent and therefore equatorial phosphines.

2.3.3 *cct*- $\text{RuH}_2(\text{CO})_2(\text{PPh}_3)_2$

Although in the present work *cct*- $\text{RuH}_2(\text{CO})_2(\text{PPh}_3)_2$ (**3**) was prepared from $\text{Ru}(\text{CO})_2(\text{PPh}_3)_3$ (**2**), as indicated in equation 2.11,



complex **3** was known¹⁷⁸ (equation 2.12) well before **2** was first synthesized.¹⁷³



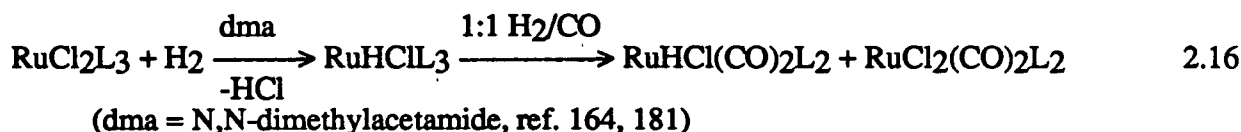
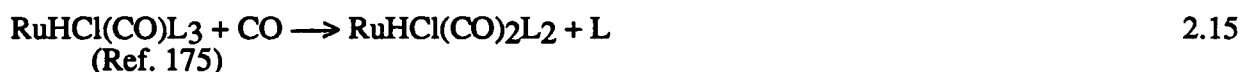
$\text{Ru}(\text{CO})_2(\text{PPh}_3)_3$ (1.2 g, 1.2 mmol) was dissolved in THF (50 mL) under H_2 (1 atm) and stirred for 30 min. The yellow colour faded, but reintensified when the volume of the solvent was reduced by vacuum distillation. Hydrogen was reintroduced. After the yellow colour had faded again, hexanes (40 mL) were added to induce precipitation. The suspension was filtered and the white product dried in a vacuum at room temperature for several days; yield 95%. Elem. Anal. Calcd. for $\text{C}_{38}\text{H}_{32}\text{O}_2\text{P}_2\text{Ru}$: C, 66.8; H, 4.7. Found: C, 67.1; 4.8. IR (Nujol) 2012, 1977 cm^{-1} $\nu(\text{CO})$; 1880, 1825 cm^{-1} $\nu(\text{Ru-H})$; IR (CH_2Cl_2) 2017, 1977 cm^{-1} $\nu(\text{CO})$; IR (THF) 2019, 1981 cm^{-1} $\nu(\text{CO})$; $^{31}\text{P}\{^1\text{H}\}$ NMR (C_6D_6) δ 56.29 ppm (s). ^1H NMR (C_6D_6) δ -6.34 (t, 2H,

$J_{\text{PH}}=23.4$ Hz, Ru-H), 7.05 (multi, 18H, *m*-, *p*-Ph), 7.90 ppm (multi, 12H, *o*-Ph). The UV/vis. absorbance was negligible between 625 and 350 nm, rising steeply at lower wavelengths. The IR frequencies, hydride chemical shift, and the $2J_{\text{PH}}$ value are close to the reported values.¹⁷⁴

The white product has two carbonyl stretching bands in the IR spectrum, indicating *cis* carbonyls (C_{2v} symmetry). The complex contains magnetically equivalent hydride ligands and magnetically equivalent phosphorus atoms, as indicated by the high field triplet in the ^1H NMR spectrum. Therefore two structures are possible; *cct* and *tcc*. L'Epplattienier and Calderazzo¹⁷⁸ favoured the former, but presented no evidence. Because the ^1H NMR signal of the *o*-phenyl protons is separated from that of the *m*- and *p*-phenyl signals by greater than 0.5 ppm, a phenomenon associated with *trans* phosphines¹⁸⁰, then the observed isomer is believed to be *cct*- $\text{RuH}_2(\text{CO})_2(\text{PPh}_3)_2$.

2.3.4 *cct*- $\text{RuH}(\text{Cl})(\text{CO})_2(\text{PPh}_3)_2$

The complex $\text{RuH}(\text{Cl})(\text{CO})_2(\text{PPh}_3)_2$ (**4**) has been synthesised from $\text{RuHCl}(\text{CO})(\text{PPh}_3)_3$ and, in the method used here, from $\text{RuCl}_2(\text{PPh}_3)_3$.



$\text{RuCl}_2(\text{PPh}_3)_3$ (0.40 g, 0.42 mol) was dissolved in 10 mL of degassed dma under H_2 (1 atm), giving a red-brown solution. After 30 min, the hydrogen atmosphere was replaced with CO (1 atm). The solution turned yellow within 5 min. After another 30 min, the solvent volume was reduced by vacuum distillation, and methanol (20 mL) added. The resulting white precipitate was filtered and dried under vacuum. The yield was 40%. $^{31}\text{P}\{^1\text{H}\}$ NMR (C_6D_6) δ 38.43 ppm

(s). ^1H NMR (C_6D_6) δ -3.86 ppm (t, $J_{\text{PH}}=19.2$ Hz, Ru-H), 7.04 (multi, *m*- and *p*-phenyl), 7.99 (multi, *o*-phenyl). The NMR data match those reported by Dekleva¹⁸² for *cct*- $\text{RuH}(\text{Cl})(\text{CO})_2(\text{PPh}_3)_2$, synthesized from $\text{RuH}(\text{Cl})(\text{PPh}_3)_3$ in CH_2Cl_2 under CO.

The wide difference in chemical shifts between the *m/p*- and the *o*-phenyl signals indicates the presence of *trans* phosphine ligands; the structure is therefore *cct*. Joshi and James¹⁸³ reached the same conclusion based on the ^{13}C NMR spectrum of a sample of **4** formed by hydrogenolysis of a norbornenolyl derivative.

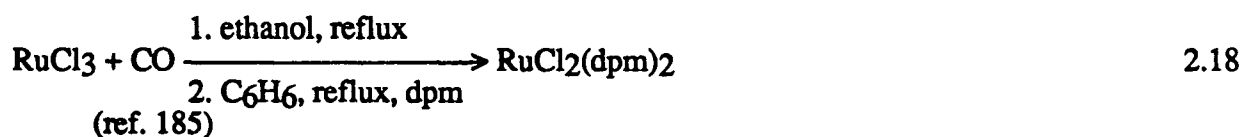
In the ^1H NMR spectrum of **4**, the ratio of the peak areas of the hydride versus the phenyl proton signals is 1:21, although 1:30 is the theoretical value. The difference is caused by the longer T_1 values of the phenyl protons, which do not allow for complete relaxation between pulses. The same effect is observed in an analytically pure sample of the similar complex *cct*- $\text{RuH}(\text{SEt})(\text{CO})_2(\text{PPh}_3)_2$ (Chapter 3), for which the hydride:phenyl peak area ratio is also 1:21 under the same NMR conditions.

As noted, the second step of the synthesis involved exposure of the solution to CO and not the 1:1 H_2/CO mixture recommended earlier.¹⁶⁴ The use of CO alone is reported¹⁶⁴ to give *tcc*- $\text{RuCl}_2(\text{CO})_2(\text{PPh}_3)_2$. However, in our hands, the pure CO treatment reproducibly gave pure *cct*- $\text{RuHCl}(\text{CO})_2(\text{PPh}_3)_2$; the reason for the differing results is not known.

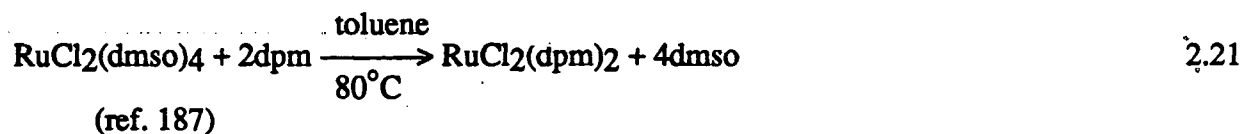
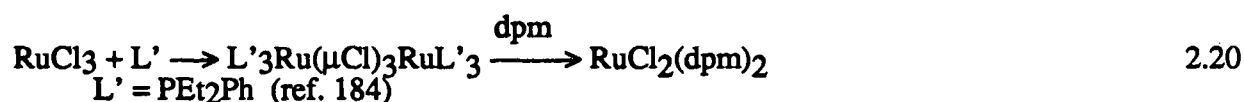
2.3.5 *cis*- and *trans*- $\text{RuCl}_2(\text{dpm})_2$

The *cis* (**5**) and *trans* (**6**) isomers of the complex $\text{RuCl}_2(\text{dpm})_2$ can be differentiated by ^1H and $^{31}\text{P}\{^1\text{H}\}$ NMR spectroscopy. The ratio of isomers depends on the synthetic method. Those reported to produce the *trans* isomer are:





The reactions reported to form the *cis* isomer are:



Although no X-ray crystal structure of either isomer has been reported, that of the related complex *trans*-RuCl₂(Ph₂PCH₂AsPh₂)₂ has been described by Balch *et al.*¹⁸⁸

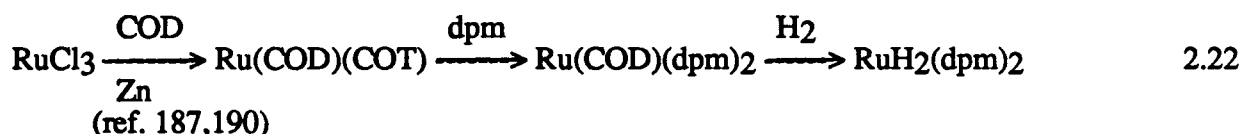
A sample of **5** was kindly donated by Dr. C.-L. Lee, who had prepared it by the method of Chaudret *et al.*^{187a}; A solution of RuCl₃·3H₂O (2 g, 8 mmol) in dmsO (30 mL) was refluxed for 30 min, during which time it turned yellow/orange. After reduction of the volume to 10 mL, and addition of a large excess of acetone, a yellow precipitate of *cis*-RuCl₂(dmsO)₄ formed. This was collected by filtration and dried under vacuum. A refluxing 100 mL toluene solution of this product (1 g, 2 mmol) and dpm (1.6 g, 4.2 mmol) turned bright yellow over 2 h. The solution was then allowed to cool, and diethyl ether (100 mL) was added. Filtration afforded a yellow product. ³¹P{¹H} NMR (C₆D₆) -0.44 ppm (t), -26.72 ppm (t). Similar ³¹P{¹H} NMR shifts and coupling constant have been reported.¹⁸⁷

A mixture of **5** and **6** was also synthesized and donated by Dr. C.-L. Lee; RuCl₃·3H₂O (3 g, 10 mmol) in methanol (250 mL) was refluxed for 2 h, with hydrogen gas bubbling through the solvent. The resulting solution was transferred into a boiling mixture of methanol, dpm (9.2 g,

24 mmol), and 37% aqueous formaldehyde (7 mL). Refluxing was continued for another hour, after which the solution was cooled to room temperature and filtered. The yellow compound was reprecipitated twice from CH₂Cl₂/petroleum ether. ³¹P{¹H} (CD₂Cl₂) δ -0.35 (t, J_{PP}=35.9 Hz, **5**), -8.03 (s, **6**), -26.38 ppm (t, J_{PP}=35.9 Hz, **5**). The integration showed that 70% of the mixture was the *trans* isomer **6**. The ³¹P{¹H} NMR chemical shift of **6** in CH₂Cl₂ is -6.9 ppm,¹⁸⁶ relative to P(OMe)₃ at 141 ppm downfield of 85% H₃PO₄.

2.3.6 RuH₂(dpm)₂

Difficulties encountered in the synthesis of RuH₂(dpm)₂ (**7**) have no doubt restricted its use in experimental chemistry. The complex cannot be formed by the reactions of dpm with RuH₂(PPh₃)₄, or LiAlH₄ with RuCl₂(dpm)₂ (**5** or **6**), which instead form RuH₂(dpm)(PPh₃)₂¹⁸⁷ and RuHCl(dpm)₂,¹⁸⁹ respectively. The reaction of NaBH₄ with **5** produced mostly RuH(η¹BH₄)(dpm)₂ with some Ru(η¹BH₄)₂(dpm)₂ (Section 2.3.7). The only successful method to date requires the preparation of the air-sensitive compound Ru(COD)(COT) (COD=1,5-cyclooctadiene, COT=1,3,5-cyclooctatriene).



A 20 mL ethanol solution of COD (17 mL, 140 mmol) and RuCl₃·3H₂O (0.7 g, 2.7 mmol) was refluxed under argon for 20 min. Zn dust (6 g), activated by washing with water, 2% HCl, EtOH, and dry Et₂O, was added. The resulting mixture was refluxed for 45 min, filtered, and dried to a gelatinous residue by overnight evaporation under vacuum. The solubles from this residue were extracted by washing with pentane (100 mL), and passing the resulting solution through a 20 cm neutral alumina column (Brockmann Activity II 80-200 mesh). The volume of the yellow filtrate was reduced to 5 mL by vacuum transfer. The solution was cooled in a dry

ice/acetone bath overnight, resulting in the formation of yellow crystals.¹⁹¹ A 20 mL toluene solution of dpm (640 mg, 1.7 mmol) was added to the product. After overnight exposure to H₂, the solution was reduced in volume by vacuum transfer of most of the solvent, and hexanes (20 mL) were added to encourage the formation of the yellow precipitate, which was collected by filtration.¹⁹¹ The overall yield is typically low (10-40%), and attempts by Dr. C.-L. Lee to perform increased-scale syntheses resulted in lower, not higher yields.

Characterization of *cis*- and *trans*-RuH₂(dpm)₂: Elem. Anal. Calcd. for RuP₄C₅₀H₄₆: C, 68.9; H, 5.3. Found: C, 68.9; H, 5.2.

¹H NMR (C₆D₆)¹⁹¹ δ -7.58 (dq, ²J_{transPH} = 73 Hz, ²J_{cisPH} = 18 Hz, RuH of *cis*-isomer), -4.80 (qn, ²J_{cisPH} = 19 Hz, RuH of *trans*-isomer), 4.10 (multi, CH₂ of *cis*-isomer), 4.63 (multi, CH₂ of *trans*-isomer), 4.81 ppm (multi, CH₂ of *cis*-isomer).

³¹P{¹H} NMR (C₆D₆)¹⁹¹ δ 14.06 (t, ²J_{cisPP} = 19.3 Hz, *cis*-isomer), 9.11 (s, *trans*-isomer), 0.57 ppm (t, ²J_{cisPP} = 18.8 Hz).

Similar ¹H NMR data has been reported.⁴⁷ The product is always formed as a 1:4 mixture of the *trans* and *cis* isomers.¹⁸⁷ Although this was the synthetic method used by G. Rastar and the present author to prepare samples for the present study, the reaction of NaBH₄ with **5** was investigated as a possible alternate route (Section 2.3.7).

2.3.7 An Attempted New Synthesis of RuH₂(dpm)₂: The Synthesis of *trans*-RuH(η¹BH₄)(dpm)₂

Hydrogen was bubbled through a suspension of *cis*-RuCl₂(dpm)₂ (0.5 g, 0.5 mmol) in benzene (30 mL) and methanol (50 mL) for 10 min. Fresh sodium borohydride (2 g, 50 mmol) was added in 3 portions over 5 min. Hydrogen was bubbled through the resulting mixture for 1 h, after which methanol (100 mL) was added. The white product isolated by filtration was washed with methanol (20 mL) and dried under vacuum at room temperature. The yield was 0.45 g. The spectroscopic analysis of the product is consistent with RuH(η¹BH₄)(dpm)₂ (**8**),

although the presence of some $\text{Ru}(\eta^1\text{BH}_4)_2(\text{dpm})_2$ is suggested by the FAB/MS data. Reprecipitation from methanol/benzene resulted in partial conversion to $\text{RuH}_2(\text{dpm})_2$. As a result, the elemental analysis was of an unpurified sample.



Elem. Anal.; calcd. for $\text{C}_{50}\text{H}_{49}\text{BP}_4\text{Ru}$: C, 67.8; H, 5.6. Found: C, 65.2; H, 5.5.

FT-IR (Nujol or HCB): 2397 cm^{-1} ($\nu(\text{B-H}_t)$, $\nu_D/\nu_H = 0.755$); 2346 ($\nu(\text{B-H}_t)$, 0.754); 1788 ($\nu(\text{B-H}_b)$ or $\nu(\text{Ru-H}_t)$, 0.732); 1069 cm^{-1} ($\delta(\text{BH}_3)$, 0.723);

^1H NMR (C_6D_6 , 20°C) δ -10.60 (qn, 1H, $^2J_{\text{PH}} = 19.5$ Hz, Ru-H), -1.05 (br, 4H, BH_4), 4.53 (dt, 2H, $^2J_{\text{HaHb}} = 14$ Hz, $^2J_{\text{PH}} = 3$ Hz, CH_a (methylene)), 4.97 (dt, 2H, $^2J_{\text{HaHb}} = 14$ Hz, $^2J_{\text{PH}} = 4$ Hz, CH_b (methylene)), 6.88 (multi, 12H, *m-p*-Ph), 7.07 (multi, 12H, *m-p*-Ph), 7.46 (s, 8H, *o*-Ph), 7.71 ppm (s, 8H, *o*-Ph);

^1H NMR ($\text{C}_6\text{D}_5\text{CD}_3$, -89°C) δ -10.5 (br, RuH), -9.0 (br, Ru- H_b -B);

^1H NMR T_1 values ($\text{C}_6\text{D}_5\text{CD}_3$, 20°C) 0.36 s (BH_4), 0.56 s (RuH), ($\text{C}_6\text{D}_5\text{CD}_3$, -58°C) 0.26 s (BH_4), 0.35 s (RuH);

$^{31}\text{P}\{^1\text{H}\}$ NMR (C_6D_6 , 20°C) δ 2.43 ppm (s);

^{11}B NMR (C_6D_6 , 20°C) δ -2 (br, major), 46 (br, minor), -46 ppm (br, minor);

FAB/MS (*p*-nitrobenzylalcohol) *m/e* 1036 $\{\text{RuH}(\text{BH}_4)(\text{dpm})_2 \cdot \text{O}_2\text{NC}_6\text{H}_4\text{CH}_2\text{OH}\}$; 1008 $\{\text{RuH}(\text{BH}_4)(\text{dpm})_2 \cdot \text{O}_2\text{NC}_6\text{H}_4\}$; 900 $\{\text{Ru}(\text{BH}_4)_2(\text{dpm})_2\}$; 885 $\{\text{RuH}(\text{BH}_4)(\text{dpm})_2\}$; 869 $\{\text{Ru}(\text{dpm})_2\}$; 501 $\{\text{RuH}(\text{BH}_4)(\text{dpm})\}$; plus 20 other fragments (Table 2.1, Fig. 2.3).

The ^1H NMR spectrum of the product (Fig. 2.4) resembles that of *trans*- $[\text{RuH}(\eta^2\text{H}_2)(\text{dppe})_2]\text{BF}_4$,¹⁹² which has a broad peak at -4.6 ppm (H_2) and a quintet at -10.0 ppm ($J_{\text{PH}}=16$ Hz) in acetone- d_6 . However, the T_1 measurements and the microanalysis, which showed the virtual absence of chlorine, eliminate the possibility of the product being *trans*- $[\text{RuH}(\eta^2\text{H}_2)(\text{dpm})_2]\text{Cl}$. Further, the THF and the benzene solutions of the product do not conduct at room temperature.

Table 2.1 Fragments detected in the FAB/mass spectrum of Ru(H)(BH₄)(dpm)₂

Observed m/z	Expected m/z	Fragment Allocation
1036	1038	RuH(BH ₄)(dpm) ₂ + O ₂ NC ₆ H ₄ CH ₂ OH
1008	1007	RuH(BH ₄)(dpm) ₂ + O ₂ NC ₆ H ₄
900	900	Ru(BH ₄) ₂ (dpm) ₂
885	885	RuH(BH ₄)(dpm) ₂
869	869	Ru(dpm) ₂
791	792	Ru(dpm)(PPh ₂ CH ₂ PPh)
717	715	Ru(dpm)(PPh ₂ CH ₂ P)
685	684	Ru(dpm)(PPh ₂ CH ₂)
669	670	Ru(dpm)(PPh ₂)
607	607	Ru(dpm)(PPhCH ₂)
593	593	Ru(dpm)(PPh)
531	530	Ru(dpm)(PCH ₂)
515	516	Ru(dpm)(P)
501	501	RuH(BH ₄)(dpm)
485	485	Ru(dpm)
468	468	Ru(BH ₄)(PPh ₂ CH ₂ PPh)(PCH ₂)
439	439	Ru(PPh ₂ CH ₂ PPh)(P)
417		
407	408	Ru(PPh ₂ CH ₂ PPh)
393	394	Ru(PPh ₂)(PPh)
363	362	Ru(PPh ₂ CH ₂ PPh)(P)
331	331	Ru(PPh ₂ CH ₂ P)
315	317	Ru(PPh ₂)
285	285	Ru(PPhCH ₂ P)(P)
285	286	Ru(PPh ₂)
253	254	Ru(PPhCH ₂ P)

TABLE 2.2 ¹H NMR DATA FOR *trans*-RuH(X)(dpm)₂^a

X	H _a	H _b	H _t	J _{PH_a}	J _{PH_b}	J _{HaHb}	J _{PH_t}	solvent	ref.
H	4.6	4.6	-4.8	n.a.	n.a.	n.a.	18.9	C ₆ D ₆	b
H	-	-	-4.7	n.a.	n.a.	n.a.	19.7	CD ₂ Cl ₂	187
SH	4.5	5.2	-9.5	3	-	16	19	C ₆ D ₆	c
SPh	4.3	4.8	-10.9	3.3	-	13.8	19.9	C ₆ D ₆	c
SBz	4.4	5.2	-10.2	3.2	-	13.5	20.0	C ₆ D ₆	c
BH ₄	4.5	5.0	-10.6	3.1	4.2	14.2	19.5	C ₆ D ₆	d
Cl	-	-	-14.1	-	-	-	19.7	CD ₂ Cl ₂	187
H ₂ O	4.6	5.2	-18.8	3.5	3.5	11.5	19.1	(CD ₃) ₂ CO	187
CO	5.4	5.4	-	-	-	-	-	CD ₃ OD	185

^a n.a. = not applicable

H_a, H_b = methylene protons

H_t = terminal hydride

Coupling constants and chemical shift in Hz and ppm, respectively

^b Section 2.3.6 of this work

^c Section 3.4 of this work

^d Section 2.3.7 of this work

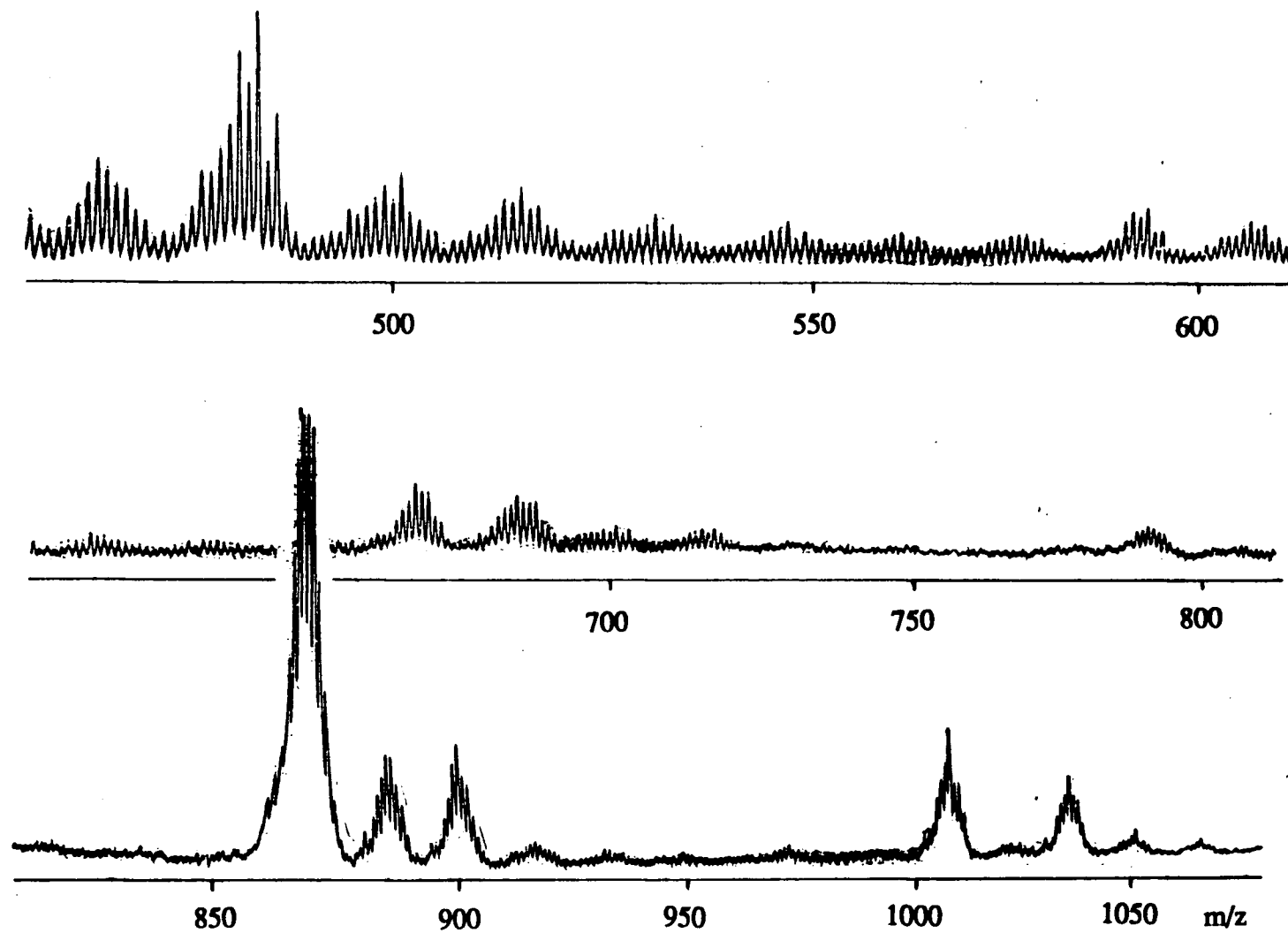


Fig. 2.3 FAB mass spectrum of $\text{RuH}(\text{BH}_4)(\text{dpm})_2$ in *p*-nitrobenzyl alcohol.

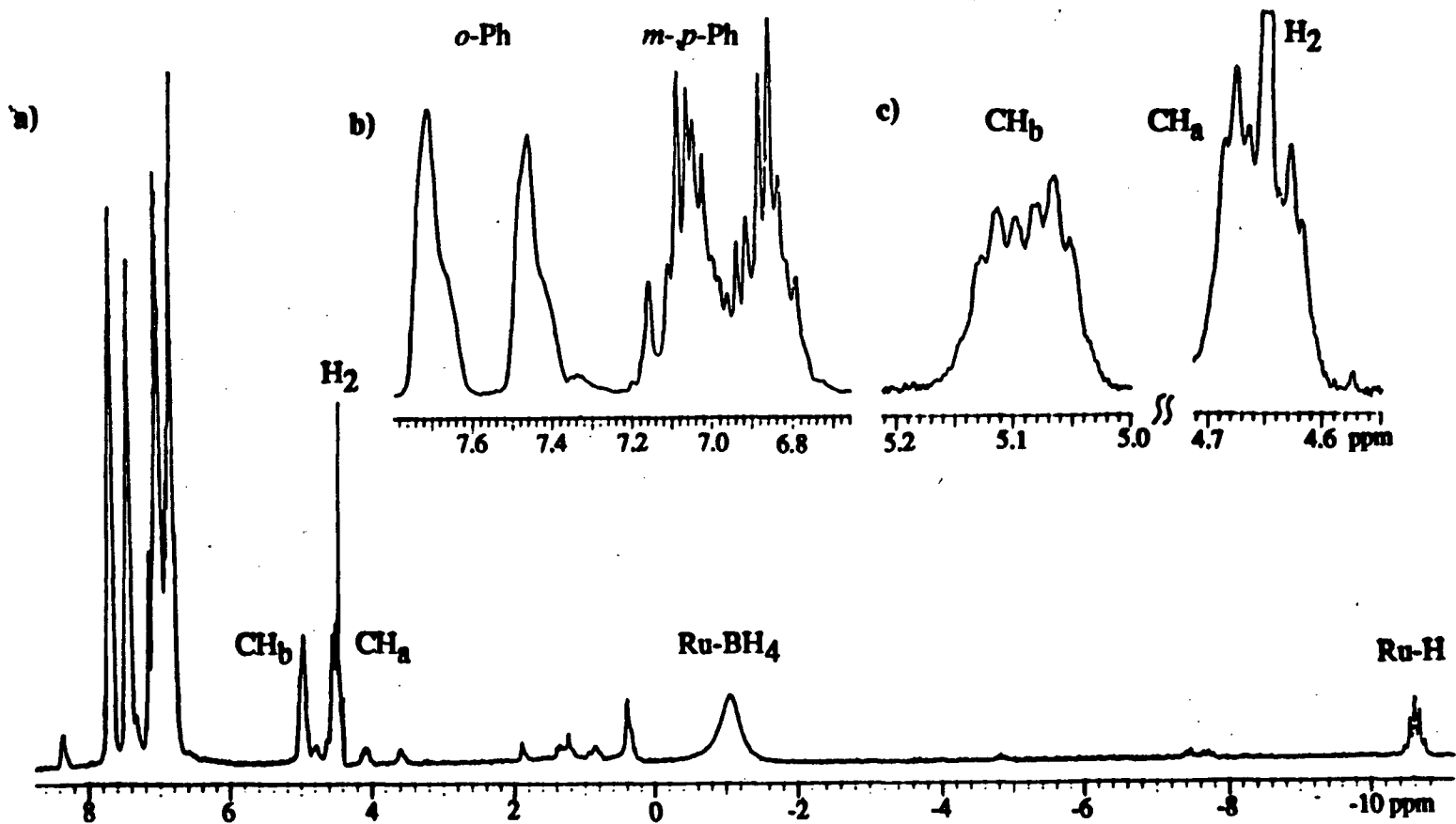


Fig. 2.4 ^1H NMR spectrum of $\text{RuH}(\text{BH}_4)(\text{dpm})_2$ under H_2 at 20°C , 300 MHz
a) full spectrum (solvent = C_6D_6)
b) phenyl region (C_6D_6)
c) methylene region ($\text{C}_6\text{D}_5\text{CD}_3$)

The methylene region of the ^1H NMR spectrum contains an ABX_2 pattern, consistent with a *trans*- $\text{Ru}(\text{X})(\text{Y})(\text{dpm})_2$ structure, and the coupling constants and chemical shifts are comparable to those in similar complexes (Table 2.2). In the phenyl region, two multiplets are observed for the *o*-phenyl protons, and two for the *m*- and *p*-phenyl protons, compared to only one of each type for **6**. The complexes of the formula *trans*- $\text{RuX}_2(\text{dpm})_2$ are of D_{4h} symmetry, and have equivalent phenyl groups. In contrast, *trans*- $\text{RuX}(\text{Y})(\text{dpm})_2$ complexes (C_{4v}) such as **8** have phenyl groups in two different environments; four in the hemisphere of the X, and four in the hemisphere of the Y ligand.

The linewidth of the broad peak in the ^1H NMR spectrum increases as the temperature decreases, while the terminal hydride remains at -10.5 ppm, although the quintet pattern is not resolved at lower temperatures (Fig. 2.5). At -79°C , the broad peak is barely visible, and a new broad peak at -9.0 ppm appears. These changes are believed to result from the slowing down of the exchange between the BH_t (terminal) hydrogens and the hydrogen(s) bridging the Ru and B atoms, the new peak being due to the bridging hydrogen. At -89°C the integral of that peak has increased to half that of the quintet at higher field. At even lower temperatures, where the peak would be better resolved, the area should be equal to that of the quintet, assuming $\nu^1\text{BH}_4$ coordination. The peak for the terminal borohydride hydrogen atoms, if it were close to that of B_2H_6 ($\delta = 4$ ppm),^{193a,194} would be obscured by the solvent. The slowing of the exchange has been observed in only a few borohydride complexes.¹⁹³

The ^1H NMR spectrum of a toluene- d_8 solution of the complex changed irreversibly at temperatures greater than 50°C ; the principal product was **7**.



The complex *trans*- $\text{RuD}(\text{BD}_4)(\text{dpm})_2$ was synthesized from **5** and NaBD_4 under H_2 . The ^1H NMR spectrum of this product indicates 88% deuteration at the hydride and borohydride positions. This suggests that H_2 played no role in the reaction, and indeed later experiments

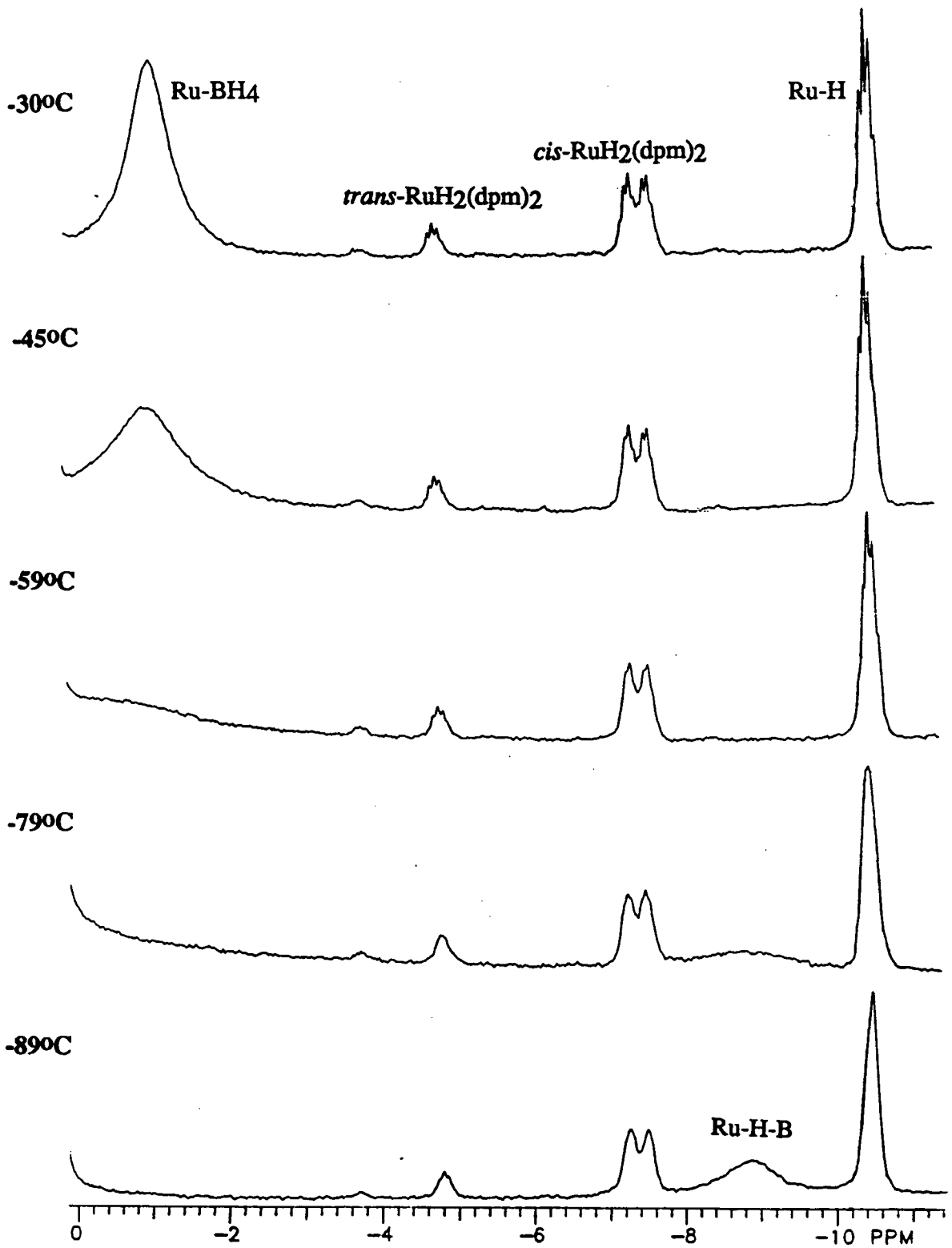
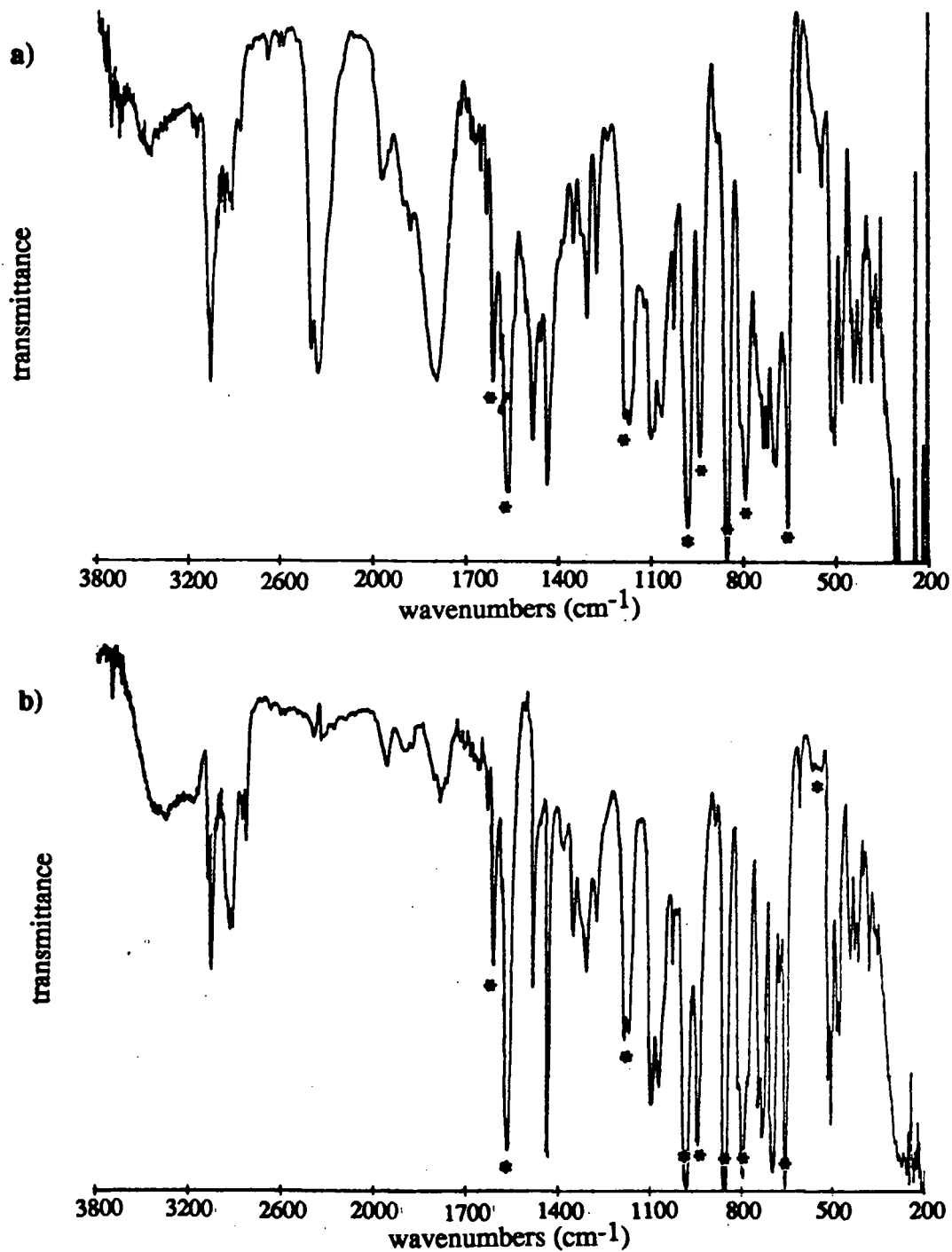


Fig. 2.5 ^1H NMR (300 MHz) spectra of $\text{RuH}(\text{BH}_4)(\text{dpm})_2$ in $\text{C}_6\text{D}_5\text{CD}_3$ below ambient temperatures.

Fig. 2.6 FT-IR spectra of HCB mulls of a) $\text{RuH}(\text{BH}_4)(\text{dpm})_2$ and b) $\text{RuD}(\text{BD}_4)(\text{dpm})_2$ (88 % deuteration). The peaks due to HCB are marked with asterisks.

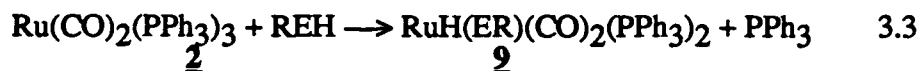


therefore somewhat ambiguous, but structure II, a 20 electron, seven-coordinate species, is considered unlikely. The monodentate borohydride complex $\text{FeH}(\text{HBH}_3)(\text{dmpe})_2$, which has been structurally characterized as type I, has IR bands (cm^{-1}) at 2340 ($\nu(\text{B-H}_t)$), 2030 ($\nu(\text{Fe-H}_b)$, $\nu(\text{B-H}_b)$), 1788 ($\nu(\text{Fe-H}_t)$) and 1045 (BH_3 def.).¹⁹⁷

Ruthenium borohydride complexes which have been reported include $\text{RuH}(\text{BH}_4)(\text{PR}_3)_3$ ($\text{PR}_3 = \text{PPh}_3$,¹⁹⁸⁻²⁰⁰ PPh_2Me ,²⁰¹ PPhMe_2 ,²⁰² or PMe_3 ²⁰³), $\text{RuH}(\eta^2\text{BH}_4)(\text{CO})(\text{PR}_3)_2$ ($\text{PR}_3 = \text{PPh}_3$,²⁰⁰ P^iPr_3 , $\text{PMe}(\text{tBu})_2$ ²⁰⁴), $\text{RuH}(\text{BH}_4)(\text{CO})_2(\text{PCy}_3)_2$ ²⁰⁰, $\text{CpRu}(\text{BH}_4)(\text{PR}_3)_2$ ($\text{Cp} = \text{C}_5\text{H}_5$ or C_5Me_5 , $\text{R} = \text{Ph}$,²⁰⁵ Me , Et , Cy ²⁰⁶), and $\text{Ru}_3(\text{CO})_9(\text{H})(\text{BH}_4)$ ²⁰⁷.

Although $\text{RuH}(\text{BH}_4)(\text{dpm})_2$ reacts with Lewis bases such as thiophene and amines to form $\text{RuH}_2(\text{dpm})_2$, this route is not of higher yield or greater reliability than the preparation of the latter complex from $\text{Ru}(\text{COD})(\text{COT})$.

Note added in proof: Bianchini et al.³⁰² have very recently reported the synthesis of $\text{RuH}(\eta^1\text{BH}_4)(\text{PP}_3)$ from $\text{RuCl}_2(\text{PP}_3)$ and NaBH_4 ($\text{PP}_3 = \text{P}\{\text{CH}_2\text{CH}_2\text{PPh}_2\}_3$). The variable temperature ^1H NMR spectra of the complex bear a strong resemblance to those of $\text{RuH}(\eta^1\text{BH}_4)(\text{dpm})_2$.



ER = 9a SH, 9b SC₆H_{4p}CH₃, 9c SCH₃, 9d SCH₂CH₃, 9e SCH₂C₆H₅, 9f SC₆H_{4o}CH₃,
9g SC₆H_{4m}CH₃, 9h SeC₆H₅, 9i SC₆H₅, or 9j SC₆F₅

are complete within minutes at room temperature, and form a series of products with the formula RuH(ER)(CO)₂(PPh₃)₂ (9), the characterization of which is described in the following section.

Complex 2 failed to react with ethanol (85 mM) in THF. Alcohols are structurally similar to thiols, but are much less acidic (*pK_a*'s 3.5 to 5.5 units higher). We shall see in Section 3.5 that the more acidic thiols bind more strongly in these systems than the less acidic thiols.

3.2 THE CHARACTERIZATION OF RuH(ER)(CO)₂(PPh₃)₂

Analytically pure samples of several of the title complexes (9a, 9c-h) have been isolated. The carbon analyses of 9b and 9i were 1% low. In addition, 9j was isolated but not purified, and samples of RuH(SCH₂CH₃)(CO)₂(PPh₂Py)₂ (11d) (where Py = -2-C₅H₄N) and RuH(SCH₂CH₃)(CO)₂(P(C₆H_{4p}CH₃)₃)₂ (12d) were prepared *in situ* in C₆D₆ in order to make comparisons with their NMR spectra.

The ¹H NMR spectra of 9 (Figs. 3.1 and 3.2, and Table 3.1) contain a high field triplet due to the hydride ligand, split by two equivalent phosphines. The coupling constant ²J_{PH} is within the range 19.5 to 20.5 Hz in C₆D₆, comparable to those of other complexes with phosphines *cis* to hydride ligands, such as *mer*-RuH₂(CO)(PPh₃)₃ (*cis* ²J_{PH}=16, 29, 30 Hz, *trans* ²J_{PH}=74 Hz),²⁰⁸

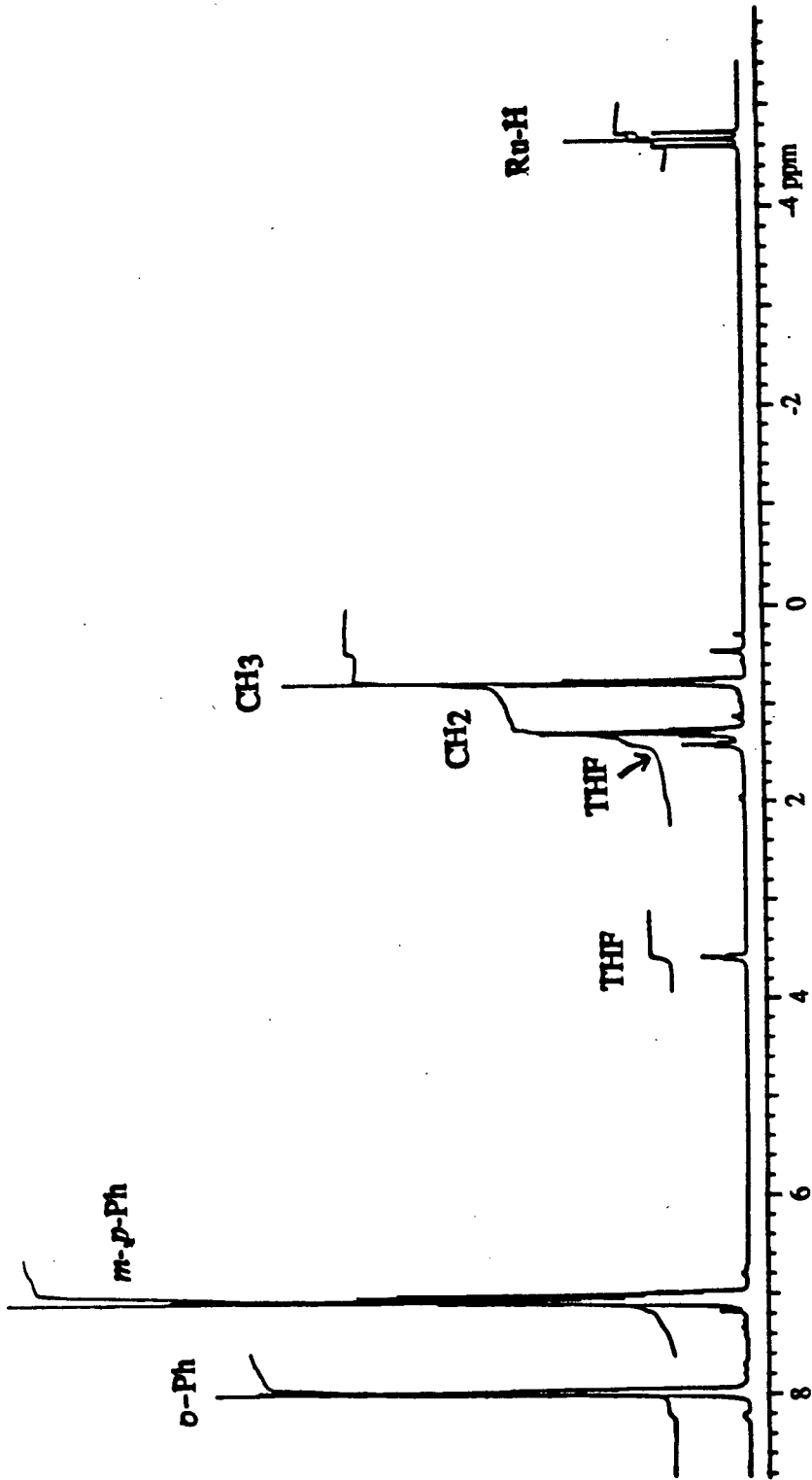


Fig. 3.1 1H NMR spectrum of *cct*-RuH(SeEt)(CO)₂(PPh₃)₂ in C₆D₆ at 20°C and 300 MHz.

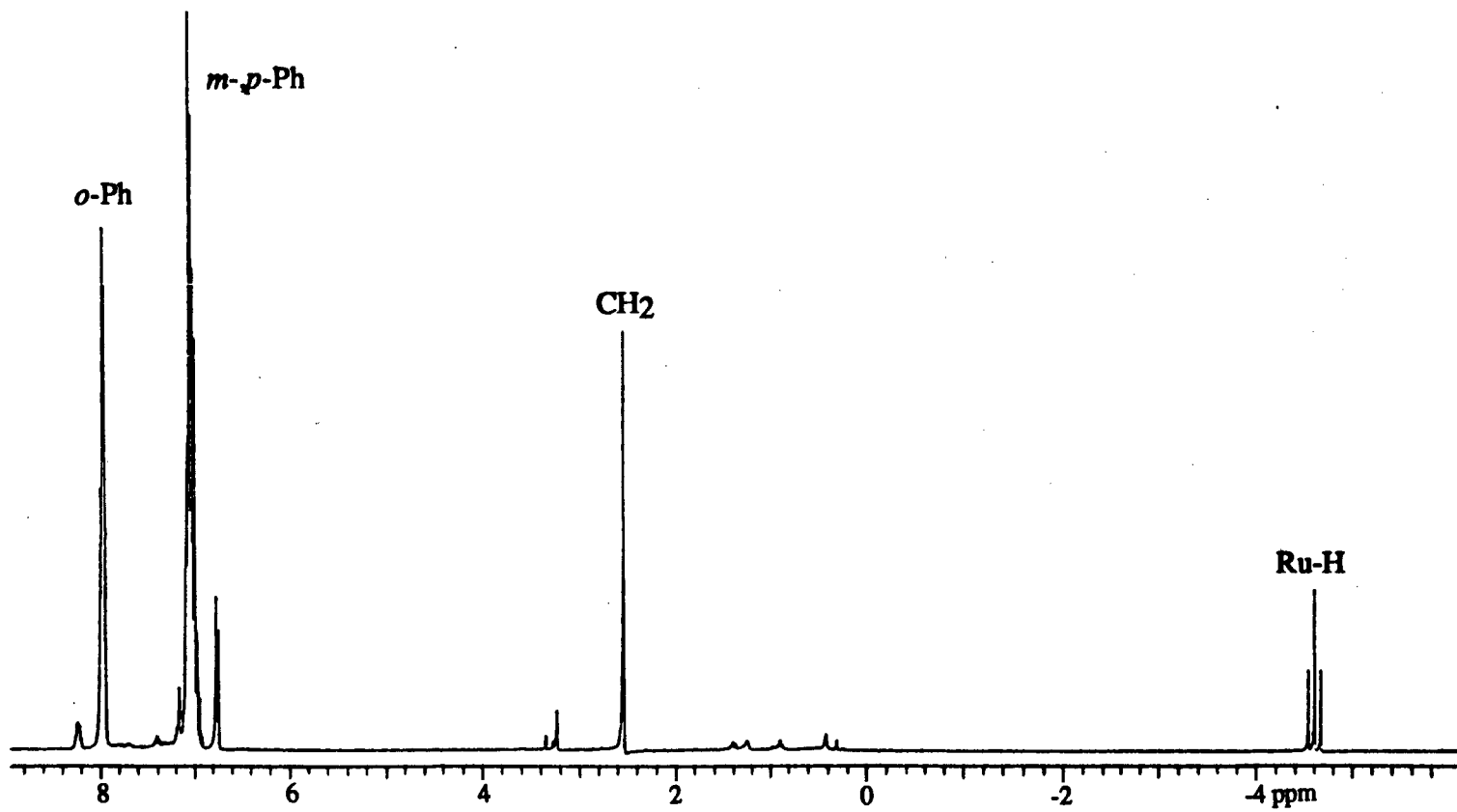


Fig. 3.2 ^1H NMR spectrum of *cct*- $\text{RuH}(\text{SCH}_2\text{Ph})(\text{CO})_2(\text{PPh}_3)_2$ (**2e**) in C_6D_6 at 20°C and 300 MHz.

Table 3.1 $^{31}\text{P}\{^1\text{H}\}$ and ^1H NMR Data for *cct*-RuH(ER)(CO) $_2$ (PPh $_3$) $_2$ Complexes in C $_6$ D $_6$ at 20°C and 300 MHz.

9	ER	$^{31}\text{P}_a$	Ru-H^b	$2J_{\text{PH}}$	CH$_3$	Other
9a	SH	42.01	-4.79	20.1	-	-3.00 (t, $^3J_{\text{PH}}=4.9$, $^3J_{\text{HH}}=3$, SH)
9c	SCH $_3$	37.14	-4.68	20.5	1.04	-
9d	SCH $_2$ CH $_3$	37.25	-4.67	20.4	0.77	1.28 (q, $^3J_{\text{HH}}=7.4$, CH $_2$)
9e	SCH $_2$ C $_6$ H $_5$	37.09	-4.63	20.3	-	2.53 (s, CH $_2$)
9i	SC $_6$ H $_5$	37.26	-4.32	19.5	-	-
9j	SC $_6$ F $_5$	38.45	-4.31	19.5	-	-
9b	SC $_6$ H $_4p$ CH $_3$	37.43	-4.33	19.5	2.04	-
9g	SC $_6$ H $_4m$ CH $_3$	37.39	-4.36	19.5	1.93	-
9f	SC $_6$ H $_4o$ CH $_3$	36.55	-4.23	19.5	2.19	-
9h	SeC $_6$ H $_5$	36.98	-4.75	19.8	-	-

a singlet.

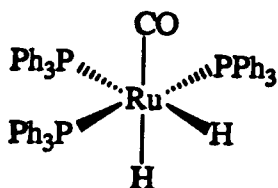
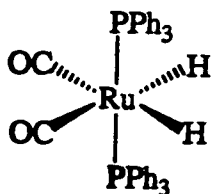
b triplet, except for that of **9a**, which is a doublet of triplets ($^3J_{\text{HH}} = 3$ Hz).

Table 3.2 FT-IR Data for *cct*-RuH(ER)(CO) $_2$ (PPh $_3$) $_2$ Complexes in Nujol, HCB, or CH $_2$ Cl $_2$ at room temperature.^a

9	ER	Nujol $\nu(\text{CO})$	$\nu(\text{RuH})$	HCB $\nu(\text{CO})$	$\nu(\text{RuH})$	CH$_2$Cl$_2$^b $\nu(\text{CO})$
9a	SH	2029, 1984	1901			2035, 1979
9c	SCH $_3$	2021, 1970	1899	2023, 1971	1902	
9d	SCH $_2$ CH $_3$	2025, 1964	1925			2029, 1971
9e	SCH $_2$ C $_6$ H $_5$	2019, 1981	b			
9i	SC $_6$ H $_5$	2030, 1981	1920			
9b	SC $_6$ H $_4p$ CH $_3$	2021, 1987	1900	2021, 1987	1900	2033, 1975
9g	SC $_6$ H $_4m$ CH $_3$	2026, 1983	1906			2035, 1975
9f	SC $_6$ H $_4o$ CH $_3$	2025, 1991	1900			2035, 1977
9h	SeC $_6$ H $_5$	2027, 1978	1919			

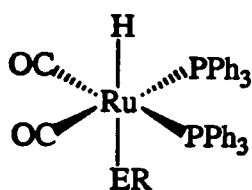
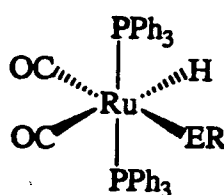
a All frequencies in units of cm $^{-1}$.

b $\nu(\text{RuH})$ not detected.

*mer*-RuH₂(CO)(PPh₃)₃*cis*-RuH₂(CO)₂(PPh₃)₂

cis-RuH₂(CO)₂(PPh₃)₂ (*cis* ²J_{PH}=23.4 Hz, Section 2.3.3), and others.^{178,187} The ³¹P{¹H} NMR spectra of **2** consist of a sharp singlet, indicating equivalent phosphines and a lack of rapid exchange with free phosphine.

The IR spectra of **2** in Nujol mull (Fig. 3.3) include two carbonyl stretch bands of unequal intensity, one in the range 2019 to 2030 and the other in the range 1964 to 1991 cm⁻¹, and a single ν(Ru-H) stretch at 1899 to 1925 cm⁻¹; the exact frequencies are listed in Table 3.2. In CH₂Cl₂ solution, the ν(CO) bands appear at 2035 and 1979 (ER=SH) or 2029 and 1971 cm⁻¹ (ER=SC₂H₅), and the ν(Ru-H) band is not detected. The presence of two carbonyl bands in the IR spectra indicates that the carbonyls have *cis* positions in both solid state and in solution. There are two possibilities for the structure of **2** in solution, given that the phosphine ligands are equivalent and *cis* to the hydride ligand, and the carbonyl ligands are mutually *cis*:

*tcc**cct*

The relative positions of the phosphines were determined by ¹H and ¹³C{¹H} NMR spectroscopy. If the two PPh₃ ligands are *trans*, the ¹³C{¹H} NMR signal of the phosphorus-bound carbons should be a triplet, and the chemical shift difference between the *o*- and the *m/p*-phenyl signals in the ¹H NMR spectrum should be greater than 0.5 ppm. Conversely, if the two PPh₃ ligands are *cis*, then the ¹³C NMR signal should be a doublet,¹⁷¹ while the ¹H NMR

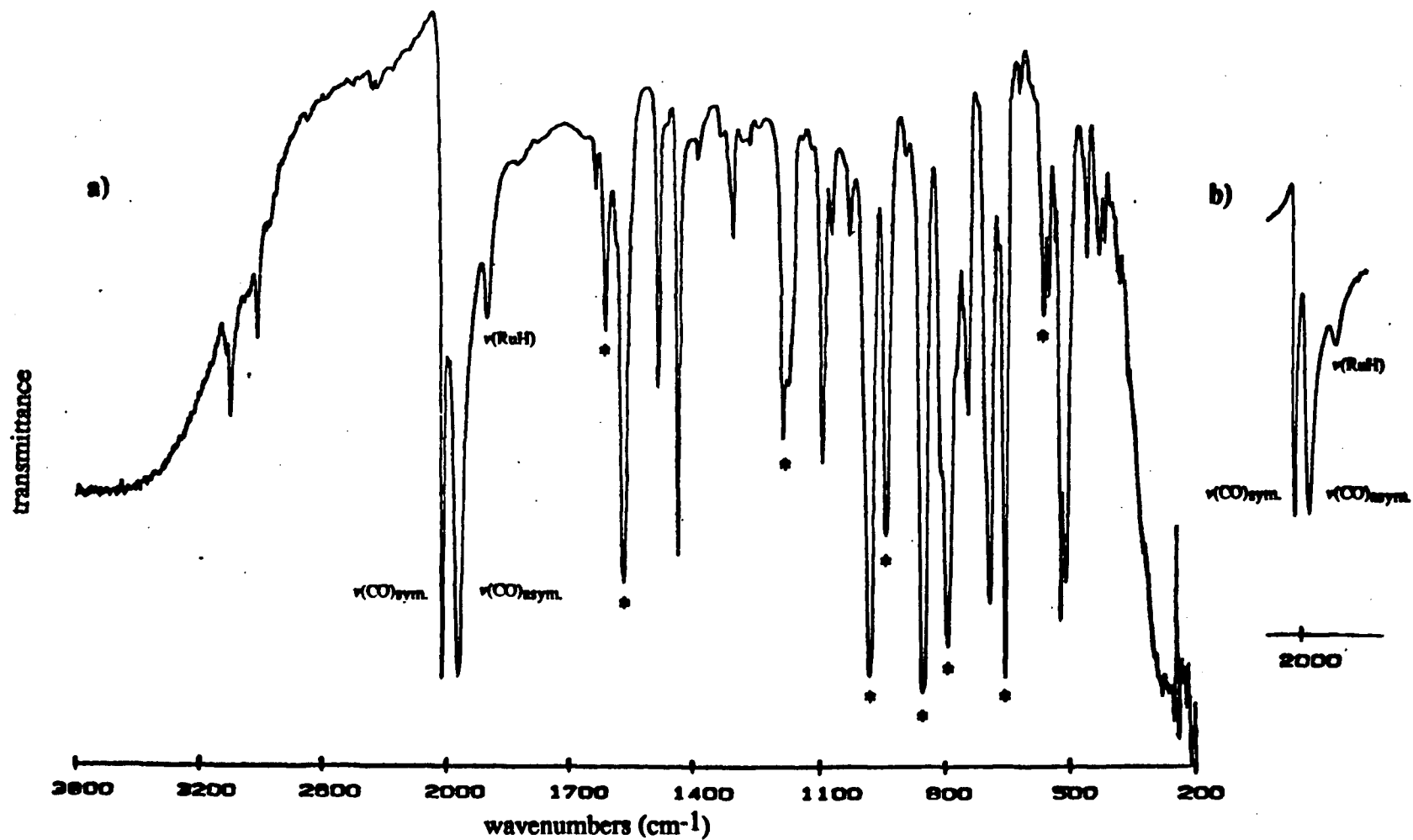


Fig. 3.3 a) The FT-IR spectrum of *cct*-RuH(SMe)(CO)₂(PPh₃)₂ (**9c**) in HCB. The peaks due to HCB are marked with asterisks. b) The carbonyl region of the corresponding spectrum of *cct*-RuH(SPh)(CO)₂(PPh₃)₂ (**9i**).

chemical shift difference should be less than 0.5 ppm.¹⁸⁰ The ^{13}C spectrum (Fig. 3.4) of $\text{RuH}(\text{SC}_2\text{H}_5)(\text{CO})_2(\text{PPh}_3)_2$ in CD_2Cl_2 shows triplets at 135.6 (t, $|J_{\text{CP}}+J_{\text{CP}'}|=23.3$, P-C), 134.6 (t, $|J_{\text{CP}}+J_{\text{CP}'}|=5.9$, *o*-Ph), 128.2 (t, $|J_{\text{CP}}+J_{\text{CP}'}|=4.4$, *m*-Ph), and 130.1 ppm (s, *p*-Ph). The ^1H NMR chemical shift difference between the *o*- and *m/p*-phenyl signals of complexes **2a-j** in C_6D_6 is 0.9 ppm. These observations show that the phosphine ligands are *trans*, and therefore that **2** exists as the *cct* isomer in solution.

The solid state structure of **2b** was investigated by X-ray crystallography, and was shown to be the *cct* isomer (Figs. 3.5 and 3.6 and Tables 3.3 and 3.4).²⁰⁹ No other monomeric ruthenium hydrido thiolato complex has been crystallographically characterized, although the structure of a triruthenium complex has been reported.⁹⁸ Some deviations from the octahedral geometry at the metal are due to the four ligands *cis* to the hydride ligand crowding the hydride. The P-Ru-P bond angle is 172.6° , and the C(1)-Ru-S bond angle is 167.2° .

The Ru-S bond length (2.458 Å) is similar to that for the thiolate ligand (2.453 Å) *trans* to a carbonyl in the complex $\text{Ru}(\text{pyS})_2(\text{CO})_2(\text{PPh}_3)_2$ (pyS=*o*-SC₅H₄N).^{210,211} Shorter Ru^{II}-S bonds (2.406 to 2.429 Å) exist in thiolate ligands *trans* to weaker π acceptors than CO, such as phosphine or thiolate groups,²¹⁰⁻¹² although an apparent exception is $(\text{PhMe}_2\text{P})_3\text{Ru}(\mu\text{SH})_3\text{Ru}(\text{PMe}_2\text{Ph})_2(\text{SH})$ with a terminal Ru-S (*trans* to a bridging SH ligand) bond length of 2.44 Å.²¹³ The M^{II}-S-C bond angle is large (113.6°) in **2b**, as it is in other complexes with thiolates *trans* to carbonyls, such as $\text{Fe}(\text{SPh})_2(\text{CO})_2(\text{dppe})$ (112.4 to 114.9°).²¹⁴ Smaller angles (107.7 to 109.6°) are found in complexes with thiolates *trans* to phosphine or thiolate ligands.^{210-2,214}

The length (1.875 Å) of the Ru-C bond *trans* to the thiolate ligand in **2b** is slightly shorter than that found in $\text{Ru}(\text{pyS})_2(\text{CO})_2(\text{PPh}_3)$ (1.895 Å),²¹¹ possibly because of the intramolecular interactions which exist in the pyridyl complex. The Ru-C bond *trans* to hydride is 1.945 Å in **2b**, (cf. 1.970 Å in $[\text{RuH}(\text{H}_2\text{O})(\text{CO})_2(\text{PPh}_3)_2]^+$),²¹⁵ longer than that *trans* to the thiolate because of the strong *trans* influence of hydride ligands.²¹⁶ The aquo complex shows

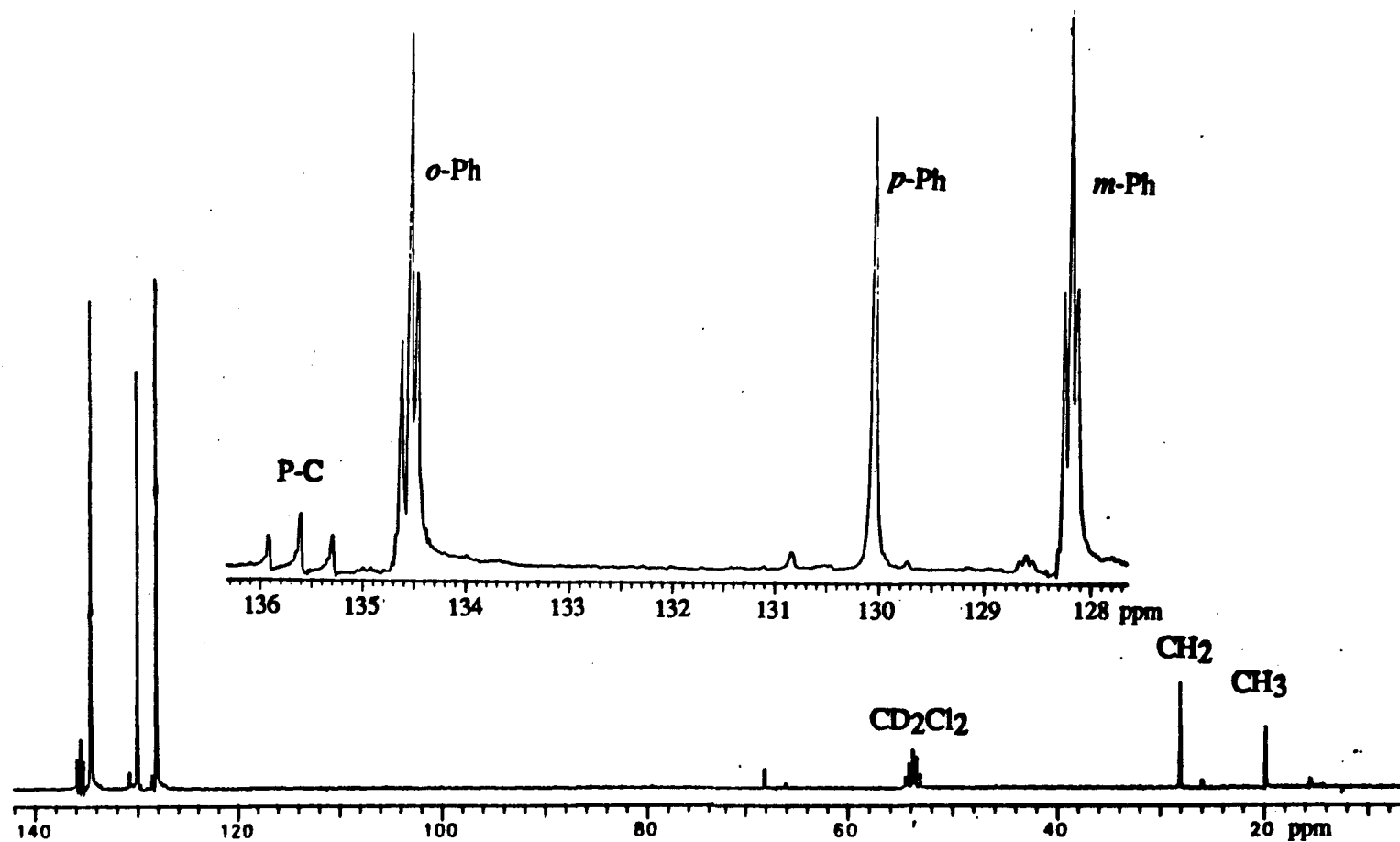


Fig. 3.4 $^{13}\text{C}\{^1\text{H}\}$ NMR spectrum of *cct*-RuH(SEt)(CO)₂(PPh₃)₂ (9d) in CD₂Cl₂ at 20°C and 75 MHz, as provided by Dr. C.-L. Lee. Inset shows an expansion of the phenyl region.

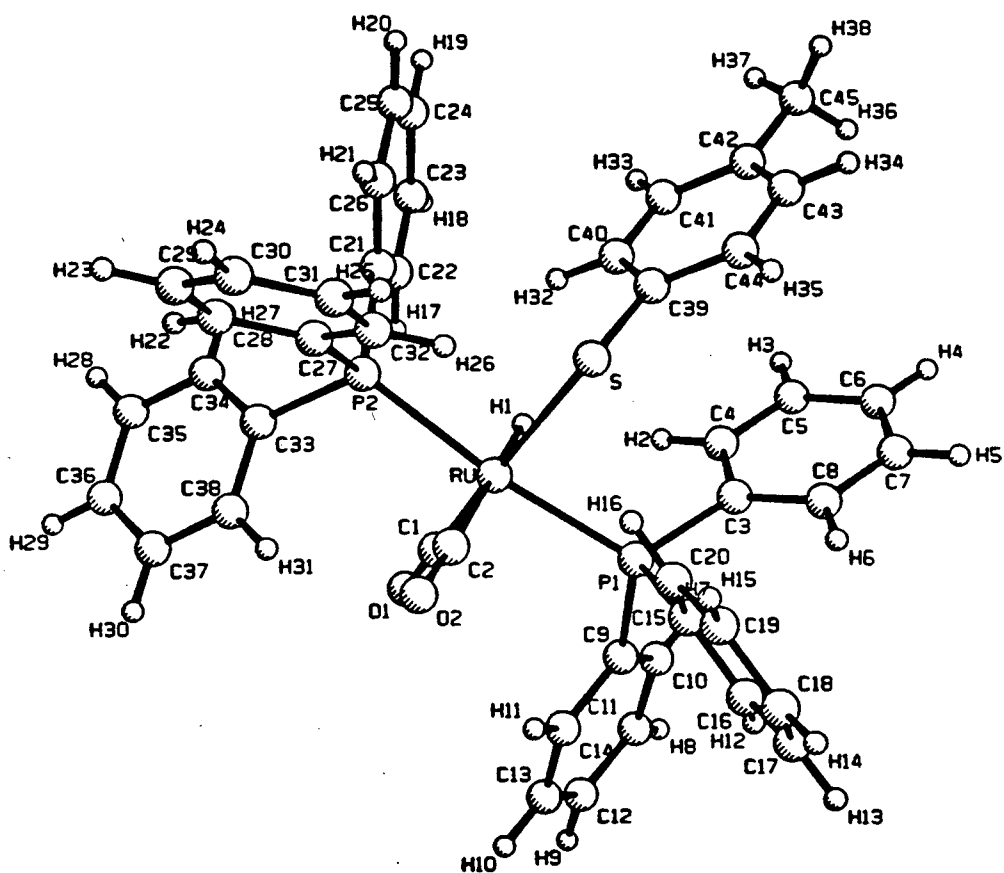


Fig. 3.5 X-ray crystallographic structure of *cct*-RuH(SC₆H₄pCH₃)(CO)₂(PPh₃)₂ (**9b**).

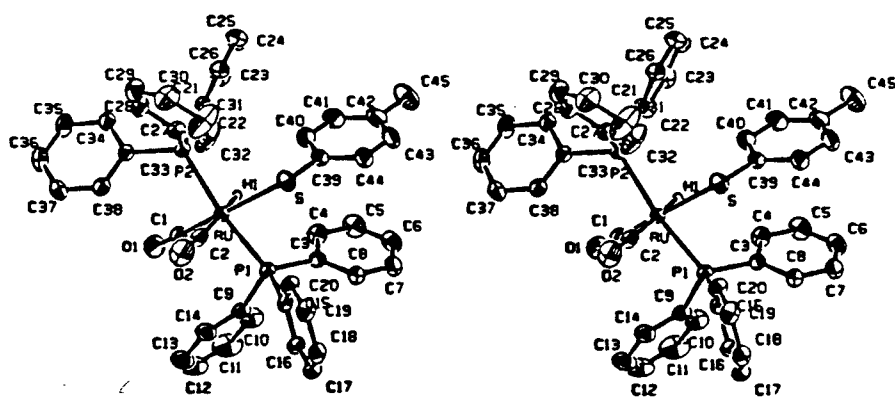


Fig. 3.6 Stereo-view of the structure of *cct*-RuH(SC₆H₄pCH₃)(CO)₂(PPh₃)₂ (**9b**). Hydrogen atoms (other than hydride) omitted for clarity.

Table 3.3 Selected bond lengths (Å) with estimated standard deviations in parentheses, for RuH(SC₆H₄pCH₃)(CO)₂(PPh₃)₂ (9b).

atom	atom	distance	atom	atom	distance
Ru	H(1)	1.58 (3)	P(1)	C(9)	1.835 (3)
Ru	C(1)	1.875 (3)	P(1)	C(15)	1.836 (2)
Ru	C(2)	1.945 (3)	P(2)	C(21)	1.825 (3)
Ru	P(1)	2.361 (1)	P(2)	C(33)	1.834 (3)
Ru	P(2)	2.381 (1)	P(2)	C(27)	1.837 (3)
Ru	S	2.458 (1)	O(1)	C(1)	1.136 (3)
S	C(39)	1.769 (3)	O(2)	C(2)	1.135 (3)
P(1)	C(3)	1.828 (3)			

Table 3.4 Selected bond angles (°) with estimated standard deviations in parentheses, for RuH(SC₆H₄pCH₃)(CO)₂(PPh₃)₂ (9b).

atom	atom	atom	angle	atom	atom	atom	angle
H(1)	Ru	C(1)	81 (1)	C(39)	S	Ru	113.6 (1)
H(1)	Ru	C(2)	176 (1)	C(3)	P(1)	C(9)	105.4 (1)
H(1)	Ru	P(1)	87 (1)	C(3)	P(1)	C(15)	102.3 (1)
H(1)	Ru	P(2)	88 (1)	C(3)	P(1)	Ru	117.53 (9)
H(1)	Ru	S	87 (1)	C(9)	P(1)	C(15)	101.1 (1)
C(1)	Ru	C(2)	96.0 (1)	C(9)	P(1)	Ru	111.35 (8)
C(1)	Ru	P(1)	92.80 (9)	C(15)	P(1)	Ru	117.30 (8)
C(1)	Ru	P(2)	91.59 (9)	C(21)	P(2)	C(33)	103.3 (1)
C(1)	Ru	S	167.2 (1)	C(21)	P(2)	C(27)	104.4 (1)
C(2)	Ru	P(1)	93.79 (8)	C(21)	P(2)	Ru	115.49 (8)
C(2)	Ru	P(2)	91.64 (8)	C(33)	P(2)	C(27)	101.2 (1)
C(2)	Ru	S	96.7 (1)	C(33)	P(2)	Ru	113.98 (8)
P(1)	Ru	P(2)	172.63 (3)	C(27)	P(2)	Ru	116.71 (9)
P(1)	Ru	S	84.04 (4)	O(1)	C(1)	Ru	174.3 (3)
P(2)	Ru	S	90.39 (4)	O(2)	C(2)	Ru	173.4 (3)

Table 3.5 ³¹P{¹H} and ¹H NMR Data for RuH(SET)(CO)₂L₂.

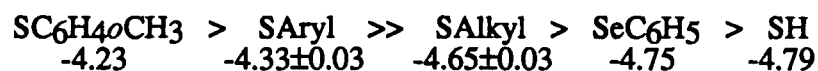
L ^a	³¹ P δ	¹ H δ RuH	² J _{PH}	CH ₂	CH ₃	³ J _{HH}
Ptol ₃ (12)	35.17	-4.52	20.2	1.46	0.86	7.2
PPh ₃ (9d)	37.25	-4.67	20.4	1.28	0.77	7.3
PPh ₂ Py (11)	39.76	-4.06	20.7	0.97	0.79	7.2

^a Ph=C₆H₅ tol=C₆H₄pCH₃ Py=-2-C₅H₅N

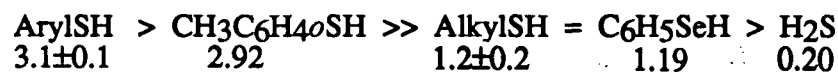
inequivalent Ru-P bond lengths that result from crystal packing effects.²¹⁵ The Ru-P bond lengths in **9b** are essentially equivalent, and match closely those in related complexes.^{215,217}

The Ru-H bond length in **9b** is slightly shorter (1.58 Å) than those found in [RuH(H₂O)(CO)₂(PPh₃)₂]⁺ (1.7 Å),²¹⁵ RuH(Cl)(PPh₃)₃ (1.7 Å),^{218a} and *trans*-RuH(Cl)(diop)₂ (1.65 Å)^{218b} (diop = 4,5-bis((diphenylphosphino)methyl)-2,2-dimethyl-1,3-dioxolane).

The effects of changes in the ER group on the NMR spectra of these complexes correlate with differences in electron-withdrawing ability and steric bulk. The chemical shift (δ) of the hydride ligand (Table 3.1) decreases as the thiolate ligand is changed in the order:

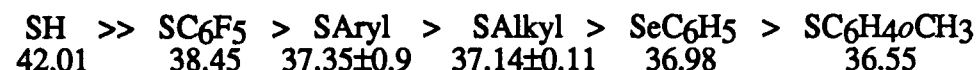


This order is consistent with an electronic effect, and is almost the same as that observed for the acidic protons of the free thiols themselves in the same solvent, C₆D₆.



The coupling constant ²J_{PH} (Table 3.1) is less variable than the chemical shift, having values of 19.5 (SAryl), 19.8 (SePh), 20.1 (SH) and 20.4 ± 0.1 Hz (SAlkyl). The chemical shift and the coupling constant provide a reliable indication of the nature of the R group in complexes of the formula RuH(SR)(CO)₂(PPh₃)₂.

The chemical shift of the ³¹P{¹H} NMR singlet varies in a different order, with the ER = SH and SC₆H₄oCH₃ positions completely reversed compared to the previous sequence,



presumably because of the steric effect of these ER groups on the Ru-P distance. The ³¹P chemical shift of *cis*-RuX(Y)(CO)₂(PPh₃)₂ complexes depends strongly and inversely on the Ru-P bond length, which in turn depends on the bulk of the X and Y ligands (Fig 3.7). This

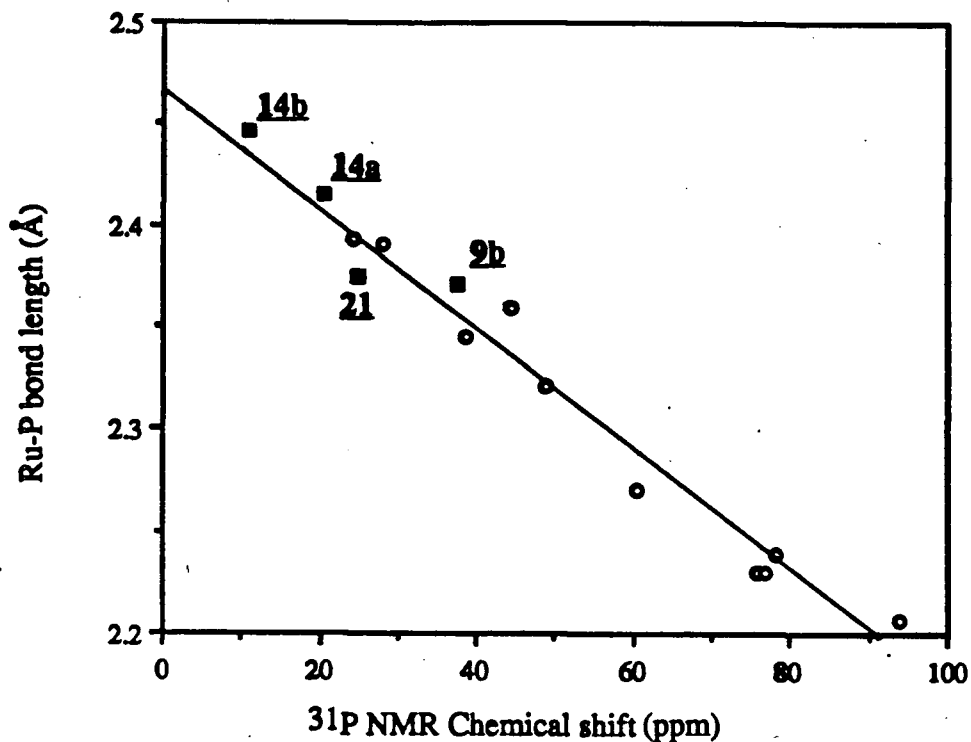


Fig. 3.7 Relationship between the ^{31}P NMR chemical shift and the Ru-P bond length of thiolato-phosphine ruthenium complexes (■). The line is that fitted by Dekleva¹⁸² to data for triarylphosphine ruthenium complexes (○).

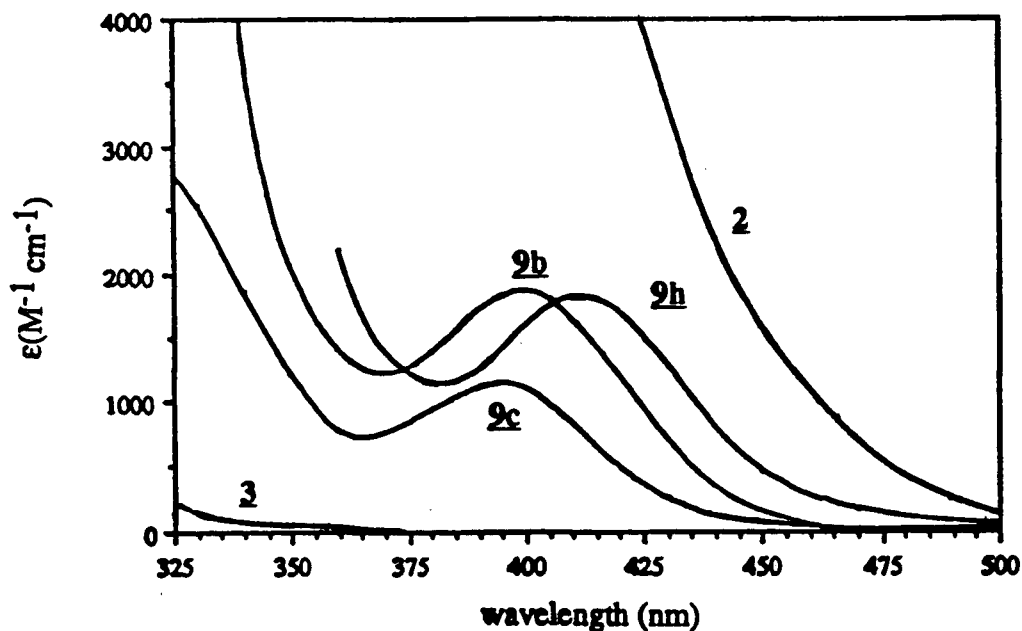


Fig. 3.8 The UV/vis. spectra of *cis*- $\text{RuH}(\text{ER})(\text{CO})_2(\text{PPh}_3)_2$ (**9**) in THF at room temperature, where ER = $\text{SC}_6\text{H}_4\text{pCH}_3$ (**9b**), SCH_3 (**9c**), or SeC_6H_5 (**9h**). The spectra of $\text{Ru}(\text{CO})_2(\text{PPh}_3)_3$ (**2**) and $\text{RuH}_2(\text{CO})_2(\text{PPh}_3)_2$ (**3**) are included for comparison.

correlation was reported for a series of ruthenium hydrido, chloro, and/or acetato phosphine complexes.¹⁸² The bond lengths and chemical shifts of the four thiolato complexes **9b**, **14a**, **14b** (Section 4.2), and **21** (Section 5.3) fit the reported correlation well. As has been observed for RuH(Cl)(CO)₂(PPh₃)₂ with the dichloro- and dihydrido- analogues (**1** and **3**),¹⁸² the ³¹P chemical shift of RuH(SR)(CO)₂(PPh₃)₂ (42.01 for **9a**) is within a few ppm of the average (38.35) of the chemical shifts of Ru(SR)₂(CO)₂(PPh₃)₂ (20.40 for R=H, Section 4.2) and RuH₂(CO)₂(PPh₃)₂ (56.29 ppm).

The effect of changes in the phosphine ligand of RuH(SCH₂CH₃)(CO)₂(PR₃)₂ on the ¹H NMR spectra is summarized in Table 3.5. The three complexes **9d**, **11**, and **12** have similar spectra, presumably because PPh₃, PPh₂Py, and P(C₆H₄pCH₃)₃ are similar in nature.

There is no apparent trend in $\nu(\text{Ru-H})$ in the IR spectra in Nujol. The symmetric $\nu(\text{CO})$ band is randomly scattered within a narrow 11 cm⁻¹ range, while the asymmetric $\nu(\text{CO})$ band varies over a wider 27 cm⁻¹ range, in the following order for RuH(X)(CO)₂(PPh₃)₂ in Nujol (the range of $\nu(\text{CO})$ values observed for CH₂Cl₂ solutions of **9** is much narrower):

X = SPhoMe > SPhpMe > SH \equiv SPhmMe > SPh \equiv
asym. $\nu(\text{CO})$ 1991 1987 1984 1983 1981

SCH₂Ph \equiv Br¹⁶⁴ > SePh > H > SMe >> SEt
 1981 1980 1978 1975 1970 1964

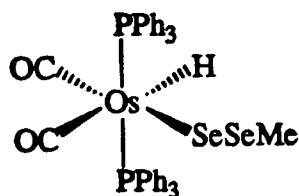
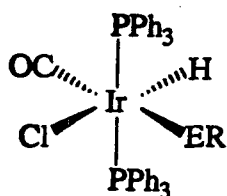
The π backbonding from Ru to the CO π^* antibonding orbitals, which lowers the $\nu(\text{CO})$, is seen to be stronger in alkyl vs. aryl thiolato complexes; the difference is attributed to the π -acceptor ability of the aromatic rings.

The UV/visible spectra of these complexes (Fig 3.8) contain a strong absorbance near 400 nm, which is most probably due to a thiolate ligand-to-metal charge transfer.²¹⁹ The extinction coefficient and λ_{max} are somewhat higher in the spectra of the aryl vs. alkyl thiolate complexes. The λ_{max} is particularly high in the selenolate complex.

ER	=	SeC ₆ H ₅	>	SC ₆ H ₄ pCH ₃	=	SC ₆ H ₅	>>	SCH ₂ C ₆ H ₅	>	SCH ₃	>	SC ₂ H ₅
ϵ (M ⁻¹ cm ⁻¹)	=	1900		1900		1900		1300		1100		1000
λ_{\max} (nm)	=	411		398		397		393		395		396

The small and unpredictable effect of changes in the R group on the charge transfer bands of thiolato complexes has been observed previously in studies of *trans*-Tc(SR)₂(dmpe)₂ⁿ⁺ (n=0,1)^{220a} and MoL₄ⁿ⁻ (L=dithio acid or 1,1-dithiolate ligand, n=2,3,4).^{220b}

Reported complexes similar in structure to **2** include the following Ir⁷⁹ and Os²²¹ complexes.



where E = S, Se; R = H, C₃H₇, C₄H₉, C₆H₅

3.3 THE REACTION OF RuH₂(CO)₂(PPh₃)₂ WITH H₂S AND THIOLS

As was shown in the previous report from these laboratories,⁸⁶ the dihydride complex *cis*-RuH₂(CO)₂(PPh₃)₂ (**3**) reacts with H₂S or thiols at room temperature, giving complete conversion to RuH(SR)(CO)₂(PPh₃)₂ (**2**, R = H, alkyl or aryl) within 2 h.



The H₂ produced in this reaction was qualitatively detected by gas chromatography and quantitatively measured in a gas-uptake experiment. After 50 min at 30°C, the gas production due to reaction 3.4 had slowed to a value of 1.2 equivalents/Ru.

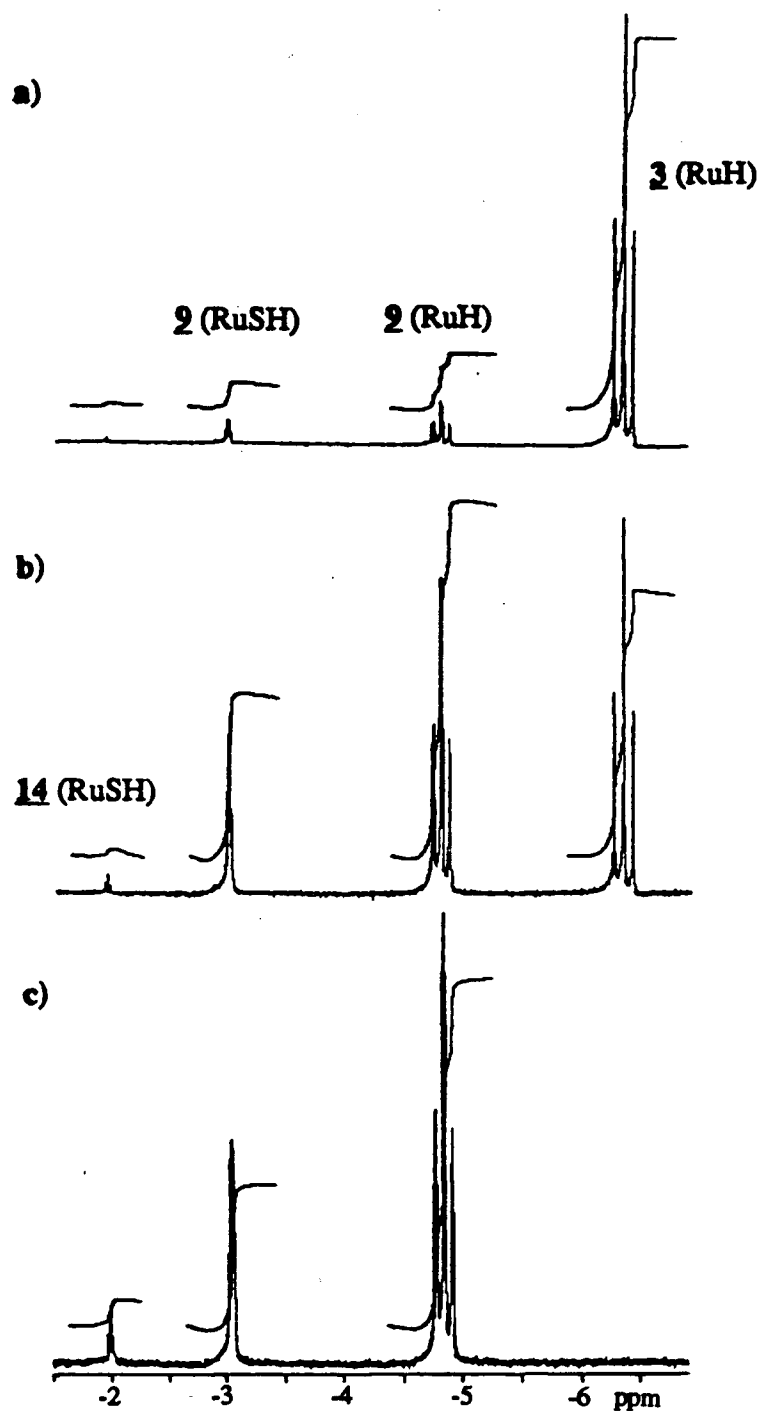


Fig. 3.9 ^1H NMR spectra acquired during the reaction of $cct\text{-RuH}_2(\text{CO})_2(\text{PPh}_3)_2$ (3, 10 mM) with H_2S (1 atm.) in C_6D_6 .

- a) after 2 to 9 minutes at 25°C
- b) after 34 to 39 minutes at 25°C
- c) after raising the temperature to 50°C .

The reaction of **3** with excess H₂S was monitored by ¹H NMR spectroscopy (Fig. 3.9). The *pseudo*-first order log plot is linear for 3 half-lives, and the observed rate constant (at 25.0°C in C₆D₆) is 5.7 x 10⁻⁴ s⁻¹.

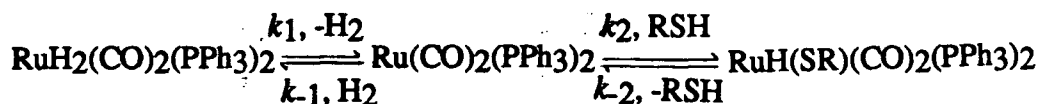
The rate of the reaction with ethanethiol in THF was monitored by the change in absorption at 400 nm in the visible spectrum (Fig. 3.10). Because the spectra of **3** and **9** do not cross (Fig. 3.8), no isosbestic points are observed. If the reaction occurs under *pseudo*-first order conditions (large excess of EtSH), the log plot (Fig. 3.11) is linear for 4 half-lives. Shaking the vessel between absorbance measurements has no effect on the rate. Over the range 0.36 to 2.86 mM **3** at 95 mM EtSH and 26°C, the rate constant is invariant (Fig. 3.12), which shows that the rate is first order with respect to [**3**].

The observed rate constant does not vary with changes in the thiol concentration. At 1 mM **3** the observed rate constant is essentially unchanged (Fig. 3.13) even though the thiol concentration was changed from 45 to 190 mM. The rate of reaction is therefore independent of [EtSH]. The value of the rate constant at 26°C is 6.7(±0.2) x 10⁻⁴ s⁻¹ (average of 11 results).

Corresponding results were obtained in the reaction with *p*-thiocresol. The reaction is again *pseudo*-first order (Fig. 3.14), with the average rate constant slightly lower, at 6.2 (±0.4) x 10⁻⁴ s⁻¹ (average of 11 results). Again, the observed rate constant is independent of the concentration of **3** (Fig 3.15) over the range of 0.045 to 0.96 mM **3** at 95 mM thiocresol, and independent of [CH₃*p*C₆H₄SH] (Fig 3.16) over the range 9.5 to 110 mM at 0.93 mM **3**. The rate law for both systems is therefore

$$\frac{-d[\mathbf{3}]}{dt} = k[\mathbf{3}]$$

which implies that the first and rate determining step of the mechanism is loss of H₂.



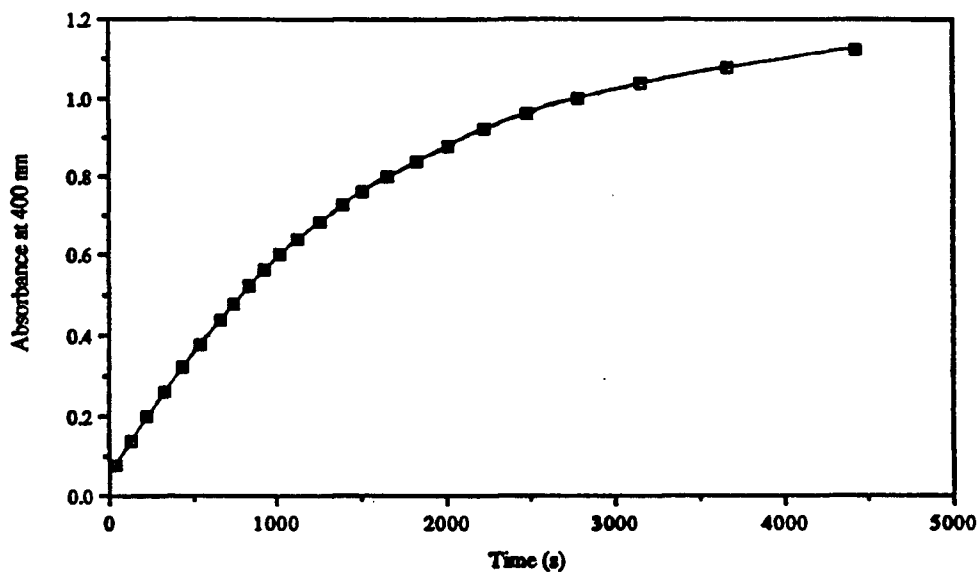


Fig. 3.10 Plot of absorbance at 400 nm versus time during the reaction of *cct*-RuH₂(CO)₂(PPh₃)₂ (**3**, 1.0 mM) with ethanethiol (95 mM) in THF at 26°C.

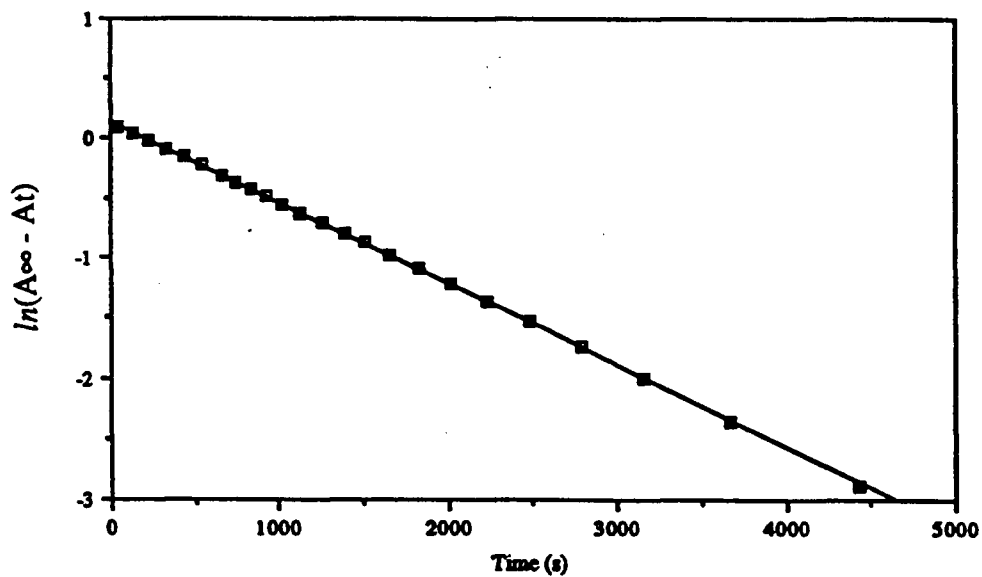


Fig. 3.11 Logarithmic plot of absorbance at 400 nm vs. time for the reaction of *cct*-RuH₂(CO)₂(PPh₃)₂ (**3**, 1.0 mM) with ethanethiol (95 mM) in THF at 26°C.

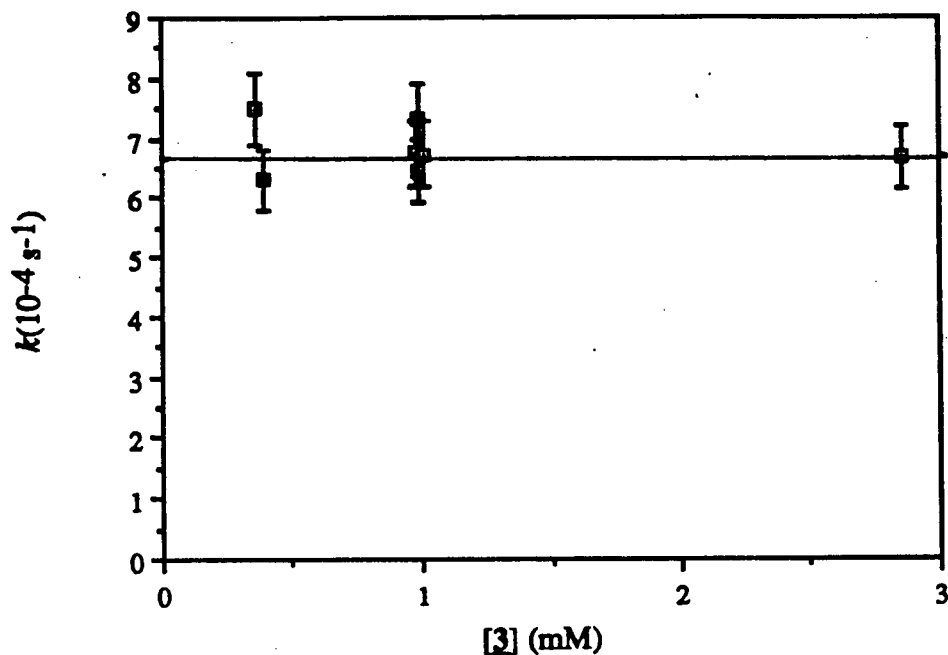


Fig. 3.12 Dependence of the pseudo-first order rate constant on the concentration of *cct*-RuH₂(CO)₂(PPh₃)₂ (**3**) for the reaction with ethanethiol (95 mM) in THF at 26°C. Bars indicate estimated error (8 %) on individual measurements of *k*.

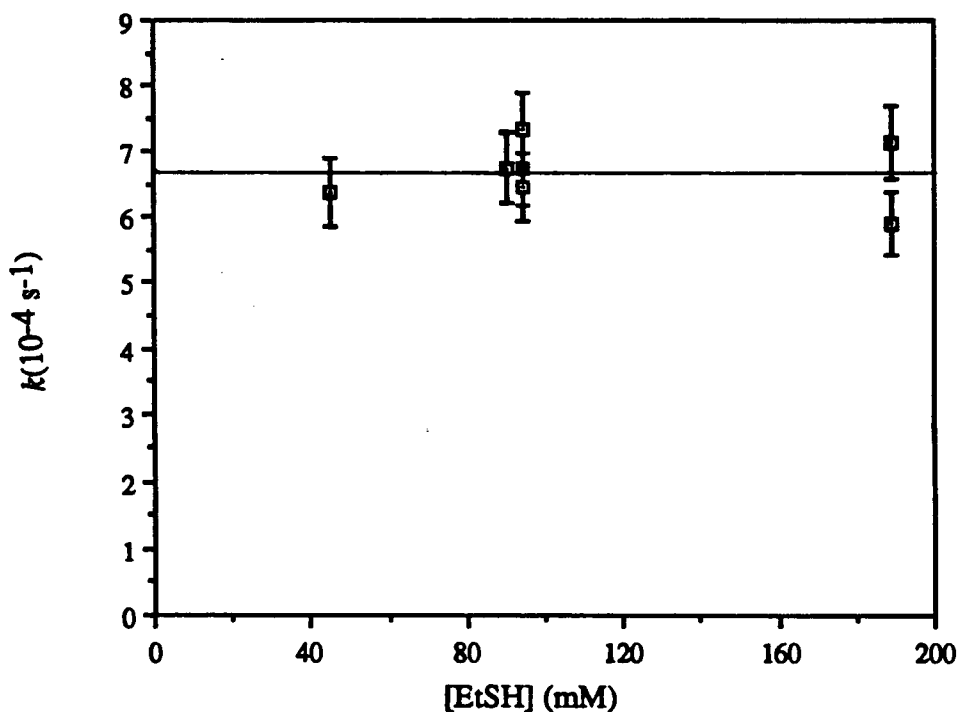


Fig. 3.13 Dependence of the pseudo-first order rate constant on the thiol concentration for the reaction of *cct*-RuH₂(CO)₂(PPh₃)₂ (**3**, 1.0 mM) with ethanethiol in THF at 26°C. Bars indicate estimated error (8 %) on individual measurements of *k*.

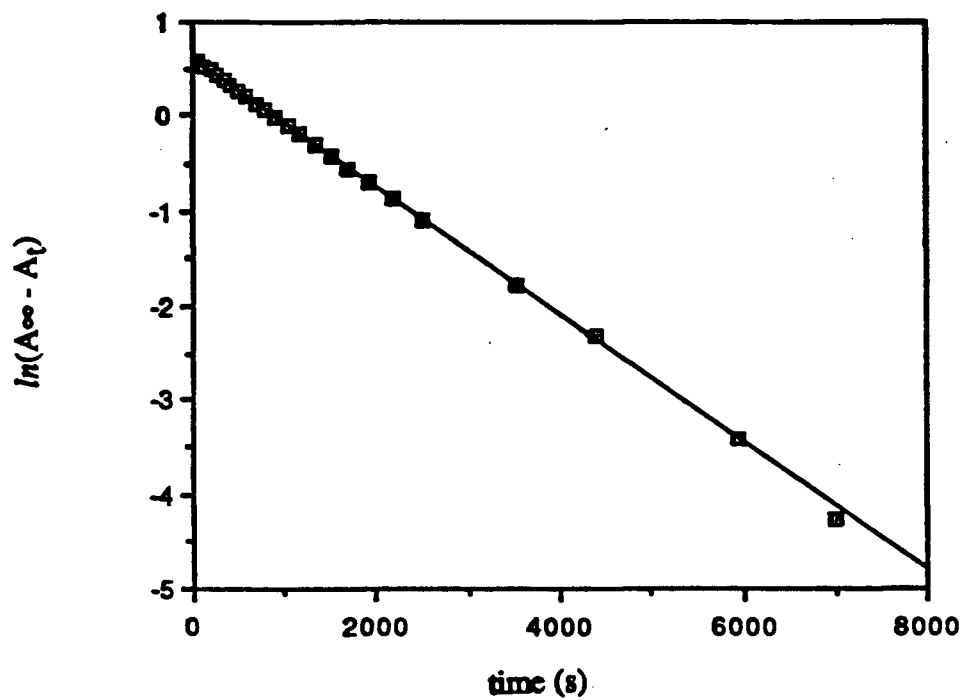


Fig. 3.14 Logarithmic plot of absorbance at 400 nm vs. time for the reaction of *cct*- $\text{RuH}_2(\text{CO})_2(\text{PPh}_3)_2$ (**3**, 1.0 mM) and *p*-thiocresol (91 mM) in THF at 26°C.

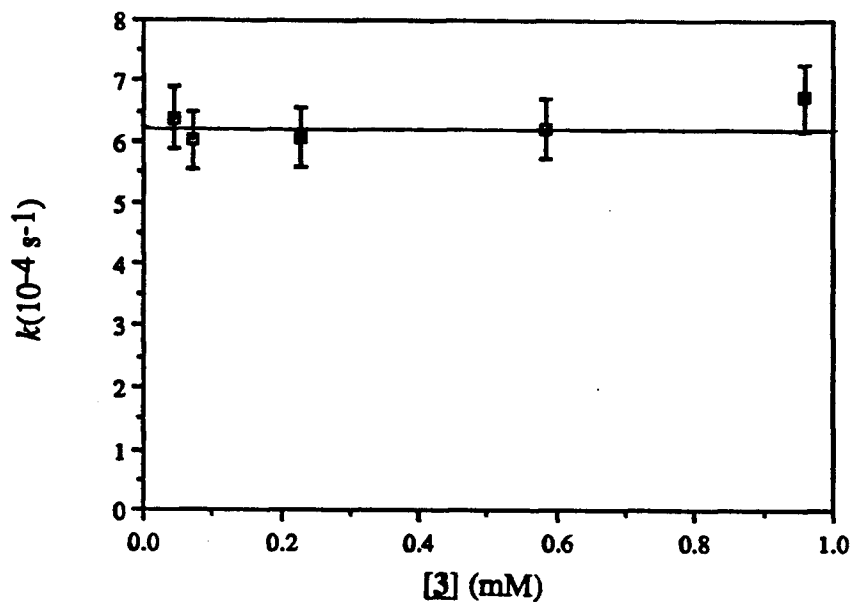


Fig. 3.15 Dependence of the pseudo-first order rate constant on the concentration of *cct*-RuH₂(CO)₂(PPh₃)₂ (**3**) for the reaction with *p*-thiocresol (92 mM) in THF at 26°C. Bars indicate estimated error (8 %) on individual measurements of *k*.

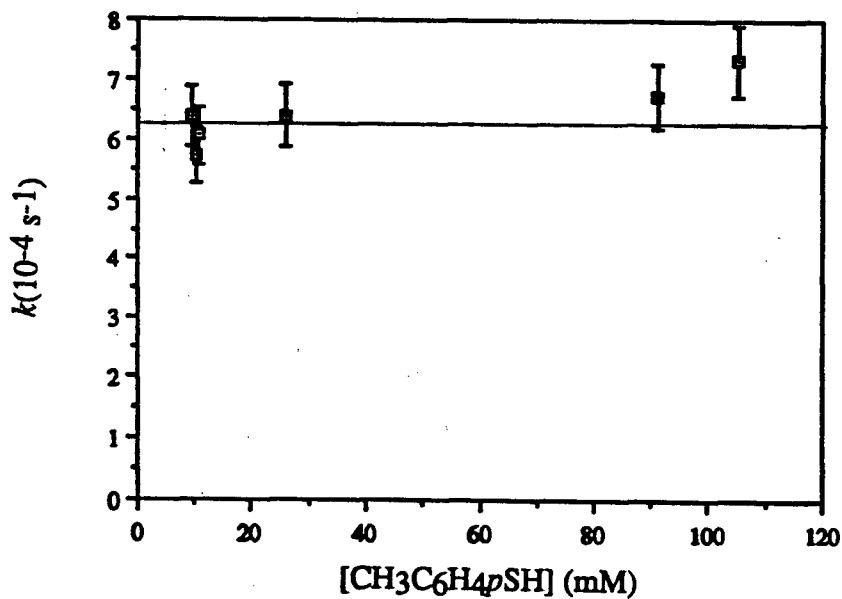


Fig. 3.16 Dependence of the pseudo-first order rate constant on thiol concentration for the reaction of *cct*-RuH₂(CO)₂(PPh₃)₂ (**3**, 0.93 mM) with *p*-thiocresol in THF at 26°C. Bars indicate estimated error (8 %) on individual measurements of *k*.

The unobserved intermediate "Ru(CO)₂(PPh₃)₂" has been previously invoked to explain the mechanism of the reaction of Ru(CO)₂(PPh₃)₃ with a variety of ligands.¹⁷³

The full rate law for this mechanism is:

$$\frac{-d[3]}{dt} = \frac{k_2[\text{RSH}]\{k_1[3] + k_{-2}[9]\}}{k_{-1}[\text{H}_2] + k_2[\text{RSH}]} - k_{-2}[9]$$

If one assumes that $k_{-1}[\text{H}_2]$ is much less than $k_2[\text{RSH}]$ when RSH is present in excess, then this rate law simplifies to

$$\frac{-d[3]}{dt} = k_1[3]$$

consistent with the observed data.

The rate of the reaction with 95 mM EtSH is unchanged if one substitutes the argon atmosphere with H₂ (1 atm). This allows us to put a lower limit on the ratio of k_2/k_{-1} . The concentration of H₂ in benzene can be calculated from published data²²² to be 14.4 mM under these conditions. If $k_2[\text{RSH}] \gg k_{-1}[\text{H}_2]$, then $k_2/k_{-1} \gg 0.15$. However, under 24 atm of H₂, the reaction is reversed, in that the dihydride can be formed from 9 in the absence of free thiol (Chapter 6).

The temperature dependence of the rate (Fig 3.17) allows the calculation of ΔH^\ddagger and ΔS^\ddagger values (Table 3.6), which do not differ significantly between the reactions with ethanethiol and *p*-thiocresol. The essentially zero ΔS^\ddagger value is consistent with an activated complex similar in structure to Ru(*n*²H₂)(CO)₂(PPh₃)₂. A small but positive ΔS is expected for the change from a "static metal dihydride" to a rotor-like *n*²-H₂ complex.²²³ The ΔH^\ddagger values (90 kJ mol⁻¹) for the reactions of 3 are approximately what one would predict for the cleavage of two Ru-H bonds (about 250 kJ mol⁻¹ each)²²⁴ and the formation of an H₂ molecule (H-H bond = 436 kJ mol⁻¹).²²⁵ This again is consistent with an activated complex similar in structure to Ru(*n*²H₂)(CO)₂(PPh₃)₂, assuming that the decrease in the H-H bond energy of the latter,

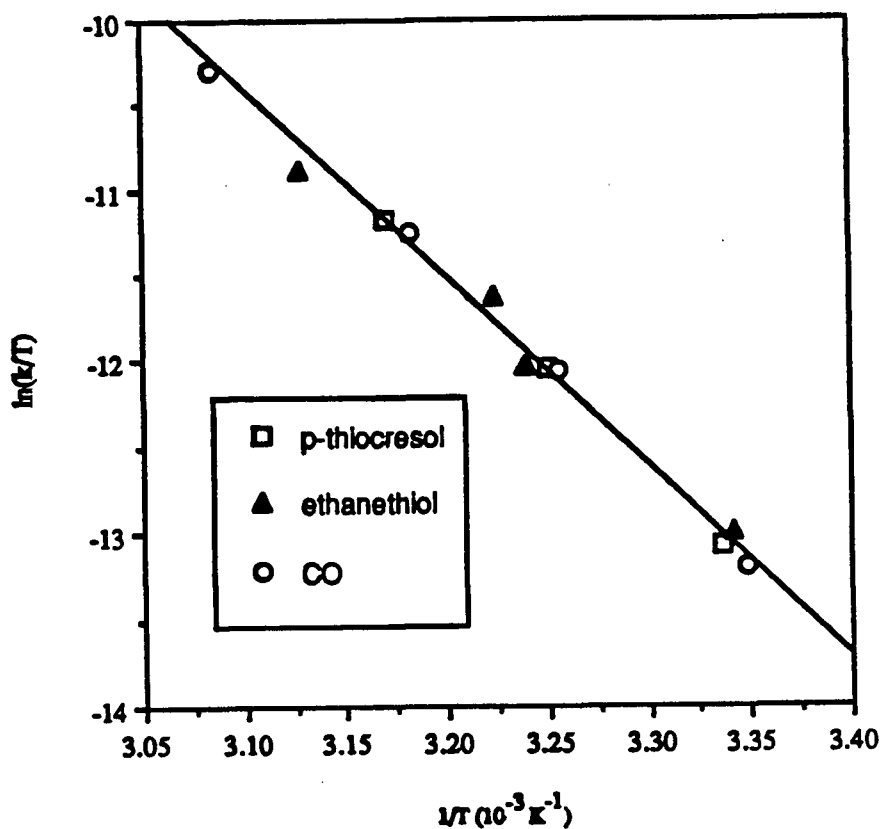


Fig. 3.17 Eyring Plot for the Reactions of *cct*- $\text{RuH}_2(\text{CO})_2(\text{PPh}_3)_2$ (**3**) with several reagents (Table 3.6).

Table 3.6 Kinetic Data for the Reactions of $\text{RuH}_2(\text{CO})_2(\text{PPh}_3)_2$ (**3**) with Various Reagents in C_6D_6 at 26°C .^a

Reagent	$k(\text{s}^{-1})$	ΔH^\ddagger	ΔS^\ddagger	ΔG^\ddagger
$\text{CH}_3\text{C}_6\text{H}_4\text{pSH}$	$6.2(\pm 0.6) \times 10^{-4}$	96 (± 8)	10 (± 30)	92 (± 17)
$\text{CH}_3\text{CH}_2\text{SH}$	$6.7(\pm 0.4) \times 10^{-4}$	84 (± 8)	-30 (± 30)	92 (± 17)
CO	$6.5(\pm 0.2) \times 10^{-4}$	92 (± 8)	-20 (± 30)	96 (± 17)
PPh_3	$6.4(\pm 0.7) \times 10^{-4}$	-	-	-

^a The units for the activation parameters are kJ mol^{-1} for ΔH^\ddagger and ΔG^\ddagger , and $\text{J K}^{-1} \text{ mol}^{-1}$ for ΔS^\ddagger .

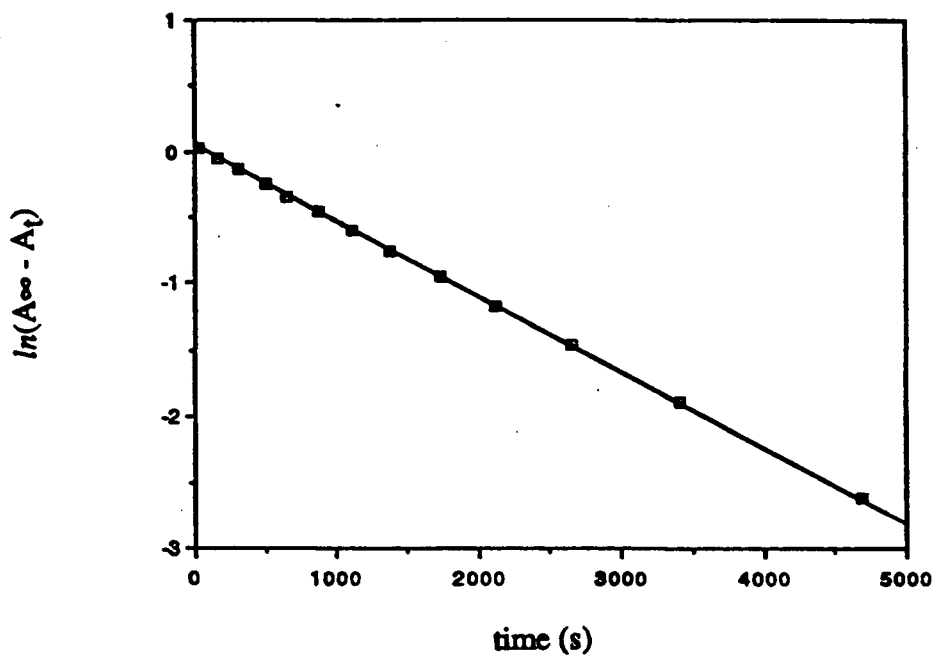


Fig. 3.18 Logarithmic plot of absorbance at 350 nm vs. time for the reaction of *cct*- $\text{RuH}_2(\text{CO})_2(\text{PPh}_3)_2$ (**3**, 1.1×10^{-3} M) with CO (1 atm) in THF at 26°C.

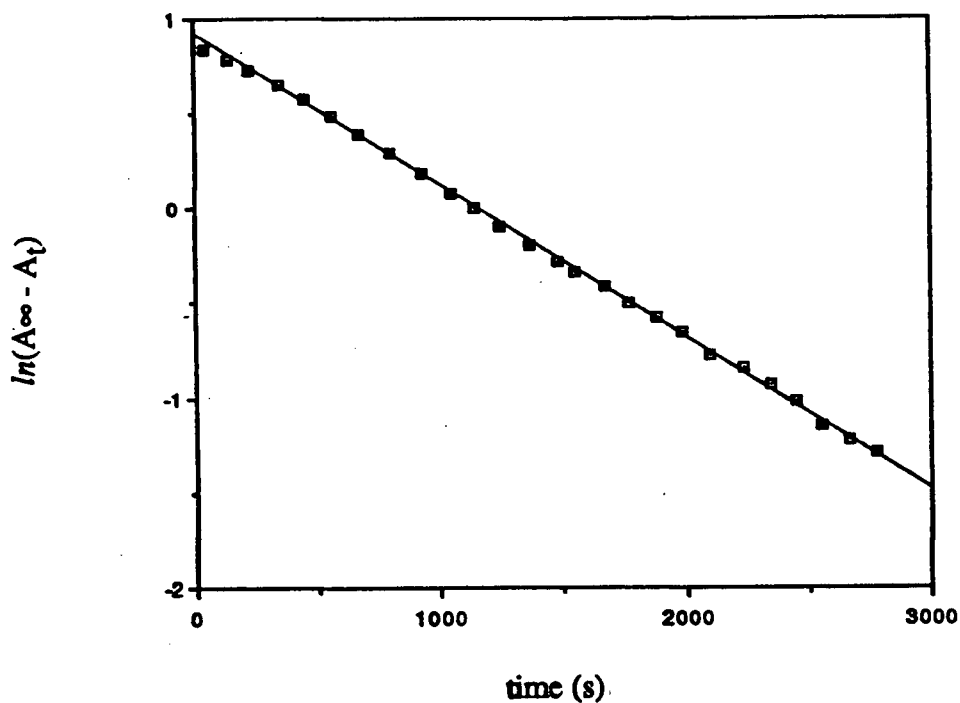


Fig. 3.19 Logarithmic plot of absorbance at 400 nm vs. time for the reaction of *cct*- $\text{RuH}_2(\text{CO})_2(\text{PPh}_3)_2$ (**3**, 6×10^{-4} M) and PPh_3 (0.38 M) in THF at 26°C.

presented some technical difficulties. When monitored by UV/visible spectroscopy under N_2 at 26°C and 400 nm, the reaction did not go to completion unless the cell was stirred or shaken between absorbance measurements. Monitoring the reaction by measuring the gas production in the "gas-uptake" apparatus was tried, because the apparatus allows for shaking. The amount of gas produced (1.0 equivalents/Ru) and the $^{31}P\{^1H\}$ NMR spectra showed the reaction to be complete after 3 days. However, the *pseudo*-first order log plots of gas evolution were not linear. These problems probably resulted from the back reaction, which is rapid at this temperature under 1 atm of H_2 (in the absence of added phosphine), and may be significant under the conditions used for reaction 3.6 if the diffusion of the H_2 product into the gas phase is slow. If this is the case, and if the rate law is similar to that for thiols, then $k_{-1}[H_2]$ is of the same magnitude as $k_2[PPh_3]$ after the generation of some H_2 , and therefore k_{-1} must be one to two orders of magnitude larger than k_2 (assuming $[H_2] = 1/2 [3]_0 = 0.5$ mM, $[PPh_3] = 60$ mM). Therefore, the rate of the reaction of the intermediate, $Ru(CO)_2(PPh_3)_2$, with EtSH is one or more magnitudes faster than the reaction of the same intermediate with PPh_3 .

Under conditions designed to guarantee that $k_{-1}[H_2]$ is much less than $k_2[PPh_3]$, namely $[PPh_3]/[3]$ greater than 130 and vigorous shaking between absorbance measurements to ensure H_2 removal, the *pseudo*-first order log plot is linear for 3 half-lives (Fig. 3.19). At 0.33 mM of the dihydride, and 50 mM PPh_3 , the rate constant is $6.4 (\pm 0.7) \times 10^{-4} s^{-1}$ (average of 3 experiments), and at 375 mM PPh_3 , the rate constant was $6.5 \times 10^{-4} s^{-1}$ (single experiment).

Therefore, the observed rate law and suggested mechanism for the reactions with CO and PPh_3 correspond to those for the thiol reactions. As predicted by the mechanism, the observed *pseudo*-first order rate constant k is independent of the concentration or nature of the added reagent, and corresponds to k_1 .

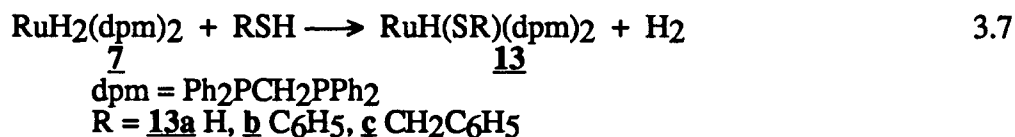
Of the three products of these reactions, only one, $Ru(CO)_2(PPh_3)_3$, can be converted back into **3** by the application of 1 atm of H_2 to its solution (in the absence of free phosphine).¹⁷⁷ The other two, $RuH(SR)(CO)_2(PPh_3)_2$ (Section 6.1.4) and $Ru(CO)_3(PPh_3)_2$,¹⁷⁸ require

elevated pressures for conversion back to **3**.

$\text{RuH}_2(\text{CO})_2(\text{PPh}_3)_2$ failed to react with methanol (247 mM) in THF within 1 h.

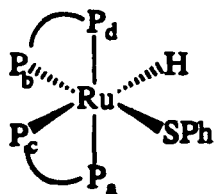
3.4 THE REACTION OF $\text{RuH}_2(\text{dpm})_2$ WITH H_2S AND THIOLS

The mixture of *cis*- and *trans*- $\text{RuH}_2(\text{dpm})_2$ (**7**) reacts too quickly with H_2S (reaction 3.7, $\text{R}=\text{H}$) at room temperature to monitor the course of the reaction accurately by NMR spectroscopy.¹⁹¹



The product of the reaction with H_2S is exclusively *trans*- $\text{RuH}(\text{SH})(\text{dpm})_2$ (Fig. 3.20).

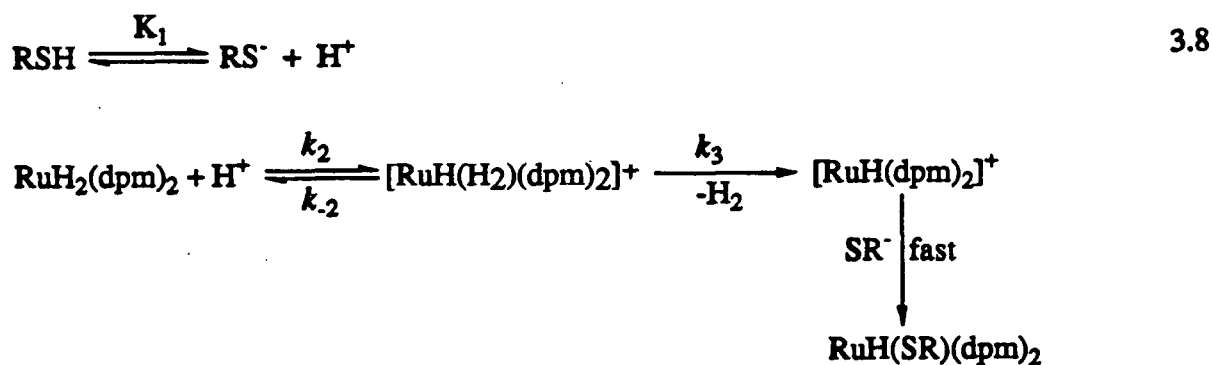
Reaction 3.7 ($\text{R} = \text{Ph}, \text{CH}_2\text{Ph}$) produces 1:5 mixtures of *cis*- and *trans*- $\text{RuH}(\text{SR})(\text{dpm})_2$. These complexes are easily identified by their characteristic ^1H and $^{31}\text{P}\{^1\text{H}\}$ NMR spectra (Figs. 3.21 through 3.23, and Table 3.7). The hydride region of the ^1H NMR spectrum contains quintets for the *trans*-complexes and AX_2YZ (doublet of doublet of triplet) patterns for the *cis* complexes. The $^2J_{\text{transPH}}$ couplings are 90 to 100 Hz, while the $^2J_{\text{cisPH}}$ coupling constants are 16 to 23 Hz, typical values for such constants.²⁰⁸ The $^{31}\text{P}\{^1\text{H}\}$ NMR spectrum (Fig. 3.23) contains a strong singlet for the major product, *trans*-**13**, and four weak multiplets for *cis*-**13**, corresponding to the four different phosphine atoms in the molecule. The following assignments for *cis*- $\text{RuH}(\text{SPh})(\text{dpm})_2$ in toluene- d_8 are consistent with the NMR spectra, but have not been confirmed by decoupling experiments. The $^2J_{\text{cisPP}}$ values are assumed to be negative, following a generalization suggested by Baker and Field²²⁶ that this is usually the case (an opposing view has been expressed by Bookham *et al.*).²²⁷



$\delta\text{H} = -6.29$ ppm	$\delta\text{P}_\text{c} = -15.86$ ppm
$\delta\text{P}_\text{a} = 4.44$ ppm	$\delta\text{P}_\text{d} = -15.96$ ppm
$\delta\text{P}_\text{b} = 7.67$ ppm	
$J_\text{PaPb} = -20$ Hz	$J_\text{PbPc} = -24$ Hz
$J_\text{PaPc} = -26$ Hz	$J_\text{PbPd} = -51$ Hz
$J_\text{PaPd} = 330$ Hz	$J_\text{PcPd} = -24$ Hz
$J_\text{PbH} = 24.1$ Hz	$J_\text{PcH} = 91.5$ Hz
$J_\text{PaH} = J_\text{PdH} = 16.3$ Hz	

The reaction with thiophenol (Fig. 3.24) is an order of magnitude faster at 25°C than that with α -toluenethiol (Fig. 3.25). There is too much scatter in the data to conclude that the rate of loss of *cis*- $\text{RuH}_2(\text{dpm})_2$ is *pseudo*-first order. However, it is clear that the rate depended strongly on the thiol concentration (Fig. 3.25).

A mechanism consistent with a dependence on the nature and concentration of thiol is the following, in which the *cis*- and *trans*- $\text{RuH}_2(\text{dpm})_2$ reactants are treated as one species.



Assuming a steady state condition for the unobserved molecular hydrogen species $[\text{RuH}(\text{H}_2)(\text{dpm})_2]^+$, and assuming that K_1 is small, the rate law for this mechanism is:

$$\frac{d[\text{13}]}{dt} = \frac{k_2 k_3 K_1^{1/2} [\text{7}] [\text{RSH}]^{1/2}}{k_{-2} + k_3}$$

However, the mechanism is incomplete because of the question of the nature of the equilibrium between *cis*- and *trans*- $\text{RuH}_2(\text{dpm})_2$ at room temperature. According to Chaudret *et*

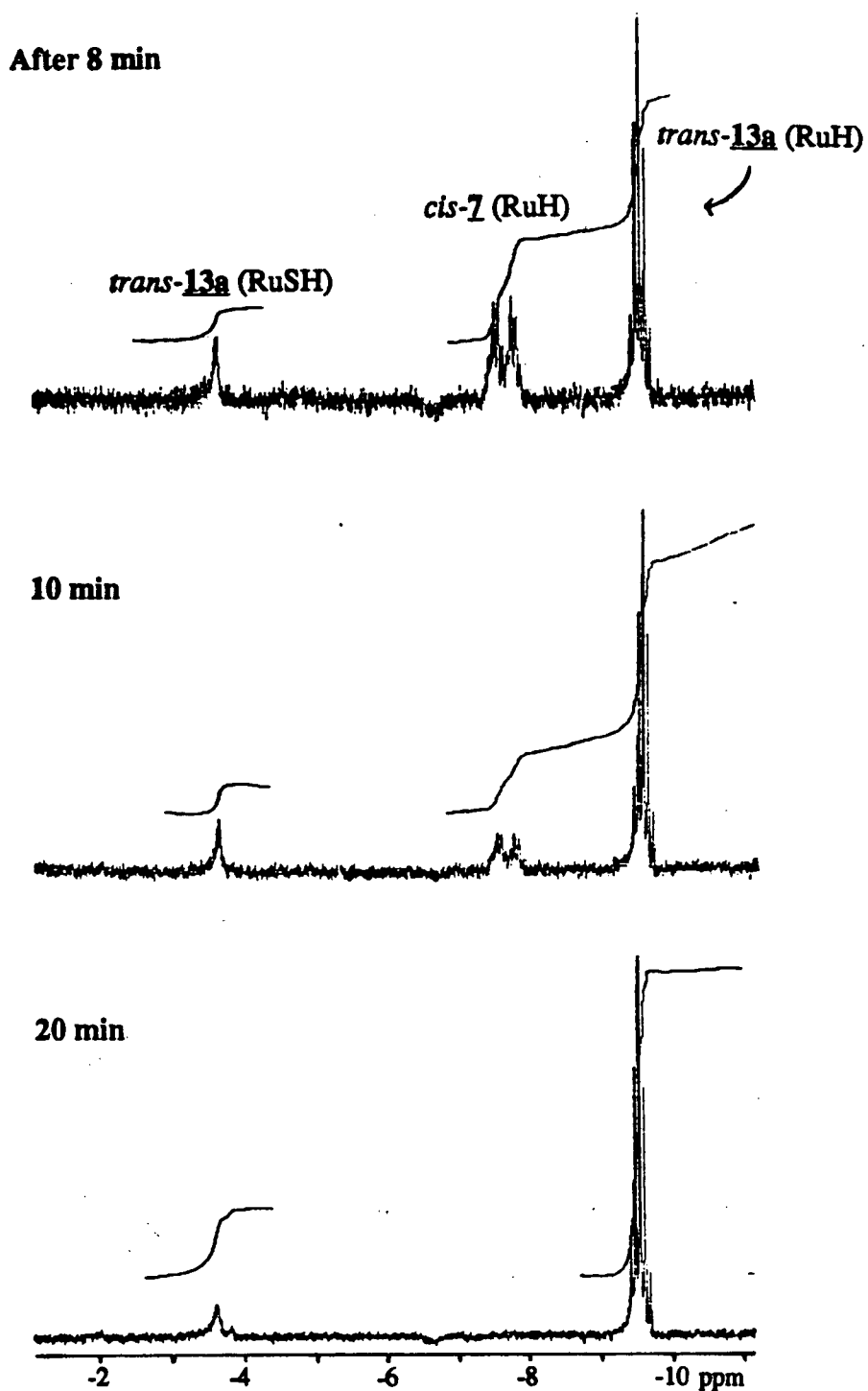


Fig. 3.20 a) ^1H NMR spectra (hydride region) for the reaction of *cis*- and *trans*- $\text{RuH}_2(\text{dpm})_2$ (11 mM) with H_2S in C_6D_6 at 25°C and 300 MHz.¹⁹¹

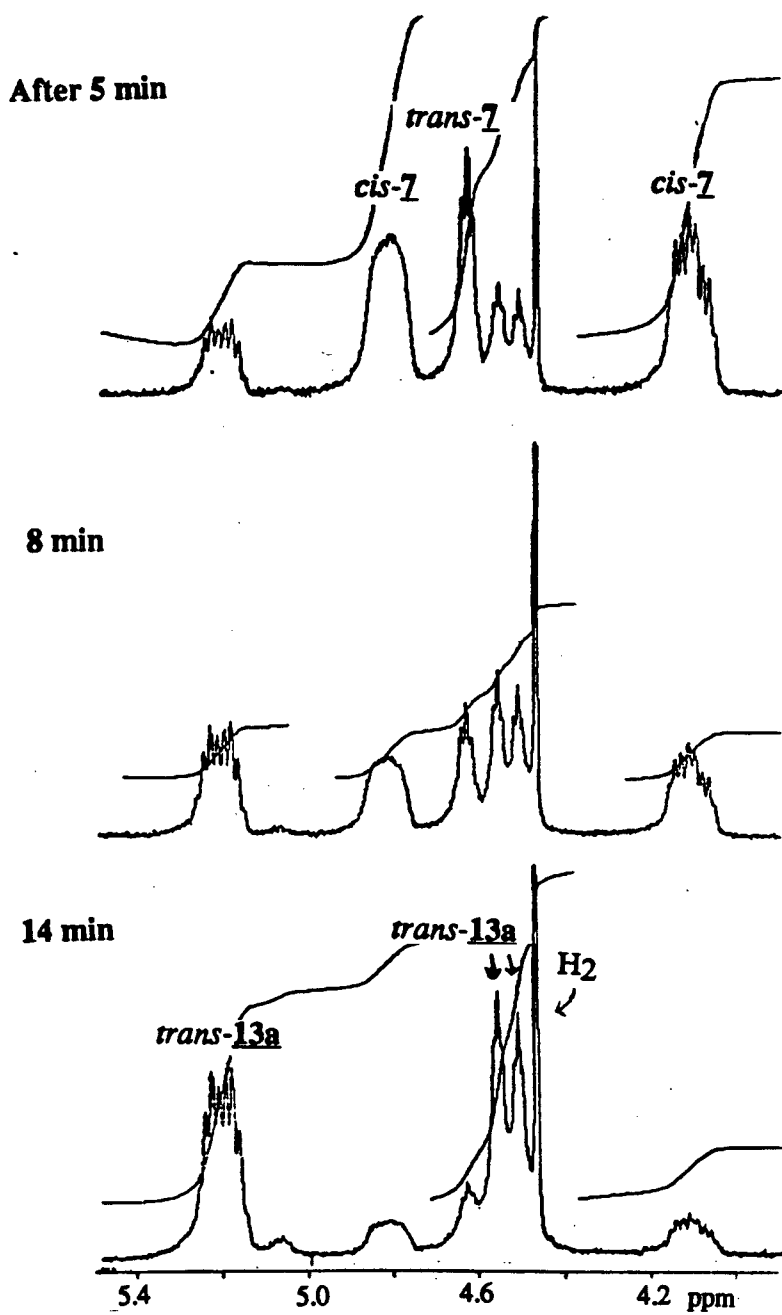


Fig. 3.20 b) ¹H NMR spectra (methylene region) for the reaction of *cis*- and *trans*-RuH₂(dpm)₂ (11 mM) with H₂S in C₆D₆ at 25°C and 300 MHz.¹⁹¹

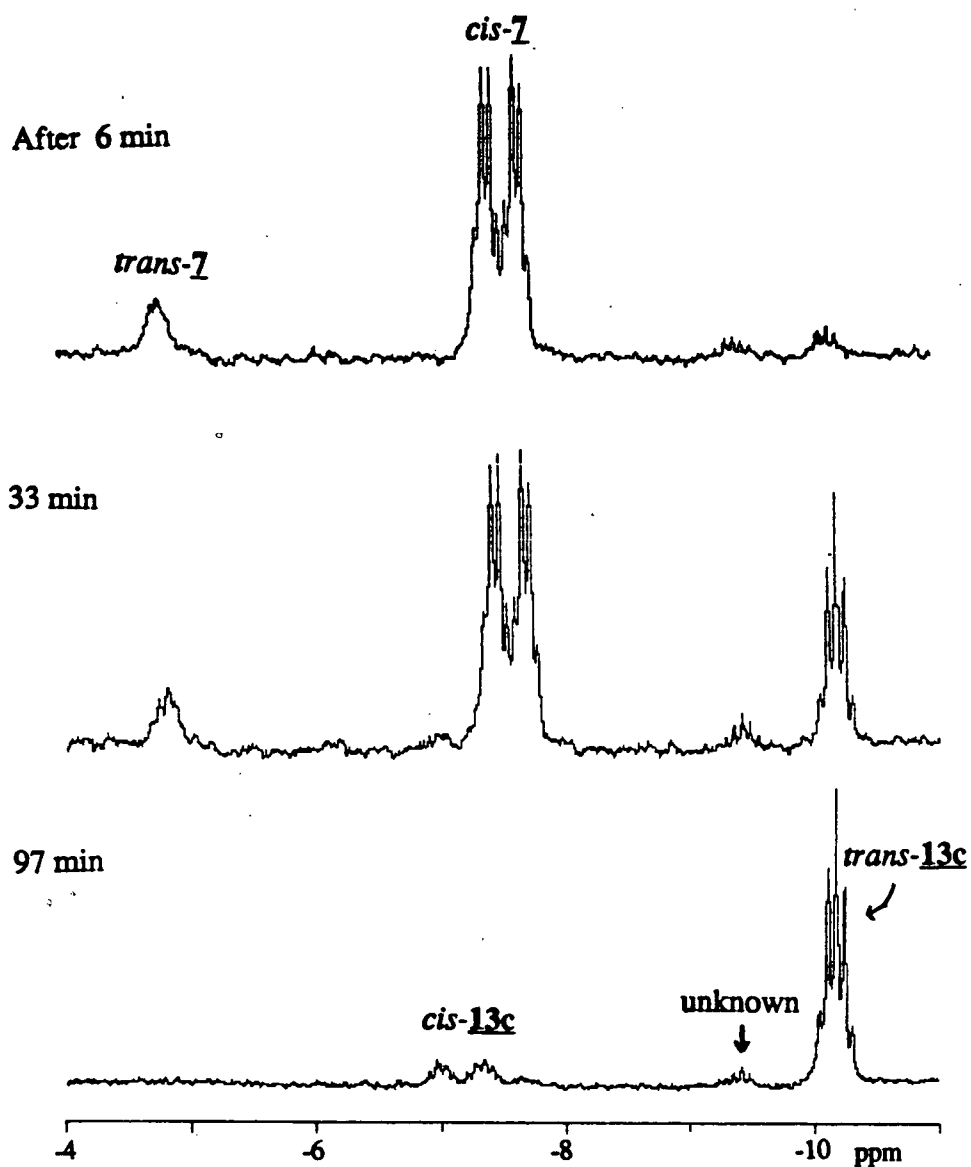


Fig. 3.21 ^1H NMR spectra (hydride region) for the reaction of $\text{RuH}_2(\text{dpm})_2$ (4.1 mM) with PhCH_2SH (280 mM) in C_6D_6 at 25.0°C .

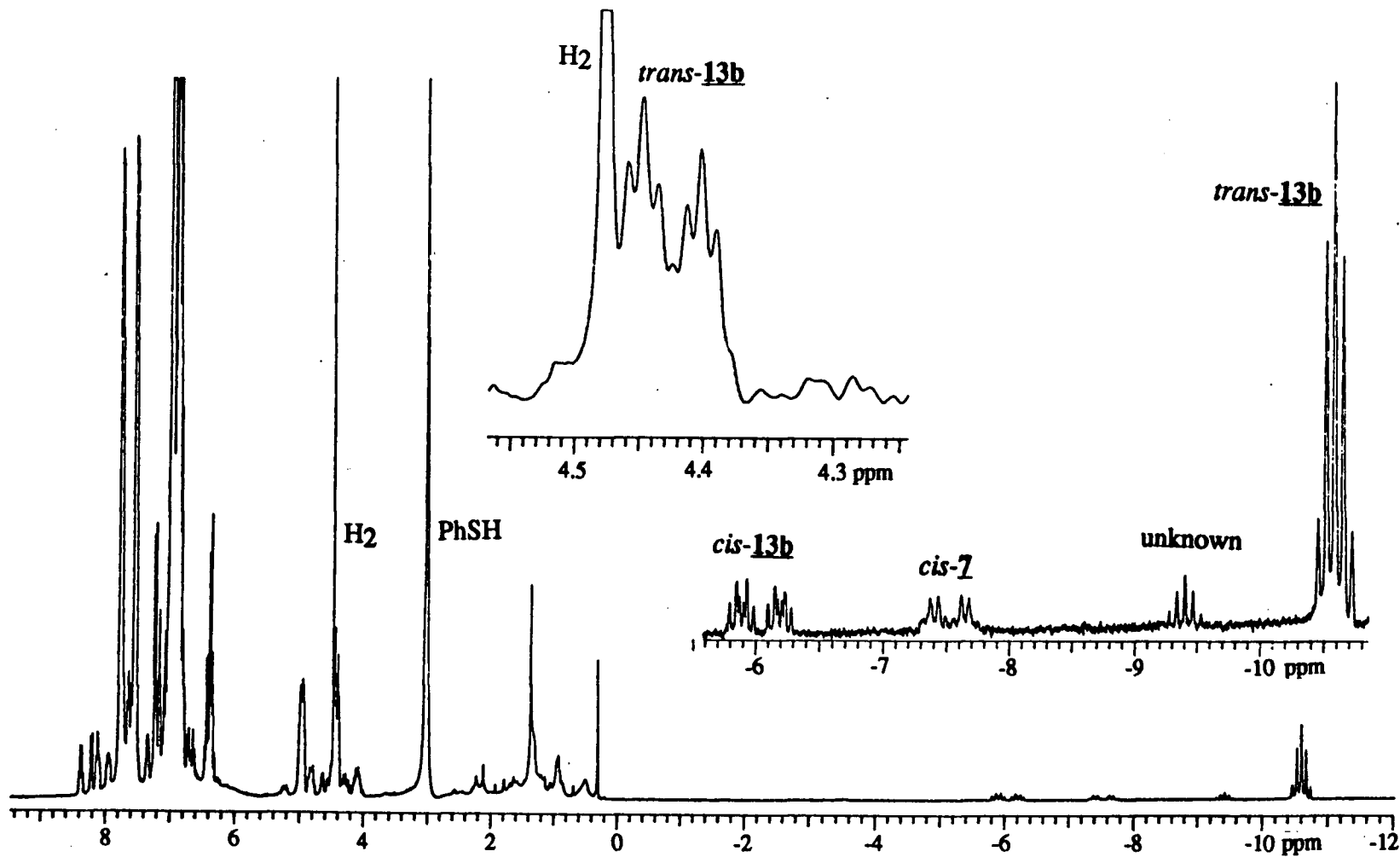


Fig. 3.22 ^1H NMR spectrum (300 MHz) of a sample of $\text{RuH}(\text{SPh})(\text{dpm})_2$ prepared *in situ* from $\text{RuH}_2(\text{dpm})_2$ and thiophenol in C_6D_6 , with expanded views of the hydride region and part of the methylene region.

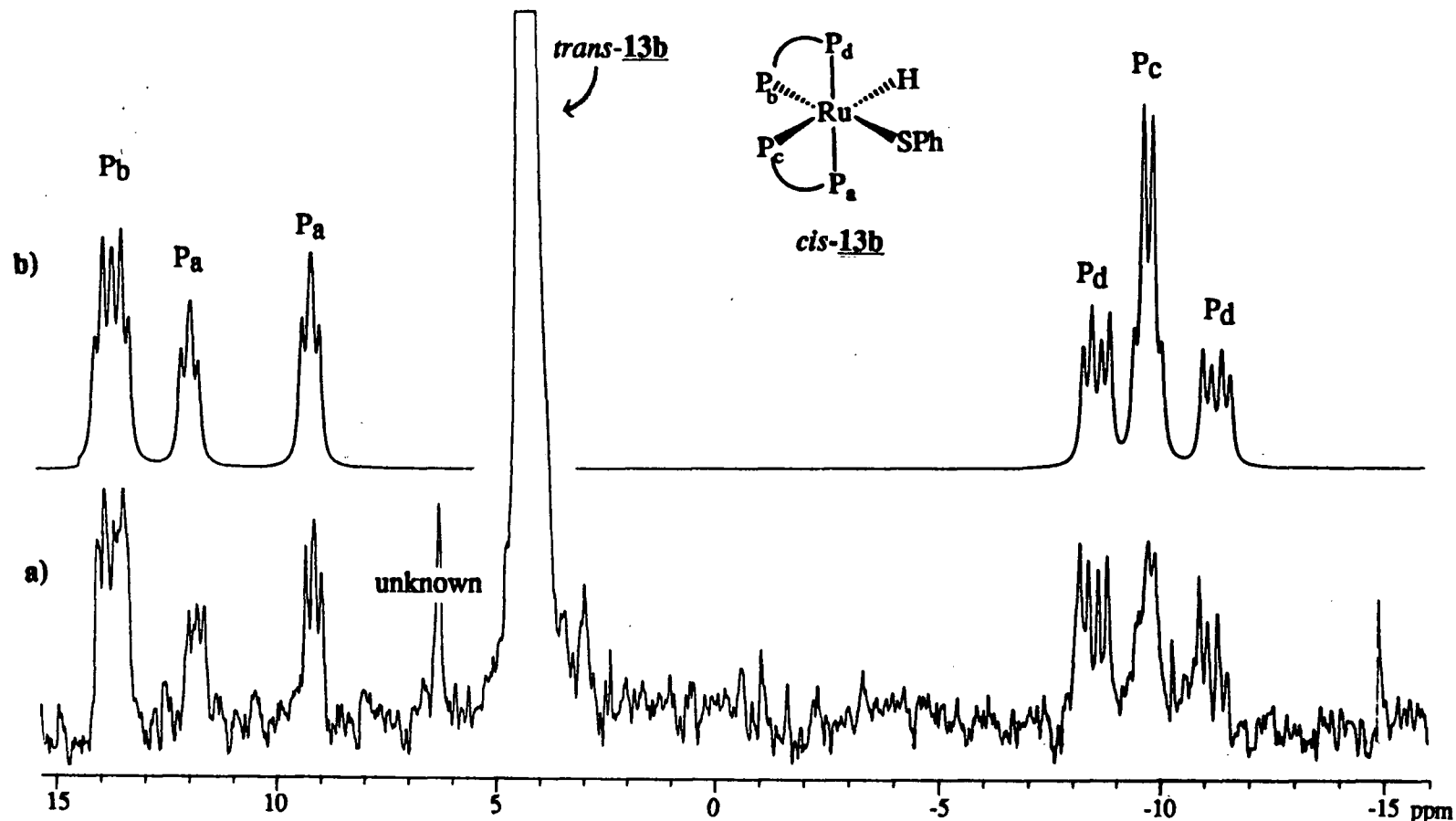


Fig. 3.23 a) $^{31}\text{P}\{^1\text{H}\}$ NMR spectrum (expanded vertical scale) of a sample of $\text{RuH}(\text{SPh})(\text{dpm})_2$ (**13b**) prepared *in situ* from $\text{RuH}_2(\text{dpm})_2$ and thiophenol in toluene- d_8 .

b) Simulated spectrum for *cis-13b*.

Table 3.7 NMR Data for Ru(X)(Y)(dpm)₂ Complexes in C₆D₆ solution.^aa) *trans* isomers

XY	³¹ P	Ru-H ^b	² J _{PH}	PCH ₂ P	SH
(H) ₂ ^c	9.11	-4.80	18.9	4.63	
H(SH) ^d	0.39	-9.46	19	4.56, 5.23	-3.55 (br)
H(SPh) ^e	-2.06	-10.86	19.9	4.27, 4.78	
H(SBz) ^d	-1.68	-10.16	20.0	4.44, 5.19	
(SH) ₂	-7.05	-	-	5.10	-3.73(t, ³ J _{PH} =5.7)

b) *cis* isomers

XY	³¹ P	² J _{pp}	Ru-H ^f	² J _{PH}	PCH ₂ P	SH
(H) ₂ ^c	14.06	28.4	-7.53	72.7, 18.3	4.10, 4.81	-
	0.57	29.6				
H(SPh) ^d	v.i.	v.i.	-6.29	92, 24, 16	n.r.	-
H(SBz) ^d	n.r.	n.r.	-7.17	101	n.r.	-
(SH) ₂	-5.93	28.5	-	-	4.62, 5.10	-1.92
	-22.65	26.5				

^a Bz=CH₂C₆H₅, n.r.=not resolved, v.i.=vide infra (the ³¹P{¹H} NMR spectrum of *cis*-RuH(SPh)(dpm)₂ is described in Section 3.4).

^b quintets.

^c The NMR spectra of RuH₂(dpm)₂ have been reported previously.¹⁸⁷
cis-RuH(SH)(dpm)₂ was not observed.

^d prepared *in situ*.

^e prepared *in situ* in toluene-d₈.

^f ddt.

al.,¹⁸⁷ the *cis:trans* ratio of a prepared sample in solution is constant over a wide range of temperatures, which suggests that the isomerization reaction is very slow or nonexistent. However, they concluded that there was a temperature-independent equilibrium between the isomers because the reactions with HBF₄/H₂O and CH₂Cl₂ gave only the *trans* isomers of the products [RuH(H₂O)(dpm)₂]⁺ and RuH(Cl)(dpm)₂, respectively. In general, complexes of the type MH₂(PR₃)₄ and MH₂L₂ (L=chelating diphosphine) are stereochemically non-rigid.²²⁸ Although the *trans*-MH₂L₂ complexes can be generated *in situ*,²²⁹ *via* deprotonation of the molecular H₂ species,



the subsequent isomerization to the *cis* complexes is rapid at room temperature. It is therefore believed that *cis*- and *trans*-7 are in equilibrium at room temperature, and one or both of them react with the proton from the thiol to form [RuH(*n*²H₂)(dpm)₂]⁺.

During the reaction with thiol, the ratio of *cis:trans* 7 does not change over time, even as the concentrations of each decline. This ratio is 6.7 (±1) : 1 (average of 11 measurements), somewhat higher than the ratio observed in the absence of thiol. This could be caused by a situation wherein the reaction of *trans*-7 with H⁺ is faster than both the reaction of *cis*-7 with H⁺ and the isomerization of *cis*-7 to *trans*-7.

The ratio of the isomers of the product is constant during the reaction (Fig. 3.24) and up to 4 h after reaction 3.7 was complete. The two isomers of RuH(SR)(dpm)₂ are possibly being formed independently by parallel reactions, or as a single isomer, the other isomer being produced by a rapid equilibrium between the isomers. The latter possibility is less likely, because other than the dihydrides, most six-coordinate compounds are non-fluxional.²²⁸

The proposed mechanism has to take into account the possible equilibrium between the isomers of the dihydride 7. Scheme 3.1 shows the suggested mechanism.

After a study of the related reaction,

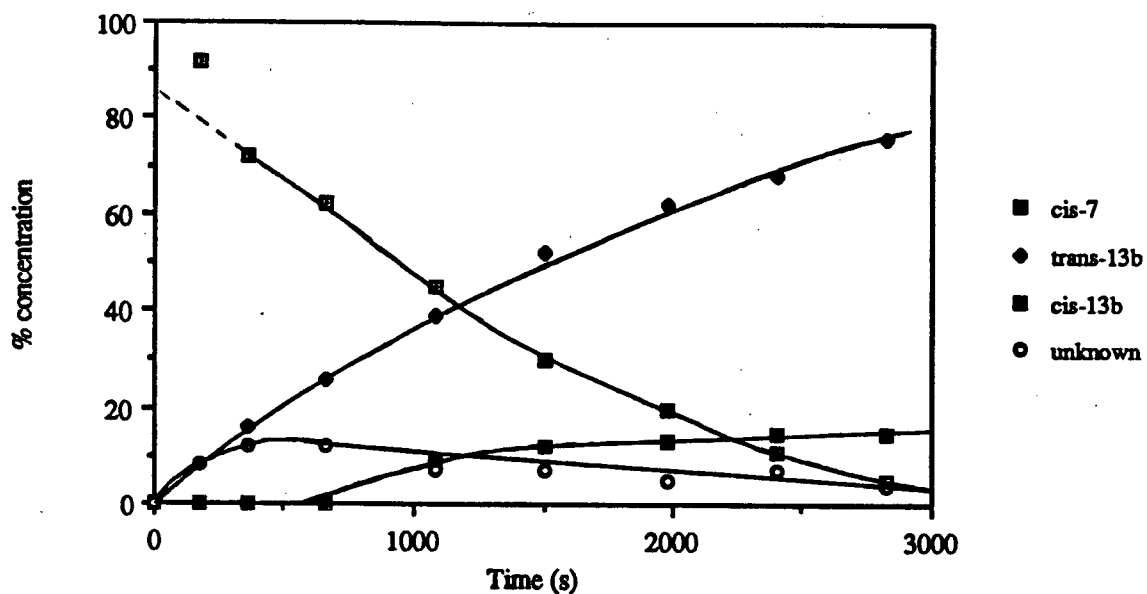


Fig. 3.24 Time dependence of concentrations during the reaction of $\text{RuH}_2(\text{dpm})_2$ (4.6 mM) with thiophenol (70 mM) in C_6D_6 at 25°C. Dashed line shows an extrapolation to the concentration of *cis*-7 in a solution of 7 in C_6D_6 .

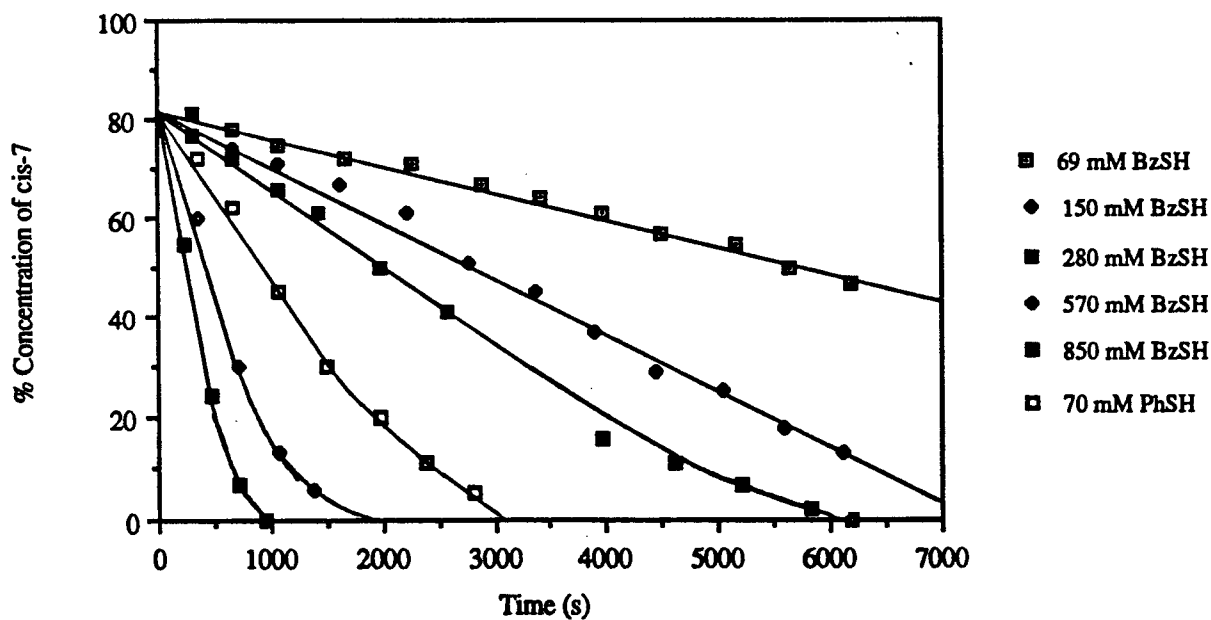
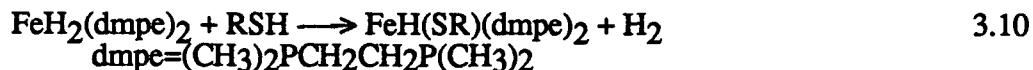
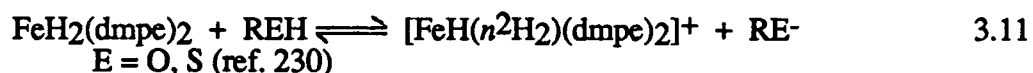


Fig. 3.25 Time dependence of the concentration of *cis*- $\text{RuH}_2(\text{dpm})_2$ (*cis*-7) in the reaction with thiols in C_6D_6 at 25°C and $[\text{7}]_0 = 4.2$ mM.

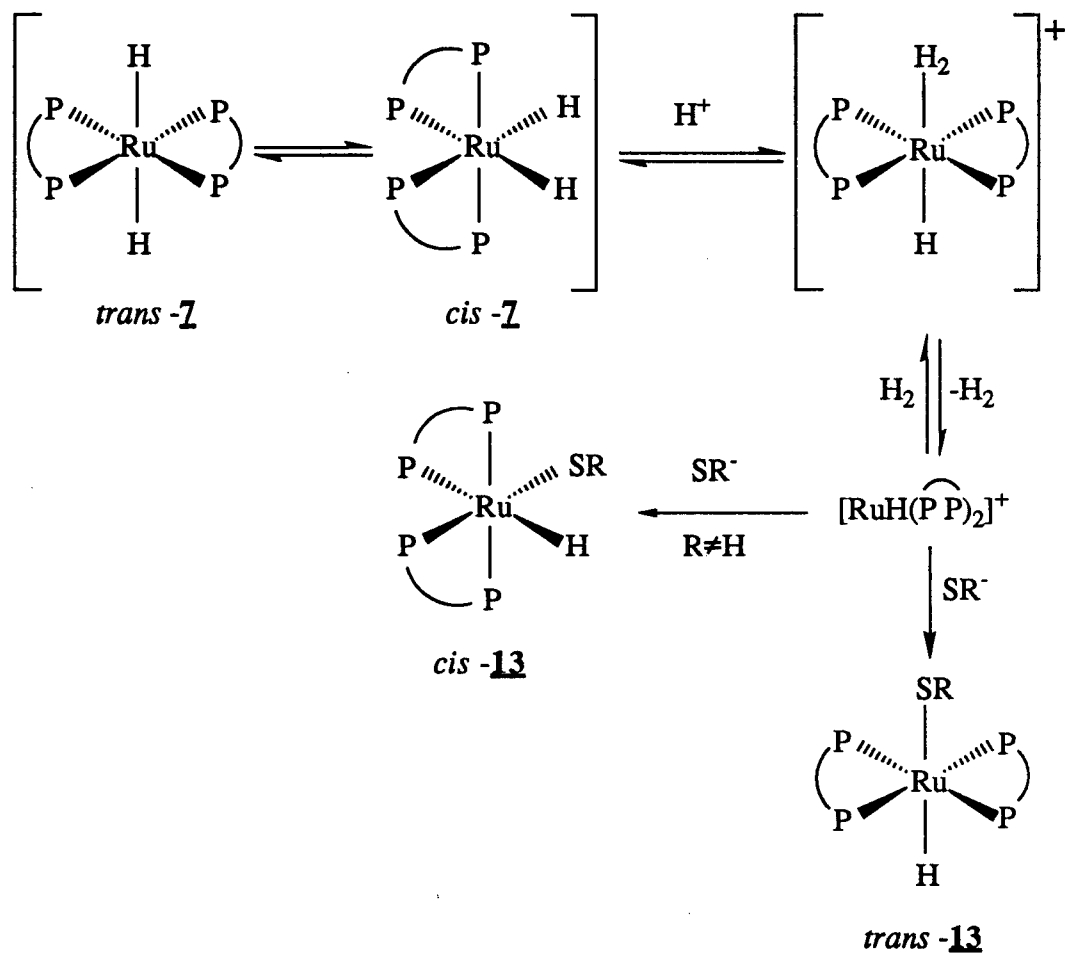


Boyd *et al.*²³⁰ proposed a mechanism analogous to that in Scheme 3.1 because they observed the intermediate *trans*-[FeH(*n*²H₂)(dmpe)₂]⁺ during the reactions with thiols²³⁰ and alcohols,²³¹ and because the hydride ligands of FeH₂(dmpe)₂ exchanged with added D₂ in the presence of alkanethiols.



In the present ruthenium system, [RuH(*n*²H₂)(dpm)₂]⁺ is not detected, although a minor intermediate is observed, which reaches a maximum concentration (in the reaction with thiophenol) of 12% after 0.5 half-lives (Figs. 3.22 and 3.24). This unknown species appears in lower concentrations in the reaction with α -toluenethiol, but not at all in the reaction with H₂S. The species also appears in the ¹H spectrum of a mixture of RuH₂(dpm)₂ and *p*-toluenesulphonic acid (Fig. 3.26). It is seen in each case as a quintet (δ -9.6 ppm, ²J_{PH} = 19.3 Hz in toluene-d₈) in the hydride region of the ¹H NMR spectrum, indicative of a complex of the type *trans*-RuH(X)(dpm)₂. The unknown is not *trans*-[RuH(H₂O)(dpm)₂]⁺, because this complex resonates at a higher field.¹⁸⁷ There was no peak in the ¹H NMR spectrum consistent with a molecular hydrogen ligand, even at lower temperatures, suggesting that the unknown is not *trans*-[RuH(*n*²H₂)(dpm)₂]⁺. An inversion-recovery experiment was designed which produces a spectrum with positive peaks for all of the protons which have T₁ relaxation times less than 60 ms. Most molecular hydrogen complexes have T₁'s of less than 100 ms at high field strengths, unless exchange is occurring with a terminal hydride ligand,²³²⁻³ and indeed such ruthenium complexes have particularly low T₁ values.^{232,234} No positive peak was observed within the range δ +10 to -10 ppm, when a spectrum was acquired with this pulse sequence during a reaction of RuH₂(dpm)₂ with PhSH. Thus, there is no direct evidence for the presence of [RuH(*n*²H₂)(dpm)₂]⁺. It is possible, however, that the *n*²H₂ peak is not observed

Scheme 3.1 Proposed mechanism for the reaction of $\text{RuH}_2(\text{dpm})_2$ with thiols, based on that proposed by Boyd *et al.*²²⁹



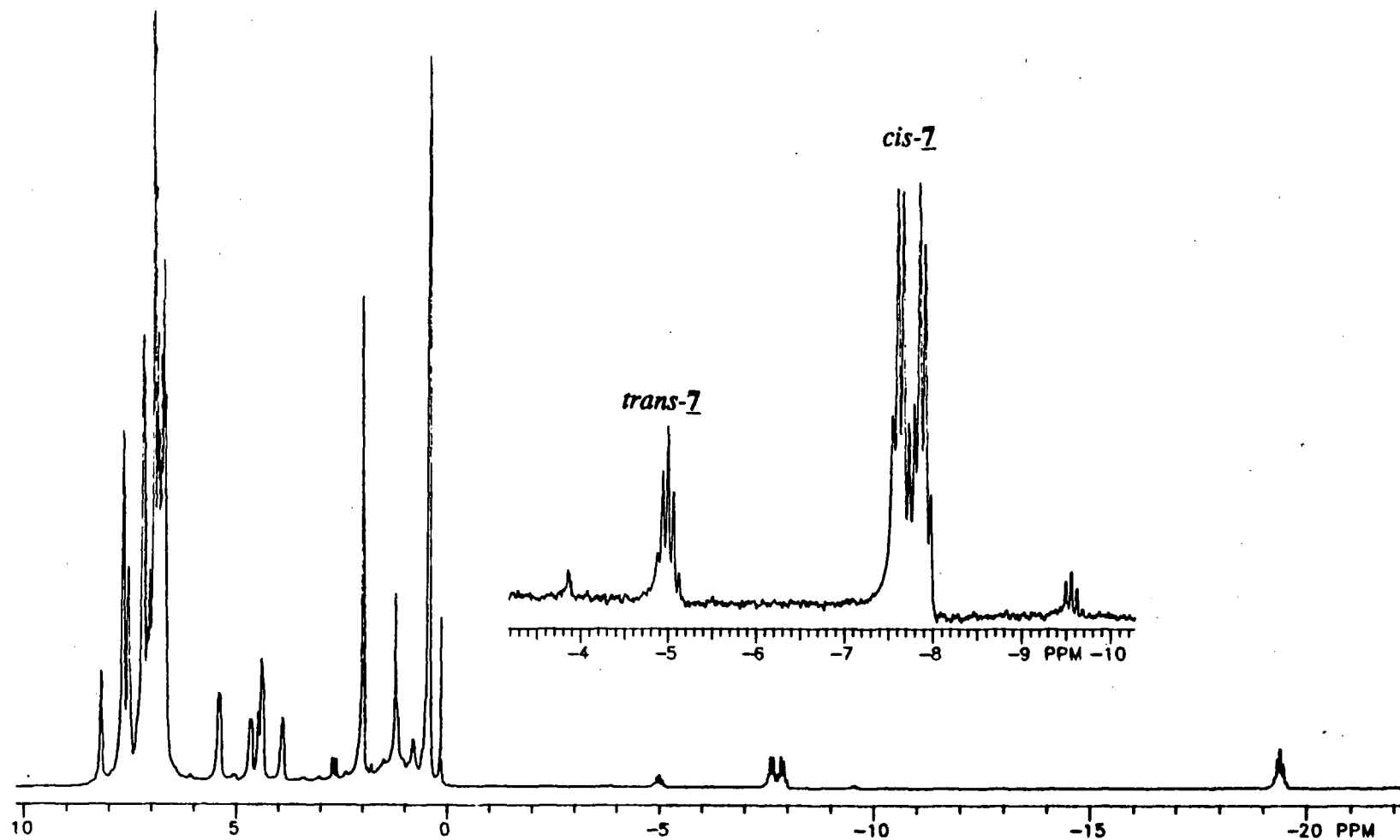
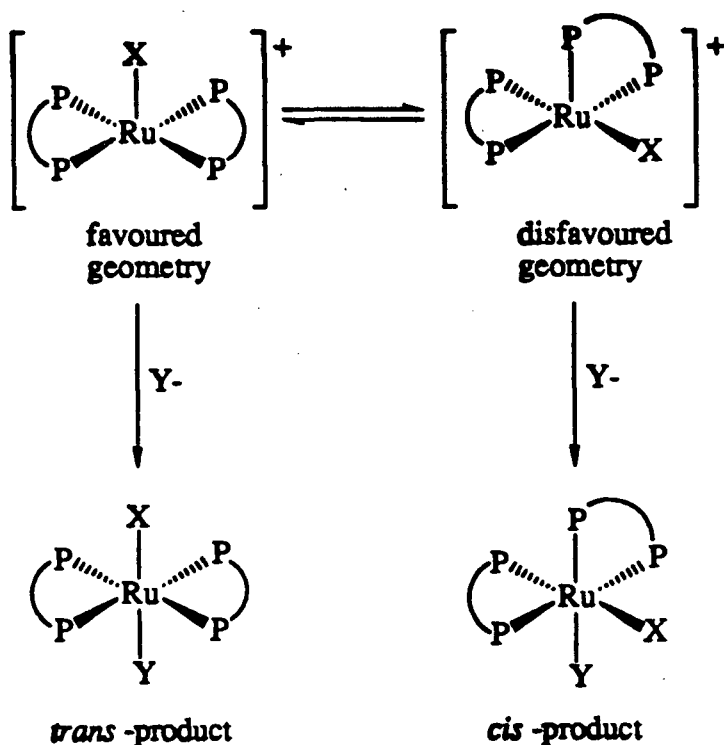


Fig. 3.26 The ^1H NMR spectrum (hydride region) acquired during the reaction of $\text{RuH}_2(\text{dpm})_2$ (7.9 mM) with *p*-toluenesulphonic acid (200 mM). The products have not been identified.

because it is broad, or that the unknown complex is $[\text{RuH}(\text{dpm})_2]^+$, in analogy to the intermediate proposed by Boyd *et al.*²³⁰

The difference in the mechanisms for the reactions of $\text{RuH}_2(\text{dpm})_2$ (**7**) and $\text{RuH}_2(\text{CO})_2(\text{PPh}_3)_2$ (**3**) with thiols is believed to result from the more basic hydride ligands of the former complex. Thus, the hydride ligands of both *cis*- and *trans*-**7** exchange with 4% CD_3OD in C_6D_6 in 10 min at room temperature, while the intensity of the hydride signals in the ^1H NMR spectrum of **3** under the same conditions does not decrease significantly even after 2 h. The exchange reaction of **7** with CD_3OD probably proceeds by an equilibrium analogous to reaction 3.11. The acidity of $n^2\text{H}_2$ complexes is decreased by increased electron density at the metal centre.^{229,235} Such complexes containing electron-withdrawing ancillary ligands, such as $[\text{Ru}(n^5\text{C}_5(\text{CH}_3)_5)(n^2\text{H}_2)(\text{CO})_2]^+$ ($pK_a = -5$)²³⁶ are much more acidic than complexes containing electron-donating ligands such as $[\text{Ru}(n^5\text{C}_5\text{H}_5)(n^2\text{H}_2)(\text{dpm})]^+$ ($pK_a = 7.1$).²³⁵ Complex **3** is probably insufficiently basic to be protonated by a thiol.

Why is the *trans* isomer of $\text{RuH}(\text{X})(\text{dpm})_2$ observed exclusively ($\text{X}=\text{SH}$ and BH_4 in this work, H_2O ¹⁸⁷ and Cl ¹⁸⁷), or predominantly ($\text{X}=\text{SPh}$ and SBz), but $\text{RuH}_2(\text{dpm})_2$ is predominantly *cis*? This tendency of $\text{RuH}(\text{X})(\text{dpm})_2$ to exist solely or predominantly as a *trans* complex has been noted previously.²³⁷ Of the complexes of this type, it is likely that only $\text{RuH}_2(\text{dpm})_2$ is fluxional in solution at room temperature, although the process is slow on the NMR time-scale. Its geometry therefore depends on thermodynamic factors such as steric interactions between PPh_2 groups (favouring *trans*), and the *trans*-influence of the hydride ligands (favouring *cis* geometry). Obviously, the latter effect is stronger; of the 12 dihydrido phosphine ruthenium complexes studied by Meakin *et al.*,²²⁸ nine are exclusively *cis* in solution, and the other three are predominantly *cis*. The remaining $\text{RuX}(\text{Y})(\text{dpm})_2$ complexes, with the possible exception of $\text{RuH}(\text{BH}_4)(\text{dpm})_2$, are probably geometrically rigid. The factors which determine the observed geometry are therefore kinetic rather than thermodynamic, and depend on the mechanism of the formation reaction. The preponderance of *trans* products is

Scheme 3.2 A partial mechanism for the formation of RuX(Y)(dpm)₂ complexes.

consistent with mechanisms involving 5-coordinate square-pyramidal $[\text{RuX}(\text{dpm})_2]^+$ intermediates. Of the two possible geometries for such intermediates, that with 4 rather than 3 equatorial phosphines is sterically favoured. The *trans* product is therefore expected to be the major product (Scheme 3.2), unless Y or X is large. If X is large, then the other intermediate will be favoured, and a *cis* product obtained. If Y is large, then the reaction yielding the *trans*-product will be slower than the reaction yielding the *cis*-product.

3.5 THE THIOL EXCHANGE REACTIONS OF *cct*-RuH(SR)(CO)₂(PPh₃)₂

The title complexes (9) exchange with added thiols.



3.12

For example, the reaction of *cct*-RuH(SEt)(CO)₂(PPh₃)₂ (**9d**) with thiophenol generates *cct*-RuH(SPh)(CO)₂(PPh₃)₂ (**9i**) and free ethanethiol; both products are detected by ¹H NMR spectroscopy (Fig. 3.27).

The reaction of *cct*-RuH₂(CO)₂(PPh₃)₂ (**3**) with a mixture of 5 equivalents each of ethanethiol and thiophenol initially produces a mixture of **9i** and **9d**, but the final product is almost exclusively **9i**. The reactions of **3** with various binary mixtures of thiols were monitored by ¹H and/or ³¹P{¹H} NMR spectroscopy in C₆D₆ at 50°C (Fig. 3.28) to determine the equilibrium constants for reaction 3.12. The observed equilibrium constants (±10%) are 2.2 (R/R'=C₆H₄*p*CH₃/C₆H₅), 71 (CH₂CH₃/C₆H₅), and 8.4 (CH₂CH₃/CH₂C₆H₅). To confirm that equilibrium had been reached, the equilibrium between **9i** and **9d** (R/R'=CH₂CH₃/C₆H₅) was approached from the "other side" by adding EtSH to a solution of **9i**. After one hour, no further reaction was detected. Although equilibrium may not have been reached in this experiment, the *K*_{obs} value calculated from the results (83) serves as an upper limit for *K*_{eq}.

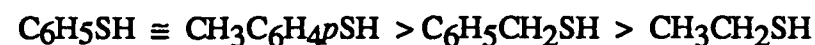
Comparisons of the thermodynamic stability of complexes of the formula *cct*-RuH(SR)(CO)₂(PPh₃)₂ (**9**) can be more easily made if the equilibrium constants are recalculated as *K*_{eq} values for reaction 3.12 where R=Et.

$$K_{eq} = \frac{[\text{RuH}(\text{SR}')(\text{CO})_2(\text{PPh}_3)_2][\text{EtSH}]}{[\text{RuH}(\text{SEt})(\text{CO})_2(\text{PPh}_3)_2][\text{R}'\text{SH}]}$$

These *K*_{eq} values decrease in the following order:

$$\begin{array}{cccc} \text{R}' = \text{C}_6\text{H}_5 & > & \text{C}_6\text{H}_4\text{pCH}_3 & > & \text{CH}_2\text{C}_6\text{H}_5 & > & \text{CH}_2\text{CH}_3 \\ K_{eq} = 71 & & 32 & & 8.4 & & 1 \end{array}$$

It is clear that the thermodynamic stability of **9** depends on the nature of the thiolate group, the aryl thiolato complexes being more stable than the alkyl thiolato complexes. This order of stability is similar to the order of acidity of the free thiols in aqueous solution,



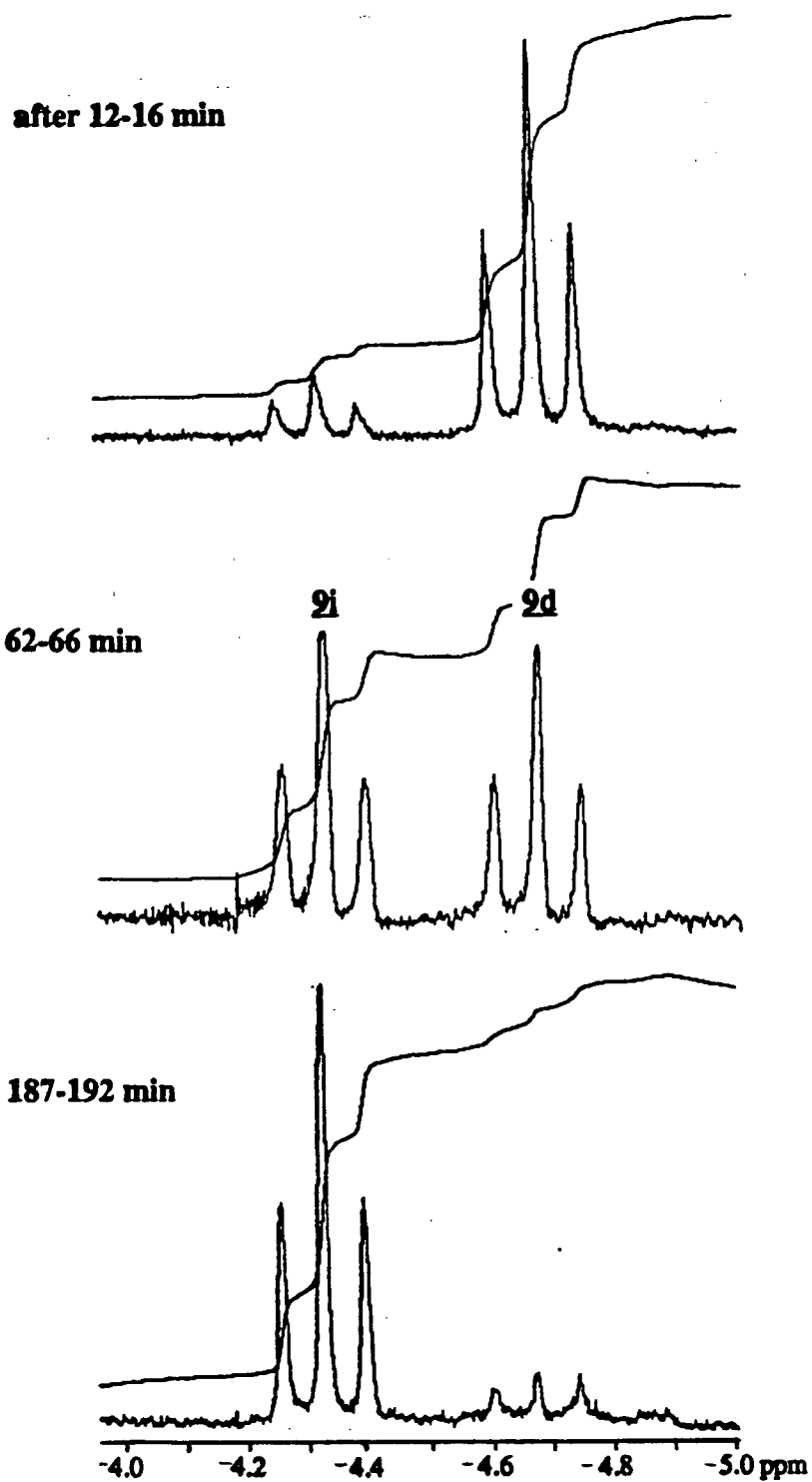


Fig. 3.27 ^1H NMR spectra acquired during the reaction of *cct*- $\text{RuH}(\text{SET})(\text{CO})_2(\text{PPh}_3)_2$ (8 mM) with thiophenol (1500 mM) in C_6D_6 at 22°C .

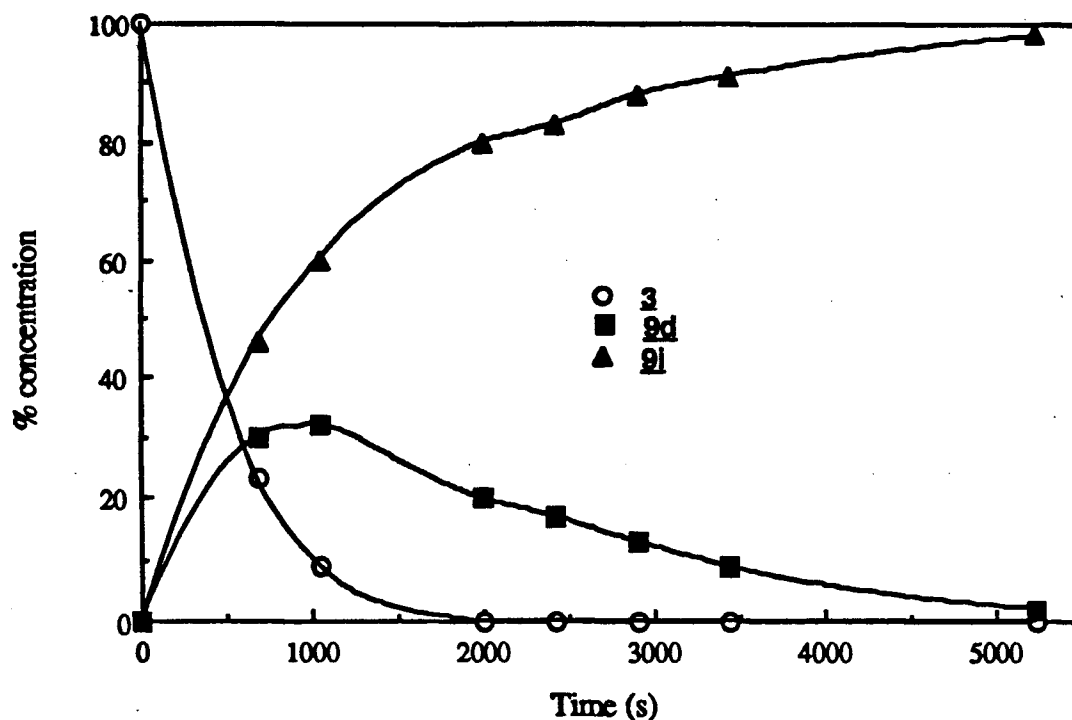


Fig. 3.28 Time dependence of concentrations during the reaction of *cct*-RuH₂(CO)₂(PPh₃)₂ (9.9 mM) with PhSH (1.6 M) and EtSH (2.5 M) in C₆D₆ at 36°C.

Table 3.8 Published *pK_a* Values for Selected Thiols in Aqueous Solution.

Thiol	<i>pK_a</i>	T(°C)	Ref.
H ₂ S	7.0	25	238
	7.0	25	239
	7.04	18	240
	7.06	25	241
	7.24	25	242
CH ₃ SH	10.70	25	243
CH ₃ CH ₂ SH	9.61	25	245
	10.50	20	244
	10.60	25	242
	10.61	25	243
(CH ₃) ₂ CHSH	10.9	25	239
	10.86	25	243
C ₆ H ₅ CH ₂ SH	9.4	25	239
	10.7	25	243
C ₆ H ₅ SH	6.43	25	245
	6.5	25	239
	7.78	20	244
	7.8	a	246
	8.3	25	242
CH ₃ C ₆ H ₄ <i>o</i> SH	6.64	25	243
CH ₃ C ₆ H ₄ <i>m</i> SH	6.58	25	243
CH ₃ C ₆ H ₄ <i>p</i> SH	6.52	25	243
C ₆ F ₅ SH	2.68	25	245

a not available.

although the published values of the pK_a 's of thiols show some variation; the value for thiophenol in particular varies widely (Table 3.8). The most stable complexes in the series **9** are those with the least basic thiolate ligands. The reason for this trend is not known. The same type of relationship between the acidity of a free thiol and its tendency to replace a thiolate ligand was observed by Que *et al.*,²⁴⁷ during studies of the thiol exchange reactions of an iron tetramer.



They noted that acidity is not the only factor involved. For example, sulphur ligands such as ethanethiolate bind much more strongly than oxygen ligands such as *p*-cresolate, despite the fact that the two reagents are equally basic.

The *pseudo*-first order rate constant for the forward step of the reaction of **9d** with thiophenol (reaction 3.12, R=Et, R'=Ph) in C_6D_6 at $22(\pm 1)^\circ\text{C}$ is essentially independent of **[9d]**. The rate constant is $1.9 \times 10^{-4} \text{ s}^{-1}$ at 1.8 mM **9d** (single result) and $2.0(\pm 0.2) \times 10^{-4} \text{ s}^{-1}$ at 9 mM (average of 4 results). The *pseudo*-first order log plot of **[9d]** is linear for 3 half-lives (Fig. 3.29). The rate is also independent of the thiophenol concentration (Fig. 3.30) over the range 0.12 M to 3.4 M.

$$\frac{-d[\mathbf{9d}]}{dt} = k[\mathbf{9d}]$$

The rate constants and rate law are identical for the reactions of **9** with R'SH (reaction 3.12), with CO (Section 6.1.2), and with $\text{P}(\text{C}_6\text{H}_4\text{pCH}_3)_3$ (Section 6.1.1). The mechanisms for all three of these reactions are thought to begin with elimination of PPh_3 , followed by coordination of R'SH, CO, or $\text{P}(\text{C}_6\text{H}_4\text{pCH}_3)_3$, respectively. If this is the case, then the mechanism for reaction 3.12 may be that in Scheme 3.3. The expected rate law, assuming that the back reactions with rate constants k_{-2} and k_{-3} are negligible, and reaction step k_4 is rapid, is

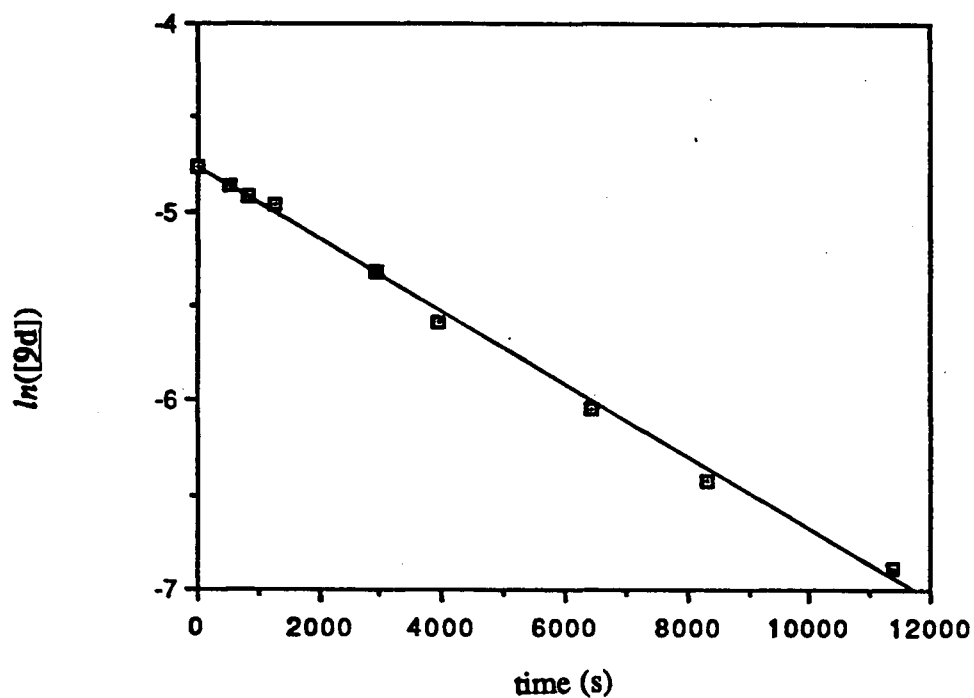


Fig. 3.29 Logarithmic plot of the concentration of **9d** versus time during the reaction of *cct*-RuH(SEt)(CO)₂(PPh₃)₂ (**9d**, 8.5 mM) and PhSH (1.5 M) in C₆D₆ at 22°C.

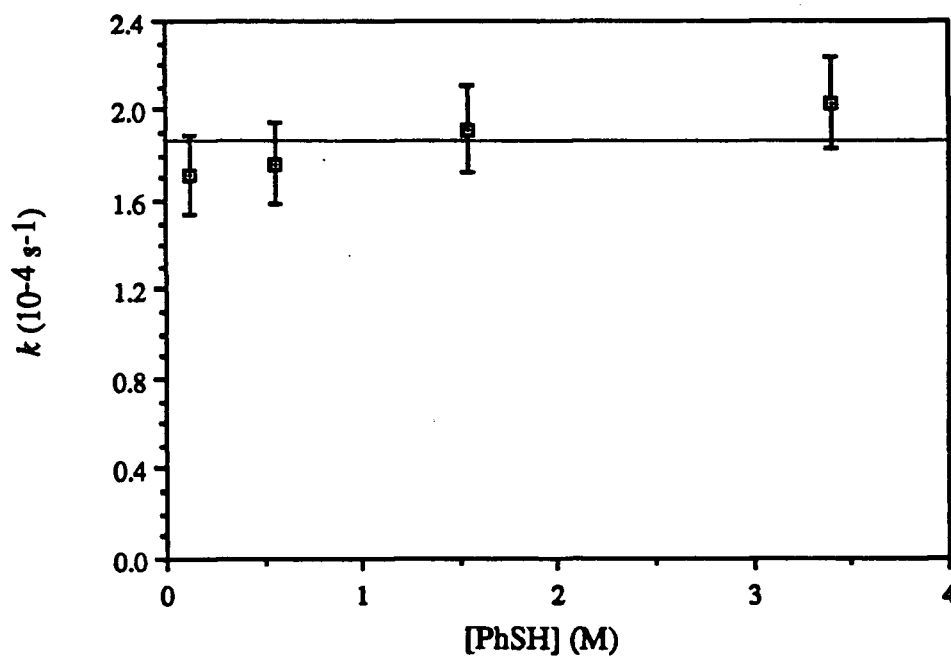
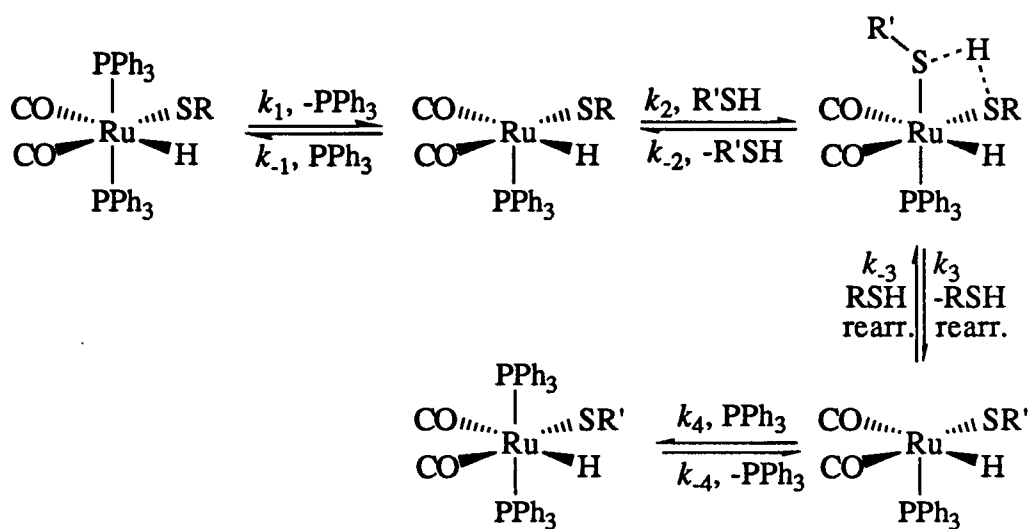


Fig. 3.30 Dependence of the pseudo-first order rate constant on [PhSH] for the reaction with *cct*-RuH(SEt)(CO)₂(PPh₃)₂ (9 mM) in C₆D₆ at 22°C. Bars indicate estimated error (10 %) on individual measurements of k .

Scheme 3.3 The proposed mechanism for the reaction of $\text{RuH}(\text{SR})(\text{CO})_2(\text{PPh}_3)_2$ (**2**) with $\text{R}'\text{SH}$.



$$\text{rate} = \frac{k_1 k_2 [\mathbf{9}][\text{R}'\text{SH}]}{k_{-1}[\text{PPh}_3] + k_2[\text{R}'\text{SH}]}$$

or, if $k_{-1}[\text{PPh}_3] \ll k_2[\text{R}'\text{SH}]$,

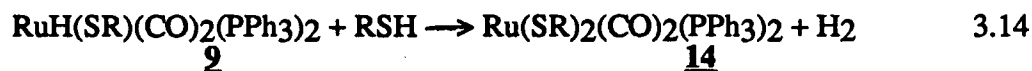
$$\text{rate} = k_1[\mathbf{9}]$$

as observed. If PPh₃ were added in sufficiently high concentrations, then a decrease in the rate would be observed. In fact, only a small decrease in the rate constant (2.1×10^{-3} , 1.7×10^{-3} , and $1.8 \times 10^{-3} \text{ s}^{-1}$ ($\pm 10\%$) at [PPh₃]=0, 260, and 660 mM, respectively) is observed for the reaction of **9c** (R=Me, [**9**]₀=6 mM) with PhSH (80 mM) in C₆D₆, monitored by NMR spectroscopy at 40°C. This result suggests that $k_{-1} \ll k_2$.

The thiol proton in the proposed intermediate [RuH(SR)(RSH)(CO)₂(PPh₃)] may be equally bonded to the two sulphur atoms, in the same way as the sodium atom in the complex [Ru(CO)₂(PPh₃)(μSEt)₂(μ₃SEt)Na(THF)]₂ (Section 5.2) is shared by three sulphurs on the same ruthenium centre. Similar sharing of a proton by a thiolate and a chloride ligand on the same metal centre is observed in the complex Ru(HCl)(buS₄)(PPh₃) (buS₄²⁻ = 1,2-bis((3,5-di-*tert*-butyl-2-mercapto-phenyl)thio)ethanato(2-)).²⁴⁹ The structure of this complex is shown in Section 7.2.

3.6 THE SLOWER REACTION OF RuH(SR)(CO)₂(PPh₃)₂ WITH H₂S AND THIOLS

The reactions of free R'SH with RuH(SR)(CO)₂(PPh₃)₂ (**9**) result in substitution, by R'S-, of either the thiolate ligand (reaction 3.12), or the hydride ligand (reaction 3.14). The latter reaction, which is significantly slower, forms a *bis*-thiolato complex (**14**, Section 4.2).



The new complex **14** can therefore be prepared in one "pot," *via* **9**, from the reaction of Ru(CO)₂(PPh₃)₃ (**2**) or RuH₂(CO)₂(PPh₃)₂ (**3**) with thiols. For example, **2** reacts with excess

PhSH in THF at room temperature to produce $\text{RuH(SPh)(CO)}_2(\text{PPh}_3)_2$ within 5 min (100% conversion, reaction 3.3), and $\text{Ru(SPh)}_2(\text{CO)}_2(\text{PPh}_3)_2$ after 3 days (46%, reaction 3.14).

Because of the extremely slow rate of reaction 3.14 and the further reaction of **14** ($\text{R} \neq \text{H}$) under conditions of heat or light (Chapter 6), reaction 3.14 was not successfully monitored kinetically or used as the synthetic route to **14** (except for $\text{R} = \text{H}$). As Chapter 4 describes, the reaction of disulphides with $\text{Ru(CO)}_2(\text{PPh}_3)_3$ is the preparative route of choice for **14** ($\text{R} = \text{aryl}$). The characterization of **14** is therefore described in that chapter.

The reaction of **3** with acetic acid²⁵⁰



probably proceeds *via* $\text{RuH(OAc)(CO)}_2(\text{PPh}_3)_2$, if the chemistry is analogous to that observed with thiols. However, there was no mention, in the report, of any attempt to detect or isolate the acetato(hydrido)-intermediate, which has since been observed in the present work (Chapter 2).

Reaction 3.14 ($\text{R} = \text{H}$) was followed by NMR spectroscopy at 60°C (Fig. 3.31). The starting material, $\text{RuH(SH)(CO)}_2(\text{PPh}_3)_2$ (**9a**), is easily generated *in-situ* by the reaction of **3** with excess H_2S at 60°C for 3 min. The **9a** thus generated reacts with H_2S more slowly. After 40 min (almost 2 half-lives), free PPh_3 is observed, indicating some decomposition or side-reaction is occurring. Up to this point, the reaction has a half-life of approximately 1400 s, assuming *pseudo*-first order behaviour. For comparison, reaction 3.4 (which forms **9** from $\text{RuH}_2(\text{CO})_2(\text{PPh}_3)_2$ and H_2S or RSH) has a half-life of 24 s at this temperature in THF (calculated by extrapolation of data acquired between 26 and 46°C).

Although these preliminary data do not include the dependence of the rate on $[\text{H}_2\text{S}]$, it is possible to speculate on the mechanism of reaction 3.14. Reductive elimination of thiol from $\text{RuH(SR)(CO)}_2(\text{PPh}_3)_2$ cannot be the first step, as this would subsequently lead to the re-formation of the starting material (i.e. no reaction would occur). The first steps of three possible mechanisms are protonation of the hydride (Scheme 3.4), elimination of PPh_3 (Scheme 3.5), or (less likely) elimination of CO.

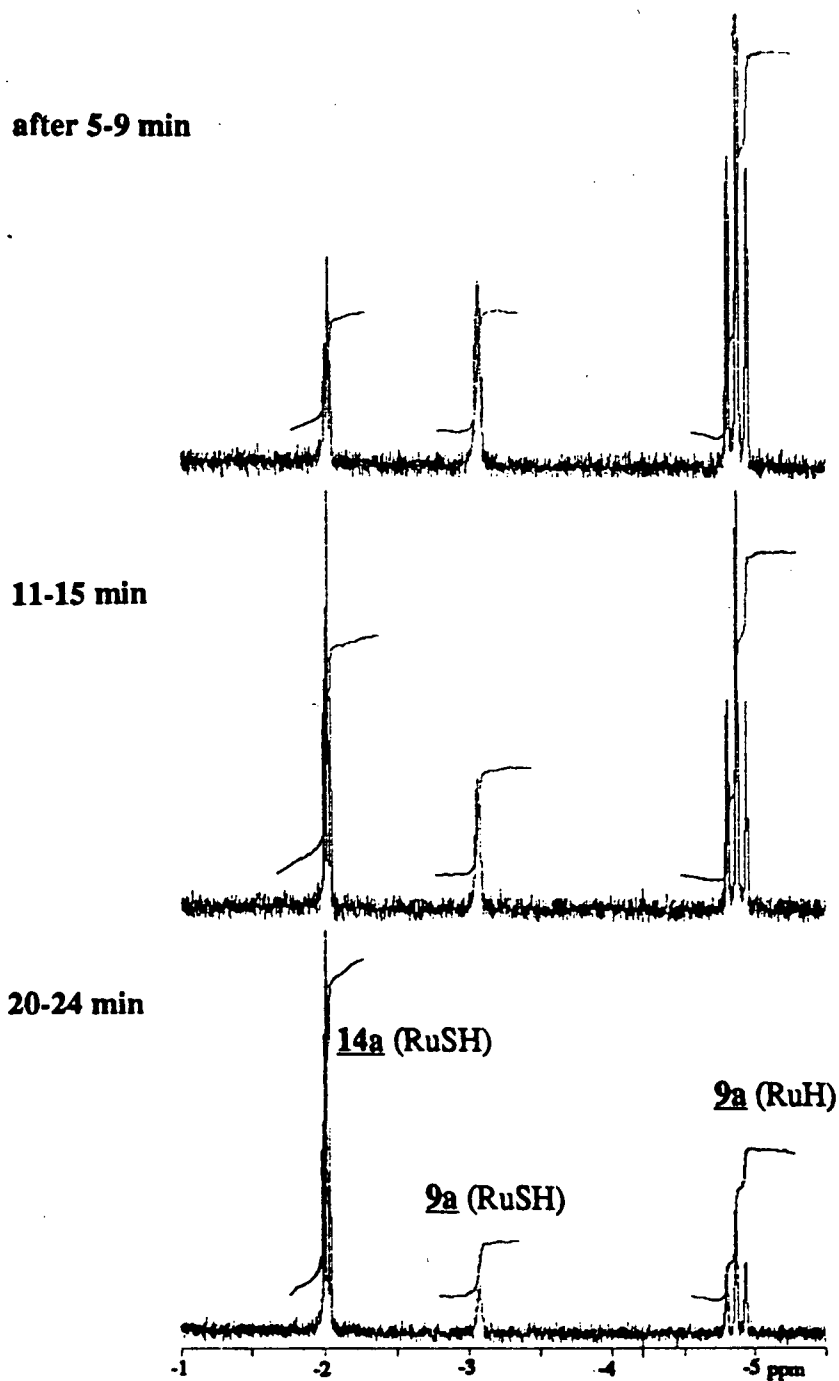
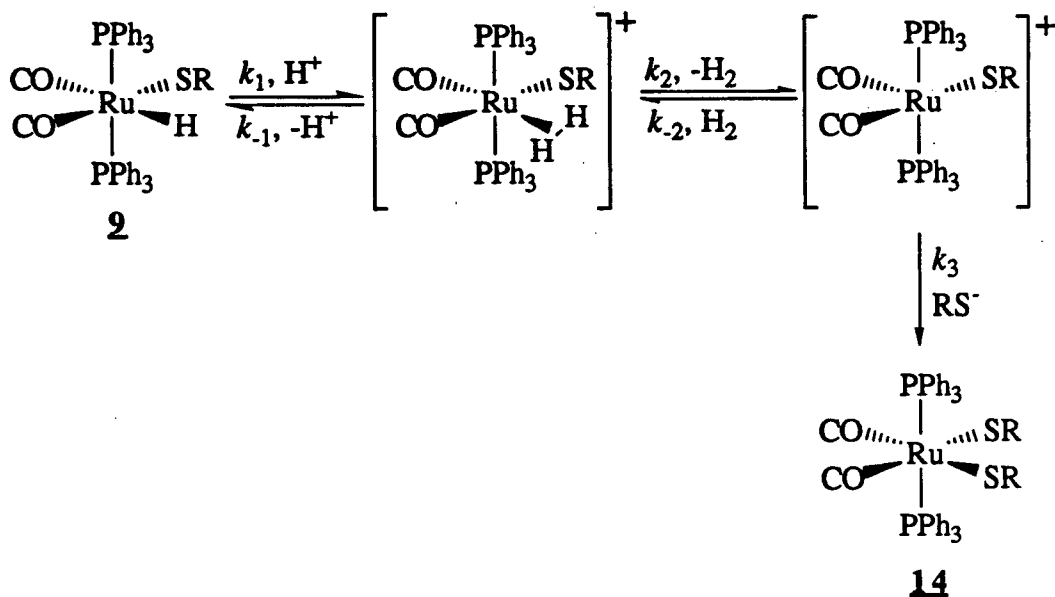
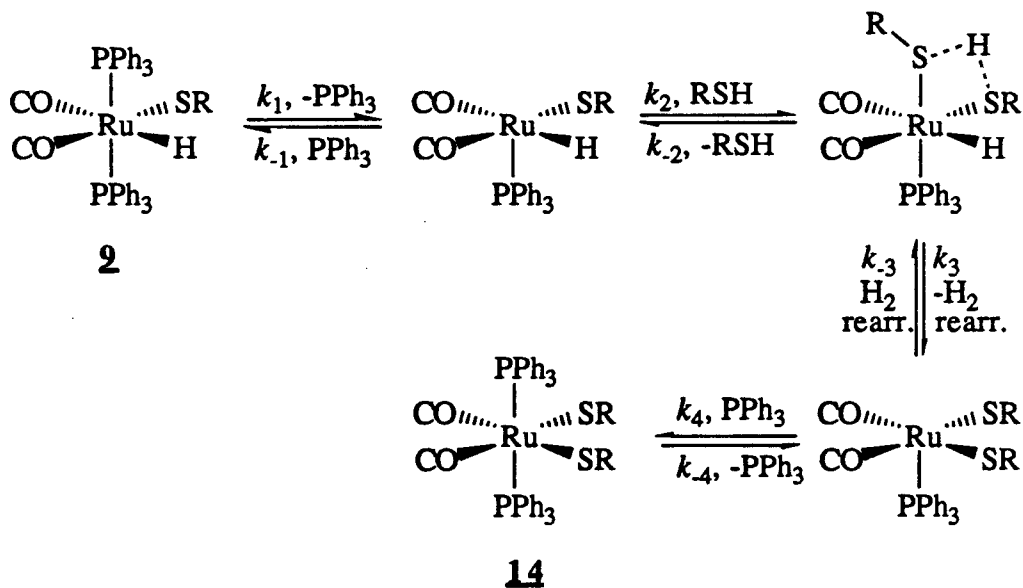


Fig. 3.31 ^1H NMR spectra acquired during the reaction of *cct*-RuH(SH)(CO) $_2$ (PPh $_3$) $_2$ (9a) with H $_2$ S in C $_6$ D $_6$ at 60°C.

Scheme 3.4 A mechanism for the reaction of $\text{RuH}(\text{SR})(\text{CO})_2(\text{PPh}_3)_2$ (**9**) with RSH , in which the first step is protonation of the hydride.



Scheme 3.5 A possible mechanism for the reaction of $\text{RuH}(\text{SR})(\text{CO})_2(\text{PPh}_3)_2$ (**9**) with RSH , in which the first step is dissociation of PPh_3 from the complex.



The first of these mechanisms involves the formation of a molecular hydrogen complex, $[\text{Ru}(\eta^2\text{H}_2)(\text{SR})(\text{CO})_2(\text{PPh}_3)_2]^+$. Two types of experiments to detect this complex or the chloro analogue were performed.

a) The reactions of acids such as alcohols,²⁵¹ $\text{HBF}_4/\text{Et}_2\text{O}$,^{192,236} and $\text{H}_2\text{C}(\text{SO}_2\text{CF}_3)_2$ ²⁵² have been used to protonate hydrides to form molecular hydrogen complexes. Attempts at the protonation of $\text{RuH}(\text{SC}_6\text{H}_4\text{pCH}_3)(\text{CO})_2(\text{PPh}_3)_2$ by $\text{HBF}_4/\text{Et}_2\text{O}$, $\text{HBF}_4/\text{H}_2\text{O}$ or HCl (aqueous) failed to produce evidence of a molecular hydrogen complex (Section 6.1.5).

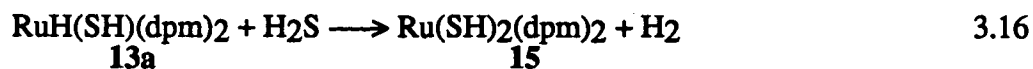
b) Metathesis reactions of transition metal chloro-complexes with NaBPh_4 under H_2 gas have also been used to generate molecular hydrogen complexes.²⁵³ A mixture of $\text{RuCl}_2(\text{CO})_2(\text{PPh}_3)_2$ and NaBPh_4 in acetone under H_2 was passed through diatomaceous earth after reacting at room temperature for 90 min, and a white solid was precipitated by removal of some of the solvent under vacuum. The $^{31}\text{P}\{^1\text{H}\}$ NMR spectrum shows that the only phosphorus-containing compound in the recovered solid was $\text{RuCl}_2(\text{CO})_2(\text{PPh}_3)_2$.

The failure to produce a $\eta^2\text{H}_2$ complex may result from the insufficient basicity of the hydride ligand of **9**. As described in Section 3.4, the presence of carbonyl ligands greatly decreases the basicity of hydrido-complexes. The intermediate $\eta^2\text{H}_2$ complex shown in Scheme 3.4 is therefore unlikely.

The mechanisms which involve initial loss of CO or PPh_3 do not require a $\eta^2\text{H}_2$ complex as an intermediate. Because the phosphine ligands of **9** are known to be labile (Section 6.1.1), the latter mechanism (Scheme 3.5) is considered more likely. It involves the same initial steps and the same intermediate, $[\text{RuH}(\text{SR})(\text{RSH})(\text{CO})_2(\text{PPh}_3)]$, which were proposed for the reaction of **9** with $\text{R}'\text{SH}$ (reaction 3.12, Scheme 3.3). The intermediate therefore represents the branching point of the two reactions. If thiol is eliminated (which is statistically favoured), then the product will be **9**; if H_2 is eliminated, then the product will be $\text{Ru}(\text{SR})_2(\text{CO})_2(\text{PPh}_3)_2$ (**14**).

3.7 THE REACTION OF RuH(SH)(dpm)₂ WITH H₂S

The title complex (**13**) probably undergoes thiol exchange reactions in a manner similar to reaction 3.12, although experiments to confirm this were not performed. The title complex also reacts with H₂S and presumably other thiols to produce a *bis*-thiolate complex (**15**, cf. reaction 3.14).



The reaction of *trans*-RuH(SH)(dpm)₂ (**13a**) with H₂S was monitored by NMR spectroscopy (Fig. 3.32). A C₆D₆ solution of RuH₂(dpm)₂ (7.4 mM) under H₂S (1 atm) reacts within 3 min at 60°C to form **13a**, which reacts more slowly (T_{1/2} = 20 min) to form a 1:1.8 mixture of *cis*- and *trans*-**15**. The H₂ produced in the reaction was detected by ¹H NMR spectroscopy. The rate of disappearance of the hydride signal of **13a** is *pseudo*-first order, with a log plot linear over more than 3 half-lives (Fig. 3.33). The rate dependence on [H₂S] was not determined.

The ¹H NMR spectrum of **15** in C₆D₆ (Fig. 3.32) contains two signals at -1.92 and -3.74 ppm for the *cis* and *trans* isomers, respectively. The former signal is a complicated multiplet, but the latter is a simple quintet (³J_{PH}=5.6 Hz) due to the *cis* coupling of the SH group of *trans*-**15** to four equivalent phosphorus atoms. The methylene signal of the *trans* complex appears at 5.10 ppm, while the *cis* complex has two methylene multiplets: one at 4.62 and the other under the peak at 5.10 ppm.

The ³¹P{¹H} NMR spectrum of the *cis/trans* mixture (Fig. 3.34) contains a singlet (*trans*-**15**) at -7.05 ppm, and two triplets (*cis*-**15**) at -5.93 (2J_{pp}=28.5 Hz) and -22.65 ppm (2J_{pp}=26.5 Hz).

As previously mentioned, six-coordinate complexes are generally not fluxional. Although iron(II) and ruthenium(II) phosphine dihydrides have been found to be exceptions,²²⁸ there is no reason to suppose that **15** is fluxional. In fact, the observation of a different *cis:trans* ratio (2:1) in the filtrate from reaction 3.16²⁵⁴ shows that the isomerization reactions between the isomers of **15** are slow at room temperature.

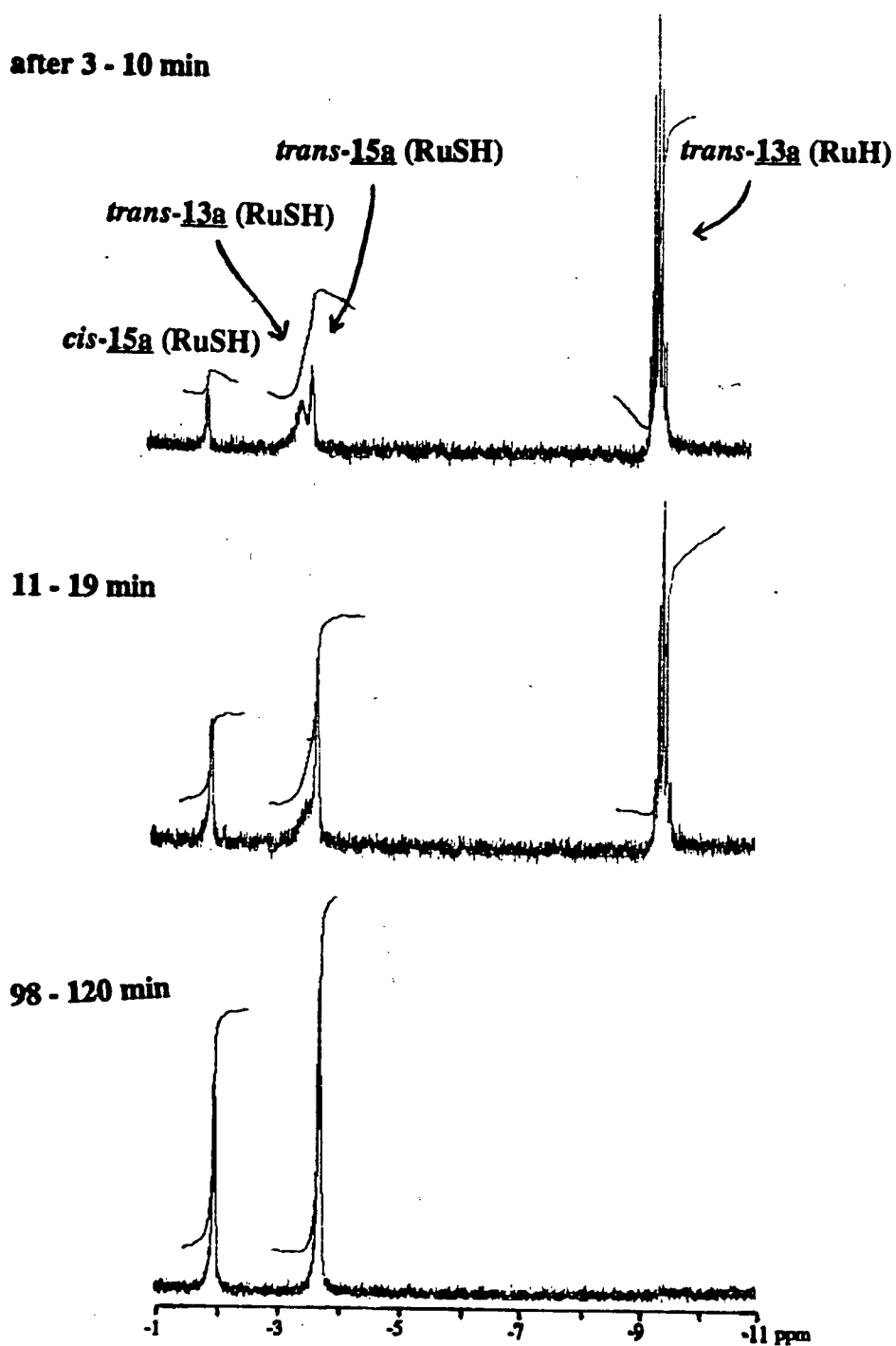


Fig. 3.32 a) ^1H NMR spectra (hydride region) acquired during the reaction of RuH(SH)(dpm)_2 (13a, 7.4 mM) with H_2S in C_6D_6 at 60.0°C .

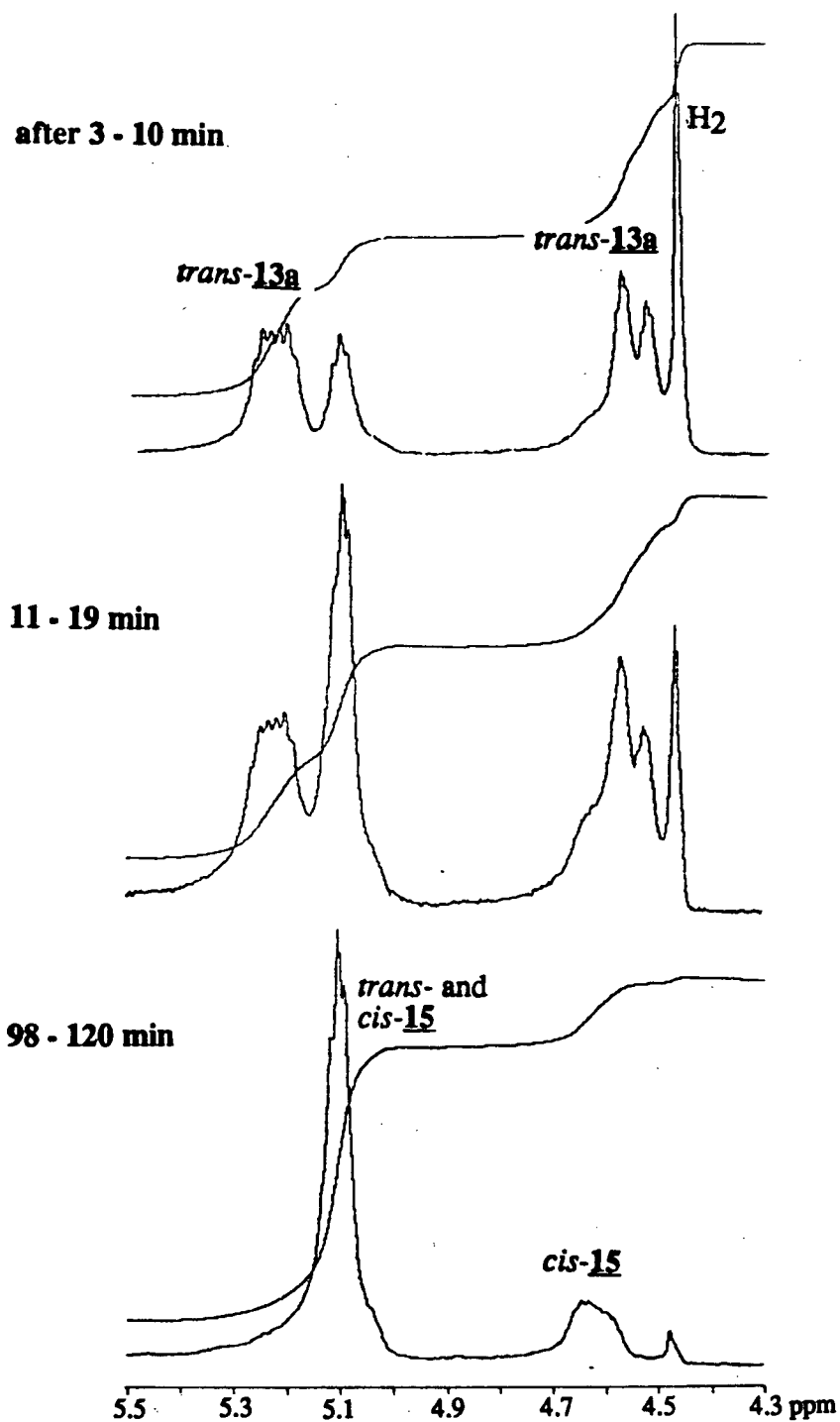


Fig. 3.32 b) ¹H NMR spectra (methylene region) acquired during the reaction of RuH(SH)(dpm)₂ (13a, 7.4 mM) with H₂S in C₆D₆ at 60.0°C.

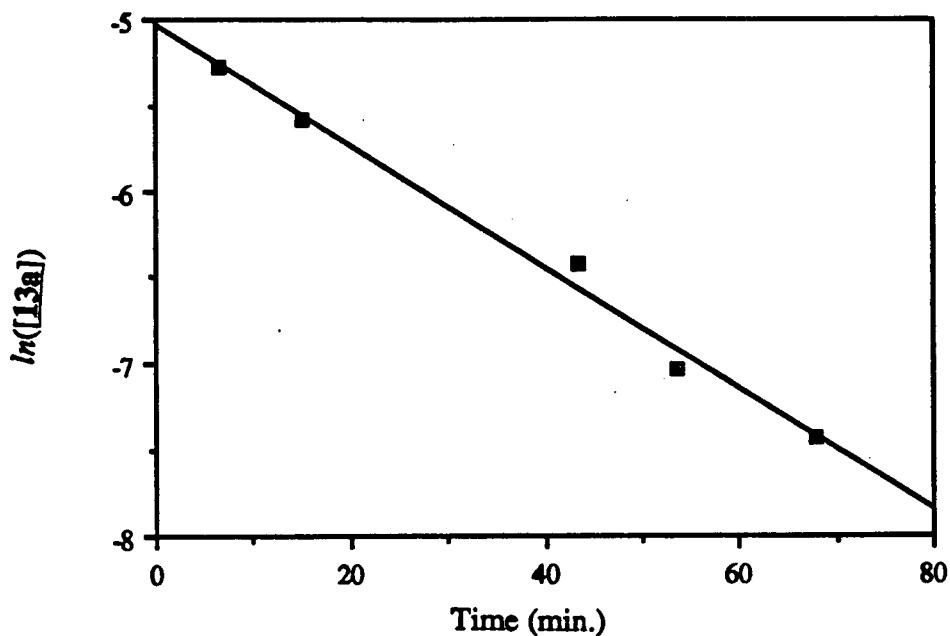


Fig. 3.33 Logarithmic plot of concentration of *trans*-RuH(SH)(dpm)₂ (**13a**) during the reaction of that compound (7.4 mM) with H₂S (1 atm) at 60.0°C in C₆D₆.

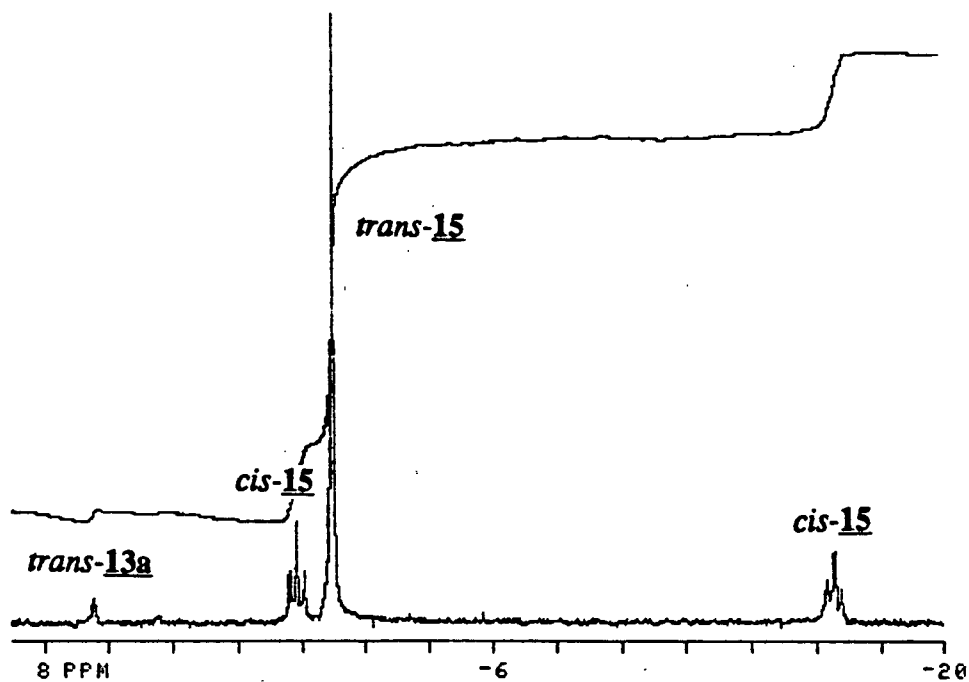


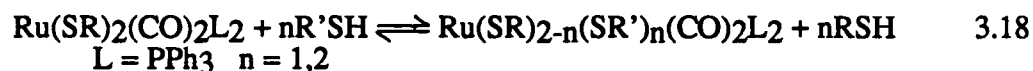
Fig. 3.34 The ³¹P{¹H} NMR spectrum of Ru(SH)₂(dpm)₂ (**15**) in C₆D₆ (δ with reference to PPh₃ in C₆D₆)

The reaction of *trans*-RuH(BH₄)(dpm)₂ (Section 2.3.7, 0.4 g) with H₂S (1 atm) in THF (30 mL) over 5 days at room temperature²⁵⁴ produces a similar mixture of *cis*- and *trans*-15 (*cis*:*trans* = 1:2, yield = 80%).



3.8 THE THIOL EXCHANGE REACTIONS OF *cct*-Ru(SR)₂(CO)₂(PPh₃)₂

The title compound (14) reacts with added thiols to exchange the thiolate groups, in a reaction reminiscent of that with *cct*-RuH(SR)(CO)₂(PPh₃)₂ (reaction 3.12).



For example, the reaction of *cct*-Ru(SC₆H₄*p*CH₃)₂(CO)₂(PPh₃)₂ (14b, 6 mM) in C₆D₆ with H₂S (1 atm) at room temperature is complete within 5 min, giving pure *cct*-Ru(SH)₂(CO)₂(PPh₃)₂ (14a). However, the reaction of 14b (6 mM) with excess EtSH at room temperature produces equilibrium mixtures of the 14b, *cct*-Ru(SCH₂CH₃)(SC₆H₄*p*CH₃)(CO)₂(PPh₃)₂ (14bd), and *cct*-Ru(SCH₂CH₃)₂(CO)₂(PPh₃)₂ (14d) within 20 min, after which the ratio is unchanging (monitored for a further 50 min). The 14b:14bd:14d ratio is 24:52:24 or 10:45:45 after the addition of 260 or 960 mM EtSH, respectively. The *p*-thiocresol produced in the reaction is clearly detected in the ¹H NMR spectrum. From three experiments of this type, rough estimates of the two equilibrium constants were calculated.

$$K_1 = \frac{[\text{Ru}(\text{SEt})(\text{Stol})(\text{CO})_2(\text{PPh}_3)_2][\text{tolSH}]}{[\text{Ru}(\text{Stol})_2(\text{CO})_2(\text{PPh}_3)_2][\text{EtSH}]}$$

$$K_2 = \frac{[\text{Ru}(\text{SEt})_2(\text{CO})_2(\text{PPh}_3)_2][\text{tolSH}]}{[\text{Ru}(\text{SEt})(\text{Stol})(\text{CO})_2(\text{PPh}_3)_2][\text{EtSH}]}$$

where Et = CH₂CH₃ and tol = C₆H₄*p*CH₃

At 20°C, these constants were 4×10^{-2} and 1×10^{-2} ($\pm 25\%$), respectively.

The Ru(SH)₂(CO)₂(PPh₃)₂ complex (**14a**, 5.7 mM) reacts with *p*-thiocresol (220 mM) in C₆D₆ (1 mL) at 21°C to produce Ru(SH)(SC₆H₄*p*CH₃)(CO)₂(PPh₃)₂ (**14ab**) (56% conversion) and Ru(SC₆H₄*p*CH₃)₂(CO)₂(PPh₃)₂ (**14b**) (10%) after 140 min. The reaction of **14a** with thiophenol is similar (Fig. 3.35 and 3.37). However, with 1500 equivalents of ethanethiol, no reaction is observed even after several hours. This is probably a result of the greater binding strength of the more acidic thiols such as H₂S and the aryl thiols (Section 3.5). The mixed products of the reactions of **14a** with thiols are detected by ³¹P{¹H} and ¹H NMR spectroscopy (Fig. 3.35 and Table 4.1 on page 159).

The reaction of **14a** (0.70 mM) with thiophenol (2.0 mM) can also be followed by UV (Fig. 3.36). Isosbestic points are observed for the first 10 min at 367 nm ($\epsilon = 2100$) and 386 nm ($\epsilon = 1830$), because only Ru(SPh)₂(CO)₂(PPh₃)₂ (**14i**) is produced in the first 10 to 20 min, with no trace (NMR evidence) of Ru(SH)(SPh)(CO)₂(PPh₃)₂ (**14ai**). The rate constant at 25°C is $2.3 \times 10^{-3} \text{ s}^{-1}$, significantly higher than the result in C₆D₆ ($4.2 \times 10^{-4} \text{ s}^{-1}$, see below).

The rate of the same reaction of **14a** with PhSH was also monitored by ³¹P{¹H} NMR spectroscopy at 25.00°C. At low [PhSH], the monosubstituted product (**14ai**) is produced more quickly and in greater amounts than the disubstituted product (**14i**, Fig. 3.37a). The reaction does not proceed to completion presumably because an equilibrium is attained. Since H₂S is very soluble in benzene²⁵⁵, a significant amount of the H₂S produced in the reaction must remain in solution. At high [PhSH], the rate of loss of **14a** is *pseudo*-first order (Fig. 3.37c,d). The log plot (Fig. 3.38) is linear for 2.5 half-lives, with a *pseudo*-first order rate constant of $4.0 \times 10^{-4} \text{ s}^{-1}$. Because first order behaviour is not observed over the full range of thiol concentrations tested, the initial rate method was adopted for the kinetic study. The rate constant was calculated from the initial rate of loss of **14a** as determined from the ³¹P{¹H} NMR spectra. This rate constant is independent of [PhSH] (77 to 1700 mM), although it decreases slightly at very high concentrations of thiol (Fig. 3.39). The average value is $4.2 (\pm 0.3) \times 10^{-4} \text{ s}^{-1}$ (average of 5 results). If extra PPh₃ is added, the rate decreases and becomes dependent on [PhSH] (Fig.

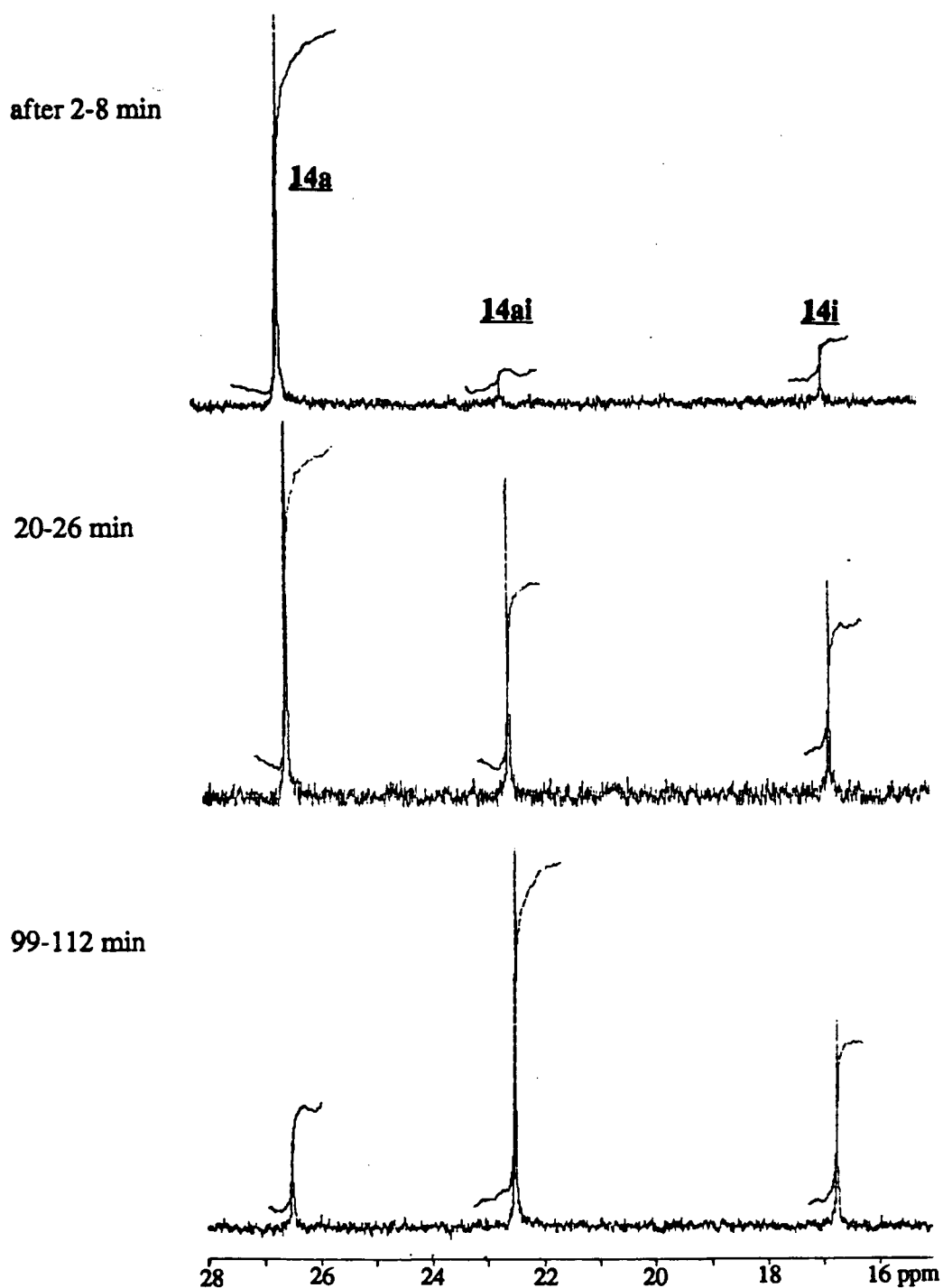


Fig. 3.35 $^{31}\text{P}\{^1\text{H}\}$ NMR spectra acquired during the reaction of *cis*- $\text{Ru}(\text{SH})_2(\text{CO})_2(\text{PPh}_3)_2$ (**14a**, 9.4 mM) with PhSH (700 mM) at 25°C in C_6D_6 . Chemical shift shown with respect to PPh_3 in C_6D_6 .

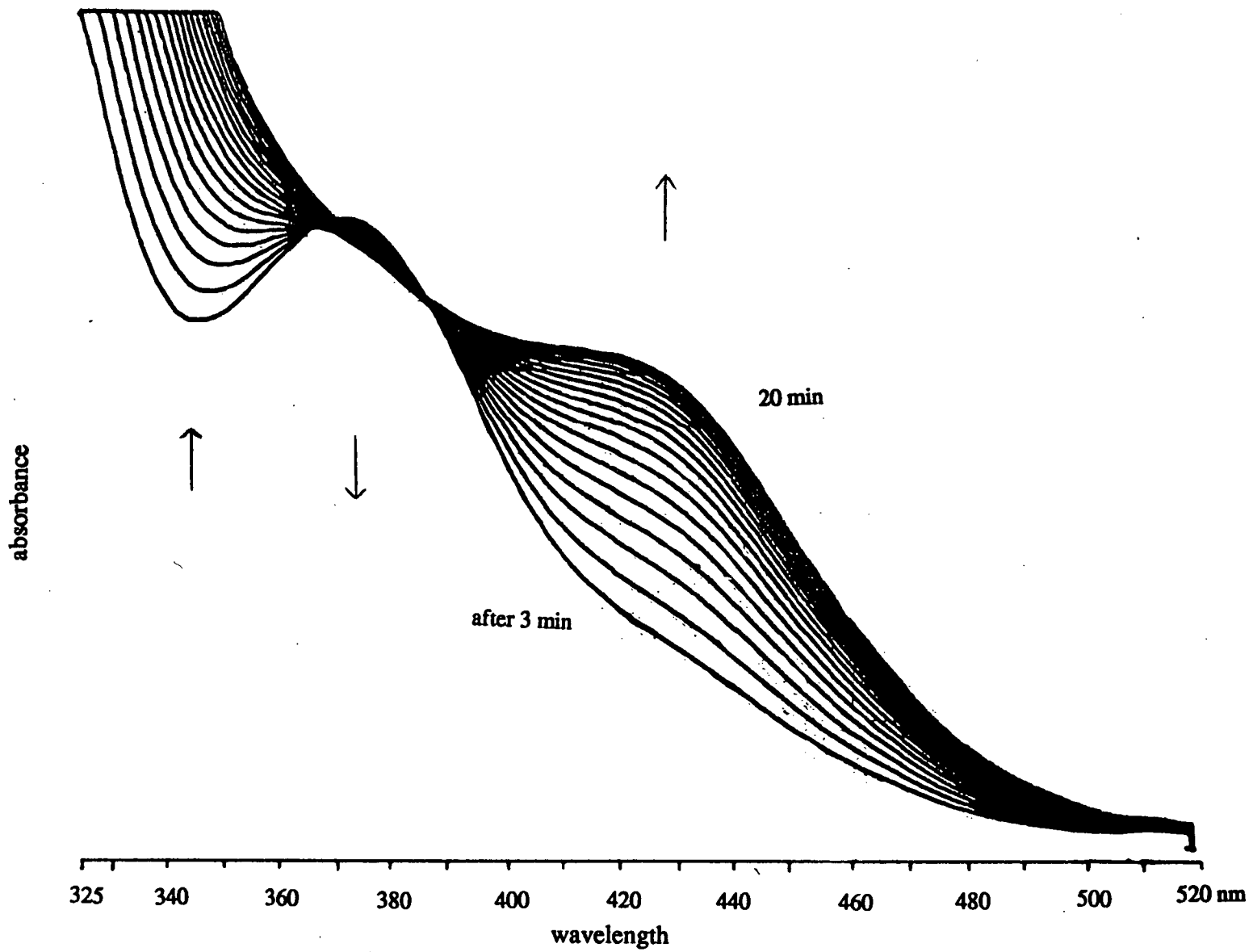


Fig. 3.36 UV/vis. spectra acquired at 1 min intervals during the reaction of *cct*-Ru(SH)₂(CO)₂(PPh₃)₂ (**14a**, 0.70 mM) with PhSH (2.0 M) at 25°C in THF.

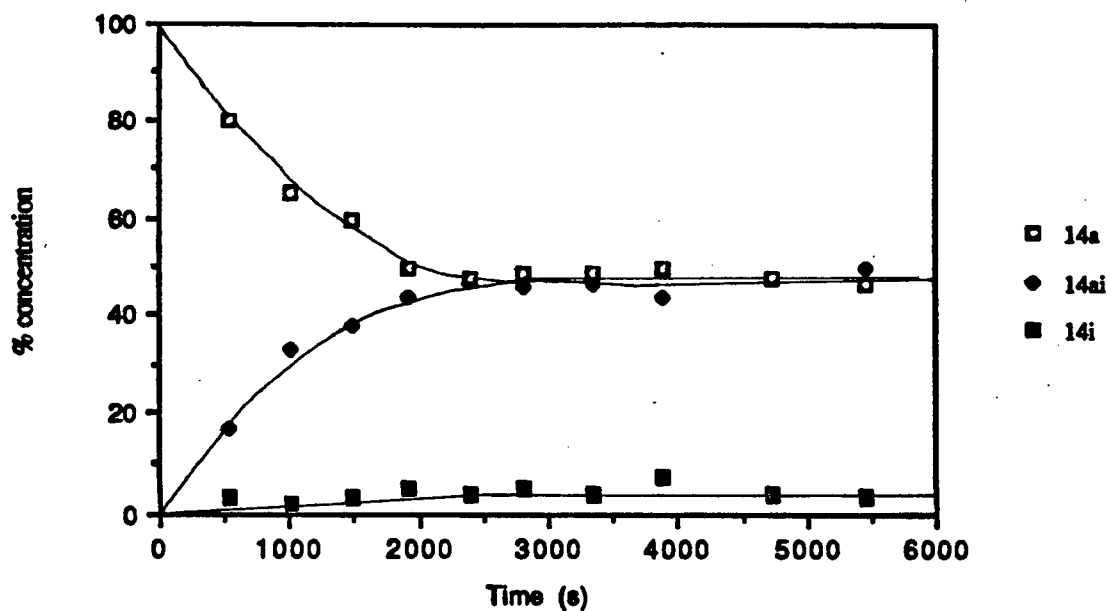
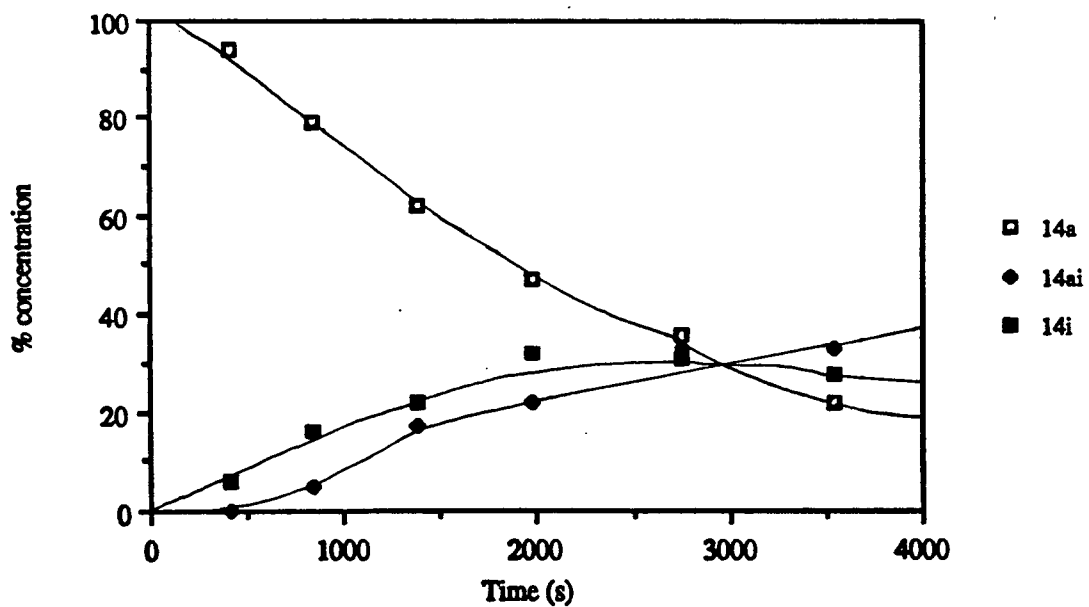
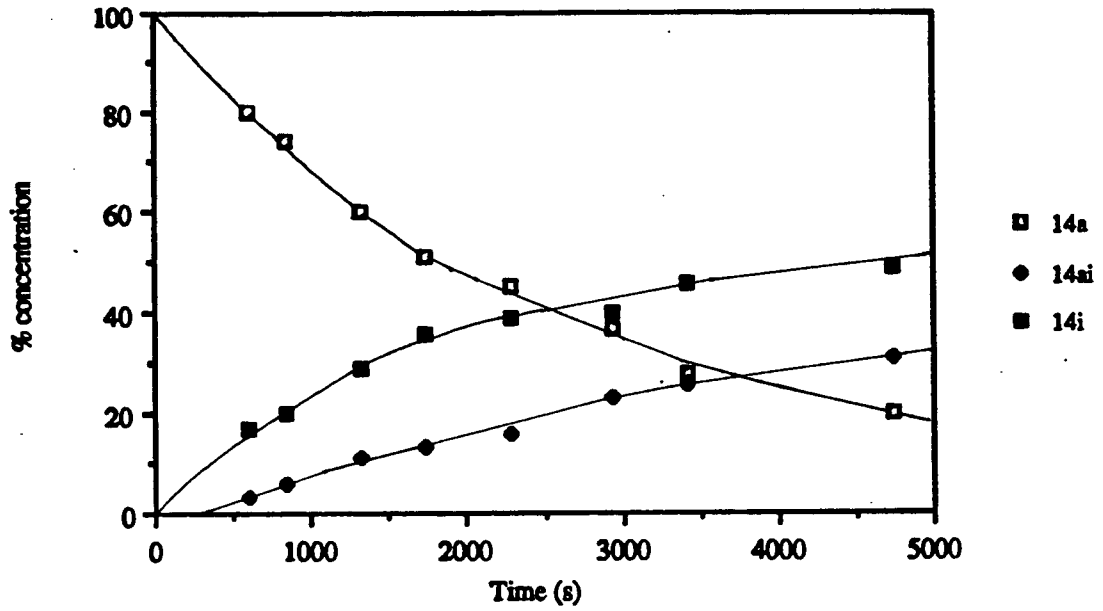


Fig. 3.37 Time dependence of the concentrations of species detected by $^{31}\text{P}\{^1\text{H}\}$ NMR during the reaction of *cct*-Ru(SH) $_2$ (CO) $_2$ (PPh $_3$) $_2$ (14a, 6 mM) with PhSH at 25°C in C $_6$ D $_6$.

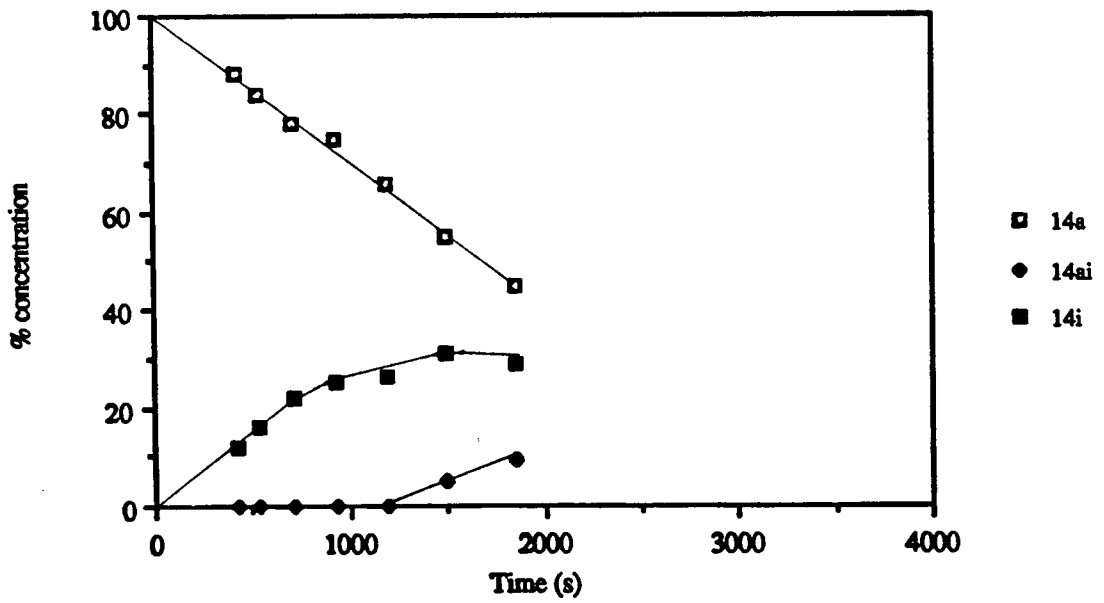
a) at 77 mM PhSH



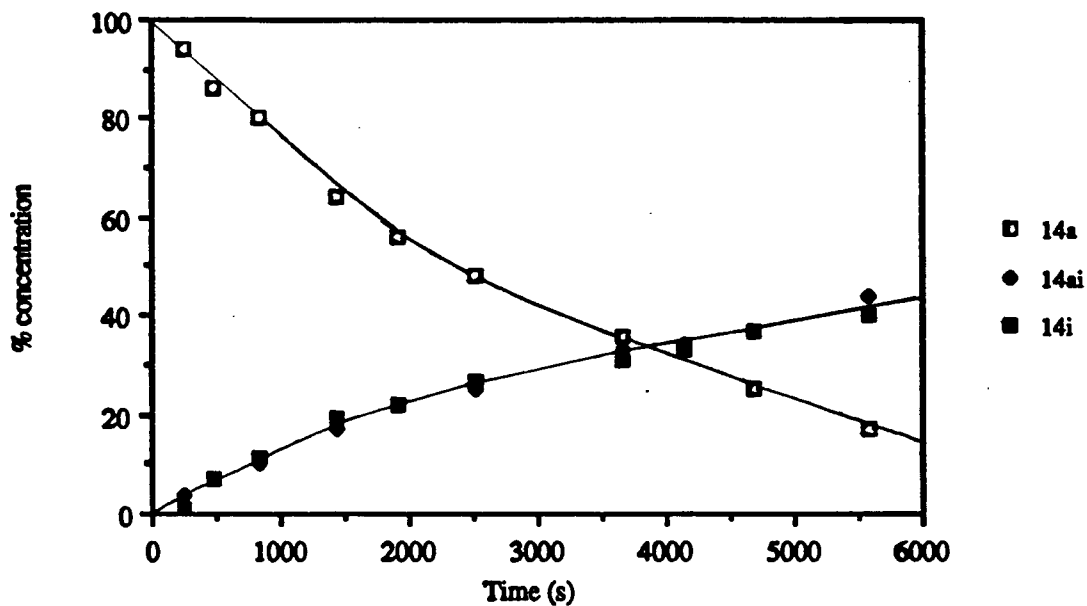
b) at 690 mM PhSH



c) at 1700 mM PhSH



d) at 2900 mM PhSH



e) at 810 mM PhSH and 470 mM PPh₃

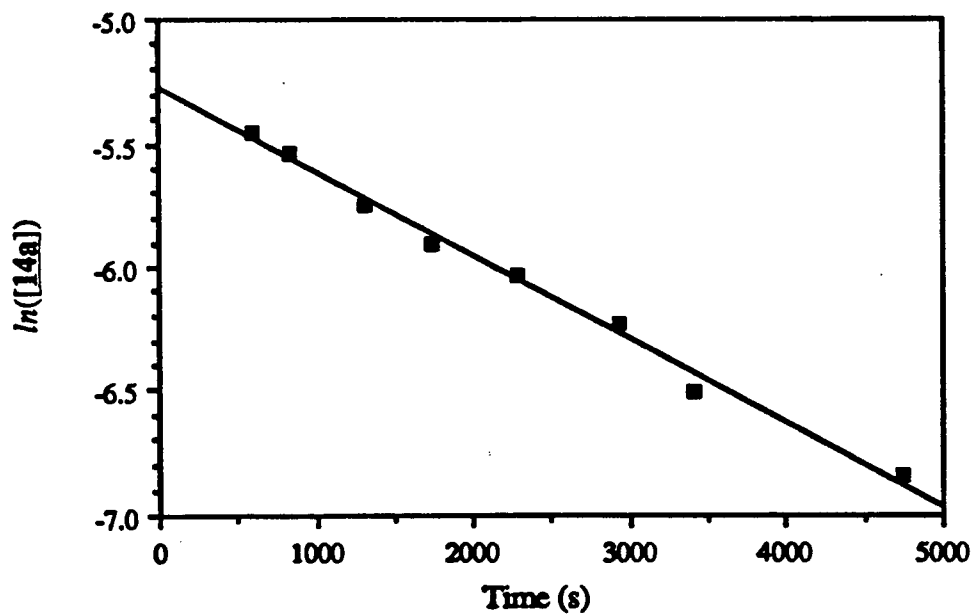


Fig. 3.38 The log plot of the concentration of *cct*-Ru(SH)₂(CO)₂(PPh₃)₂ (**14a**) during its reaction (5.3 mM Ru) with thiophenol (1.7 M) in C₆D₆ at 25°C.

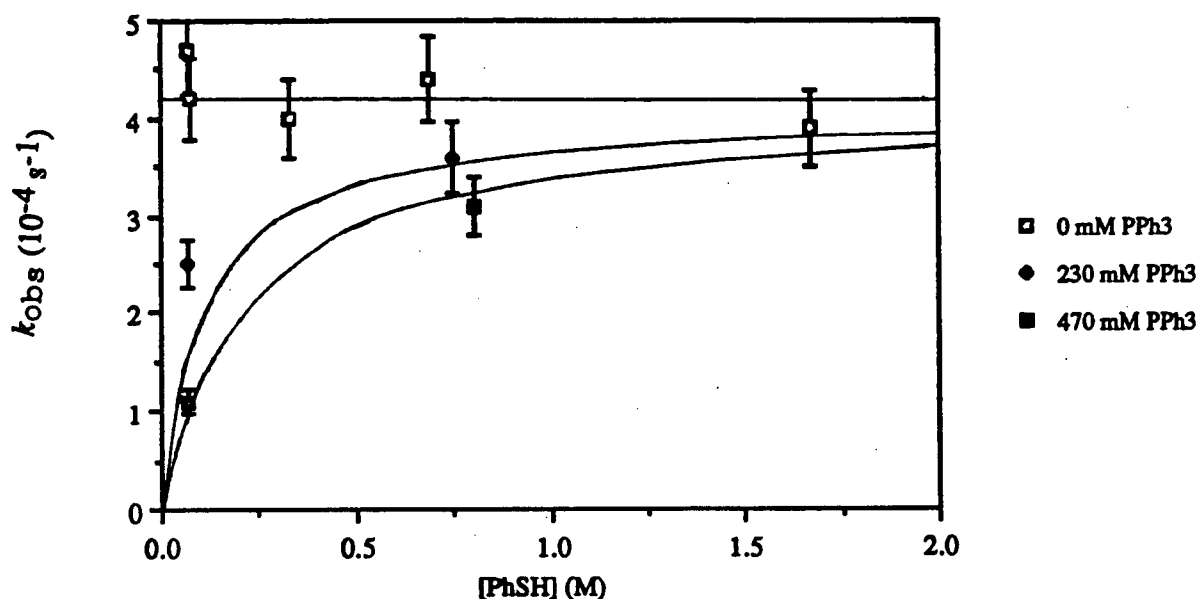


Fig. 3.39 The dependence on $[\text{PhSH}]$ of the observed initial rate constant for the loss of $cis\text{-Ru}(\text{SH})_2(\text{CO})_2(\text{PPh}_3)_2$ (**14a**) during the reaction with PhSH at several concentrations of added PPh_3 . Bars indicate estimated error (10 %) on individual measurements of k .

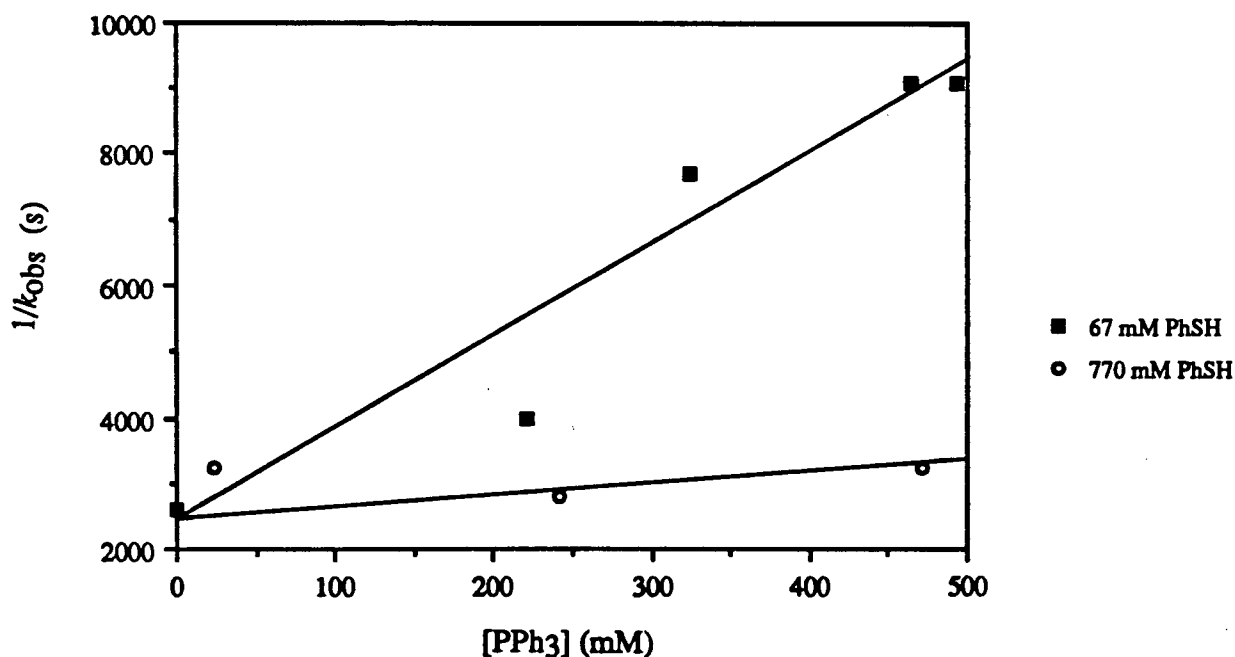
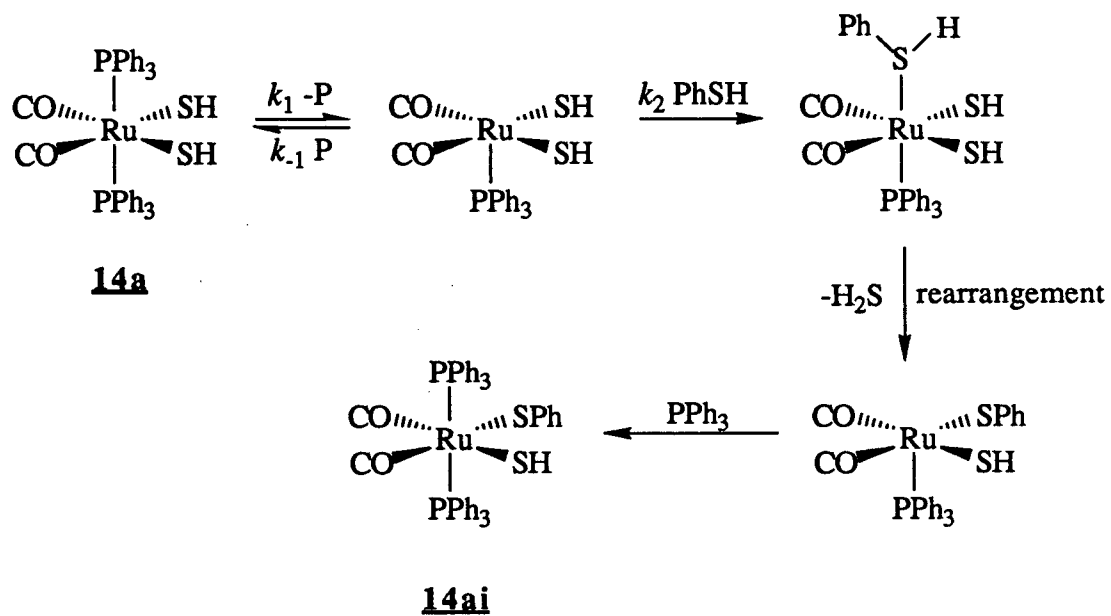


Fig. 3.40 Phosphine dependence of the inverse of the observed initial rate constant for the loss of $cis\text{-Ru}(\text{SH})_2(\text{CO})_2(\text{PPh}_3)_2$ (**14a**, 6 mM) during the reaction with PhSH at several $[\text{PhSH}]$. The lines are drawn from a fixed point at $[\text{PPh}_3]=0$ mM based on data from experiments with no added phosphine.

Scheme 3.6 The proposed mechanism for the first step of the reaction of $\text{Ru}(\text{SH})_2(\text{CO})_2(\text{PPh}_3)_2$ (**14a**) with PhSH .



3.39). A mechanism consistent with these observations is shown in Scheme 3.6. The proton in the intermediate complex $\text{Ru}(\text{SH})_2(\text{PhSH})(\text{CO})_2(\text{PPh}_3)$ probably is shared by all three thiolate groups, rather than being simply attached to one of them. This kind of intermediate was discussed in Section 3.5. The rate law predicted by the mechanism in Scheme 3.6, assuming that k_{-2} is negligible, is:

$$\frac{-d[\mathbf{14a}]}{dt} = \frac{k_1 k_2 [\text{PhSH}][\mathbf{14a}]}{k_{-1}[\text{PPh}_3] + k_2[\text{PhSH}]}$$

Under *pseudo*-first order conditions, $[\text{PhSH}]$ is essentially constant during the reaction. PPh_3 is neither produced nor consumed in the reaction and $[\text{PPh}_3]$ is therefore constant. Thus the observed initial rate constant k_{obs} is given by

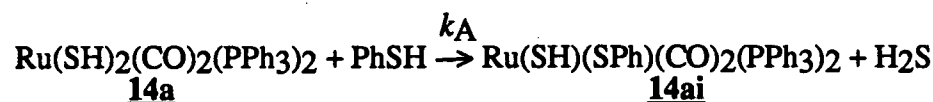
$$k_{\text{obs}} = \frac{k_1 k_2 [\text{PhSH}]}{k_{-1}[\text{PPh}_3] + k_2[\text{PhSH}]}$$

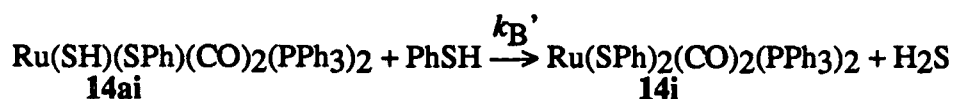
or

$$\frac{1}{k_{\text{obs}}} = \frac{k_{-1}[\text{PPh}_3]}{k_1 k_2 [\text{PhSH}]} + \frac{1}{k_2}$$

A plot of $1/k_{\text{obs}}$ against $[\text{PPh}_3]$ should be a straight line with a slope inversely proportional to $[\text{PhSH}]$. Although there is considerable scatter in the data, this is perhaps the case (Fig. 3.40). The slope of the line drawn through the data for 67 mM PhSH is 14000, giving a value for k_{-1}/k_2 of 0.4. The slope for 770 mM PhSH is 1800, giving a value for k_{-1}/k_2 of 0.6. The average value is 0.5.

During the reaction of $\mathbf{14a}$ with low $[\text{PhSH}]$, $\mathbf{14ai}$ is produced at a higher initial rate than $\mathbf{14i}$. It was initially supposed that $\mathbf{14ai}$ may be an intermediate in the formation of $\mathbf{14i}$. The reaction equations would therefore be the following.





However, at high [PhSH] (Fig. 3.37c,d), 14i is observed first, and the appearance of 14ai is considerably delayed. The rate constant for the second step was calculated, assuming that a) the first substitution reaction is first order with respect to [14a] and independent of [PhSH], b) the second substitution reaction is first order with respect to [14ai] and n^{th} order with respect to [PhSH], and c) n and [PhSH] are constant with respect to time. The rate equations, based on these assumptions, are:

$$-\frac{d[\text{14a}]}{dt} = k_A[\text{14a}] \quad \frac{d[\text{14i}]}{dt} = k_B'[\text{14ai}][\text{PhSH}]^n = k_B[\text{14ai}]$$

where $k_B = k_B'[\text{PhSH}]^n$.

The integrated rate laws for this type of system are known.²⁵⁶



$$\frac{[\text{14a}]_t}{[\text{14a}]_0} = \exp(-k_A t)$$

$$\frac{[\text{14ai}]_t}{[\text{14a}]_0} = \frac{k_A \{\exp(-k_A t) - \exp(-k_B t)\}}{k_B - k_A}$$

$$\frac{[\text{14i}]_t}{[\text{14a}]_0} = 1 + \frac{k_B \exp(-k_A t) - k_A \exp(-k_B t)}{k_A - k_B}$$

The value of k_A is already known ($k_A = k_1 = 4.2 \times 10^{-4} \text{ s}^{-1}$). For each experiment, the plots of the observed and predicted concentrations of $\text{Ru}(\text{SH})_2(\text{CO})_2(\text{PPh}_3)_2$ (14a), $\text{Ru}(\text{SH})(\text{SPh})(\text{CO})_2(\text{PPh}_3)_2$ (14ai), and $\text{Ru}(\text{SPh})_2(\text{CO})_2(\text{PPh}_3)_2$ (14i) were compared for several values of k_B . The best value for k_B was taken to be that which produced the best fit of the predicted concentration curve (calculated using the above equations) to the observed curve in the

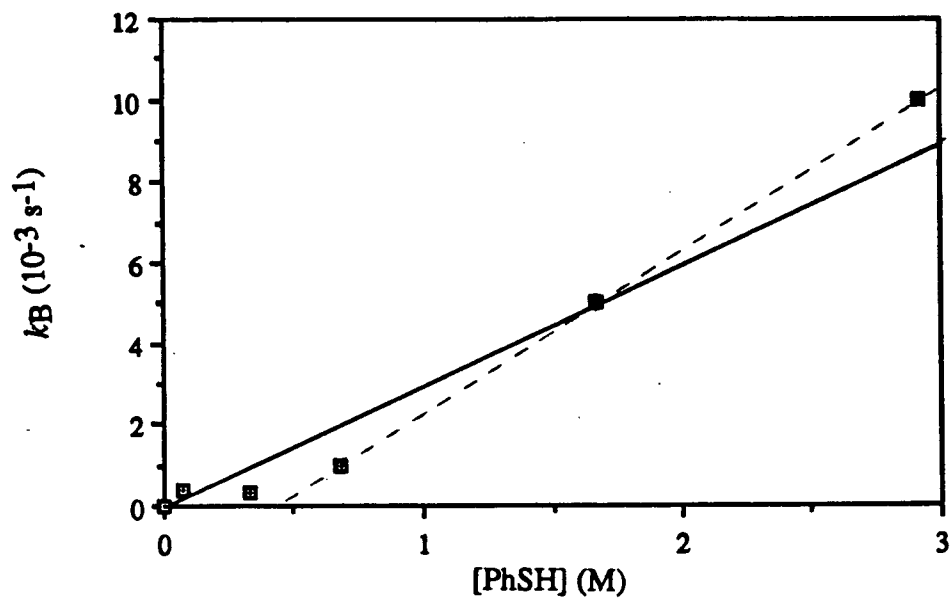


Fig. 3.41 Thiol dependence of the calculated rate constant k_B for the second step of the reaction of *cct*- $\text{Ru}(\text{SH})_2(\text{CO})_2(\text{PPh}_3)_2$ with thiophenol at 25°C in C_6D_6 . Solid line assumes a first-order dependence at all $[\text{PhSH}]$. Dashed line shows an incorrect interpretation of the rate dependency.

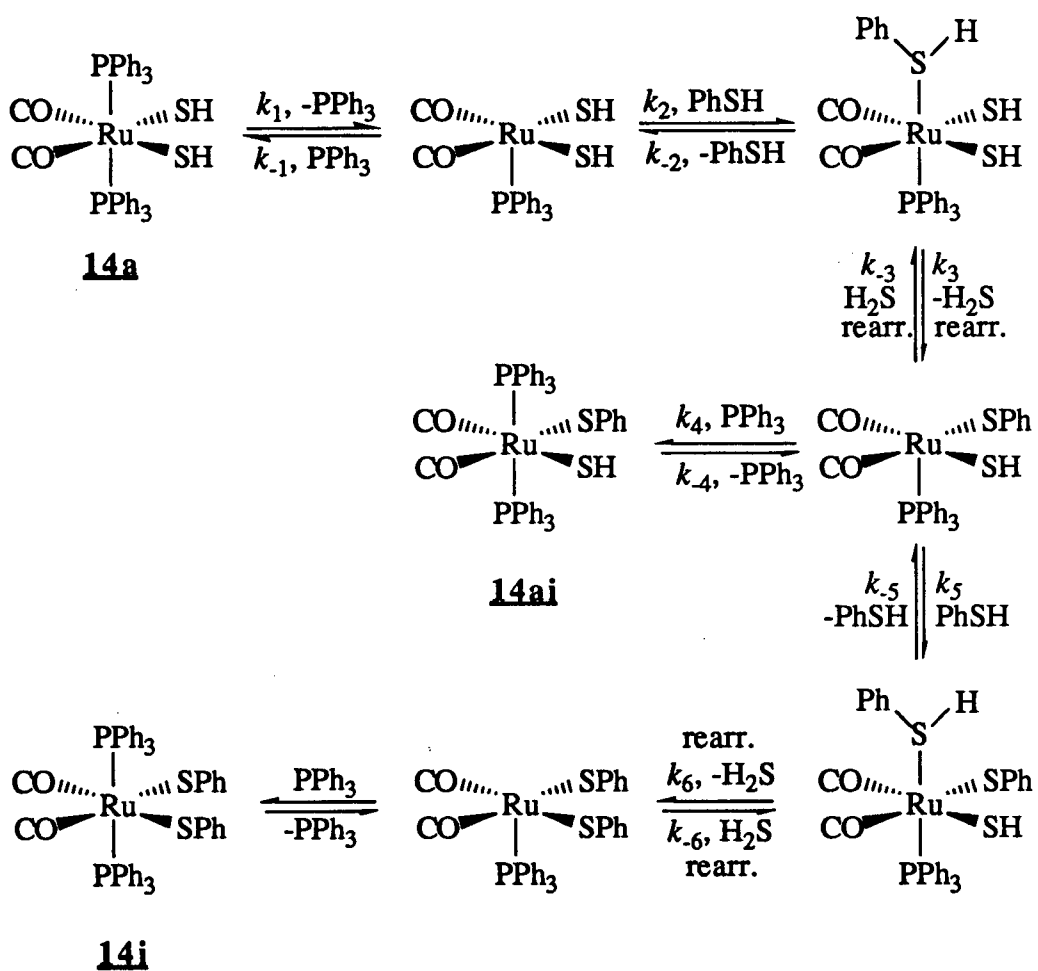
initial rate region (the first two data points, Fig. 3.37). It is tempting to interpret the plot of the [PhSH] dependence of the k_B values (Fig. 3.41) as showing n to be 0 at low thiol concentrations, and 1 at high thiol concentrations. The error on each point, although difficult to estimate, is probably too large for this interpretation, and the sloping line for a supposed first-order dependence on [PhSH] (dotted line in Fig. 3.41) should extrapolate back to the origin, which it fails to do. It is clear, however, that the value of k_B depends on [PhSH]. This indicates that either

- i) the reaction of 14ai with PhSH is dependent on [PhSH], and is sufficiently fast at high [PhSH] that 14ai is not observed, or
- ii) 14ai is not an intermediate in the formation of 14i under these conditions.

The first possibility is counter-intuitive, because one would expect that the mechanism of the reaction of 14ai with PhSH would correspond to that of 14a with PhSH. A mechanism consistent with the second possibility and with the mechanism proposed for the loss of 14a (Scheme 3.6) is shown in Scheme 3.7. According to this mechanism, the unobserved five-coordinate complex $[\text{Ru}(\text{SH})(\text{SPh})(\text{CO})_2(\text{PPh}_3)]$ is an intermediate for which PPh_3 and PhSH compete to form 14ai (directly) and 14i (via other intermediates), respectively. This accounts for the observation that high [PhSH] favours early formation of 14i (Figs. 3.37b,c,d), while added PPh_3 increases the initial rate of formation of 14ai at the expense of 14i (Fig. 3.37e).

With this mechanism, we can now interpret the observed dependence of k_B on [PhSH] (Fig. 3.41). At very low [PhSH], k_B should be independent of [PhSH], because in this region, the pathway via 14ai is predominant. The value of k_B in this range should therefore equal that of k_{-4} . As mentioned earlier, the flattened region at low [PhSH] in Fig. 3.41 is believed to result from scatter in the data, although it is interesting that the lowest observed value of k_B ($4 \times 10^{-4} \text{ s}^{-1}$) is very close to the value of k_1 ($3.8 \times 10^{-4} \text{ s}^{-1}$). Because 14a and 14ai are so similar, the values of k_{-4} and k_1 are expected to be similar. At higher [PhSH], the other pathway should be predominant. That is, 14i is formed without 14ai having been an intermediate. The value of $k_B/[\text{PhSH}]$ in this region ($3 \times 10^{-3} \text{ M}^{-1} \text{ s}^{-1}$) is presumably that of k_5 .

Scheme 3.7 The proposed mechanism for the reaction of $\text{Ru}(\text{SH})_2(\text{CO})_2(\text{PPh}_3)_2$ (**14a**) with PhSH.



As we have seen, if one assumes that k_{-2} is negligible, then one can calculate that k_{-1}/k_2 is approximately 0.5. This leads one to speculate about the value of k_4/k_5 . Both ratios are concerned with competing reactions of PPh_3 and PhSH for a five-coordinate intermediate. If k_4/k_5 were also approximately 0.5, or even if k_4 and k_5 were of the same magnitude, then under the conditions of excess added thiol and no added phosphine, $k_5[\text{PhSH}]$ would be far greater than $k_4[\text{PPh}_3]$, and therefore no **14ai** would have been observed in the initial rate region. That the initial rate of production of **14ai** is significant at 77 mM PhSH (Fig. 3.37a) suggests that k_4/k_5 is much larger than k_{-1}/k_2 or that k_{-5} is larger than k_{-2} . It is difficult to explain why k_4/k_5 should be larger than k_{-1}/k_2 , but it is clear why k_{-5} should be larger than k_{-2} . For statistical and steric reasons, the thiol which is ejected from $\text{Ru}(\text{SPh})(\text{SH})(\text{PhSH})(\text{CO})_2(\text{PPh}_3)$ is more likely to be PhSH (k_{-5}) than H_2S (k_6). The corresponding complex $\text{Ru}(\text{SH})_2(\text{PhSH})(\text{CO})_2(\text{PPh}_3)$ is more likely, for statistical reasons, to eliminate H_2S (k_3) than PhSH (k_{-2}). Also, the steric crowding which might encourage elimination of PhSH from $\text{Ru}(\text{SPh})(\text{SH})(\text{PhSH})(\text{CO})_2(\text{PPh}_3)$ is weaker in $\text{Ru}(\text{SH})_2(\text{PhSH})(\text{CO})_2(\text{PPh}_3)$. These arguments suggest that k_{-5} should be larger than k_{-2} .

Why does *cct*- $\text{Ru}(\text{SC}_6\text{H}_4\text{pCH}_3)_2(\text{CO})_2(\text{PPh}_3)_2$ (**14b**) react more quickly with thiols than does *cct*- $\text{Ru}(\text{SH})_2(\text{CO})_2(\text{PPh}_3)_2$ (**14a**)? The rate determining step in Scheme 3.5 and 3.6 is dissociation of PPh_3 from the complex. It is possible that the bulky thiolate groups in **14b** labilize the phosphine. This is supported by the observation (Section 6.2.2) that the phosphine-exchange reaction of **14b** with $\text{P}(\text{C}_6\text{H}_4\text{pCH}_3)_3$ proceeds more quickly than that of **14a**.

3.9 THE REACTIONS OF OTHER CARBONYL(PHOSPHINE)RUTHENIUM(0) COMPLEXES WITH H_2S AND THIOLS

The bisphosphine tricarbonyl complex $\text{Ru}(\text{CO})_3(\text{PPh}_3)_2$, (**10**), is much less reactive than $\text{Ru}(\text{CO})_2(\text{PPh}_3)_3$ (**2**). After 3 h in refluxing THF under H_2S , only 6% of a sample of **10** had

been converted to *cct*-RuH(SH)(CO)₂(PPh₃)₂, of which half had reacted further (reaction 3.14) to produce *cct*-Ru(SH)₂(CO)₂(PPh₃)₂.²⁵⁴



The only related reactions which have been reported previously are the reaction of Ru(CO)₃(PPh₃)₂ with pyridine-2-thiol, producing Ru(pyS)₂(CO)(PPh₃),²¹¹ and reaction 3.20:



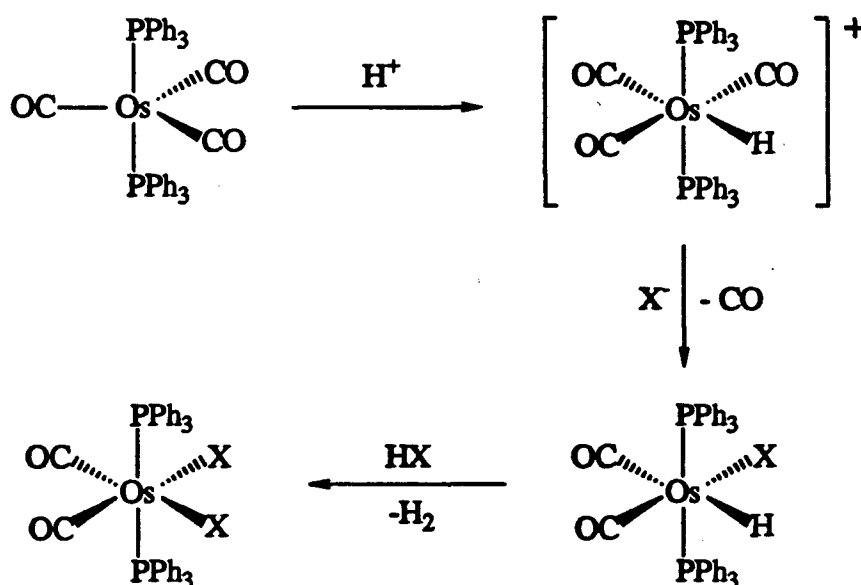
M=Os, X=Cl, Br, I (ref. 257a)

M=Ru, X=Cl, Br (ref. 257b), OCOR (ref. 257b,c,d)

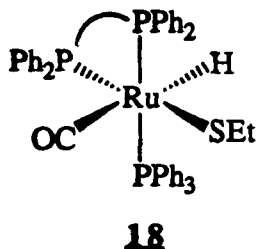
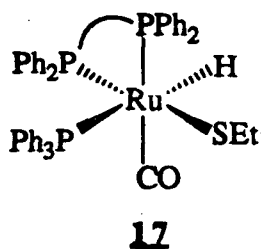
A mechanism proposed^{257a} for this reaction (Scheme 3.8) was supported by the isolation of complexes of the formula [OsX(CO)₃(PPh₃)₂]⁺X⁻ (X=Br, I, I₃)^{257a} and

OsH(Cl)(CO)₂(PPh₃)₂.^{257e} The mechanism of reaction 3.19 may parallel that in Scheme 3.8.

Scheme 3.8 A mechanism proposed by Collman and Roper^{257a} for the reaction of Os(CO)₃(PPh₃)₂ with HX (X=Cl, Br, I).



Samples of the complex $\text{Ru}(\text{CO})_2(\text{PPh}_3)(\text{dpm})$ (**16**), kindly supplied by Dr. C.-L. Lee, react with thiols to form mixtures of thiolate complexes (Figs. 3.42 and 3.43). The major product has not been identified. Three identified minor products of the reaction with ethanethiol in THF are *cis*- $\text{RuH}(\text{SCH}_2\text{CH}_3)(\text{CO})_2(\text{PPh}_3)_2$ (**9d**) and two isomers of $\text{RuH}(\text{SCH}_2\text{CH}_3)(\text{CO})(\text{PPh}_3)(\text{dpm})$, one (**17**) containing a $^2J_{\text{transPH}}$ coupling, and the other (**18**) containing only $^2J_{\text{cisPH}}$ couplings. These three products are detected in the hydride region of the ^1H NMR spectrum. The integrals of the hydride signals are in a ratio **9d**:**17**:**18** of 120:2.3:1. The peaks due to **16** and **9d** comprise 28% and 13% of the $^{31}\text{P}\{^1\text{H}\}$ NMR signal, respectively. It is not clear which peaks in the $^{31}\text{P}\{^1\text{H}\}$ NMR spectrum correspond to **17** and **18**. Possible structures for these isomers are shown below.



The detection of **17**, **18**, and **9d** shows that loss of a carbonyl ligand and exchange of the phosphine ligands are significant reactions. The existence of three labile ligands on the starting complex **16** make this system too complicated to be amenable to a full study of its reactivity and kinetics.

Results obtained in the reaction of **16** with H_2 are summarized in the experimental section at the end of this chapter. The products of the reaction include trace amounts of *cis*- $\text{RuH}_2(\text{CO})_2(\text{PPh}_3)_2$, and several unidentified species.

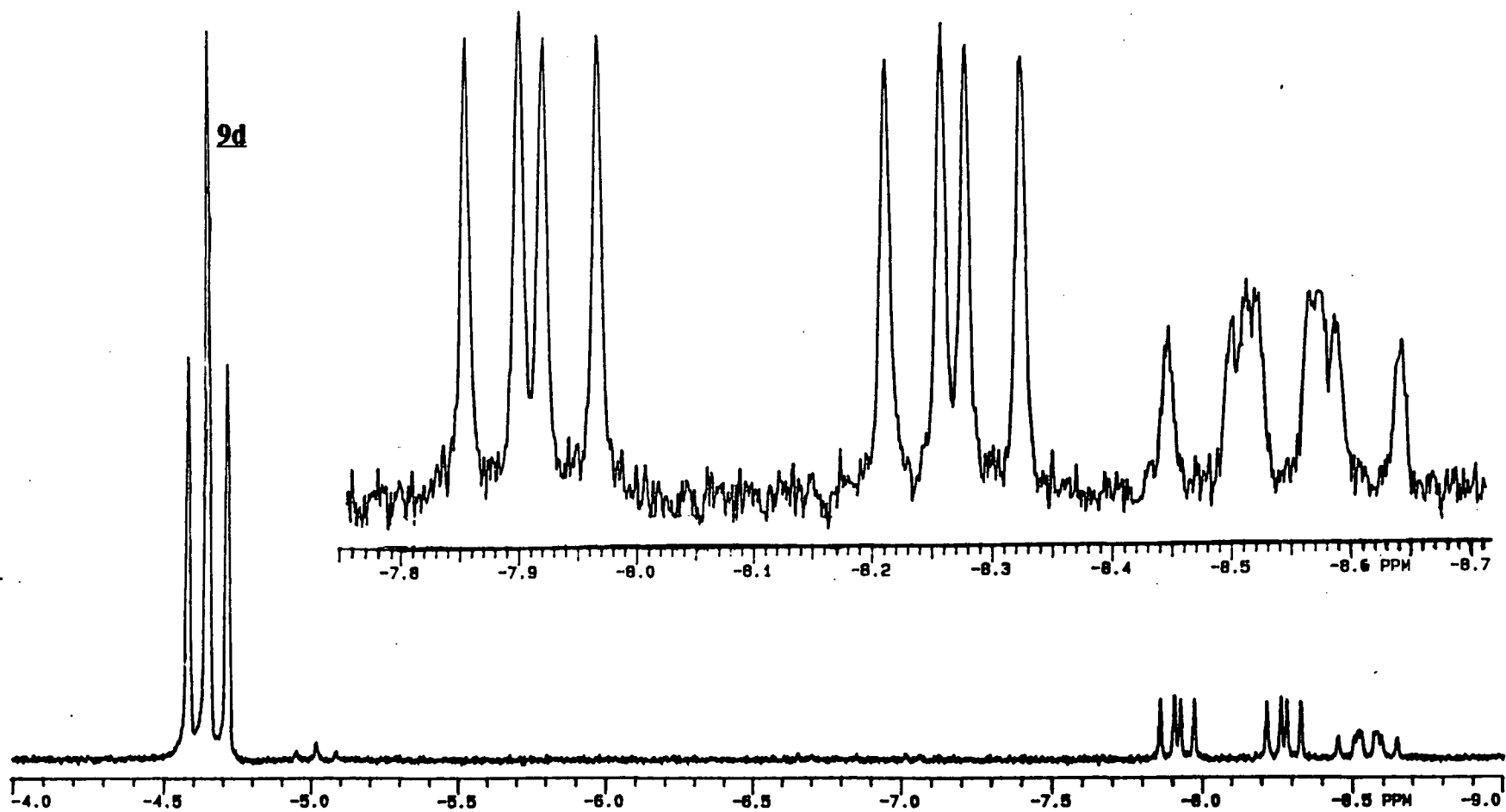


Fig. 3.42 ^1H NMR spectrum (hydride region) of the products of the reaction of $\text{Ru}(\text{CO})_2(\text{dpm})(\text{PPh}_3)$ with ethanethiol.

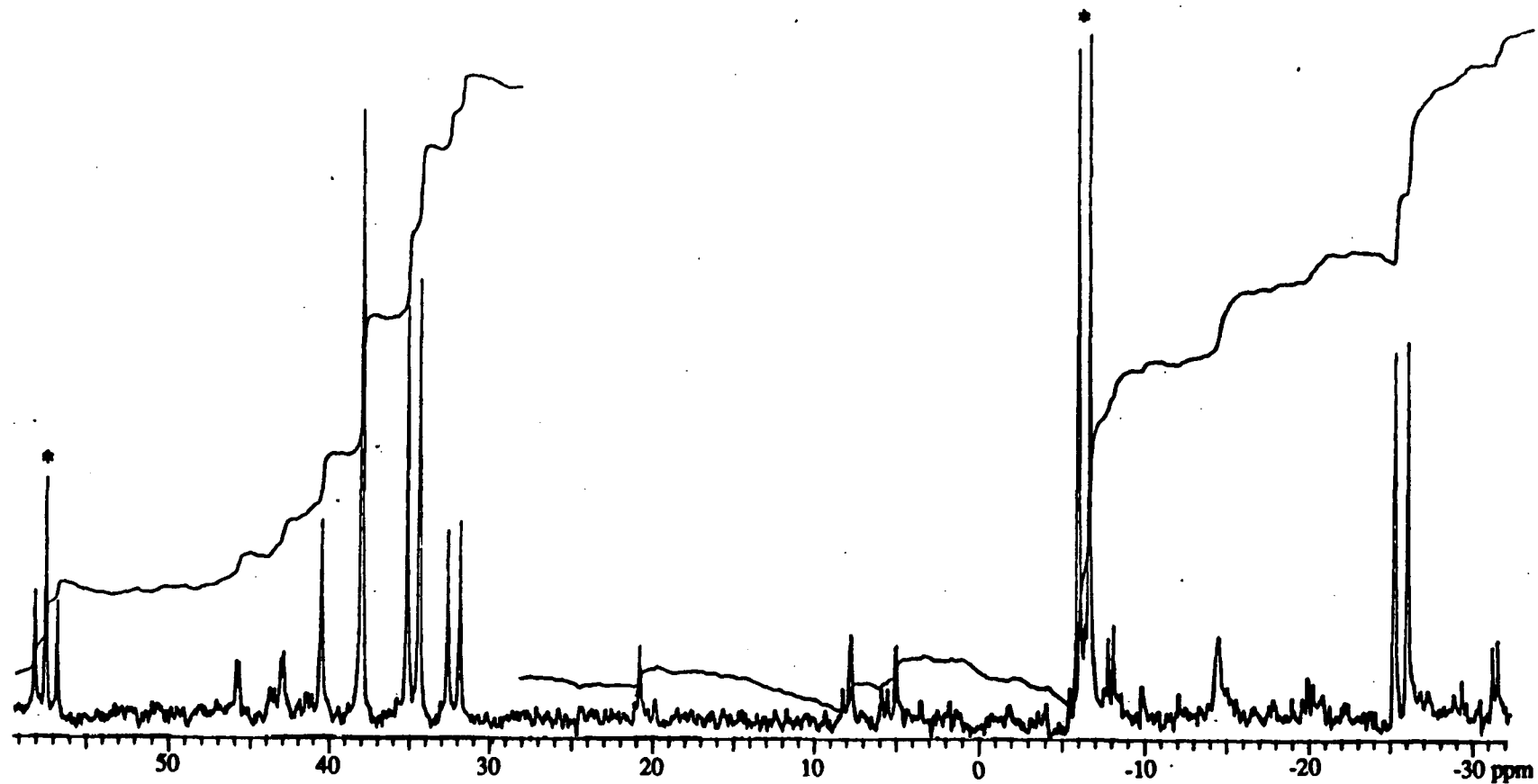


Fig. 3.43 $^{31}\text{P}\{^1\text{H}\}$ NMR spectrum of the products of the reaction of $\text{Ru}(\text{CO})_2(\text{dpm})(\text{PPh}_3)$ with ethanethiol. The signals due to unreacted starting material are indicated with asterisks.

3.10 EXPERIMENTAL DETAILS

The reaction of $\text{Ru}(\text{CO})_2(\text{PPh}_3)_3$ with hydrogen sulphide, thiols and selenols over several hours: Complex $\text{Ru}(\text{CO})_2(\text{PPh}_3)_3$ (**2**) (400 mg, 0.4 mmol) in THF (50 mL) was reacted with a) gaseous H_2S (1 atm) at -35°C for 2 h,⁸⁶ b) under gaseous MeSH (1 atm) at room temperature for 3 h, c) with excess (e.g. 8 equivalents) dissolved thiol at room temperature for 3 h, or d) with one equivalent of phenyl selenol for 1.5 h at room temperature. The product was precipitated by reduction of the solvent volume by vacuum distillation followed by addition of 100 mL hexanes, producing 40-95% yields of a) a pale tan powder, or b,c,d) a yellow powder, which analyzed for $\text{RuH}(\text{ER})(\text{CO})_2(\text{PPh}_3)_2$ (**9**). The same products can be similarly prepared from the reactions of *cct*- $\text{RuH}_2(\text{CO})_2(\text{PPh}_3)_2$ with H_2S or thiols. Elem. Anal.:

9a (ER=SH) Calcd. for $\text{C}_{38}\text{H}_{32}\text{O}_2\text{P}_2\text{RuS}$: C, 63.8; H, 4.5; S, 4.5. Found: C, 63.8; H, 4.7; S, 4.6.

9b (ER= $\text{SC}_6\text{H}_4\text{pCH}_3$) Calcd. for $\text{C}_{45}\text{H}_{38}\text{O}_2\text{P}_2\text{RuS}$: C, 67.1; H, 4.8; S, 4.0. Found: C, 66.1; H, 4.8; S, 4.3

9c (ER= SCH_3) Calcd. for $\text{C}_{39}\text{H}_{34}\text{O}_2\text{P}_2\text{RuS}$: C, 64.2; H, 4.7; S, 4.4. Found: C, 63.9; H, 4.8; S, 4.4.

9d (ER= SCH_2CH_3) Calcd. for $\text{C}_{40}\text{H}_{36}\text{O}_2\text{P}_2\text{RuS}$: C, 64.6; H, 4.9; S, 4.3. Found: C, 64.8; H, 5.1; S, 4.5.

9e (ER= $\text{SCH}_2\text{C}_6\text{H}_5$) Calcd. for $\text{C}_{45}\text{H}_{38}\text{O}_2\text{P}_2\text{RuS}$: C, 67.1; H, 4.8; S, 4.0. Found: C, 67.0; H, 4.9; S, 4.3.

9f (ER= $\text{SC}_6\text{H}_4\text{oCH}_3$) Calcd. for $\text{C}_{45}\text{H}_{38}\text{O}_2\text{P}_2\text{RuS}$: C, 67.1; H, 4.8; S, 4.0. Found: C, 66.7; H, 4.8; S, 4.3.

9g (ER= $\text{SC}_6\text{H}_4\text{mCH}_3$) Calcd. for $\text{C}_{45}\text{H}_{38}\text{O}_2\text{P}_2\text{RuS}$: C, 67.1; H, 4.8; S, 4.0. Found: C, 66.7; H, 4.3; S, 3.5.

9h (ER= SeC_6H_5) Calcd. for $\text{C}_{44}\text{H}_{36}\text{O}_2\text{P}_2\text{RuSe}$: C, 63.0; H, 4.3. Found: C, 63.3; H, 4.6.

9i (ER=SC₆H₅) Calcd. for C₄₄H₃₆O₂P₂RuS: C, 66.7; H, 4.6. Found: C, 65.8; H, 4.8. The NMR and IR spectra of these complexes are described and shown in Section 3.2 and summarized in Tables 3.1, 3.2, and 3.5. A sample of **9j** (ER=C₆F₅) was obtained, as confirmed by NMR spectroscopy, but an elemental analysis was not performed. The *cct*-RuD(SC₆H₅)(CO)₂(PPh₃)₂ complex was synthesized from **2** and PhSD. Samples of *cct*-RuH(SCH₂CH₃)(CO)₂(PR₃)₂ (PR₃=PPh₂Py, or P(C₆H₄*p*CH₃)₃) were prepared in a similar manner from the corresponding *tris*-phosphine complexes, Ru(CO)₂(PPh₂Py)₃ and Ru(CO)₂(P(C₆H₄*p*CH₃))₃. The latter precursor was supplied by Dr. C.-L. Lee. The former precursor, Ru(CO)₂(PPh₂Py)₃ was prepared by Mr. M. Prystay, from [RuCl₂(CO)₃]₂ and PPh₂Py, followed by sodium amalgam reduction of the resulting *cct*-RuCl₂(CO)₂(PPh₂Py)₂.²⁵⁸

The non-reaction of Ru(CO)₂(PPh₃)₃ with ethanol: Ru(CO)₂(PPh₃)₃ (12 mg, 13 μmol) and ethanol (50 μL, 0.9 mmol) failed to react within 2 days in 10 mL THF at room temperature. The solvents were removed by vacuum distillation, and the unreacted solid, redissolved in C₆D₆, was identified by ³¹P{¹H} NMR spectroscopy.

The X-ray crystallographic analysis of *cct*-RuH(SC₆H₄*p*CH₃)(CO)₂(PPh₃)₂:

Crystals of **9b** suitable for X-ray crystallography were prepared by diffusion of hexanes into a saturated solution of the complex in THF, under Ar. The crystallographic data were acquired and analysed by Dr. S. J. Rettig of this department.

The final unit-cell parameters were obtained by least-squares on the setting angles for 25 reflections with 2θ = 31.1-35.6°. The intensities of three standard reflections, measured every 200 reflections throughout the data collection, were essentially constant. The data were processed^{259a} and corrected for Lorentz and polarization effects and absorption (empirical, based on azimuthal scans for four reflections).

The structure analysis was initiated in the centrosymmetric space group $P\bar{1}$, the choice being confirmed by the subsequent successful solution and refinement of the structure. The structure was solved by conventional heavy atom methods, the coordinates of the Ru, P, and S atoms being determined from the Patterson functions and those of the remaining non-hydrogen atoms from subsequent difference Fourier syntheses. All non-hydrogen atoms were refined with anisotropic thermal parameters. Hydrogen atoms were fixed in idealized positions ($d_{C-H} = 0.98 \text{ \AA}$, $B_H = 1.2 B_{\text{bonded atom}}$), except for the metal hydride which was refined with an isotropic thermal parameter. Neutral atom scattering factors and anomalous dispersion corrections for the non-hydrogen atoms were taken from the International Tables for X-Ray Crystallography.^{259b} Final atomic coordinates and equivalent isotropic thermal parameters [$B_{eq} = 4/3 \sum_i \sum_j b_{ij}(a_i a_j)$], bond lengths, and bond angles appear in Appendix 2, and Tables 3.3 and 3.4, respectively. Other crystallographic data for this structure and the other structures described in this work are presented in Appendix 1.²⁰⁹

The reaction of *cct*-RuH₂(CO)₂(PPh₃)₂ (3**) with thiols:** The preparation of **9** from **3** was carried out in the same manner as described for the synthesis from **2** (see above), except that reaction times of 3 to 4 h were required.

To confirm the production of H₂ from the reaction, *p*-thiocresol (50 mg, 0.2 mmol) was added to a 1 mL saturated solution of **3** in THF in an NMR tube. After 2 h, and again after 25 h, 0.2 mL samples of the vapour phase were injected onto a molecular sieve column. A strong H₂ peak was observed each time.

The amount of H₂ produced was determined by following the reaction between **3** (35 μmol) and PhSH (290 μmol) in a constant pressure uptake apparatus at 30 °C. After 50 min, the gas evolution measured had levelled off and corresponded to 40 μmoles of gas.

The reaction of **3** with H₂S was also monitored by ¹H NMR spectroscopy. A sample of **3** (4.17 mg, 10.3 mM) was dissolved in C₆D₆ (0.6 mL) under Ar in an NMR tube and

the Ar atmosphere was promptly replaced by flushing H₂S through syringe needles inserted into the septum seal of the NMR tube. The sample tube was inserted into the NMR probe, which was maintained at 25.0°C. Successive spectra were acquired at a rate of one every 6 min, with every third being of the ³¹P rather than ¹H region of the NMR spectrum, in order to confirm that no products other than **2a** were forming. The concentrations of **3** and **2a** were calculated from the metal hydride signals in the ¹H NMR spectra.

The reaction of *cct*-RuH₂(CO)₂(PPh₃)₂ (3**) with CO:** The reaction of **3** (0.25 to 1.1 mM) with CO (1 atm) in THF was monitored at 350 nm, where the product Ru(CO)₃(PPh₃)₂ (**10**, ε=930 M⁻¹ cm⁻¹) absorbs more strongly than **3** (ε=70 M⁻¹ cm⁻¹). The results at 41°C are described on page 86. Reactions at 25°C under N₂ with sufficient CO injected through a septum to give a CO partial pressure of 0.09 atm had virtually the same first order rate constant (5.4 × 10⁻⁴ s⁻¹) as reactions under a full atmosphere of CO (5.6 × 10⁻⁴ s⁻¹). The ³¹P NMR chemical shift of the product (55.1 ppm) was identical to that reported by Dekleva,¹⁸² after correction for the different reference (all of the ³¹P NMR chemical shifts in Dekleva's work are exactly 1.5 ppm downfield of those observed in the present study, presumably because of a difference in the reference point).

The reaction of *cct*-RuH₂(CO)₂(PPh₃)₂ (3**) with PPh₃:** The reaction of **3** (0.34 mM) with PPh₃ (47 to 380 mM) in THF was monitored at 25°C and 400 nm, where the product **2** (ε=6000 M⁻¹ cm⁻¹) absorbs much more strongly than **3** (ε=40 M⁻¹ cm⁻¹). The plots of ln(A_∞-A) versus time are linear for experiments with ratios of [PPh₃]:[**3**] of 130 or greater. To insure proper mixing, particularly for the H₂ co-product, the cell was quickly inverted four times between each measurement, or approximately every 25 seconds. *Pseudo*-first order kinetics were also observed if Ar was bubbled through the cell between measurements. The identity of the Ru product of the reaction,

$\text{Ru}(\text{CO})_2(\text{PPh}_3)_3$ (**2**), was confirmed by comparing the $^{31}\text{P}\{^1\text{H}\}$ NMR spectrum of the product to that of a C_6D_6 solution of a known sample of **2** (Section 2.3.2).

The non-reaction of *cct*- $\text{RuH}_2(\text{CO})_2(\text{PPh}_3)_2$ (3**) with methanol:**

MeOH (70 μl , mmol) and **3** (8 mg, 12 μmol) in THF (7 mL) failed to react within an hour. The solvents were removed by vacuum distillation, and the starting material was identified by its $^{31}\text{P}\{^1\text{H}\}$ and ^1H NMR spectra.

The reaction of *cct*- $\text{RuH}_2(\text{CO})_2(\text{PPh}_3)_2$ (3**) with acetic acid:**

Acetic acid (50 μL , 870 μmol) and **3** (23 mg, 34 μmol) were mixed in THF (10 mL) for 24 h at room temperature, during which no colour appeared. The volatiles were then removed by evacuation. The ^1H and $^{31}\text{P}\{^1\text{H}\}$ NMR spectra of the residue redissolved in C_6D_6 showed signals for a major product consistent with *cct*- $\text{RuH}(\text{OAc})(\text{CO})_2(\text{PPh}_3)_2$. ^1H NMR (C_6D_6) δ -3.68 ppm (t, 1H, $^2J_{\text{PH}} = 19.0$ Hz, Ru-H), 1.40 ppm (s, 3H, CH_3); $^{31}\text{P}\{^1\text{H}\}$ (C_6D_6) δ 45.24 ppm. These data match closely those found by Dekleva¹⁸² for *cct*- $\text{RuH}(\text{OCOPh})(\text{CO})_2(\text{PPh}_3)_2$ (^1H NMR (C_6D_6) δ -3.52 ppm (t, $^2J_{\text{PH}} = 20$ Hz, Ru-H); $^{31}\text{P}\{^1\text{H}\}$ (C_6D_6) corrected δ 44.8 ppm). The acetate made in the present study was not purified or analysed, and contained 10 % each (measured by ^{31}P NMR) of *cct*- $\text{RuH}_2(\text{CO})_2(\text{PPh}_3)_2$, $\text{Ru}(\text{CO})_3(\text{PPh}_3)_2$, and an unknown (singlet at 44.63 ppm).

The reaction of *cis*- and *trans*- $\text{RuH}_2(\text{dpm})_2$ (7**) with thiols:** A sample of **7** (6.0 mg, 6.9 μmol) was dissolved in C_6D_6 (0.5 mL) in an NMR tube under Ar, and the tube was capped with a septum. The gas phase of the NMR tube was then flushed with H_2S . The progress of the reaction was followed by NMR spectroscopy. The ^1H and $^{31}\text{P}\{^1\text{H}\}$ spectra after 45 min showed almost complete conversion to a new complex, believed to be *trans*- $\text{RuH}(\text{SH})(\text{dpm})_2$ (**13a**). ^1H NMR (C_6D_6) δ -9.46 (qn, $^2J_{\text{PH}} = 19$ Hz, Ru-H),

-3.55 (br, Ru-SH), 4.54 (dt, $^2J_{\text{HH}} = 16$ Hz, $^2J_{\text{PH}} = 3$ Hz, CH₂), and 5.21 ppm (multi, CH₂); $^{31}\text{P}\{^1\text{H}\}$ NMR (C₆D₆) δ 0.40 ppm (s).

The corresponding reaction of **7** with thiols was monitored by dissolving **7** (6.0 mg, 6.9 μmol) in C₆D₆ or toluene-d₈ (0.5 mL) in an NMR tube under Ar, and capping the tube with a septum. After an NMR spectrum of this sample had been acquired and the temperature of the probe had reached a steady 25°C, PhSH (4 μL , 70 mM) or PhCH₂SH (5 to 60 μL , 70 to 850 mM) was injected through the septum. The progress of the reaction was followed by NMR spectroscopy. Three products were observed. Two of these, *trans*- and *cis*-RuH(SR)(dpm)₂ (**13**) could be identified from their NMR spectra. *trans*-RuH(SPh)(dpm)₂ (*trans*-**13b**): ^1H NMR (toluene-d₈) δ -10.86 (qn, 1H, $^2J_{\text{PH}} = 19.9$ Hz, Ru-H), 4.27 (dt, 2H, $^2J_{\text{HH}} = 13.8$ Hz, $^2J_{\text{PH}} = 3.3$, CH₂), and 4.78 (multi, 2H, CH₂); $^{31}\text{P}\{^1\text{H}\}$ NMR δ -2.06 ppm (s).

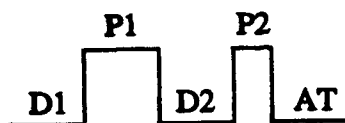
cis-RuH(SPh)(dpm)₂ (*cis*-**13b**): ^1H NMR (toluene-d₈) δ -6.29 ppm (ddt, $^2J_{\text{transPH}} = 91.5$ Hz, $^2J_{\text{cisPH}} = 24.1, 16.3$ Hz, Ru-H). The $^{31}\text{P}\{^1\text{H}\}$ NMR spectrum of the toluene-d₈ solution of this product is described in Section 3.4 and shown in Fig. 3.23.

trans-RuH(SCH₂Ph)(dpm)₂ (*trans*-**13c**): ^1H NMR (C₆D₆) δ -10.16 (qn, $^2J_{\text{PH}} = 20.0$ Hz, Ru-H), 4.44 (dt, $^2J_{\text{HH}} = 13.5$ Hz, $^2J_{\text{PH}} = 3.2$, CH₂), and 5.19 (multi, CH₂); $^{31}\text{P}\{^1\text{H}\}$ NMR δ -1.68 ppm (s).

cis-RuH(SCH₂Ph)(dpm)₂ (*cis*-**13e**): ^1H NMR (C₆D₆) δ -7.17 ppm (d of q, $^2J_{\text{transPH}} = 97$ Hz, $^2J_{\text{cisPH}} = 20$ Hz, Ru-H). The peaks for this complex were not resolved in the $^{31}\text{P}\{^1\text{H}\}$ NMR spectrum of the toluene-d₈ solution of the *cis*- and *trans*-**13c** mixture.

Unknown minor product: ^1H NMR (C₆D₆) δ -9.41 ppm (qn, $^2J_{\text{PH}} = 19.4$ Hz, Ru-H); $^{31}\text{P}\{^1\text{H}\}$ NMR (C₆D₆) δ 0.20 ppm (s). ^1H NMR (toluene-d₈) δ -9.66 ppm (qn, $^2J_{\text{PH}} = 19.2$ Hz, Ru-H); $^{31}\text{P}\{^1\text{H}\}$ NMR (toluene-d₈) δ 0.15 ppm (s). This unknown product, in the reaction with PhSH, reached a maximum of up to 12 % and thereafter declined. In the reaction with PhCH₂SH, the same product was observed, although at lower and more constant concentrations. The structure of this product remains unassigned.

An inversion-recovery NMR experiment with the following pulse sequence



where D1 = 1.00 s delay time
 D2 = 60 ms delay time
 P1 = 0.092 ms = 180° pulse
 P2 = 0.046 ms = 90° pulse
 AT = 1.36 s acquisition time

shows a positive peak for protons with T_1 values of less than 60 ms. During a reaction of **7** (2.3 mg, 4.5 mM) and PhSH (4 μ L, 70 mM) in C_6D_6 (0.6 mL) at 20°C, spectra were acquired using this pulse sequence. Only negative peaks were observed.

The reaction of *cis*- and *trans*- $RuH_2(dpm)_2$ (7**) with *p*-toluenesulphonic acid:**

Complex **7** (5.0 mg, 5.7 μ mol) and *p*-toluenesulphonic acid (28 mg, 150 μ mol) reacted in deuterated toluene (0.7 mL) at room temperature to form several products within a few minutes. A major product, a minor product, and unreacted *cis*- and *trans*- $RuH_2(dpm)_2$ were evident in the 1H and $^{31}P\{^1H\}$ NMR spectra. The major product was possibly $RuH(SO_3C_6H_4pCH_3)(dpm)_2$. 1H NMR (toluene- d_8) δ -19.40 ppm (qn, $^2J_{PH} = 19.7$ Hz, Ru-H), 4.39 (multi, CH_2), and 5.40 (multi, CH_2); $^{31}P\{^1H\}$ NMR (toluene- d_8) δ -3.00 ppm (s). The minor product had the same NMR spectra as the unknown product observed in the reaction with thiols. 1H NMR (toluene- d_8) δ -9.56 ppm (qn, $^2J_{PH} = 19.2$ Hz, Ru-H); $^{31}P\{^1H\}$ NMR (toluene- d_8) δ 0.20 ppm (s).

The reactions of *cis*- and *trans*- $RuH_2(dpm)_2$ (7**) and *cct*- $RuH_2(CO)_2(PPh_3)_2$ (**3**)**

with deuterated methanol: A C_6D_6 solution of each of **7** and **3** (4 mM) was prepared under Ar, and a 1H NMR spectrum of the sample acquired while the probe temperature equilibrated to 25°C. Enough CD_3OD was then injected to make a 4% v/v CD_3OD/C_6D_6 mixture. The decay in intensity of the peaks in the 1H NMR spectrum

was then observed with successive acquisitions using constant experimental parameters. The results are summarized in Section 3.4.

The reactions of *cct*-RuH₂(CO)₂(PPh₃)₂ (3**) with binary mixtures of thiols:**

Complex **3** (6.3 mg, 9.2 μmol), PhSH (4.7 μL, 9.2 μmol) and EtSH (3.4 μL, 9.2 μmol) were stirred in THF (7 mL) overnight at room temperature. The solvent was removed by evaporation under vacuum, and the residual solid redissolved in C₆D₆. ¹H and ³¹P{¹H} NMR spectra showed that the product was *cct*-RuH(SPh)(CO)₂(PPh₃)₂ (**9i**).

This experiment was repeated ([**3**] = 10 mM, [EtSH] = 2.3 mM, [PhSH] = 1.62 mM) in an NMR tube to allow *in situ* monitoring of the reaction by ¹H NMR spectroscopy at 35.5°C. Complex **3** was consumed, producing both **9i** and *cct*-RuH(SEt)(CO)₂(PPh₃)₂ (**9d**), the latter reaching a maximum of 32% and thereafter decreasing. After 50 min, no trace of **3** remained. After 100 min, the yield of **9i** was 98%, the remainder being **9d**.

Several such reactions were performed, with several different mixtures of thiols. The concentrations of thiols were chosen so as to produce a fairly even mixture of thiolate products, that is, the major product was not over 80% of the mixture.

The reaction of *cct*-RuH(SEt)(CO)₂(PPh₃)₂ (9d**) with thiophenol:** Complex **9d** (1.8 or 8.4 mM) and PhSH (0.12 to 3.4 M) were dissolved in C₆D₆ (0.7 mL) in an NMR tube. ¹H NMR spectra were acquired every 8-20 min, for about 3 half-lives (190 min). Concentrations were calculated from the integration of the hydride signals. The observed rate constant, *k*_{obs}, was determined from the plot of ln[**9d**] vs. time, which was linear (Fig. 3.29). One equivalent of free EtSH was detected by ¹H NMR spectroscopy.

The reaction over 3 days of Ru(CO)₂(PPh₃)₃ (2**) with thiophenol:** Complex **2** (86 mg, 91 μmol) and PhSH (190 μL, 1.3 mmol) were left for 3 days at room temperature in THF solution (10 mL). The solvent was then removed by vacuum distillation, and the orange

oily residue redissolved in C_6D_6 . The $^{31}P\{^1H\}$ NMR spectrum shows that the product mixture contained (other than free PPh_3): *cct*- $RuH(SPh)(CO)_2(PPh_3)_2$ (**9i**, 37.26 ppm, 40% of ^{31}P signal), *cct*- $Ru(SPh)_2(CO)_2(PPh_3)_2$ (**14i**, 10.73 ppm, 55%), and an unknown (23.88 ppm, 5%). None of the starting complex (**2**) remained.

The same experiment, but with 300 mg of complex **2** and 0.5 mL PhSH, resulted in 90% conversion (based on ^{31}P NMR signal integration) to **14i**.²⁵⁴

A similar experiment with *m*-thiocresol (0.3 mL, 2.5 mmol) gave only 55% conversion to the *bis*-thiolato complex **14g**, the other product being the mono-thiolato derivative **9g**. No signal for **2** was detected in the $^{31}P\{^1H\}$ NMR spectrum.²⁵⁴

The overnight reaction of $Ru(CO)_2(PPh_3)_3$ with H_2S : $Ru(CO)_2(PPh_3)_3$ (400 mg, 0.42 mmol) under H_2S (1 atm) in THF (20 mL), was stirred overnight at room temperature. The volume of solvent was reduced to 10 mL by vacuum transfer, and hexanes (150 mL) were added to induce precipitation. The isolated product had a $^{31}P\{^1H\}$ NMR spectrum identical to that of a sample of *cct*- $Ru(SH)_2(CO)_2(PPh_3)_2$ synthesised from *cct*- $RuH_2(CO)_2(PPh_3)_2$ and H_2S (see below).²⁵⁴

The overnight reaction of *cct*- $RuH_2(CO)_2(PPh_3)_2$ (3**) with H_2S :** Complex **3** (400 mg, 0.6 mmol) in THF (30 mL) was exposed to H_2S overnight at room temperature. The solution was then reduced in volume by vacuum transfer; a solid, precipitated by addition of hexanes (150 mL), was filtered off and collected as a yellow powder (76% yield).²⁵⁴ The identity of the product, *cct*- $Ru(SH)_2(CO)_2(PPh_3)_2$, was determined from the NMR spectra, the analysis, and the X-ray crystal structure (Section 4.2). Elem. Anal. Calcd. for $C_{38}H_{32}O_2P_2RuS_2$: C, 61.0 H, 4.3 S, 8.6. Found: C, 60.4 H, 4.5 S, 8.7. 1H NMR (C_6D_6) δ -1.93 ppm (t, $^3J_{PH} = 6.8$, Ru-SH), 6.95 (multi, *m/p*-Ph), 8.15 (multi, *o*-Ph); $^{31}P\{^1H\}$ NMR (C_6D_6) δ 20.45 ppm (s). For more complete details of the characterization, refer to Section 4.2.

Kinetic monitoring of the reaction of *cct*-RuH(SH)(CO)₂(PPh₃)₂ (9a**) with H₂S:**

Complex **9a** was generated *in situ* from the reaction of **3** with H₂S at 60°C. The concentrations of **9a** and the final product *cct*-Ru(SH)₂(CO)₂(PPh₃)₂ (**14a**) were calculated from their respective SH peak integrals. The experiment was stopped at the stage when PPh₃ was detected in the ³¹P{¹H} NMR spectrum, which occurred after 40-50 min at 60°C.

The non-reaction of *cct*-RuCl₂(CO)₂(PPh₃)₂ (1**) with NaBPh₄:** Complex **1** (0.109 g, 145 μmol) and NaBPh₄ (50 mg, 146 μmol) were mixed in acetone (25 mL, distilled, freeze-thaw degassed three times under H₂) under H₂ (1 atm) at room temperature. After 90 min, the suspension was filtered through diatomaceous earth. The volume of the clear and colourless filtrate was reduced to 5 mL by vacuum distillation. The white precipitate thus formed was filtered and redissolved in C₆D₆. The ³¹P{¹H} NMR spectrum showed that this material was unreacted *cct*-RuCl₂(CO)₂(PPh₃)₂.

The reaction of *trans*-RuH(SH)(dpm)₂ (13a**) with H₂S:** Complex **13a** was generated *in situ* by dissolving *trans*- and *cis*- RuH₂(dpm)₂ (**7**, 4.3 mg, 7.4 mM) in C₆D₆ (0.5 mL) in an NMR tube under Ar, capping the tube with a septum, and flushing the gas phase of the NMR tube with H₂S. The tube was then placed into the NMR probe, which was maintained at 60°C. Successive spectra were acquired at a rate of one every 10 min, with every fourth being of the ³¹P rather than ¹H region of the NMR spectrum. The ¹H NMR spectrum after 100 min showed almost complete conversion to a 1:1.8 mixture of *cis*- and *trans*-Ru(SH)₂(dpm)₂ (*cis*- and *trans*-**15**).

***trans*-Ru(SH)₂(dpm)₂ (*trans*-**15**):** ¹H NMR (C₆D₆) δ -3.73 ppm (t, ³J_{PH} = 5.7 Hz, SH), 5.10 ppm (unresolved multi, CH₂); ³¹P{¹H} NMR (C₆D₆) δ -7.05 ppm (s).

cis-Ru(SH)₂(dpm)₂ (*cis*-**15**): ¹H NMR (C₆D₆) δ -1.92 ppm (s, SH), 4.62 ppm (unresolved multi, CH₂), 5.10 ppm (unresolved multi, CH₂); ³¹P{¹H} NMR (C₆D₆) δ -5.93 ppm (t, ²J_{PP} = 28.5 Hz), -22.65 ppm (t, ²J_{PP} = 28.4 Hz).

Cis- and *trans*-**15** were isolated²⁵⁴ from the reaction of **7** (300 mg, 0.34 mmol) with H₂S (saturated solution) in THF (30 mL) after 24 h at room temperature. The yellow precipitate thus formed was collected by filtration. Elem. Anal.: Calcd. for C₅₀H₄₆P₄RuS₂: C, 64.2; H, 5.0. Found: C, 63.6; H, 5.0. The precipitate contained only 5% of the *trans* isomer, while the solid precipitated from the filtrate contained 33% of the *trans* isomer.

The reaction of *trans*-RuH(BH₄)(dpm)₂ with H₂S, using similar methods, produced a 1:2 mixture of *cis*- and *trans*-**15**.²⁵⁴

The reaction of *cct*-Ru(SC₆H₄pCH₃)₂(CO)₂(PPh₃)₂ (**14b**) with H₂S: Complex **14b** (3 mg, 3.3 μmol) was dissolved in C₆D₆ (0.5 mL) and exposed to H₂S at room temperature. The complex had been converted entirely to *cct*-Ru(SH)₂(CO)₂(PPh₃)₂ by the time the first ³¹P{¹H} NMR spectrum had been acquired, within 5 min after the start of the reaction.

The reaction of *cct*-Ru(SC₆H₄pCH₃)₂(CO)₂(PPh₃)₂ (**14b**) with ethanethiol: A saturated C₆D₆ solution of **14b** was prepared in an NMR tube under Ar, the tube being capped with a septum. EtSH (24 μL, 0.32 mmol) was injected through the septum, and the tube was placed into the NMR probe at 20°C. Successive spectra were acquired at a rate of one every 6 min, with every third being of the ¹H rather than ³¹P region of the NMR spectrum. The ³¹P{¹H} NMR spectra after 26 min no longer changed. The solution contained 75% **14b** and 25% *cct*-Ru(SC₂H₅)(SC₆H₄pCH₃)(CO)₂(PPh₃)₂ (**14bd**), based on the ³¹P NMR integration. After 70 min, more EtSH (77 μL, 1.0 mmol) was added, which shifted the equilibrium. After 200 min, the product mixture was 11%

14b (δ 10.90 ppm), 44% **14bd** (11.00 ppm), and 45% *cct*-Ru(SC₂H₅)₂(CO)₂(PPh₃)₂ (**14d**, 11.18 ppm).

This experiment was repeated three times, but with 6 mM of the starting complex and three different concentrations of ethanethiol (260 to 1530 mM). Approximate K_{eq} values at 20°C (Section 3.8) were calculated from the ¹H NMR spectra: $K_1 = 4(\pm 1.4) \times 10^{-2}$, $K_2 = 1(\pm 0.2) \times 10^{-2}$.

The reaction of *cct*-Ru(SH)₂(CO)₂(PPh₃)₂ (**14a**) with thiols: *p*-Thiocresol (2.8 mg, 0.223 M) and **14a** (4.2 mg, 5.7 mM) were dissolved in C₆D₆ (1 mL) in an NMR tube under Ar. Successive ³¹P{¹H} NMR spectra were acquired at 21°C, each taking 11 min. By 2 h, the concentrations of the complexes had converged to 34% **14a**, 56% *cct*-Ru(SH)(SC₆H₄*p*CH₃)(CO)₂(PPh₃)₂ (**14ab**) and 10% *cct*-Ru(SC₆H₄*p*CH₃)₂(CO)₂(PPh₃)₂ (**14b**).

A sample of **14a** (4 mg, 7 mM) was dissolved in C₆D₆ (0.8 mL) in an NMR tube under Ar, and PhSH (6 to 180 μ L, 7.7×10^{-2} M to 2.0 M) was injected, before the start of monitoring by ³¹P{¹H} NMR spectroscopy at 21°C. The results of these experiments are described in detail in Section 3.8.

Ethanethiol (0.25 mL, 3.3 mmol) and **14a** (3 mg, 4.0 μ mol) were dissolved in C₆D₆ and the reaction monitored *in situ* by ³¹P{¹H} NMR spectroscopy at room temperature. By 20 min, no change had been observed in the spectra.

The reaction of Ru(CO)₃(PPh₃)₂ (10**) with H₂S:** The precursor complex **10** was supplied by Dr. C.-L. Lee, who prepared it by the reaction of Ru(CO)₂(PPh₃)₃ with CO.¹⁷⁷ A refluxing THF (40 mL) solution of **10** (600 mg, 0.85 mmol), after being under H₂S (1 atm) for 3 h, was evaporated to dryness, the reaction giving 5-10% conversion to *cct*-RuH(SH)(CO)₂(PPh₃)₂ (**9a**) and **14a**, as determined by ³¹P NMR spectroscopy, the remainder being unreacted starting material.²⁵⁴

The reaction of Ru(CO)₂(dpm)(PPh₃) (16**) with thiols:** The precursor complex, **16**, was supplied by Dr. C.-L. Lee, who prepared it by the reaction of Ru(CO)₂(PPh₃)₃ with dpm (synthesis and characterization, including the crystallographically-determined structure of the 1,1-bis(diphenylphosphino)ethane (dpm-Me) analogue, to be published). Ethanethiol (98 μ L, 1.3 mmol) and **16** (16 mg, 19 μ mol) were stirred in THF (5 mL) for 5 h at room temperature, after which the volatiles were removed by vacuum distillation. The hydride region of the ¹H NMR spectrum of the residue in C₆D₆ contained three patterns at δ -4.65 (t, ²J_{PH} = 19.8 Hz, RuH of **9d**), -8.09 (ddd, ²J_{transPH} = 107, ²J_{cisPH} = 20.1, 13.8 Hz, RuH of **17**), -8.55 ppm (ddd, ²J_{cisPH} = 21.7, 20.1, 16.3 Hz, RuH of **18**). The ³¹P{¹H} NMR spectrum contained a large number of unidentified peaks, in addition to those for **16** and **9d**. The relative intensities of the peaks mentioned above are described in Section 3.9

Thiophenol (10 μ L, 97 μ mol) and **16** (7 mg, 9.0 μ mol) were dissolved in C₆D₆. After 10 min, two singlets in the ³¹P{¹H} NMR spectrum were observed, in addition to the peaks for the starting complex. The largest, at 15% of the integral, was of an unknown complex (at -9.67 ppm), while the smallest, barely detectable by ³¹P{¹H} NMR spectroscopy, was *cis*-RuH(SPh)(CO)₂(PPh₃)₂ (**9i**, 37 ppm). The identity of this latter product was confirmed by the ¹H NMR spectrum, which shows a triplet at -4.54 ppm (²J_{PH} = 19.8 Hz). No other hydride signal was observed.

The reaction of Ru(CO)₂(dpm)(PPh₃) (16**) with H₂:** A sample of Ru(CO)₂(dpm)(PPh₃) (7.4 mg, 9 μ mol) was stirred in THF (5 mL) under H₂ for two days at room temperature. Hexanes were added to the light brown solution to induce precipitation of a product which was collected by filtration. The ³¹P{¹H} NMR spectrum (C₆D₆) contained many peaks, all unidentified. The metal-hydride region of the ¹H NMR spectrum contained four weak patterns, at δ -5.30 (m, unidentified), -6.33

(t, $^2J_{\text{PH}} = 23.3$ Hz, *cis*- $\text{RuH}_2(\text{CO})_2(\text{PPh}_3)_2$), -8.43 (ddd, $^2J_{\text{cisPH}} = 22.1, 14.1,$ and 4.0 Hz, unidentified), and -8.14 ppm (ddd, $^2J_{\text{cisPH}} = 21.8, 13.6,$ and 4.1 Hz, unidentified).

4. REACTIONS OF CARBONYL (PHOSPHINE) RUTHENIUM COMPLEXES WITH DISULPHIDES, THIOETHERS, AND RELATED REAGENTS

4.1 THE REACTIONS OF Ru(CO)₂(PPh₃)₃ WITH DISULPHIDES

The reaction of **2** with *p*-tolyl disulphide (equation 4.1, R = C₆H₄*p*CH₃),



briefly mentioned in a previous publication from this laboratory,⁸⁶ proceeds cleanly in THF, giving an isolable product, **14b** (R=C₆H₄*p*CH₃). The same product is detected by ³¹P{¹H} NMR spectroscopy after the reactions of *p*-tolyl disulphide with *cct*-RuH(SEt)(CO)₂(PPh₃)₂ (**9d**, Section 4.4), and *p*-thiocresol with *cct*-RuH₂(CO)₂(PPh₃)₂ (**3**, Section 3.6).

Both **14b** and the related complex *cct*-Ru(SH)₂(CO)₂(PPh₃)₂ (**14a**) have been fully characterized (Section 4.2). Other examples of *cct*-Ru(SR)₂(CO)₂(PPh₃)₂ complexes have been synthesized in this laboratory (Section 4.2) and other isomers have since been reported in the literature.²⁶⁰

The reaction of **2** (7.5 mM) with *p*-tolyl disulphide (210 mM) at 18°C in C₆D₆, monitored by ³¹P{¹H} NMR (Fig. 4.1), has a *pseudo*-first order rate constant of 1.2 x 10⁻³ s⁻¹ and a half-life of 560 s (9.4 min). In the presence of a large amount of 1,1-dicyclopropylethylene (2.1 M), a thiyl-radical trap,²⁶¹ the reaction rate is unchanged, suggesting that the reaction mechanism does not involve free radicals. After the reaction of **2** with *p*-tolyl disulphide in the presence of added phosphine, *cct*-RuH(SC₆H₄*p*CH₃)(CO)₂(PPh₃)₂ (**9b**) and Ph₃PO are observed in addition to **14b**. This may be due to a side-reaction involving trace water.²⁶²



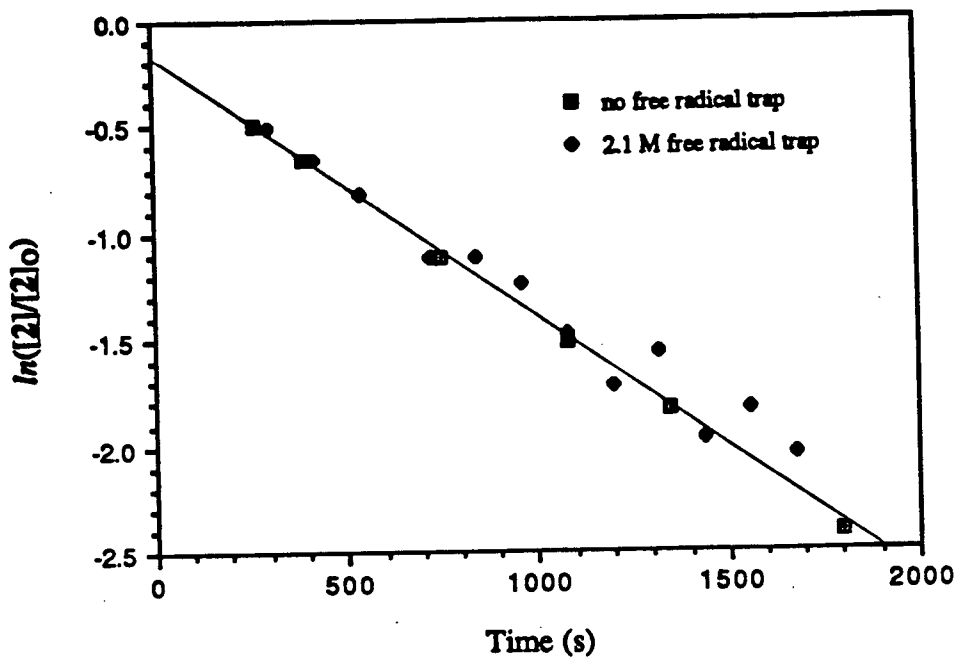
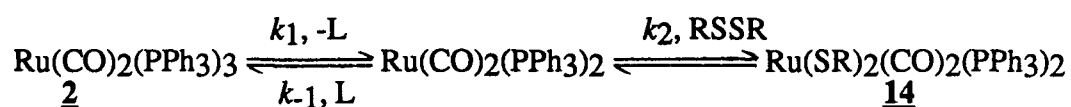


Fig. 4.1 The logarithmic dependence of the concentration of $\text{Ru}(\text{CO})_2(\text{PPh}_3)_3$ ($[\text{2}]_0 = 7.5$ mM) versus time during its reaction with *p*-tolyl disulphide (210 mM) in C_6D_6 at 18°C with or without a thiyl radical trap (1,1-dicyclopropylthylene).

The reaction of 2 with *p*-tolyl disulphide in THF, monitored by UV at 26°C, has an isosbestic point at 426 nm (Fig. 4.2), which decays because of a subsequent reaction which results in a UV spectrum having no maximum between 350 and 550 nm. This subsequent reaction, which is an order of magnitude slower than reaction 4.1, will be more fully described in Section 6.2.1. Because the subsequent reaction has an isosbestic at 395 nm, this wavelength was chosen for the collection of absorbance data for the measurement of the initial rate of reaction 4.1. This rate, calculated from the absorbances and the ϵ values of isolated samples of 2 and 14b, increases with [2], although the scatter in the data is greater than expected (Fig. 4.3). The dependence of the observed initial rate on [RSSR] is first order at low [RSSR] (< 4 mM), decreasing to zero order at high [RSSR] (Fig. 4.4a). This is qualitatively consistent with the following mechanism.



$$\frac{d[\text{14}]}{dt} = \frac{k_1 k_2 [\text{2}][\text{RSSR}]}{k_{-1}[\text{L}] + k_2[\text{RSSR}]}$$

The observed initial rate constant at high [RSSR] ($k_{\text{obs}} = 7 \times 10^{-3} \text{ s}^{-1}$) should correspond to k_1 . The same constant can be calculated from the plot of the inverse of the rate equation (Fig. 4.4b). However, the value of k_1 determined from the reaction of $\text{Ru(CO)}_2(\text{PPh}_3)_3$ with CO is $4 \times 10^{-2} \text{ s}^{-1}$ (single experiment at 1.0 mM 2 and 1 atm CO in THF at 26°C). The reason for this discrepancy is not known. Reaction 4.1 is not sufficiently clean for accurate kinetic data. The proposed mechanism should therefore be considered as tentative.

The initial concentration of PPh_3 must be less than 0.05 mM because the concentration of PPh_3 in solutions of $\text{Ru(CO)}_2(\text{PPh}_3)_3$ is not detectable by ^{31}P NMR. Thus, it is possible to place a lower limit of 80 on the value of k_{-1}/k_2 , although the exact value cannot be determined because the conventional method¹⁷² requires addition of excess PPh_3 , which causes a side reaction to occur. Values of k_{-1}/k_2 have been determined for the corresponding mechanisms of the reactions of 2 with CO and H_2 (0.043 and 0.15, respectively, at 24°C in dma).¹⁷² The

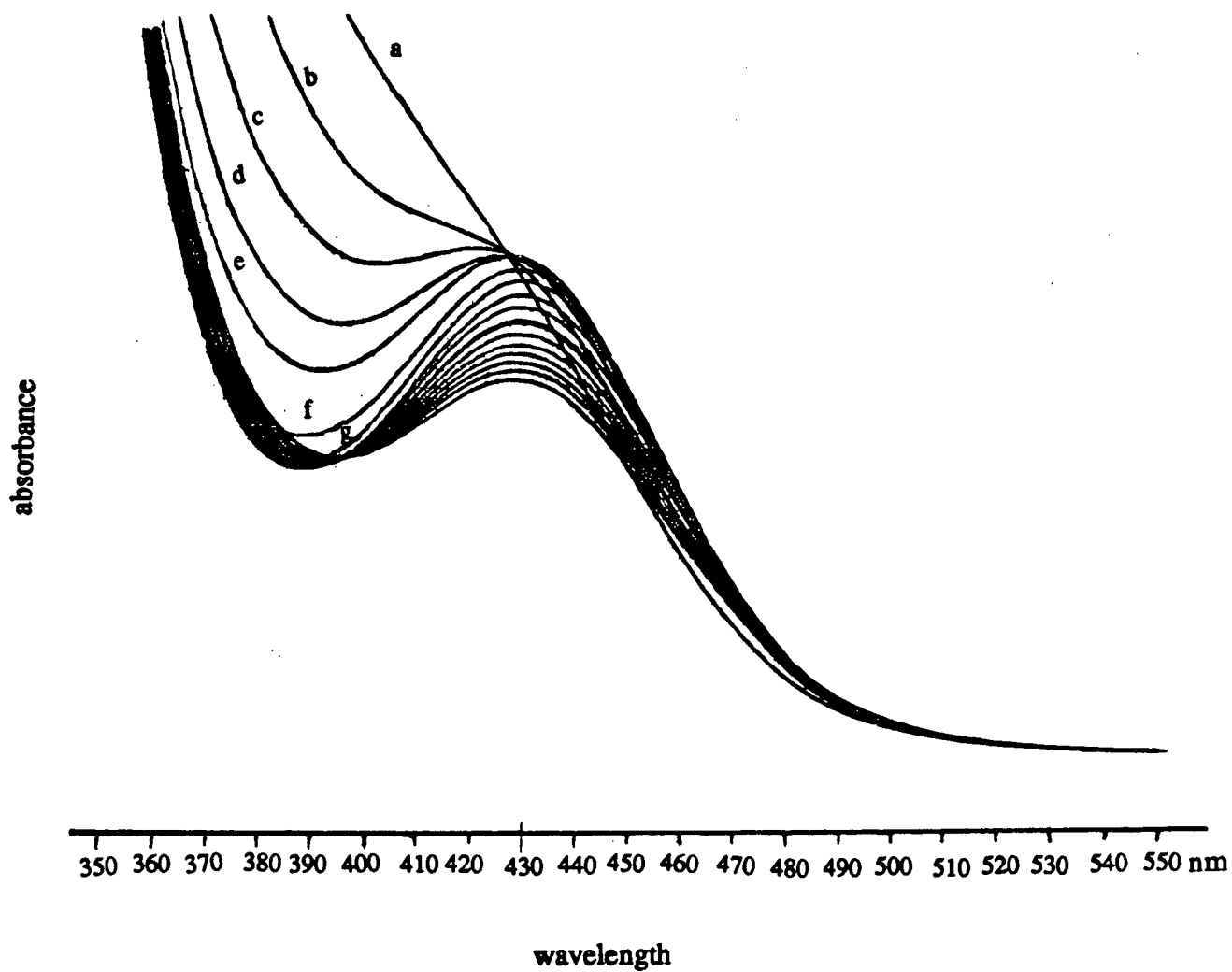


Fig. 4.2 The UV/visible absorption spectrum of a solution of $\text{Ru}(\text{CO})_2(\text{PPh}_3)_3$ (0.60 mM) and *p*-tolyldisulphide (8.2 mM) in THF at 26°C a) after 70 s, b) 190 s, c) 320 s, d) 460 s, e) 620 s, f) 990 s, g) 1440 s, and thereafter every 600 s.

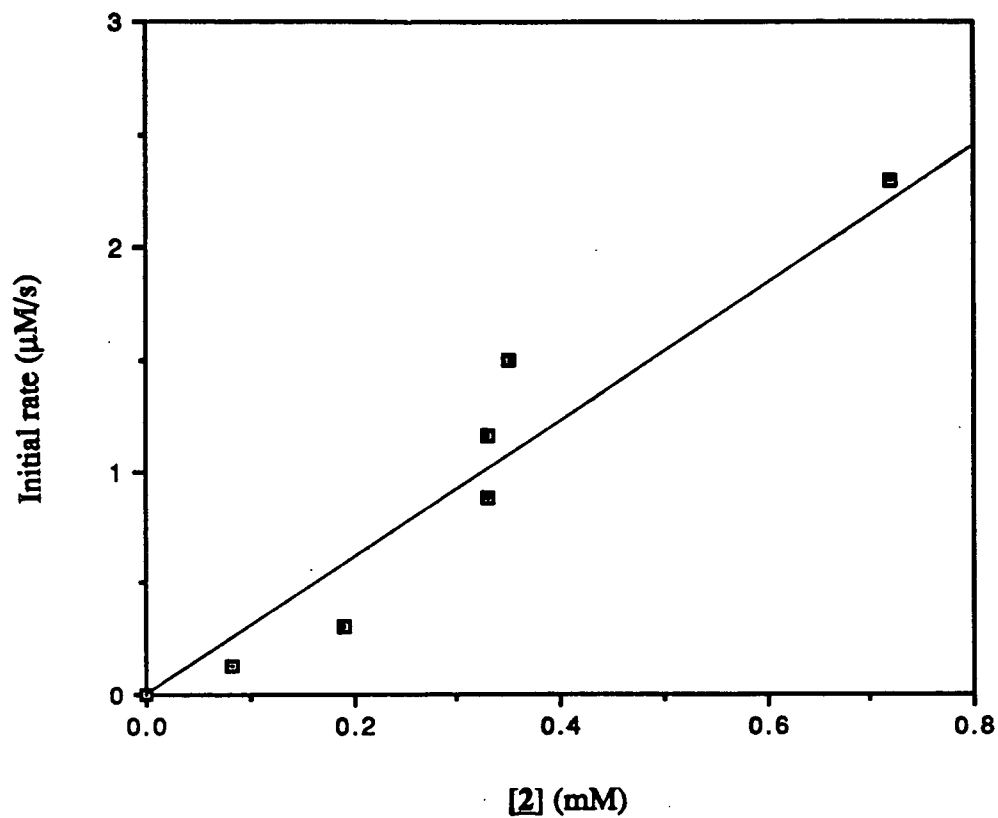


Fig. 4.3 The dependence on [2] of the initial rate of the reaction $\text{Ru}(\text{CO})_2(\text{PPh}_3)_3$ (2) with *p*-tolyldisulphide (8 mM) in THF at 26°C.

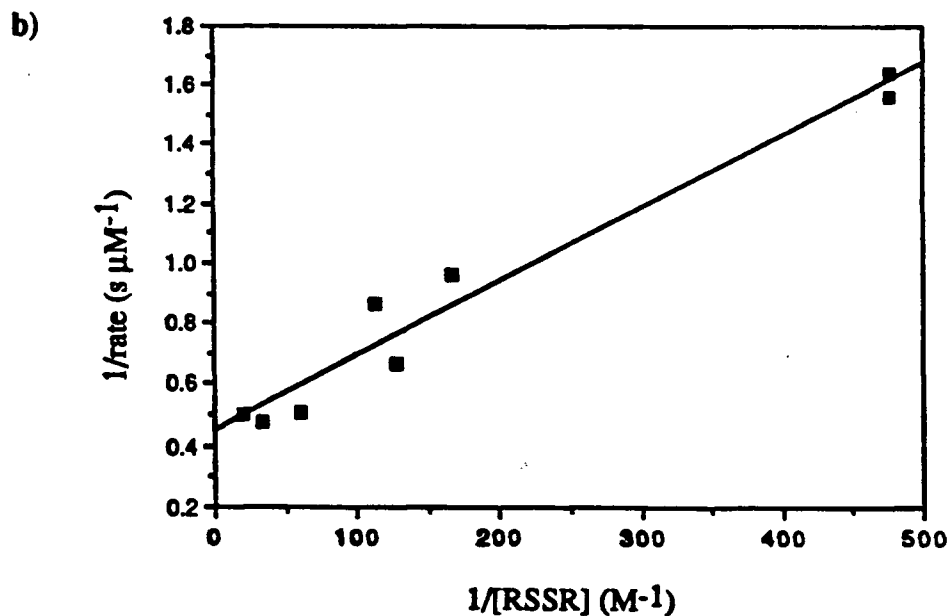
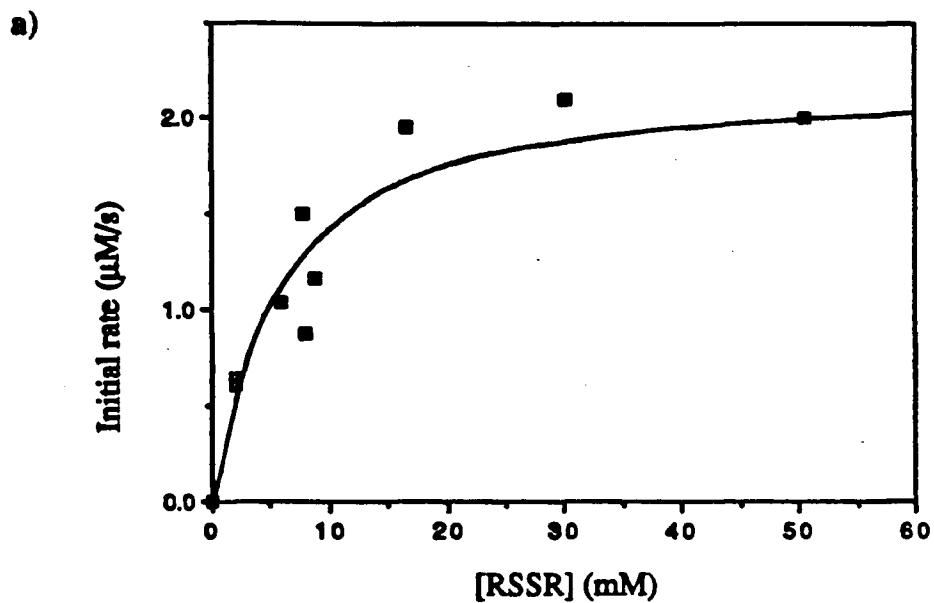


Fig. 4.4 a) The dependence on [RSSR] of the initial rate of the reaction of $\text{Ru}(\text{CO})_2(\text{PPh}_3)_3$ (2, 0.34 mM) with *p*-tolyl disulphide in THF at 26°C, showing the line which corresponds to the best-fit straight line in Fig. 4.4b.

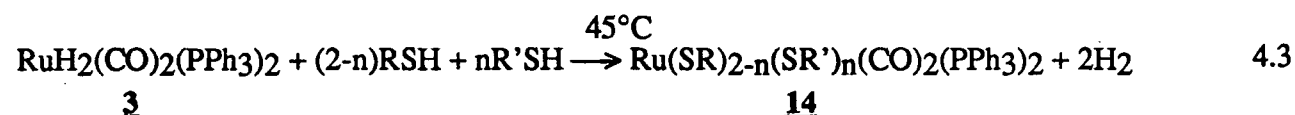
b) Plot of $1/(\text{initial rate})$ against $1/[\text{RSSR}]$ for the same reaction, including the best-fit straight line.

reaction of the unobserved intermediate $\text{Ru}(\text{CO})_2(\text{PPh}_3)_2$ with *p*-tolyl disulphide is therefore three orders of magnitude slower than with CO or H₂, if one neglects the effect of solvent.

The reaction of **2** with ethyl disulphide is neither as fast nor as clean as that with *p*-tolyl disulphide, producing *cct*-RuH(SEt)(CO)₂(PPh₃)₂ (**9c**, 6 % by ³¹P NMR) and *cct*-Ru(SEt)₂(CO)₂(PPh₃)₂ (**14c**, 12 %) after 110 min at room temperature in C₆D₆. The rate of the *k*₂ step in the reaction with EtSSEt must be even slower than the rate with *p*-tolyl disulphide, as expected for the oxidative addition of a weaker Lewis acid.

4.2 THE CHARACTERIZATION OF *cct*-Ru(SR)₂(CO)₂(PPh₃)₂

The complex *cct*-Ru(SC₆H₄*p*CH₃)₂(CO)₂(PPh₃)₂ (**14b**) was synthesized from Ru(CO)₂(PPh₃)₃ (**2**) and *p*-tolyl disulphide (Section 4.1), while *cct*-Ru(SH)₂(CO)₂(PPh₃)₂ (**14a**) was synthesized from **2** or *cct*-RuH₂(CO)₂(PPh₃)₂ (**3**) and H₂S (Sections 3.1 and 3.3). Both **14a** and **14b** have been fully characterized, and analyze correctly. The structures of both have been determined by X-ray crystallography. In addition, several other members of the series *cct*-Ru(SR)₂(CO)₂(PPh₃)₂ (Table 4.1) have been observed *in situ* by ¹H and ³¹P{¹H} NMR spectroscopy during the reactions of **14a** or **14b** with R'SH (reaction 3.18) or the reactions of *cct*-RuH₂(CO)₂(PPh₃)₂ (**3**) with binary mixtures of thiols in large excess (reaction 4.3, cf. sections 3.5, 3.6).



The ³¹P NMR chemical shift of **14** depends very little on the nature of the thiolate group, with the exceptions of complexes containing the -SH and -SC₆F₅ ligands, which have signals significantly further downfield (Table 4.1). The observed spectra show that the ³¹P chemical

Table 4.1 NMR Spectroscopic Data for Complexes of the Series *cct*-Ru(SR)(SR')(CO)₂(PPh₃)₂^a

	R	R'	31p δ obs. ^b	31p δ calc. ^c	¹ H NMR ^d
14a	H	H	20.40 ^e	21.47	-1.93 (t, ³ J _{PH} =6.8, SH)
14ab	H	C ₆ H ₄ <i>p</i> CH ₃	16.62 ^f	16.17	-1.82 (t, ³ J _{PH} =7.1, SH)
14ai	H	C ₆ H ₅	16.56 ^f	16.07	-1.82 (t, ³ J _{PH} =7.3, SH)
14j	C ₆ F ₅	C ₆ F ₅	18.30 ^g	18.25	-
14ij	C ₆ F ₅	C ₆ H ₅	14.42 ^g	14.46	-
14d	CH ₂ CH ₃	CH ₂ CH ₃	11.25 ^e	11.21	1.16 (t, ³ J _{HH} =7.4, CH ₃) 1.97 (q, ³ J _{HH} =7.4, CH ₂)
14bd	CH ₂ CH ₃	C ₆ H ₄ <i>p</i> CH ₃	11.00 ^f	11.04	
14b	C ₆ H ₄ <i>p</i> CH ₃	C ₆ H ₄ <i>p</i> CH ₃	10.90 ^e	10.87	6.54 (d, ³ J _{HH} =8.1, <i>o</i> -Ph) 6.86 (d, ³ J _{HH} =8.2, <i>m</i> -Ph) 2.03 (s, CH ₃)
14bi	C ₆ H ₄ <i>p</i> CH ₃	C ₆ H ₅	10.78 ^g	10.77	-
14i	C ₆ H ₅	C ₆ H ₅	10.69 ^g	10.67	-

a C₆D₆ solutions at room temperature.

b observed chemical shift (ppm), with reference to 85 % H₃PO₄ in H₂O.

c calculated from the empirical equation presented in Section 4.2.

d ppm, with reference to TMS in C₆D₆. Coupling constants are given in Hz. Data are for the protons of the thiolate ligands only.

e isolated sample.

f generated *in situ* via reaction 3.18.

g generated *in situ* via reaction 4.3.

shift (δ) of *cct*-Ru(SR)(SR')(CO)₂(PPh₃)₂ in C₆D₆ at room temperature is roughly predicted by the following simple additivity rule.

$$\delta = 10.67 \text{ ppm} + X(\text{R}) + X(\text{R}')$$

$$\text{where } \begin{array}{l} \text{R} = \text{H} > \text{C}_6\text{F}_5 > \text{CH}_2\text{CH}_3 > \text{C}_6\text{H}_4\text{pCH}_3 > \text{C}_6\text{H}_5 \\ \text{X} = 5.4 & 3.79 & 0.27 & 0.10 & 0.00 \text{ ppm} \end{array}$$

The error is ± 0.06 ppm except for the complexes containing the -SH ligand. The chemical shifts of **14** in CD₂Cl₂ are 21.91 (R=H), 11.43 (R=Ph), 11.39 (R=C₆H₄pCH₃), and 11.77 ppm (R=C₆H₄mCH₃), not significantly different from those in C₆D₆. The ³¹P chemical shifts in CDCl₃ of the *cct*-Ru(SR)₂(CO)₂(PPh₃)₂ complexes isolated by Catala *et al.*^{260b} were reported relative to P(OMe)₃. After conversion to shifts relative to 85 % H₃PO₄ (assuming that the signal of P(OMe)₃ appears at 141 ppm²⁶³), the reported shifts of these complexes are 22.8 (R=Me), 39.6 (*t*Bu), 26.6 (C₆F₄H), and 29.4 ppm (C₆F₅, **14j**). It is not known why the chemical shift reported by Catala *et al.* for **14j** and that in the present study differ by more than 10 ppm. The spread of the chemical shifts are similar in the two studies. The difference between the chemical shifts of *cct*-Ru(SR)₂(CO)₂(PPh₃)₂ (R=Me and C₆F₅) in CDCl₃ is 6.6 ppm,^{260b} very similar to the difference (R=Et vs. C₆F₅) of 7.05 ppm in C₆D₆ found in the present study.

The ¹H NMR test described in Section 2.3.3, applied to the spectra of **14a** and **14b** (Fig. 4.5), proves that the PPh₃ ligands of those complexes are in *trans* positions. The mercapto signals of **14a** are triplets, 1.07 ppm downfield of the same signal in *cct*-RuH(SH)(CO)₂(PPh₃)₂ (**9a**). The methyl signal of **14b** is at the same chemical shift (2.03 ppm) as its hydrido-thiolato analogue **9b**.

The FT-IR spectra of **14** (Fig. 4.6) contain two strong $\nu(\text{CO})$ bands at 2046 and 1981 cm⁻¹ (**14a**)¹²⁶ or at 2028 and 1968 cm⁻¹ (R=**14b**)²⁵⁴, suggesting that both complexes contain *cis*-carbonyls, and therefore that both are *cct* isomers in solution. The *cct* isomer is the most stable of the isomers of *cct*-RuCl₂(CO)₂(PR₃)₂.¹⁶⁹

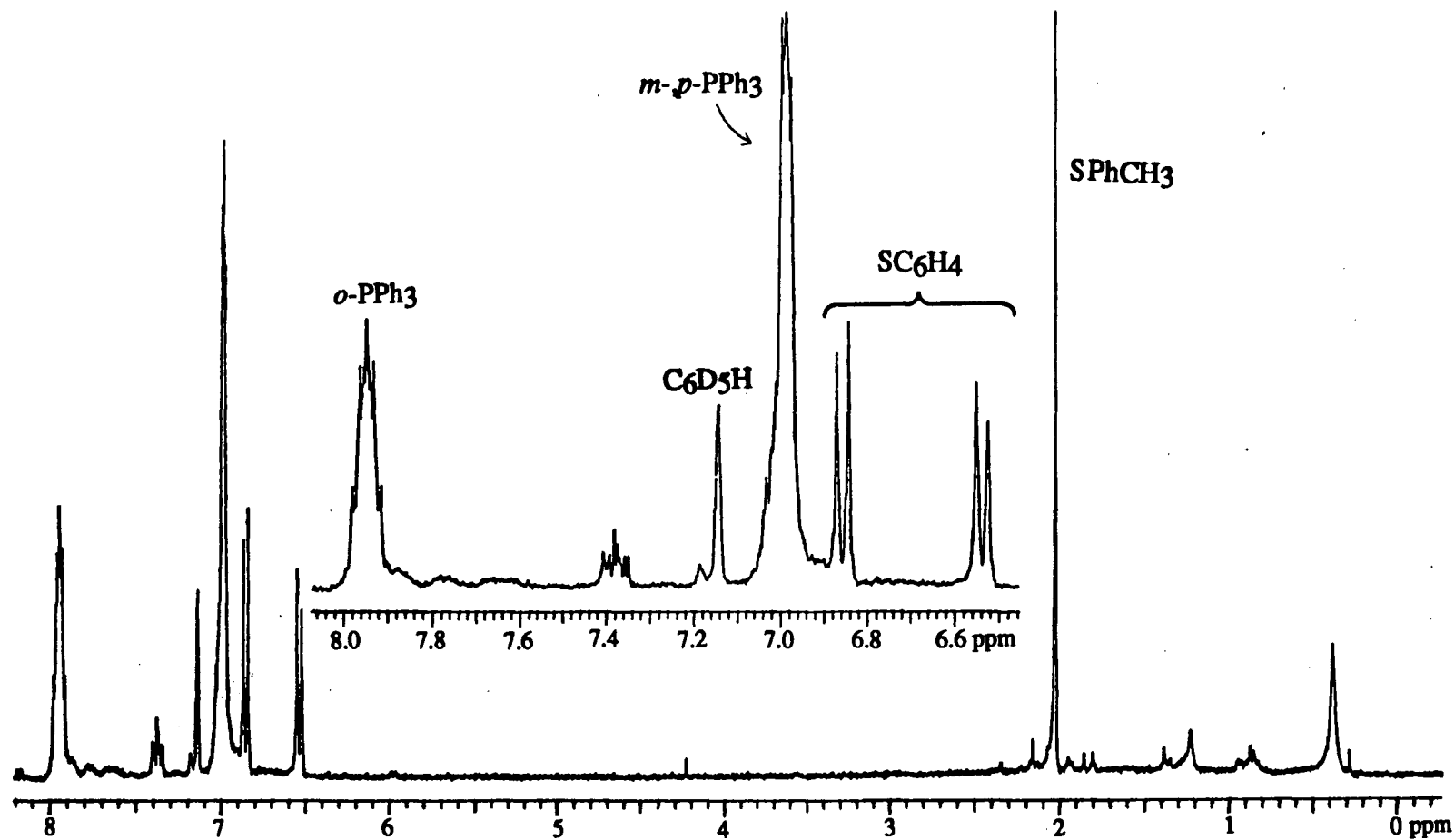


Fig. 4.5 ^1H NMR spectrum of $cct\text{-Ru}(\text{SC}_6\text{H}_4\text{pCH}_3)_2(\text{CO})_2(\text{PPh}_3)_2$ (**9b**), in C_6D_6 , with an expanded view of the phenyl region.

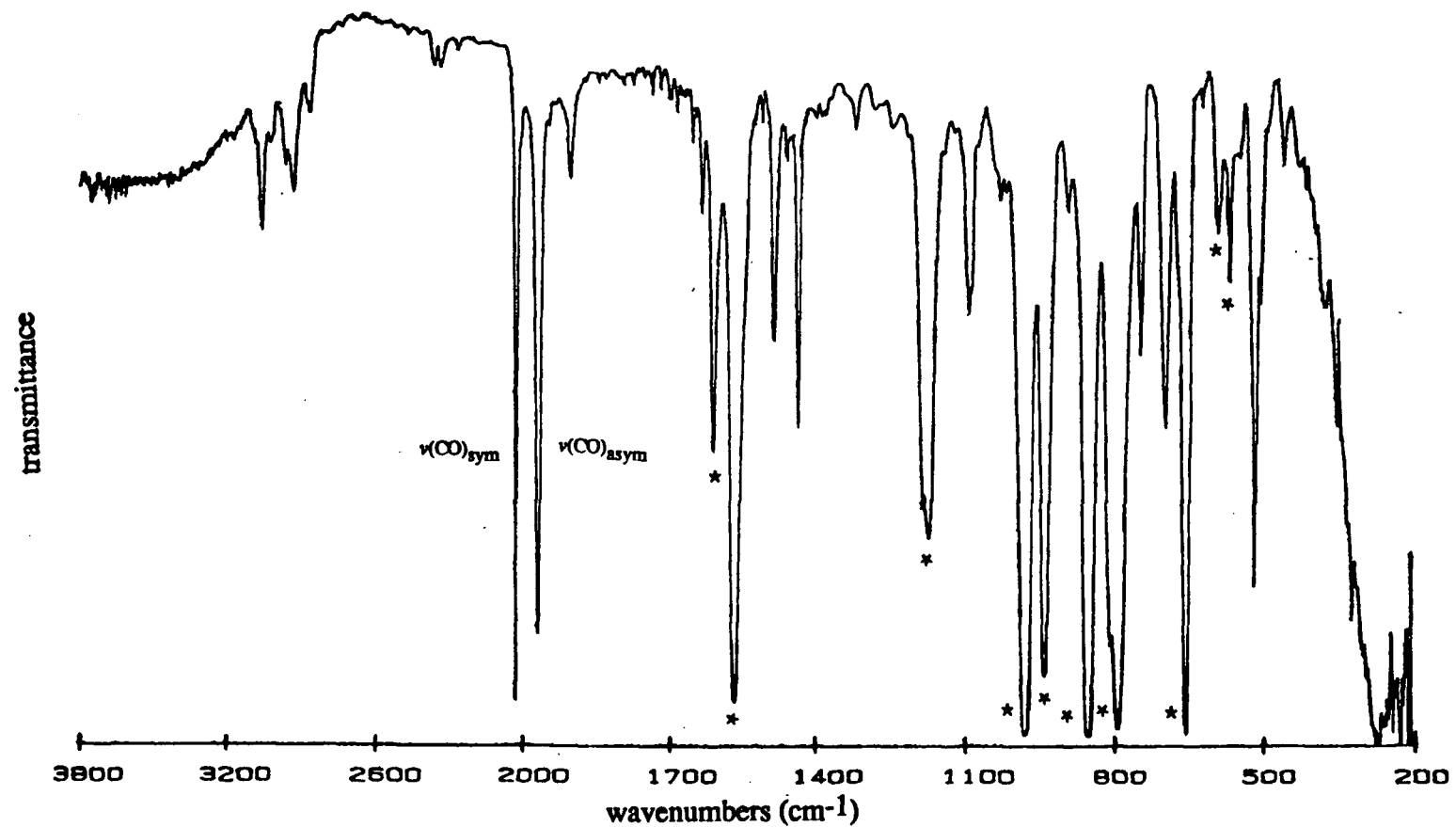


Fig. 4.6 FT-IR spectrum of *cct*- $\text{Ru}(\text{SC}_6\text{H}_4\text{pCH}_3)_2(\text{CO})_2(\text{PPh}_3)_2$ in HCB. The peaks due to HCB are indicated with asterisks.

The UV/vis spectrum of **14** contains a maximum at 371 ($\epsilon = 2460$, **14a**) or 430 nm ($\epsilon = 3040 \text{ M}^{-1} \text{ cm}^{-1}$, **14b**), which causes the yellow colour. The absorption is probably caused by the same ligand-to-metal charge transfer which caused the similar band in the spectrum of *cct*-RuH(SR)(CO)₂(PPh₃)₂ (Section 3.2).

The solid state X-ray crystal structure of **14b** (Fig. 4.7) was investigated by Dr. S. Rettig,²⁰⁹ and can be compared to the previously solved structure of a crystal of **14a** (Fig. 4.8) synthesized in this lab.²⁶⁴ Both were shown to be of *cct* geometry. Bond lengths, bond angles, and other crystallographic data are listed in Tables 4.2 through 4.5 and Appendices 1 and 3. Related complexes for which X-ray crystal structures have been reported include *ccc*-Os(SC₆F₅)₂(CO)₂(PEt₂Ph)₂^{260d} and *cct*-Ru(OCOPh)₂(CO)₂(PPh₃)₂.^{257d}

The observed deviations from octahedral geometry around the Ru centre of **14b** are due to the PPh₃ groups crowding the carbonyls in order to avoid the bulky thiolate ligands. The carbonyls therefore are slightly further apart (91.6°), and the thiolates closer together (83.05°) than expected for octahedral geometry. This effect is not observed in **14a** (angles: C-Ru-C 89.1°, S-Ru-S 92.2°)²⁶⁴ because the mercapto ligands are considerably less bulky than the thiolates in **14b**. The proximity of the S atoms in **14b** (3.26 Å) but not **14a** (3.56 Å)²⁶⁴ is probably caused by the bulky *p*-tolyl groups which point away from each other. The S atoms are not so close together as to indicate S-S attractive interactions, which have been reported for some *cis*-thiolate complexes. "S-S contacts are invariably shorter when the sulphur lone pairs (assuming approximate *sp*³ hybridizations) are oriented so as to allow overlap, resulting in an interaction which would normally be considered repulsive."²⁶⁵ Visual inspection of the structure of **14b** shows that the thiolate ligands are oriented so as to allow almost no lone pair overlap. In both complexes, and in *ccc*-Fe(SPh)₂(CO)₂(dppe) (dppe = 1,2-bis{diphenylphosphino}ethane, S-S distance is 3.23 Å),²¹⁴ the S-S interatomic distance is considerably longer than observed for S-S bonds such as in *cct*-Os(η^2 S₂Me)(CO)₂(PPh₃)₂ (2.022 Å).¹¹⁸

The lengths of the Ru-S, Ru-C, and C-O bonds of **14a**, **14b**, and *cct*-RuH(SC₆H₄*p*CH₃)(CO)₂(PPh₃)₂ (**9b**, Section 3.2) are similar. The S-C bond lengths of

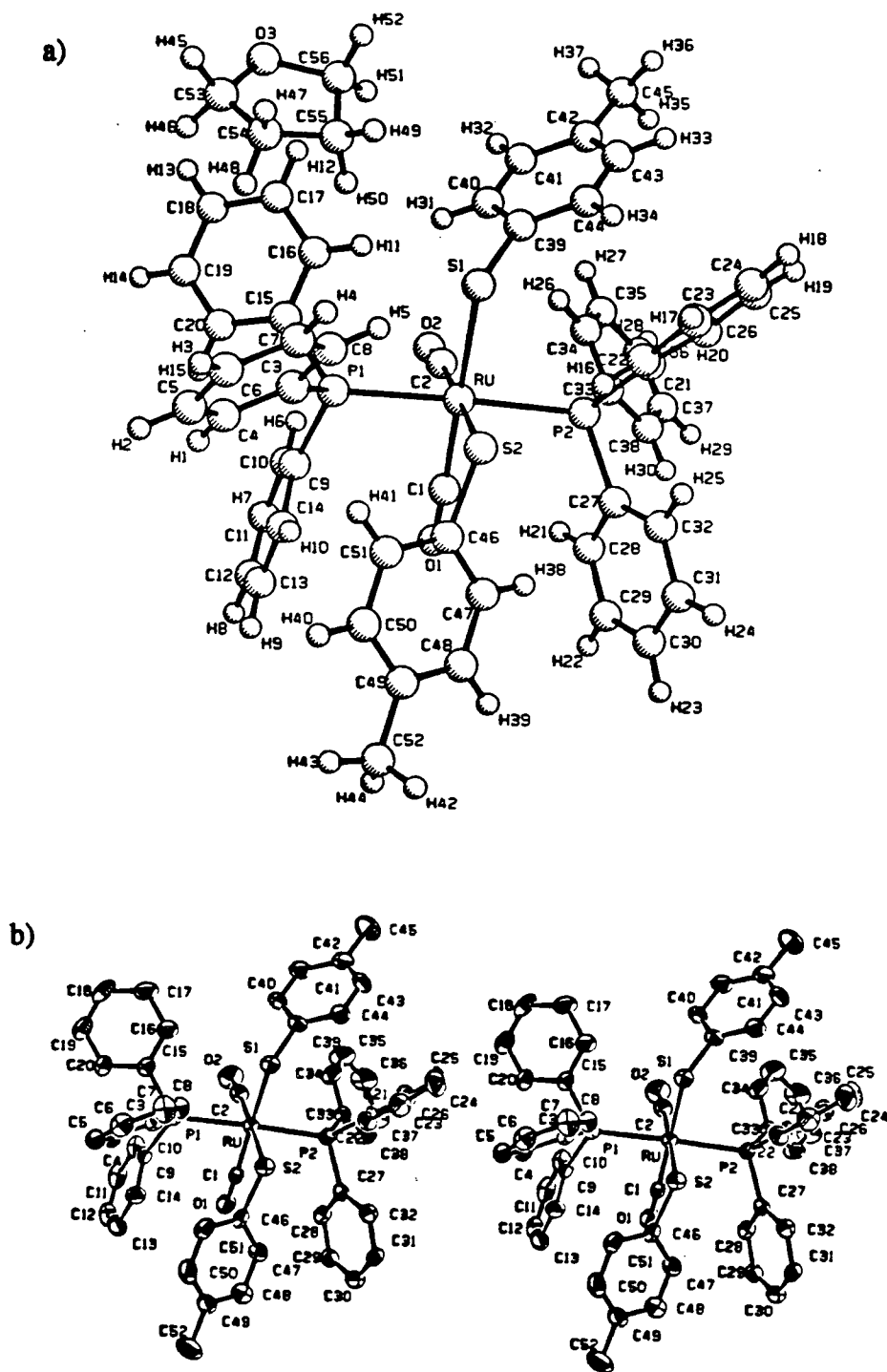


Fig. 4.7 a) The structure of *cct*-Ru(SC₆H₄pCH₃)₂(CO)₂(PPh₃)₂ (**14b**), showing co-crystallised THF molecule, and b) a stereoscopic view of the same structure, with hydrogen atoms and the THF molecule omitted for clarity.

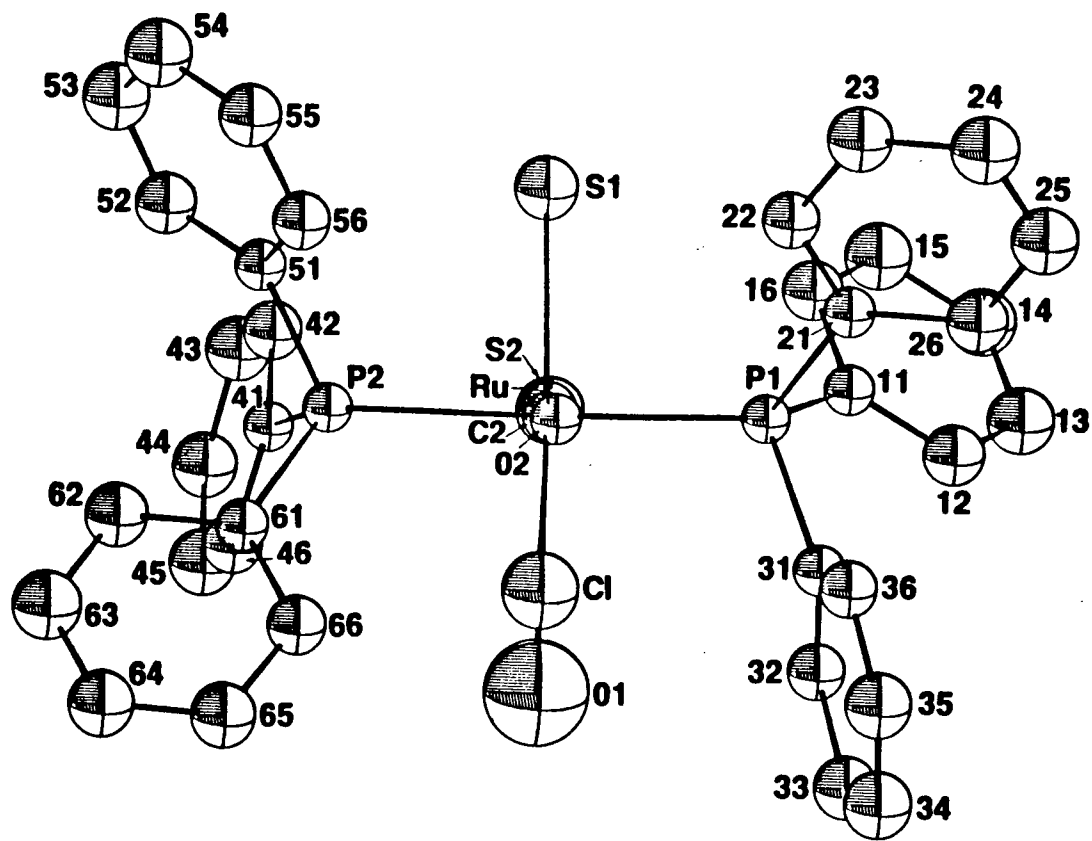


Fig. 4.8 The structure of $\text{Ru}(\text{SH})_2(\text{CO})_2(\text{PPh}_3)_2 \cdot 2.264$ Hydrogen atoms are omitted for clarity.

Table 4.2 Selected bond lengths (Å) with estimated standard deviations in parentheses, for *cct*-Ru(SC₆H₄pCH₃)₂(CO)₂(PPh₃)₂ (14b).²⁰⁹

atom	atom	distance	atom	atom	distance
Ru	C(2)	1.863 (8)	P(1)	C(9)	1.814 (8)
Ru	C(1)	1.900 (8)	P(1)	C(15)	1.838 (8)
Ru	P(1)	2.444 (2)	P(1)	C(3)	1.841 (7)
Ru	P(2)	2.449 (2)	P(2)	C(33)	1.826 (7)
Ru	S(2)	2.450 (2)	P(2)	C(27)	1.833 (7)
Ru	S(1)	2.470 (2)	P(2)	C(21)	1.841 (7)
S(1)	C(39)	1.788 (7)	O(1)	C(1)	1.129 (7)
S(2)	C(46)	1.778 (8)	O(2)	C(2)	1.148 (8)

Table 4.3 Selected bond angles (°) with estimated standard deviations in parentheses, for *cct*-Ru(SC₆H₄pCH₃)₂(CO)₂(PPh₃)₂ (14b).²⁰⁹

atom	atom	atom	angle	atom	atom	atom	angle
C(2)	Ru	C(1)	91.6 (3)	C(46)	S(2)	Ru	113.6 (2)
C(2)	Ru	P(1)	86.8 (2)	C(9)	P(1)	C(15)	103.2 (4)
C(2)	Ru	P(2)	94.8 (2)	C(9)	P(1)	C(3)	106.3 (3)
C(2)	Ru	S(2)	178.1 (2)	C(9)	P(1)	Ru	107.0 (2)
C(2)	Ru	S(1)	95.9 (2)	C(15)	P(1)	C(3)	98.4 (3)
C(1)	Ru	P(1)	88.3 (2)	C(15)	P(1)	Ru	119.3 (3)
C(1)	Ru	P(2)	90.1 (2)	C(3)	P(1)	Ru	120.7 (2)
C(1)	Ru	S(2)	89.4 (2)	C(33)	P(2)	C(27)	103.1 (3)
C(1)	Ru	S(1)	172.3 (2)	C(33)	P(2)	C(21)	101.9 (3)
P(1)	Ru	P(2)	177.8 (1)	C(33)	P(2)	Ru	114.3 (3)
P(1)	Ru	S(2)	91.62 (8)	C(27)	P(2)	C(21)	103.5 (3)
P(1)	Ru	S(1)	90.64 (8)	C(27)	P(2)	Ru	113.0 (2)
P(2)	Ru	S(2)	86.87 (8)	C(21)	P(2)	Ru	119.1 (2)
P(2)	Ru	S(1)	90.74 (8)	O(1)	C(1)	Ru	176.7 (6)
S(2)	Ru	S(1)	83.05 (7)	O(2)	C(2)	Ru	174.2 (7)
C(39)	S(1)	Ru	113.0 (2)				

Table 4.4 Selected bond lengths (Å) with estimated standard deviations in parentheses, for *cct*-Ru(SH)₂(CO)₂(PPh₃)₂ (14a).²⁶⁴

atom	atom	distance	atom	atom	distance
Ru	P(1)	2.411 (1)	Ru	P(2)	2.418 (2)
Ru	S(1)	2.472 (2)	Ru	S(2)	2.470 (2)
Ru	C(1)	1.891 (8)	Ru	C(2)	1.891 (7)
S(1)	H(1)	1.0 (2)	S(2)	H(2)	1.2 (1)
P(1)	C(11)	1.846 (6)	P(1)	C(21)	1.846 (8)
P(1)	C(31)	1.832 (6)	P(2)	C(41)	1.835 (7)
P(2)	C(41)	1.835 (7)	P(2)	C(51)	1.836 (9)
P(2)	C(61)	1.841 (4)	C(1)	O(1)	1.12 (1)
C(2)	O(2)	1.12 (1)			

Table 4.5 Selected bond angles (°) with estimated standard deviations in parentheses, for *cct*-Ru(SH)₂(CO)₂(PPh₃)₂ (14a).²⁶⁴

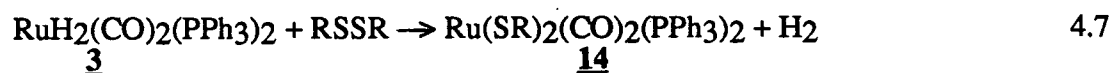
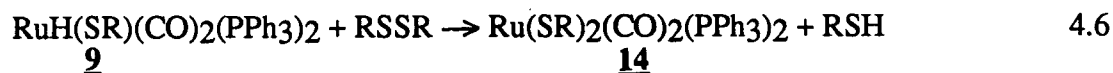
atom	atom	atom	angle	atom	atom	atom	angle
P(1)	Ru	P(2)	175.57 (7)	P(1)	Ru	S(1)	91.0 (1)
P(1)	Ru	S(2)	85.4 (1)	P(1)	Ru	C(1)	91.2 (2)
P(1)	Ru	C(2)	92.0 (1)	P(2)	Ru	S(1)	87.5 (1)
P(2)	Ru	S(2)	90.5 (1)	P(2)	Ru	C(1)	90.6 (2)
P(2)	Ru	C(2)	92.1 (1)	S(1)	Ru	S(2)	92.2 (1)
S(1)	Ru	C(1)	175.6 (2)	S(1)	Ru	C(2)	86.9 (2)
S(2)	Ru	C(1)	91.8 (2)	S(2)	Ru	C(2)	177.3 (1)
C(1)	Ru	C(2)	89.1 (2)	Ru	S(1)	H(1)	84 (12)
Ru	S(2)	H(2)	99 (14)	Ru	P(1)	C(11)	117.1 (1)
Ru	P(1)	C(21)	120.3 (1)	Ru	P(1)	C(31)	109.9 (1)
C(11)	P(1)	C(21)	99.7 (3)	C(11)	P(1)	C(31)	105.1 (3)
C(21)	P(1)	C(31)	102.8 (3)	Ru	P(2)	C(41)	108.5 (3)
Ru	P(2)	C(51)	117.1 (2)	Ru	P(2)	C(61)	120.0 (3)
C(41)	P(2)	C(51)	106.3 (3)	C(41)	P(2)	C(61)	102.0 (3)
C(51)	P(2)	C(61)	101.1 (3)	Ru	C(1)	O(1)	176.8 (7)
Ru	C(2)	O(2)	178.1 (9)				



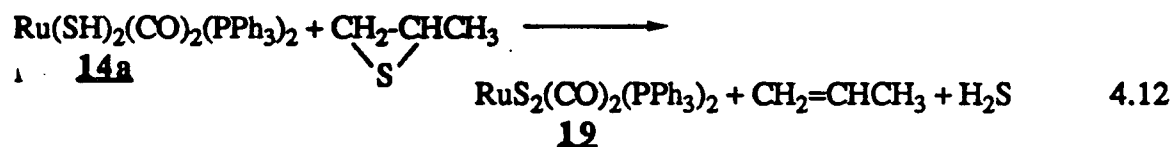
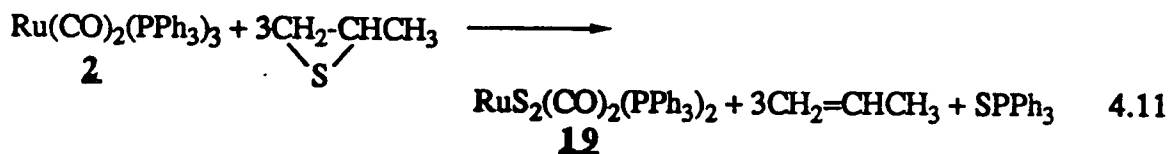
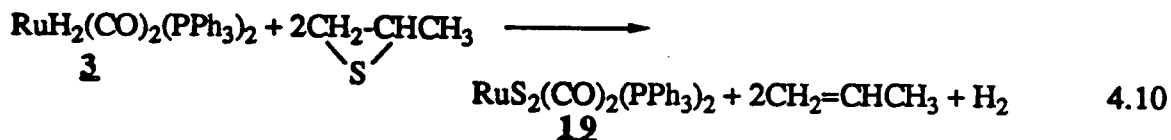
The evidence for this was the detection of RSH (0.02 mmol) after a 5 h reaction of a THF solution (40 mL) of the dihydride (0.41 mmol) and *p*-tolyl disulphide (0.41 mmol).^{126,266}

Although the suggested sequence of reactions is reasonable, it is not unequivocal that the detection of a small amount of thiol is evidence for reaction 4.5; the thiol could instead have been produced by reaction 4.6 (see below).

The reaction of **3** with an 18-fold excess of *p*-tolyl disulphide in C₆D₆ was monitored by NMR at 45°C. After 1 h, the conversion to **9b** was 84 %. If the reaction is monitored at room temperature, a small amount (less than 11 %) of **14b** is observed while the reaction to **9b** proceeds. No *p*-thiocresol was detected in the ¹H NMR spectrum during this time, possibly because reaction 3.4 is faster than reaction 4.4; the concentration of thiol never reaches a level sufficient for detection. The production of the *bis*-thiolate complex **14b** is evidence for reaction 4.6 (to be described in Section 4.4), although a small amount of this product could have been produced by reaction 4.7, for which no independent evidence exists.



The rate of reaction 4.4, monitored by either NMR or UV/vis spectroscopy is neither reproducible nor *pseudo*-first order, not surprising considering that reactions 3.4, 4.5, 4.6 and possibly 4.7 are all occurring in the same solution. No isosbestic points are observed because the UV/vis spectra of **3** and **9b** do not have cross-over points. The mechanism of reaction 4.4 was not determined.



The production of SPPh_3 in reaction 4.11 (identified by $^{31}\text{P}\{^1\text{H}\}$ NMR spectroscopy) suggests the possibility of reaction 4.13.



but propylene sulphide and PPh_3 in C_6D_6 fail to react within 12 h at room temperature.

Oxidation of the phosphine to the phosphine sulphide must therefore involve the ruthenium complex.

In the present work, reaction 4.10 (using a large excess of thioether) was monitored by $^{31}\text{P}\{^1\text{H}\}$ NMR spectroscopy at 21°C , and initially two sulphur-containing complexes were observed, **19** (22 % of the ^{31}P NMR signal after 10 min) and *cis*- $\text{RuH}(\text{SR})(\text{CO})_2(\text{PPh}_3)_2$ (**9**, 10 %, R unknown). After 160 min, the signals due to these species had increased to 53 % and 29 %, respectively, while SPPh_3 started to appear (12 % of the ^{31}P NMR signal). After 7 days, the sole product detected in the ^{31}P NMR spectrum was SPPh_3 . The rate of loss of **3**, as measured by ^{31}P NMR spectroscopy, was not *pseudo*-first order. The initial rate constant was calculated from the concentrations of **3** and **9** (determined from the ^{31}P NMR peak integration) assuming the initial rate is first order in [**3**]. The value of this rate constant ($6.0 \times 10^{-4} \text{ s}^{-1}$ at 21°C) is similar to that of the reaction of **3** with thiols (Section 3.3), and is therefore consistent with a mechanism involving reductive elimination of H_2 as the first and rate determining step. Similar

$^{31}\text{P}\{^1\text{H}\}$ NMR experiments monitoring the reaction of **2** with propylene sulphide showed that reaction 4.11 is complete after 3 min at 25°C in C_6D_6 .

4.6 THE NON-REACTIONS OF CARBONYL (PHOSPHINE) RUTHENIUM COMPLEXES WITH UNSTRAINED THIOETHERS

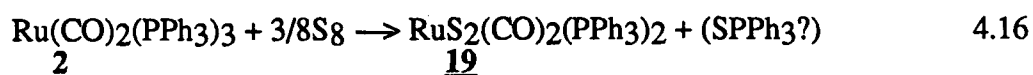
The two complexes $\text{Ru}(\text{CO})_2(\text{PPh}_3)_3$ (**2**)²⁵⁴ and *cct*- $\text{RuH}_2(\text{CO})_2(\text{PPh}_3)_2$ (**3**) fail to react with thioethers such as MeSMe, PhSPh, and dibenzothiophene.



A 35-fold excess of freshly distilled thiophene reacts with **3** at room temperature to produce *cct*- $\text{RuH}(\text{SR})(\text{CO})_2(\text{PPh}_3)_2$ (2% conversion, R=unknown alkyl group) after three days. This reaction is probably due to a trace (0.5ppth, calculated from the extent of conversion of **3** to **9**) of thiol which was not removed by the distillation. At least four C₄-thiols have boiling points²⁶⁷ within 20° of that of thiophene.

4.7 THE REACTIONS OF CARBONYL(PHOSPHINE)RUTHENIUM COMPLEXES WITH OTHER NEUTRAL SULPHUR-CONTAINING REAGENTS

The reaction of $\text{Ru}(\text{CO})_2(\text{PPh}_3)_3$ (**2**) with elemental sulphur in benzene has been reported, although the fate of the extra phosphine ligand was not mentioned.^{118a}



The same product complex (**19**) is observed, along with SPPH_3 , after the reaction of sulphur with $cis\text{-Ru}(\text{SH})_2(\text{CO})_2(\text{PPh}_3)_2$.²⁵⁴

Dibenzyl trisulphide has been used to oxidize bridging thiolate groups to sulphides.²⁶⁸ The trisulphide reacts with $cis\text{-Ru}(\text{SC}_6\text{H}_4\text{pCH}_3)_2(\text{CO})_2(\text{PPh}_3)_2$ (**14b**) relatively quickly at room temperature, giving SPPH_3 and a host of minor products (<3 % each) after 40 min. The trisulphide reacts with **2** or **3** more slowly, producing SPPH_3 , and two unknowns with ^{31}P NMR singlets with chemical shifts (34.67 and 31.34 ppm in C_6D_6) different from those of any of the related complexes that have been previously isolated, such as $cis\text{-Ru}(\text{SR})_2(\text{CO})_2(\text{PPh}_3)_2$ (R=H or CH_2Ph), $cis\text{-RuH}(\text{SR})(\text{CO})_2(\text{PPh}_3)_2$, or $cis\text{-RuS}_2(\text{CO})_2(\text{PPh}_3)_2$. The desulphurization of trisulphides by triphenyl phosphine, giving disulphides and SPPH_3 , has been reported.²⁶⁹

4.8 EXPERIMENTAL DETAILS

The reaction of $\text{Ru}(\text{CO})_2(\text{PPh}_3)_3$ (2**) with *p*-tolyl disulphide:** Complex **2** (140 mg, 0.15 mmol) and the disulphide (91 mg, 0.36 mmol) were dissolved in THF (20 mL) in a Schlenk tube wrapped with foil in darkness at room temperature. The solution remained orange throughout the reaction. After 4.5 h, the volume of the solution was reduced to 5 mL by vacuum distillation, and hexanes (60 mL) were added to induce precipitation. The collected yellow solid was $cis\text{-Ru}(\text{SC}_6\text{H}_4\text{pCH}_3)_2(\text{CO})_2(\text{PPh}_3)_2$ (**14b**, 85 % yield). Elem. Anal. Calcd. for $\text{C}_{52}\text{H}_{44}\text{O}_2\text{P}_2\text{RuS}_2$: C, 67.3; H, 4.8; S, 6.9. Found: C, 67.3; H, 4.7; S, 6.8. UV/vis max (0.25 mM in THF) 430 nm (ϵ 3000 $\text{M}^{-1}\text{cm}^{-1}$); FT-IR (Nujol) 2028, 1968 cm^{-1} ($\nu(\text{C}=\text{O})$); (HCB) : 2029, 1971 cm^{-1} ; ^1H NMR (C_6D_6) δ 2.03 (s, 6H, CH_3), 6.54 (d, 4H, $^3J_{\text{HH}} = 8.1$ Hz, SC_6H_4), 6.86 (d, 4H, $^3J_{\text{HH}} = 8.2$ Hz, SC_6H_4), 6.99 (m, 18H, *p*-,*m*- PPh_3), 7.95 ppm (m, 12H, *o*- PPh_3); $^{13}\text{C}\{^1\text{H}\}$ NMR (C_6D_6) 20.90 ppm (s, CH_3); $^{31}\text{P}\{^1\text{H}\}$ NMR (C_6D_6) 10.95 ppm (s).

A crystal of **14b** suitable for X-ray crystallography was prepared by diffusion of hexanes into a concentrated THF solution under Ar in darkness. The collection and analysis of the

crystallographic data were performed by Dr. S. J. Rettig of this department.²⁰⁹ The final unit-cell parameters were obtained by least-squares on the setting angles for 25 reflections with $2\theta = 10.0\text{-}16.0^\circ$. The intensities of three standard reflections, measured every 200 reflections throughout the data collection, were essentially constant. The data were processed^{259a} and corrected for Lorentz and polarization effects, and absorption (empirical, based on azimuthal scans for four reflections).²⁰⁹

The structure analysis was initiated in the centrosymmetric space group $P\bar{1}$, the choice being confirmed by the subsequent successful solution and refinement of the structure. The structure was solved by conventional heavy atom methods, the coordinates of the Ru, P, and S atoms being determined from the Patterson functions and those of the remaining non-hydrogen atoms from subsequent difference Fourier syntheses. The asymmetric unit contains one tetrahydrofuran solvate molecule in addition to the complex molecule. All non-hydrogen atoms were refined with anisotropic thermal parameters. Hydrogen atoms were fixed in idealized positions ($d_{C-H} = 0.98 \text{ \AA}$, $B_H = 1.2 B_{\text{bonded atom}}$). Neutral atom scattering factors and anomalous dispersion corrections for the non-hydrogen atoms were taken from the International Tables for X-Ray Crystallography.^{259b} Final atomic coordinates and equivalent isotropic thermal parameters [$B_{eq} = 4/3 \sum_i \sum_j b_{ij} (a_i a_j)$], bond lengths, and bond angles²⁰⁹ appear in Appendix 3, and Tables 4.2 and 4.3 respectively. Other crystallographic data for this structure and the other structures described in this work are presented in Appendix 1.²⁰⁹

The reaction of $\text{Ru}(\text{CO})_2(\text{PPh}_3)_3$ (2**) with ethyl disulphide:** A sample of **2** (3.3 mg, 7.1 mM) was dissolved in C_6D_6 (0.46 mL) in an NMR tube at room temperature under Ar, and EtSSEt (36 μL , 592 mM) was added to start the reaction. After 30 min, *cct*- $\text{RuH}(\text{SEt})(\text{CO})_2(\text{PPh}_3)_2$ (**9d**, 4 % conversion), *cct*- $\text{Ru}(\text{SEt})_2(\text{CO})_2(\text{PPh}_3)_2$ (**14d**, 6 %), and PPh_3 were detected by $^{31}\text{P}\{^1\text{H}\}$ NMR spectroscopy. After 110 minutes, these conversions had increased to 6 and 12 %, respectively.

Monitoring the reaction of Ru(CO)₂(PPh₃)₃ (2**) with *p*-tolyl disulphide by ³¹P{¹H} NMR spectroscopy:**

a) without added PPh₃: Complex **2** (4.2 mg, 7.5 mM) and *p*-tolyl disulphide (31.7 mg, 210 mM) were dissolved in C₆D₆ (0.46 mL) in an NMR tube at 18°C under Ar. After 30 min, *cct*-Ru(SC₆H₄*p*CH₃)₂(CO)₂(PPh₃)₂ (**14b**, 91 % conversion) and PPh₃ were observed. After 60 min, the conversion had increased to 99 %. The *pseudo*-first order log plot was linear, with some scatter (Fig. 4.1); the rate constant was 1.2 x 10⁻³ s⁻¹.

b) with added PPh₃: Complex **2** (2.7 mg, 4.1 mM), *p*-tolyl disulphide (15.7 mg, 91 mM), and PPh₃ (23.7 mg, 130 mM) were dissolved in C₆D₆ (0.70 mL) in an NMR tube at 26°C under Ar. After 30 min, *cct*-RuH(SC₆H₄*p*CH₃)(CO)₂(PPh₃)₂ (**9b**, 6 % conversion), **14b** (8 %), and OPPh₃ (5 % of the ³¹P NMR signal) were observed, in addition to the signals for the starting materials. After 30 min at 50°C, these conversions had increased to 41, 45, and 10 %, for **9b**, **14b**, and OPPh₃ respectively (the integration of the signal for OPPh₃ cannot be assumed to accurately represent the concentration of that species, because of its large T₁ value).

c) with added 1,1-dicyclopropylethylene: Complex **2** (4.6 mg, 7.3 mM), and *p*-tolyl disulphide (31.8 mg, 200 mM) were dissolved in a mixture of C₆D₆ (0.49 mL) and 1,1-dicyclopropylethylene (0.13 mL, 2.1 M) in an NMR tube at 18°C under Ar. After 5, 14, and 28 min, **14b** (40, 67, and 87 % conversion) and PPh₃ were observed. The *pseudo*-first order log plot was linear (Fig. 4.1), with more scatter than observed without the free radical trap; the rate constant was 1.1 x 10⁻³ s⁻¹.

The reaction of *cct*-RuH₂(CO)₂(PPh₃)₂ (3**) with mixtures of thiols:** Complex **3** (4.6 mg, 8.4 mM) and *p*-thiocresol (24.4 mg, 246 mM) were dissolved in C₆D₆ under Ar in an NMR tube, which was capped with a septum. Thiophenol (20 μL, 244 mM) was injected through the septum. After 400 min at 21°C, the products were *cct*-RuH(SC₆H₅)(CO)₂(PPh₃)₂ (³¹P{¹H} NMR δ 37.24 ppm, 46 %), *cct*-RuH(SC₆H₄*p*CH₃)(CO)₂(PPh₃)₂ (37.42 ppm, 21 %), *cct*-Ru(SC₆H₅)₂(CO)₂(PPh₃)₂ (10.69 ppm, 12 %), *cct*-Ru(SC₆H₅)(SC₆H₄*p*CH₃)(CO)₂(PPh₃)₂

(10.78 ppm, 15 %), and *cct*-Ru(SC₆H₄*p*CH₃)₂(CO)₂(PPh₃)₂ (10.90 ppm, 6 %). Experiments with other mixtures of thiols were performed in a similar manner.

The reaction of *cct*-RuH₂(CO)₂(PPh₃)₂ (3**) with *p*-tolyl disulphide:**

a) 21°C: Complex **3** (1.7 mg, 3.9 mM) and *p*-tolyl disulphide (20 mg, 130 mM) were dissolved in C₆D₆ (0.63 mL) in an NMR tube under Ar. The reaction was monitored by ³¹P{¹H} NMR spectroscopy, with the temperature of the sample being maintained at 21±1°C. After 40 min, 4 h, and 14 h, the species detected were **3** (55, 38, and 10 %), *cct*-RuH(SC₆H₄*p*CH₃)(CO)₂(PPh₃)₂ (42, 57, and 74 %), and *cct*-Ru(SC₆H₄*p*CH₃)₂(CO)₂(PPh₃)₂ (3, 5, and 11 %).

b) 45°C: Complex **3** (3.5 mg, 7.3 mM) and *p*-tolyl disulphide (23 mg, 130 mM) were dissolved in C₆D₆ (0.69 mL) in an NMR tube under Ar. The reaction was monitored by ³¹P{¹H} NMR spectroscopy, with the temperature of the sample being maintained at 45°C. After 30 min and 1 h, the species detected were **3** (33 and 16 %), and *cct*-RuH(SC₆H₄*p*CH₃)(CO)₂(PPh₃)₂ (67 and 84 %).

The reaction of *cct*-RuH(SR)(CO)₂(PPh₃)₂ with *p*-tolyl disulphide: a) over minutes: A sample of *cct*-RuH(SMe)(CO)₂(PPh₃)₂ (**9c**, 8.0 mg, 17 mM) and *p*-tolyl disulphide (39 mg, 250 mM) were dissolved in C₆D₆ (0.65 mL) in an NMR tube under Ar. The reaction was monitored by ¹H and ³¹P{¹H} NMR spectroscopy at 45°C. After 12 and 55 min, the species detected were unreacted **9c** (66 and 10 % of the hydride region of the ¹H NMR spectrum) and *cct*-RuH(SC₆H₄*p*CH₃)(CO)₂(PPh₃)₂ (34 and 90 %). Only four spectra were acquired, not enough to confirm that the rate of loss of **9c** was first order. However, assuming *pseudo*-first order behaviour, the observed rate constant was 1.4 x 10⁻³ s⁻¹, corresponding to a half-life of 8.3 min.

b) over days: A sample of *cct*-RuH(SEt)(CO)₂(PPh₃)₂ (14 mg, 19 μmol) and *p*-tolyl disulphide (123 mg, 500 μmol) were dissolved in THF (10 mL) in a Schlenk tube under Ar. The yellow

solution turned to a more orange colour over 2 days at room temperature. The solvent was removed by vacuum filtration, and the residue was redissolved in C_6D_6 . The $^{31}P\{^1H\}$ NMR spectrum revealed the presence of *cct*-Ru(SC₆H₄pCH₃)₂(CO)₂(PPh₃)₂ (**14b**, 38 % of the signal), PPh₃ (15 %), and unknown species which generated nine signals (<7 % each), most of which are also observed when solutions of *cct*-Ru(SC₆H₄pCH₃)₂(CO)₂(PPh₃)₂ are irradiated with 430 nm light (Section 6.2.1).

The reaction of *cct*-RuH₂(CO)₂(PPh₃)₂ (3**) with propylene sulphide:** A sample of **3** (3.6 mg, 12 mM) was dissolved in a mixture of CD₂Cl₂ (0.44 mL) and propylene sulphide (0.10 mL, 2.9 M) in an NMR tube under Ar. The reaction was monitored by $^{31}P\{^1H\}$ NMR at room temperature (21°C). The species detected after 10 min, 38 min, 160 min, and 7 days were **3** (64, 39, 7, and 0 % of the signal), *cct*-RuS₂(CO)₂(PPh₃)₂ (22, 31, 53, and 0%), an unknown complex with ^{31}P and 1H NMR signals similar to those of *cct*-RuH(SR)(CO)₂(PPh₃)₂ (10, 25, 29, and 0 %), and SPPH₃ (0, 4, 12, and 100 %). The chemical shifts of these four species were 56.19, 39.35, 38.36, and 42.86 ppm, respectively. The hydride region of the 1H NMR spectrum contained triplets at -6.3 and -3.8 ppm, consistent with the presence of unreacted **3** and *cct*-RuH(SR)(CO)₂(PPh₃)₂. Similar results were obtained when C_6D_6 was used as the solvent.

The reaction of Ru(CO)₂(PPh₃)₃ (2**) with propylene sulphide:** Propylene sulphide (50 μ L, 1.1 M) was added to a solution of **2** (2.4 mg, 4.5 mM) in C_6D_6 (0.57 mL) at room temperature. A $^{31}P\{^1H\}$ NMR spectrum acquired three minutes later detected three species; SPPH₃ (δ 41.97 ppm, 30 % of signal), *cct*-RuS₂(CO)₂(PPh₃)₂ (39.76 ppm, 30 %), and an unknown complex (37.07 ppm, 40 %) with ^{31}P and 1H NMR signals consistent with *cct*-RuH(SR)(CO)₂(PPh₃)₂ (1H NMR δ -4.77 ppm, t, $^2J_{PH} = 20.4$ Hz, R unknown but probably alkyl based on the 1H NMR data).

The non-reaction of *cct*-RuH₂(CO)₂(PPh₃)₂ (3**) with unstrained thioethers:**

a) PhSPh: A sample of **3** (110 mg, 7.9 mM) was dissolved in a mixture of THF (20 mL) and PhSPh (0.6 mL, 180 mM) and the solution was stirred for 2 days under Ar at room temperature. The volume of the solvent was reduced to 10 mL by vacuum distillation and hexanes (30 mL) were added to the remainder to induce precipitation. The off-white solid collected by filtration was shown by ³¹P{¹H} NMR spectroscopy to be unreacted **3**.

b) MeSMe:²⁵⁴ A sample of **3** (400 mg, 14.6 mM) was dissolved in a mixture of THF (40 mL) and MeSMe (0.5 mL, 170 mM) and the solution was stirred for a day at room temperature under N₂. The solvent was removed by vacuum distillation. ³¹P{¹H} NMR spectroscopy of the residue in C₆D₆ showed the presence of unreacted **3** and a small amount of *cct*-RuO₂(CO)₂(PPh₃)₂ (identified by comparison of the ³¹P NMR chemical shift to that reported by Dekleva¹⁸²).

c) thiophene: A sample of **3** (140 mg, 10 mM) was dissolved in a mixture of THF (20 mL) and thiophene (0.8 mL, 500 mM) and the solution was stirred for 3 days under Ar at room temperature. The volume of the solution was reduced to 5 mL by vacuum distillation and hexanes (20 mL) were added to the remainder to induce precipitation. The off-white solid collected by filtration was shown by ³¹P{¹H} NMR spectroscopy (C₆D₆) to be **3** (98 %) and *cct*-RuH(SR)(CO)₂(PPh₃)₂ (**9**, 2 %, R unknown). The ¹H NMR spectrum contained a weak triplet at -4.6 ppm (**9**), in addition to the triplet at -6.3 due to the dihydride (**3**).

d) dibenzothiophene: A sample of **3** (20 mg, 2.8 mM) and dibenzothiophene (154 mg, 84 mM) were dissolved in THF (10 mL) and the solution was left for four days under Ar at room temperature. The solvent was then removed by vacuum distillation, leaving a residue of **3** (identified by ³¹P{¹H} NMR spectroscopy).

The reactions of Ru(CO)₂(PPh₃)₃ and *cct*-RuH₂(CO)₂(PPh₃)₂ with di benzyl trisulphide:
Ru(CO)₂(PPh₃)₃ (150 mg, 7.9 mM) and dibenzyl trisulphide (286 mg, 51 mM) were dissolved in THF (20 mL) and the solution was stirred for 1 day. The volume of the solution was reduced

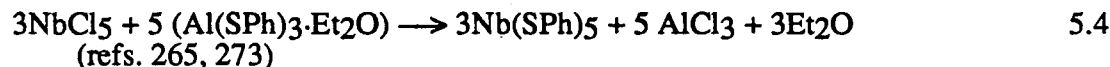
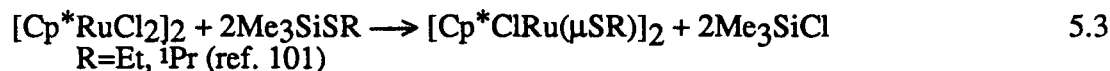
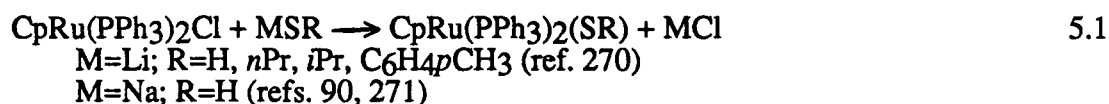
to 10 mL by vacuum distillation and hexanes (20 mL) were added to the remainder to induce precipitation of a yellow solid. This product was isolated by filtration and washed with hexanes (20 mL). The $^{31}\text{P}\{^1\text{H}\}$ NMR spectrum (C_6D_6) of the product contained three peaks at 42.08 ppm (SPPH₃, 10 % of integral), 34.67 ppm (unknown, 20 %), and 31.34 ppm (unknown, 70 %). The filtrate was dried by vacuum distillation. The $^{31}\text{P}\{^1\text{H}\}$ NMR spectrum (C_6D_6) of the residue contained the same three peaks but with different intensities (73, 25, and 2 %, respectively). The reaction of the trisulphide with *cct*-RuH₂(CO)₂(PPh₃)₂ gave similar results.

The reaction of *cct*-Ru(SC₆H₄*p*CH₃)₂(CO)₂(PPh₃)₂ (14b**) with di benzyl trisulphide:** a sample of **14b** (160 mg, 1.8 mM) and dibenzyl trisulphide (286 mg, 11.6 mM) were dissolved in THF (20 mL) under Ar in a darkened room. After 40 min, the solvent was removed by vacuum distillation. The $^{31}\text{P}\{^1\text{H}\}$ NMR spectrum (C_6D_6) of the yellow residue redissolved in C_6D_6 showed that the major phosphorus-containing product was SPPH₃. Thirteen other signals were observed, although the integration of each of these peaks was less than 3 % of the total.

5 THE METATHESIS REACTIONS OF CHLORORUTHENIUM COMPLEXES WITH THIOLATE SALTS

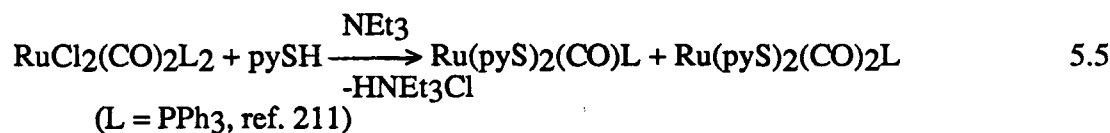
5.1 INTRODUCTION

The metathesis reactions of transition metal chlorides with thiolate salts are common synthetic routes for the preparation of thiolate complexes. The driving force for the reaction is the precipitation of an insoluble salt (e.g. NaCl) or the formation of a volatile product (e.g. Me₃SiCl). The following reactions illustrate the variety of thiolate salts that have been used.

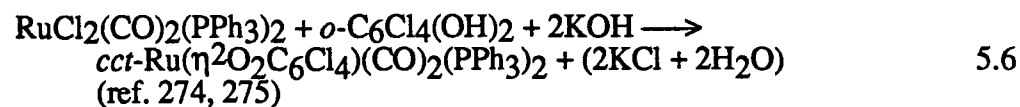


Other commonly used reagents include the potassium, lead(II) and mercury(II) thiolate salts.²⁶⁵

An alternative method involves addition of a base and a thiol to the solution of the chloro-transition metal complex.

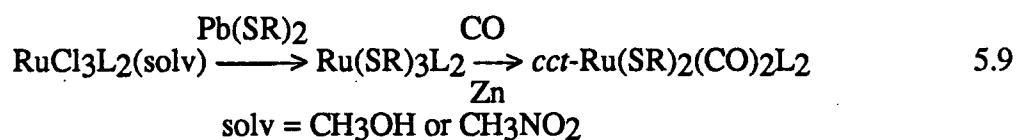
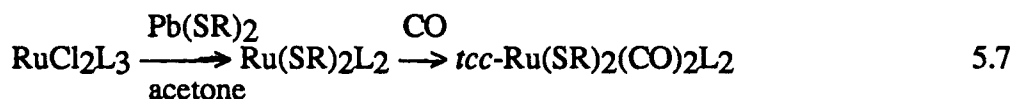


Metathesis is also used in the following related reaction with alcohols.



Catala *et al.* have reported^{260,276} the metathesis reactions of several (chloro)-phosphine ruthenium complexes with thiolate salts. The thiolato (phosphine) products react with CO to

produce isomers of $\text{Ru}(\text{SR})_2(\text{CO})_2(\text{PPh}_3)_2$. Although the authors report results with several lead thiolates and four different phosphines, only the results with PPh_3 (L) and $\text{Pb}(\text{SC}_6\text{F}_5)_2$ are summarized below.



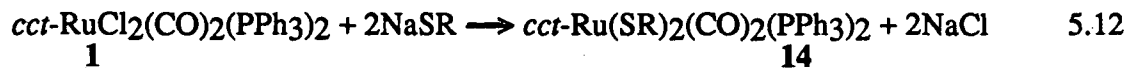
It is not clear in reference 276 whether reactions 5.7 and 5.8 occur under different conditions or whether both products are observed simultaneously. In addition, the same group^{260b} report the metathesis reaction of $\text{tcc-RuCl}_2(\text{CO})_2(\text{PPh}_3)_2$ to form the same isomer of the *bis*-thiolate complex.



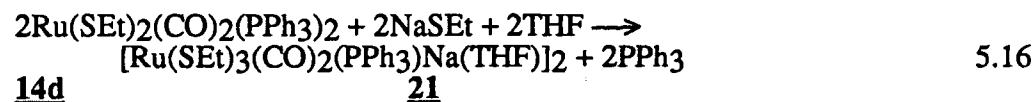
Metathesis reactions followed or preceded by carbonylation reactions are viable alternatives to the reactions of $\text{Ru}(\text{CO})_2(\text{PPh}_3)_3$ with thiols or disulphides for the synthesis of $\text{cct-Ru}(\text{SAryl})_2(\text{CO})_2(\text{PPh}_3)_2$. For the alkyl analogues, metathesis reactions appear to be the only successful route.

5.2 THE REACTIONS OF *cct*-RuCl₂(CO)₂(PPh₃)₂ WITH SODIUM THIOLATES

The metathesis reaction of *cct*-RuCl₂(CO)₂(PPh₃)₂ (**1**) with sodium *p*-thiocresolate proceeds cleanly in acetone, the pure product being identified by comparing its ¹H and ³¹P{¹H} NMR spectra with those of a sample prepared from Ru(CO)₂(PPh₃)₃ and *p*-tolyl disulphide.



The metathesis reaction of **1** with sodium ethanethiolate in acetone produces the desired complex, *cct*-Ru(SEt)₂(CO)₂(PPh₃)₂ (**14d**), but isolation and reprecipitation of this product were plagued by the formation of intractable oils. The same reaction in THF generates **14d** and two new products *cct*-RuCl(SEt)(CO)₂(PPh₃)₂ (**20**) and [Ru(SEt)₃(CO)₂(PPh₃)Na(THF)]₂ (**21**) in varying ratios depending on the amount and freshness of thiolate used. If two equivalents are used, less than 10 % conversion to **20** is observed. If a large excess of thiolate is used, the exclusive product is **21**. At intermediate concentrations of thiolate, mixtures of **14d**, **20**, and **21** are observed. It is likely that reactions 5.14 through 5.16 occur consecutively.

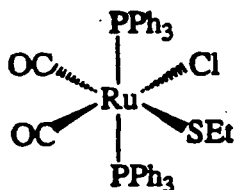


The lability of the phosphine ligands of *cct*-Ru(SR)₂(CO)₂(PPh₃)₂ (**14**) has already been demonstrated (Section 3.8). Reaction 5.16 may simply proceed by elimination of PPh₃ followed by coordination of a third thiolate ligand. The full characterization of **21** is described in Section 5.3.

The two other products *cct*-RuCl(SEt)(CO)₂(PPh₃)₂ (**20**) and *cct*-Ru(SEt)₂(CO)₂(PPh₃)₂ (**14d**) have virtually identical solubility, and have not been successfully separated. However,

samples in which one or the other was predominant were obtained by reacting $\text{RuCl}_2(\text{CO})_2(\text{PPh}_3)_2$ (**1**) with different concentrations of thiolate.

A sample of *cis*- $\text{RuCl}(\text{SEt})(\text{CO})_2(\text{PPh}_3)_2$ (**20**) containing only 2 % of **14d** (estimated by NMR spectroscopy) was characterized. The integration of the ^1H NMR spectrum (Fig. 5.1a) shows that the ligands PPh_3 and SEt are present in a 2:1 ratio. The chemical shift difference between the *o*- and the *m/p*-phenyl signals is 1.2 ppm, clearly indicating *trans* phosphines. The $^{31}\text{P}\{^1\text{H}\}$ NMR signal of **20** is a singlet at 14.54 ppm, intermediate in position between those of *cis*- $\text{RuCl}_2(\text{CO})_2(\text{PPh}_3)_2$ (**1**, 15.66 ppm) and *cis*- $\text{Ru}(\text{SEt})_2(\text{CO})_2(\text{PPh}_3)_2$ (**14d**, 11.27 ppm). Two $\nu(\text{CO})$ stretching bands in the infrared spectrum of **20** (Fig. 5.2a) indicate *cis* carbonyls. Therefore, the geometry of the complex is the same as that of the starting material.



The FAB-Mass spectrum of **20** (Fig. 5.3 and Table 5.1) contains the molecular peak and several identifiable fragments. The carbon analysis is low.

A sample of $\text{Ru}(\text{SEt})_2(\text{CO})_2(\text{PPh}_3)_2$ (**14d**) containing 20 % of **20** was characterized. The integration of the ^1H NMR spectrum (Fig. 5.1b) shows that the ligands PPh_3 and SEt are present in a 1:1 ratio. The chemical shift difference between the *o*- and the *m/p*-phenyl signals is 1.2 ppm, indicating *trans* phosphines. The $^{31}\text{P}\{^1\text{H}\}$ NMR signal of **14d** (Table 5.2) is at 11.18 ppm, slightly higher than those of the *bis*-(aryl thiolato) derivatives such as **14b** (Section 4.2). The same signal is observed after the reactions of $\text{Ru}(\text{CO})_2(\text{PPh}_3)_3$ with excess ethanethiol or ethyl disulphide, and the reaction of *cis*- $\text{Ru}(\text{SC}_6\text{H}_4\text{pCH}_3)_2(\text{CO})_2(\text{PPh}_3)_2$ (**14b**) with ethanethiol (see Chapters 3 and 4). The infrared spectrum of the mixture of **14d** and **20** contains two $\nu(\text{CO})$ bands due to **14d** (Fig. 5.2b), indicating *cis* carbonyls. The structure is again *cis*.

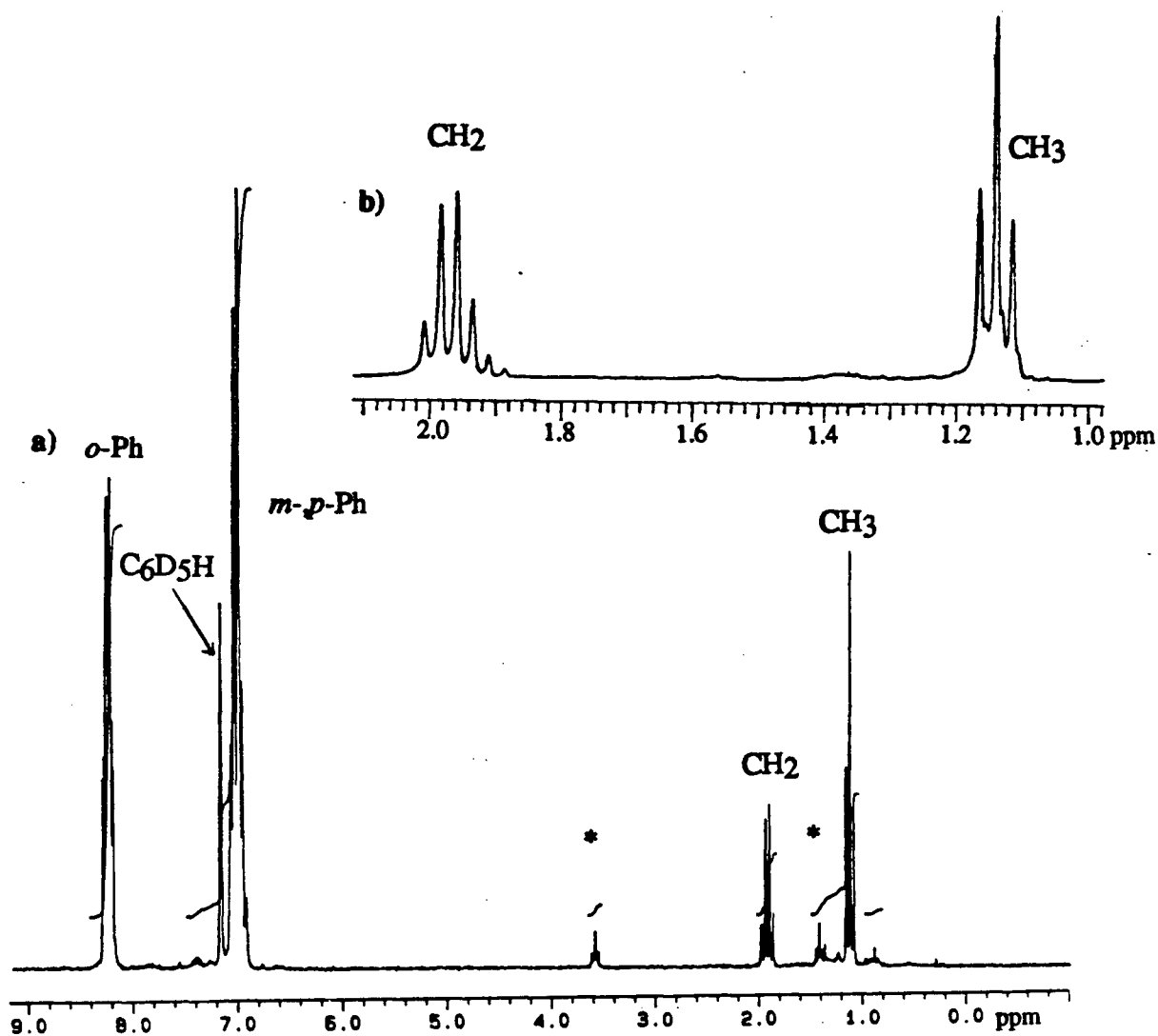


Fig. 5.1 a) ¹H NMR spectrum (200 MHz, C₆D₆ solution) of *cct*-RuCl(SET)(CO)₂(PPh₃)₂. The signals for THF are indicated by asterisks.
 b) Expanded region of the ¹H NMR spectrum (300 MHz, C₆D₆ solution) of a sample of *cct*-Ru(SET)₂(CO)₂(PPh₃)₂ containing 20% of *cct*-RuCl(SET)(CO)₂(PPh₃)₂.

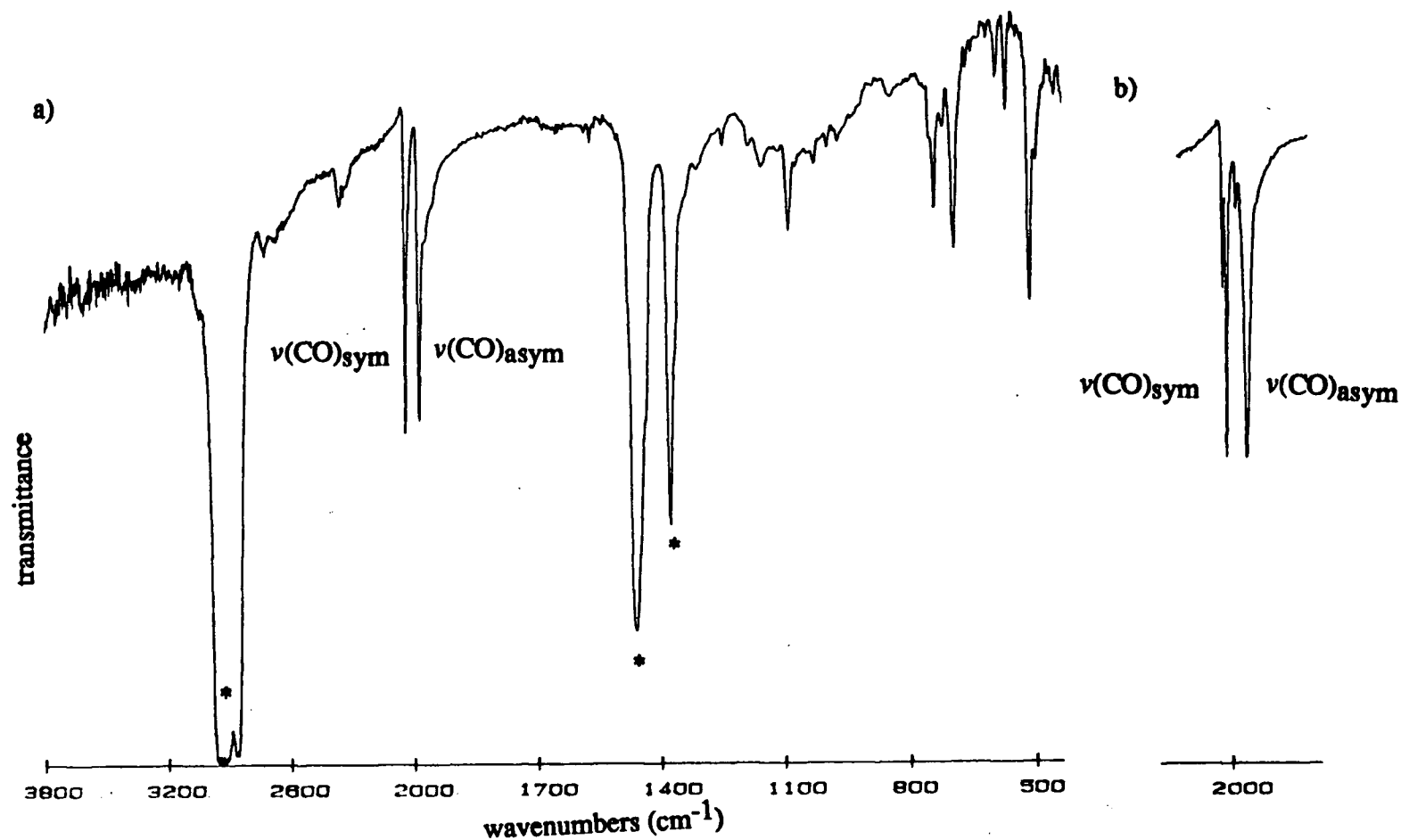


Fig. 5.2 a) The FT-IR spectrum of $cct\text{-RuCl}(\text{SET})(\text{CO})_2(\text{PPh}_3)_2$ in a Nujol mull. The signals for Nujol are indicated by asterisks.
 b) Carbonyl region of the FT-IR spectrum of a sample of $cct\text{-Ru}(\text{SET})_2(\text{CO})_2(\text{PPh}_3)_2$ containing 20% of $cct\text{-RuCl}(\text{SET})(\text{CO})_2(\text{PPh}_3)_2$, in a Nujol mull.

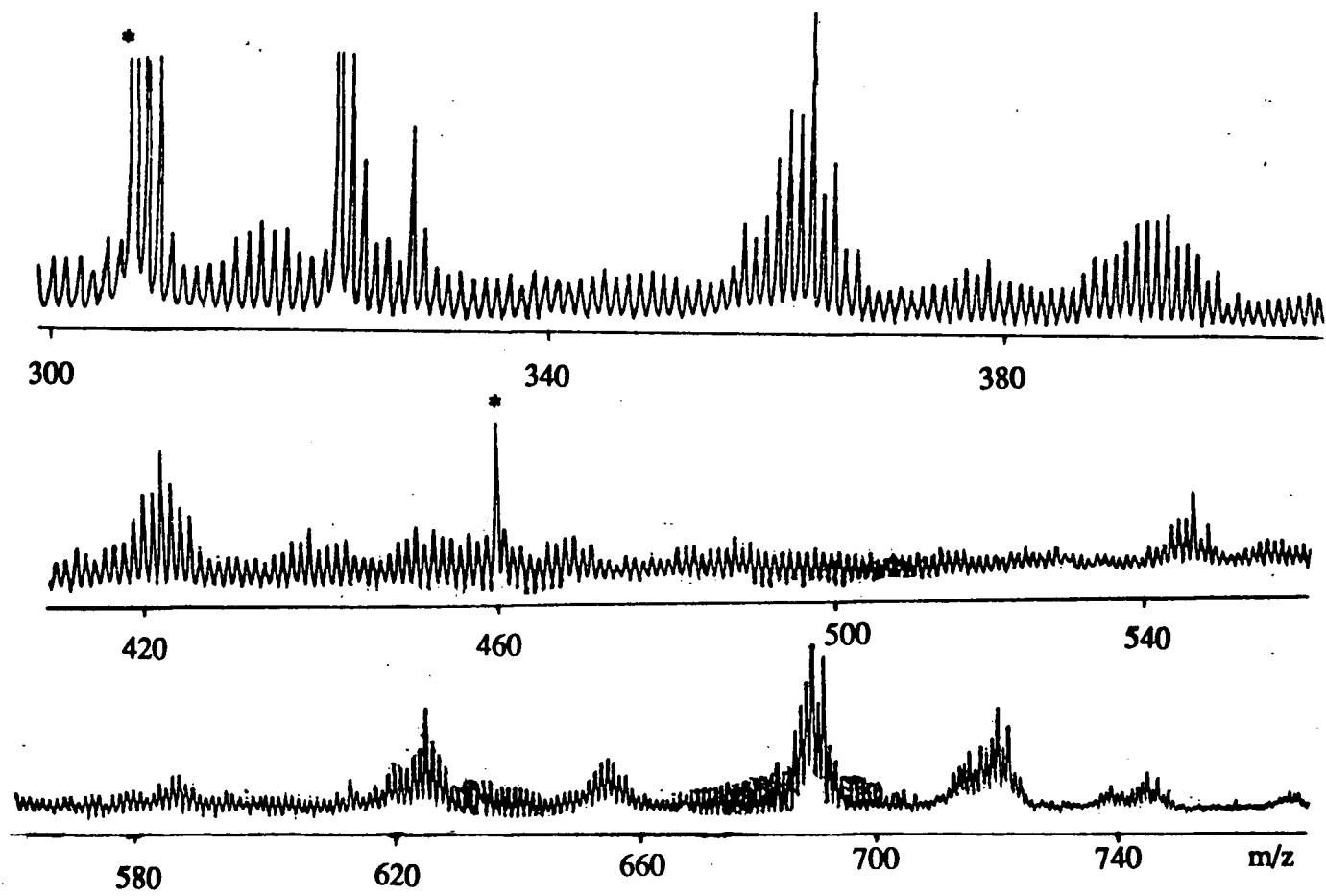


Fig. 5.3 The FAB-Mass spectrum of *cct*-RuCl(SET)(CO)₂(PPh₃)₂ in a *p*-nitrobenzyl alcohol matrix. The peaks due to the matrix are indicated by asterisks.

Table 5.1 Fragments Detected in the FAB-Mass Spectrum of *cct*-RuCl(SEt)(CO)₂(PPh₃)₂

<i>m/z</i>	Allocation	Fragmentation
778	RuCl(SEt)(CO) ₂ (PPh ₃) ₂	M
750	RuCl(SEt)(CO)(PPh ₃) ₂	M-CO
722	RuCl(SEt)(PPh ₃) ₂	M-2CO
689	RuCl(CO)(PPh ₃) ₂	M-CO-SEt
654	Ru(CO)(PPh ₃) ₂	M-CO-SEt-Cl
625	Ru(PPh ₃) ₂	M-2CO-SEt-Cl
547	Ru(PPh ₃)(PPh ₂)	M-2CO-SEt-Cl-Ph
423	Ru(SEt)(PPh ₃)	M-2CO-Cl-PPh ₃
396	RuCl(PPh ₃) ^a	M-2CO-SEt-PPh ₃
363	Ru(PPh ₃)	M-2CO-SEt-Cl-PPh ₃

^a Fragment has a predicted *m/z* two units above that observed. All others have predicted values within one unit of those observed.

Table 5.2 NMR^a and IR^b Spectral Data for Ru(X)(SEt)(CO)₂(PPh₃)₂.

X	31P NMR δ PPh ₃	1H NMR δ CH ₂ δ CH ₃		$^3J_{\text{HH}}$	<i>sym.</i> $\nu(\text{CO})$	<i>asym.</i> $\nu(\text{CO})$
Hc	37.25	1.28	0.77	7.4 Hz	2025 cm ⁻¹	1964 cm ⁻¹
Cl	14.54	1.92	1.13	7.4	2042	1987
SEt	11.18	1.97	1.16	7.4	2022	1963
SPhpMed ^d	11.00	-	-	-	-	-

^a C₆D₆ solutions at room temperature using a 300 MHz spectrometer.

^b Nujol mulls.

^c Section 3.2

^d Section 3.8

The spectroscopic data for the series $cct\text{-Ru(X)(SEt)(CO)}_2(\text{PPh}_3)_2$ are summarized in Table 5.2. The ^1H NMR shifts of the ethyl group in $cct\text{-RuH(SEt)(CO)}_2(\text{PPh}_3)_2$ are at significantly higher field than those in the other complexes because H^- is not as electron withdrawing as Cl^- or SR^- .

5.3 THE CHARACTERIZATION OF $[\text{Ru(SEt)}_3(\text{CO})_2(\text{PPh}_3)\text{Na(THF)}]_2$

The $^{31}\text{P}\{^1\text{H}\}$ NMR signal of the title complex (**21**) is a singlet ($w_{1/2} = 8$ Hz at 18°C in toluene- d_8), which broadens at lower temperatures ($w_{1/2} = 29$ Hz at -58°C , 120 Hz at -78°C ; all data at 121 MHz). In C_6D_6 , the peak is asymmetric, which suggests the possibility of two peaks and therefore two environments for the P atoms in the complex.

The ^1H NMR spectrum (Figs. 5.4 and 5.6a) is complicated, and can only be assigned with the help of a COSY experiment (Fig. 5.5) or selective homonuclear decoupling experiments (Fig. 5.6). The CH_3 region contains two triplets at 1.40 and 1.59 ppm (in C_6D_6) in a ratio of 2:1. There are therefore two different kinds of ethyl group, which will be referred to as (a) and (b) respectively. The CH_3 peak of Et(a) coincides with one of the two resonances of THF, which is present in the sample. The ratio of the ligands $\text{PPh}_3 : \text{THF} : \text{Et(a)} : \text{Et(b)}$ is 1:1:2:1, based on the integration. The methylene region is quite complicated, due to overlapping signals, second order spectra, and inequivalence of geminal methylene protons. Irradiation of the CH_3 resonances simplifies the signals to two AB patterns. The two doublets for $\text{CH}_2(\text{a})$ evident in Fig. 5.6c are at 2.72 and 2.95 ppm. The $^2J_{\text{HH}}$ coupling constant in Et(a) is 9.0 Hz. The AB pattern for $\text{CH}_2(\text{b})$ is second order, so that only the two central peaks of the pattern are observed (Fig. 5.6b). A simple AB pattern consists of four lines, of which the outer two are short and of equal intensity, and the inner two are tall and of equal intensity. The ratio of the intensities of the outside peaks relative to those of the inside peaks can be calculated using the following formulae.²⁷⁷

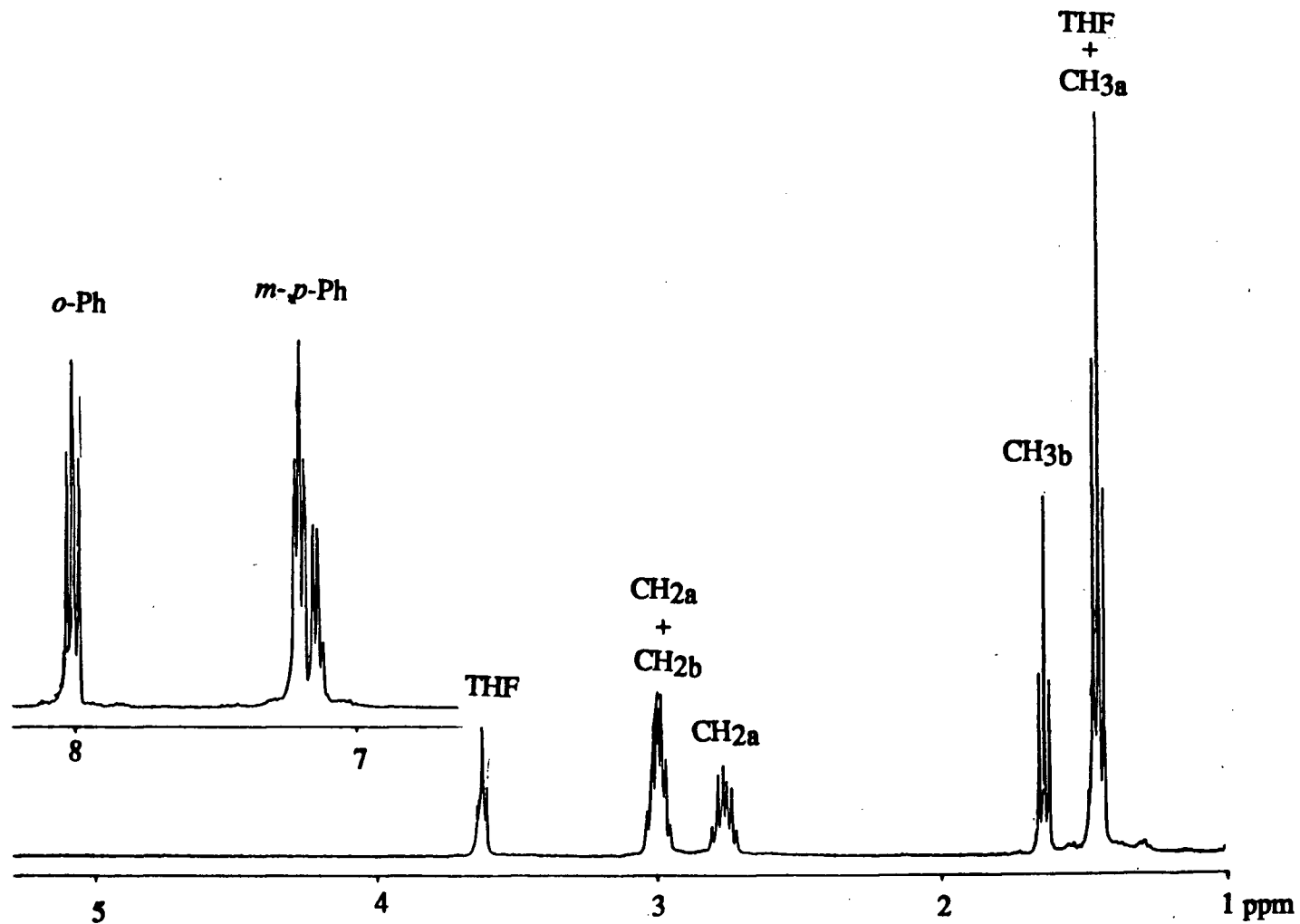


Fig. 5.4 The ^1H NMR spectrum (400 MHz) of a C_6D_6 solution of $[(\text{CO})_2(\text{PPh}_3)\text{Ru}(\text{SCH}_2\text{CH}_3)_3\text{Na}(\text{THF})_2]$ at 20°C .

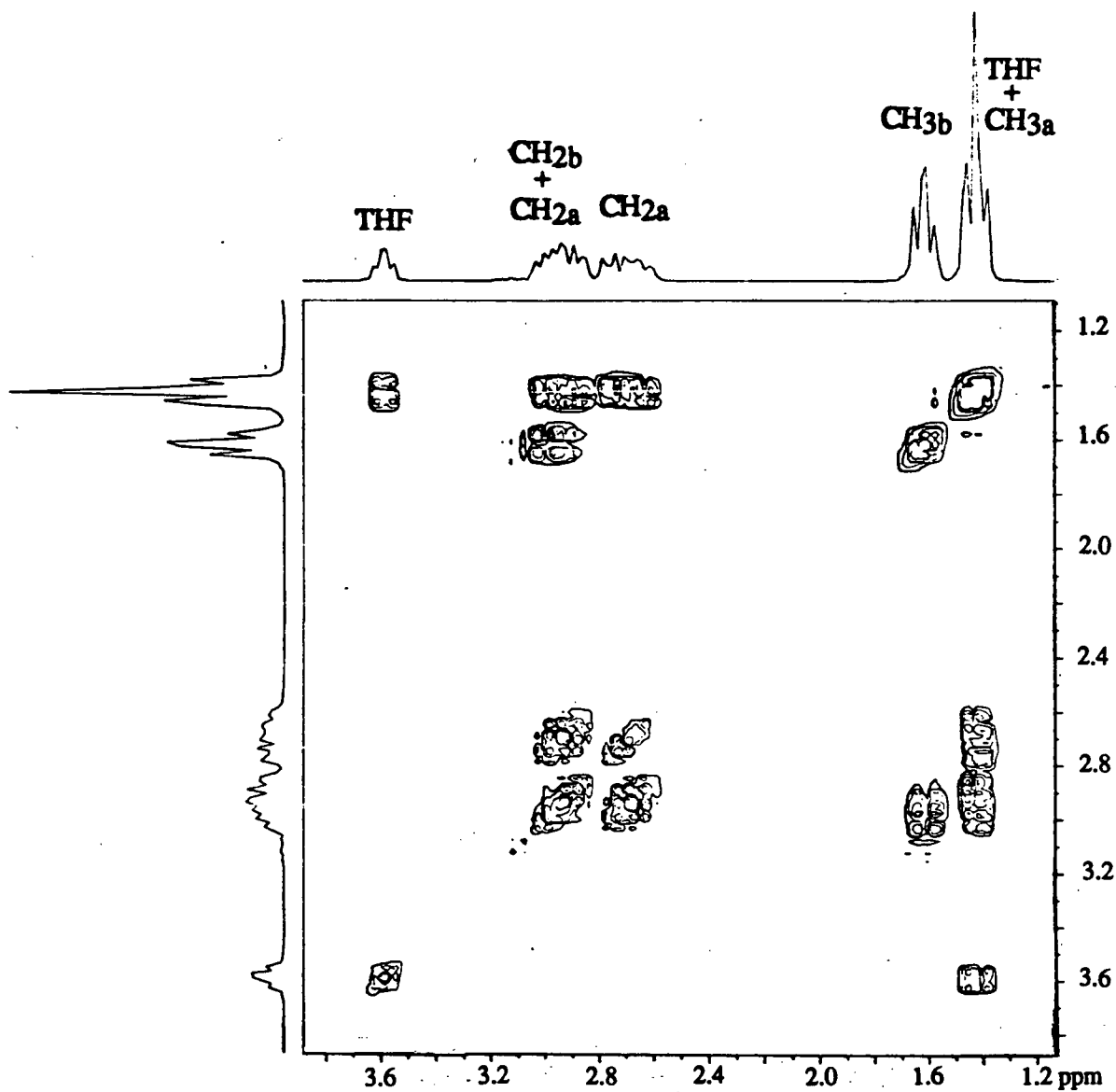


Fig. 5.5 The ^1H COSY NMR plot (400 MHz) for a C_6D_6 solution of $[(\text{CO})_2(\text{PPh}_3)\text{Ru}(\text{SCH}_2\text{CH}_3)_3\text{Na}(\text{THF})_2]$.

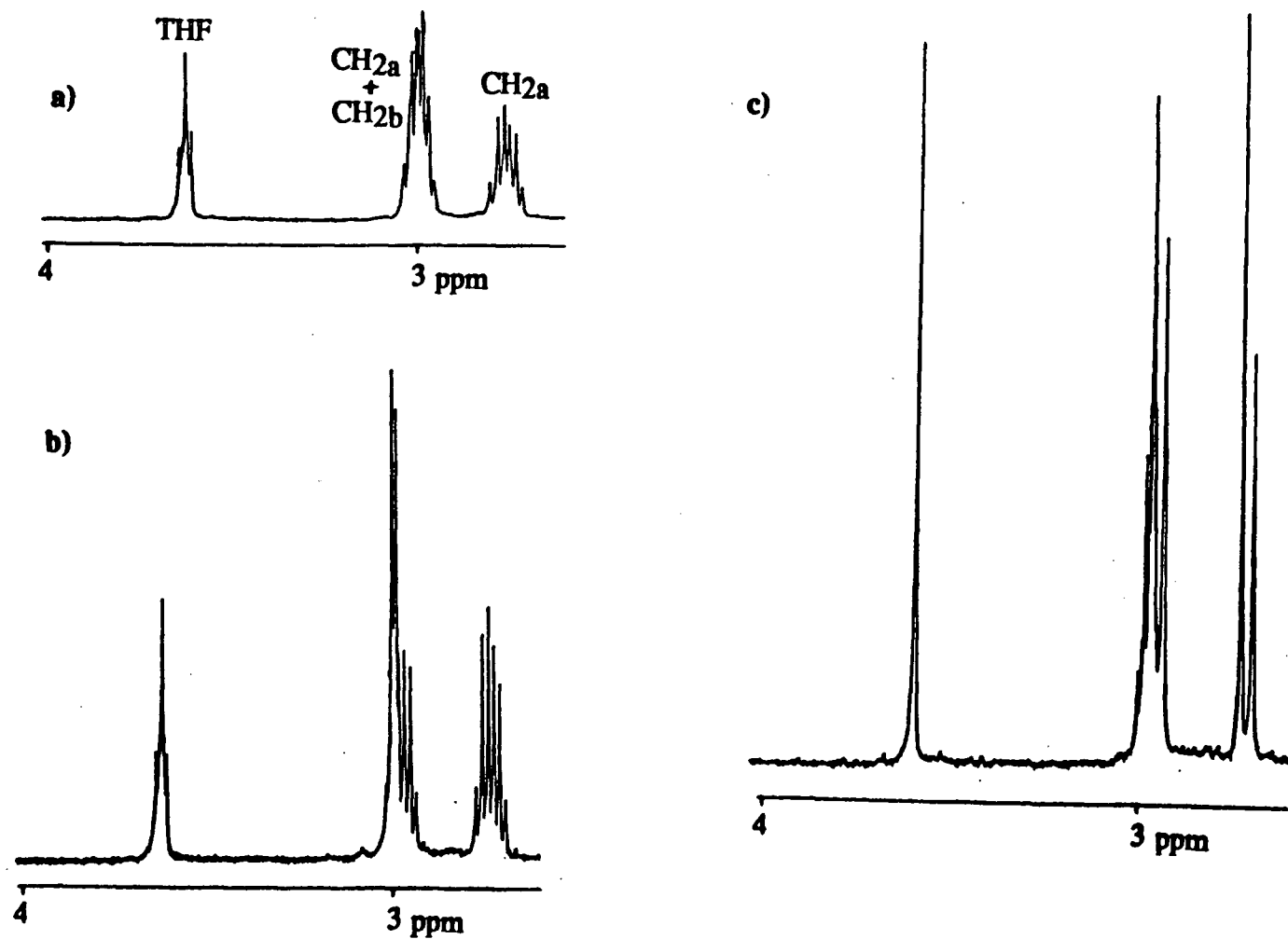


Fig. 5.6 The methylene region of ^1H NMR spectra of a C_6D_6 solution of $[(\text{CO})_2(\text{PPh}_3)\text{Ru}(\text{SCH}_2\text{CH}_3)_3\text{Na}(\text{THF})]_2$ at 400 MHz, with
 a) no decoupling,
 b) selective decoupling at 1.59 ppm (CH_3b), or
 c) selective decoupling at 1.40 ppm (CH_3a and THF).



$$\frac{I(A1)}{I(A2)} = \frac{D-J}{D+J}$$

$$D = ((\nu_A - \nu_B)^2 + J^2)^{1/2}$$

$$\nu_{A2} = 1/2 (\nu_A + \nu_B - J + D)$$

$$\nu_{B1} = 1/2 (\nu_A + \nu_B + J - D)$$

Assuming that J is again 9 Hz, and taking 2.976 and 2.987 ppm as the positions of the two central peaks (ν_{A2} and ν_{B1}), then the relative intensities of the outside peaks compared to the inside peaks is calculated to be 16%; the outside peaks are therefore too small to be detected in the selective decoupling experiment or in the cross-sections of the COSY.

The methylene region of the ^1H NMR spectrum (300 MHz) of **21** in C_6D_6 was accurately simulated (Fig. 5.7) using the following data:

CH ₃ (a):	1.41 ppm, t, $^3J_{\text{HH}} = 7.6$ Hz
CH ₃ (b):	1.59 ppm, t, $^3J_{\text{HH}} = 7.3$ Hz
CH ₂ (a):	2.708 ppm, d of q, $^2J_{\text{HH}} = 9.0$ Hz, $^3J_{\text{HH}} = 7.4$ Hz
	2.962 ppm, d of q, $^2J_{\text{HH}} = 9.0$ Hz, $^3J_{\text{HH}} = 7.4$ Hz
CH ₂ (b):	2.953 ppm, d of q, $^2J_{\text{HH}} = 9.0$ Hz, $^3J_{\text{HH}} = 7.3$ Hz
	2.987 ppm, d of q, $^2J_{\text{HH}} = 9.0$ Hz, $^3J_{\text{HH}} = 7.4$ Hz

The peak positions in the simulated spectra match those in the observed spectrum within 0.005 ppm.

The infrared spectrum of **21** in Nujol (Fig. 5.8) contains two $\nu(\text{CO})$ bands at 2014 and 1952 cm^{-1} , suggesting *cis* carbonyls. In solution, the equivalent thiolates must be those *trans* to the carbonyls (assuming a *fac* arrangement of thiolates), and are assigned to the Et(a) signals in the NMR spectra. The observations described to this point are consistent with any structure containing $\text{Ru}(\text{SEt})_3(\text{CO})_2(\text{PPh}_3)$ units. The compound does not conduct in THF solution (up to 1 mM), whereas tetrabutylammonium iodide, a 1:1 electrolyte, has a conductivity of 1 Mho at 0.2 mM in THF. The ruthenium could not have been oxidized to the paramagnetic trivalent state, because the peaks in the ^1H NMR spectrum would have been broadened and shifted. Therefore the complex must contain one bound extraneous counter-ion per Ru atom. The elemental

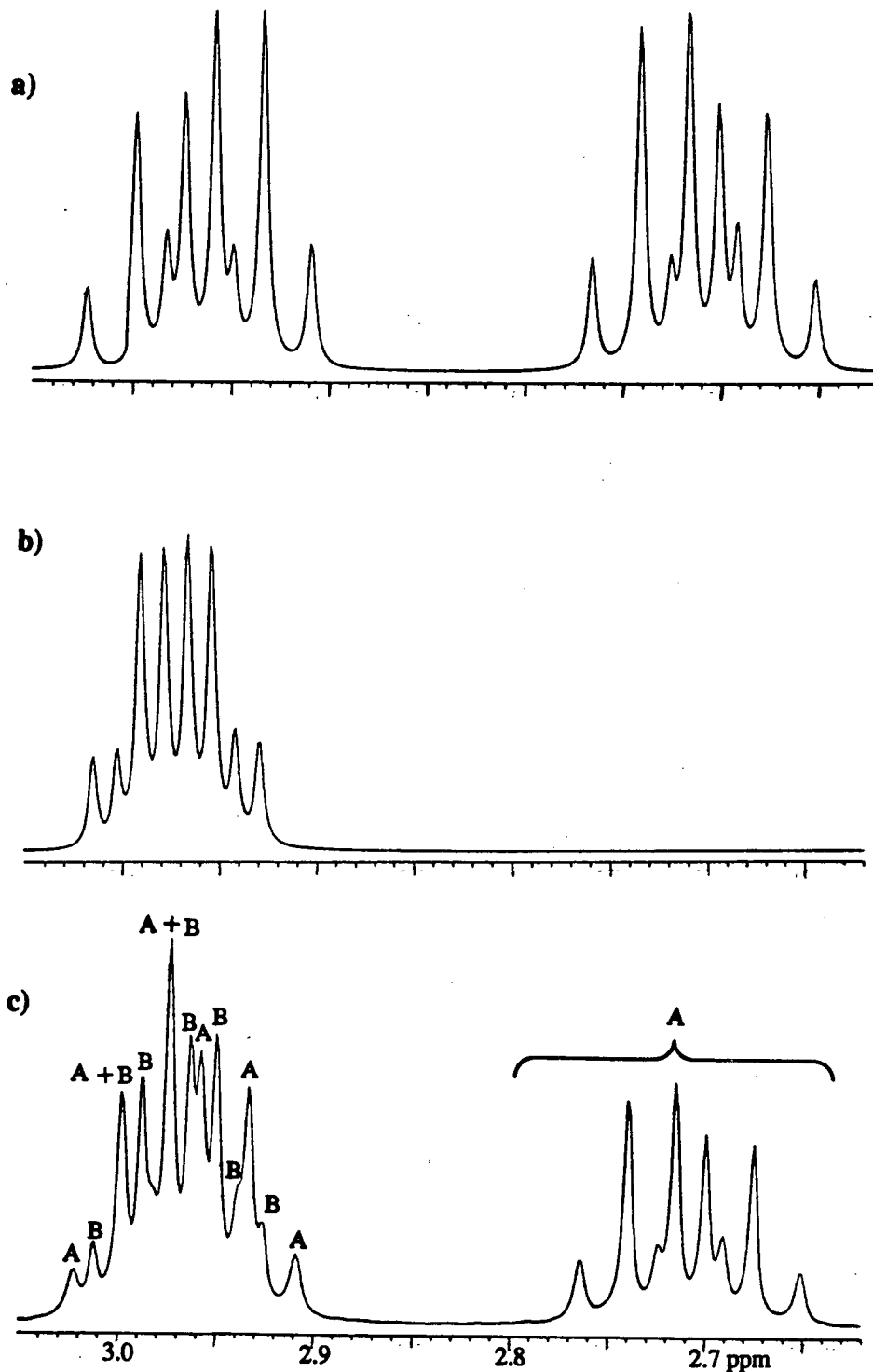


Fig. 5.7 Simulated ^1H NMR spectra (300 MHz) of a) the CH_2a protons, and b) the CH_2b protons of $[(\text{CO})_2(\text{PPh}_3)\text{Ru}(\text{SCH}_2\text{CH}_3)_3\text{Na}(\text{THF})]_2$. The peak positions match within 0.005 ppm of those in the observed spectrum (c) of the same complex in C_6D_6 . The CH_2a and CH_2b protons are identified with the letters "A" and "B", respectively.

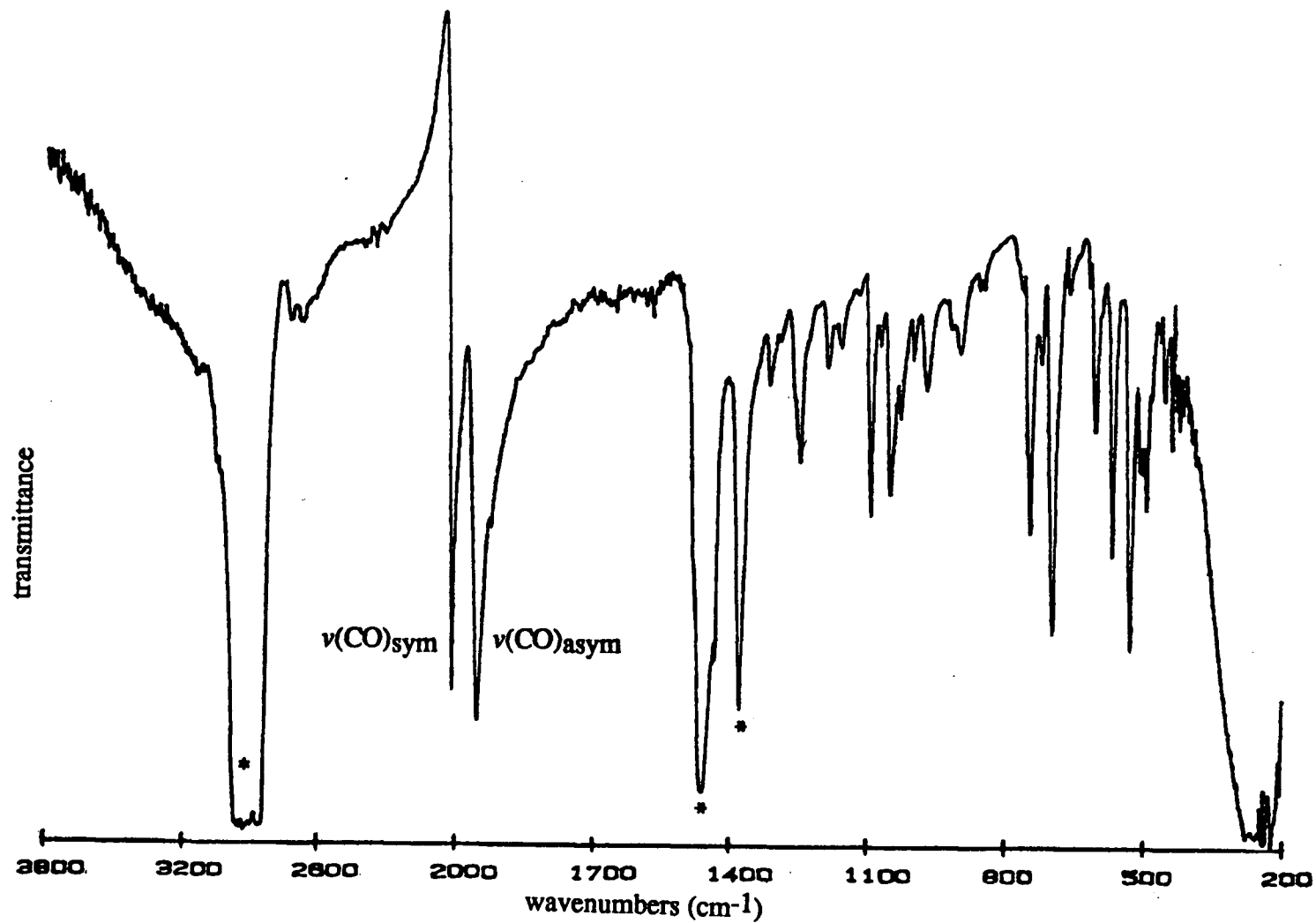


Fig. 5.8 The FT-IR spectrum of $[(\text{CO})_2(\text{PPh}_3)\text{Ru}(\mu_3\text{Set})_2(\mu_3\text{Set})\text{Na}(\text{THF})_2]$ in Nujol. The peaks for Nujol are indicated by asterisks.

analysis and FAB-MS (Fig. 5.9 and Table 5.3) are consistent with, and the X-ray structure confirms, the formula $[(PPh_3)(CO)_2Ru(\mu_2SEt)_2(\mu_3SEt)Na(THF)]_2$ (**21**).

The FAB Mass Spectrum of **21** (Fig. 5.9) contains many peaks assignable to fragments of this molecule (Table 5.3). The peak corresponding to the highest m/e value is that of the dimer minus one THF moiety.

The X-ray structure of **21** is shown in figures 5.10 to 5.12. The bond lengths, angles, and other data are listed in tables 5.4, 5.5, and Appendix B, respectively. The structure contains a crystallographically imposed centre of symmetry, and thus only one half of the atoms are labelled in Figures 5.11 and 5.12.

Each sodium atom is bound to three thiolate ligands of one $Ru(SEt)_3(CO)_2(PPh_3)$ fragment, one thiolate of the other fragment, and a THF molecule. The sodium atoms therefore have a coordination number of five, the sixth site being blocked by a phenyl group of the phosphine ligand. The coordination geometry at the Na is a distorted square pyramid. The *cis* S-Na-S angles are 71 or 72°, except those involving S^{2*} , because the sodium atom is shifted towards the empty site away from the centre of the square pyramid. The *cis* S-Na-O angles are all greater than 90° because the THF is leaning towards the empty sixth site. The Na-S bond lengths ($Na^{1-}S^1$, $Na^{1-}S^3$, and $Na^{1*}-S^3$) are 2.82 to 2.84 Å, comparable to the length of the same bond in NaSMe (2.8 Å).²⁷⁸ The $Na^{1-}S^2$ bond is slightly longer (3.0 Å) than the others, and can be classed as secondary bridging.⁹²

There are three types of thiolates present; one (S^1) *trans* to the phosphine and doubly bridging, one (S^3) *trans* to a carbonyl and doubly bridging, and one (S^2) *trans* to a carbonyl and triply bridging. The Ru-S bond lengths for the thiolate ligands ($SEt(a)$) *trans* to carbonyls (2.474, 2.467 Å) are virtually identical to those in the structures described in previous chapters. The Ru-S and the S-C bond lengths for the thiolate ligand ($SEt(b)$) *trans* to the phosphine (2.434 and 1.746 Å, respectively) are somewhat shorter than in the $SEt(a)$ ligands because of the *trans* influence of the phosphine ligand. The Ru-S bond length of a similar thiolate ligand in $Ru(pyS)_2(CO)_2(PPh_3)$ is comparable (2.42 Å).²¹⁰ The S-C(sp^3) bond lengths of **21** are longer

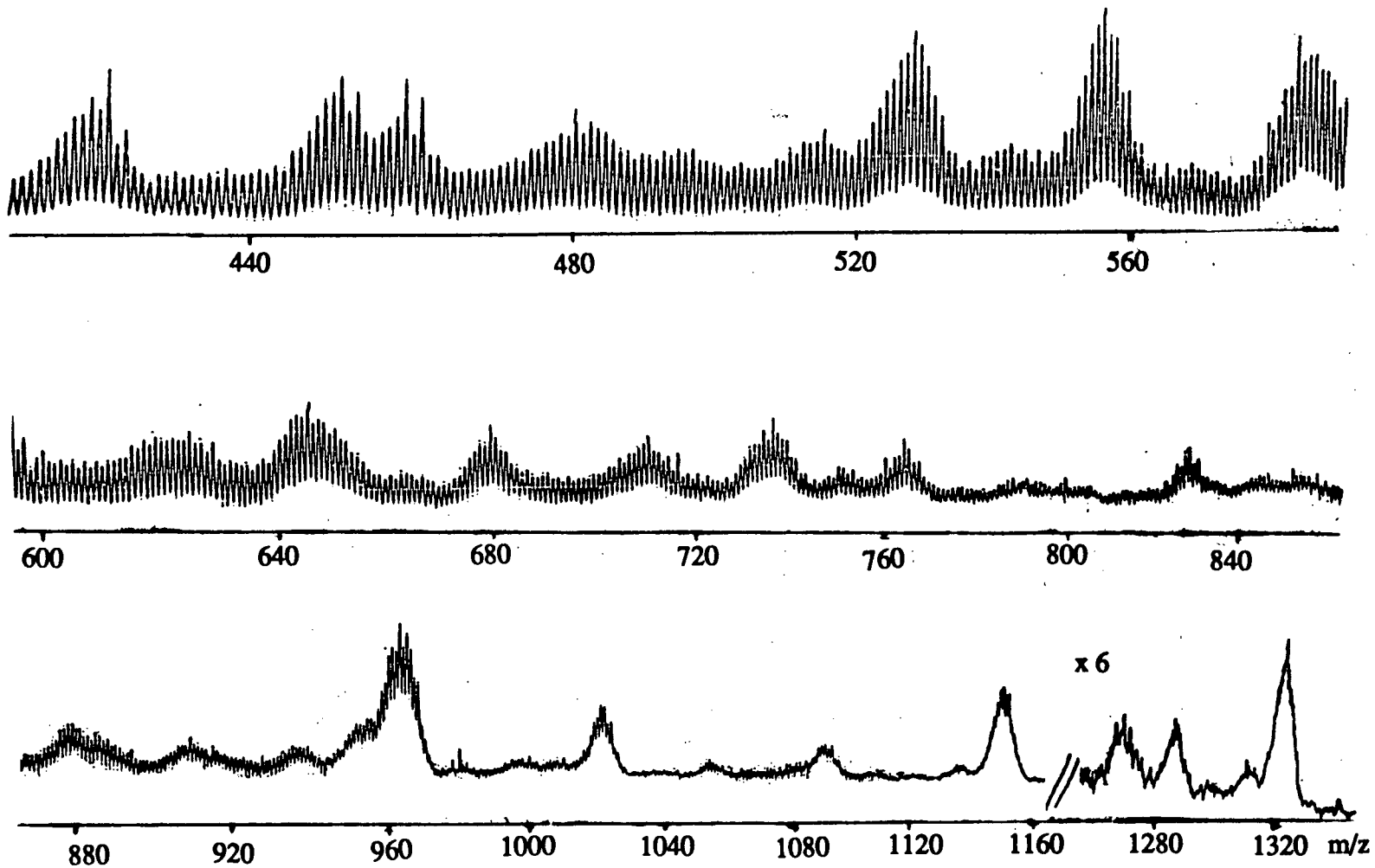


Fig. 5.9 The FAB-Mass spectrum of $[(\text{CO})_2(\text{PPh}_3)\text{Ru}(\mu\text{SEt})_2(\mu_3\text{SEt})\text{Na}(\text{THF})]_2$ in a *p*-nitrobenzyl alcohol matrix.

Table 5.3 Fragments Detected in the FAB-Mass Spectrum of [(PPh₃)(CO)₂Ru(μ₂SEt)₂(μ₃SEt)Na(THF)]₂

m/z	Allocation	Fragmentation
1326	Ru ₂ (SEt) ₆ (CO) ₄ (PPh ₃) ₂ Na ₂ (THF) ^a	M-THF
1289		
1269	Ru ₂ (SEt) ₆ (CO) ₂ (PPh ₃) ₂ Na ₂ (THF)	M-2CO-THF
1147	Ru ₂ (SEt) ₄ (CO) ₂ (PPh ₃) ₂ Na ₂ (THF)	M-2SEt-2CO-THF
1088	Ru ₂ (SEt) ₄ (PPh ₃) ₂ Na ₂ (THF) ^a	M-2SEt-4CO-THF
1022	Ru ₂ (SEt) ₄ (CO)(PPh ₃) ₂ Na	M-2SEt-3CO-Na-2THF
	Ru ₂ (SEt) ₆ (PPh ₃)Na ₂ (THF) ₂	M-4CO-PPh ₃
964	Ru ₂ (SEt) ₆ (CO) ₃ (PPh ₃)Na ₂ ^a	M-CO-PPh ₃ -2THF
829	Ru ₂ (SEt) ₄ (PPh ₃)Na ₂ (THF)	M-2SEt-4CO-PPh ₃ -THF
765		
737	Ru ₂ (SEt) ₅ (CO) ₄ Na ₂ (THF)	M-SEt-2PPh ₃ -THF
646	Ru(SEt)(CO) ₂ (PPh ₃)Na(THF) ₂	M-Ru-5SEt-2CO-PPh ₃ -Na
587		
557		
529		
451	Ru(SEt)(CO)(PPh ₃)	M-Ru-5SEt-3CO-PPh ₃ -2Na-2THF
423	Ru(SEt)(PPh ₃)	M-Ru-5SEt-4CO-PPh ₃ -2Na-2THF
363	Ru(PPh ₃)	M-Ru-6SEt-4CO-PPh ₃ -2Na-2THF
319	Ru(SEt) ₂ Na(THF)	M-Ru-4SEt-4CO-2PPh ₃ -Na-THF
285	Ru(SEt) ₃	M-Ru-3SEt-4CO-2PPh ₃ -2Na-2THF
263	PPh ₃	M-2Ru-6SEt-4CO-PPh ₃ -2Na-2THF
241	Ru(SEt)(CO) ₂ Na	M-Ru-5SEt-3CO-2PPh ₃ -Na-2THF

^a Indicated fragments have a predicted m/z value two or three units below those observed. All others have predicted values within one unit of those observed.

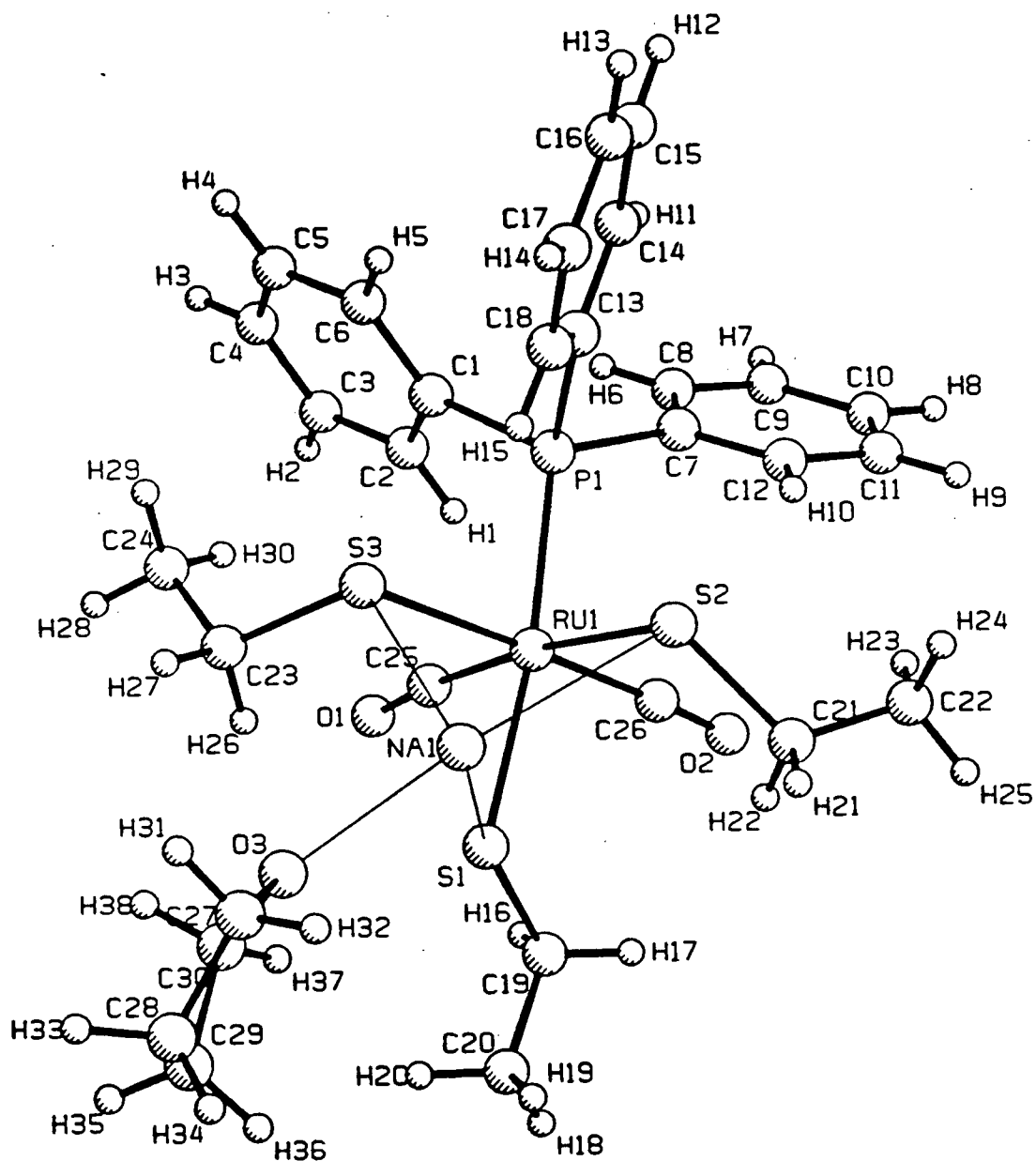


Fig. 5.10 The structure of one half of a molecule of $[(\text{CO})_2(\text{PPh}_3)\text{Ru}(\mu\text{SEt})_2(\mu_3\text{SEt})\text{Na}(\text{THF})]_2$.

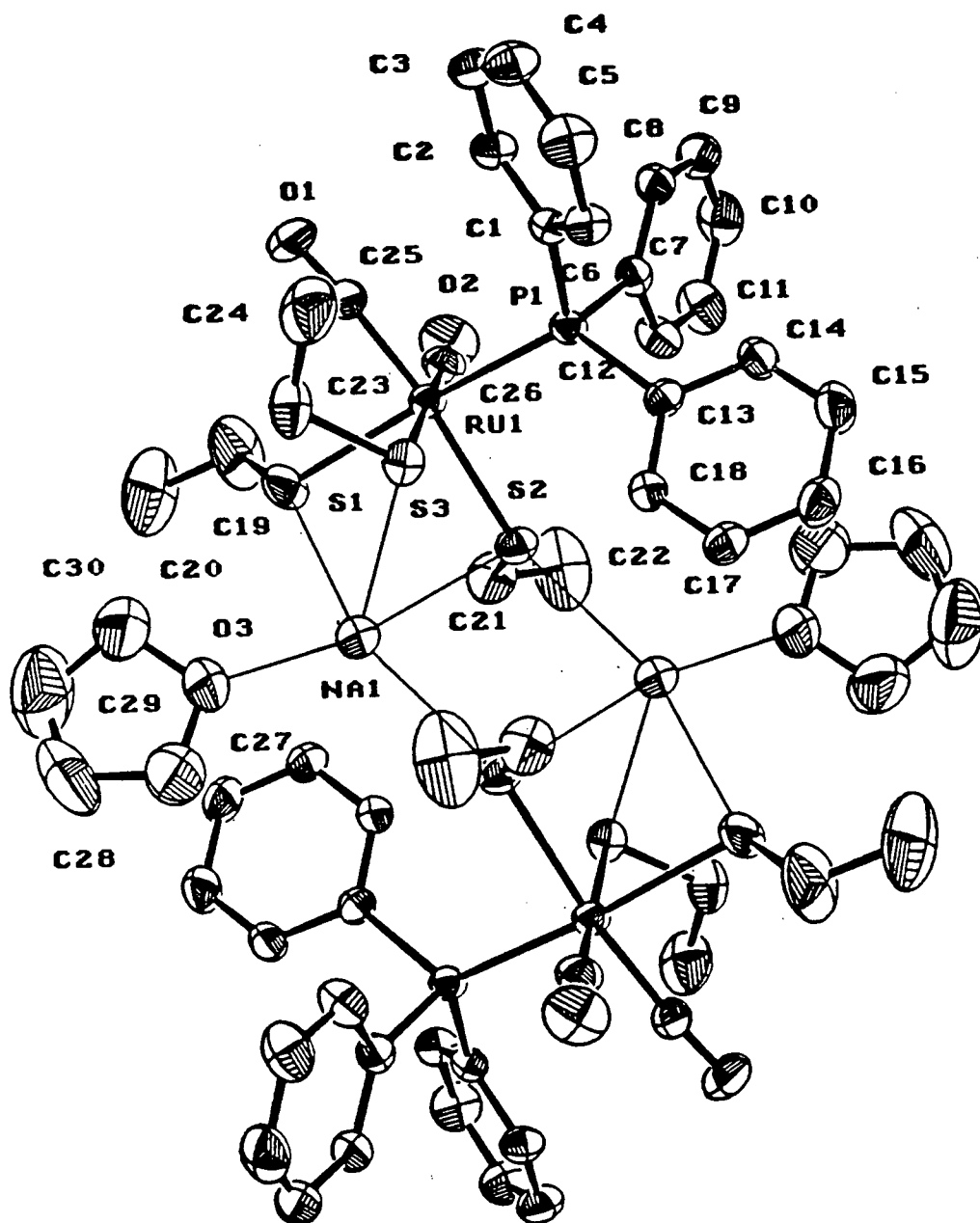


Fig. 5.11 The structure of $[(\text{CO})_2(\text{PPh}_3)\text{Ru}(\mu\text{SEt})_2(\mu_3\text{SEt})\text{Na}(\text{THF})]_2$.
Hydrogen atoms omitted for clarity.

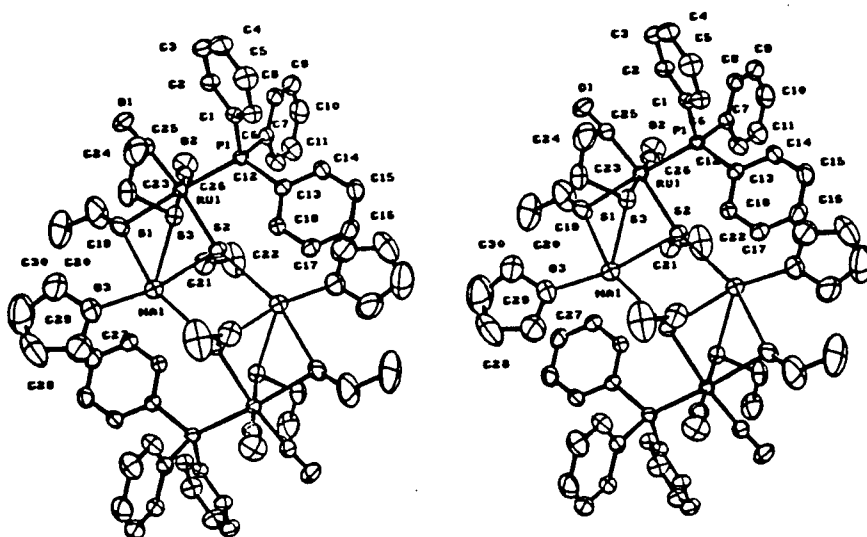


Fig. 5.12 Stereoscopic view of the structure of $[(\text{CO})_2(\text{PPh}_3)\text{Ru}(\mu_3\text{SEt})_2(\mu_3\text{SEt})\text{Na}(\text{THF})]_2$.
Hydrogen atoms omitted for clarity.

Table 5.4 Selected bond lengths (Å) with estimated standard deviations in parentheses for 21.209

atom	atom	distance	atom	atom	distance
Ru(1)	S(1)	2.434(2)	S(2)	C(21)	1.819(5)
Ru(1)	S(2)	2.474(1)	S(3)	Na(1)	2.821(2)
Ru(1)	S(3)	2.467(1)	S(3)	C(23)	1.825(5)
Ru(1)	P(1)	2.375(1)	P(1)	C(1)	1.839(4)
Ru(1)	C(25)	1.865(5)	P(1)	C(7)	1.834(4)
Ru(1)	C(26)	1.877(5)	P(1)	C(13)	1.840(4)
S(1)	Na(1)	2.824(2)	Na(1)	O(3)	2.365(5)
S(1)	C(19)	1.746(7)	O(1)	C(25)	1.144(5)
S(2)	Na(1)	3.019(2)	O(2)	C(26)	1.146(5)
S(2)	Na(1)*	2.839(2)			

* denotes symmetry operation: 1-x, -y, -z.

Table 5.5 Selected bond angles (°) with estimated standard deviations in parentheses, for 21.209

atom	atom	atom	angle	atom	atom	atom	angle
S(1)	Ru(1)	S(2)	88.46(5)	Ru(1)	S(3)	Na(1)	85.91(6)
S(1)	Ru(1)	S(3)	84.60(5)	Ru(1)	S(3)	C(23)	109.4(2)
S(1)	Ru(1)	P(1)	170.79(5)	Na(1)	S(3)	C(23)	109.3(2)
S(1)	Ru(1)	C(25)	84.6(1)	Ru(1)	P(1)	C(1)	114.2(1)
S(1)	Ru(1)	C(26)	93.4(1)	Ru(1)	P(1)	C(7)	112.3(1)
S(2)	Ru(1)	S(3)	88.47(5)	Ru(1)	P(1)	C(13)	120.6(1)
S(2)	Ru(1)	P(1)	90.33(5)	C(1)	P(1)	C(7)	104.8(2)
S(2)	Ru(1)	C(25)	173.0(1)	C(1)	P(1)	C(13)	102.6(2)
S(2)	Ru(1)	C(26)	89.2(1)	C(7)	P(1)	C(13)	100.4(2)
S(3)	Ru(1)	P(1)	86.25(5)	S(1)	Na(1)	S(2)	71.64(6)
S(3)	Ru(1)	C(25)	91.6(2)	S(1)	Na(1)	S(1)*	157.14(9)
S(3)	Ru(1)	C(26)	176.9(1)	S(1)	Na(1)	S(3)	71.50(6)
P(1)	Ru(1)	C(25)	96.6(1)	S(1)	Na(1)	O(3)	95.3(1)
P(1)	Ru(1)	C(26)	95.7(1)	S(2)	Na(1)	S(2)*	85.79(7)
C(25)	Ru(1)	C(26)	90.5(2)	S(2)	Na(1)	S(3)	72.25(6)
Ru(1)	S(1)	Na(1)	86.45(6)	S(2)	Na(1)	O(3)	166.9(1)
Ru(1)	S(1)	C(19)	114.0(3)	S(2)*	Na(1)	S(3)	105.59(8)
Na(1)	S(1)	C(19)	147.9(3)	S(2)*	Na(1)	O(3)	107.3(1)
Ru(1)	S(2)	Na(1)	81.57(5)	S(3)	Na(1)	O(3)	104.2(1)
Ru(1)	S(2)	Na(1)*	145.88(6)	Na(1)	O(3)	C(27)	129.1(5)
Ru(1)	S(2)	C(21)	110.1(2)	Na(1)	O(3)	C(30)	123.0(5)
Na(1)	S(2)	Na(1)*	94.21(7)	C(27)	O(3)	C(30)	106.2(6)
Na(1)	S(2)	C(21)	103.7(2)	Ru(1)	C(25)	O(1)	173.8(4)
Na(1)*	S(2)	C(21)	103.8(2)	Ru(1)	C(26)	O(2)	176.8(5)

* denotes symmetry operation: 1-x, -y, -z.

than the S-C(sp²) bond lengths for the structures of *cct*-RuH(SC₆H₄pCH₃)(CO)₂(PPh₃)₂ (**9b**) and *cct*-Ru(SC₆H₄pCH₃)₂(CO)₂(PPh₃)₂ (**14b**) described in Chapters 3 and 4.

The Ru-C and C-O bond lengths of **21** are comparable to those in carbonyls *trans* to thiolates in **9b**, **14b**, and **14a** (Chapter 4). The Ru-P bond length is 2.375 Å, slightly shorter than in the other complexes, probably because the *trans* influence of thiolates is weaker than that of phosphines.

The CP/MAS (cross-polarized, magic angle spinning) solid-state ¹³C NMR spectrum of **21** (Fig. 5.13a) contains two strong peaks for the THF molecule (68.2 and 25.6 ppm), one of which partly obscures the methylene region. Two peaks are observed on either side of the THF peak, at 26.9 and 24.6 ppm. However, three peaks are expected, because there are three different ethyl groups in the solid state structure. It is possible that the third peak is obscured by the THF resonance. The methyl region clearly contains three signals, as expected. An NQS (Non-Quaternary Suppression) solid state ¹³C NMR experiment was performed to confirm the identification of the three high field peaks as methyl peaks (Fig. 5.13b). In such an experiment, strongly dipolar-coupled nuclei such as CH or CH₂ carbons are suppressed, while quaternary carbons and carbons in rapidly moving groups (e.g. CH₃ groups) are detected.²⁷⁹ The three high field peaks due to CH₃ groups are detected, in addition to the strong THF peak at 25.5 ppm. From the latter observation, one can conclude that the β carbons of the THF ligand are mobile, as suggested by the size of their thermal ellipsoids (Fig. 5.11). The THF ligand is therefore "wagging." The peaks were assigned by analogy to the solution ¹³C{¹H} NMR spectrum (see below).

The solution ¹³C{¹H} NMR spectrum of **21** (Fig. 5.14) was assigned with the help of an APT (Attached Proton Test) experiment (Fig. 5.15) and a HETCOR (¹³C/¹H NMR Heteronuclear Correlation) experiment (Fig. 5.16). The HETCOR plot allows direct correlation of the ¹³C{¹H} NMR signals with the assigned peaks of the ¹H NMR spectrum. The methylene region of the ¹³C{¹H} NMR spectrum again contains resonances due to the THF molecule, at 67.8 and 25.7 ppm. Also in the methylene region are a larger peak at 25.2 ppm and a smaller

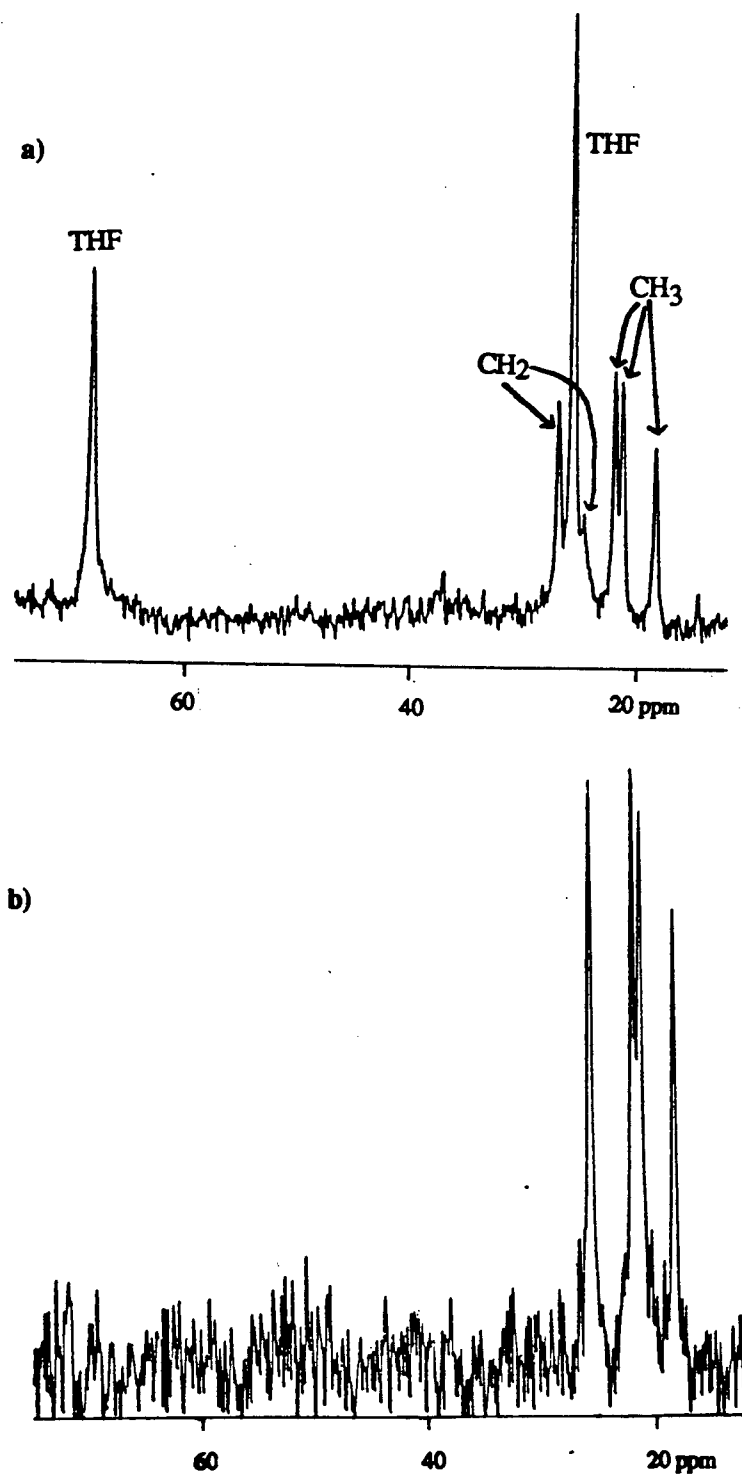


Fig. 5.13 a) ^{13}C solid state (CP/MAS) NMR spectrum of $[(\text{CO})_2(\text{PPh}_3)\text{Ru}(\mu\text{SEt})_2(\mu_3\text{SEt})\text{Na}(\text{THF})]_2$.
b) ^{13}C solid state (CP/MAS) NQS NMR spectrum of $[(\text{CO})_2(\text{PPh}_3)\text{Ru}(\mu\text{SEt})_2(\mu_3\text{SEt})\text{Na}(\text{THF})]_2$.

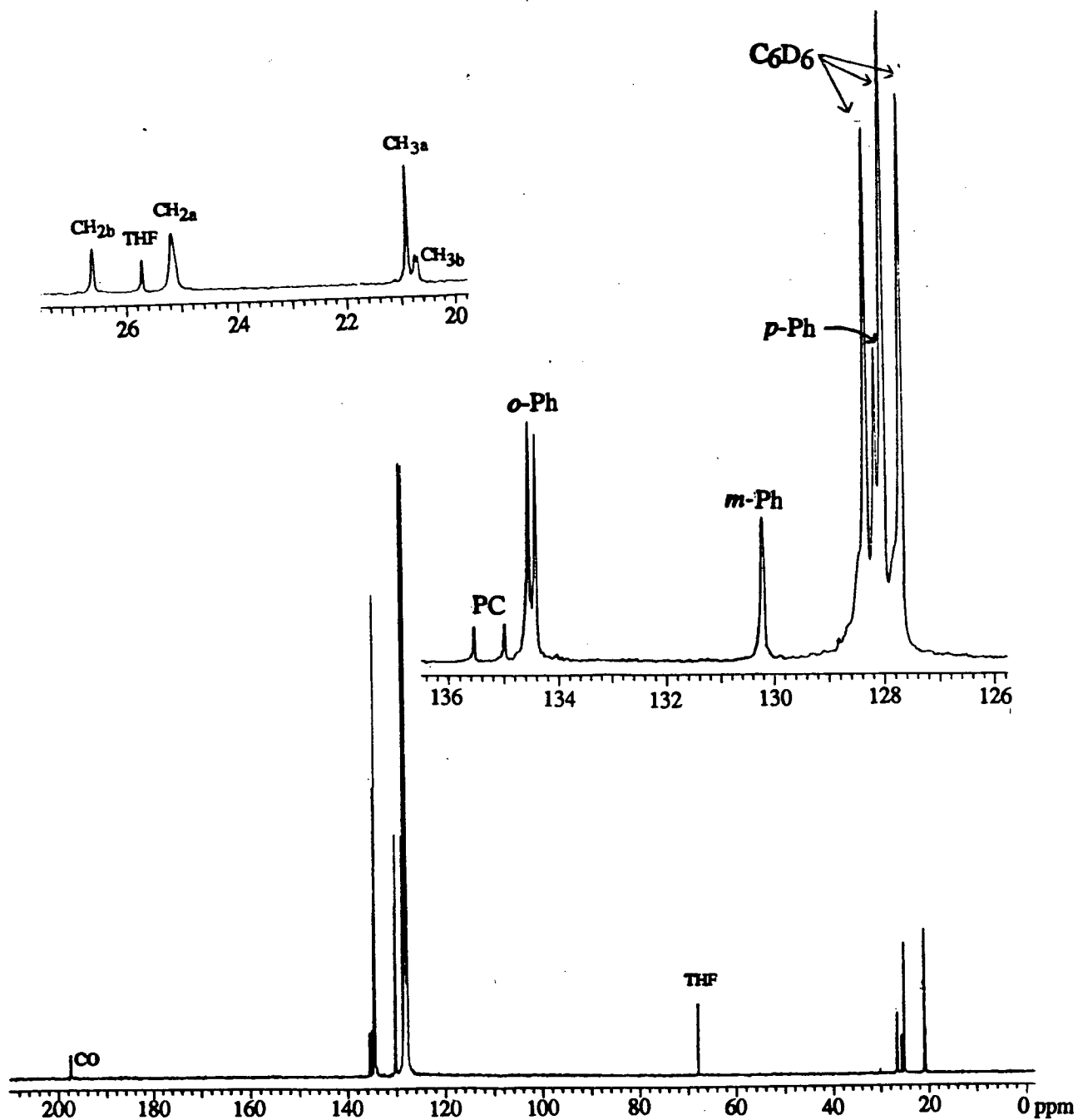


Fig. 5.14 $^{13}\text{C}\{^1\text{H}\}$ NMR spectrum of $[\text{Ru}(\text{CO})_2(\text{PPh}_3)\text{Ru}(\text{SET})_3\text{Na}(\text{THF})]_2$ in C_6D_6 at 20°C and 75 MHz .

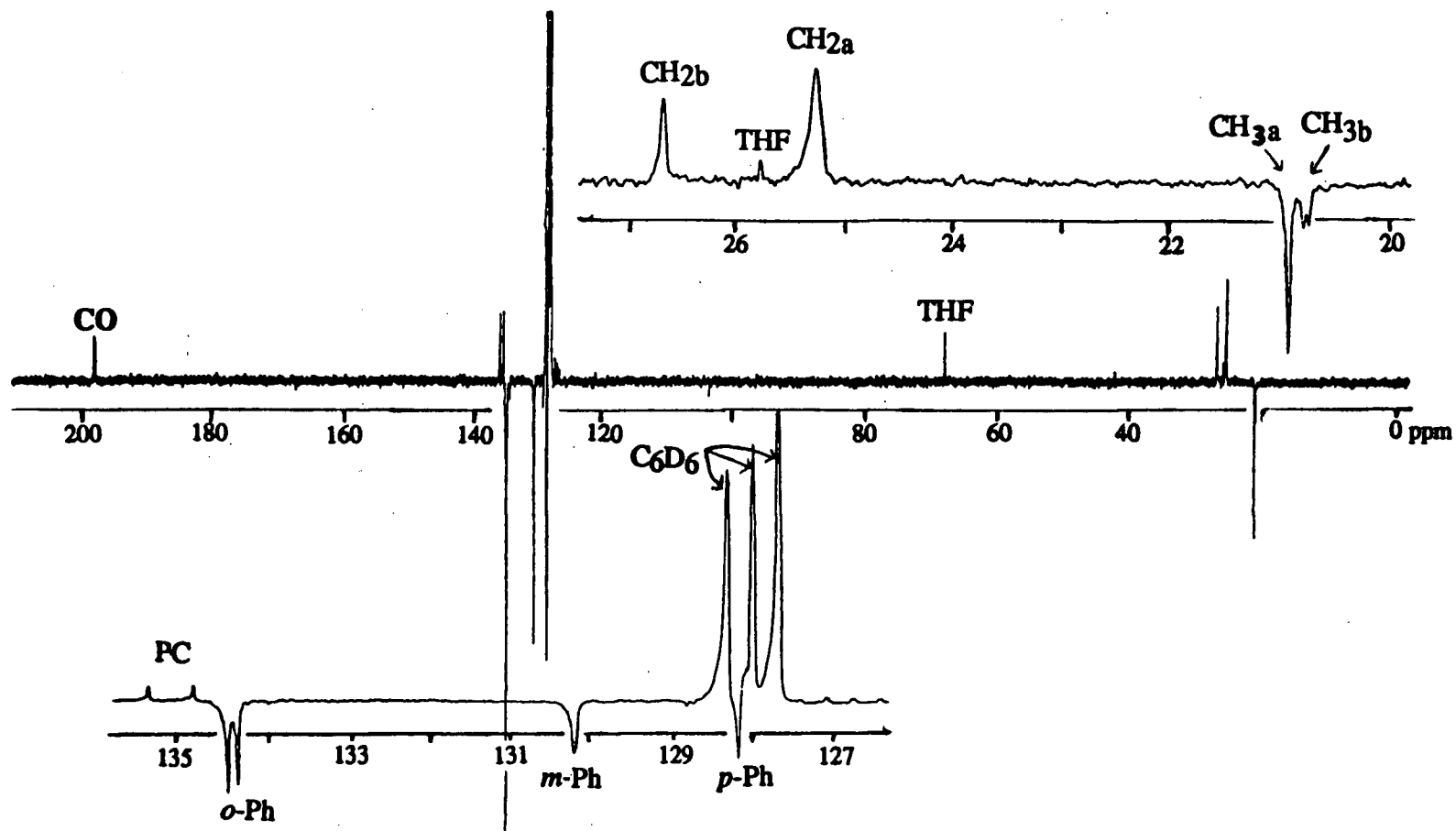


Fig. 5.15 ^{13}C APT NMR spectrum of $[\text{Ru}(\text{CO})_2(\text{PPh}_3)\text{Ru}(\text{SET})_3\text{Na}(\text{THF})]_2$ in C_6D_6 at 20°C and 75 MHz .

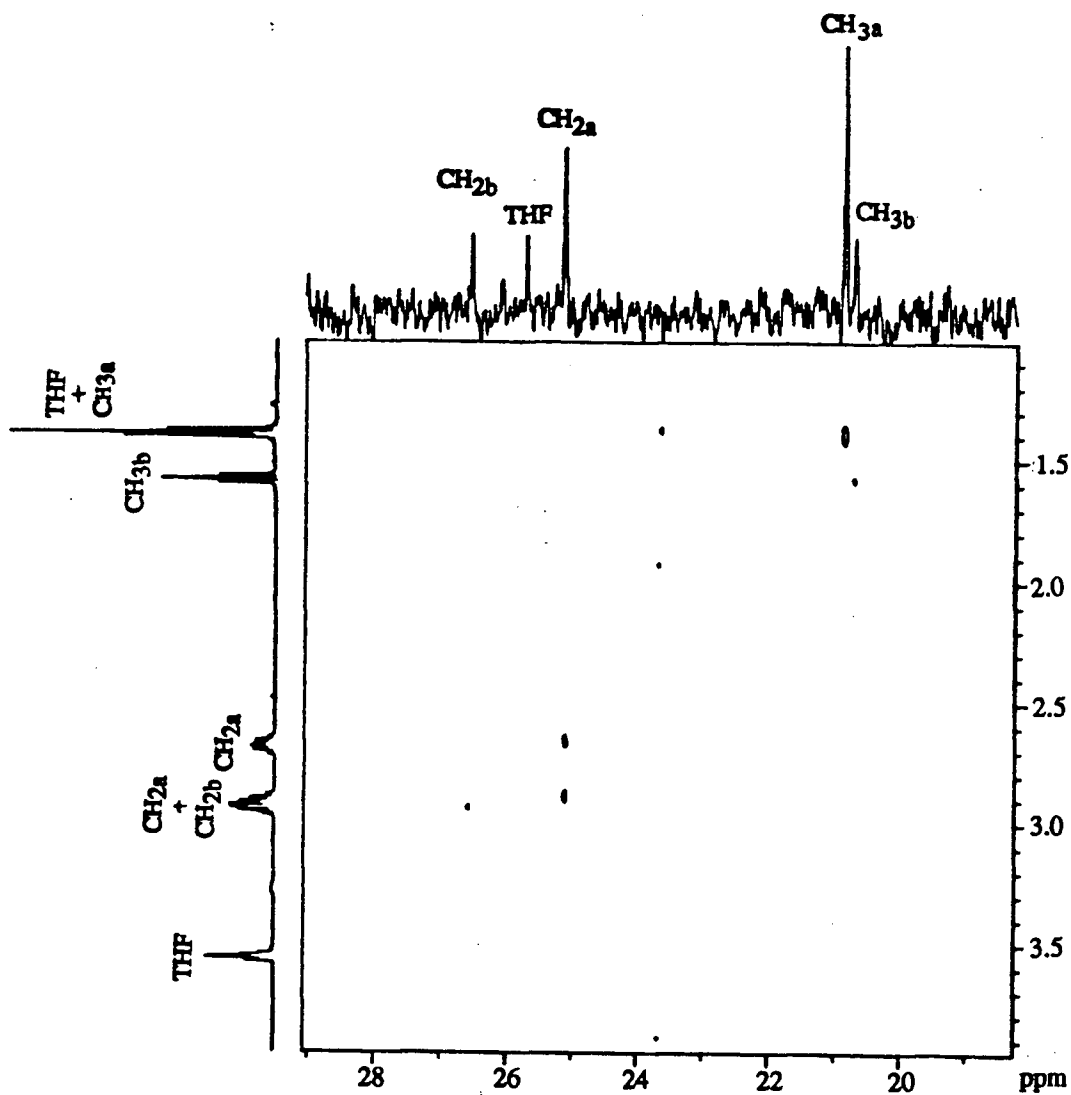


Fig. 5.16 The Heteronuclear Correlation ($^{13}\text{C}/^1\text{H}$) NMR plot for $[\text{Ru}(\text{CO})_2(\text{PPh}_3)\text{Ru}(\mu_3\text{SEt})_2(\mu_3\text{SEt})\text{Na}(\text{THF})_2]$ in C_6D_6 at 125 MHz. Points along the line defined by $^{13}\text{C} \delta = 23.5$ ppm are believed to be artifacts.

peak at 26.6 ppm representing CH₂(a) and CH₂(b), respectively. The fact that only two such peaks are detected supports the conclusion from the ¹H NMR spectral data that the two Et(a) groups are equivalent in solution on the NMR time-scale. The methyl region of the solution ¹³C{¹H} NMR spectrum contains a tall peak for the CH₃(a) groups, again confirming their equivalence. However, the small signal for the CH₃(b) groups appears split in the ¹³C{¹H} and APT spectra at 75 MHz, but not in the ¹³C{¹H} NMR spectrum at 125 MHz. The reason for this splitting is not known. The ¹H NMR spectrum is unequivocal in demonstrating that there is only one type of CH₃(b) group in the solution. The ¹³C{¹H} NMR spectral assignments for the phenyl region are based on the assumption that the J_{PC} coupling constant decreases in the order P-bound, *o*-, *m*-, *p*-phenyl carbons.

The lack of conductivity in solution indicates that the sodium atoms do not dissociate from the complex. The solution NMR spectra of **21** do not reveal whether the complex exists as a dimer or monomer in solution. It is neither sufficiently stable for a determination of the molecular weight by the Signer method,²⁸⁰ nor sufficiently soluble for a solvent freezing-point depression experiment. However, we know that the structure is not identical to that of the solid state because the Et(a) groups are equivalent in solution and not in the solid state.

For the two Et(a) groups attached to S² and S³ to be chemically equivalent, as observed in the solution spectra, a mirror plane would have to exist between them. Because the positions of Et(b), THF and the Na atoms are not on this plane, these three groups must be in rapid motion across it to create such a mirror plane. In other words, the following motions must occur rapidly on the NMR time-scale.

1) Inversion at the chiral sulphur atom S¹ would bring Et(b) across the mirror plane.

Inversion at S² or S³ is not required, nor is it likely because it would bring the Et(a) groups into collision with the phenyl rings of the phosphine.

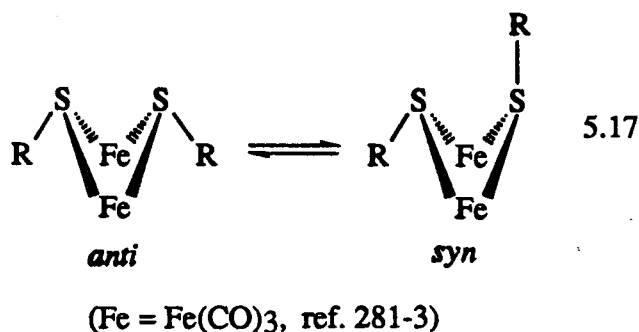
2) Rapid back-and-forth motion of Na^{1*} between S² and S³, and Na¹ between S^{2*} and S^{3*}.

If the complex were a monomer in solution, then symmetry would only require that the Na¹-S² and Na¹-S³ bonds be equivalent.

3) Rapid motion of the THF molecule between the sites *trans* to S^2 and S^3 . If the complex were a dimer in solution, this motion would not be possible without dissociation of the THF ligand because of hindrance from the phenyl rings. This motion would also have to occur simultaneously with motion 2, so that the site to which the THF is travelling would no longer be blocked by a phenyl group. Alternatively, the two THF ligands could be completely dissociated from the sodium atoms in solution. The ^1H and $^{13}\text{C}\{^1\text{H}\}$ NMR chemical shifts of the THF protons and carbons are not significantly different from those of THF alone in C_6D_6 . This is consistent with but not proof of THF dissociation.

The situation is made more complicated by the fact that the methylene protons of $\text{CH}_2(\text{b})$ (C^{19}) are not equivalent. If the mirror plane exists, then these protons should be equivalent. Therefore inversion at S^1 (motion 1) is probably not occurring rapidly on the NMR time-scale. It is not clear whether or not motions 2 and 3 are occurring. However, it seems unlikely that the Et(a) protons could appear to be equivalent without at least motion 2 being rapid on the NMR time-scale.

Studies on the effect of the R group on the rate of the *anti* to *syn* isomerization of $[\text{Fe}(\text{CO})_3(\mu\text{SR})]_2$ (equation 5.17)

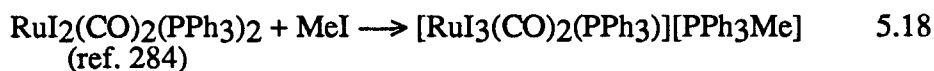


have shown that bulkier and aromatic thiolates invert more quickly. The rate constant for the conversion of the *anti* to the *syn* isomer, in toluene solution at 35°C, range from $1.1 \times 10^{-5} \text{ s}^{-1}$ ($\text{R}=\text{Me}$)²⁸¹ or $2.4 \times 10^{-4} \text{ s}^{-1}$ ($\text{R}=\text{Ph}$) to 0.6 s^{-1} ($\text{R}=\text{tBu}$)²⁸² or higher²⁸³ for very bulky groups. The ethyl derivative undergoes this net inversion process only marginally faster than the methyl derivative.²⁸¹ The mechanism is probably *via* Fe-S bond cleavage. Although the thiolates in

$[(\text{PPh}_3)(\text{CO})_2\text{Ru}(\text{SEt})_3\text{Na}(\text{THF})]_2$ (**21**) and $[\text{Fe}(\text{CO})_3(\mu\text{SEt})]_2$ are not in identical environments, it seems reasonable that the inversion process in **21** is not rapid on the NMR time-scale.

The variable temperature ^1H NMR spectra of **21** shed little light on the problem of motion within the molecule. At temperatures greater than 60°C , changes in the appearance of the spectrum are rapid and irreversible. The signals due to THF (1.4 to 1.6 ppm) and an unknown complex presumably resulting from the decomposition of **21** (2.15 ppm) become more intense relative to the peaks of the dimer, which become amorphous. The ^1H NMR spectrum is not restored to its original appearance after the solution is cooled to 20°C , and only PPh_3 can be detected in the $^{31}\text{P}\{^1\text{H}\}$ NMR spectrum. The ^1H NMR spectrum of a fresh sample at -78°C shows the peaks of **21** (but not those of THF or toluene- d_7) to be greatly broadened (Fig. 5.17). This effect may result from a slowing of internal motions within the dimer. Spectra at even lower temperatures would be required to confirm this, although toluene- d_8 has too high a freezing point (-93°C) to be used in such experiments.

The only other compound containing $[\text{RuX}_3(\text{CO})_2(\text{PPh}_3)]^-$ fragments ($\text{X}=\text{halide}$ or *pseudo-halide*), which has been mentioned in the literature, is $[\text{RuI}_3(\text{CO})_2(\text{PPh}_3)][\text{PPh}_3\text{Me}]$.



The related anions $[\text{RuX}_3(\text{CO})_3]^-$ ($\text{X}=\text{Cl}, \text{Br}, \text{I}$)^{285,286} and $[\text{RuCl}_3(\text{CO})(\text{PPh}_3)_2]^-$ ²⁸⁷ have also been reported.

The structure of **21** is unique in that the two Ru centres are connected to each other by a network of six bridging thiolate ligands and two sodium atoms; four thiolates ($\text{S1}, \text{S3}, \text{S1}^*$, and S3^*) bridge one Ru and one Na, while two thiolates (S2 and S2^*) triply bridge one Ru and two Na atoms. Such triple bridging of thiolates between transition metal and alkali metal ions is unprecedented. The recently reported anionic species $[\text{Na}\{\text{Ru}(\text{CO})_2(\text{Se}_4)_2\}_2]^{3-}$ contains Se atoms (of Se_4^{2-} ligands) bridging Ru and Na atoms,²⁸⁸ while examples of alkyl thiolate ligands bridging three Ru atoms are known.²⁸⁹ More generally, there are few examples of transition

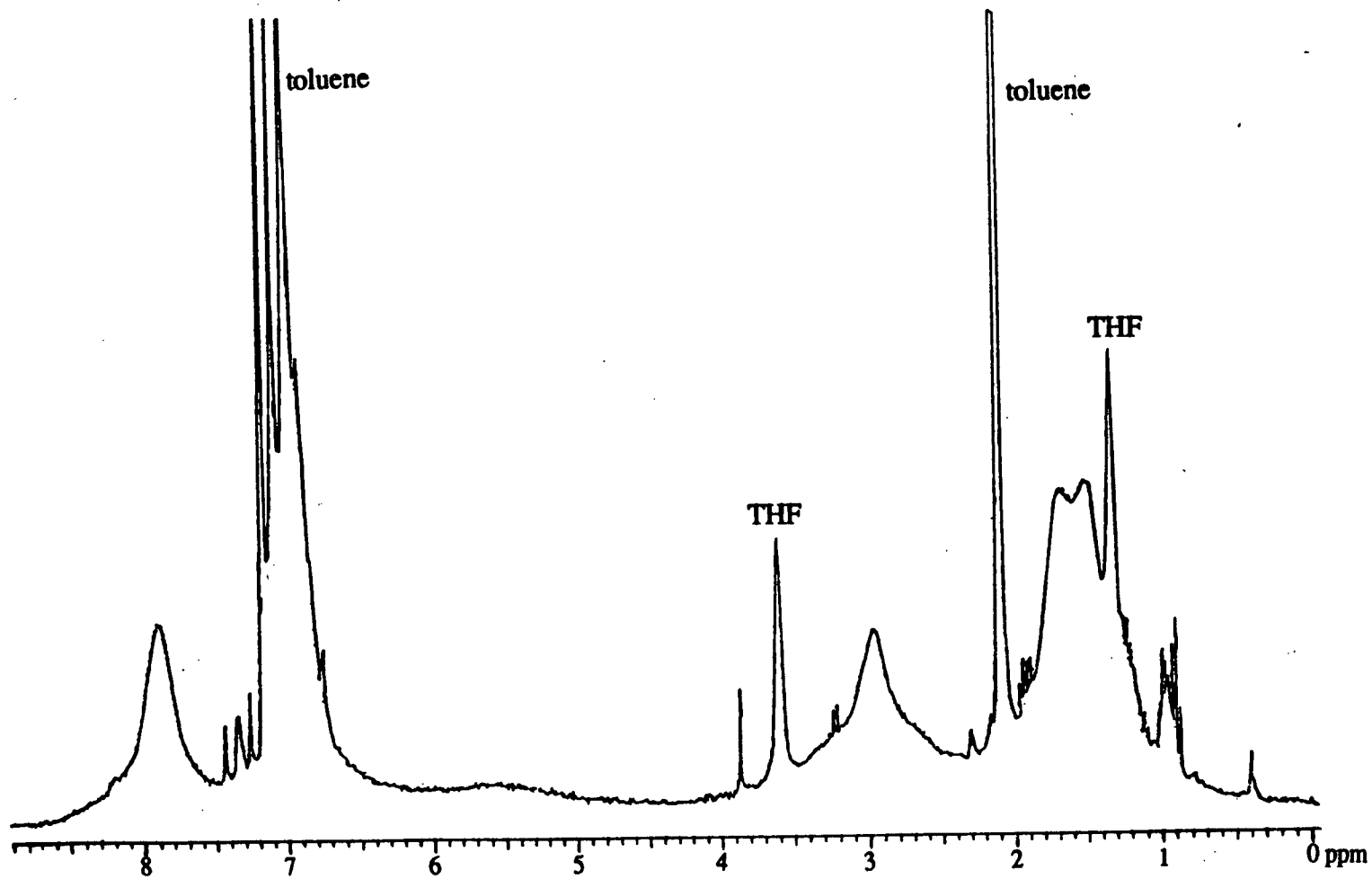
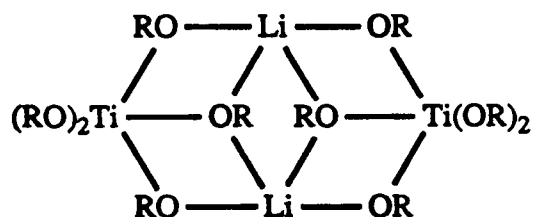


Fig. 5.17 The ^1H NMR spectrum of $[\text{Ru}(\text{CO})_2(\text{PPh}_3)\text{Ru}(\mu_3\text{SEt})_2(\mu_3\text{SEt})\text{Na}(\text{THF})_2]$ in toluene- d_8 at -78°C

metal complexes containing alkali metal cations "trapped" *via* bridging thiolate ligands:

$(C_5Me_5)_2Lu(\mu S^tBu)_2Li(THF)_2$,²⁹⁰⁻¹ $[Li(dme)]_4[U(edt)_4]$ (dme = 1,2-dimethoxyethane, edt = 1,2-ethylenedithiolate),²⁹² and $(SC_6H_4pCH_3)_3Nb(\mu SC_6H_4pCH_3)_3Na(THF)_3$.²⁹³ There are many more examples of trapped alkali metal cations in alkoxide chemistry, particularly as by-products of metathesis reactions using alkoxide salts; these have been described in reviews of "double metal alkoxides" (complexes containing alkoxide ligands bridging two different metals).²⁹⁴ Double metal thiolates have not been reviewed. No previous Na/Ru double metal alkoxide or thiolate is known to us. Perhaps the mostly closely parallel alkoxide complex is $Li_2Ti_2(OiPr)_{10}$, the structure of which has recently been determined.²⁹⁵



Organic complexes containing alkali metal cations trapped by sulphur atoms are rare. Almost all of the reports covering crown thioether metal complexes deal exclusively with transition metals.²⁹⁶ No X-ray structure of a appears to have been reported. Comparisons between sodium crown-thioether complexes and 21, which represents an "inorganic crown thioether," will have to wait for the completion of the crystal structure of an example of a sodium crown-thioether complex. In the vast literature of the oxygen-containing crown ether ligands, there is, of course, an abundance of structures of sodium complexes.²⁹⁷⁻³⁰⁰

5.4 THE REACTIONS OF OTHER RUTHENIUM CHLORO COMPLEXES WITH SODIUM THIOLATES

The reaction of a $\text{RuCl}_3/\text{PPh}_3$ mixture with excess NaSEt under CO in refluxing MeOH produces a mixture of 10 to 20% each of $cct\text{-RuCl}_2(\text{CO})_2(\text{PPh}_3)_2$ (**1**), $cct\text{-RuCl}(\text{SEt})(\text{CO})_2(\text{PPh}_3)_2$ (**20**), $cct\text{-Ru}(\text{SEt})_2(\text{CO})_2(\text{PPh}_3)_2$ (**14d**), and a product with the same ^{31}P chemical shift as $[(\text{PPh}_3)(\text{CO})_2\text{Ru}(\text{SEt})_3\text{Na}(\text{THF})]_2$, plus smaller amounts of several unidentified products. This experiment was attempted because of a report of the synthesis of $cct\text{-Ru}(\text{SC}_6\text{F}_5)_2(\text{CO})_2(\text{PMePh}_2)_2$ directly from RuCl_3 .^{260b} With optimization of conditions, this method perhaps could provide a short-cut to the synthesis of these thiolato (carbonyl) phosphine complexes.

The complex $cct\text{-RuH}(\text{Cl})(\text{CO})_2(\text{PPh}_3)_2$ reacts with one equivalent of $\text{NaSC}_6\text{H}_5\text{pCH}_3$ in acetone to give 56% conversion to $cct\text{-RuH}(\text{SC}_6\text{H}_4\text{pCH}_3)(\text{CO})_2(\text{PPh}_3)_2$.



If excess thiolate is used, 90% conversion to $cct\text{-Ru}(\text{SC}_6\text{H}_4\text{pCH}_3)_2(\text{CO})_2(\text{PPh}_3)_2$ (**14b**) is observed. The reactions of $\text{Ru}(\text{CO})_2(\text{PPh}_3)_3$ and $cct\text{-RuH}_2(\text{CO})_2(\text{PPh}_3)_2$ with thiols are the preferred synthetic routes to **9** because in these reactions the formation of the *bis*-thiolate product is easier to control.

A mixture of *cis*- and *trans*- $\text{RuCl}_2(\text{dpm})_2$ (**5** and **6**) does not react with NaSEt . The role of the bulky phenyl rings of $\text{RuH}(\text{Cl})(\text{dppe})_2$ ($\text{dppe}=\text{Ph}_2\text{PCH}_2\text{CH}_2\text{PPh}_2$) has been cited to explain its non-reaction with LiAlH_4 .¹⁸⁹ However, *cis*- $\text{RuCl}_2(\text{dpm})_2$ reacts easily with NaBH_4 (Chapter 2), possibly because the BH_4^- anion is considerably smaller than AlH_4^- and SEt^- .

5.5 EXPERIMENTAL DETAILS

The reaction of *cct*-RuCl₂(CO)₂(PPh₃)₂ (1**) with NaSC₆H₄pCH₃:** A white acetone (40 mL) suspension of **1** (140 mg, 0.18 mmol) and the thiolate salt (56 mg, 0.38 mmol) under CO (1 atm) turned yellow within one minute at room temperature. The suspension was filtered, after being stirred overnight. The solid was discarded and the volume of the yellow filtrate was reduced to 10 mL by vacuum distillation. MeOH (approx. 30 mL) was added to encourage precipitation. The solid product collected by filtration was pure *cct*-Ru(SC₆H₄pCH₃)₂(CO)₂(PPh₃)₂ (**14b**), according to the ³¹P{¹H} and ¹H NMR spectra, which are identical to those of a known sample of that complex prepared from Ru(CO)₂(PPh₃)₃ and the disulphide (Sections 4.1 and 4.2).

The reaction of *cct*-RuCl₂(CO)₂(PPh₃)₂ (1**) and NaSEt in acetone:** A white acetone (20 mL) suspension of **1** (450 mg, 0.60 mmol) and the thiolate salt (120 mg, 1.4 mmol) under CO (1 atm) turned yellow within one minute at room temperature. The suspension was stirred overnight and then filtered through diatomaceous earth. The volume of the yellow filtrate was reduced to 5 mL by vacuum distillation. MeOH (30 mL) was added to encourage precipitation, and the vessel left for 2 h at 0°C. During this time, a yellow precipitate formed. The suspension was filtered. The collected solid product was a mixture of *cct*-Ru(SC₂H₅)₂(CO)₂(PPh₃)₂ (**14d**) and PPh₃ according to the ³¹P{¹H} NMR spectrum of the C₆D₆ solution of this product. All attempts at purifying this complex, or repeating the reaction, resulted in yellow or brown oils which contained the same product.

The reaction of *cct*-RuCl₂(CO)₂(PPh₃)₂ (1**) and NaSEt in THF:** A yellow THF (100 mL) suspension of **1** (520 mg, 0.70 mmol) and the thiolate salt (1.4 g, 17 mmol) under Ar was stirred for 1 h at room temperature, filtered, and the solid discarded. The yellow filtrate was evaporated to dryness. The products from two such reactions were dissolved together in THF (10 mL). The volume of the solution was reduced to 3 mL by vacuum distillation, and hexanes (15 mL) were

added to induce precipitation. The suspension was filtered and the collected yellow solid was washed with 15 mL of cooled hexanes. The overall yield was 53%. The NMR spectra show the product to be pure $[(PPh_3)(CO)_2Ru(SEt)_3Na(THF)]_2$ (**21**). If only 2-3 equivalents of NaSEt were used, significant amounts of **1** remained after several hours. By using intermediate amounts of NaSEt and 15 min reaction times, mixtures of *cct*- $RuCl(SEt)(CO)_2(PPh_3)_2$ (**20**) and *cct*- $Ru(SEt)_2(CO)_2(PPh_3)_2$ (**14d**) were obtained.

Characterization of *cct*- $RuCl(SEt)(CO)_2(PPh_3)_2$ (20**, containing 2% **14d** based on the $^{31}P\{^1H\}$ NMR spectrum):** Elem. Anal.: Calcd. for $C_{40}H_{35}ClO_2P_2RuS$: C, 61.7; H, 4.5.

Found: C, 60.6; H, 4.6. 1H NMR (C_6D_6 , 300 MHz) δ 1.13 (t, 3H, $^3J_{HH} = 7.4$ Hz, CH_3), 1.92 (q, 2H, $^3J_{HH} = 7.3$ Hz, CH_2), 7.0 (multi, 18H, *m*-/*p*-Ph), 8.25 ppm (multi, 12H, *o*-Ph); $^{31}P\{^1H\}$ NMR (C_6D_6 , 121 MHz) δ 14.54 ppm (s); IR (Nujol) 2042, 1988 cm^{-1} ($\nu(CO)$).

Characterization of *cct*- $Ru(SEt)_2(CO)_2(PPh_3)_2$ (14d**, containing 20 % of **20** based on the $^{31}P\{^1H\}$ NMR spectrum, listing resonances due to the major component only):** 1H NMR

(C_6D_6 , 300 MHz) δ 1.16 (t, 6H, $^3J_{HH} = 7.4$ Hz, CH_3), 1.97 (q, 4H, $^3J_{HH} = 7.4$ Hz, CH_2), 7.04 (multi, 18H, *m*-/*p*-Ph), 8.22 (multi, 12H, *o*-Ph); $^{31}P\{^1H\}$ NMR (C_6D_6 , 121 MHz) δ 11.18 ppm (s); IR (Nujol) 2022, 1963 cm^{-1} ($\nu(CO)$).

Characterization of $[(PPh_3)(CO)_2Ru(\mu_2SEt)_2(\mu_3SEt)Na(THF)]_2$ (21**):** Elem. Anal.: Calcd. for $C_{60}H_{76}Na_2O_6P_2Ru_2S_6$: C, 51.6; H, 5.5; S, 13.8. Found: C, 51.7; H, 5.5; S, 14.1. 1H NMR

(C_6D_6) δ 1.41 (t, 12H, $^3J_{HH} = 7.6$ Hz, $CH_3(a)$), 1.41 (multi, 8H, β - CH_2 of THF), 1.59 (t, 6H, $^3J_{HH} = 7.3$ Hz, $CH_3(b)$), 2.71 (d of q, 8H, $^2J_{HH} = 9.0$, $^3J_{HH} = 7.3$ Hz, $CH_2(a)$), 2.95 (d of q, 8H, $^2J_{HH} = 9.0$, $^3J_{HH} = 7.5$ Hz, $CH_2(a)$), 2.97 (d of q, 4H, $^2J_{HH} = 9.0$, $^3J_{HH} = 7.3$ Hz, $CH_2(b)$), 2.98 (d of q, 4H, $^2J_{HH} = 9.0$, $^3J_{HH} = 7.5$ Hz, $CH_2(b)$), 3.57 ppm (multi, 8H, α - CH_2 of THF), 7.06 (multi, 6H, *p*-Ph), 7.15 (t, 12H, $^3J_{HH} = 7.0$, *m*-Ph), 7.96 ppm (t, 12H, $^3J_{HH} = 8.8$ Hz, *o*-Ph); $^{13}C\{^1H\}$ NMR (C_6D_6 , 75 MHz) δ 20.73 ($CH_3(b)$), 20.89 ($CH_3(a)$), 25.16 ($CH_2(a)$), 25.71 (β -C of THF), 26.62 ($CH_2(b)$), 67.85 (α -C of THF), 128.16 (*p*-Ph), 130.22 (*m*-Ph), 134.50 (d, $J_{PC} = 9.4$ Hz, *o*-Ph), 135.28 (d, $J_{PC} = 41.9$ Hz, P-C), 197.48 ppm (CO); $^{31}P\{^1H\}$ NMR

(C₆D₆, 121 MHz) δ 25.05 ppm (s); IR (Nujol) 2014, 1952 cm⁻¹ (ν (CO)). Solutions of **21** (up to 1 mM) in THF had no detectable conductance at room temperature under argon.

A crystal of [(PPh₃)(CO)₂Ru(μ ₂SEt)₂(μ ₃SEt)Na(THF)]₂ (**21**) suitable for X-ray crystallography was prepared by diffusion of hexanes into a concentrated THF solution under Ar in darkness. The structure analysis was performed by Dr. S. J. Rettig.²⁰⁹ The final unit-cell parameters were obtained by least-squares on the setting angles for 25 reflections with $2\theta = 20.0$ - 26.5° . The intensities of three standard reflections, measured every 200 reflections throughout the data collection, decayed uniformly by 12%. The data were processed^{259a} and corrected for Lorentz and polarization effects, decay, and absorption (empirical, based on azimuthal scans for four reflections).²⁰⁹

The structure analysis was initiated in the centrosymmetric space group $P\bar{1}$, the choice being confirmed by the subsequent successful solution and refinement of the structure. The structure was solved by conventional heavy atom methods, the coordinates of the Ru, P, and S atoms being determined from the Patterson functions and those of the remaining non-hydrogen atoms from subsequent difference Fourier syntheses. The complex has crystallographically imposed symmetry. All non-hydrogen atoms were refined with anisotropic thermal parameters. Hydrogen atoms were fixed in idealized positions ($d_{C-H} = 0.98$ Å, $B_H = 1.2$ B bonded atom). Neutral atom scattering factors and anomalous dispersion corrections for the non-hydrogen atoms were taken from the International Tables for X-Ray Crystallography.^{259b} Final atomic coordinates and equivalent isotropic thermal parameters [$B_{eq} = 4/3 \sum_i \sum_j b_{ij}(a_i a_j)$], bond lengths, and bond angles appear in Appendix 4, and Tables 5.4 and 5.5 respectively. Other crystallographic data for this structure and the other structures described in this work are presented in Appendix 1.²⁰⁹

The reaction of RuCl₃ with PPh₃ and NaSEt: RuCl₃ (300 mg, 0.96 mmol) and PPh₃ (1.43 g, 5.4 mmol) were allowed to react in refluxing MeOH (30 mL) under N₂ for 15 min. During this time, the solution turned from brown to dark green. After the solution had cooled, NaSEt (155

mg, 1.8 mmol) was added, and CO introduced. The brown colour returned immediately, but again slowly changed to dark green. After 30 min, the volatiles were removed by vacuum distillation, leaving a yellow/brown unpurified product. The $^{31}\text{P}\{^1\text{H}\}$ NMR spectrum (C_6D_6) shows that this product contained, in addition to PPh_3 , *cct*- $\text{RuCl}_2(\text{CO})_2(\text{PPh}_3)_2$ (**1**, 20 % of ^{31}P NMR signal excluding that of free PPh_3), *cct*- $\text{RuCl}(\text{SEt})(\text{CO})_2(\text{PPh}_3)_2$ (**20**, 7 %), *cct*- $\text{Ru}(\text{SEt})_2(\text{CO})_2(\text{PPh}_3)_2$ (**14d**, 19 %), a product having the same chemical shift as $[(\text{PPh}_3)(\text{CO})_2\text{Ru}(\text{SEt})_3\text{Na}(\text{THF})]_2$ (16 %), and several unknowns at lower concentrations.

The reaction of *cct*- $\text{RuH}(\text{Cl})(\text{CO})_2(\text{PPh}_3)_2$ (4**) and $\text{NaSC}_6\text{H}_4\text{pCH}_3$:** Complex **1** (72 mg, 0.10 mol) and the thiolate salt (18 mg, 0.12 mmol) reacted very quickly in acetone (20 mL) at room temperature under Ar, the white solution turning yellow within minutes. After 2 h, the volatiles were removed by vacuum distillation, leaving a yellow powder. This unpurified product was dried overnight, and then redissolved in C_6D_6 . The $^{31}\text{P}\{^1\text{H}\}$ NMR spectrum (121 MHz) shows that the product mixture contained unreacted **4** (20 % of ^{31}P NMR signal), *cct*- $\text{RuH}(\text{SC}_6\text{H}_4\text{pCH}_3)(\text{CO})_2(\text{PPh}_3)_2$ (**9b**, 60 %), *cct*- $\text{Ru}(\text{SC}_6\text{H}_4\text{pCH}_3)_2(\text{CO})_2(\text{PPh}_3)_2$ (**14b**, 10 %), and small (<5 %) amounts of PPh_3 , $\text{Ru}(\text{CO})_2(\text{PPh}_3)_3$ (**2**), and $\text{Ru}(\text{CO})_3(\text{PPh}_3)_2$ (**10**). The ^1H NMR spectrum confirms the identification of the major product and the starting material.

The overnight reaction of **4** with three equivalents of $\text{NaSC}_6\text{H}_4\text{pCH}_3$ produced a mixture of **14b** (90 %) and **9b** (10 %).

The attempted reaction of *trans*- $\text{RuCl}_2(\text{dpm})_2$ (6**) with NaSEt :** Complex **6** (140 mg, 0.15 mmol) failed to react with NaSEt (120 mg, 1.6 mmol) in acetone (25 mL) at room temperature. After one day, the suspension was washed through diatomaceous earth with THF (20 mL). The volume of the filtrate was reduced to 6 mL, and hexanes (20 mL) were added to induce precipitation. The collected yellow powder was unreacted starting material (identification by

$^{31}\text{P}\{^1\text{H}\}$ NMR spectroscopy).³⁰¹ The same result was obtained from a similar experiment with $\text{NaSC}_6\text{H}_4\text{pCH}_3$.

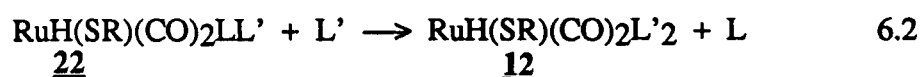
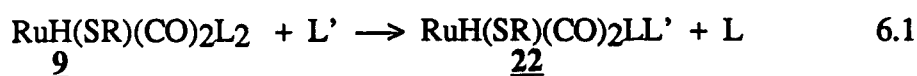
6. THE REACTIONS OF THIOLATO RUTHENIUM(II) COMPLEXES WITH NON-SULPHUR-CONTAINING REAGENTS

Comparisons between the reactions described in this chapter and those of the preceding chapters allow for greater insight into the mechanisms of the reactions and the conditions under which Ru-S bonds may be broken. The latter information is required before a catalytic cycle for desulphurization can be designed.

6.1 THE REACTIONS OF *cct*-RuH(SR)(CO)₂(PPh₃)₂ (**9**)

6.1.1 P(C₆H₄*p*CH₃)₃

The complex *cct*-RuH(SR)(CO)₂(PPh₃)₂ (**9**) reacts with P(C₆H₄*p*CH₃)₃ to produce a complex (**22**) of a structure similar to that of **9** but containing inequivalent phosphines (¹H and ³¹P{¹H} NMR spectral evidence). This product reacts further to produce a third complex (**12**), again of a structure similar to **9**, but containing equivalent phosphines. Based on the similarity of the NMR spectra of these complexes with those of the PPh₃ analogues, it is believed that the structures are *cct*-RuH(SR)(CO)₂(PPh₃)(P(C₆H₄*p*CH₃)₃) (**22**) and *cct*-RuH(SR)(CO)₂(P(C₆H₄*p*CH₃)₃)₂ (**12**). The ethyl derivative of the latter (**12d**) has been independently synthesized *via* the reaction of Ru(CO)₂(P(C₆H₄*p*CH₃)₃)₃ with ethanethiol (Sections 3.1 and 3.2). The sequence of reactions between **9e** and P(C₆H₄*p*CH₃)₃ is the following:



$L = \text{PPh}_3$, $L' = \text{P}(\text{C}_6\text{H}_4\text{pCH}_3)_3$, $R = \text{CH}_2\text{C}_6\text{H}_5$, $\text{C}_6\text{H}_4\text{pCH}_3$

The reaction of **9e** ($R = \text{CH}_2\text{C}_6\text{H}_5$) with $\text{P}(\text{C}_6\text{H}_4\text{pCH}_3)_3$ (L') was followed by $^{31}\text{P}\{^1\text{H}\}$ and ^1H NMR spectroscopy (Figs. 6.1 to 6.3) in C_6D_6 at 45°C under *pseudo*-first order conditions (large excess of L'). The rate of loss of **9e** is *pseudo*-first order, the log plot being linear for at least 3 half-lives (Fig. 6.4) and has an observed rate constant of $1.1 (\pm 0.1) \times 10^{-3} \text{ s}^{-1}$ (average of 5 results, at $[\mathbf{9e}] = 11 \text{ mM}$). The rate constant for the corresponding reaction of *cis*- $\text{RuH}(\text{SC}_6\text{H}_4\text{pCH}_3)(\text{CO})_2(\text{PPh}_3)_2$ (**9b**) is $7.0 \times 10^{-4} \text{ s}^{-1}$ (single experiment). The observed rate constant (for **9e**) is independent of the concentration of L' (94 to 502 mM, at $[\mathbf{9e}] = 11 \text{ mM}$) or **9e** ($k_{\text{obs}} = 1.2 \times 10^{-3} \text{ s}^{-1}$ at $[\mathbf{9e}] = 2.65 \text{ mM}$ and 130 mM L'). The rate law is simply:

$$-\frac{d[\mathbf{9e}]}{dt} = k_1[\mathbf{9e}] \quad \text{where } k_1 = 1.1 \times 10^{-3} \text{ s}^{-1}.$$

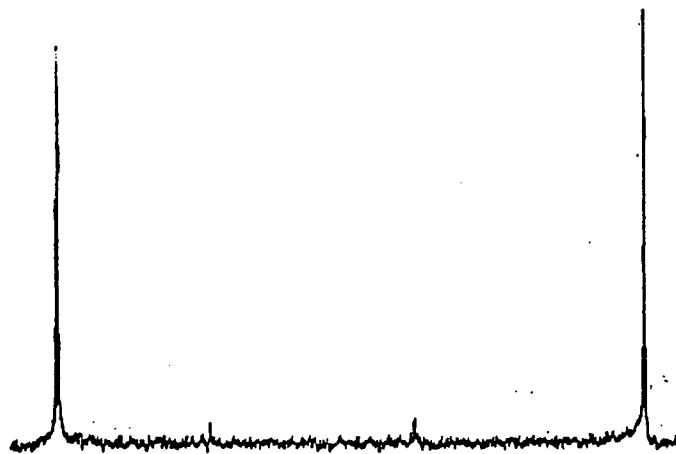
It therefore seems likely that the first step of reaction 6.1 is the rate determining dissociation of the phosphine L (Scheme 6.1), although other less likely mechanisms are possible, such as initial reductive elimination of thiol. The rate law for the loss of **9e**, assuming a steady state for $\text{RuH}(\text{SR})(\text{CO})_2L$ (in Scheme 6.1), is the following:

$$-\frac{d[\mathbf{9e}]}{dt} = k_1[\mathbf{9e}] - \frac{k_{-1}[L]\{k_1[\mathbf{9e}] + k_{-2}[\mathbf{22}]\}}{k_2[L'] + k_{-1}[L]}$$

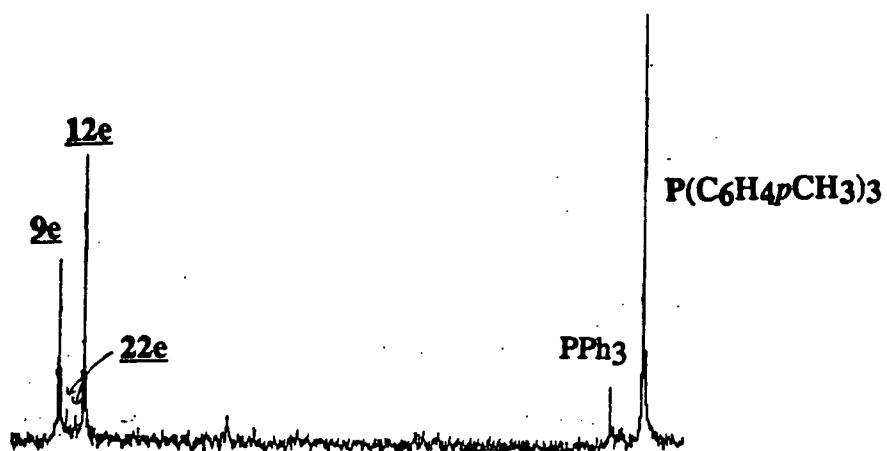
That reaction 6.1 goes to completion implies that the rate of the k_{-2} reaction is negligible (i.e. $k_{-2}[\mathbf{22}] \ll k_1[\mathbf{9e}]$), and thus if one assumes that $k_{-1}[L] \ll k_2[L']$ then the second term in the rate law is insignificant. This assumption appears to be valid during at least the first two half-lives if L' is present in large excess; this accounts for the observed *pseudo*-first order behaviour.

Reaction 6.2 must be significantly faster than reaction 6.1, because complex **22** never appears in large amounts (Fig. 6.3). The rate law for the proposed mechanism of reaction 6.2 (Scheme 6.1) is the following:

after 5 min.



26 min



49 min

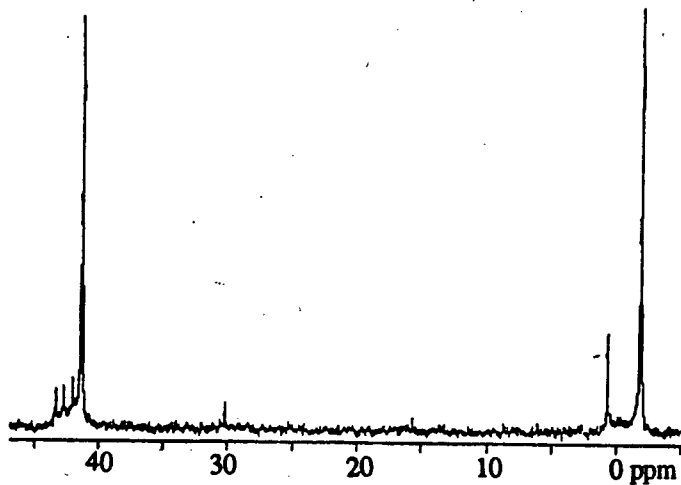


Fig. 6.1 $^{31}\text{P}\{^1\text{H}\}$ NMR spectra acquired during the reaction of *cct*-Ru(SCH₂Ph)(CO)₂(PPh₃)₂ (9e, 11 mM) with P(C₆H₄pCH₃)₃ (94 mM) in C₆D₆ at 45°C. Chemical shift scale is relative to PPh₃ in C₆D₆.

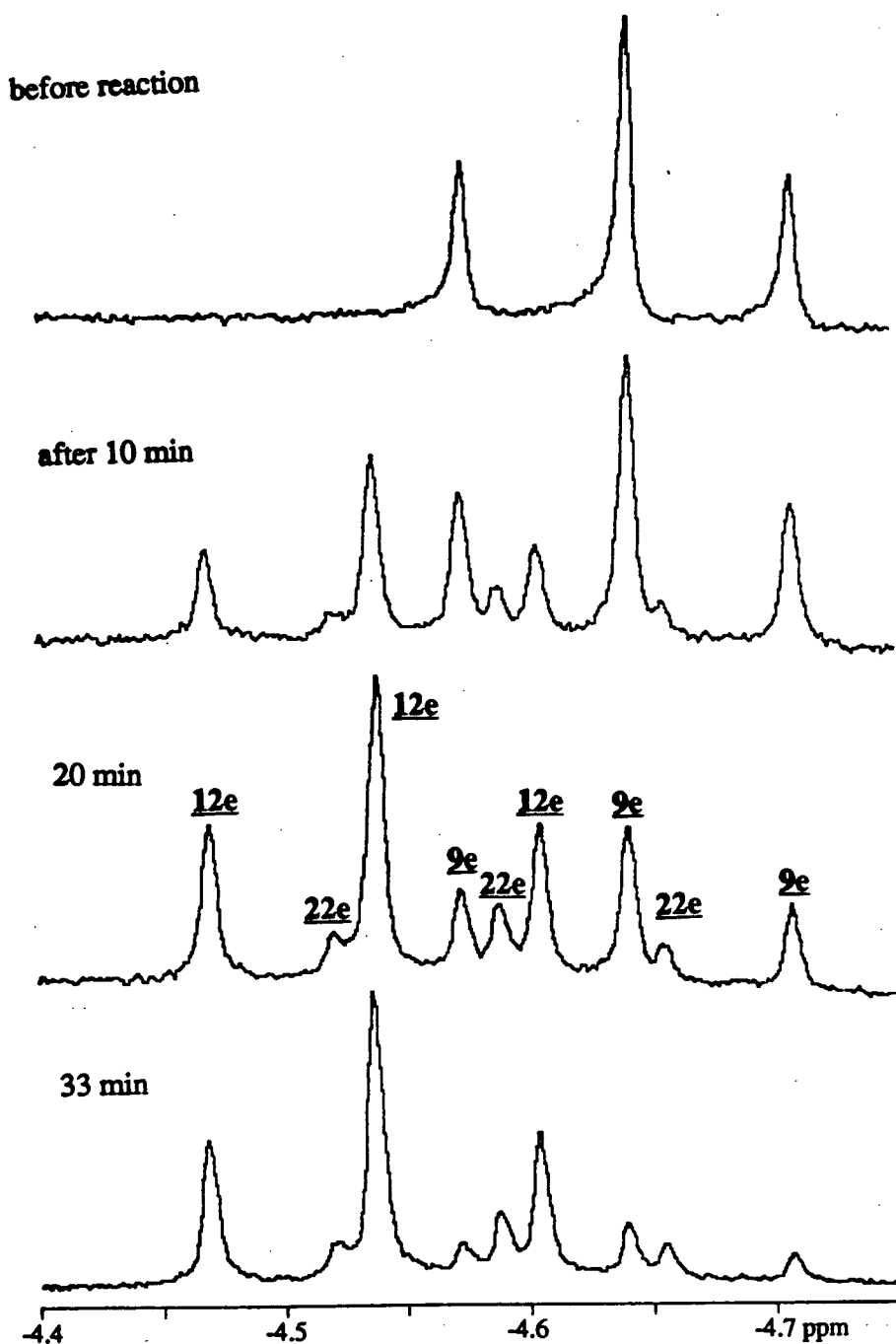


Fig. 6.2 ^1H NMR spectra (hydride region) acquired during the reaction of *cis*- $\text{RuH}(\text{SCH}_2\text{Ph})(\text{CO})_2(\text{PPh}_3)_2$ ($9e$, 11 mM) with $\text{P}(\text{C}_6\text{H}_4\text{pCH}_3)_3$ (94 mM) in C_6D_6 at 45°C .

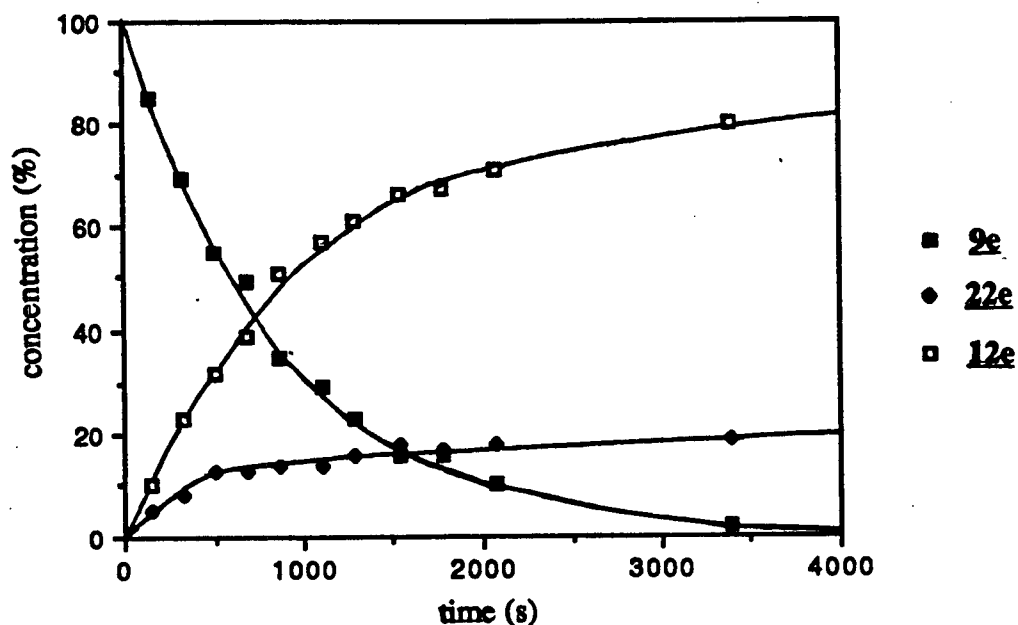


Fig. 6.3 Time dependence of the concentrations of observed complexes during the reaction of *cct*-RuH(SCH₂Ph)(CO)₂(PPh₃)₂ (**9e**, 12 mM) with P(C₆H₄*p*CH₃)₃ (120 mM) in C₆D₆ at 45°C.

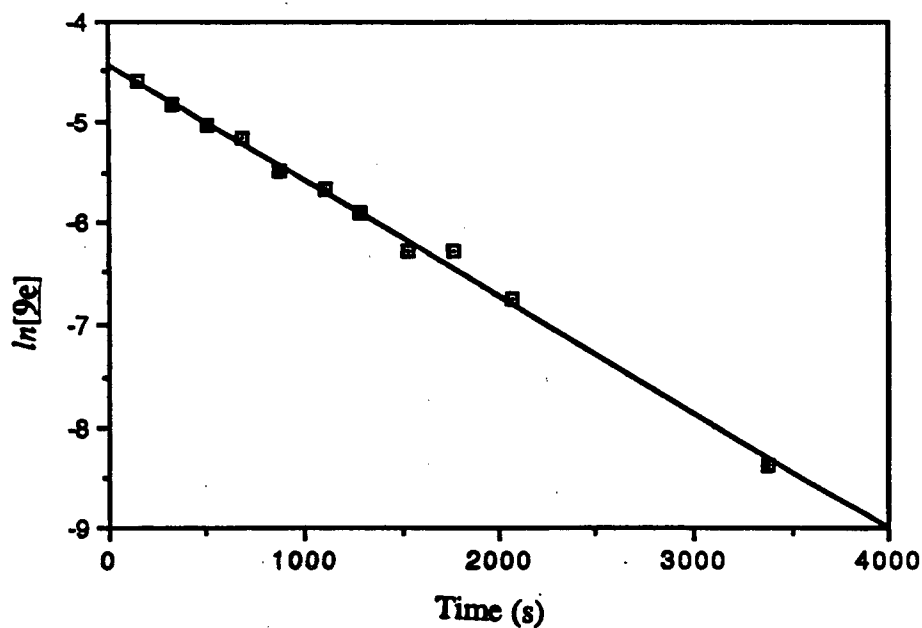
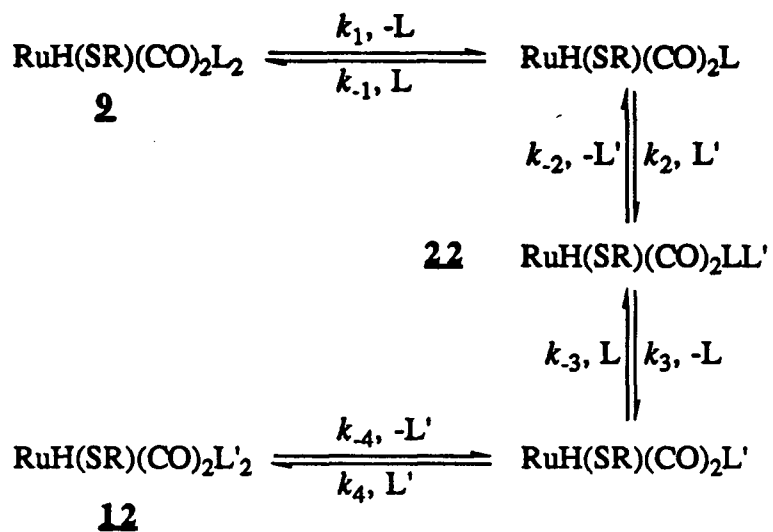


Fig. 6.4 Log plot of [9e] during the reaction of *cct*-RuH(SCH₂Ph)(CO)₂(PPh₃)₂ (**9e**, 12 mM) with P(C₆H₄*p*CH₃)₃ (120 mM) in C₆D₆ at 45°C.

Scheme 6.1 A proposed mechanism for the reaction of $\text{RuH}(\text{SR})(\text{CO})_2(\text{PPh}_3)_2$ with $\text{P}(\text{C}_6\text{H}_4\text{pCH}_3)_3$ ($\text{L}=\text{PPh}_3$, $\text{L}'=\text{P}(\text{C}_6\text{H}_4\text{pCH}_3)_3$).



$$\frac{d[12]}{dt} = \frac{k_4[L']\{k_3[22] + k_{-4}[12]\}}{k_4[L'] + k_{-3}[L]} - k_{-4}[12]$$

This rate law simplifies if one assumes that $k_4[L'] \gg k_{-3}[L]$ in the presence of excess L' .

$$\frac{d[12]}{dt} = k_3[22]$$

The value of k_3 could then be determined by plotting $d[12]/dt$ vs. $[22]$. The values of $d[12]/dt$ are easily determined from the tangents to the plot of $[12]$ against time (Fig. 6.3). The resulting plot should be a straight line of positive slope k_3 , if the assumption of a negligible back reaction ($k_{-3}[L]$) is correct. In fact, a decreasing trend is observed (Fig. 6.5), suggesting that the $k_{-3}[L]$ back reaction is significant. Because all back-reactions are negligible at the start of the reaction, an approximate value of k_3 can be obtained from the y-intercept of this plot. The value thus obtained (0.01 s^{-1}) shows that k_3 is an order of magnitude greater than k_1 .

If PPh_3 (L , 100 mM) is added to the reaction of $\underline{9e}$ (11 mM) with $\text{P}(\text{C}_6\text{H}_4\text{pCH}_3)_3$ (L' , 110 mM) at 45°C in C_6D_6 , a mixture of three complexes, $\underline{9}$, $\underline{22}$, and $\underline{12}$ is obtained (Fig. 6.6). Because reaction 6.1 does not go to completion, the back reaction must be significant under these conditions. It is not surprising, therefore, that *pseudo*-first order behaviour is not observed. The fact that the initial rate is unchanged suggests that $k_{-1}/k_2 \ll 1$.

p-Tolyl phosphine (L'), more basic than PPh_3 , may labilize the phosphine *trans* to it by increasing the electron density at the metal centre, thereby promoting formation of the activated complex *en route* from $\underline{22}$ to $\underline{12}$. The observation that k_3 is greater than k_1 suggests that reaction 6.2 may reach an equilibrium before reaction 6.1. This can be checked by plotting Q_1 and Q_2 against time for the experiment described above, in which both L and L' were present in excess, where:

$$Q_1 = \frac{[22][L]}{[9][L']}$$

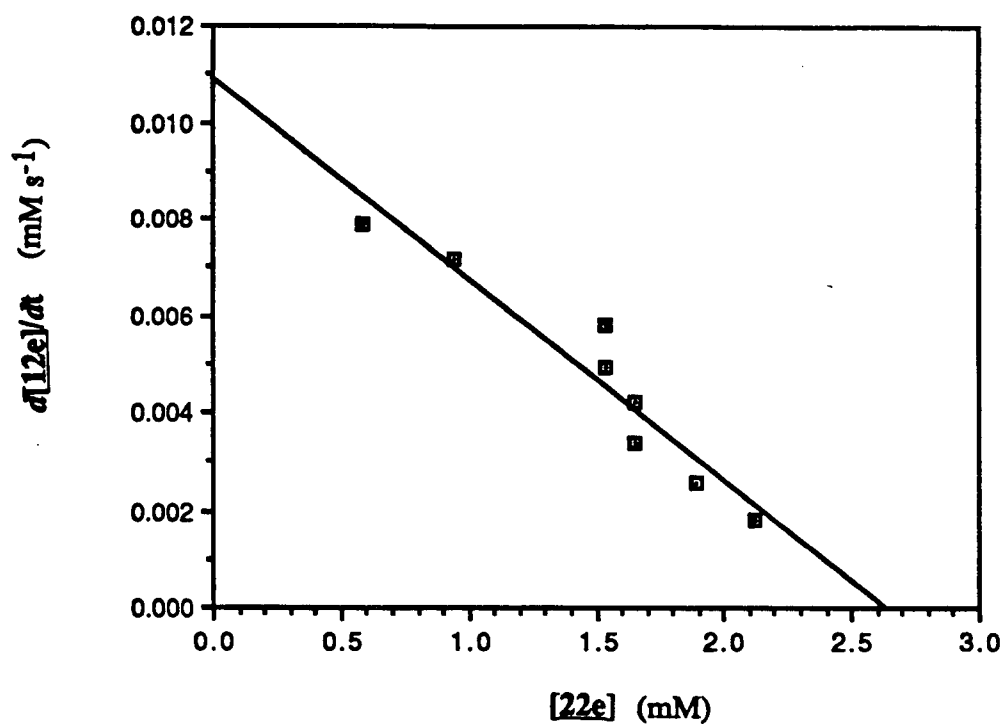


Fig. 6.5 The dependence of $d[12e]/dt$ on $[22e]$ during the reaction of *cis*- $\text{RuH}(\text{SCH}_2\text{Ph})(\text{CO})_2(\text{PPh}_3)_2$ (**9e**, 12 mM) with $\text{P}(\text{C}_6\text{H}_4\text{pCH}_3)_3$ (120 mM) in C_6D_6 at 45°C.

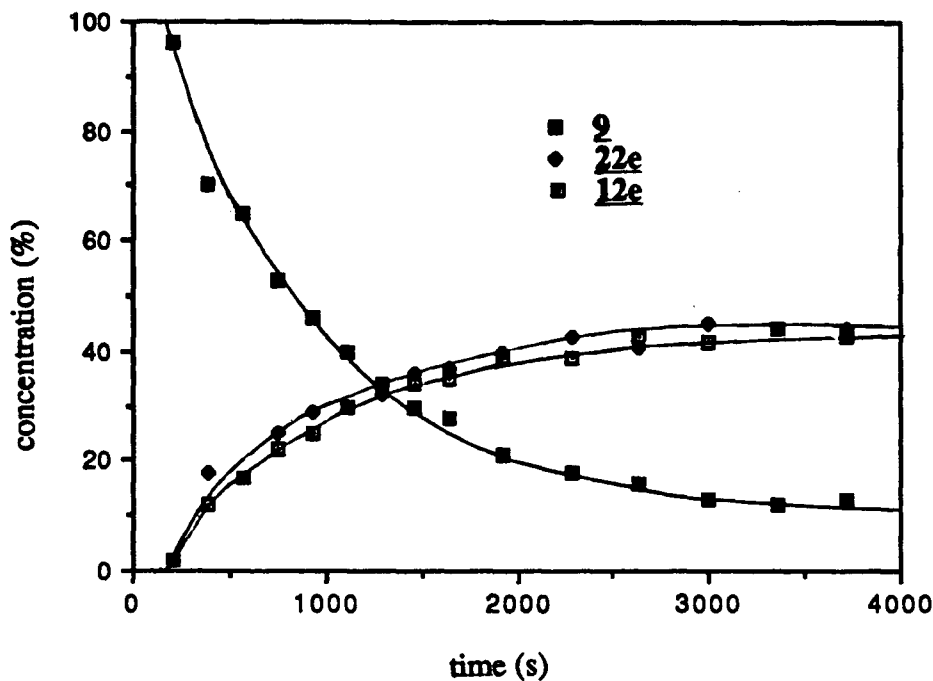


Fig. 6.6 Time dependence of the concentrations of observed complexes during the reaction of *cct*-RuH(SCH₂Ph)(CO)₂(PPh₃)₂ (**9e**, 11 mM) with P(C₆H₄*p*CH₃)₃ (110 mM) in the presence of PPh₃ (100 mM) in C₆D₆ at 45°C.

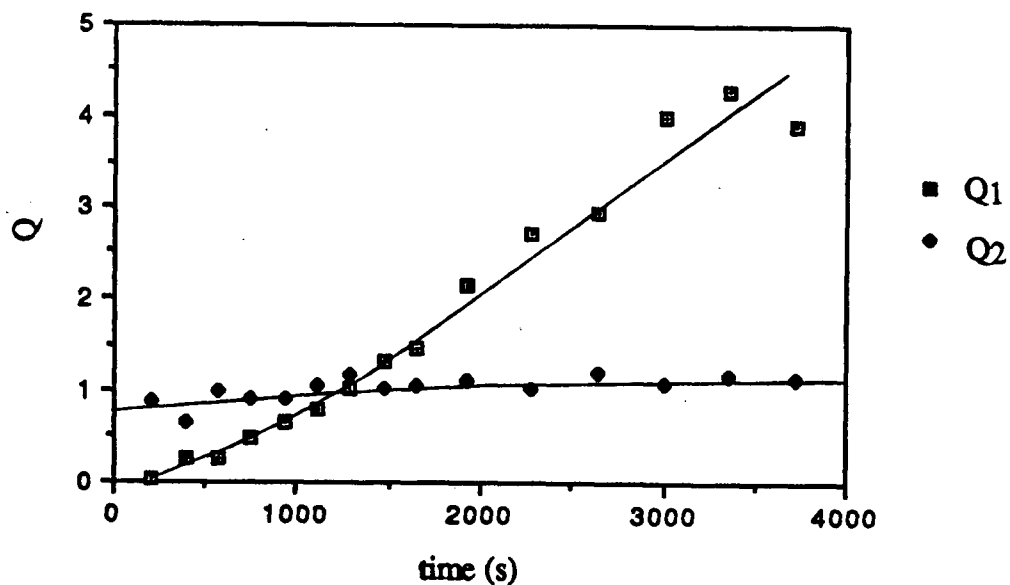
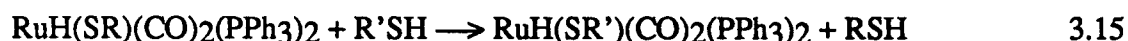


Fig. 6.7 Time dependence of Q1 and Q2 (defined in Section 6.1.1) during the reaction of RuH(SCH₂Ph)(CO)₂(PPh₃)₂ (**9e**, 11 mM) with P(C₆H₄*p*CH₃)₃ (110 mM) in the presence of PPh₃ (100 mM) in C₆D₆ at 45°C.

$$Q_2 = \frac{[12][L]}{[22][L']}$$

In fact, Q_1 varies over time (Fig. 6.7), while Q_2 settles quickly to a value of approximately 1.2. The equilibrium constants for reactions 6.1 and 6.2 are thus $K_1 > 4$ and $K_2 = 1.2$.

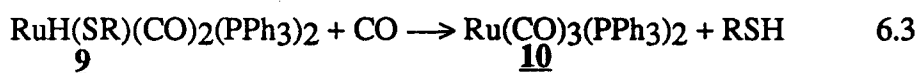
The rate of the exchange reaction of **9** with thiols (Section 3.5)



has the same simplified rate law and rate constant ($1.0 \times 10^{-3} \text{ s}^{-1}$ at 45°C in C_6D_6 , $\text{R}=\text{CH}_2\text{C}_6\text{H}_5$, $\text{R}'=\text{C}_6\text{H}_5$) as reaction 6.1, suggesting that the rate determining steps of the two reactions are the same.

6.1.2 CO

The reactions of several complexes of the series *cct*- $\text{RuH}(\text{SR})(\text{CO})_2(\text{PPh}_3)_2$ (**9**) with CO (1 atm) to give $\text{Ru}(\text{CO})_3(\text{PPh}_3)_2$



in THF at several temperatures was monitored by UV/vis. spectroscopy (Fig. 6.8). Under *pseudo*-first order conditions (1 atm CO) the *pseudo*-first order log plot is linear for 3 half-lives (Fig. 6.9). The observed rate constant is independent of the pressure of CO (760 to 6 torr for $\text{R}=\text{Et}$, at 26°C), but is dependent on the choice of thiolate group. The rate law and rate constants (all at 55°C) are as follows.

$$-\frac{d[\mathbf{9}]}{dt} = k[\mathbf{9}]$$

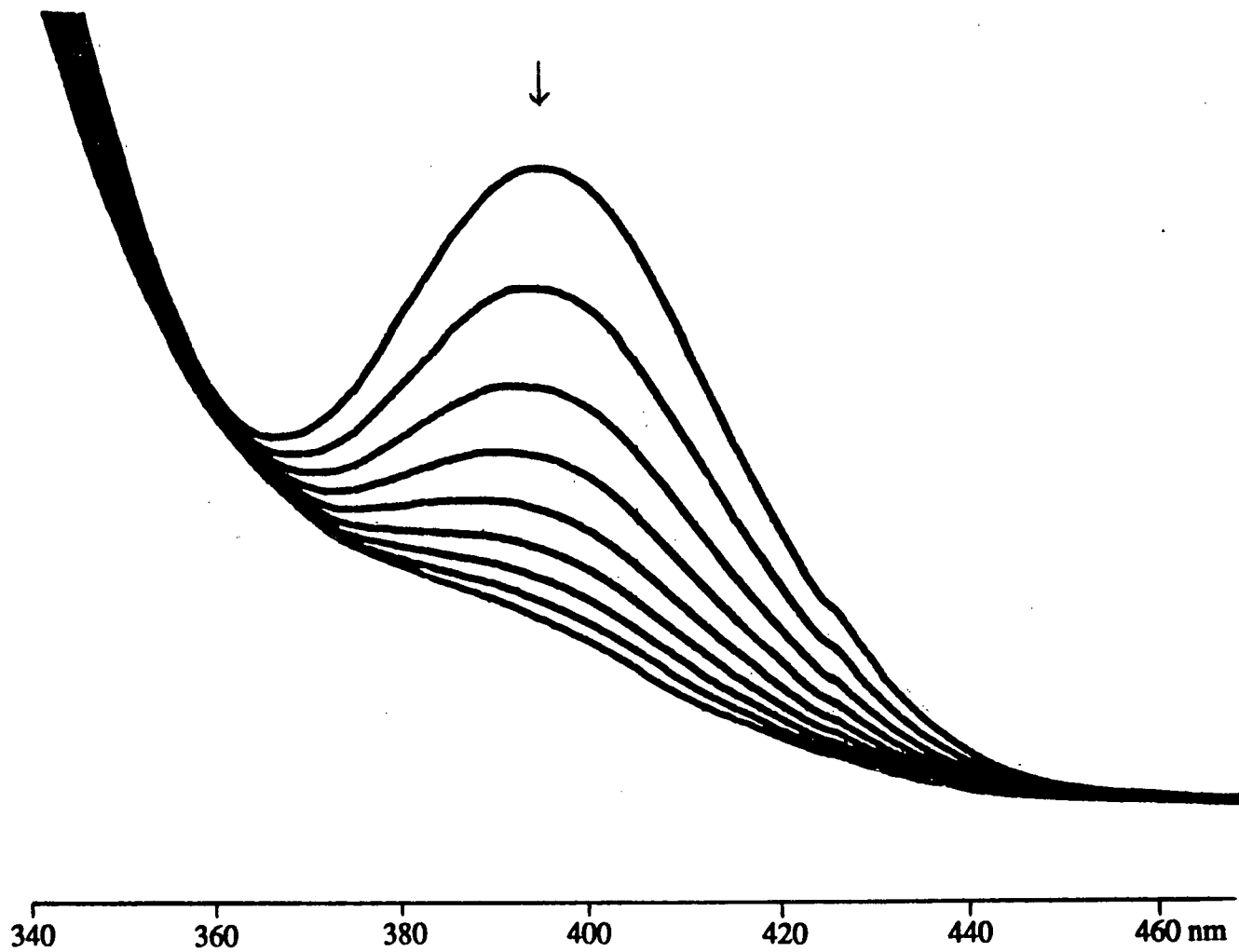


Fig. 6.8 UV/vis. spectra acquired every 900 s during the reaction of *cct*-RuH(SET)(CO)₂(PPh₃)₂ (0.9 mM) and CO (1 atm) in THF at 26°C.

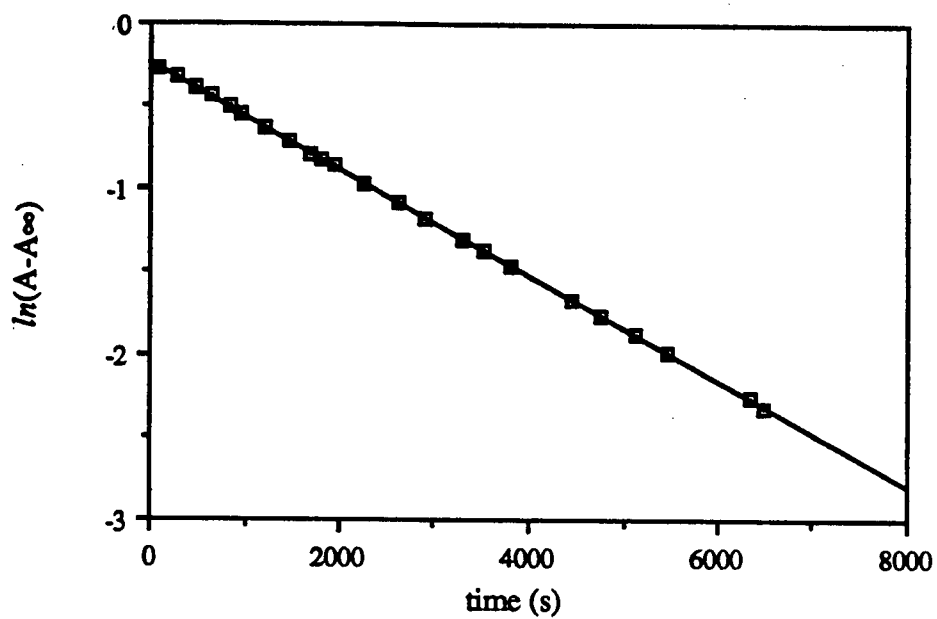
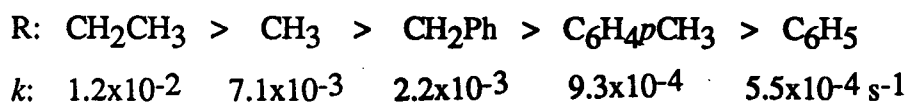


Fig. 6.9 Logarithmic plot of absorbance at 400 nm versus time for the reaction of *cct*-RuH(SET)(CO)₂(PPh₃)₂ (**9e**, 0.9 mM) and CO (1 atm) in THF at 26.5°C.



The temperature dependence of these rate constants has also been determined (Fig. 6.10). Because the rate law and rate constant of the reaction of **9d** with CO (reaction 6.3, R=Et) extrapolated to 22°C ($1.8 \times 10^{-4} \text{ s}^{-1}$) are the same (within the experimental error) as those for the reaction of **9d** with PhSH (reaction 3.12, Section 3.5) at the same temperature ($1.9 \times 10^{-4} \text{ s}^{-1}$), then the two reactions most likely proceed by analogous mechanisms. As explained in Sections 6.1.1 and 3.5, these mechanisms probably involve loss of a phosphine ligand as the first step. The subsequent steps of the mechanism of reaction 6.3 are co-ordination of CO and elimination of thiol, but the order in which they occur is not known. The path which leads to a 3-coordinate species (elimination of thiol before coordination of CO) seems less likely. The proposed mechanism is shown in Scheme 6.2.

Attempts to test the effect of a large excess of PPh₃ on the rate of reaction 6.3 were hindered by the occurrence of a side reaction of **9** with PPh₃ (Section 6.1.3).

The enthalpies of activation are $120 \pm 20 \text{ kJ/mol}$ for **9b** (R=C₆H₄pCH₃) and $100 \pm 10 \text{ kJ mol}^{-1}$ for **9d** (R=C₂H₅), consistent with the suggestion (Section 6.1.1) that increased electron density at the metal centre increases the rate of reaction by stabilizing the activated complex $\{\text{RuH}(\text{SR})(\text{CO})_2(\text{PPh}_3)\}^\ddagger$. Ethanethiolate, a more basic ligand than thiophenolate, would increase the electron density.

The large error inherent in the calculation of the entropy of activation (40 ± 40 and $20 \pm 25 \text{ J mol}^{-1} \text{ K}^{-1}$ for **9b** and **9d**, respectively) precludes any conclusion about the possible effect of the nature of the thiolate group on ΔS^\ddagger . However, it is clear that the entropy of activation is positive, as expected for a dissociative mechanism. The enthalpy term is mainly responsible for the difference in rates between the reactions of **8b** (R=C₆H₄pCH₃) and **8d** (CH₂CH₃) at this temperature.

It has now been established that reactions 6.1, 6.3, and 3.15 all proceed via the same rate determining step, suggested to be the initial dissociation of PPh₃ from the Ru centre. Further

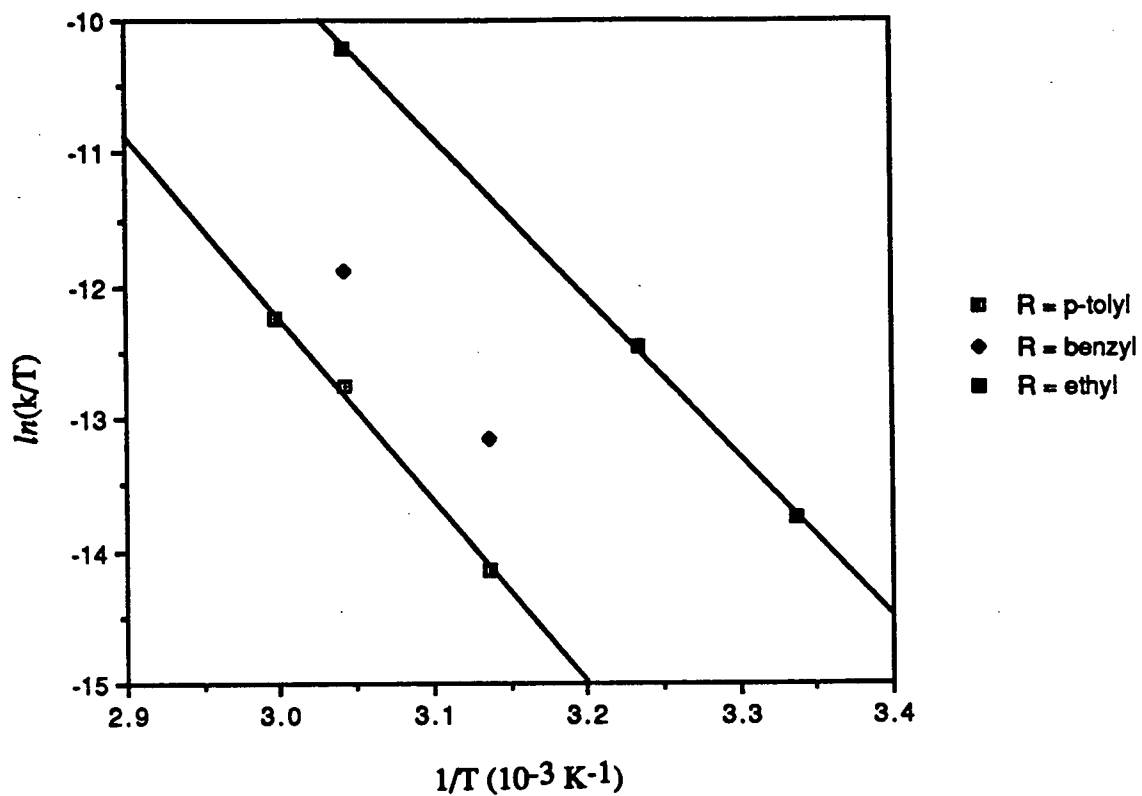
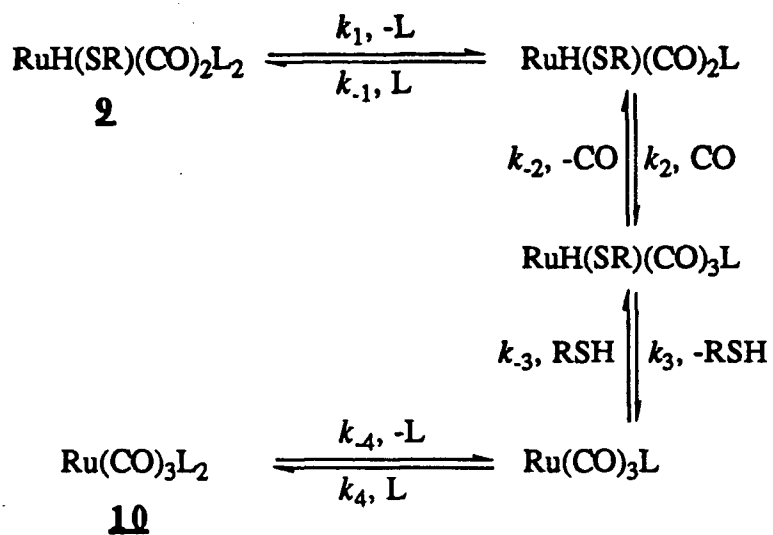


Fig. 6.10 Eyring plot for the reactions of *cct*- $\text{RuH}(\text{SR})(\text{CO})_2(\text{PPh}_3)_2$ (**9**) with CO (1 atm) in THF, where R = $\text{C}_6\text{H}_4\text{CH}_3$ (**9b**), $\text{CH}_2\text{C}_6\text{H}_5$ (**9c**), or CH_2CH_3 (**9d**).

Scheme 6.2 A proposed mechanism for the reaction of $\text{RuH}(\text{SR})(\text{CO})_2(\text{PPh}_3)_2$ with CO ($\text{L} = \text{PPh}_3$).

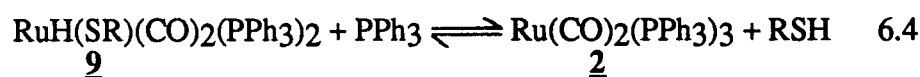


evidence for this is the magnitude of the effect on the rate of reaction 6.1 when the phosphine *trans* to the dissociating ligand has *p*-methyl substituents; the rate is increased ten-fold. This strong an effect is consistent with a *trans* effect, rather than a *cis* effect. That is, if the rate determining step were initial reductive elimination of thiol, then the effect of a change in the phosphine in the *cis* position would not be as large as that observed. The evidence, therefore, supports a rate determining step of PPh₃ dissociation. However, *cct*-RuH(SC₆H₄*p*CH₃)(CO)₂(PPh₃)₂ reacts 1.7 times faster with CO than does *cct*-RuH(SC₆H₅)(CO)₂(PPh₃)₂. If the rate-determining step were initial dissociation of PPh₃, then this would constitute a *cis*-effect. It is not possible to evaluate whether 1.7 is a reasonable value because the magnitudes of the *cis*-effects of thiolate ligands on the rate of elimination of phosphines have not been previously reported. If the first and rate-determining step is reductive elimination of thiol, then a large rate difference is expected. The argument for initial phosphine loss is considered stronger because the *trans*-effect of the phosphine is more pronounced, and because the mechanisms of the reactions of **9** are expected to be analogous to those of **14**. In the latter system (Section 3.8 and 6.2.2), the evidence for initial phosphine loss includes kinetic measurements of the inhibition by added PPh₃ of the reaction of **14** with thiols.

Reaction 6.3 is the reverse of reaction 3.19 (Section 3.9), the kinetics and mechanism of which are not known.

6.1.3 PPh₃

A large excess of PPh₃ in THF at room temperature converts *cct*-RuH(SEt)(CO)₂(PPh₃)₂ (**9d**) to Ru(CO)₂(PPh₃)₃ (**2**, 26 % conversion after 4 h, 100 % after 4 days).



This reaction parallels reaction 3.12 (Section 3.5) in that HCl acts in the same manner as a thiol. As shown in Section 3.5, the most acidic thiols react preferentially, and thus the high reactivity of HCl seems reasonable. Reaction 6.6 is highly favourable, and the reverse reaction would require a very large excess of thiol (or in a more practical sense an excess of NaSR, *cf.* Section 5.4).

The products of the reaction of *cct*-RuH(SC₆H₅)(CO)₂(PPh₃)₂ (3.3 μmol) in C₆D₆ (0.6 mL) with HBF₄/H₂O (50 μL, 300 μmol) at room temperature have not been identified. However, the ¹H (Fig. 6.11) and ³¹P{¹H} NMR spectra are consistent with a major product of the formula *cct*-RuH(X)(CO)₂(PPh₃)₂ (where X is unknown). A broad peak at 1.5 ppm in the ¹H NMR spectrum has the correct integral and chemical shift²¹⁵ for the aquo ligand of *cct*-[RuH(H₂O)(CO)₂(PPh₃)₂]⁺, suggesting that this is the major product. The same product is not observed when HBF₄/Et₂O is used as the protonating agent. Instead, a large number of unassigned peaks is observed in the ³¹P{¹H} NMR spectrum.

6.1.6 CD₃OD

The hydrido and mercapto hydrogen atoms of *cct*-RuH(SH)(CO)₂(PPh₃)₂ (**9a**) undergo deuterium exchange with 4% v/v CD₃OD in C₆D₆ (Fig. 6.12).



The first-order rate constants, at 19°C, are 4.1 × 10⁻⁵ and 2.9 × 10⁻⁴ s⁻¹, respectively (Fig. 6.13). Of the two hydrogens, the mercapto hydrogen exchanges more rapidly, suggesting that it is exchanging intermolecularly with the D⁺ ions in the solution, possibly with the following mechanism:

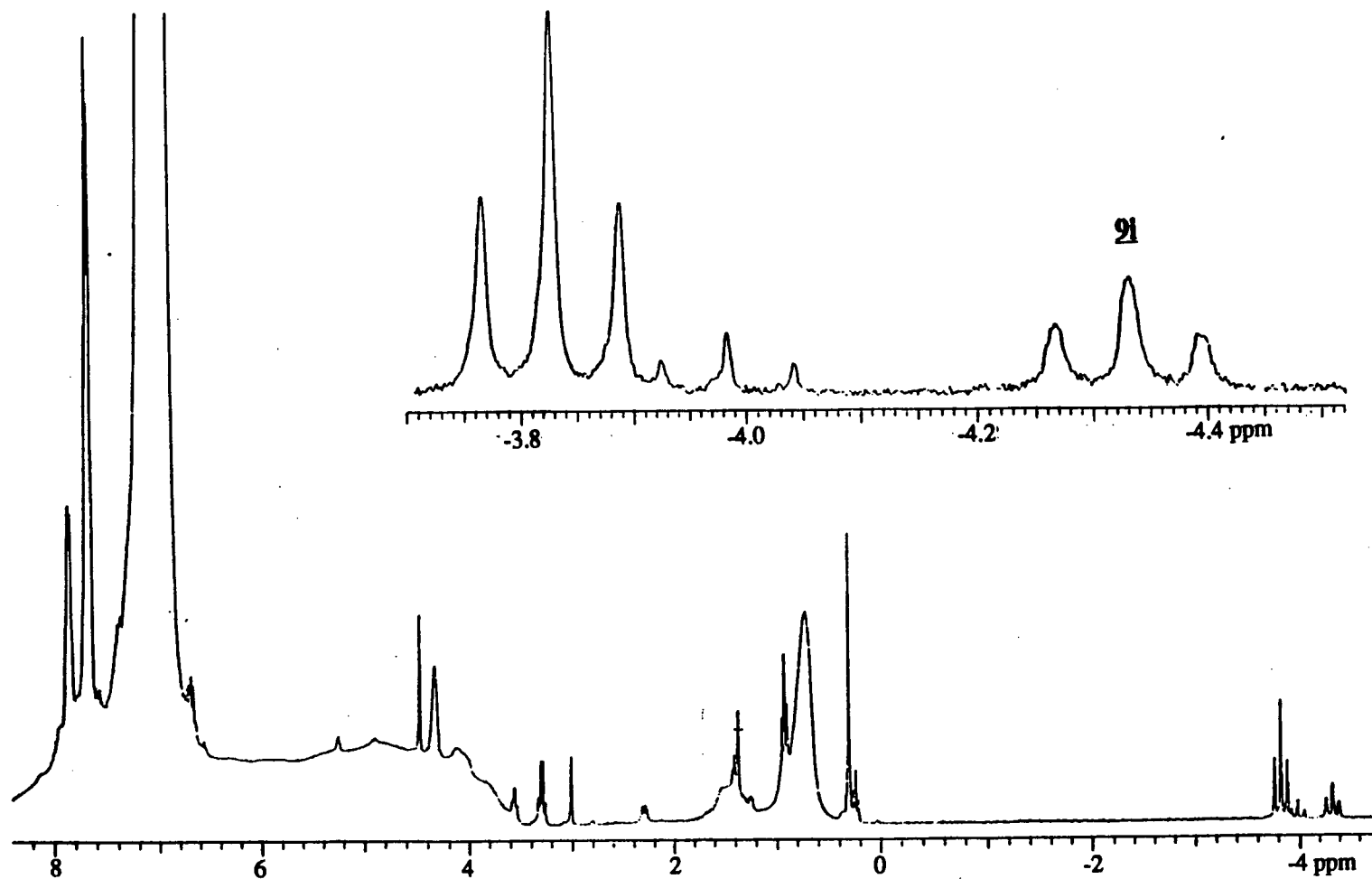


Fig. 6.11 ^1H NMR spectrum acquired 30 min after the start of the reaction of *cct*- $\text{RuH}(\text{SC}_6\text{H}_5)(\text{CO})_2(\text{PPh}_3)_2$ (**9i**, 5.6 mM) with excess $\text{HBF}_4/\text{H}_2\text{O}$ (50 μL) in C_6D_6 at room temperature.

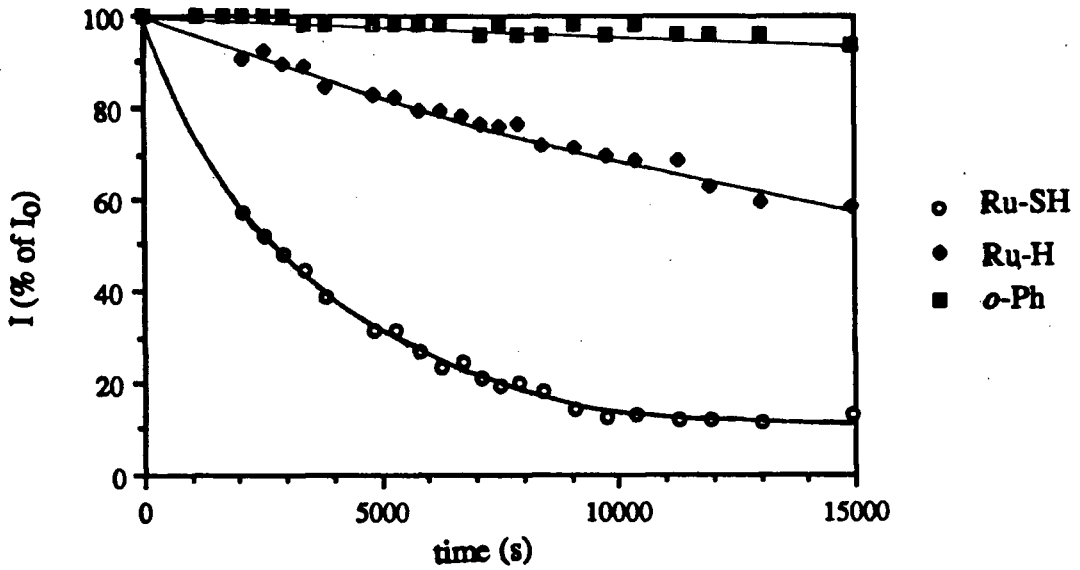


Fig. 6.12 The time dependence of the intensity (I) of the ^1H NMR signals due to *cct*-RuH(SH)(CO)₂(PPh₃)₂ (4.4 mM) in 4% v/v CD₃OD/C₆D₆ at 19°C.

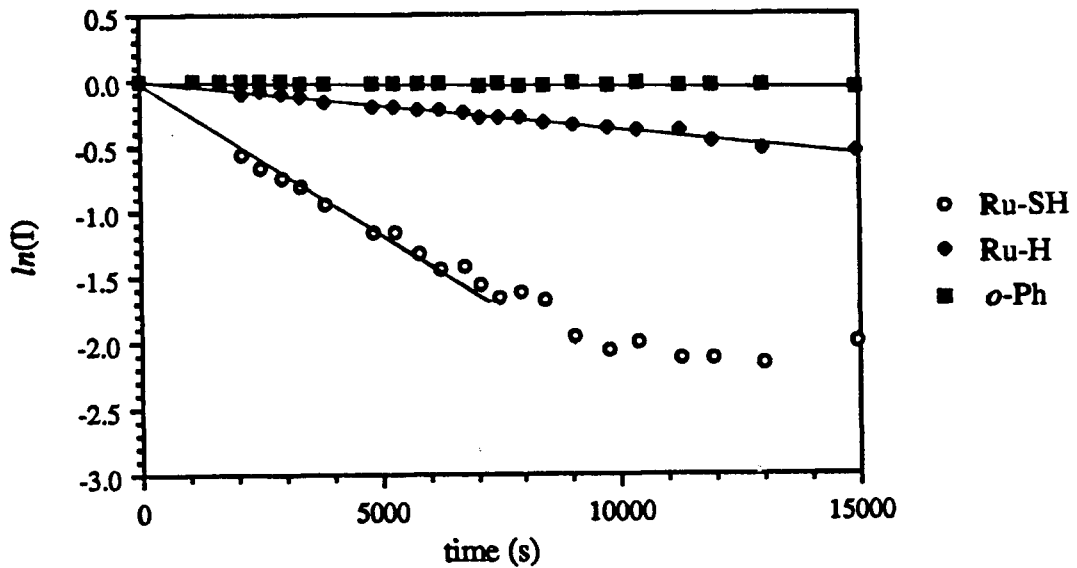
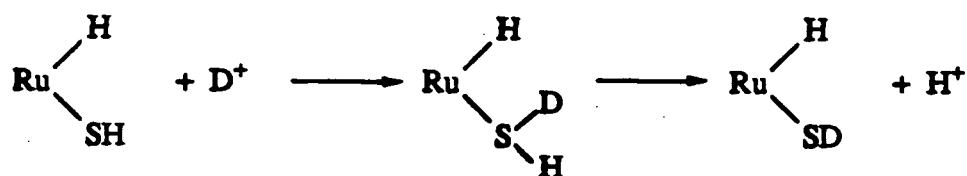
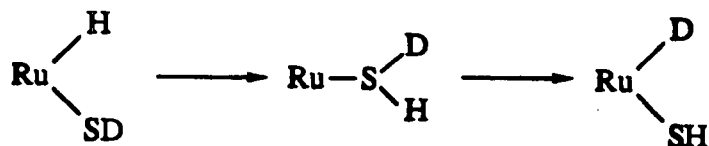


Fig. 6.13 The log plot of the intensity of the ^1H NMR signals due to *cct*-RuH(SH)(CO)₂(PPh₃)₂ (4.4 mM) in 4% v/v CD₃OD/C₆D₆ at 19°C.



The mercapto hydrogens of *cis*-Ru(SH)₂(CO)₂(PPh₃)₂ (**14a**) also exchange with 4% CD₃OD in CD₂Cl₂ (Section 6.2.4), showing that the exchange does not require a hydride *cis* to the mercapto group. The hydrido hydrogen of **9a** is either exchanging intermolecularly or intramolecularly. The intermolecular exchange process is unlikely, because *cis*-RuH₂(CO)₂(PPh₃)₂ shows no exchange in 4% CD₃OD in C₆D₆ even after 2 h (Section 3.4). The intramolecular exchange could take place in the following manner:



Osakada *et al.*³⁰⁴ have reported on the H/D exchange of the hydrido and mercapto hydrogens of RuH(SH)(PPh₃)₃ with 4% CD₃OD in CD₂Cl₂. It appears from Figure 2 of their report that the rate of the exchange of the hydrido hydrogen is faster than that of the mercapto hydrogen. However, the authors of the report concluded the reverse, and therefore, that the mercapto hydrogen alone was exchanging with the CD₃OD, and the deuteration at the hydridic site was *via* intramolecular exchange. They cited the lack of H/D exchange of the complexes RuH(SPh)(PPh₃)₃ and RuH(Cl)(PPh₃)₃, and the observation of intramolecular exchange in PtH(SH)(PPh₃)₂ by Ugo *et al.*⁸² The conclusions in the RuH(SH)(PPh₃)₃ system are therefore analogous to those in the *cis*-RuH(SH)(CO)₂(PPh₃)₂ system.

The ¹H NMR spectral data (Fig. 6.12) also show a slight decrease in the intensity of the *o*-phenyl proton signal, a phenomenon not observed with the *m*- and *p*-phenyl signals. The mechanism by which *o*-hydrogen exchange could occur is not known for this system.

6.2 THE REACTIONS OF *cct*-Ru(SR)₂(CO)₂(PPh₃)₂ (**14**)

All of the observations of the reactivity of these bis-thiolate complexes (**14**) toward H₂, thiols, and phosphines suggest that the reactivity of **14** and associated mechanisms are similar to those of the hydrido-thiolato complexes (**9**). The lability of the phosphines in **14** has already been noted (Sections 3.8 and 5.2). A major difference in reactivity between species of types **9** and **14** is the instability of solutions of **14** (but not **14a**) in solution .

6.2.1 Light

Tetrahydrofuran solutions of *cct*-Ru(SC₆H₄pCH₃)₂(CO)₂(PPh₃)₂ (**14b**) under Ar, when exposed to light at 430 nm in the UV/vis. spectrometer exhibit a changing spectrum with an isosbestic point at 395±2 nm (Fig. 6.14). Unfortunately, the products have not been identified unambiguously, with the exception of PPh₃. The presence of added water or O₂ (1 atm) had no effect on the spectral changes, including the isosbestic wavelength.

Two samples of **14b** (4.4 mM in C₆D₆) in NMR tubes at room temperature were analyzed by ³¹P{¹H} NMR spectroscopy after 8 h of darkness for one sample and 8 h under a Hanovia UV lamp for the other. Both samples were exposed to room light immediately before and during the NMR spectrum acquisition. The amount of unreacted starting material remaining in the former "dark" sample (70 %) compared to the latter (2 %) shows that the reaction being observed is promoted by exposure to light.

In attempts to identify the products of this reaction, a FAB mass spectrum was acquired of the solid product obtained from one such reaction using a THF solution under a Hanovia lamp for 90 minutes (Fig. 6.15). The strong peak at *m/z* = 1149 (±5) must represent a fragment containing at least two Ru atoms, unless it is Ru(PPh₃)₄. The match between the observed and predicted isotopic patterns is poor for Ru(PPh₃)₄, but fair for two Ru₂ and one Ru₃ complexes (Fig. 6.16).

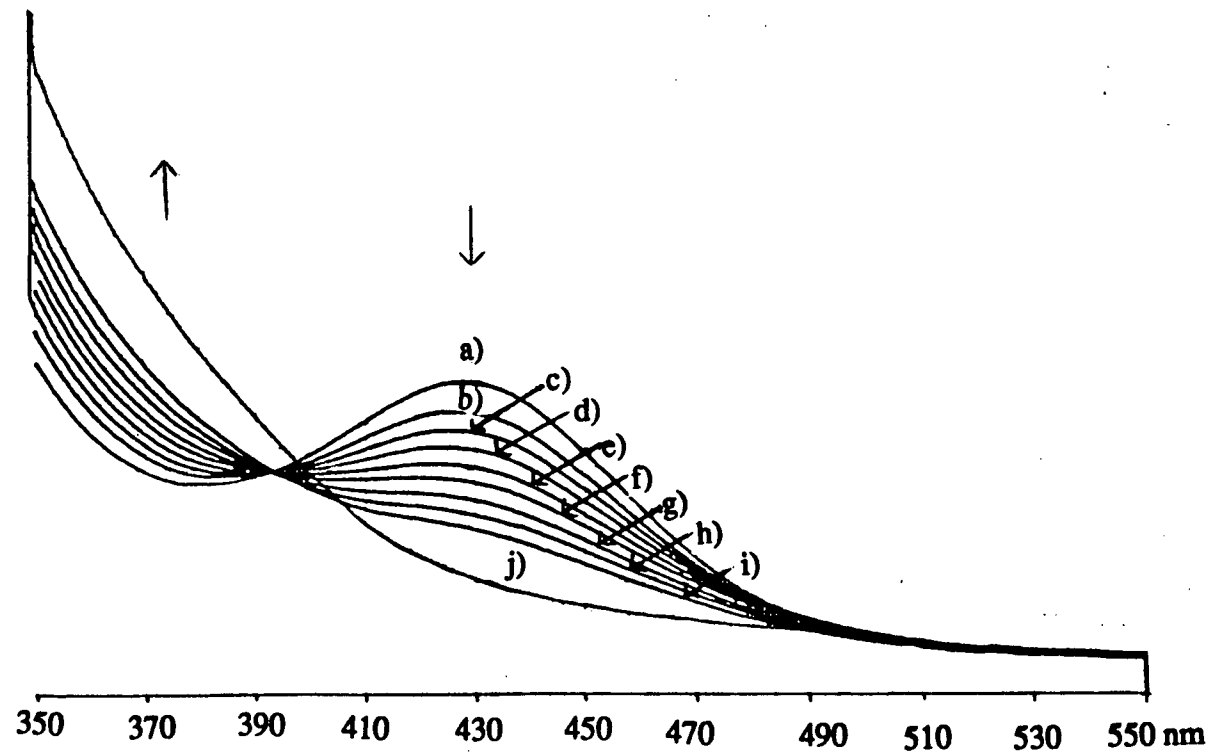


Fig. 6.14 UV/vis. absorbance spectra of a THF solution of $cct\text{-Ru}(\text{SC}_6\text{H}_4p\text{CH}_3)_2(\text{CO})_2(\text{PPh}_3)_2$ (0.32 mM) at 25°C being irradiated at 430 nm (between spectral acquisitions), after a) 50, b) 300, c) 600, d) 1,200, e) 2,100, f) 3,300, g) 5,400, h) 8,000, i) 13,000 and j) 240,000 s.

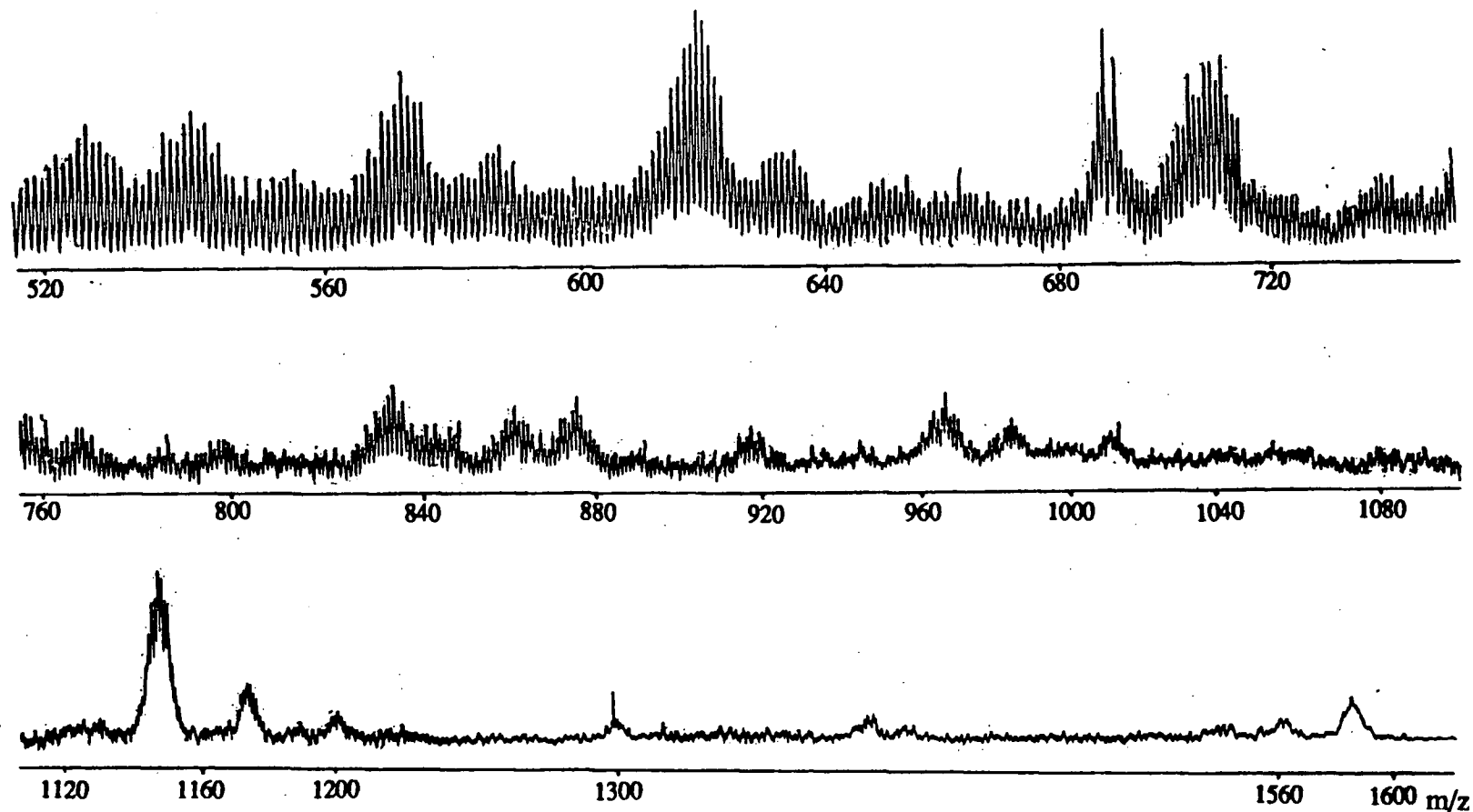


Fig. 6.15 FAB Mass Spectrum of the solid residue from a THF solution of *cct*-Ru(SC₆H₄pCH₃)₂(CO)₂(PPh₃)₂ irradiated for 90 min under a Hanovia lamp.

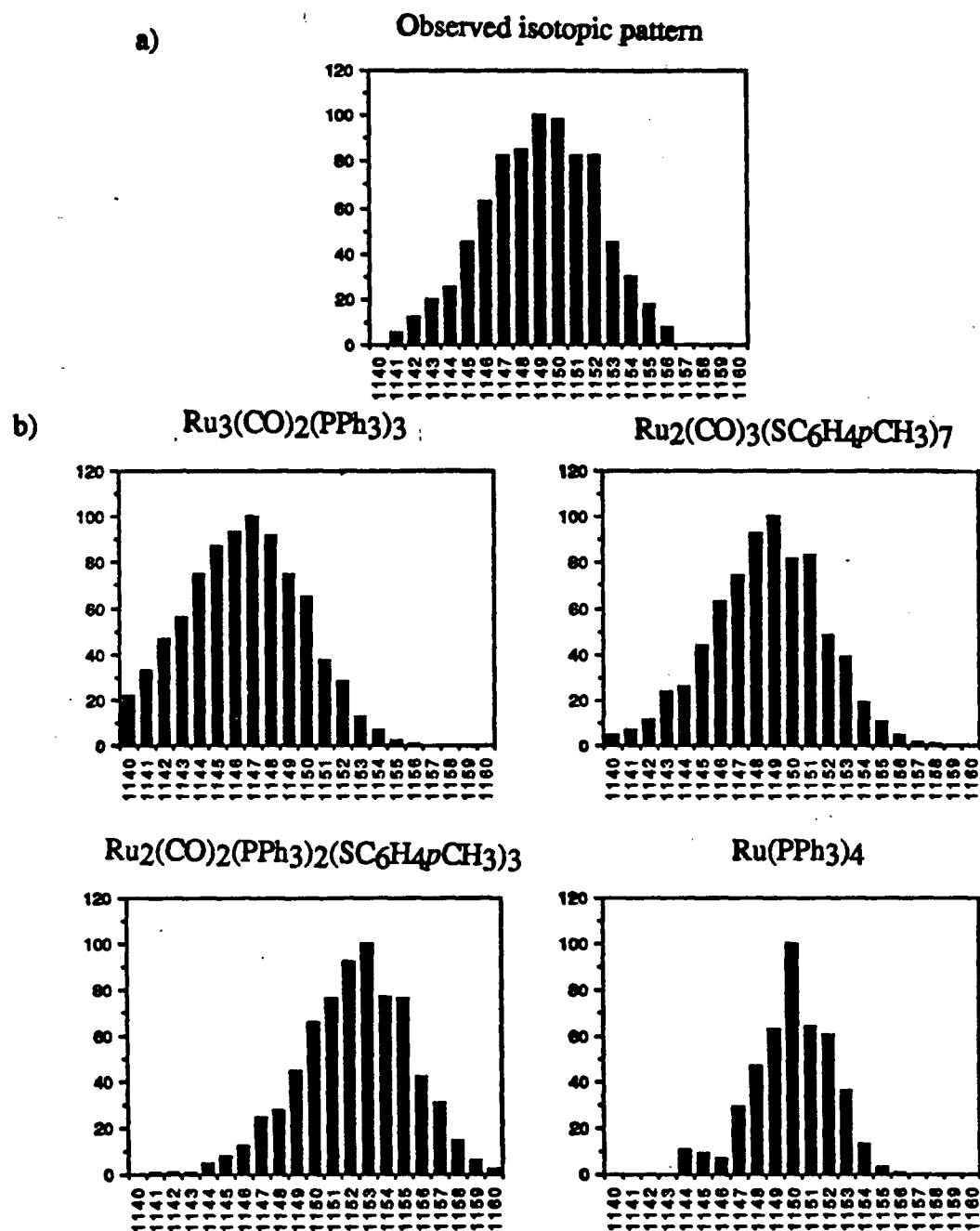
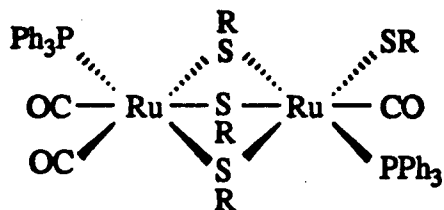


Fig. 6.16 a) Observed isotopic pattern for the fragment $m/z = 1149 \pm 5$, and b) the predicted isotopic patterns for four possible formulations for the fragment.

If the suggested fragmentation trees (shown in Scheme 6.3) are correct, then the most likely formula for the fragment at $m/z = 1149$ ($\text{Ru}_2(\text{SC}_6\text{H}_4p\text{CH}_3)_3(\text{CO})_2(\text{PPh}_3)_2$) suggests that the unfragmented molecule could be $\text{Ru}_2(\text{SC}_6\text{H}_4p\text{CH}_3)_4(\text{CO})_3(\text{PPh}_3)_2$ ($m/z = 1300$).



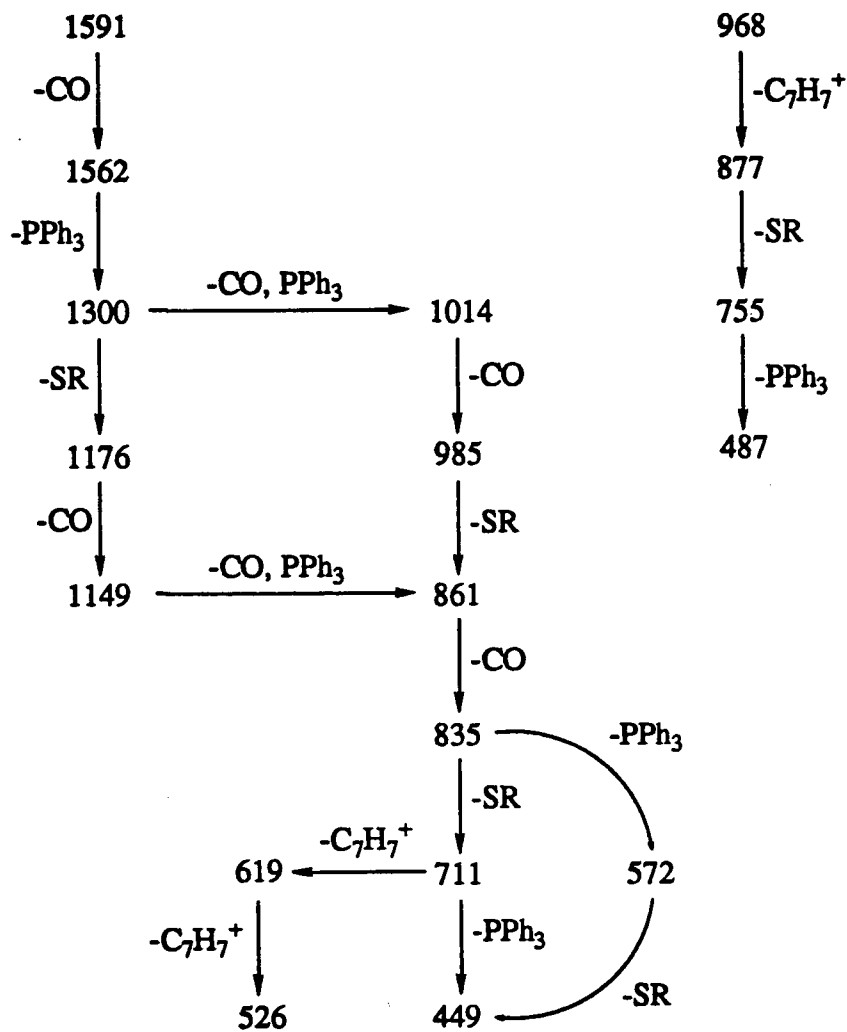
If this were the case, however, then the suggested connections in Scheme 6.3 between the peak at 1300 and the peaks at 1562 and 1591 would have to be incorrect.

The suggested triply thiolate-bridged complex would have two singlet peaks in the $^{31}\text{P}\{^1\text{H}\}$ NMR spectrum and three $\nu(\text{CO})$ bands in the IR spectrum. The $^{31}\text{P}\{^1\text{H}\}$ NMR spectrum of the sample submitted for the FAB/mass spectroscopy contains several peaks, including two at 32.84 and 42.84 ppm of roughly equal intensity. The same two peaks were observed in the $^{31}\text{P}\{^1\text{H}\}$ NMR spectra of isolated product mixtures from many similar reactions. The IR spectrum contains three $\nu(\text{CO})$ bands at frequencies (2034, 1977, and 1941) different from those of *cct*- $\text{Ru}(\text{SC}_6\text{H}_4p\text{CH}_3)_2(\text{CO})_2(\text{PPh}_3)_2$ (2028, 1968 cm^{-1}). It is not certain whether the three $\nu(\text{CO})$ bands are due to the same complex which gives rise to the NMR and FAB/MS signals already discussed.

Precedents for the triply-bridged type of complex include $[(\text{PMe}_2\text{Ph})_3\text{Ru}(\mu\text{SMe})_3\text{Ru}(\text{PMe}_2\text{Ph})_3]^+^{305}$ and $[(\text{CO})_3\text{Fe}(\mu\text{SMe})_3\text{Fe}(\text{CO})_3]^+^{306}$ while several of the series $\text{L}_3\text{Ru}(\mu\text{Cl})_3\text{Ru}(\text{Cl})\text{L}_2^{234,307}$ have been reported. In addition, $[(\text{CO})_2(\text{PPh}_3)\text{Ru}(\mu\text{SEt})_3\text{Na}(\text{THF})]_2$ (described in Section 5.3) has a similar structure and is formed *via* a similar *cct*- $\text{Ru}(\text{SR})_2(\text{CO})_2(\text{PPh}_3)_2$ precursor (**14d**).

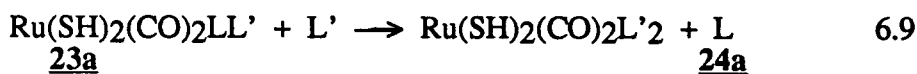
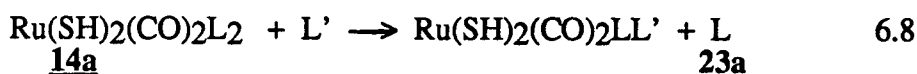
In summary, the products of the light-induced decomposition reaction of *cct*- $\text{Ru}(\text{SR})_2(\text{CO})_2(\text{PPh}_3)_2$ cannot be identified with certainty, beyond the fact that at least one of them contains two or more Ru atoms. A possible formulation for one of the products is suggested.

Scheme 6.3 Suggested fragmentation trees for the FAB mass spectrum of the products from the light-induced decomposition of *cct*-Ru(SC₆H₄pCH₃)₂(CO)₂(PPh₃)₂ (**14b**).

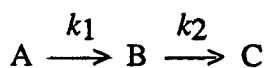


6.2.2 P(C₆H₄pCH₃)₃

The complex *cct*-Ru(SH)₂(CO)₂(PPh₃)₂ (**14a**) reacts with P(C₆H₄pCH₃)₃ in C₆D₆ at 25°C to produce two previously unknown complexes of structures similar to **14a**, the NMR data (Figs. 6.17 and 6.18) being consistent with the following reactions (L=PPh₃, L'=P(C₆H₄pCH₃)₃, all complexes *cct*):



The rates of these sequential reactions were followed by ¹H NMR spectroscopy (Figs. 6.18 and 6.19). The observed concentrations match exactly those predicted for the system



for over 4 half-lives of the first reaction (with $k_1 = 6 \times 10^{-4}$ and $k_2 = 5 \times 10^{-4} \text{ s}^{-1}$ at 25°C). This shows that in contrast to the mechanism of the reaction of the phosphine with a hydrido-thiolato analogue described in Section 6.1.1 (reactions 6.1 and 6.2), the rates of the reverse reactions shown in equations 6.8 and 6.9 are negligible for at least four half-lives.

The complex *cct*-Ru(SC₆H₄pCH₃)₂(CO)₂(PPh₃)₂ (**14b**) reacts much more quickly than **14a** with L', giving complete conversion to a new product of structure similar to **24a** by the time the first NMR spectrum can be taken, 3 minutes after the start of the reaction. The new complex is presumably *cct*-Ru(SC₆H₄pCH₃)₂(CO)₂{P(C₆H₄pCH₃)₃}₂ (**24b**). The difference in rates suggests that the phosphines of **14b** must be considerably more labile than those of **14a**. This is consistent with the difference in rates of the reactions of **14a** and **14b** with thiols (Section 3.8).

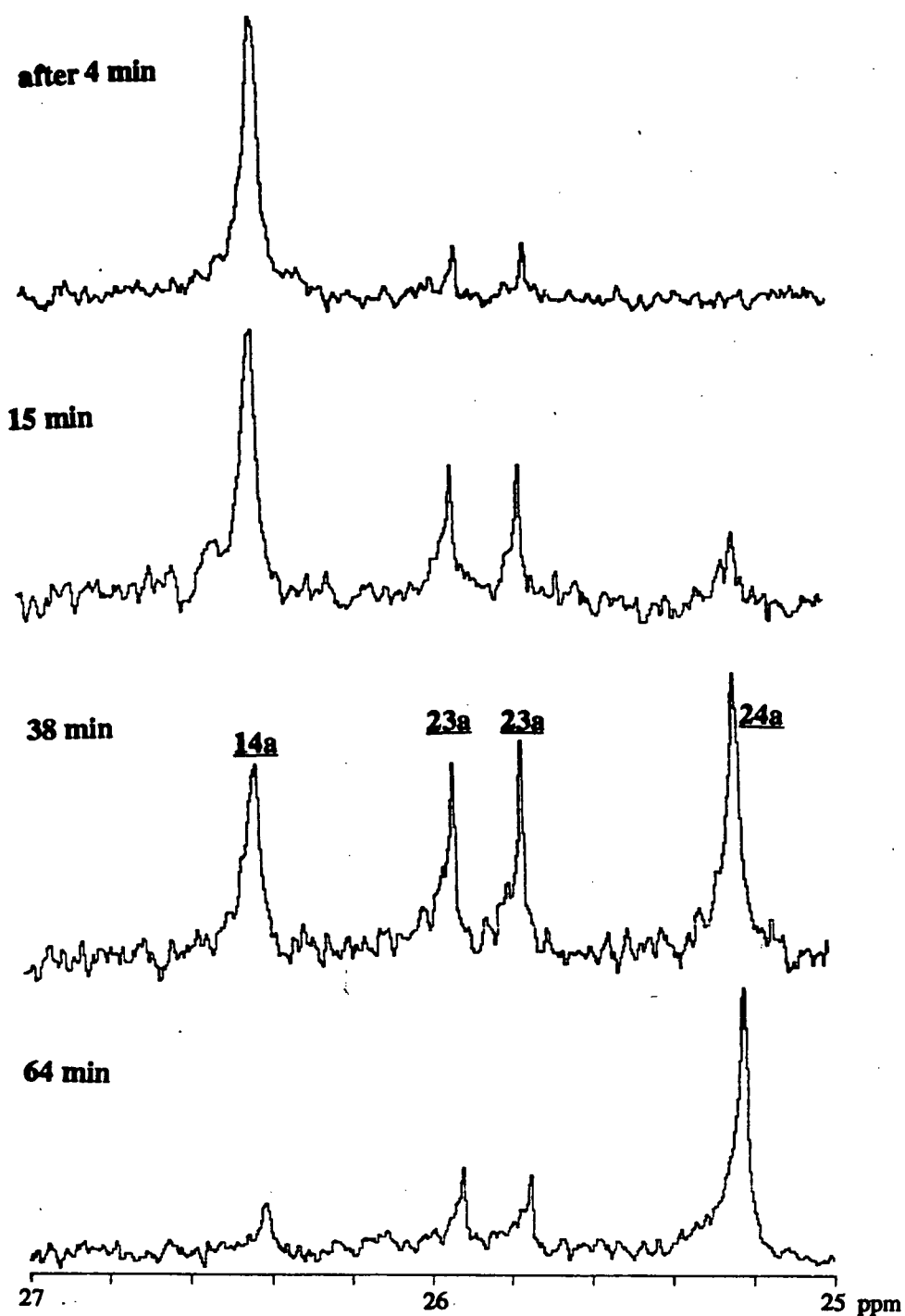


Fig. 6.17 $^{31}\text{P}\{^1\text{H}\}$ NMR spectra acquired during the reaction of *cis*- $\text{Ru}(\text{SH})_2(\text{CO})_2(\text{PPh}_3)_2$ (**14a**, 8.3 mM) with $\text{P}(\text{C}_6\text{H}_4\text{pCH}_3)_3$ (230 mM) in C_6D_6 at 25°C . Chemical shift scale is relative to PPh_3 in C_6D_6 .

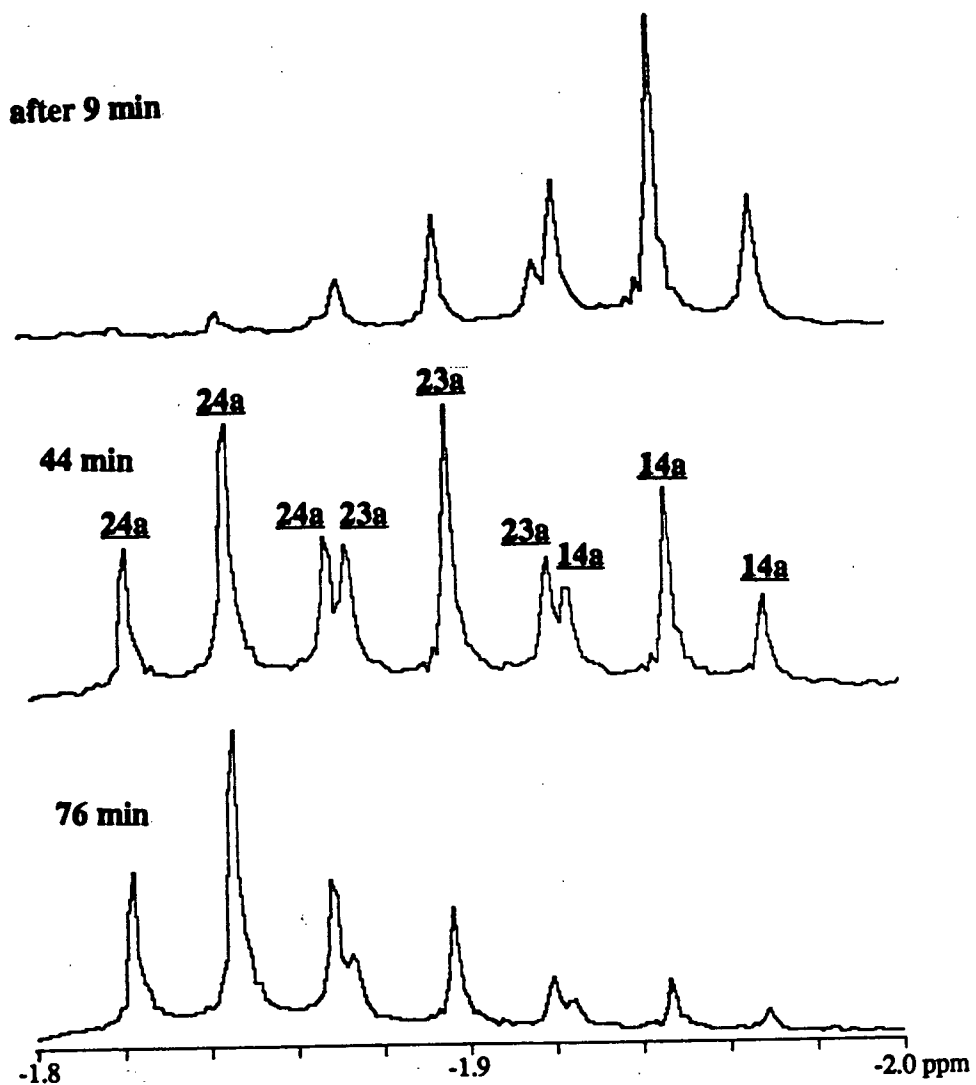


Fig. 6.18 ^1H NMR spectra acquired during the reaction of $cis\text{-Ru}(\text{SH})_2(\text{CO})_2(\text{PPh}_3)_2$ (**14a**, 8.3 mM) with $\text{P}(\text{C}_6\text{H}_4\text{pCH}_3)_3$ (230 mM) in C_6D_6 at 25°C .

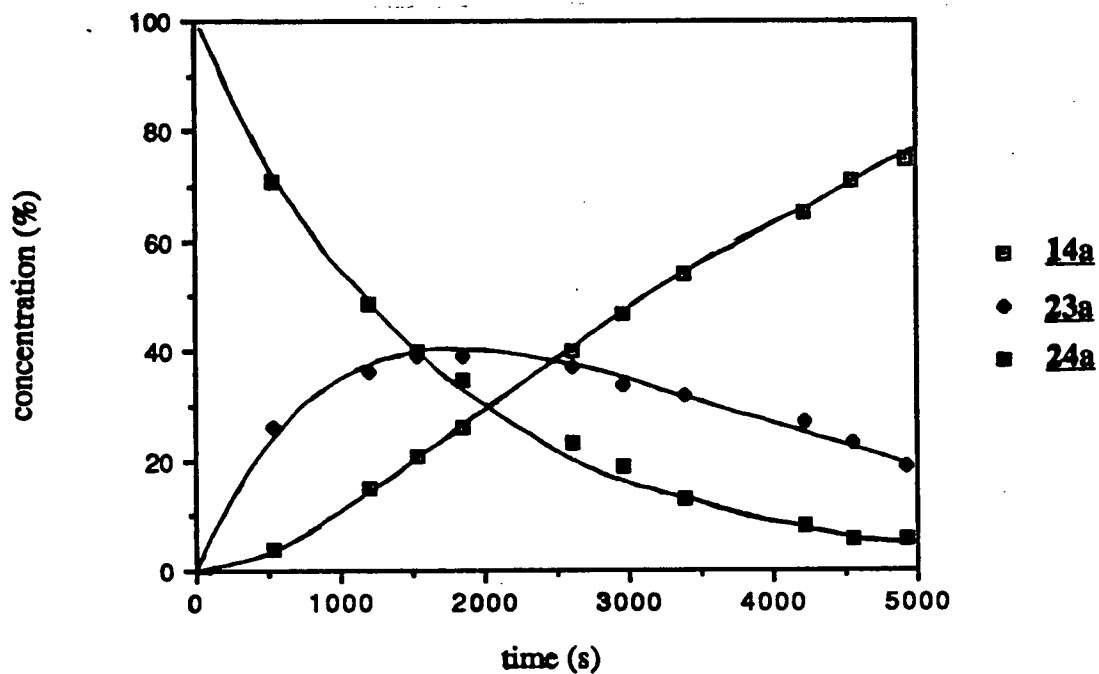
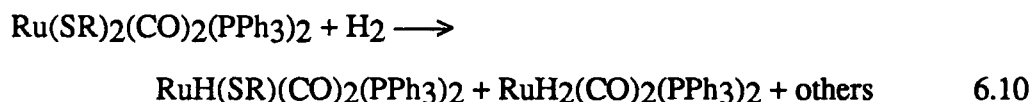


Fig. 6.19 The time dependence of the concentrations of the observed complexes during the reaction of *cct*-Ru(SH)₂(CO)₂(PPh₃)₂ (**14a**, 8.3 mM) with P(C₆H₄pCH₃)₃ (230 mM) in C₆D₆ at 25°C.

6.2.3 H₂

A toluene solution of *cct*-Ru(SC₆H₄pCH₃)₂(CO)₂(PPh₃)₂ (**14b**) was exposed to 24 atm of H₂ at room temperature for 100 min. The ¹H and ³¹P{¹H} NMR spectra of the isolated product mixture in C₆D₆ (Figs. 6.20 and 6.21) showed that the solution contained unreacted **14b** (20 % of the ³¹P NMR signal), the major product *cct*-RuH(SC₆H₄pCH₃)(CO)₂(PPh₃)₂ (**9b**, 45 %), *cct*-RuH₂(CO)₂(PPh₃)₂ (**3**, 1 %), and several unknowns. The hydride region of the ¹H NMR spectrum contained, in addition to the expected peaks for **9b** and **3**, a triplet at -10.19 ppm (²J_{PH}=15.9 Hz) and a doublet of doublets at -6.40 ppm (²J_{transPH}=96.9, ²J_{cisPH}=28.2 Hz). Complexes which could give rise to the latter pattern are *ccc*- or *ctc*-RuH(SR)(CO)₂(PPh₃)₂. Neither of these isomers have been observed, although *ccc*-Ru(SC₆F₅)₂(CO)₂(PPh₃)₂ is known.^{260b}



Attempts to detect or isolate the organic products of the reaction were not made, except for the observation that the singlet (3.02 ppm) in the ¹H NMR spectrum which corresponds to the mercapto proton of *p*-thiocresol is very small indeed (Fig. 6.20), suggesting that the thiol is not the major organic product.

6.2.4 CD₃OD

The mercapto hydrogens of *cct*-Ru(SH)₂(CO)₂(PPh₃)₂ (**14a**) exchanged with 4% CD₃OD in CD₂Cl₂ (Fig. 6.22), probably by the same mechanism as that proposed for reaction 6.7.



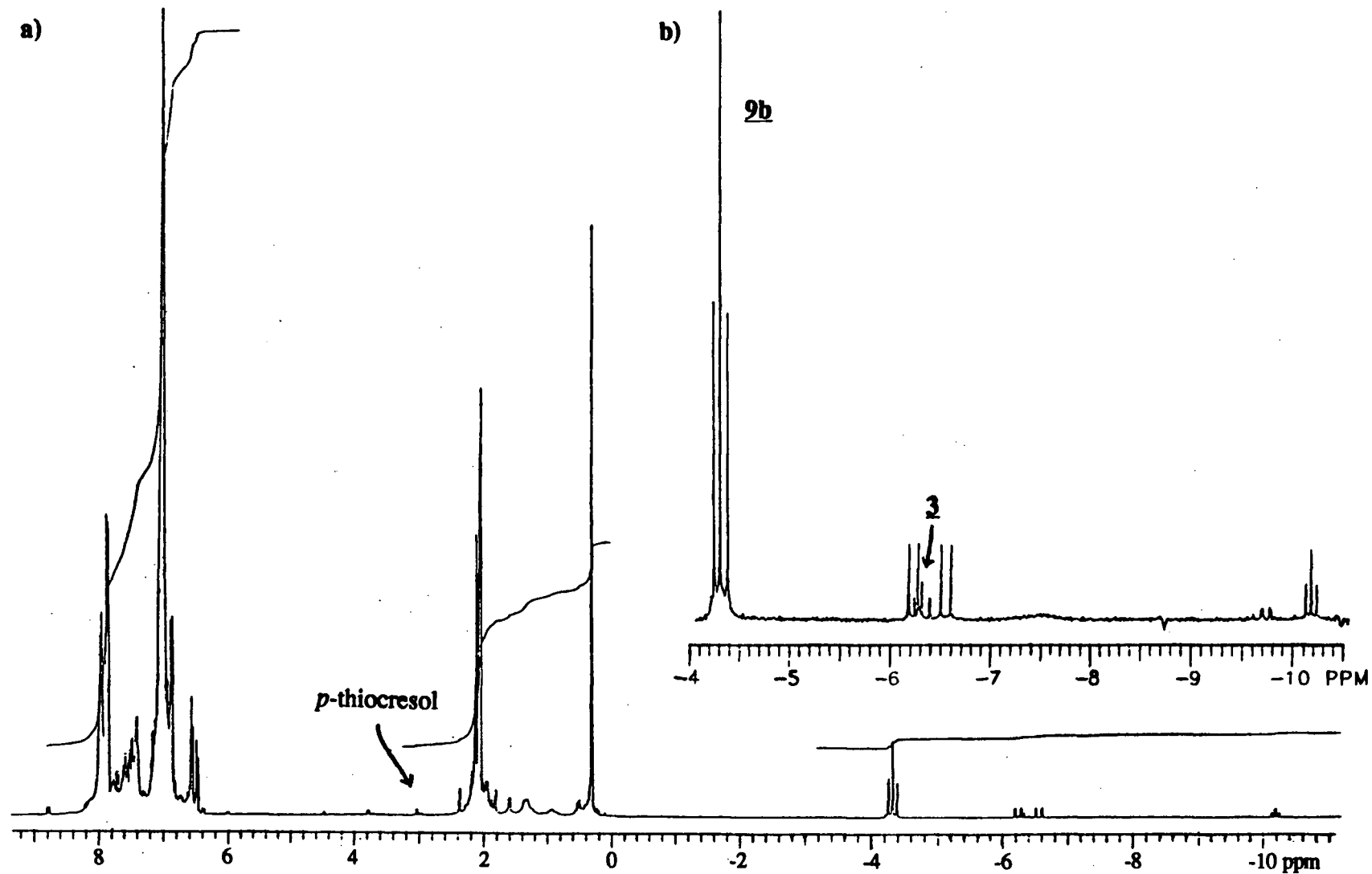


Fig. 6.20 a) ^1H NMR spectrum of a C_6D_6 solution of the product from the reaction of a THF solution of $cis\text{-Ru}(\text{SC}_6\text{H}_4\text{pCH}_3)_2(\text{CO})_2(\text{PPh}_3)_2$ with H_2 (24 atm).
 b) Expanded view of the hydride region of the same spectrum.

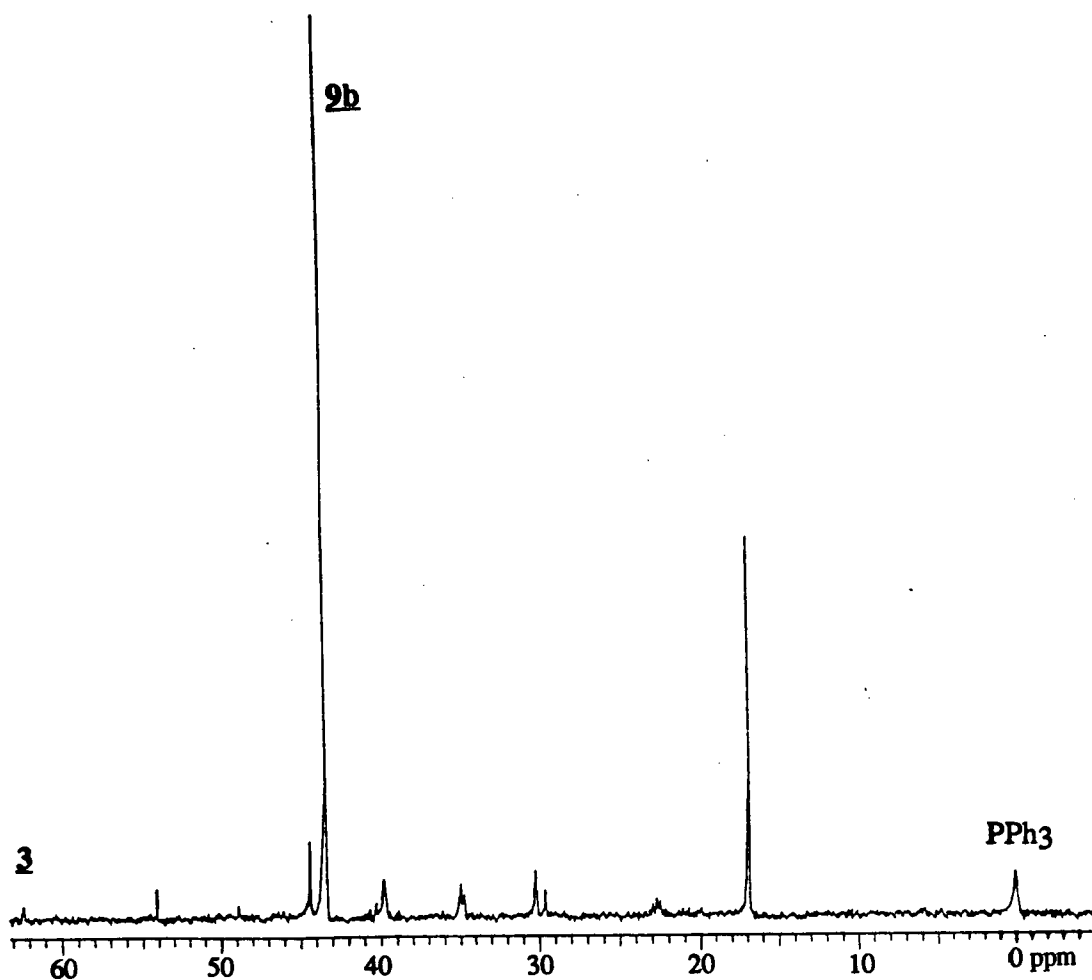


Fig. 6.21 $^{31}\text{P}\{^1\text{H}\}$ NMR spectrum of a C_6D_6 solution of the product from the reaction of a THF solution of *cct*- $\text{Ru}(\text{SC}_6\text{H}_4\text{pCH}_3)_2(\text{CO})_2(\text{PPh}_3)_2$ with H_2 (24 atm). Chemical shift scale is shown relative to PPh_3 in C_6D_6 .

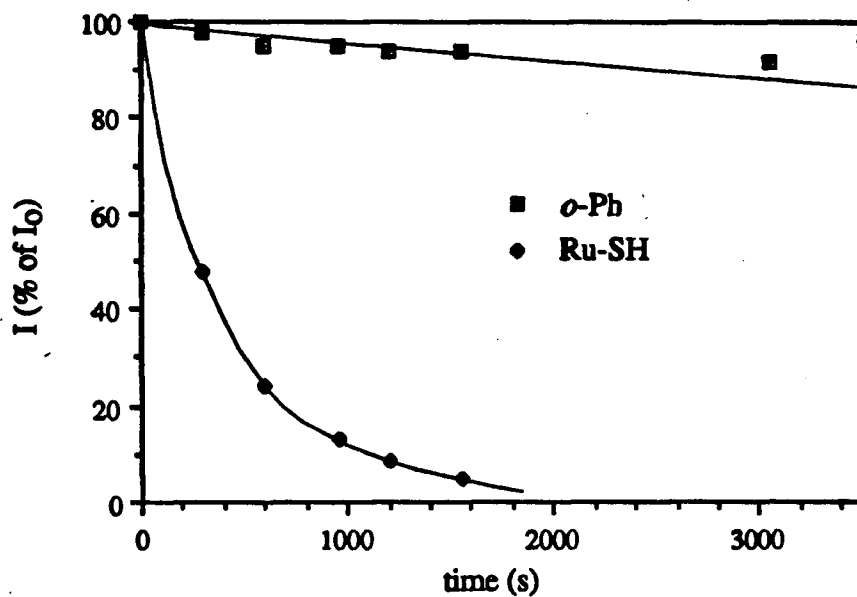


Fig. 6.22 The time dependence of the intensity (I) of the ^1H NMR signals due to *cis*- $\text{Ru}(\text{SH})_2(\text{CO})_2(\text{PPh}_3)_2$ (3.3 mM) in 4% v/v $\text{CD}_3\text{OD}/\text{C}_6\text{D}_6$ at 25°C .

Once again, a significant decrease in the intensity of the signal for the *o*-phenyl proton was observed, although the mechanism by which such an exchange may occur is not known.

6.3 EXPERIMENTAL DETAILS

The reaction of *cct*-RuH(SR)(CO)₂(PPh₃)₂ with P(C₆H₄*p*CH₃)₃:

The reagents were placed in an NMR tube within a wide-mouth Schlenk tube. The latter tube was evacuated and Ar introduced at 1 atm. C₆D₆ (0.6 mL) was added into the NMR tube, which was then sealed with a septum. The tube was inserted into the pre-warmed NMR probe (45°C), at which point the reaction was considered to have started. The change in reaction was monitored by ¹H NMR spectroscopy, with the assumption that the T₁'s of the hydride ligands on the complexes observed were the same (Section 2.2.3). The products were not isolated, but were identified by comparison of their ¹H and ³¹P{¹H} NMR spectra with those of the corresponding starting complex.

cct-RuH(SCH₂C₆H₄)(CO)₂(PPh₃){P(C₆H₄*p*CH₃)₃}: ¹H NMR (C₆D₆) δ -4.58 ppm (t, ²J_{PH} = 20.3 Hz, RuH); ³¹P{¹H} NMR (C₆D₆) δ 36.49, 35.83 ppm (both single peaks, considered to be the centre two peaks of an AB pattern with the two outlying peaks unobserved, ²J_{PP} unknown).

cct-RuH(SCH₂C₆H₄)(CO)₂{P(C₆H₄*p*CH₃)₃}: ¹H NMR (C₆D₆) δ -4.53 ppm (t, ²J_{PH} = 20.2 Hz, RuH); ³¹P{¹H} NMR (C₆D₆) δ 35.17 ppm (s).

cct-RuH(SC₆H₄*p*CH₃)(CO)₂(PPh₃){P(C₆H₄*p*CH₃)₃}: not detected

cct-RuH(SC₆H₄*p*CH₃)(CO)₂{P(C₆H₄*p*CH₃)₃}: ¹H NMR (C₆D₆) δ -4.22 ppm (t, ²J_{PH} = 19.7 Hz, RuH); ³¹P{¹H} NMR (C₆D₆) δ 35.09 ppm (s).

The reaction of *cct*-RuH(SCH₂CH₃)(CO)₂(PPh₃)₂ (**9d**) with PPh₃: The complex (6.7 mg, 1.3 mM) and PPh₃ (270 mg, 150 mM) were dissolved in THF (7 mL). After 4 h at room

temperature, the solvent was removed by vacuum distillation, and the residue redissolved in C_6D_6 . The $^{31}P\{^1H\}$ NMR spectrum contained signals for $Ru(CO)_2(PPh_3)_3$ (**2**, 30 % of the ^{31}P signal excluding the free PPh_3 or its oxide), the starting materials, and a small amount of $OPPh_3$. The conversion to **2** was calculated to be 26 %, using correction factors determined from the $^{31}P\{^1H\}$ NMR spectrum of a known mixture of **2** and *cct*- $RuH(SR)(CO)_2(PPh_3)_2$.

The $^{31}P\{^1H\}$ NMR spectrum of the residue from a similar reaction ($[9d] = 2.2$ mM, $[PPh_3] = 78$ mM) of 4 days duration contained no signal for **9d**. Conversion to **2** was therefore complete.

The reaction of *cct*- $RuH(SCH_3)(CO)_2(PPh_3)_2$ (9c**) with H_2 :** A solution of **9c** (8 mg, 2.3 mM) in THF (5 mL) was exposed to H_2 (60 atm) for 25 h in a glass-lined steel vessel. After depressurization, the solution was transferred by syringe into an Ar-filled Schlenk tube through a septum. The volatiles were removed by vacuum distillation, and the solid residue redissolved in C_6D_6 . The $^{31}P\{^1H\}$ NMR spectrum contained signals for *cct*- $RuH_2(CO)_2(PPh_3)_2$ (δ 56.33 ppm, 86 % of the total signal), unreacted **9c** (37.05 ppm, 5 %), $Ru(CO)_2(PPh_3)_3$ (49.25, 2 %), and *cct*- $RuO_2(CO)_2(PPh_3)_2$ (33.93 ppm, 8 %).

The reaction of *cct*- $RuH(SCH_2C_6H_5)(CO)_2(PPh_3)_2$ (9e**) with HCl:** Complex **9e** (6.9 mg, 8.6 mol) was dissolved in a heterogeneous mixture of C_6D_6 (0.6 mL) and aqueous concentrated HCl (0.05 mL, 0.6 mmol). The reaction was monitored by $^{31}P\{^1H\}$ and 1H NMR spectroscopies. After 10 min at room temperature, the $^{31}P\{^1H\}$ NMR spectrum of the solution showed the presence of *cct*- $RuH(Cl)(CO)_2(PPh_3)_2$ (38.43 ppm, 84 % of the total signal), unreacted **9e** (37.09 ppm, 5 %), and an unknown (38.76 ppm, 11 %). A 1H NMR spectrum was acquired from 15 to 48 min after the start of the reaction. In addition to the triplet for *cct*- $RuH(Cl)(CO)_2(PPh_3)_2$ (δ -3.86 ppm, $^2J_{PH} = 19.1$ Hz, 76 % of the integral of the hydride region), two other triplets of unidentified species were observed, at δ -5.25 ppm ($^2J_{PH} = 16.7$ Hz, 7 %) and -13.31 ppm ($^2J_{PH} = 15.4$ ppm, 16 %). The triplet of the starting complex was not observed at this time.

The reaction of *cct*-RuH(SC₆H₅)(CO)₂(PPh₃)₂ (9i**) with HBF₄:**

A heterogeneous mixture of aqueous HBF₄ (50 μL, 48 wt. %, 300 μmol) and a 0.6 mL C₆D₆ solution of *cct*-RuH(SC₆H₅)(CO)₂(PPh₃)₂ (3.3 μmol) was prepared under argon at room temperature. The ³¹P{¹H} NMR spectrum acquired after 20 min showed singlets for unreacted **9i** (37.19 ppm, 25 %) and an unidentified product (41.71 ppm, 75 %). The ¹H NMR spectrum (Fig. 6.11) acquired after 30 min contained three triplets, for **9i** (-4.33 ppm, ²J_{PH} = 19.3 Hz, 27 %), the major product (-3.83 ppm, ²J_{PH} = 18.3 Hz, 68 %), and a second unknown (-3.98 ppm, ²J_{PH} = 17.6 Hz, 5 %). A broad peak at 1.5 ppm in the ¹H NMR spectrum has the correct integral and chemical shift²¹⁵ for the aquo ligand of *cct*-[RuH(H₂O)(CO)₂(PPh₃)₂]⁺, suggesting that this could be the major product.

The reaction of *cct*-RuH(SC₆H₄*p*CH₃)(CO)₂(PPh₃)₂ (**9b**, 9.2 μmol) with HBF₄/Et₂O (0.2 mL, 1 mmol) in toluene-*d*₈ (0.6 mL) at 1°C was monitored by NMR spectroscopy. After 4 min, the ³¹P{¹H} NMR spectrum showed singlets at 38.6 ppm (unassigned, 63% of the integration), 37.8 ppm (**9b**, 15%) and 18.9 ppm (unassigned, 18%), in addition to a large number of very small unassigned peaks. After 30 min, the integrals of the three major peaks had changed to 26, 10, and 46%, respectively, while the size of the smaller peaks had increased. The hydride region of the ¹H NMR spectrum contains an unassigned triplet at -5.1 ppm.

The reaction of *cct*-RuH(SH)(CO)₂(PPh₃)₂ with CD₃OD: Complex **9a** (2.1 mg, 4.4 mM) was dissolved in C₆D₆ (0.66 mL) under Ar in a septum-sealed NMR tube. CD₃OD (26 μL) was injected to start the reaction. Successive ¹H NMR spectra, acquired every 7-10 min, showed a decrease in the signals of the *o*-phenyl (7.91 ppm), mercapto (-3.01 ppm) and hydrido (-4.83 ppm) hydrogens. The temperature was maintained at 19°C. The results are further described in section 6.1.6.

The light-induced reaction of *cct*-Ru(SC₆H₄pCH₃)₂(CO)₂(PPh₃)₂ (14b**):** Complex **14b** (18 mg, 0.32 mM) was dissolved in THF (6 mL) in a quartz cell under Ar. A UV/vis. spectrum (Fig. 6.14) was acquired after 50, 290, 610, 1200, 2100, 3300, 5400, 8000, 13,000, and 240,000 s, the absorbance at 430 nm being monitored continuously until 15,000 s, except during spectral acquisition (100 s per acquisition). The temperature was maintained at 25.5°C. The rate of change in absorbance decreased over time, but was not first- or second-order. An isosbestic point was observed at 393 nm. The spectrum acquired after 240,000 s showed a departure from the isosbestic. The solvent was removed from the sample by vacuum distillation, and the residue was redissolved in C₆D₆ for analysis by NMR. Five unassigned peaks were present, at 24.22, 24.23, 32.82, 32.87, and 42.88 ppm, each with approximately 20 % of the total integral. A similar experiment with only 4 h reaction time produced a ³¹P{¹H} NMR spectrum with peaks for unreacted **14b** (60 %), PPh₃ (6 %), and unknowns at 23.60 (9%), 24.16 (12 %, possibly OPPh₃), 34.31 (5 %), and 34.82 ppm (6 %).

A sample of *cct*-Ru(SC₆H₄pCH₃)₂(CO)₂(PPh₃)₂ (**14b**, 63 g, 4.5 mM) was dissolved in THF (15 mL) in a Pyrex Schlenk tube under Ar. The tube was held 15 cm from a Hanovia lamp for 90 min without cooling the sample solution, during which time the yellow/orange solution turned orange/red. The temperature of the solution did not increase significantly above room temperature. The volatiles were then removed by vacuum distillation, and some of the residue redissolved in C₆D₆. The ³¹P{¹H} NMR spectrum contained signals for unreacted **14b** (30 %), PPh₃ (8 %), and unknowns at 13.90 (28 %), 24.18 (5 %), 32.84 (11 %), and 42.84 ppm (16 %). The FT-IR spectrum of the crushed residue in Nujol contained three ν(CO) bands, at 2034, 1977, and 1941 cm⁻¹. The residue was submitted for FAB/MS.

The reaction of *cct*-Ru(SH)₂(CO)₂(PPh₃)₂ (14a**) with P(C₆H₄pCH₃)₃:**

Complex **14a** (2.8 mg, 8.3 mM) and P(C₆H₄pCH₃)₃ (31.8 mg, 230 mM) were placed in an NMR tube within a wide-mouth Schlenk tube. The latter tube was evacuated and Ar introduced. C₆D₆ (0.46 mL) was added to the NMR tube, which was then sealed with a septum and cooled

in liquid N₂. After being transported to the NMR room, the tube was warmed to the melting point of benzene, and inserted into the pre-warmed NMR probe (25°C). At this point the reaction was considered to have started. The change in reaction was monitored by ¹H NMR spectroscopy, with the assumption that the T₁'s of the mercapto hydrogens on the three reactant and product complexes were the same (Section 2.2.3). The products were not isolated, but were identified by comparison of their ¹H and ³¹P{¹H} NMR spectra with those of the starting complex **14a**.

cct-Ru(SH)₂(CO)₂(PPh₃){P(C₆H₄*p*CH₃)₃} (**23a**): ¹H NMR (C₆D₆) δ -1.90 ppm (t, ³J_{PH} = 6.9 Hz, SH); ³¹P{¹H} NMR (C₆D₆) δ 19.70, 19.87 ppm (both single peaks, considered to be the centre two peaks of an AB pattern with the two outlying peaks unobserved, ²J_{PP} unknown).

cct-Ru(SH)₂(CO)₂{P(C₆H₄*p*CH₃)₃}₂ (**24a**): ¹H NMR (C₆D₆) δ -1.85 ppm (t, ³J_{PH} = 7.1 Hz, SH); ³¹P{¹H} NMR (C₆D₆) δ 19.18 ppm (s).

The reaction of *cct*-Ru(SC₆H₄*p*CH₃)₂(CO)₂(PPh₃)₂ (**14b**) with P(C₆H₄*p*CH₃)₃: The method described above was adopted for studying the title reaction. However, the reaction was complete by the time the first ³¹P{¹H} NMR spectrum was acquired (3 min). Only three peaks were observed; those of P(C₆H₄*p*CH₃)₃, PPh₃ (-6.05 ppm), and the product (9.93 ppm). The last mentioned is 1 ppm upfield of the position of the starting material, and therefore probably results from the *cct*-Ru(SC₆H₄*p*CH₃)₂(CO)₂{P(C₆H₄*p*CH₃)₃}₂ complex (**24b**).

The reaction of *cct*-Ru(SC₆H₄*p*CH₃)₂(CO)₂(PPh₃)₂ (**14b**) with H₂: A toluene solution (50 mL) of **14b** (42 mg, 0.90 mM) was exposed to H₂ (24 atm) at room temperature for 100 min in a glass-lined steel vessel. After depressurization, the solution was transferred by syringe into an Ar-filled Schlenk tube through a septum. After the volatiles were removed, the solid products were redissolved in C₆D₆ and analyzed by ¹H and ³¹P{¹H} NMR spectroscopies. The spectra indicated the presence of **14b** (20 % of the ³¹P NMR signal),

cct-RuH(SC₆H₄*p*CH₃)(CO)₂(PPh₃)₂ (**9b**, 45 %), *cct*-RuH₂(CO)₂(PPh₃)₂ (**3**, 1 %), and several

unknowns. The hydride region of the ^1H NMR spectrum contained triplets at -4.33 (**9b**, $^2J_{\text{PH}}=19.7$, 71 %), -6.33 (**3**, $^2J_{\text{PH}}=23.4$, 4 %), and at -10.19 ppm (unknown, $^2J_{\text{PH}}=15.9$ Hz, 8 %) and a doublet of doublets at -6.40 ppm (unknown, $^2J_{\text{transPH}}=96.9$, $^2J_{\text{cisPH}}=28.2$ Hz, 17 %).

The reaction of *cct*-Ru(SH)₂(CO)₂(PPh₃)₂ (14a**) with CD₃OD:** Complex **14a** (2.1 mg, 3.3 mM) was dissolved in C₆D₆ (0.85 mL) under Ar in a septum-sealed NMR tube. CD₃OD (34 μL) was injected to start the reaction. Successive ^1H NMR spectra, acquired every 6 min, showed a rapid decrease in the intensity of the mercapto (-1.97 ppm) hydrogen signal, and a slower decrease in the intensity of the *o*-phenyl signal. The temperature was maintained at 25°C.

7. GENERAL CONCLUSIONS AND RECOMMENDATIONS FOR FUTURE RESEARCH

7.1 Potential Applications for the Complexes in Sulphur Chemistry

The dihydride complex *cct*-RuH₂(CO)₂(PPh₃)₂ is not a likely catalyst for hydrodesulphurization (HDS) because none of its reactions with sulphur containing compounds, other than propylene sulphide, resulted in S-C bond cleavage. As discussed previously (Section 1.3), S-C bonds, especially those found in thiophenes, are more difficult to cleave than S-H and S-S bonds. The mechanism for such a S-C bond cleavage reaction with thioethers would almost certainly involve a thioether complex as an intermediate. In general, thioether transition metal complexes are unstable, usually with respect to dissociation of the thioether from the metal rather than decomposition *via* C-S bond cleavage.

The *cct*-RuH₂(CO)₂(PPh₃)₂ complex is a potential catalyst for disulphide reduction (reaction 7.1) because reactions 4.4 and 6.5 together constitute a catalytic cycle for this reaction.



Problems which could be encountered include significant back reactions (reverse of reactions 4.4 and 6.5) under conditions of excess H₂ and thiol, and loss of the catalyst *via* production of *cct*-Ru(SR)₂(CO)₂(PPh₃)₂ (reactions 4.7 and 4.9) and its subsequent decomposition (Section 6.2.1).

Reduction of disulphides to thiols is practiced in organic chemistry as the last step in the synthesis of thiols, if the direct synthesis of the thiol gives lower yields or is less safe than synthesis *via* the disulphide. In addition, unstable thiols are often stored as the disulphide.³⁰⁹

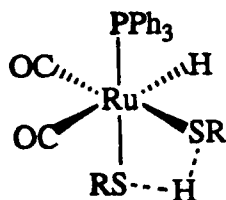
Stoichiometric methods for the reduction of disulphides have been reviewed.³⁰⁹ The reduction of disulphides by *o*-methylbenzaldehyde and methanol is catalyzed by 3,3'-tetramethylene-bridged 4-methylthiazolium bromide.³¹⁰ Thioredoxin and thioredoxin reductase together catalyse the reduction of disulphides in mammalian cells.³¹¹ The reverse reaction, oxidation of thiols to disulphides, is catalyzed by several transition metal complexes.^{312,313}

A potential non-catalytic application of the chemistry described in this thesis is the non-oxidative extraction of thiols from petroleum. Such a process would require two steps; extraction of the thiols by passing the oil fraction over a supported transition metal complex such as a derivative of $cct\text{-RuH}_2(\text{CO})_2(\text{PPh}_3)_2$, followed by regeneration of the same complex from the thiolate, $cct\text{-RuH}(\text{SR})(\text{CO})_2(\text{PPh}_3)_2$, by applying high pressures of hydrogen. Obviously, any complex containing either Ru or PPh_3 would be too expensive for such an application. However, similar applications (both oxidative and non-oxidative) for unsupported iron carbonyls have been suggested,³¹⁴ although cost remains a problem even in the iron system. Leaching of a supported transition metal catalyst, or incomplete separation of an unsupported catalyst, would also create problems of heavy-metal contamination of the fuel product.³¹⁴

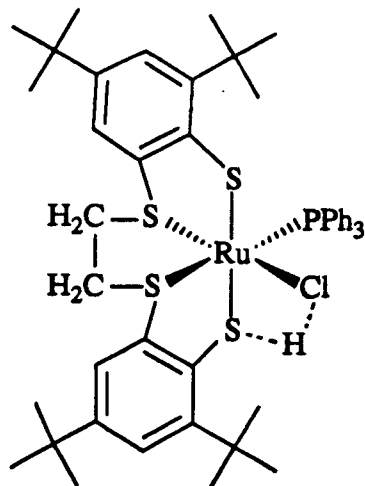
7.2 Parallels to Surface Chemistry

The hydrido thiolato complex $cct\text{-RuH}(\text{SR})(\text{CO})_2(\text{PPh}_3)_2$ has parallels in the chemistry of thiols on transition metal surfaces. In most cases of thiol adsorption to such surfaces, cleavage of the S-H bond occurs and thiolato species are detected.³¹⁵⁻⁹ The fate of the hydrogen atom is rarely reported. However, after H_2S adsorption on a Ru(110) surface, mixtures of H_2S , SH, S, and H species are detected, depending on the coverage.³²⁰ Examples of adsorption of thiols on the surface without S-H bond cleavage are reported to exist at low temperatures.^{317,319} The instability of S-bonded thiols is also recognized in transition metal solution chemistry. No such M-S(H)R species was directly observed in the present work.

A related type of complex, in which two or possibly three thiolate ligands share a proton, is proposed as an intermediate in the thiol exchange reactions of *cct*-RuH(SR)(CO)₂(PPh₃)₂ and *cct*-Ru(SR)₂(CO)₂(PPh₃)₂ (reactions 3.12 and 3.18).



The type of bonding illustrated above may exist on the surface of HDS catalysts. The formation of such species on the surface would be associated with adsorption or liberation of 1/2 to 2/3 of the hydrogen from the adsorbed thiol. Isolated metal complexes with structures containing H⁺ or other cations trapped by thiolate groups are [Ru(CO)₂(PPh₃)(μSEt)₂(μ₃SEt)Na(THF)]₂ (Section 5.2) and Ru(ClH)(buS₄)(PPh₃) (buS₄²⁻ = 1,2-bis((3,5-di-*tert*-butyl-2-mercapto-phenyl)thio)ethanato,²⁴⁹ the latter being shown below.



7.3 Conclusions

One of the phosphine ligands of $\text{Ru}(\text{CO})_2(\text{PPh}_3)_3$ (**2**) is quickly displaced by thiols and disulphides, producing species of the type $cis\text{-RuH}(\text{SR})(\text{CO})_2(\text{PPh}_3)_2$ (**9**) and $cis\text{-Ru}(\text{SR})_2(\text{CO})_2(\text{PPh}_3)_2$ (**14**), respectively. The kinetics of the disulphide reaction are consistent with a two-step mechanism involving elimination of PPh_3 followed by oxidative addition of RSSR . Similar mechanisms have been proposed in earlier studies of the related reactions of **2** with CO and H_2 .¹⁷² Complex **2** fails to react with unstrained thioethers.

Reactions of the related complex $\text{Ru}(\text{CO})_2(\text{PPh}_3)(\text{dpm})$ (**16**, $\text{dpm} = \text{bis}(\text{diphenylphosphino})\text{methane}$) are complicated by the lability of all of the three different ligands. Reactions of this complex with thiols produce mixtures of thiolate complexes.

The two dihydrides $cis\text{-RuH}_2(\text{CO})_2(\text{PPh}_3)_2$ (**3**) and $\text{RuH}_2(\text{dpm})_2$, as a *cis/trans* mixture (**7**), react with thiols to produce the hydrido-thiolato complexes $cis\text{-RuH}(\text{SR})(\text{CO})_2(\text{PPh}_3)_2$ (**9**) and $\text{RuH}(\text{SR})(\text{dpm})_2$ (**13**), respectively. The mechanism appears to depend on the basicity of the hydride ligands; the more basic dihydride, **7**, is probably protonated by the thiol, giving an unobserved molecular hydrogen intermediate. The reaction rate depends on the acidity and concentration of the thiol. The less basic dihydride, **3**, reacts by slow reductive elimination of H_2 followed by rapid oxidative addition of thiol, the rate being independent of the nature or concentration of the thiol. The same rate constant, rate law, and activation parameters are found for the reaction of **3** with thiols, CO or PPh_3 . The reaction of **3** with RSSR produces mostly **9**, with small amounts of **14** that increase with time. The mechanism of the reaction with RSSR was not determined.

The hydrido-thiolato complexes $cis\text{-RuH}(\text{SR})(\text{CO})_2(\text{PPh}_3)_2$ (**9**) are well characterized for a variety of R groups. The related complex $cis\text{-RuH}(\text{SePh})(\text{CO})_2(\text{PPh}_3)_2$ was also synthesized. The reactions of **9** with other thiols, $\text{P}(\text{C}_6\text{H}_4\text{pCH}_3)_3$, CO , RSSR , HCl , PPh_3 , and H_2 , are also reported. The first three of these reactions share the same rate law and rate constant, the common rate determining step probably being initial loss of PPh_3 . The rate constant depends

strongly on the choice of thiolate group, with the complexes containing the more basic thiolate groups reacting faster. The entropy and enthalpy of activation for the reaction of **9b** ($R=C_6H_4pCH_3$) with CO are higher than those for the same reaction of **9d** ($R=CH_2CH_3$), although the error in the entropy values is large. The difference in enthalpy is mainly responsible for the difference in rate. Some equilibrium constants for the exchange reactions of **9d** ($R=CH_2CH_3$) with other thiols were determined, the K_{eq} values increasing with the acidity of the incoming thiol.

The reactions of *cct*-Ru(SC₆H₄*p*CH₃)₂(CO)₂(PPh₃)₂ (**14b**) are complicated by the extreme lability of the phosphine ligands. The complex in solution is unstable in the presence of light, exchanges phosphines rapidly with added P(C₆H₄*p*CH₃)₃, exchanges thiolate groups with added thiols, and is converted by high pressures of H₂ to a mixture of **9b** and **3**.

The X-ray crystallographic structures of *cct*-RuH(SC₆H₄*p*CH₃)(CO)₂(PPh₃)₂ (**9b**) and *cct*-Ru(SC₆H₄*p*CH₃)₂(CO)₂(PPh₃)₂ (**14b**) show that the Ru-P bond lengths in **14b** are longer, consistent with the higher lability of the phosphines of that complex. The phosphine ligands of Ru(SH)₂(CO)₂(PPh₃)₂ (**14a**) on the other hand are less labile, and the Ru-P bond lengths shorter, than in **14b**. Complex **14a** is stable in solution in the presence of light, and exchanges phosphines more slowly with added P(C₆H₄*p*CH₃)₃.

The mercapto hydrogens of **9a** ($R=H$) and **14a** exchange with the acidic deuterons of added CD₃OD. The hydridic and ortho-phenyl hydrogens exchange more slowly, presumably by intramolecular processes.

Intermediates proposed for the mechanism of the thiol exchange reactions of **9** and **14** contain two or three thiolate groups sharing a proton. A related complex, containing three thiolate groups on a ruthenium centre sharing a sodium cation, was isolated and fully characterized. In the solid state, this [Ru(CO)₂(PPh₃)(μSEt)₂(μ₃SEt)Na(THF)]₂ complex exists in dimeric form, and is formed as a by-product from the synthesis of **14d** ($R=Et$) from *cct*-RuCl₂(CO)₂(PPh₃)₂ and sodium ethanethiolate. In acetone, **9b** and **14b** can be formed cleanly from

cct-RuHCl(CO)₂(PPh₃)₂ and *cct*-RuCl₂(CO)₂(PPh₃)₂, respectively, by reaction with ethanethiolate.

Complex **3** could be used as a catalyst for the reduction of disulphides by H₂, or as a recyclable reagent for the non-oxidative extraction of thiols from thiol-containing mixtures such as oil fractions. However, the cost of RuCl₃ and PPh₃ is too high to allow such direct applications. The chemistry described above will help instead to guide future researchers to related complexes with higher activity and lower costs, and systems that more closely parallel the processes occurring on the surfaces of industrial HDS catalysts.

7.4 Recommendations for Future Research

As has been suggested recently by another group,⁹⁰ the redox chemistry of *cct*-RuH(SH)(CO)₂(PPh₃)₂, *cct*-Ru(SH)₂(CO)₂(PPh₃)₂ and *cct*-RuS₂(CO)₂(PPh₃)₂ should be investigated. Initial experiments during the present research, but not otherwise reported here, show that high pressures of H₂ (24 atm) over CH₂Cl₂ solutions of *cct*-RuS₂(CO)₂(PPh₃)₂ for 2 h at room temperature do not cause formation of *cct*-RuH₂(CO)₂(PPh₃)₂ or *cct*-Ru(SH)₂(CO)₂(PPh₃)₂. However, such reactions may possibly be achieved in the presence of acid, because of the ease of electrophilic attack on the S₂²⁻ ligand.^{118,221,321-2}

Research should focus on complexes which are capable of cleaving unstrained S-C bonds. The most likely candidates are bimetallic complexes containing at least one transition metal which bonds strongly with sulphur. One such complex, (CO)₃Mo(μH)₂(dpm)₂Ru(CO)₂³²³ has some similarities to the complexes described in the present work. However, for closer parallels to industrial HDS catalysts, a Co/Mo bimetallic complex should be used. If the observations summarized in Figure 1.5 (p. 16)⁴⁷ can be extrapolated to solution chemistry, then a Co/Mo complex would have greater potential for HDS activity than a Ru/Mo complex.⁴⁷ Sulphido-

bridged Co/Mo clusters have been synthesised,³²⁴⁻⁶ but only from the reactions of Mo sulphide complexes with Co carbonyl complexes, rather than by the insertion of S into Co-Mo bonds.

The catalytic activity of *cct*-RuH₂(CO)₂(PPh₃)₂ for the reduction of disulphides to thiols under pressures of H₂ should be investigated.

8. REFERENCES

- (1) R. Angelici, *Acc. Chem. Res.*, **21**, 387 (1988).
- (2) L. Thurneisser Zum Thurn, "Quinta Essentia," Ossenbruck, Munster, 1570.
- (3) J. M. Stillman, "The Story of Alchemy and Early Chemistry," Dover Publ. Inc., New York, N. Y., 1960, pp 61 and 241.
- (4) J. R. Partington, "A History of Chemistry," Vol. I, MacMillan and Co. Ltd., London, 1970, pp 211 and 222.
- (5) R. Leclercq, in "Sulfur in Organic and Inorganic Chemistry," Vol. II, A. Senning, Ed., Marcel Dekker Inc., New York, N. Y., 1972, Chapter 19, pp 207-210.
- (6) C. S. Hurlbut Jr. and C. Klein, "Manual of Mineralogy," 19th ed, John Wiley and Sons, New York, N. Y., 1977, pp 230-231.
- (7) M. B. Hocking, "Modern Chemical Technology and Emission Control," Springer Verlag, Berlin, 1985, p 153.
- (8) C. J. Thompson, in "Organic Sulfur Chemistry," 9th Int'l. Symp. on Org. Sulfur Chem., Riga, U.S.S.R., June 1980, R. Kh. Freidlina and A. E. Skorova, Eds., IUPAC (Organic Chemistry Division), Pergamon Press, Oxford, 1981, pp 189-208.
- (9) J. G. Speight, "The Chemistry and Technology of Petroleum," Marcel Dekker Inc., New York, N. Y., 1980, pp 344-345 and 377-380.
- (10) G. D. Galpern, in "Thiophene and Its Derivatives," Pt. I, S. Gronowitz, Ed., Vol. 44 of the series "The Chemistry of Heterocyclic Compounds," A. Weissberger and E. C. Taylor, Series Eds., John Wiley and Sons, New York, N. Y., 1985, Chapter 4, p 326.
- (11) R. A. Meyers, "Coal Desulfurization," Marcel Dekker Inc., New York, N. Y., 1977, pp 3-4.
- (12) D. C. Nunenkamp, in "Coal Desulfurization Prior to Combustion," R. C. Eliot, Ed., Noyes Data Corp., Park Ridge, N. J., 1978, Chapter 1.
- (13) A. Attar and G. G. Hendrickson, in "Coal Structure," R. A. Meyers, Ed., Academic Press, New York, N. Y., 1982, Chapter 5.
- (14) K. Wark and C. F. Warner, "Air Pollution: Its Origin and Control," 2nd ed., Harper and Row Publishers, New York, N. Y., 1981, p 349.
- (15) G. A. Maw, in "Sulfur in Organic and Inorganic Chemistry," Vol. II, A. Senning, Ed., Marcel Dekker Inc., New York, N. Y., 1972, Chapter 15, p 115.
- (16) K. K. Andersen and D. T. Bernstein, *J. Chem. Educ.*, **55**, 159 (1978).
- (17) R. J. Huxtable, "Biochemistry of Sulphur," Plenum Press, New York, N. Y., 1986, p 269.
- (18) F. Bohlmann and C. Zdero, in "Thiophene and Its Derivatives," Pt. I, S. Gronowitz, Ed., Vol. 44 of the series "The Chemistry of Heterocyclic Compounds," A. Weissberger and

E. C. Taylor, Series Eds., John Wiley and Sons, New York, N. Y., 1985, Chapter 3, pp 261-262.

- (19) T. Yamanaka, in "Metalloproteins," S. Otsuka and T. Yamanaka, Eds., Vol. 8 of "Bioactive Molecules," Elsevier, Amsterdam, 1988, Chapter 5.8.
- (20) E. T. Adman, in "Metalloproteins Part 1: Metal Proteins with Redox Roles," P. M. Harrison, Ed., MacMillan, Houndmills, U. K., 1985, Chapter 1.
- (21) Y. Kojima, in "Metalloproteins," S. Otsuka and T. Yamanaka, Eds., Vol. 8 of "Bioactive Molecules," Elsevier, Amsterdam, 1988, Chapter 17.
- (22) M. Nozaki, in "Metalloproteins," S. Otsuka and T. Yamanaka, Eds., Vol. 8 of "Bioactive Molecules," Elsevier, Amsterdam, 1988, Chapter 9.7.
- (23) N. Ueyama and A. Nakamura, in "Metalloproteins," S. Otsuka and T. Yamanaka, Eds., Vol. 8 of "Bioactive Molecules," Elsevier, Amsterdam, 1988, Chapter 5.10.
- (24) H. Blumberg, A. Eisen, A. Sledziewski, D. Bader, and E. T. Young, *Nature*, **328**, 443 (1987).
- (25) B. A. Averill, in "Metal Clusters in Proteins," L. Que Jr., Ed., ACS Symposium Series 372, American Chemical Society, Washington, 1987, Ch. 13.
- (26) N. Ueyama and A. Nakamura, in "Metalloproteins," S. Otsuka and T. Yamanaka, Eds., Vol. 8 of "Bioactive Molecules," Elsevier, Amsterdam, 1988, Chapter 5.9.
- (27) R. H. Holm and J. A. Ibers, in "Iron Sulfur Proteins," Vol. III, W. Lovenberg, Ed., Academic Press, New York, N. Y., 1977, Chapter 7.
- (28) T. E. Wolff, P. P. Bower, R. B. Frankel, and R. H. Holm, *J. Am. Chem. Soc.*, **102**, 4694 (1980).
- (29) N. Ueyama, A. Nakamura, and S. Otsuka, in "Metalloproteins," S. Otsuka and T. Yamanaka, Eds., Vol. 8 of "Bioactive Molecules," Elsevier, Amsterdam, 1988, Chapter 10.1.
- (30) "Nomenclature of Organic Chemistry, Sections A, B, C, D, E, F and H," Commission on Nomenclature of Organic Chemistry, Organic Chemistry Division, IUPAC, Pergamon Press, Oxford, 1979, pp 210-228.
- (31) "Nomenclature of Organic Chemistry, Sections A, B, C, D, E, F and H," Commission on Nomenclature of Organic Chemistry, Organic Chemistry Division, IUPAC, Pergamon Press, Oxford, 1979, pp 337-341.
- (32) A. B. Roy and P. A. Trudinger, "The Biochemistry of Inorganic Compounds of Sulphur," Cambridge University Press, London, 1970.
- (33) C. E. Jahnig, in "Kirk-Othmer Encyclopedia of Chemical Technology," 3rd ed, Vol. 17, M. Grayson and D. Eckroth, Eds., John Wiley and Sons, New York, N. Y., p 219.
- (34) A. K. Lahiri and H. R. Thilakan, in "Corrosion in Fertilizer and Petroleum Industry," proceedings of a short course organized by the Corrosion Advisory Bureau at

Udyogamandal, December 1968, K. N. P. Rao and A. K. Lahiri, Eds., Corrosion Advisory Bureau, Jamshedpur, India.

- (35) J. G. Speight, "The Desulfurization of Heavy Oils and Residua," Marcel Dekker Inc., New York, N. Y., 1981, p 87.
- (36) J. G. Speight, "The Desulfurization of Heavy Oils and Residua," Marcel Dekker Inc., New York, N. Y., 1981, p ii.
- (37) "Petroleum Processing Handbook," W. F. Bland and R. L. Davidson, Eds., McGraw-Hill Book Co., New York, N. Y., 1967, pp 3-116 and 3-125.
- (38) "Sulfur Oxides," Committee on Sulfur Oxides, Board of Toxicology and Environmental Health Hazards, Assembly of Life Sciences, National Research Council, National Academy of Sciences, Washington, D. C., 1978, p 3.
- (39) a) Errata to "Hydrogen Sulfide in the Atmospheric Environment: Scientific Criteria for Assessing its Effects on Environment Quality," National Research Council of Canada Associate Committee on Scientific Criteria for Environmental Quality, Publ. No. NRCC 18467 of the Environmental Secretariat, Ottawa, Ont., 1981. b) "Emissions and Trends of Common Air Contaminants in Canada: 1970 to 1980," Report EPS 7/AP/17, Environment Canada, Ottawa, Ontario, 1986, pp 7-10.
- (40) M. Katz, in "Sulphur and Its Inorganic Derivatives in the Canadian Environment," National Research Council of Canada Associate Committee on Scientific Criteria for Environmental Quality, Publ. No. NRCC 15015 of the Environmental Secretariat, Ottawa, Ont., 1977.
- (41) P. B. Venuto and E. T. Habib Jr., "Fluid Catalytic Cracking with Zeolite Catalysts," Marcel Dekker Inc., New York, N. Y., 1979.
- (42) J. E. Yocom and J. B. Upham, in "Air Pollution," 3rd ed., Vol. II, A. C. Stern, Ed., Academic Press, New York, N. Y., 1977, p 83.
- (43) R. J. Campagna, J. A. Frayer, and R. T. Sebulsky, in "Encyclopedia of Chemical Processing and Design," Vol. 15, J. J. McKetta and W. A. Cunningham, Eds., Marcel Dekker Inc., New York, N. Y., p 225.
- (44) W. G. Dukek, in "Kirk-Othmer Encyclopedia of Chemical Technology," 3rd ed, Vol. 6, M. Grayson and D. Eckroth, Eds., John Wiley and Sons, New York, N. Y., p 335.
- (45) C. E. Jahnig, in "Kirk-Othmer Encyclopedia of Chemical Technology," 3rd ed, Vol. 17, M. Grayson and D. Eckroth, Eds., John Wiley and Sons, New York, N. Y., p 201.
- (46) B. C. Gates, J. R. Katzer, and G. C. A. Schuit, "Chemistry of Catalytic Processes," McGraw Hill Book Co., New York, N. Y., 1979, pp 390-447.
- (47) R. R. Chianelli, *Catal. Rev.*, **26**, 361 (1984).
- (48) S. Harris and R. R. Chianelli, *J. Catal.*, **86**, 400 (1984).
- (49) T. A. Pecoraro and R. R. Chianelli, *J. Catal.*, **67**, 430 (1981).
- (50) S. Kolboe and C. H. Amberg, *Can. J. Chem.*, **44**, 2623, (1966).

- (51) D. E. Nicholson, *Anal. Chem.*, **34**, 371 (1962).
- (52) J. Joffre, P. Geneste, and D. A. Lerner, *J. Catal.*, **97**, 543 (1986).
- (53) G. H. Singhal, R. L. Espino, and J. E. Sobel, *J. Catal.*, **67**, 446 (1981).
- (54) S. C. Huckett, L. L. Miller, R. A. Jacobsen, and R. J. Angelici, *Organometallics*, **7**, 686 (1988).
- (55) C.-M. J. Wang and R. J. Angelici, *Organometallics*, **9**, 1770 (1990).
- (56) S. C. Huckett and R. J. Angelici, *Organometallics*, **7**, 1491 (1988).
- (57) M. Draganjac, C. J. Ruffing, and T. B. Rauchfuss, *Organometallics*, **4**, 1909 (1985).
- (58) J. D. Goodrich, P. N. Nicholas, and J. P. Selegue, *Inorg. Chem.*, **26**, 3424 (1987).
- (59) R. Cordone, W. D. Harman, and H. Taube, *J. Am. Chem. Soc.*, **111**, 5969 (1989).
- (60) M. G. Choi and R. J. Angelici, *J. Am. Chem. Soc.*, **111**, 8753 (1989).
- (61) J. Chen and R. J. Angelici, *Organometallics*, **8**, 2277 (1989).
- (62) G. Spies and R. J. Angelici, *J. Am. Chem. Soc.*, **107**, 5569 (1985).
- (63) P. Desikan and C. H. Amberg, *Can. J. Chem.*, **42**, 843 (1964).
- (64) G. N. Givens and P. B. Venuto, *Prepr. Am. Chem. Soc. Div. Pet. Chem.*, **15**, A183 (1970), as reported in B. C. Gates, J. R. Katzer, and G. C. A. Schuit, "Chemistry of Catalytic Processes," McGraw Hill Book Co., New York, N. Y., 1979, pp 390-447.
- (65) J. Devanneaux and J. Maurin, *J. Catal.*, **69**, 202 (1981).
- (66) J. M. J. G. Lipsch and G. C. A. Schuit, *J. Catal.*, **15**, 179 (1969).
- (67) H. Kwart, G. C. A. Schuit, and B. C. Gates, *J. Catal.*, **61**, 128 (1980).
- (68) D. A. Lesch, J. W. Richardson, R. A. Jacobsen, and R. J. Angelici, *J. Am. Chem. Soc.*, **106**, 2901 (1984).
- (69) A. J. Gellman, M. E. Bussell, and G. A. Somorjai, *J. Catal.*, **107**, 103 (1987).
- (70) S. Kolboe, *Can. J. Chem.*, **47**, 352, (1969).
- (71) S. W. Cowley, Ph. D. thesis, Southern Illinois University, 1975, as reported in H. Kwart, G. C. A. Schuit, and B. C. Gates, *J. Catal.*, **61**, 128 (1980).
- (72) J. W. Hachgenei and R. J. Angelici, *J. Organomet. Chem.*, **355**, 359 (1988).
- (73) N. N. Sauer, E. J. Markel, G. L. Schrader, and R. J. Angelici, *J. Catal.*, **117**, 295 (1989).
- (74) D. F. McMillen and D. M. Golden, *Annu. Rev. Phys. Chem.*, **33**, 493 (1982).

- (75) S. W. Benson, *Chem. Rev.*, **78**, 23 (1978).
- (76) H. Singer and G. Wilkinson, *J. Chem. Soc. (A)*, 2516 (1968).
- (77) L. Vaska, *J. Am. Chem. Soc.*, **88**, 5325 (1966).
- (78) A. M. Mueting, P. Boyle, and L. H. Pignolet, *Inorg. Chem.* **23**, 44 (1984).
- (79) M. Hsieh, R. Zingaro, and V. Krishnan, *Int. J. Sulfur. Chem. (A)*, **1**, 197 (1971).
- (80) C. V. Senoff, *Can. J. Chem.*, **48**, 2444 (1970).
- (81) D. Morelli, A. Segre, R. Ugo, G. LaMonica, S. Cenini, F. Conti, and F. Bonati, *J. Chem. Soc., Chem. Commun.*, 524 (1967).
- (82) R. Ugo, G. LaMonica, S. Cenini, A. Segre, and F. Conti, *J. Chem. Soc. (A)*, 522 (1971).
- (83) J. Chatt, J. P. Lloyd, and R. L. Richards, *J. Chem. Soc., Dalton Trans.*, 566 (1976).
- (84) R. A. Henderson, D. L. Hughes, R. L. Richards, and C. Shortman, *J. Chem. Soc., Dalton Trans.*, 1115, (1987).
- (85) C. Shortman and R. L. Richards, *J. Organomet. Chem.*, **286**, C3 (1985).
- (86) C.-L. Lee, J. Chisholm, B. R. James, D. A. Nelson, and M. A. Lilga, *Inorg. Chim. Acta*, **121**, L7 (1986).
- (87) M. Y. Darensbourg, W.-F. Liaw, and C. G. Riordan, *J. Am. Chem. Soc.*, **111**, 8051 (1989).
- (88) C. G. Kuehn and H. Taube, *J. Am. Chem. Soc.*, **98**, 3 (1976).
- (89) G. C. Christoph and M. Tolbert, Abstracts, Am. Cryst. Assoc. Meeting, March 1980, Abstract P6.
- (90) J. Amarasekera and T. B. Rauchfuss, *Inorg. Chem.*, **28**, 3875 (1989).
- (91) J. P. Collman, T. N. Sorrell, K. O. Hodgson, A. K. Kulshrestha, and C. E. Strousse, *J. Am. Chem. Soc.*, **99**, 5180 (1977).
- (92) I. G. Dance, *Polyhedron*, **5**, 1037 (1986).
- (93) A. M. Mueting, P. Boyle, and L. H. Pignolet, *Inorg. Chem.*, **23**, 44 (1984).
- (94) J. L. Herde and C. V. Senoff, *Can. J. Chem.*, **51**, 1016 (1973).
- (95) K. Osakada, T. Yamamoto, A. Yamamoto, A. Takenaka, and Y. Sasada, *Inorg. Chim. Acta*, **105**, L9 (1985).
- (96) N. S. Nametkin, V. D. Tyurin, and M. A. Kukina, *J. Organomet. Chem.*, **149**, 355 (1978).
- (97) K. Farmery and M. Kilner, *J. Chem. Soc. (A)*, 634 (1970).
- (98) M. R. Churchill, J. W. Ziller, and J. B. Keister, *J. Organomet. Chem.*, **297**, 93 (1985).

- (99) G. R. Crooks, B. F. G. Johnson, J. Lewis, and I. C. Williams, *J. Chem. Soc. (A)*, 797 (1969).
- (100) J. R. Fisher, A. J. Mills, S. Sumner, M. P. Brown, M. A. Thomson, R. J. Puddephatt, A. A. Frew, L. M. Muir, and K. W. Muir, *Organometallics*, **1**, 1421 (1982).
- (101) S. Dev, K. Imagawa, Y. Mizobe, G. Cheng, Y. Wakatsuki, H. Yamazaki, and M. Hidai, *Organometallics*, **8**, 1232 (1989).
- (102) C.-L. Lee, G. Besenyei, B. R. James, D. A. Nelson, and M. A. Lilga, *J. Chem. Soc., Chem. Commun.*, 1175 (1985).
- (103) G. Besenyei, C.-L. Lee, J. Gulinski, S. J. Rettig, B. R. James, D. A. Nelson, and M. A. Lilga, *Inorg. Chem.*, **26**, 3622 (1987).
- (104) G. Besenyei, C.-L. Lee, and B. R. James, *J. Chem. Soc., Chem. Commun.*, 1750 (1986).
- (105) A. F. Barnabas, D. Sallin, and B. R. James, *Can. J. Chem.*, **67**, 2009 (1989).
- (106) M. C. Jennings and R. J. Puddephatt, *Inorg. Chem.*, **27**, 4280 (1988).
- (107) W. Hieber and K. Kaiser, *Z. Naturforsch., Teil B*, **24**, 778 (1969).
- (108) U. Berger and J. Strahle, *Z. Anorg. Allg. Chem.*, **516**, 19 (1984).
- (109) M. A. Walters and J. C. Dewan, *Inorg. Chem.*, **25**, 4889 (1986).
- (110) P. M. Treichel, M. S. Schmidt, P. C. Nakagaki, and E. K. Rublein, *J. Organomet. Chem.*, **311**, 193 (1986).
- (111) N. Kuhn and H. Schumann, *J. Organomet. Chem.*, **287**, 345 (1985).
- (112) P. M. Treichel, L. D. Rosenhein, and M. S. Schmidt, *Inorg. Chem.*, **22**, 3960 (1983).
- (113) W. F. Liaw, C. Kim, M. Y. Darensbourg, and A. L. Rheingold, *J. Am. Chem. Soc.*, **111**, 3591 (1989).
- (114) B. Chaudret and R. Poilblanc, *Inorg. Chim. Acta*, **34**, L209 (1979).
- (115) J. A. M. Canich, F. A. Cotton, K. R. Dunbar, and L. R. Falvello, *Inorg. Chem.*, **27**, 804 (1988).
- (116) S. D. Killops and S. A. R. Knox, *J. Chem. Soc., Dalton Trans.*, 1260 (1978).
- (117) K. W. Lee and T. L. Brown, *Inorg. Chem.*, **26**, 1852 (1987).
- (118) a) G. R. Clark, D. R. Russell, W. R. Roper, and A. Walker, *J. Organomet. Chem.*, **136**, C1 (1977), b) G. R. Clark and D. R. Russell, *J. Organomet. Chem.*, **173**, 377 (1979).
- (119) J. Amarasekera, T. B. Rauchfuss, and A. L. Rheingold, *Inorg. Chem.*, **26**, 2017 (1987).
- (120) J. Amarasekera, T. B. Rauchfuss, and S. R. Wilson, *Inorg. Chem.*, **26**, 3328 (1987).

- (121) M. A. El-Hinnawi, M. L. Sumadi, F. T. Esmadi, I. Jibril, W. Imhof, and G. Huttner, *J. Organomet. Chem.*, **377**, 373 (1989).
- (122) G. Tainturier, M. Fahim, and B. Gautheron, *J. Organomet. Chem.*, **373**, 193 (1989).
- (123) M. Fahim and G. Tainturier, *J. Organomet. Chem.*, **301**, C45 (1986).
- (124) V. M. Schmidt and G. G. Hoffmann, *Z. Anorg. Allg. Chem.*, **464**, 209 (1980).
- (125) S. Evans, P. Legzdins, S. Rettig, L. Sanchez, and J. Trotter, *Organometallics*, **6**, 7 (1987).
- (126) P. Legzdins and L. Sanchez, *J. Am. Chem. Soc.*, **107**, 5525 (1985).
- (127) K. Krogh-Jespersen, X. Zhang, J. D. Westbrook, R. Fikar, K. Nayak, W. L. Kwik, J. A. Potenza, and H. J. Schugar, *J. Am. Chem. Soc.*, **111**, 4082 (1989).
- (128) R. Kroener, M. J. Heeg, and E. Deutsch, *Inorg. Chem.*, **27**, 558 (1988).
- (129) J. Amarasekera, T. B. Rauchfuss, and S. R. Wilson, *J. Am. Chem. Soc.*, **110**, 2332 (1988).
- (130) J. Chatt, G. J. Leigh, and A. P. Storace, *J. Chem. Soc. (A)*, 1380 (1971).
- (131) J. E. Fergusson, J. D. Karran, and S. Seevaratnam, *J. Chem. Soc.*, 2627 (1965).
- (132) J. S. Jaswal, S. J. Rettig, and B. R. James, *Can. J. Chem.*, **68**, 1808 (1990).
- (133) S. R. Cooper, *Acc. Chem. Res.*, **21**, 141 (1988).
- (134) S. Jang, L. M. Atagi, and J. M. Mayer, *J. Am. Chem. Soc.*, **112**, 6413 (1990).
- (135) M. C. Jennings and R. J. Puddephatt, *Inorg. Chem.*, **27**, 4280 (1988).
- (136) M. D. Fryzuk and D. H. McConville, *Inorg. Chem.*, **28**, 1613 (1989).
- (137) K. Osakada, K. Matsumoto, T. Yamamoto, and A. Yamamoto, *Organometallics*, **4**, 857 (1985).
- (138) K. Osakada, T. Chiba, Y. Nakamura, T. Yamamoto, and A. Yamamoto, *J. Chem. Soc., Chem. Commun.*, 1589 (1986).
- (139) T. Yamamoto, M. Akimoto, O. Saito, and A. Yamamoto, *Organometallics*, **5**, 1559 (1986).
- (140) T. Yamamoto, M. Akimoto, and A. Yamamoto, *Chem. Lett.*, 1725 (1983).
- (141) K. Osakada, M. Maeda, Y. Nakamura, T. Yamamoto, and A. Yamamoto, *J. Chem. Soc., Chem. Commun.*, 442 (1986).
- (142) E. Wenkert, M. E. Shepard, and A. T. McPhail, *J. Chem. Soc., Chem. Commun.*, 1390 (1986).
- (143) W. Danzer, W. P. Fehlhammer, A. T. Liu, G. Thiel, and W. Beck, *Chem. Ber.*, **115**, 1682 (1982).
- (144) J. J. Eisch, L. E. Hallenbeck, and K. I. Han, *J. Org. Chem.*, **48**, 2963 (1983).

- (145) H. D. Kaesz, R. B. King, T. A. Manuel, L. D. Nichols, and F. G. A. Stone, *J. Am. Chem. Soc.*, **82**, 4749 (1960).
- (146) A. E. Ogilvy, M. Draganjac, T. B. Rauchfuss, and S. R. Wilson, *Organometallics*, **7**, 1171 (1988).
- (147) G. H. Kosolapoff and L. Maier, "Organic Phosphorus Compounds," 2nd ed, Wiley Interscience, New York, N. Y., 1972, p 130.
- (148) B. M. Mattson, PEEKS 1982 computer program, Creighton University, Omaha, Nebraska, 1982.
- (149) B. R. James and G. L. Rempel, *Can. J. Chem.*, **44**, 233 (1966).
- (150) A. J. Chalk and J. Halpern, *J. Am. Chem. Soc.*, **81**, 5846 (1959).
- (151) P. S. Pregosin, in "Phosphorus 31 NMR Spectroscopy in Stereochemical Analysis," J. G. Verkade and L. D. Quin, Eds., V. C. H. Publishers, Deerfield Beach, Florida, 1987, pp 466-72.
- (152) A. E. Derome, "Modern NMR Techniques for Chemistry Research," Pergamon Press, Oxford, 1987, pp 168-9.
- (153) S. Jans-Burli and P. S. Pregosin, *Magn. Res. in Chem.*, **23**, 198 (1985).
- (154) E. S. Swinbourne, "Analysis of Kinetic Data," Thomas Nelson & Sons, Ltd., London, 1971, pp 79-83.
- (155) G. H. McKinnon, C. J. Backhouse, and A. H. Kalantar, *Int. J. Chem. Kinet.*, **16**, 1427 (1984).
- (156) E. A. Guggenheim, *Philos. Mag.*, **2**, 538 (1926).
- (157) F. J. Kezdy, J. Jaz, and A. Bruylants, *Bull. Soc. Chim. Belg.*, **67**, 687 (1958).
- (158) P. C. Mangelsdorf II, *J. Appl. Phys.*, **30**, 442 (1959).
- (159) E. S. Swinbourne, *J. Chem. Soc.*, 2371 (1960).
- (160) B. Borderie, D. Lavabre, G. Levy, and J. C. Micheau, *J. Chem. Educ.*, **67**, 459 (1990).
- (161) N. C. Thomas, *Coord. Chem. Rev.*, **70**, 121 (1986).
- (162) E. A. Seddon and K. R. Seddon, "The Chemistry of Ruthenium," Elsevier, Amsterdam, 1984, pp 622-647.
- (163) T. A. Stephenson and G. Wilkinson, *J. Inorg. Nucl. Chem.*, **28**, 945 (1966).
- (164) B. R. James, L. D. Markham, B. C. Hui, and G. L. Rempel, *J. Chem. Soc., Dalton Trans.*, 2247 (1973).
- (165) D. R. Fahey, *J. Org. Chem.*, **38**, 80 (1973).

- (166) M. I. Bruce and F. G. A. Stone, *J. Chem. Soc. (A)*, 1238 (1967).
- (167) F. Piacenti, M. Bianchi, E. Benedetti, and G. Braca, *Inorg. Chem.*, **7**, 1815 (1968).
- (168) C. F. J. Barnard, J. A. Daniels, J. Jeffery, and R. J. Mawby, *J. Chem. Soc., Dalton Trans.*, 953 (1976).
- (169) D. W. Krassowski, J. H. Nelson, K. R. Brower, D. Hauenstein, and R. A. Jacobson, *Inorg. Chem.*, **27**, 4294 (1988).
- (170) D. W. Krassowski, K. Reimer, H. E. LeMay Jr., and J. H. Nelson, *Inorg. Chem.*, **27**, 4307 (1988).
- (171) B. E. Mann, B. L. Shaw, and R. E. Stainbank, *J. Chem. Soc., Chem. Commun.*, 151 (1972).
- (172) D. A. Nelson, R. T. Hallen, C.-L. Lee, and B. R. James, in "Recent Developments in Separation Science," Vol. IX, N. N. Li and J. M. Calo, Eds., CRC Press, Boca Raton, Florida, 1986, pp 1-14.
- (173) B. E. Cavit, K. R. Grundy, and W. R. Roper, *J. Chem. Soc. Chem. Commun.*, 60 (1972).
- (174) S. Cenini, F. Porta, and M. Pizzotti, *Inorg. Chim. Acta*, **20**, 119 (1976).
- (175) K. R. Grundy, *Inorg. Chim. Acta*, **53**, L225 (1981).
- (176) E. O. Sherman Jr. and P. R. Schreiner, *J. Chem. Soc., Chem. Commun.*, 3 (1976).
- (177) F. Porta, S. Cenini, S. Giordano, and M. Pizzotti, *J. Organomet. Chem.*, **150**, 261 (1978).
- (178) F. L'Eplattenier and F. Calderazzo, *Inorg. Chem.*, **7**, 1290 (1968).
- (179) J. D. Cotton, M. I. Bruce, and F. G. A. Stone, *J. Chem. Soc. (A)*, 2162 (1968).
- (180) D. S. Moore and S. D. Robinson, *Inorg. Chim. Acta*, **53**, L171 (1981).
- (181) B. R. James and L. D. Markham, *Inorg. Nucl. Chem. Lett.*, **7**, 373 (1971).
- (182) T. W. Dekleva, Ph. D. Thesis, University of British Columbia, Vancouver, B. C., 1983.
- (183) A. J. Joshi and B. R. James, *Organometallics*, **9**, 199 (1990).
- (184) J. Chatt and R. G. Hayter, *J. Chem. Soc.*, 896 (1961).
- (185) J. T. Mague and J. P. Mitchener, *Inorg. Chem.*, **11**, 2714 (1972).
- (186) R. Mason, D. W. Meek, and G. R. Scollary, *Inorg. Chim. Acta*, **16**, L11 (1976).
- (187) a) B. Chaudret, G. Commenges, and R. Poilblanc, *J. Chem. Soc., Dalton Trans.*, 1635 (1984), b) I. P. Evans, A. Spencer, and G. Wilkinson, *J. Chem. Soc., Dalton Trans.*, 204 (1973).
- (188) A. L. Balch, M. M. Olmstead, P. E. Ready, and S. P. Rowley, *Inorg. Chem.*, **27**, 4289 (1988).

- (189) J. Chatt and R. G. Hayter, *J. Chem. Soc.*, 2605 (1961).
- (190) P. Pertici, G. Vitulli, M. Paci, and L. Porri, *J. Chem. Soc., Dalton Trans.*, 1962 (1980).
- (191) G. Rastar, B. Sc. Thesis, University of British Columbia, Vancouver, B. C., 1990.
- (192) R. H. Morris, J. F. Sawyer, M. Shiralian, and J. D. Zubkowski, *J. Am. Chem. Soc.*, **107**, 5581 (1985).
- (193) a) T. J. Marks and W. J. Kennelly, *J. Am. Chem. Soc.*, **97**, 1439 (1975), b) T. J. Marks and J. R. Kolb, *Chem. Rev.*, **77**, 263 (1977).
- (194) T. C. Farrar, R. B. Johannesen, and T. D. Coyle, *J. Chem. Phys.*, **49**, 281 (1968).
- (195) H. D. Empsall, E. Mentzer, and B. L. Shaw, *J. Chem. Soc., Chem. Comm.*, 861 (1975).
- (196) D. G. Holah, A. N. Hughes, B. C. Hui, and K. Wright, *Can. J. Chem.*, **52**, 2990 (1974).
- (197) M. V. Baker and L. D. Field, *J. Chem. Soc., Chem. Commun.*, 996 (1984).
- (198) D. G. Holah, A. N. Hughes, B. C. Hui, and C. T. Kan, *J. Catal.*, **48**, 340 (1977).
- (199) D. G. Holah, A. N. Hughes, B. C. Hui, and K. Wright, *Inorg. Nucl. Chem. Lett.*, **9**, 835 (1973).
- (200) D. G. Holah, A. N. Hughes, and B. C. Hui, *Can. J. Chem.*, **54**, 320 (1976).
- (201) R. H. Crabtree and A. J. Pearman, *J. Organomet. Chem.*, **157**, 335 (1978).
- (202) J. W. Bruno, J. C. Hoffman, and K. G. Caulton, *Inorg. Chim. Acta*, **89**, 167 (1984).
- (203) J. A. Slatter, G. Wilkinson, M. Thornton-Pratt, and M. B. Hursthouse, *J. Chem. Soc., Dalton Trans.*, 8, 1731 (1984).
- (204) H. Werner, M. A. Estervelas, V. Meyer, and B. Wrackmeyer, *Chem. Ber.*, **120**, 11 (1987).
- (205) T. Wilczewski, M. Bochenska, and J. F. Biernat, *J. Organomet. Chem.*, **215**, 87 (1981).
- (206) H. Suzuki, D. H. Lee, N. Oshima, and Y. Moro-uka, *Organometallics*, **6**, 1569 (1987).
- (207) A. K. Chipperfield and C. E. Housecraft, *J. Organomet. Chem.*, **349**, C17 (1988).
- (208) P. S. Hallman, B. R. McGarvey, and G. Wilkinson, *J. Chem. Soc. (A)*, 3143 (1968).
- (209) S. J. Rettig, personal communication, 1989.
- (210) P. Mura, B. G. Olby, and S. D. Robinson, *Inorg. Chim. Acta*, **98**, L21 (1985).
- (211) P. Mura, B. G. Olby, and S. D. Robinson, *J. Chem. Soc., Dalton Trans.*, 2101 (1985).
- (212) S. Jeannin, Y. Jeannin, and G. Lavigne, *Transition Met. Chem.*, **1**, 192 (1976).
- (213) K. Osakada, T. Yamamoto, A. Yamamoto, A. Takenaka, and Y. Sasada, *Inorg. Chim. Acta*, **105**, L9 (1985).

- (214) J. Takacs, L. Marko, and L. Parkanyi, *J. Organomet. Chem.*, **361**, 109 (1989).
- (215) S. M. Boniface, G. R. Clark, T. J. Collins, and W. R. Roper, *J. Organomet. Chem.*, **206**, 109 (1981).
- (216) A. Pidcock, R. E. Richards, and L. M. Venanzi, *J. Chem. Soc. (A)*, 1707 (1966).
- (217) R. A. Sánchez-Delgado, U. Thewalt, N. Valencia, A. Andriollo, R. L. Marquez-Silva, J. Puga, H. Schollhorn, H. P. Klein, and B. Fontal, *Inorg. Chem.*, **25**, 1097 (1986).
- (218) a) A. C. Skapski and P. G. H. Troughton, *J. Chem. Soc., Chem. Commun.*, 1230 (1968), b) R. G. Ball and J. Trotter, *Inorg. Chem.*, **20**, 261 (1981).
- (219) A. E. Keskinen and C. V. Senoff, *J. Organomet. Chem.*, **37**, 201 (1972).
- (220) a) T. Konno, J. R. Kirchhoff, W. R. Heineman, and E. Deutsch, *Inorg. Chem.*, **28**, 1174 (1989), b) P. G. Perkins and F. A. Schultz, *Inorg. Chem.*, **22**, 1133 (1983).
- (221) D. H. Farrar, K. R. Grundy, N. C. Payne, W. R. Roper, and A. Walker, *J. Am. Chem. Soc.*, **101**, 6577 (1979).
- (222) C. L. Young (Ed.), *Solubility Data Series*, **5/6**, IUPAC, Pergamon Press (1981).
- (223) M. S. Chinn and D. M. Heinekey, *J. Am. Chem. Soc.*, **112**, 5166 (1990).
- (224) M. Tilset and V. D. Parker, *J. Am. Chem. Soc.*, **111**, 6711 (1989).
- (225) G. Herzberg, *J. Mol. Spectrosc.*, **33**, 147 (1970).
- (226) M. V. Baker and L. D. Field, *Inorg. Chem.*, **26**, 2010 (1987).
- (227) J. L. Bookham, X. L. R. Fontaine, J. D. Kennedy, and W. McFarlane, *Inorg. Chem.*, **27**, 1111 (1988).
- (228) P. Meakin, E. L. Muetterties, and J. P. Jesson, *J. Am. Chem. Soc.*, **95**, 75 (1973).
- (229) M. T. Bautista, E. P. Cappellani, G. Jia, P. A. Maltby, and R. H. Morris, 1st C.I.C. Congress, Halifax, N. S., July 1990, Paper 231.
- (230) S. E. Boyd, L. D. Field, T. W. Hambley, and D. J. Young, *Inorg. Chem.*, **29**, 1496 (1990).
- (231) M. V. Baker, L. D. Field, and D. J. Young, *J. Chem. Soc., Chem. Comm.*, 546 (1988).
- (232) D. G. Hamilton and R. H. Crabtree, *J. Am. Chem. Soc.*, **110**, 4126 (1988).
- (233) S. Antoniutti, G. Albertin, P. Amendola, and E. Bordignon, *J. Chem. Soc., Chem. Commun.*, 229 (1989).
- (234) A. J. Joshi and B. R. James, *J. Chem. Soc., Chem. Commun.*, 1785 (1989).
- (235) G. Jia and R. H. Morris, *Inorg. Chem.*, **29**, 581 (1990).

- (236) M. S. Chinn, D. M. Heinekey, N. G. Payne, and C. D. Sofield, *Organometallics*, **8**, 1824 (1989).
- (237) A. P. Ginsberg, *Trans. Met. Chem.*, **1**, 111 (1965).
- (238) G. Valensi, J. van Muylder, and M. Pourbaix in "Atlas d'Equilibres Electrochimiques," M. Pourbaix, Ed., Gauthier-Villars, Paris & Co., 1963, p 546.
- (239) M. M. Kreevoy, E. T. Harper, R. E. Duvall, H. S. Wilgus III, and L. T. Ditsch, *J. Am. Chem. Soc.*, **82**, 4899 (1960).
- (240) D. R. Lide, Ed., "Handbook of Chemistry and Physics," 71st ed, CRC Press, Boca Raton, Florida, 1990, p 8-37.
- (241) H. L. Loy and D. M. Himmelbau, *J. Phys. Chem.*, **65**, 264 (1961).
- (242) A. Ohno and S. Oae, in "Organic Chemistry of Sulfur," Plenum Press, New York, N. Y., 1977, Chapter 4, p 122.
- (243) J. A. Dean, Ed., "Lange's Handbook of Chemistry," 13th ed, McGraw Hill Book Co., New York, N. Y., 1985, pp 5-18 to 5-60.
- (244) J. P. Danehy and C. J. Noel, *J. Am. Chem. Soc.*, **82**, 2511 (1960).
- (245) W. P. Jencks and K. Salvesen, *J. Am. Chem. Soc.*, **93**, 4433 (1971).
- (246) G. Schwarzenbach and H. Egli, *Helv. Chim. Acta.*, **17**, 1176 (1934).
- (247) L. Que Jr., M. A. Bobrik, J. A. Ibers, and R. H. Holm, *J. Am. Chem. Soc.*, **96**, 4168 (1974).
- (248) G. R. Dukes and R. H. Holm, *J. Am. Chem. Soc.*, **97**, 528 (1975).
- (249) D. Sellman, I. Barth, and M. Moll, *Inorg. Chem.*, **29**, 176 (1990).
- (250) P. Frediani, M. Bianchi, A. Salvini, and F. Piacenti, 6th Int'l. Symp. on Homog. Cat., 1988, Vancouver, B. C., Poster P-137.
- (251) M. V. Baker, L. D. Field, and D. J. Young, *J. Chem. Soc., Chem. Commun.*, 546 (1988).
- (252) A. R. Siedle, R. A. Newmark, G. A. Korba, L. H. Pignolet, and P. D. Boyle, *Inorg. Chem.*, **27**, 1593 (1988).
- (253) M. Bautista, K. A. Earl, R. H. Morris, and A. Sella, *J. Am. Chem. Soc.*, **109**, 3780 (1987).
- (254) C.-L. Lee and B. R. James, unpublished results.
- (255) P. G. T. Fogg and C. L. Young, (Eds.), *Solubility Data Series*, **32**, IUPAC, Pergamon Press, Oxford, 1988.
- (256) C. Capellos and B. H. J. Bielski, "Kinetic Systems," Robert E. Krieger Publishing Co., Huntington, N. Y., 1980, pp 46-58.
- (257) a) J. P. Collman and W. R. Roper, *J. Am. Chem. Soc.*, **88**, 3504 (1966), b) J. P. Collman and W. R. Roper, *J. Am. Chem. Soc.*, **87**, 4008 (1965), c) S. D. Robinson and M. F.

Uttley, *J. Chem. Soc., Dalton Trans.*, 1912 (1973), d) M. Rotem, Z. Stein, and Y. Shvo, *J. Organomet. Chem.*, **387**, 95 (1990), e) A. Ouedeman, F. van Rantwijk, and H. van Bekkum, *J. Coord. Chem.*, **4**, 1 (1974).

- (258) a) M. Prystay, C.-L. Lee, P. Jessop, and B. R. James, unpublished results, b) M. Prystay, B. Sc. Thesis, University of British Columbia, 1988.
- (259) a) TEXSAN/TEXRAY structural analysis package which includes versions of the following: DIRDIF, direct methods for difference structures, by P. T. Beurskens; ORFLS, full matrix least squares, and ORFFE, function and errors, by W. R. Busing, K. O. Martin, and H. A. Levy; ORTEP II, illustrations, by C. K. Johnson, b) "International Tables for X-ray Crystallography," Vol. IV, Kynoch Press, Birmingham, U. K., (present distributor: Kluwer Academic Publishers, Dordrecht, The Netherlands), 1974, pp 99-102 and 149.
- (260) a) R. M. Catala, D. Cruz-Garriz, P. Terreros, H. Torrens, A. Hills, D. L. Hughes, and R. L. Richards, *J. Organomet. Chem.*, **328**, C37 (1987), b) R. M. Catala, D. Cruz-Garriz, H. Torrens, and R. L. Richards, *J. Organomet. Chem.*, **354**, 123 (1988), c) R. M. Catala, D. Cruz-Garriz, A. Hills, D. L. Hughes, R. L. Richards, P. Sosa, and H. Torrens, *J. Chem. Soc., Chem. Commun.*, 261 (1987), d) D. Cruz-Garriz, P. Sosa, H. Torrens, A. Hills, D. L. Hughes, and R. L. Richards, *J. Chem. Soc., Dalton Trans.*, 419 (1989).
- (261) M. Campredon, J. M. Kanabus-Kaminska, and D. Griller, *J. Org. Chem.*, **53**, 5393 (1988).
- (262) L. E. Overman, D. Matzinger, E. M. O'Connor, and J. D. Overman, *J. Am. Chem. Soc.*, **96**, 6081 (1974).
- (263) M. M. Crutchfield, C. H. Dungan, and J. R. VanWazer, *Top. Phosphorus Chem.*, **5**, 1 (1967).
- (264) C.-L. Lee, B. R. James, C. J. L. Lock, and R. Faggiani, unpublished results.
- (265) P. J. Blower and J. R. Dilworth, *Coord. Chem. Rev.*, **76**, 121 (1987).
- (266) J. Chisholm, C.-L. Lee, and B. R. James, unpublished results.
- (267) R. C. Weast (Ed.), *CRC Handbook of Chemistry and Physics*, 63rd edition, Chemical Rubber Co.; Baton Rouge, Florida, 1982.
- (268) D. Coucouvanis, M. Kanatzidis, E. Simhon, and N. C. Baenziger, *J. Am. Chem. Soc.*, **104**, 1874 (1982).
- (269) D. N. Harpp and R. A. Smith, *J. Am. Chem. Soc.*, **104**, 6045 (1982).
- (270) A. Shaver, P.-Y. Plouffe, P. Bird, and E. Livingstone, *Inorg. Chem.*, **29**, 1826 (1990).
- (271) J. Amarasekera, T. B. Rauchfuss, and S. R. Wilson, *J. Chem. Soc., Chem. Commun.*, 14 (1989).
- (272) B. R. Hollebhone and R. S. Nyholm, *J. Chem. Soc. (A)*, 332 (1971).
- (273) H. Funk and M. Hessebarth, *Z. Chem.*, **6**, 227 (1966).
- (274) A. L. Balch and Y. S. Sohn, *J. Organomet. Chem.*, **30**, C31 (1971).

- (275) A. Y. Girgis, Y. S. Sohn, and A. L. Balch, *Inorg. Chem.*, **14**, 2327 (1975).
- (276) R. M. Catala, D. Cruz-Garriz, P. Sosa, P. Terreros, H. Torrens, A. Hills, D. L. Hughes, and R. L. Richards, *J. Organomet. Chem.*, **359**, 219 (1989).
- (277) F. A. Bovey, "Nuclear Magnetic Resonance Spectroscopy," Academic Press, New York, N. Y., 1969, p 94.
- (278) E. Weiss and U. Joergens, *Chem. Ber.*, **105**, 481 (1972).
- (279) S. J. Opella and M. H. Frey, *J. Am. Chem. Soc.*, **101**, 5854 (1979).
- (280) E. P. Clark, *Ind. Eng. Chem., Anal. Ed.*, **13**, 820 (1941).
- (281) P. C. Ellgen and J. N. Gerlach, *Inorg. Chem.*, **12**, 2526 (1973).
- (282) G. Natile, L. Maresca, and G. Bor, *Inorg. Chim. Acta*, **23**, 37 (1977).
- (283) X. Q. Lu, C. Y. Zhu, L. C. Song, and Y. T. Chen, *Inorg. Chim. Acta*, **143**, 55 (1988).
- (284) J. Jeffery and R. J. Mawby, *J. Organomet. Chem.*, **40**, C42 (1972).
- (285) M. J. Cleare and W. P. Griffith, *J. Chem. Soc. (A)*, 372 (1969).
- (286) R. Colton and R. H. Farthing, *Aust. J. Chem.*, **24**, 903 (1971).
- (287) P. W. Armit, W. J. Sime, and T. A. Stephenson, *J. Chem. Soc., Dalton Trans.*, 2121 (1976).
- (288) M. Draganjac, S. Dhingra, S.-P. Huang, and M. G. Kanatzidis, *Inorg. Chem.*, **29**, 590 (1990).
- (289) a) M. I. Bruce, O. B. Shawkataly, and B. K. Nicholson, *J. Organomet. Chem.*, **286**, 427 (1985), b) T. A. Creswell, J. A. K. Howard, F. G. Kennedy, S. A. R. Knox, and H. Wadepohl, *J. Chem. Soc., Dalton Trans.*, 2220 (1981).
- (290) H. Schumann, I. Albrecht, and E. Hahn, *Angew. Chem., Int. Ed. Engl.*, **24**, 985 (1985).
- (291) H. Schumann, I. Albrecht, M. Gallagher, E. Hahn, C. Muchmore, and J. Pickardt, *J. Organomet. Chem.*, **349**, 103 (1988).
- (292) K. Tatsumi, I. Matsubara, Y. Inoue, A. Nakamura, R. E. Cramer, G. J. Tagoshi, J. A. Golen, and J. W. Gilje, *Inorg. Chem.*, **29**, 4928 (1990).
- (293) S.-M. Koo, R. Bergero, A. Salifoglou, and D. Coucouvanis, *Inorg. Chem.*, **29**, 4844 (1990).
- (294) a) D. C. Bradley, R. C. Mehrotra, and D. P. Gaur, "Metal Alkoxides," Academic Press, Inc., London, 1978, pp 299-334, b) K. G. Caulton and L. G. Hubert-Pfalsgraf, *Chem. Rev.*, **90**, 969 (1990).

- (295) D. Williams, M. Hampden-Smith, A. Rheingold, C. Peden, and D. Doughty, personal communication, as reported in K. G. Caulton and L. G. Hubert-Pfalzgraf, *Chem. Rev.*, **90**, 969 (1990).
- (296) S. R. Cooper, *Acc. Chem. Res.*, **21**, 141 (1988).
- (297) M. R. Truter, *Struct. Bonding (Berlin)*, **16**, 71 (1973).
- (298) F. P. van Remoortere and F. P. Boer, *Inorg. Chem.*, **13**, 2071 (1974).
- (299) F. P. Boer, M. A. Neuman, F. P. van Remoortere, and E. C. Steiner, *Inorg. Chem.*, **13**, 2826 (1974).
- (300) A. I. Popov and J. M. Lehn, in "Coordination Chemistry of Macrocyclic Compounds," G. A. Melson (Ed.), Plenum Press, New York, N. Y., 1979, Chapter 9.
- (301) G. Rastar, P. G. Jessop, and B. R. James, unpublished results.
- (302) C. Bianchini, P. J. Perez, M. Peruzzini, F. Zanobini, A. Vacca, *Inorg. Chem.*, **30**, 279 (1991).
- (303) R. J. Angelici, *Coord. Chem. Rev.*, **105**, 61 (1990).
- (304) K. Osakada, T. Yamamoto, and A. Yamamoto, *Inorg. Chim. Acta*, **90**, L5 (1984).
- (305) T. V. Ashworth, M. J. Nolte, and E. Singleton, *J. Chem. Soc., Chem. Commun.*, 936 (1977).
- (306) A. J. Shultz and R. Eisenberg, *Inorg. Chem.*, **12**, 518 (1973).
- (307) M. Schroder and T. A. Stephenson, in "Comprehensive Coordination Chemistry," G. Wilkinson (Ed.), Pergamon Press, Oxford, 1987, pp 410-3.
- (308) E. Babaian-Kibala, F. A. Cotton, and P. A. Kibala, *Inorg. Chem.*, **29**, 4002 (1990).
- (309) J. L. Wardell, in "The Chemistry of the Thiol Group," Part 1, S. Patai (Ed.), John Wiley & Sons, London, 1974, pp 220-229.
- (310) H. Inoue and S. Tamura, *Chem. Comm.*, 858 (1986).
- (311) A. Holmgren, *J. Biol. Chem.*, **254**, 9627 (1979).
- (312) K. Sakata, S. Wada, and M. Hashimoto, *Inorg. Chim. Acta*, **148**, 7, (1988).
- (313) D. H. J. Carlson, U. S. Patent 4,206,043 (1980), as reported in *Chem. Abstr.* **108**:93920m.
- (314) V. D. Tyurin, S. P. Gubin, and N. S. Nametkin, *Proc. World Pet. Congr.*, **5**, 217 (1975).
- (315) B. A. Sexton and G. L. Nyberg, *Surf. Sci.*, **165**, 251 (1986).
- (316) L. D. Nell and S. C. Kitching, *J. Phys. Chem.*, **78**, 1648 (1974).
- (317) R. J. Koesher, J. Stohr, J. L. Gland, E. B. Kollin, and F. Sette, *Chem. Phys. Lett.*, **120**, 285 (1985).

- (318) M. R. Albert, J. P. Lu, S. L. Bernasek, S. D. Cameron, and J. L. Gland, *Surf. Sci.*, **206**, 348 (1988).
- (319) D. L. Seymour, S. Bao, C. F. McConville, M. D. Crapper, D. P. Woodruff, and R. G. Jones, *Surf. Sci.*,
- (320) G. B. Fisher, *Surf. Sci.*, **87**, 215 (1979).
- (321) J. E. Hoots and T. B. Rauchfuss, *Inorg. Chem.*, **22**, 2806 (1983).
- (322) K. Leonard, K. Plute, R. C. Haltiwanger, and M. R. DuBois, *Inorg. Chem.*, **18**, 3246 (1979).
- (323) B. Chaudret, F. Dahan, and S. Sabo, *Organometallics*, **4**, 1490 (1985).
- (324) M. Curtis and P. D. Williams, *Inorg. Chem.*, **22**, 2661 (1983).
- (325) H. Brunner and J. Wachter, *J. Organomet. Chem.*, **240**, C41 (1982).
- (326) M. D. Curtis, P. D. Williams, and W. M. Butler, *Inorg. Chem.*, **27**, 2853 (1988).

APPENDIX 1: SUMMARY OF CRYSTALLOGRAPHIC DATA

compound	9b	14b·THF	21
formula	$C_{45}H_{38}O_2P_2RuS$	$C_{36}H_{32}O_3P_2RuS_2$	$C_{60}H_{76}Na_2O_6P_2Ru_2S_6$
fw	804.86	928.06	1395.68
color, habit	yellow, irregular	yellow, prism	yellow, prism
crystal size, mm	0.30 x 0.35 x 0.50	0.15 x 0.22 x 0.46	0.10 x 0.15 x 0.35
crystal system	triclinic	triclinic	triclinic
space group	$P\bar{1}$	$P\bar{1}$	$P\bar{1}$
<i>a</i> , Å	12.340(4)	13.173(3)	12.189(3)
<i>b</i> , Å	14.948(3)	19.766(4)	13.124(3)
<i>c</i> , Å	10.684(4)	9.770(4)	12.032(4)
α , deg	90.05(3)	98.26(2)	99.70(2)
β , deg	99.27(3)	91.24(3)	110.61(2)
γ , deg	86.84(3)	78.31(2)	67.95(2)
<i>V</i> , Å ³	1942(1)	2465(1)	1668.4(8)
<i>Z</i>	2	2	1
ρ_{calc} , g/cm ³	1.38	1.25	1.39
<i>F</i> (000)	826	956	720
μ (Mo K_{α}), cm ⁻¹	5.63	4.91	7.27
transmission factors	0.947-1.00	0.926-1.00	0.946-1.00
scan type	ω -2 θ	ω -2 θ	ω -2 θ
scan range, deg in ω	1.31+0.35 tan θ	1.16+0.35 tan θ	1.26+0.35 tan θ
scan speed, deg/min	32	32	16
data collected	+ <i>h</i> , ± <i>k</i> , ± <i>l</i>	+ <i>h</i> , ± <i>k</i> , ± <i>l</i>	+ <i>h</i> , ± <i>k</i> , ± <i>l</i>
2 θ_{max} deg	60	50	55

cryst decay	negligible	negligible	12.0%
total no. of reflections	11794	9129	7986
no. of unique reflections	11310	8713	7627
R_{merge}	0.022	0.074	0.040
no. of reflcns with $I > 3\sigma(I)$	7174	3597	4252
no. of variables	464	577	352
R	0.032	0.041	0.039
R_w	0.037	0.043	0.043
gof	1.28	1.17	1.43
max Δ/σ (final cycle)	0.14	0.06	0.02
residual density $e/\text{\AA}^3$	0.55	0.54	0.84 (near Ru)

^a Temperature 294 K, Rigaku AFC6S diffractometer, Mo K_{α} radiation ($\lambda = 0.71069 \text{ \AA}$), graphite monochromator, takeoff angle 6.0° , aperture $6.0 \times 6.0 \text{ mm}$ at a distance of 285 mm from the crystal, stationary background counts at each end of the scan (scan/background time ratio 2:1), $\sigma^2(F^2) = [S^2(C + 4B) + (pF^2)^2]/Lp^2$ (S - scan rate, C - scan count, B - normalized background count, $p = 0.035$ for 1, 0.040 for 2, and 0.030 for 3), function minimized $\sum w(|F_o| - |F_c|)^2$ where $w = 4F_o^2/\sigma^2(F_o^2)$, $R = \sum ||F_o| - |F_c||/\sum |F_o|$, $R_w = (\sum w(|F_o| - |F_c|)^2/\sum w|F_o|^2)^{1/2}$, and $\text{gof} = [\sum (|F_o| - |F_c|)^2/(m-n)]^{1/2}$. Values given for R , R_w , and gof are based on those reflections with $I \geq 3\sigma(I)$.

APPENDIX 2: ATOMIC COORDINATES FOR
cis-RuH(SC₆H₄pCH₃)(CO)₂(PPh₃)₂ (9b)

Table A2.1 Final atomic coordinates (fractional) and B(eq).

atom	x	y	z	B (eq)
Ru	0.39625(2)	0.23433(1)	0.36310(2)	2.663(7)
S	0.30451(6)	0.28651(5)	0.15245(6)	4.10(3)
P(1)	0.21506(5)	0.22674(4)	0.40562(5)	2.80(2)
P(2)	0.57093(5)	0.25962(4)	0.30634(6)	2.89(2)
O(1)	0.4931(2)	0.2198(2)	0.6397(2)	6.4(1)
O(2)	0.4235(2)	0.0331(2)	0.3080(3)	7.2(1)
C(1)	0.4578(2)	0.2206(2)	0.5347(3)	4.0(1)
C(2)	0.4098(2)	0.1080(2)	0.3212(3)	4.1(1)
C(3)	0.1218(2)	0.3258(2)	0.3689(2)	3.3(1)
C(4)	0.1576(2)	0.4095(2)	0.4061(3)	4.6(1)
C(5)	0.0893(3)	0.4860(2)	0.3786(3)	5.8(2)
C(6)	-0.0150(3)	0.4796(2)	0.3142(3)	5.7(2)
C(7)	-0.0512(3)	0.3979(2)	0.2761(3)	5.2(2)
C(8)	0.0166(2)	0.3206(2)	0.3025(3)	4.3(1)
C(9)	0.2141(2)	0.2017(2)	0.5736(2)	3.4(1)
C(10)	0.1798(3)	0.2634(2)	0.6568(3)	5.2(1)
C(11)	0.1915(4)	0.2409(3)	0.7859(3)	7.5(2)
C(12)	0.2354(4)	0.1593(3)	0.8294(3)	7.1(2)
C(13)	0.2689(3)	0.0976(3)	0.7477(3)	5.8(2)
C(14)	0.2595(2)	0.1183(2)	0.6206(3)	4.5(1)
C(15)	0.1332(2)	0.1371(2)	0.3287(2)	2.97(9)
C(16)	0.0491(2)	0.1047(2)	0.3843(2)	3.6(1)
C(17)	-0.0176(2)	0.0407(2)	0.3233(3)	4.2(1)
C(18)	0.0003(2)	0.0078(2)	0.2084(3)	4.4(1)
C(19)	0.0836(2)	0.0391(2)	0.1526(3)	4.5(1)
C(20)	0.1499(2)	0.1038(2)	0.2119(2)	3.7(1)

Table A2.1 (cont.)

atom	x	y	z	B(eq)
C(21)	0.5932(2)	0.3756(2)	0.2689(2)	3.2(1)
C(22)	0.5912(2)	0.4398(2)	0.3638(3)	4.1(1)
C(23)	0.6022(3)	0.5293(2)	0.3375(3)	5.3(1)
C(24)	0.6153(3)	0.5558(2)	0.2174(4)	5.8(2)
C(25)	0.6170(3)	0.4934(2)	0.1246(3)	5.5(2)
C(26)	0.6069(2)	0.4032(2)	0.1495(3)	4.2(1)
C(27)	0.6091(2)	0.1954(2)	0.1718(2)	3.5(1)
C(28)	0.7179(2)	0.1726(2)	0.1651(3)	4.5(1)
C(29)	0.7471(3)	0.1263(2)	0.0624(3)	5.3(2)
C(30)	0.6689(3)	0.1019(3)	-0.0343(3)	6.1(2)
C(31)	0.5628(3)	0.1239(4)	-0.0291(4)	9.3(3)
C(32)	0.5318(3)	0.1698(3)	0.0737(4)	7.6(2)
C(33)	0.6875(2)	0.2290(2)	0.4309(2)	3.1(1)
C(34)	0.7742(2)	0.2838(2)	0.4650(3)	4.1(1)
C(35)	0.8616(2)	0.2563(2)	0.5575(3)	5.0(1)
C(36)	0.8636(2)	0.1755(2)	0.6177(3)	4.9(1)
C(37)	0.7784(3)	0.1196(2)	0.5830(3)	4.8(1)
C(38)	0.6909(2)	0.1465(2)	0.4907(3)	4.1(1)
C(39)	0.2654(2)	0.4023(2)	0.1460(2)	3.6(1)
C(40)	0.3239(2)	0.4682(2)	0.2124(3)	4.6(1)
C(41)	0.2911(3)	0.5577(2)	0.1958(3)	5.3(2)
C(42)	0.1987(3)	0.5857(2)	0.1115(3)	5.4(2)
C(43)	0.1404(3)	0.5200(2)	0.0443(3)	5.4(2)
C(44)	0.1715(2)	0.4300(2)	0.0611(3)	4.5(1)
C(45)	0.1629(4)	0.6837(3)	0.0915(4)	8.2(2)
H(1)	0.390(2)	0.736(2)	0.405(3)	5.4(7)

Table A2.2 Calculated hydrogen coordinates and B(iso).

atom	x	y	z	B(iso)
H(2)	0.2323	0.4146	0.4525	5.5
H(3)	0.1158	0.5447	0.4053	6.9
H(4)	-0.0636	0.5336	0.2955	6.9
H(5)	-0.1259	0.3936	0.2294	6.3
H(6)	-0.0103	0.2623	0.2740	5.1
H(7)	0.1477	0.3223	0.6261	6.2
H(8)	0.1675	0.2846	0.8456	9.0
H(9)	0.2432	0.1447	0.9199	8.5
H(10)	0.2995	0.0385	0.7793	7.0
H(11)	0.2850	0.0741	0.5626	5.4
H(12)	0.0365	0.1271	0.4673	4.3
H(13)	-0.0777	0.0189	0.3628	5.1
H(14)	-0.0463	-0.0379	0.1660	5.2
H(15)	0.0964	0.0156	0.0702	5.4
H(16)	0.2089	0.1260	0.1710	4.5
H(17)	0.5818	0.4215	0.4493	5.0
H(18)	0.6007	0.5739	0.4045	6.4
H(19)	0.6234	0.6190	0.1990	7.0
H(20)	0.6255	0.5123	0.0391	6.6
H(21)	0.6095	0.3591	0.0820	5.1
H(22)	0.7753	0.1894	0.2341	5.4
H(23)	0.8249	0.1109	0.0592	6.4
H(24)	0.6897	0.0687	-0.1067	7.3
H(25)	0.5062	0.1073	-0.0992	11.2
H(26)	0.4537	0.1840	0.0761	9.1
H(27)	0.7737	0.3423	0.4234	4.9

Table A2.2 (cont.)

atom	x	y	z	B(iso)
H(28)	0.9229	0.2953	0.5801	6.0
H(29)	0.9247	0.1573	0.6848	5.8
H(30)	0.7800	0.0608	0.6241	5.7
H(31)	0.6306	0.1067	0.4673	5.0
H(32)	0.3903	0.4509	0.2728	5.6
H(33)	0.3345	0.6025	0.2451	6.3
H(34)	0.0750	0.5377	-0.0173	6.5
H(35)	0.1271	0.3852	0.0130	5.4
H(36)	0.0973	0.6971	0.1306	9.8
H(37)	0.2223	0.7205	0.1305	9.8
H(38)	0.1458	0.6969	0.0004	9.8

APPENDIX 3: ATOMIC COORDINATES FOR
***cct*-Ru(SC₆H₄pCH₃)₂(CO)₂(PPh₃)₂ (14b)**

Table A3.1 Final atomic coordinates (fractional) and B(eq).

atom	x	y	z	B(eq)
Ru	0.13050(5)	0.21874(4)	0.32473(7)	2.66(3)
S(1)	0.1587(2)	0.2929(1)	0.1517(2)	3.6(1)
S(2)	0.1947(2)	0.1238(1)	0.1380(2)	3.7(1)
P(1)	0.3056(2)	0.2177(1)	0.4135(2)	3.0(1)
P(2)	-0.0436(1)	0.2150(1)	0.2351(2)	3.0(1)
O(1)	0.1126(4)	0.1136(3)	0.5150(5)	4.7(3)
O(2)	0.0592(5)	0.3329(3)	0.5611(6)	5.8(4)
O(3)	0.468(2)	0.4670(8)	0.171(1)	17(1)
C(1)	0.1182(5)	0.1515(4)	0.4409(7)	2.8(4)
C(2)	0.0858(6)	0.2920(4)	0.4664(8)	3.7(4)
C(3)	0.4197(6)	0.1805(4)	0.3016(7)	3.1(4)
C(4)	0.5130(6)	0.1487(4)	0.3539(8)	4.0(4)
C(5)	0.5985(6)	0.1260(4)	0.269(1)	4.4(5)
C(6)	0.5928(7)	0.1344(5)	0.132(1)	5.3(5)
C(7)	0.4999(7)	0.1665(5)	0.0802(8)	5.7(5)
C(8)	0.4141(6)	0.1897(4)	0.1632(8)	4.0(4)
C(9)	0.3199(5)	0.1696(4)	0.5599(7)	3.3(4)
C(10)	0.2799(6)	0.2019(5)	0.6875(8)	4.5(5)
C(11)	0.2801(7)	0.1658(6)	0.7988(8)	5.3(6)
C(12)	0.3212(7)	0.0952(6)	0.781(1)	5.6(6)
C(13)	0.3582(7)	0.0613(5)	0.656(1)	5.5(6)
C(14)	0.3578(6)	0.0981(4)	0.5434(8)	4.2(5)
C(15)	0.3422(5)	0.3006(4)	0.4846(8)	3.5(4)
C(16)	0.3114(6)	0.3580(5)	0.4167(9)	4.9(5)
C(17)	0.3456(8)	0.4199(4)	0.462(1)	6.1(6)

Table A3.1 (cont.)

atom	x	y	z	B(eq)
C(18)	0.4094(7)	0.4233(5)	0.576(1)	6.0(6)
C(19)	0.4409(7)	0.3663(5)	0.641(1)	5.3(5)
C(20)	0.4077(6)	0.3058(4)	0.5967(8)	4.3(5)
C(21)	-0.0744(6)	0.2335(4)	0.0578(7)	3.5(4)
C(22)	-0.0051(6)	0.2043(4)	-0.0495(8)	4.2(5)
C(23)	-0.0286(8)	0.2187(5)	-0.1814(9)	5.7(6)
C(24)	-0.1201(9)	0.2626(6)	-0.210(1)	6.6(7)
C(25)	-0.1890(7)	0.2895(5)	-0.104(1)	6.4(6)
C(26)	-0.1681(7)	0.2761(4)	0.0285(9)	4.9(5)
C(27)	-0.0793(5)	0.1302(4)	0.2372(7)	3.0(4)
C(28)	-0.0908(5)	0.1079(4)	0.3650(7)	3.1(4)
C(29)	-0.1096(6)	0.0423(4)	0.3712(8)	3.8(4)
C(30)	-0.1175(6)	-0.0024(4)	0.2516(9)	4.3(5)
C(31)	-0.1109(6)	0.0202(4)	0.1263(8)	3.9(4)
C(32)	-0.0910(6)	0.0858(4)	0.1178(7)	3.7(4)
C(33)	-0.1476(6)	0.2759(4)	0.3352(7)	3.4(4)
C(34)	-0.1390(6)	0.3446(4)	0.3693(9)	4.7(5)
C(35)	-0.2148(7)	0.3936(4)	0.447(1)	6.3(6)
C(36)	-0.3008(7)	0.3731(5)	0.489(1)	6.5(6)
C(37)	-0.3127(7)	0.3065(5)	0.452(1)	6.4(6)
C(38)	-0.2367(6)	0.2580(4)	0.3773(9)	4.6(5)
C(39)	0.0664(5)	0.3736(4)	0.1657(8)	3.4(4)
C(40)	0.0598(6)	0.4250(4)	0.2810(8)	4.2(5)
C(41)	-0.0121(7)	0.4859(4)	0.2860(9)	4.7(5)
C(42)	-0.0824(7)	0.4983(4)	0.180(1)	4.8(5)
C(43)	-0.0731(7)	0.4186(5)	0.0676(9)	5.2(5)

Table A3.1 (cont.)

atom	x	y	z	B(eq)
C(44)	-0.0002(7)	0.3862(4)	0.0576(8)	4.4(5)
C(45)	-0.1646(8)	0.5640(5)	0.187(1)	7.6(7)
C(46)	0.2398(5)	0.0419(4)	0.1963(7)	3.1(4)
C(47)	0.1718(6)	0.0026(4)	0.2349(8)	3.8(4)
C(48)	0.2081(7)	-0.0649(4)	0.2640(7)	4.5(5)
C(49)	0.3116(8)	-0.0948(4)	0.2585(9)	4.9(5)
C(50)	0.3789(7)	-0.0552(5)	0.224(1)	5.9(5)
C(51)	0.3448(6)	0.0120(4)	0.1916(8)	4.5(5)
C(52)	0.3501(9)	-0.1673(5)	0.289(1)	8.1(7)
C(53)	0.551(2)	0.409(2)	0.149(3)	21(2)
C(54)	0.523(2)	0.357(1)	0.069(4)	25(3)
C(55)	0.418(2)	0.369(1)	0.050(2)	16(2)
C(56)	0.389(2)	0.442(2)	0.084(3)	18(2)

Table A3.2 Calculated hydrogen coordinates and B(iso).

atom	x	y	z	B(iso)
H(1)	0.5181	0.1423	0.4517	4.8
H(2)	0.6643	0.1036	0.3066	5.3
H(3)	0.6539	0.1180	0.0715	6.3
H(4)	0.4953	0.1727	-0.0176	6.8
H(5)	0.3488	0.2127	0.1253	4.8
H(6)	0.2505	0.2521	0.6997	5.4
H(7)	0.2514	0.1900	0.8886	6.3
H(8)	0.3239	0.0692	0.8597	6.7
H(9)	0.3852	0.0108	0.6437	6.6
H(10)	0.3844	0.0733	0.4531	5.0
H(11)	0.2656	0.3553	0.3366	5.9
H(12)	0.3243	0.4606	0.4137	7.3
H(13)	0.4323	0.4669	0.6091	7.2
H(14)	0.4874	0.3688	0.7205	6.3
H(15)	0.4308	0.2653	0.6451	5.2
H(16)	0.0606	0.1734	-0.0315	5.0
H(17)	0.0205	0.1974	-0.2569	6.8
H(18)	-0.1349	0.2741	-0.3037	8.0
H(19)	-0.2553	0.3192	-0.1235	7.7
H(20)	-0.2189	0.2963	0.1026	5.9
H(21)	-0.0854	0.1393	0.4508	3.7
H(22)	-0.1173	0.0274	0.4612	4.5
H(23)	-0.1279	-0.0498	0.2558	5.2
H(24)	-0.1204	-0.0106	0.0411	4.6
H(25)	-0.0852	0.1005	0.0271	4.4

Table A3.2 (cont.)

atom	x	y	z	B(iso)
H(26)	-0.0778	0.3594	0.3381	5.7
H(27)	-0.2067	0.4421	0.4707	7.6
H(28)	-0.3539	0.4066	0.5458	7.8
H(29)	-0.3760	0.2927	0.4786	7.7
H(30)	-0.2461	0.2098	0.3537	5.5
H(31)	0.1069	0.4174	0.3588	5.1
H(32)	-0.0140	0.5218	0.3668	5.7
H(33)	-0.1198	0.4569	-0.0104	6.2
H(34)	0.0036	0.3516	-0.0258	5.3
H(35)	-0.2293	0.5559	0.2231	9.1
H(36)	-0.1764	0.5769	0.0937	9.1
H(37)	-0.1417	0.6018	0.2476	9.1
H(38)	0.0974	0.0227	0.2418	4.6
H(39)	0.1583	-0.0918	0.2891	5.4
H(40)	0.4534	-0.0748	0.2215	7.0
H(41)	0.3951	0.0384	0.1656	5.4
H(42)	0.3270	-0.2005	0.2171	9.7
H(43)	0.4261	-0.1770	0.2921	9.7
H(44)	0.3226	-0.1720	0.3791	9.7
H(45)	0.6089	0.4225	0.1040	24.7
H(46)	0.5749	0.3944	0.2381	24.7
H(47)	0.5576	0.3497	-0.0205	29.9
H(48)	0.5427	0.3145	0.1133	29.9
H(49)	0.4014	0.3545	-0.0471	19.4
H(50)	0.3837	0.3453	0.1102	19.4

Table A3.2 (cont.)

atom	x	y	z	B(iso)
H(51)	0.3224	0.4548	0.1348	21.2
H(52)	0.3818	0.4648	0.0003	21.2

**APPENDIX 4: ATOMIC COORDINATES FOR
 [(CO)₂(PPh₃)₂Ru(SEt)₃Na(THF)₂ (21)**

Table A4.1 Final atomic coordinates (fractional) and B(eq).

atom	x	y	z	B _{eq}
Ru(1)	0.56768(4)	0.18197(3)	0.28424(3)	3.26(2)
S(1)	0.7506(1)	0.0165(1)	0.3369(1)	6.05(8)
S(2)	0.4531(1)	0.0666(1)	0.1457(1)	4.04(6)
S(3)	0.6480(1)	0.1922(1)	0.1263(1)	4.12(6)
P(1)	0.3992(1)	0.34358(8)	0.2063(1)	3.15(6)
Na(1)	0.6960(2)	-0.0365(2)	0.0905(2)	5.0(1)
O(1)	0.7373(4)	0.2883(3)	0.4683(3)	7.3(2)
O(2)	0.4763(4)	0.1566(3)	0.4777(3)	7.2(3)
O(3)	0.9066(4)	-0.1109(4)	0.0945(4)	8.9(3)
C(1)	0.4439(4)	0.4662(3)	0.2257(4)	3.2(2)
C(2)	0.4975(4)	0.5018(4)	0.3398(4)	3.9(2)
C(3)	0.5348(5)	0.5925(4)	0.3598(4)	4.9(3)
C(4)	0.5178(5)	0.6478(4)	0.2649(5)	5.4(3)
C(5)	0.4661(5)	0.6135(4)	0.1512(5)	5.5(3)
C(6)	0.4279(4)	0.5225(4)	0.1305(4)	4.0(2)
C(7)	0.2778(4)	0.3828(4)	0.2776(4)	3.6(2)
C(8)	0.2392(4)	0.4810(4)	0.3404(4)	4.2(3)
C(9)	0.1514(5)	0.4991(5)	0.3966(5)	5.8(3)
C(10)	0.1005(5)	0.4206(6)	0.3879(5)	6.4(4)
C(11)	0.1359(5)	0.3232(5)	0.3245(6)	6.3(4)
C(12)	0.2237(5)	0.3051(4)	0.2698(5)	5.0(3)
C(13)	0.3039(4)	0.3465(3)	0.0488(4)	3.4(2)
C(14)	0.1887(4)	0.4310(4)	0.0119(4)	4.5(3)
C(15)	0.1163(5)	0.4402(4)	-0.1058(5)	5.5(3)

Table A4.1 (cont.)

atom	x	y	z	B _{eq}
C(16)	0.1583(5)	0.3618(5)	-0.1884(4)	5.4(3)
C(17)	0.2704(5)	0.2781(4)	-0.1549(4)	4.6(3)
C(18)	0.3441(4)	0.2704(3)	-0.0366(4)	3.7(2)
C(19)	0.7885(7)	-0.0265(7)	0.4795(7)	10.9(6)
C(20)	0.9046(8)	-0.1152(8)	0.5181(8)	12.9(7)
C(21)	0.4517(6)	-0.0382(4)	0.2263(5)	6.3(4)
C(22)	0.3365(7)	-0.0278(7)	0.2348(8)	11.3(6)
C(23)	0.7955(5)	0.2173(5)	0.1933(5)	6.0(3)
C(24)	0.7799(6)	0.3372(6)	0.2072(7)	8.6(5)
C(25)	0.6699(5)	0.2530(4)	0.3947(4)	4.6(3)
C(26)	0.5076(5)	0.1663(4)	0.4019(4)	4.6(3)
C(27)	0.9580(8)	-0.1873(9)	0.0214(8)	11.4(7)
C(28)	1.087(1)	-0.242(1)	0.090(1)	18(1)
C(29)	1.106(1)	-0.203(1)	0.205(1)	15(1)
C(30)	1.005(1)	-0.101(1)	0.194(1)	17(1)

Table A4.2 Calculated hydrogen coordinates and B(iso).

atom	x	y	z	B _{iso}
H(1)	0.5093	0.4621	0.4075	4.6
H(2)	0.5729	0.6169	0.4411	5.9
H(3)	0.5431	0.7127	0.2786	6.5
H(4)	0.4558	0.6530	0.0840	6.6
H(5)	0.3899	0.4985	0.0491	4.8
H(6)	0.2743	0.5383	0.3452	5.1
H(7)	0.1261	0.5681	0.4424	6.9
H(8)	0.0380	0.4336	0.4272	7.7
H(9)	0.0988	0.2671	0.3183	7.6
H(10)	0.2485	0.2358	0.2243	6.0
H(11)	0.1587	0.4849	0.0711	5.4
H(12)	0.0368	0.5008	-0.1308	6.6
H(13)	0.1068	0.3666	-0.2722	6.5
H(14)	0.2985	0.2235	-0.2145	5.5
H(15)	0.4250	0.2111	-0.0131	4.4
H(16)	0.7927	0.0365	0.5355	13.0
H(17)	0.7219	-0.0502	0.4811	13.0
H(18)	0.9197	-0.1324	0.5994	15.5
H(19)	0.9010	-0.1803	0.4652	15.5
H(20)	0.9725	-0.0936	0.5159	15.5
H(21)	0.4826	-0.1096	0.1865	7.6
H(22)	0.5088	-0.0369	0.3073	7.6
H(23)	0.3039	0.0425	0.2757	13.6
H(24)	0.2777	-0.0302	0.1549	13.6

Table A4.2 (cont.)

atom	x	y	z	B _{iso}
H(25)	0.3470	-0.0884	0.2797	13.6
H(26)	0.8364	0.1859	0.2720	7.2
H(27)	0.8485	0.1809	0.1428	7.2
H(28)	0.8619	0.3456	0.2428	10.3
H(29)	0.7391	0.3698	0.1291	10.3
H(30)	0.7284	0.3745	0.2589	10.3
H(31)	0.9543	-0.1525	-0.0465	13.7
H(32)	0.9139	-0.2403	-0.0074	13.7
H(33)	1.1424	-0.2276	0.0572	21.0
H(34)	1.1040	-0.3217	0.0864	21.0
H(35)	1.1867	-0.1916	0.2391	18.2
H(36)	1.1016	-0.2524	0.2550	18.2
H(37)	0.9790	-0.0842	0.2650	20.4
H(38)	1.0311	-0.0420	0.1835	20.4

APPENDIX 5: KINETIC DATA**Table A5.1** The reaction of *cct*-RuH₂(CO)₂(PPh₃)₂ (**3**) with *p*-thiocresol (reaction 3.4, page 77)

[3] (mM)	[RSH] (mM)	T (°C)	<i>k</i> _{obs} (s ⁻¹)
0.88	9.5	26	6.4 x 10 ⁻⁴
0.95	10	26	5.7 x 10 ⁻⁴
0.95	11	26	6.1 x 10 ⁻⁴
0.93	26	26	6.4 x 10 ⁻⁴
0.96	91	26	6.7 x 10 ⁻⁴
0.91	110	26	7.3 x 10 ⁻⁴
0.045	94	26	6.4 x 10 ⁻⁴
0.073	87	26	6.0 x 10 ⁻⁴
0.23	91	26	6.1 x 10 ⁻⁴
0.59	91	26	6.2 x 10 ⁻⁴
0.98	92	35	1.8 x 10 ⁻³
0.93	80	42	4.5 x 10 ⁻³
0.97	94	42	4.5 x 10 ⁻³

Table A5.2 The reaction of *cct*-RuH₂(CO)₂(PPh₃)₂ (**3**) with ethanethiol (reaction 3.4, page 77)

[3] (mM)	[RSH] (mM)	T (°C)	<i>k</i> _{obs} (s ⁻¹)
1.0	45	26	6.4 x 10 ⁻⁴
1.0	91	26	6.7 x 10 ⁻⁴
1.0	95	26	6.7 x 10 ⁻⁴
1.0	95	26	7.3 x 10 ⁻⁴
1.0	95	26	6.5 x 10 ⁻⁴
1.0	190	26	7.1 x 10 ⁻⁴
1.0	190	26	5.9 x 10 ⁻⁴
0.36	95	26	7.5 x 10 ⁻⁴
0.39	95	26	6.3 x 10 ⁻⁴
2.9	95	26	6.7 x 10 ⁻⁴
1.0	95	36	1.9 x 10 ⁻³
1.1	95	37	2.8 x 10 ⁻³
1.0	95	47	6.0 x 10 ⁻³
1.0	190	47	5.7 x 10 ⁻³
1.5	95	47	6.0 x 10 ⁻³

Table A5.3 The reaction of *cct*-RuH₂(CO)₂(PPh₃)₂ (**3**) with carbon monoxide (reaction 3.5, page 86)

[3] (mM)	P _{CO} (atm)	T (°C)	<i>k</i> ' _{obs} (s ⁻¹)
1.0	0.09	25	5.4 × 10 ⁻⁴
1.0	1	25	5.7 × 10 ⁻⁴
1.1	1	25	5.7 × 10 ⁻⁴
1.0	1	34	1.8 × 10 ⁻³
1.0	1	41	4.1 × 10 ⁻³
1.0	1	41	4.1 × 10 ⁻³
0.25	1	41	4.0 × 10 ⁻³
1.1	1	51	1.1 × 10 ⁻²

Table A5.4 The reaction of *cct*-RuH₂(CO)₂(PPh₃)₂ (**3**) with triphenyl phosphine (reaction 3.6, page 86)

[3] (mM)	[PPh ₃] (mM)	T (°C)	<i>k</i> _{obs} (s ⁻¹)
0.33	51	26	6.0 × 10 ⁻⁴
0.31	50	25	6.6 × 10 ⁻⁴
0.36	47	25	6.5 × 10 ⁻⁴
0.55	380	25	6.5 × 10 ⁻⁴

Table A5.5 The reaction of *cct*-RuH(SCH₂CH₃)(CO)₂(PPh₃)₂ (**9d**) with thiophenol at 22°C (reaction 3.12, page 103)

[9d] (mM)	[PhSH] (mM)	<i>k</i> _{obs} (s ⁻¹)
8.2	120	1.7 × 10 ⁻⁴
9.7	550	1.8 × 10 ⁻⁴
8.5	1500	1.9 × 10 ⁻⁴
9.5	3400	2.0 × 10 ⁻⁴
1.8	1300	1.9 × 10 ⁻⁴

Table A5.6 The reaction of *cct*-Ru(SH)₂(CO)₂(PPh₃)₂ (**14a**) with thiophenol at 25°C (reaction 3.18, page 119)

[14a] (mM)	[PhSH] (mM)	[PPh ₃] (mM)	<i>k</i> _{obs} (s ⁻¹)	<i>k</i> _B (s ⁻¹)
6.2	69	0	4.7 x 10 ⁻⁴	4 x 10 ⁻⁴
7.8	77	0	4.2 x 10 ⁻⁴	4 x 10 ⁻⁴
6.2	330	0	4.0 x 10 ⁻⁴	3 x 10 ⁻⁴
5.1	690	0	4.4 x 10 ⁻⁴	1 x 10 ⁻³
9.4	700	0	3.8 x 10 ⁻⁴	5 x 10 ⁻⁴
5.3	1700	0	3.9 x 10 ⁻⁴	5 x 10 ⁻³
4.8	2800	0	3.4 x 10 ⁻⁴	
5.3	2900	0	3.2 x 10 ⁻⁴	1 x 10 ⁻²
5.7	770	23	3.1 x 10 ⁻⁴	3 x 10 ⁻³
5.4	750	240	3.6 x 10 ⁻⁴	3 x 10 ⁻³
6.5	66	220	2.5 x 10 ⁻⁴	3 x 10 ⁻⁴
6.2	66	325	1.3 x 10 ⁻⁴	4 x 10 ⁻⁴
6.3	64	460	1.1 x 10 ⁻⁴	4 x 10 ⁻⁴
6.1	67	490	1.1 x 10 ⁻⁴	
5.9	810	470	3.1 x 10 ⁻⁴	2 x 10 ⁻³

Table A5.7 The reaction of Ru(CO)₂(PPh₃)₃ (**2**) with *p*-tolyl disulphide (RSSR) at 25°C (reaction 4.1, page 152)

[2] (mM)	[RSSR] (mM)	initial rate (M s ⁻¹)
0.34	2.1	6.4 x 10 ⁻⁷
0.31	2.1	6.1 x 10 ⁻⁷
0.33	6.0	1.0 x 10 ⁻⁶
0.35	7.8	1.5 x 10 ⁻⁶
0.33	8.8	1.1 x 10 ⁻⁶
0.36	17	2.0 x 10 ⁻⁶
0.34	30.	2.1 x 10 ⁻⁶
0.35	51	2.0 x 10 ⁻⁶
0.083	8.0	1.3 x 10 ⁻⁷
0.19	8.1	3.0 x 10 ⁻⁷
0.72	7.9	2.3 x 10 ⁻⁶
1.3	7.8	2.0 x 10 ⁻⁶
1.3	7.9	2.5 x 10 ⁻⁶

Table A5.8 The reaction of *cct*-RuH(SR)(CO)₂(PPh₃)₂ (**9**) with P(C₆H₄*p*CH₃)₃ (L') at 45°C (reactions 6.1 and 6.2, page 218)

R	[9] (mM)	[L'] (mM)	<i>k</i> _{obs} (s ⁻¹)
-CH ₂ Ph	2.7	130	1.2 x 10 ⁻³
-CH ₂ Ph	11	94	1.0 x 10 ⁻³
-CH ₂ Ph	12	120	1.1 x 10 ⁻³
-CH ₂ Ph	10.	150	1.2 x 10 ⁻³
-CH ₂ Ph	11	300	1.3 x 10 ⁻³
-CH ₂ Ph	11	500	1.0 x 10 ⁻³
-C ₆ H ₄ <i>p</i> CH ₃	12	260	7.0 x 10 ⁻⁴

Table A5.9 The reaction of *cct*-RuH(SR)(CO)₂(PPh₃)₂ (**9**) with 1 atm carbon monoxide (reaction 6.3, page 227)

R	[9] (mM)	T (°C)	<i>k</i> _{obs} (s ⁻¹)
-CH ₃	0.87	55	7.0 x 10 ⁻³
-CH ₃	1.0	55	7.2 x 10 ⁻³
-CH ₂ CH ₃	0.88	26	3.2 x 10 ⁻⁴
-CH ₂ CH ₃	0.92	35	1.2 x 10 ⁻³
-CH ₂ CH ₃	0.89	55	1.2 x 10 ⁻²
-CH ₂ Ph	0.79	45	6.1 x 10 ⁻⁴
-CH ₂ Ph	0.74	55	2.2 x 10 ⁻³
-C ₆ H ₅	0.53	55	5.5 x 10 ⁻⁴
-C ₆ H ₄ <i>p</i> CH ₃	0.86	45	2.3 x 10 ⁻⁴
-C ₆ H ₄ <i>p</i> CH ₃	1.0	55	9.3 x 10 ⁻⁴
-C ₆ H ₄ <i>p</i> CH ₃	1.0	60	1.6 x 10 ⁻³